



UNIVERSITY OF
LIVERPOOL

**An investigation of the intestinal
epithelial damage response to
cytokines produced during
inflammatory bowel disease and
sepsis**

Thesis submitted in accordance with the
requirements of the University of Liverpool
for the degree of Doctor in philosophy

Felix Irewole Ikuomola

February 2020

Declaration

I hereby declare that this thesis is a presentation of my original work. Wherever contributions of others are involved, every effort has been made to indicate this clearly, with due reference to the literature.

Work was performed under the guidance of project supervisors' Dr Carrie Duckworth* and Professor Pritchard**.

*Gastroenterology Research Unit, Department of Molecular Physiology and Cell Signalling, Institute of Systems, Molecular and Integrative Biology, University of Liverpool

** Gastroenterology Research Unit, Department of Molecular and Clinical Cancer Medicine, Institute of Systems, Molecular and Integrative Biology, University of Liverpool.

Acknowledgements

Firstly, I am truly grateful and thankful to Dr Carrie Duckworth who has supported me immensely throughout the course of my PhD studies, and without her in-depth knowledge, patience, perseverance and guidance this doctoral thesis would not have been pragmatically possible to complete.

I would like to thank her for lecturing me comprehensively in scientific writing and for the opportunity given me to participate in the UK/Northern Ireland NF-kappaB meeting of which I won one of the best poster awards (2019).

Secondly, I am also grateful to my second supervisor, Professor Mark Pritchard for his thought-provoking supervision, advice and immeasurable support throughout the scale and scope of my PhD studies and thesis preparation.

I gratefully acknowledge Juan Hernandez-Fernand from the University of Warwick for his help with proteomics. Special thanks to all members of the Henry Wellcome Laboratories at the University of Liverpool and Department of Cellular and Molecular Physiology for their help.

Last but not the least, I am very gratefully to the Almighty God for life, sustenance and provision. And I would like to thank Wendy, my beloved wife for her inspiration, encouragement and support and Alexa Bisi, my daughter for being a source of relief from stress.

Abstract

An investigation of the intestinal epithelial damage response to cytokines produced during inflammatory bowel disease and sepsis.

Felix Irewole Ikuomola

Sepsis is a life-threatening host response to severe systemic infection that can result in multi-organ dysfunction syndrome (MODS) and organ failure. Globally, there are around 30 million cases of and 6 million deaths from sepsis annually. The intestine is one of the first organs to be damaged during the sepsis-induced proinflammatory cytokine production and hyperinflammatory responses. Similar processes occur in the intestinal mucosa during active inflammatory bowel disease (IBD). Under normal physiological conditions, the intestinal epithelium promotes gut homeostasis via mechanical protection and maintenance of structural integrity, and provides a physical barrier comprised of a continuous single cell layer of intestinal epithelial cells. Intestinal barrier dysfunction or compromised intestinal integrity potentially facilitates the passage of intestinal bacteria into the gut mucosa and blood circulation. Compromised intestinal barrier function occurs as a result of excessive epithelial cell shedding and apoptosis resulting from the direct effects of pro-inflammatory cytokines such as tumour necrosis factor (TNF) on intestinal epithelia. Understanding the mechanisms responsible for intestinal barrier function break down will potentially enable future prevention and treatment of sepsis, IBD and other conditions associated with intestinal barrier disruption. Recent advances in intestinal stem cell culture have enabled the generation of three-dimensional organoid cultures of the intestinal epithelium (termed enteroids) which can auto-propagate, auto-renew and contain similar cell populations to those found in the intestinal epithelium *in vivo*. This culture system represents a more physiological model of the intestinal epithelium than has previously been achievable using standard tissue culture techniques. It enabled investigation of tissue-level dynamics and the importance of NFκB signalling specifically in the intestinal epithelium in response to TNF (chapter 3). TNF treatment was associated with asynchronous expansions and contractions, increased motility, claudin-7 remodelling, reduced epithelial thickness and early increased surface area of enteroids. The alternative NFκB signalling pathway was demonstrated to regulate the intestinal epithelial response to injury and further exploration of other cytokines known to activate alternative pathway NFκB signalling was undertaken. We identified that other activators of NFκB signalling that are upregulated in the serum of patients with inflammatory conditions, such as TWEAK and LIGHT, were also capable of initiating the enteroid damage response and that *Nfkb2*^{-/-} enteroids were resistant to these stimuli (chapter 4). Proteomic analyses were used to identify potential mechanisms responsible for altered intestinal epithelial dynamics in response to TNF including TNFaip3 and saa3. Proteomics elucidated the potential mechanistic drivers of the intestinal damage response during perturbed NFκB signalling (chapter 5). The enteroid inflammatory model was finally tested with corticosteroids, a non-steroidal anti-inflammatory drug and a natural anti-inflammatory compound found in the diet known to modulate NFκB signalling to determine whether this newly established *in vitro* model could be used to assess novel putative therapeutic interventions for sepsis and IBD (chapter 6). Further investigation is now warranted to determine the importance of TNF, other pro-inflammatory cytokines and alternative pathway NFκB signalling in regulating intestinal tissue level dynamics during health and disease and how these parameters may be modulated therapeutically to ameliorate the severity of IBD and sepsis.

Table of contents

Declaration	2
Acknowledgements	3
Abstract.....	4
List of figures	11
List of tables	15
Abbreviations	17
1 Introduction	23
1.1 Sepsis	23
1.1.1 Clinical course of sepsis	24
1.1.2 Pathogenesis of sepsis	25
1.1.3 Intestinal manifestation of sepsis	28
1.2 Therapeutic approaches for sepsis	29
1.2.1 General measures	29
1.2.2 Specific measures	30
1.2.2.1 Antimicrobial antibiotics	30
1.2.2.2 Corticosteroids	30
1.2.2.3 PRR Antagonist	32
1.2.2.4 HMGB-1 inhibitors	32
1.2.2.5 NFκB inhibitors	32
1.2.2.6 Immunosuppressants	33
1.2.2.7 Biomedical therapy	33
1.2.2.8 Natural products	34
1.2.2.9 Surgery.....	34
1.3 Inflammatory bowel diseases	35
1.4 Similarities between sepsis and inflammatory bowel diseases	36
1.5 Anatomy and physiology of the small intestine.....	37
1.6 Intestinal mucosal epithelium	39
1.6.1 Intestinal tight junctions	35
1.6.1.1 Claudins	40
1.6.1.2 Occludin	42
1.6.1.3 Junctional adhesion molecule A (JAM-A)	43

1.6.1.4 ZO-1	44
1.7 Cell dynamics of the small intestinal epithelium	45
1.7.1 Stem cells and epithelial cell turnover	45
1.7.2 Enterocytes	47
1.7.3 Paneth cells	49
1.7.4 Goblet cells	50
1.7.5 Enteroendocrine cells	51
1.7.6 Tuft cells	52
1.7.7 M-cells	52
1.8 Organoids	53
1.8.1 Organoid definition	53
1.8.2 Small intestinal epithelial organoids	53
1.8.3 Advantages of 3D enteroid models	54
1.8.4 Disadvantages of 3D enteroid models	55
1.8.5 Applications of 3D enteroids in research and medicine	55
1.9 Prominent signalling pathways involved in gut homeostasis	56
1.9.1 Wnt signalling	56
1.9.2 Bone morphogenic protein (BMP) signalling	58
1.9.3 Epidermal growth factor (EGF) signalling	59
1.9.4 Notch signalling	59
1.10 NFκB signalling	61
1.10.1 Structure of the NFκB family	61
1.10.2 Classical NFκB signalling pathway	61
1.10.3 Alternative NFκB pathway	62
1.10.4 Hybrid pathway	63
1.10.5 IκB regulation of NFκB	63
1.10.6 NFκB signalling and small intestinal homeostasis	65
1.10.7 NFκB signalling in sepsis	66
1.11 Actions of cytokines in the small intestine	68
1.11.1 Tumor necrosis factor superfamily	68
1.11.1.1 TNF	68
1.11.1.2 TWEAK	70

1.11.1.3 LIGHT	71
1.11.1.4 CD40-L	72
1.11.1.5 Lymphotoxin alpha and beta (LT α / β)	74
1.11.1.6 BAFF	75
1.11.2 IL-6	76
1.12 Intestinal cell death mechanisms	77
1.12.1 Apoptosis in the intestinal epithelium	77
1.12.1.1 Crypt apoptosis	78
1.12.1.2 Villus tip apoptosis	79
1.12.2 Apoptotic mechanisms	80
1.12.2.1 Intrinsic apoptosis	81
1.12.2.2 Extrinsic apoptosis	82
1.12.2.3 Caspase-independent apoptosis	83
1.12.3 Necrosis	84
1.12.4 Autophagy	85
1.13 Analysis of the intestinal proteome	86
1.13.1 Proteomic technologies	87
1.13.2 Proteomic analysis in the small intestine and enteroids	88
1.14 Hypothesis, aims, and objectives	89
1.14.1 Hypothesis	89
1.14.2 Aims	89
1.14.3 Objectives	89
2. Materials and methods.....	91
2.1 Animals	91
2.1.1 Wild type mice	91
2.1.2 Transgenic mice (<i>Nfkb1</i> ^{-/-} , <i>Nfkb2</i> ^{-/-} , <i>c-Rel</i> ^{-/-})	91
2.1.2.1 Generation of <i>Nfkb1</i> ^{-/-} mice	91
2.1.2.2 Generation of <i>Nfkb2</i> ^{-/-} mice	92
2.1.2.3 Generation of <i>c-Rel</i> ^{-/-} mice	92
2.2 The 3D Small intestinal enteroids	93
2.2.1 Organoid generation from crypt isolation	93
2.2.2 Organoid media	94

2.2.2.1 Intesticult media	94
2.2.2.2 Home-made individual growth factor media	94
2.2.3 Organoid passaging	94
2.2.4 Enteroid circularity	95
2.2.5 Validation of NIH ImageJ circularity measuring technique	96
2.3 CytoSmart live cell imaging	98
2.4 Alternative NFκB signalling pathway activators	99
2.4.1 TNF superfamily	99
2.4.1.1 TNF	99
2.4.1.2 TWEAK	100
2.4.1.3 LIGHT	100
2.4.1.4 CD40-L	100
2.4.1.5 LTα1/β2	100
2.4.1.6 BAFF	100
2.5 IL-6	101
2.6 Organoid preparation for proteomic analysis	101
2.7 Organoid histology	103
2.7.1 Organoid preparation for histology	103
2.7.2 Manual organoid processing	104
2.7.3 Organoid embedding	104
2.7.4 APES slide coating for immunohistochemistry	105
2.7.5 Microtomy	105
2.7.6 Immunohistochemistry	105
2.7.7 Alkaline phosphatase co-staining	107
2.8 Therapeutic experimentation	108
2.8.1 Curcumin	108
2.8.2 Prednisolone	108
2.8.3. Hydrocortisone	108
2.8.4 Flunixin meglumine	108
2.9 Reagents and solutions	108
2.10 Data and Statistics	111
3. Characterising the actions of tumour necrosis factor on enteroids	112

3.1 Introduction	112
3.2 Results	116
3.2.1 TNF induces rounding in WT enteroids	116
3.2.2 TNF-treated WT-derived enteroids show reduced epithelial thickness .	118
3.2.3 TNF treatment induces claudin-7 remodelling in WT enteroids	120
3.2.4 TNF-treated WT enteroids show asynchronous expansions and contractions	121
3.2.5 TNF treatment is associated with increased motility of enteroids	125
3.2.6 TNF-treated enteroids showed early increases in surface area	127
3.2.7 Rescued TNF-treated enteroids demonstrated no rhythmic contractions and expansions	128
3.2.8 Rescued TNF-treated enteroids show reduced motility	131
3.2.9 Forskolin-treated enteroids are associated with asynchronous expansions and contractions	132
3.2.10 Forskolin-treated enteroids demonstrated reduced mobility	134
3.2.11 Forskolin stimulates increased enteroid surface area	136
3.2.12 CFTR inhibition does not prevent TNF-induced rounding, expansion, and contraction in enteroids	137
3.2.13 Summary table of the characteristics of actions of TNF on WT enteroids	140
3.3 Discussion	140
4. The effect of alternative pathway NFκB activation on enteroids	147
4.1 Introduction	147
4.2 Results	153
4.2.1 TNF-induced phenotypic changes in enteroids is blunted following <i>Nfkb2</i> deletion	153
4.2.2 TWEAK requires <i>Nfkb2</i> signalling to cause morphological changes of enteroids	156
4.2.3 LIGHT causes increased WT enteroid circularity which is blunted following <i>Nfkb2</i> deletion	159
4.2.4 CD40-L induces moderate morphological changes in WT enteroids but less in <i>Nfkb2</i> ^{-/-} enteroids	162
4.2.5 LTα/β slightly regulates WT and <i>Nfkb2</i> ^{-/-} enteroid phenotype	164
4.2.6 BAFF does not modulate a major WT or <i>Nfkb2</i> ^{-/-} enteroid morphology	167
4.2.7 TNF and TWEAK have additive effects on WT enteroid morphology .	169

4.2.8 Other cytokines: IL-6 induced major increase in circularity of WT but reduced in <i>Nfkb2^{-/-}</i> enteroids	172
4.2.9 Summary of action of alternative pathway activators	174
4.3 Discussion	175
5 Mechanisms by which TNF may modulate enteroid morphology and dynamics.....	180
5.1 Introduction	180
5.2 Results	182
5.2.1 There are differences in the intestinal epithelial proteome following Nfkb modulation	184
5.2.2 There are changes in the enteroid proteome following TNF treatment	184
5.2.3 TNF alters the abundance of NFκB signalling pathway components in enteroids	185
5.2.4 TNF modulates the crypt and villus proteome	186
5.2.5 TNF treatment of enteroids modulates autophagy and apoptosis	190
5.2.6 TNF treatment causes perturbations in small intestinal secretory cell populations	194
5.2.7 Mechanisms by which TNF may modulate intestinal barrier function .	196
5.2.8 Determining the effects of NFκB modulation on the intestinal epithelial response to TNF-induced injury	197
5.2.9 Similarities and differences between proteomes of TNF treated enteroids and LPS-treated intestinal mucosa	200
5.2.10 Integration of proteomic analyses with known sepsis biomarkers	206
5.2.11 Hallmark analysis of TNF-treated enteroid proteomes	209
5.3 Discussion	211
6 Development of an enteroid model to test potential sepsis and inflammatory bowel disease therapeutics	218
6.1 Introduction	218
6.2 Results	222
6.2.1 Prednisolone protects against TNF-induced enteroid rounding	222
6.2.2 Hydrocortisone prevents TNF-induced enteroid injury	225
6.2.3 Flunixin meglumine protects enteroids against TNF-induced injury....	227
6.2.4 Curcumin does not protect against TNF-induced enteroid damages ...	230
6.2.5 Summary of the actions of therapeutics on TNF-treated enteroids	232
6.3 Discussion	233

7 General discussion	239
7.1 Main findings.....	242
7.1.1 TNF causes altered enteroid morphology	242
7.1.2 TNF alters tissue dynamics of the intestinal epithelium	243
7.1.3 NFκB2 signalling is important in regulating the actions of TNF in intestinal epithelia	244
7.1.4 The intestinal epithelial proteome is modulated by TNF and NFκB perturbations	244
7.1.5 Alternative pathway NFκB2 activators regulate intestinal epithelial survival	246
7.1.6 Development of an in vitro enteroid model to investigate potential sepsis and IBD therapeutics known to modulate intestinal epithelial cell-specific NFκB signalling	246
7.2 Implications for sepsis and IBD research and therapeutic intervention	248
7.3 Strengths of the study	250
7.4 Limitations of the study	251
7.5 Future directions	252
7.6 Overall conclusions	255
8 Bibliography	256
9 Outputs	302
10 Appendix (another booklet)	

List of Figures

Figure 1.1 Microbes attached to surface cell receptors trigger immune responses that result in the activation of cascades of reactions including inflammation, vasodilatation, complement pathways, coagulopathy, endothelial cell damage, and MODS thus worsening the condition of sepsis	28
Figure 1.2 Anatomy of the small intestine showing various layers from the outer serosa to the mucosa that has an interface with the intestinal lumen and microbiota	39
Figure 1.3 Diagram of junctional protein complexes showing different types of proteins involved in maintaining intestinal epithelial integrity including tight junctions, adherens junctions, desmosomes, and gap junctions	47
Figure 1.4 Diagrammatic representation of the small intestinal epithelium depicting the villus, crypt, intestinal stem cells, transit amplifying cells, Paneth cells, goblet, enteroendocrine cells, tuft cells, and enterocytes	47

Figure 1.5 The gradients of Wnt and BMP are very important in intestinal homeostasis of which WNT signal transduction ensures the sustenance of the intestinal stem cell population in the crypts while BMP signalling maintains cell location in the crypts and prevents cell proliferation	61
Figure 1.6 Schematic diagram summarising the NFκB signalling pathways involving classical, alternative, and hybrid signalling pathways	64
Figure 1.7 Flow chart of proteomic analysis showing harvest of enteroids from mouse through protein extraction and protein digestion to protein identification by mass spectrometry method and bioinformatic analysis	87
Figure 2.1 Monitoring of the growth of enteroid from embedding in Matrigel and seeding in 24-well plates with the addition of noggin, mEGF, and R-spondin containing minigut media to provide nutrition and growth factors	95
Figure 2.2 Circularity of enteroids was investigated for intra-scorer variability within the researcher	97
Figure 2.3 Determination of inter-scorer variability of 10 enteroids randomly selected from different treatment groups and quantified by three independent scorers	97
Figure 2.4 Enteroids that were generated from the mouse were cultured with growth factors and a brightfield microscope was used to capture images	98
Figure 2.5 CytoSMART live cell imaging system with the 24-well plate containing enteroids placed on it to monitor behavioural patterns and morphological changes. Both images and videos could be accessed and assessed	99
Figure 3.1 Bright field images of TNF-treated WT enteroids. A dose-dependent and time-dependent increase in TNF-treated WT enteroid circularity was observed...	117
Figure 3.2 TNF caused a dose-dependent increase in WT-derived enteroid circularity. TNF was applied to enteroids at concentrations of 0 (purple), 1 (orange), 10 (grey), 50 (yellow) and 100 (purple) ng/ml and circularity was assessed at 0, 24 and 48 hrs	118
Figure 3.3 Alkaline phosphatase counterstained with haematoxylin micrographs of 50 ng/ml TNF-treated enteroids at 0, 6, and 24 hours	119
Figure 3.4 Relative epithelial thickness of untreated and 50 ng/ml TNF-treated enteroids were compared over a time course of 0 (blue), 6 (orange) and 24 (grey) hours	119
Figure 3.5 Immunohistochemical images of enteroids stained for claudin-7 displaying intact tight junction structural architecture and remodelled junctions shown by punctate staining	121
Figure 3.6 TNF treatment induced periodic, asynchronous expansions and contractions of WT murine enteroids	123
Figure 3.7 WT enteroids were treated with 0 (A), 50 (B), 100 (C), and 200 (D) ng/ml TNF and the CytoSMART imager collected images of nine individual enteroids per treatment every 15 minutes to monitor behavioural and morphological patterns over 72 hours	125

Figure 3.8 Each enteroid migrated independently and without a defined direction. The motility of enteroids was captured by CytoSMART live cell imaging and motility patterns are presented	126
Figure 3.9 Cumulative distances covered by untreated WT control enteroids in 72 hours was while that of 50, 100 and 200 ng/ml, TNF	127
Figure 3.10 The velocity pattern of untreated WT enteroids (blue) was steady without any sudden increases. 50 (orange), 100 (grey), and 200 (yellow) ng/ml TNF-treated WT enteroids showed marked accelerations and decelerations at different times	127
Figure 3.11 TNF induced early and sudden increases in the relative net surface area of enteroids while untreated enteroids (blue) progressively increased in the net surface area	128
Figure 3.12 Rescued enteroids from the previously 50, 100, and 200 ng/ml TNF treated enteroids did not show the spikes of asynchronous expansions and contractions that they showed while in the presence of the stimulant	131
Figure 3.13 Micrographs of rescued enteroids that were previously treated with 50 ng/ml, 100 ng/ml and 200 ng/ml TNF against untreated control. Rescued enteroids did not exhibit asynchronous expansions and contractions or increased motility ..	132
Figure 3.14 Cumulative distance (μm) travelled by control (blue), 50, 100, and 200 ng/ml TNF rescued enteroids over a 72-hour period following TNF washout	132
Figure 3.15 The 5 μM Forskolin was added to WT-derived enteroids for 72 hours. CytoSMART images were captured every 15 minutes to monitor the behavioural and morphological patterns of forskolin-treated enteroids	134
Figure 3.16 Forskolin (5 μM)-treated WT enteroids migrated through the ECM in multi-directional patterns slowly and covered different distances	135
Figure 3.17 Cumulative distances covered by untreated WT enteroids in 72 hours was while that of forskolin-treated enteroids	135
Figure 3.18 The velocity of both untreated (blue) and forskolin (5 μM)-treated (orange) WT enteroids were constant without any sudden increases or decreases in the first 48 hours of observation	135
Figure 3.19 Bright field images of forskolin and TNF-treated WT enteroids. Dose-dependent and time-dependent increases were observed in the circularity of forskolin-treated WT enteroids	136
Figure 3.20 Forskolin (5 μM) induced an early and sudden increase in the net surface area of enteroids while untreated enteroids progressively increased in the net surface area at a slower rate	137
Figure 3.21 Bright field images of CFTRinh-172-treated WT enteroids. There was no observed increase in circularity at 0, 24, and 48 hours following treatment with CFTR inhibitor	138
Figure 3.22 Bright field images of TNF treated enteroids following one-hour pre-treatment with CFTRinh-172 at indicated concentrations	139

Figure 3.23 TNF causes increased enteroid circularity following CFTR inhibition Circularity analysis at 0, 24 and 48 hrs following 0, 5, 20 and 50 μ M CFTRinh-172 pre-treatment	139
Figure 4.1 Bright field images of TNF-treated WT enteroids	155
Figure 4.2 Bright field images of TNF-treated <i>Nfkb2</i> ^{-/-} enteroids	155
Figure 4.3 TNF causes a dose-dependent and time-dependent increase in WT- derived enteroid circularity (A) but a blunted increase in circularity in <i>Nfkb2</i> ^{-/-} enteroids	156
Figure 4.4 Bright field micrographs of TWEAK-treated WT enteroids	158
Figure 4.5 Bright field images of TWEAK-treated <i>Nfkb2</i> ^{-/-} enteroids	158
Figure 4.6 TWEAK induced a dose-dependent and time-dependent increase in WT- derived enteroid circularity (A) but attenuated increase in circularity in <i>Nfkb2</i> ^{-/-} enteroids	159
Figure 4.7 LIGHT-treated WT enteroid bright field micrographs	160
Figure 4.8 Bright field images of LIGHT-treated <i>Nfkb2</i> ^{-/-} enteroids	161
Figure 4.9 LIGHT induced a dose-dependent and time-dependent increase in WT- derived enteroid circularity (A) but diminished responses in circularity in <i>Nfkb2</i> ^{-/-} enteroids	161
Figure 4.10 Bright field micrographs of CD-40L-treated WT enteroids	163
Figure 4.11 Bright field images of CD40-L-treated <i>Nfkb2</i> ^{-/-} enteroids	163
Figure 4.12 CD40-L triggered a dose-dependent and time-dependent increase in WT enteroid circularity (A) more reduced responses in circularity in <i>Nfkb2</i> ^{-/-} enteroids..	164
Figure 4.13 Bright field micrographs of LT α / β -treated WT enteroids	165
Figure 4.14 Bright field images of LT α / β -treated <i>Nfkb2</i> ^{-/-} enteroids	166
Figure 4.15 LT α / β induces a minor dose-dependent and time-dependent increase in WT-derived enteroids circularity (A) and slightly appreciable responses in circularity in <i>Nfkb2</i> ^{-/-} enteroids	166
Figure 4.16 Bright field images of BAFF-treated WT enteroids	168
Figure 4.17 Bright field micrographs of BAFF-treated <i>Nfkb2</i> ^{-/-} enteroids	168
Figure 4.18 BAFF caused a minimal dose-dependent increase in WT-derived (A) and <i>Nfkb2</i> ^{-/-} (B) enteroid circularity	169
Figure 4.19 Bright field images of TWEAK-TNF-treated WT enteroids	170
Figure 4.20 TWEAK-TNF causes a dose-dependent increase in WT enteroids circularity	171
Figure 4.21 Bright field images of IL-6-treated WT enteroids	173
Figure 4.22 Bright field micrographs of IL-6-treated <i>Nfkb2</i> ^{-/-} enteroids	173

Figure 4.23 IL-6 caused a dose-dependent and time-dependent increase in WT-derived enteroid circularity (A) which was suppressed in <i>Nfkb2</i> ^{-/-} enteroids	174
Figure 5.1 Pie charts representing the total number of significantly regulated proteins that were up- (blue) and down- (orange) regulated in untreated <i>Nfkb1</i> ^{-/-} , <i>Nfkb2</i> ^{-/-} and <i>c-Rel</i> ^{-/-} enteroids when compared with untreated WT enteroids	184
Figure 5.2 Pie charts showing that the total significantly up-regulated and down-regulated proteins in murine WT, <i>Nfkb1</i> ^{-/-} , <i>Nfkb2</i> ^{-/-} and <i>c-Rel</i> ^{-/-} enteroids following 24 hours treatment with TNF 50 ng/ml in comparison respectively with untreated WT, <i>Nfkb1</i> ^{-/-} , <i>Nfkb2</i> ^{-/-} and <i>c-Rel</i> ^{-/-} enteroids of the same strains were	185
Figure 5.3 Heat map of alternative pathway protein markers of untreated versus 24-hour 50 ng/ml TNF-treated <i>Nfkb1</i> ^{-/-} , <i>Nfkb2</i> ^{-/-} and <i>c-Rel</i> ^{-/-} IE enteroids	186
Figure 5.4 Venn diagrams depicting comparisons of significant proteomic changes (up-regulated proteins and down-regulated proteins between WT and <i>Nfkb1</i> ^{-/-} , WT and <i>Nfkb2</i> ^{-/-} , and WT and <i>c-Rel</i> ^{-/-} enteroids	200
Figure 6.1 Bright field micrographs of untreated, 0.1, 1 and, 10 µmol/l prednisolone treated WT enteroids at 0, 24, 48, and 72 hours post-treatment	223
Figure 6.2 Bright field images of untreated, 0.1, 1, 10 µmol/l prednisolone 1-hour pre-treated WT enteroids stimulated by 50 ng/ml TNF for 0, 24, 48, and 72 hours ...	224
Figure 6.3 WT enteroids were treated with 0, 0.1, 1, and 10 µmol/l prednisolone alone for 0, 24, 48, and 72 hours	224
Figure 6.4 Bright field micrographs of untreated, 0.1, 1, 10 µmol/l hydrocortisone treated WT enteroids at 0, 24, 48, and 72 hours	226
Figure 6.5 Bright field images of untreated, 0.1, 1, 10 µmol/l hydrocortisone- and 50 ng/ml TNF-treated WT enteroids at 0, 24, 48, and 72 hours	226
Figure 6.6 Measurement of WT enteroid circularity was performed following treatment with 0, 0.1, 1, and 10 µmol/l hydrocortisone for 0, 24, 48, and 72 hours	227
Figure 6.7 Bright field micrographs of untreated, 0.1, 1, 10 µmol/l flunixin meglumine treated WT enteroids at 0, 24, 48, and 72 hours	228
Figure 6.8 Bright field images of untreated, 0.1, 1, 10 µmol/l flunixin meglumine and 50 ng/ml TNF-treated WT enteroids at 0, 24, 48, and 72 hours	229
Figure 6.9 WT enteroids were treated with 0, 0.1, 1 and 10 µmol/l flunixin meglumine alone for 0, 24, 48, and 72 hours	229
Figure 6.10 Bright field micrographs of untreated, 0.1, 1 and, 10 µmol/l curcumin treated WT enteroids at 0, 24, 48, and 72 hours post-treatment	231
Figure 6.11 Bright field images of untreated WT enteroids and enteroids pre-treated with 0.1, 1, 10 µmol/l curcumin for 1 hr prior to the addition of 50 ng/ml TNF	231
Figure 6.12 WT enteroid circularity values following treatment with 0, 0.1, 1, and 10 µmol/l curcumin for 0, 24, 48, and 72 hours	232
Figure 7.1 A graphical representation of the main findings of the actions of TNF on WT and <i>Nfkb2</i> ^{-/-} intestinal epithelial (IE) enteroids and quantified proteomes	255

List of tables

Table 1.1 TNF concentrations in health and diseases from the sera, stools, and tissues of patients	70
Table 1.2 Alternative pathway activators of TNF superfamily with their gene, molecular weights (M. wt), amino acid (Aa) lengths, chromosomal (Chr.) locations, and functions	70
Table 1.3 Comparison of the features of apoptosis, necrosis, and autophagy. Activation of autophagy is aimed at saving and preserving the function of cells and cellular organelles, especially the mitochondria	86
Table 2.1 Manual organoid processing steps, temperatures and times are shown from step 1 to step 11	104
Table 2.2 Different antibody concentrations utilized in probing for the proteins in the treated enteroids	107
Table 2.3 Reagents, antibodies and other materials utilised for the methods of the experiments performed in this thesis	110
Table 3.1 Phenotypic differences between untreated and TNF-treated enteroids. The growth patterns of untreated enteroids were not interrupted with asynchronous expansions and contractions as seen in TNF treated enteroids	140
Table 4.1 Alternative pathway activators with their gene, molecular weights, amino acid lengths, chromosomal locations, and functions	152
Table 4.2 The TNF superfamily, alternative pathway activators with their concentrations in health and disease	153
Table 4.3 A summarise table of different rounding responses of WT and <i>Nfkb2</i> ^{-/-} enteroids to treatment of various cytokines	174
Table 5.1 Crypt domain protein markers from untreated versus 24-hour 50 ng/ml TNF-treated WT, <i>Nfkb1</i> ^{-/-} , <i>Nfkb2</i> ^{-/-} and <i>c-Rel</i> ^{-/-} enteroids	188
Table 5.2 Villi domain protein markers from untreated versus 24-hour 50 ng/ml TNF-treated WT, <i>Nfkb1</i> ^{-/-} , <i>Nfkb2</i> ^{-/-} and <i>c-Rel</i> ^{-/-} enteroids	189
Table 5.3 Autophagy protein markers of untreated versus 24-hour 50 ng/ml TNF-treated WT, <i>Nfkb1</i> ^{-/-} , <i>Nfkb1</i> ^{-/-} and <i>c-Rel</i> ^{-/-} enteroids	191
Table 5.4 Apoptosis-related protein markers of untreated versus 24-hour 50 ng/ml TNF-treated WT, <i>Nfkb1</i> ^{-/-} , <i>Nfkb2</i> ^{-/-} and <i>c-Rel</i> ^{-/-} enteroids	193
Table 5.5 Goblet cell protein markers of untreated versus 24-hour 50 ng/ml TNF-treated WT, <i>Nfkb1</i> ^{-/-} , <i>Nfkb2</i> ^{-/-} and <i>c-Rel</i> ^{-/-} enteroids	194
Table 5.6 Paneth cell protein markers of untreated versus 24-hour 50 ng/ml TNF-treated WT, <i>Nfkb1</i> ^{-/-} , <i>Nfkb2</i> ^{-/-} and <i>c-Rel</i> ^{-/-} enteroids	195
Table 5.7 Barrier function and tight junction protein markers of untreated versus 24-hour 50 ng/ml TNF-treated <i>c-Rel</i> ^{-/-} intestinal epithelial enteroids	197

Table 5.8 Commonly under- and over-expressed proteins in <i>Nfkb2^{-/-}</i> , <i>Nfkb1^{-/-}</i> , and <i>c-Rel^{-/-}</i> all the three transgenics compared to WT after 24 hours of 50 ng/ml TNF treatment and were individually compared with the 24 hours TNF-treated WT	199
Table 5.9 Total number of proteins detected in untreated mouse enteroids and small intestinal mucosae	202
Table 5.10 Significantly over- and under-expressed proteins in enteroids and small intestinal mucosae in WT, <i>Nfkb1^{-/-}</i> , <i>Nfkb2^{-/-}</i> and <i>c-Rel^{-/-}</i>	203
Table 5.11 Similarities and differences between murine intestinal epithelial organoids and murine intestinal mucosa	204
Table 5.12 Significantly up- and down-regulated proteins in TNF-treated enteroids and their corresponding proteins in murine small intestinal mucosa treated with LPS	205
Table 5.13 Protein biomarkers of sepsis detected in WT, <i>Nfkb1^{-/-}</i> , <i>Nfkb2^{-/-}</i> and <i>c-Rel^{-/-}</i> enteroids following 24 hours treatment with TNF (50 ng/ml)	208
Table 5.14 Summary of the hallmark analysis showing the name process category, pathway description	210
Table 6.1 Prednisolone, hydrocortisone, and flunixin meglumine ameliorated TNF-induced rounding in WT enteroids at 24 hours following treatment, but curcumin did not exert any inhibitory effect at the same time point	232

Abbreviations

ABIN-1: A20 Binding and Inhibitor of NFκB
AIDS: Acquired immunodeficiency syndrome
ANOVA: Analysis of variance
AOM: Azoxymethane
Apaf-1: Apoptotic protease activating factor 1
APC: Adenomatosis polyposis coli
APES: 3-Aminopropyltriethoxysilane
ARDS: Acute respiratory distress syndrome
ATP: Adenosine triphosphate
BAFF: B-cell activating factor
BALF: Bronchoalveolar fluid
BCMA: B-cell maturation antigen
BSU: Biomedical services unit
Caco-2: Colorectal adenocarcinoma

CADASIL: Cerebral Autosomal-Dominant Arteriopathy with Sub-cortical Infarcts and Leukoencephalopathy

cAMP: Cyclic adenosine monophosphate

CAR: Coxsackie- and adenovirus receptor

CARD: Caspase activation and recruitment domain

CBC: Crypt base columnar

CD: Crohn disease

CD40-L: Cluster of differentiation 40 ligand

CDK5: Cyclin-dependent kinase 5

CFTR: Cystic fibrosis transmembrane conductance regulator

cIAP: Cellular inhibitor of apoptosis protein

CK1 α : Casein kinase 1 α

CLP: Caecal ligation puncture

CMA: Chaperone-mediated autophagy

CME: Coronary microembolization

COPD: Chronic obstructive pulmonary disease

COX-2: Cyclooxygenase-2

CRP: C-reactive protein

CYLD: Cylindromatosis

2D-DIGE: 2D difference gel electrophoresis

2DE: Two-dimensional electrophoresis

3D: Three dimensions

DAAM-1: Dishevelled-associated activator of morphogenesis 1

DAB: Diaminobenzidine

DAMP: Damage-associated molecular pattern molecule

DAVID: Database for Annotation, Visualization and Integrated Discovery

DLG5: Discs large MAGUK scaffold protein 5

DMSO: Dimethyl sulfoxide

DNA: Deoxyribonucleic acid

Dsh/Dvl: Dishevelled

DSL: Delta-Serrate-Lag

DSS: Dextran sulphate sodium

DUB: Deubiquitinases

ECM: Extracellular matrix
EDTA: Ethylenediamine tetra-acetic acid
EGF: Epithelial growth factor
ERK: Extracellular signal–regulated kinase
ES: Embryonal stem
ES: Enrichment score
ESAM: Endothelial cell-selective adhesion molecule
ESI: Electrospray ionization
ETEC: Enterotoxigenic Escherichia coli
FAN: Factor associated with neutral sphingomyelinase activation
FC: Fold count
FDR: False discovery rate
FE: Fold enrichment
FRP: Frizzled-Related Protein
Fz: Frizzled
GC: Gene count
GCR: Glucocorticoid receptor
GLUT2: Glucose transporter 2
GM-CSF: Granulocyte-macrophage colony-stimulating factor
GO: Gene ontology
GRE: Glucocorticoid response element
GSK: Glycogen synthase kinase 3
HAT: Histone acetyltransferase
HESR: Hairy and enhancer of split-related
HIV: Human immunodeficiency virus
HMGB1: High-mobility group box 1 protein
HSP: Heat shock protein
HVEM: Herpes virus entry mediator
IBD: Inflammatory bowel disease
ICAM-1: Intercellular Adhesion Molecule 1
ICAT: Isotope-coded affinity tag
ICC: Interstitial cells of Cajal

IEC: Intestinal epithelial cell

IFN: Interferon

IKK: Inhibitor of kappa B kinase

IL- Interleukin

iPSCs: induced pluripotent stem cells

IRF9: Interferon regulatory factor 9

ISGF3: IFN-stimulated gene factor 3

iTRAQ: Isobaric tags for relative and absolute quantitation

JAK: Janus kinase

JAM: Junctional adhesion molecule

JNK: c-Jun N-terminal kinase

KEGG: Kyoto Encyclopedia of Genes and Genomes

LC: Liquid chromatography

LEF: Lymphoid enhancer-binding factor 1

LGR5: Leucine-rich repeat-containing G protein–coupled receptor 5

LIGHT: Lymphotoxin exhibits inducible expression and competes with HSV glycoprotein D for binding to herpesvirus entry mediator, a receptor expressed on T lymphocytes

LPS: Lipopolysaccharide

LRP: Lipoprotein receptor-related protein

LRR: Leucine-rich repeat

LT β R: Lymphotoxin β receptor

LUBAC: Linear ubiquitin assembly complex

MAb: Monoclonal antibody

MAC: Membrane attack complexes

MAGUK: Membrane-associated guanylate kinases

MALDI: Matrix assisted laser desorption/ionization

MAPK: mitogen-activated protein kinase

MCP-1: monocyte chemoattractant protein-1

MCSF: Macrophage colony-stimulating factor

MIF: Migration-inhibitory factor

MIS: Mucosal immunity system

MODS: Multi-organ dysfunction syndrome

MS: Mass spectroscopy

MUC: Mucin

MYD88: Myeloid differentiation primary response 88 (MYD88)

n: Number of individual enteroid in the same well

N: Number of experiment performed at specified time

NEMO: NFκB essential modulator

NFκB: Nuclear factor kappa-light-chain-enhancer of activated B

NIK: NFκB-inducing kinase

NOD2: Nucleotide-binding oligomerization domain-containing protein 2

NSAID: Non-steroidal anti-inflammatory drug

OCTN1/2: Organic cation transporter novel type 1/2

PAMP: Pathogen-associated molecular pattern

PBS: Phosphate-buffered saline

PCP: Planar cell polarity

PDGFRβ: Platelet-derived growth factor receptor beta

PDZ: Post synaptic density protein, Drosophila disc large tumor suppressor (Dlg1), and Zonula occludens-1 protein

PFA: Paraformaldehyde

PGK: Phosphoglycerate kinase

PI3K: Phosphoinositide 3-kinase

PP2A: Protein phosphatase 2A

PPARγ: Peroxisome proliferator-activated receptor gamma (PPARγ)

PPRE: Peroxisome proliferation response element

PRR: Pattern recognition receptor

RANK: Receptor activator of nuclear factor κ B

RBP-J: Recombination signal binding protein for immunoglobulin kappa J

RHD: Rel homology domain

RIPK1: Receptor-interacting serine/threonine-protein kinase 1

RNS: Reactive nitrogen species

ROCK: Rho-associated kinase

ROR-2: Receptor tyrosine kinase-like orphan receptor-2

ROS: Reactive oxygen species

RTK: Receptor tyrosine kinase

SGLT: Sodium glucose transporter

SIRS: System inflammatory response syndrome

SLPI: Secretory leukoprotease inhibitor

STAT: Signal transducer and activator of transcription

TA: Transit-amplifying

TACI: Transmembrane activator and calcium modulator and cyclophilin ligand interactor

TAD: Transcriptional activation domain

TEAB: Triethylammonium bicarbonate

TCF: Transcription factors

TCR: T cell receptor

TGF- β : Transforming growth factor- β

TJP: Tight junction protein

TLR: Toll-like receptor

TMT: Tandem mass tag

TNF: Tumour necrosis factor

TNFAIP3: TNF alpha-induced protein 3

TNFR: TNF receptor

TNFRSF: TNF receptor superfamily

TNFSF: TNF superfamily

TRAF: TNF receptor-associated factor

TRAIL: TNF-related apoptosis-induced ligands

TWEAK: TNF-related weak inducer of apoptosis

UC: Ulcerative colitis

ULK: Unc-51-like kinases

V-CAM-1: Vascular cell adhesion molecule 1

WIF-1: Wnt Inhibitory Factor-1

Wnt: Wingless (Wg) (*Drosophila melanogaster* fruit fly) and integration 1 (Int1)

WT: Wild type

XHIM: X-linked immunodeficiency hyper IgM syndrome

ZO-1: Zona occludens-1

1 Introduction

1.1 Sepsis

Sepsis is an infection-induced systemic syndrome of physiologic, pathologic, and biochemical abnormalities (Singer et al, 2016). It is a life-threatening infection-host response dysregulation resulting in multi-organ dysfunction syndrome (MODS) including cognitive dysfunction and organ damage (Singer et al., 2016; Williams et al., 2013). One of the first body organs to undergo pathophysiologic derangements due to an abrupt onset and dramatic progression of sepsis is the intestine (Doig et al., 1998; Julian et al., 2011). Intestinal homeostasis is ensured by the protective, structural, and functional barrier of the intestinal epithelium (Gasbarrini & Montalto, 1999; Ley et al., 2006; O'Hara et al., 2006). There are about 100 trillion bacteria which live symbiotically in the gut (Turnbaugh et al., 2007). However, any intestinal barrier dysfunction or compromised intestinal integrity could facilitate the passage of intestinal bacteria into the blood circulation (Blikslager et al., 2007; Cani et al., 2008). This potentially, results in increased bacterial load and subsequent sepsis progression and intestinal failure (Kiesslich et al., 2012; Piton et al., 2011; Shinoda et al., 2016). Sepsis causes increased intestinal permeability with associated multi-systemic organ dysfunction in critically ill patients. (Doig et al., 1998). Globally, every year about 30 million cases of sepsis including 19.4 million severe cases are reported (Reinhart et al., 2017) and the mortality rate due to sepsis is about 6 million cases globally per year (Reinhart et al., 2017). Globally, about 3 million newborns and 1.2 million children contract sepsis respectively each year (Fleischmann-Struzek et al., 2018). Sepsis is also responsible for about 30% of cancer deaths in hospitalised patients (Mayr et al., 2014). The estimated economic burden of sepsis in the US is around \$20 billion per annum (Singer et al., 2016), while in the UK the economic

burden totals about £2.7 billion annually (Tsertsvadze et al., 2015) resulting in considerable cost to the National Health Service (NHS).

People at the early and late extremes of life are more susceptible to developing the severe complications of sepsis. Other vulnerable groups include pregnant women, hospitalised patients, asplenic individuals, and patients with autoimmune diseases, cancer, HIV/AIDS, kidney disease, and liver cirrhosis (Say et al., 2014). Key diagnostic factors of systemic inflammatory response syndrome (SIRS) include high (>38°C) or low (<36°C) temperature, tachycardia, and tachypnoea. Other clinical manifestations of sepsis include ileus, purpura fulminans, jaundice, hypotension, altered sensorium, oliguria, and dyspnoea (Dellinger et al., 2004). In sepsis, the intestine is among the first tissues to be affected with disruption of intestinal homeostasis that results in intestinal failure. Positive blood cultures observed in patients with sepsis, severe sepsis, and septic shock are respectively 17%, 25%, and 69% (Fink & Heard, 1990). The classification of sepsis has changed recently and no longer includes SIRS which can occur without sepsis or the presence of infection.

Unfortunately, there are no molecularly targeted sepsis-specific therapeutics or validated standard diagnostics, the only current treatment is supportive or symptomatic care (Singer et al., 2016). Thus, an in-depth study of sepsis that will aid in understanding the cascades of mechanism of actions and discovery of any novel therapeutic targets with potential ability to enhance intestinal protective barrier integrity and prevent intestinal barrier dysfunction should be investigated.

1.1.1 Clinical course of sepsis

Early clinical manifestations of sepsis may be subtle and difficult to diagnose, so, a high index of suspicion is paramount. In general, a patient may present with fever which is the commonest presentation of sepsis. However, patients at the extremes of life (early and late) and patients with debilitating conditions, a history of chronic

alcohol abuse or uraemia are likely to present with sepsis-induced hypothermia and an absence of fever (Hotchkiss & Karl, 2003).

Intestinal features of sepsis include abdominal pain, vomiting, bloody or non-bloody diarrhoea, distension, rigidity, guarding, reduced or absent bowel sounds, and upper gastrointestinal tract blood loss. Early clinical presentations of sepsis include increased pulse rate, increased respiratory rate, warm and dry extremities, restlessness, slight confusion, reduced urine output, and high cardiac output. Other features include low systemic vascular resistance due to the vasodilatory effect of released mediators. However, blood pressure may be normal or slightly reduced during the early stages of sepsis. Clinical features of late sepsis include a decreased level of consciousness, coma, markedly reduced urine output, tachypnoea, tachycardia, hypotension, reduced cardiac output, and cold extremities. Investigations in the diagnosis of sepsis include serum lactate, full blood count (especially white blood cells - total and differential), blood culture, urea, electrolytes, creatinine, C-reactive protein, procalcitonin, and liver function tests. Adequate administration of antibiotics within one hour of suspected sepsis (which is considered as the 'golden hour') is very important in increasing the survival of patients (Dellinger et al., 2008). When this 'golden hour' opportunity is missed, each hour delay of administration of antibiotics, decreases patient survival by about 8% (Kumar et al., 2006). The prognosis in sepsis is based on early recognition, prompt diagnosis, early administration of appropriate antibiotics, and early adequate reversal of the shock state.

1.1.2 Pathogenesis of sepsis

The pathogenesis of sepsis is not only complex, but complicated and broad (figure 1.1). It includes dysregulated inflammatory responses, a dysfunctional clotting system, imbalanced immunomodulation, autophagy, endoplasmic reticulum stress, disrupted mitochondrial organelles, and other altered pathophysiological processes.

The cascades of dysfunctional cellular and molecular responses to sepsis cumulate in multiple organ dysfunction syndrome (MODS) and eventual multiple organ failure. Pathogens such as bacteria, viruses, parasites, and fungi invade endothelial cells and elicit the host's responses of cytokine-mediated pro- and anti-inflammatory activations. The first line of defence is migration of neutrophils to the site and these recognise and phagocytose invading pathogens through the release of proteolytic enzymes and other active host defense factors. This results in activation of mononuclear/macrophage cells via the stimulation of granulocyte-macrophage colony-stimulating factor (GM-CSF), immune complexes, pathogenic microorganisms, chemical mediators, and others (Shen et al., 2017). Pro-inflammatory cytokines can trigger a cytokine storm and modulate pattern-recognition receptors (PRRs) to activate the innate immune system through the detection of damage-associated molecular patterns (DAMPs) or pathogen-associated molecular patterns (PAMPs) (Takeuchi & Akira, 2010). PRRs such as Toll-like receptors (TLRs), retinoic acid-inducible gene (RIG)-I-like receptors (RLRs), C-type lectin receptors (CLRs), and nucleotide-binding oligomerisation domain (NOD)-like receptors (NLRs) mediate stimulation of the innate immune system resulting in overexpression of associated inflammatory target genes (Raymond et al., 2017). Toll/interleukin-1 receptor (TIR) homology domains induce TLRs to interact with their ligands to activate c-Jun N-terminal kinase (JNK), p38 mitogen-activated protein kinase (MAPK), extracellular signal-regulated kinase 1/2 (ERK1/2), and nuclear factor- κ B (NF- κ B) signaling pathways via the myeloid differentiation factor 88-dependent (MyD88) pathway (Kawai & Akira, 2010). These cascades of reactions result in the synthesis of inflammatory cytokines, including tumor necrosis factor (TNF), interleukin (IL)-1, IL-6, interferon (IFN) regulatory factor 7 (IRF7), and adaptor proteins (AP) (most especially AP-1 and AP-3) (Kawai & Akira, 2010). In response to the activation of the immune system by PAMPs and DAMPs, intracellular cytosolic protein complexes of inflammasomes are assembled. Inflammasomes initiate the

cleaving of caspase-1 precursor to cause activation of caspase-1, which results in activated caspase-1 cleaving IL-1 β and IL-18 precursors thus leading to release of the proinflammatory cytokines IL-1 β and IL-18 (Lamkanfi, 2011; Qiu et al., 2019). IL-1 modulates the thermoregulatory centre of the hypothalamus to increase body temperature during sepsis, thus it is known as an endogenous pyrogen. IL-1 also induces vasodilation, hypotension, and hyperalgesia. IL-6 mediates the production of acute phase proteins such as albumin, transthyretin, transferrin, and retinol-binding protein (Huang, Cai, & Su, 2019). It is also involved in the proliferation of B-lymphocytes and neutrophils in sepsis. The interferon (IFN) regulatory factor 7 controls the tissue-damaging apoptotic effects of interferon and interferon-mediated production of reactive oxygen species (ROS) (Arens et al., 2016). Adaptor proteins are involved in coordinating protein-binding site interaction with ligands to facilitate the generation of multiple signalling complexes especially T cell receptor (TCR) and other immunomodulatory activities (Flynn, 2001; Peterson et al., 1998). The immune dysfunction in sepsis includes reduction in HLA-DR, increase in lymphocyte replication, induction of apoptosis, and increase in anti-inflammatory molecules expression (Venet & Monneret, 2018). In sepsis, there is a coordinated interaction between the inflammatory process and coagulation through which inflammation can activate the coagulation reaction resulting in an inflammatory response. Systemic responses to sepsis range from shock, hypotension, confusion, coma, disseminated intravascular coagulopathy, carbon dioxide, increased and lactic acid concentrations and, autodigestion to multiple organ dysfunction and failure (De Backer et al., 2002; Schmid-Schonbein et al., 2011).

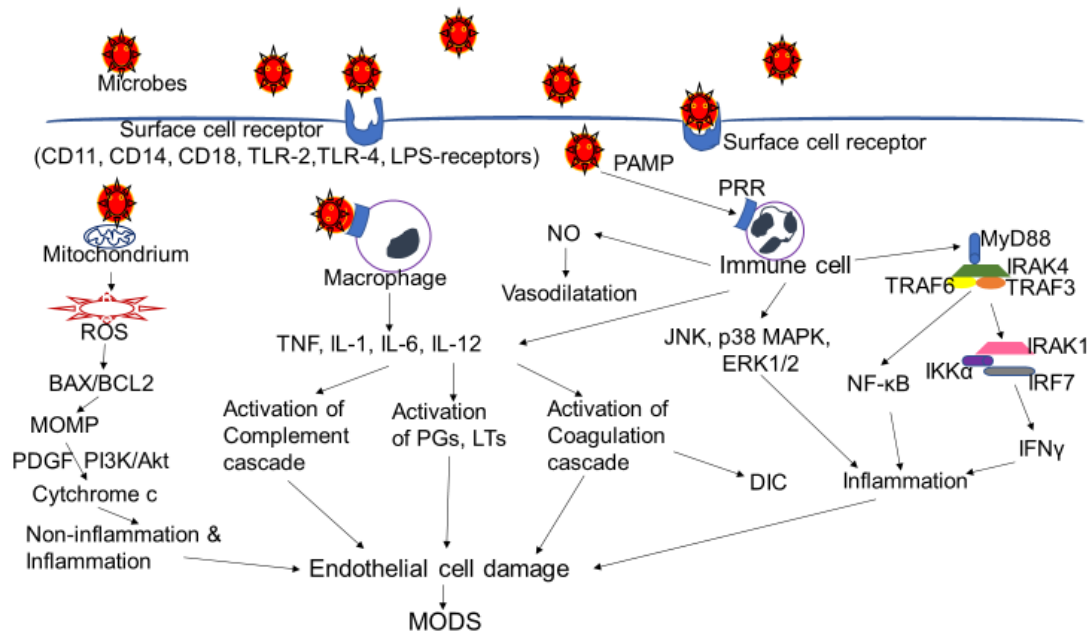


Figure 1.1 Microbes attached to surface cell receptors trigger immune responses that result in the activation of cascades of reactions including inflammation, vasodilatation, complement pathways, coagulopathy, endothelial cell damage, and MODS thus worsening the condition of sepsis. Modified from Arens et al., 2016; Kawai & Akira, 2010; Takeuchi & Akira, 2010.

1.1.3 Intestinal manifestation of sepsis

Sepsis disrupts intestinal epithelial homeostasis, including its protective and absorptive functions, and structural integrity. It also affects intestinal epithelial perfusion, enzymatic response, coagulation function, and the mucosal immune system (MIS) (Mowat & Agace, 2014). PRRs are present in intestinal epithelial cells (IECs) and intestinal macrophages and other immune cells such as neutrophils and dendritic cells (DCs). During sepsis, the presence of PAMPs such as lipopolysaccharide (LPS), bacterial DNA, and cytosine-phosphate-guanine (CpG) of bacterial microorganisms on the surface of IECs are detected by PRRs (Cerovic et al., 2014). The MIS comprises of intestinal macrophages and DCs that recognise luminal PAMPs through transepithelial dendrites (TEDs) (Cerovic et al., 2014; Haussner et al., 2019). The interaction between PAMPs and the host's PRRs and MIS results in a cytokine storm of pro-inflammatory mediators with subsequent release of reactive oxygen species (ROS), overexpression of endothelial adhesion

molecules, and additional neutrophil recruitment. The sequelae of sepsis resulting from the association of a PAMP with a PRR can provoke a cascade of reactions, including translocation of transcription factors such as nuclear factor-kappa B and activator protein-1 resulting in mediation of further increased production of pro-inflammatory proteins that can cause adverse events both locally and systemically (Wang, Bastarache & Ware, 2008). Local cellular responses to sepsis include disrupted IEC barrier functions, aggravated vasodilatation, enhanced capillary leakage, increased interstitial oedema, increased hypoxia, and necrosis of IECs, suppressed intestinal regeneration, compromised IEC repair, and facilitated bacterial translocation (Amalakuhan et al., 2016; Stadnyk, 2002). Other local effects of sepsis include compromised gut integrity, increased apoptosis, reduced proliferation, and shortened villus length (Clark et al., 2008; Dominguez et al., 2013; Williams et al., 2013).

1.2 Therapeutic approaches for sepsis

1.2.1 General measures

Supportive and symptomatic measures are among the mainstream treatments in the management of sepsis. Intravenous fluids are given for resuscitation and to ensure adequate hydration and enhance systemic function. Sufficient oxygenation is very important for maintenance of vital organ function. Intubation and mechanical support are sometimes given to patients with respiratory compromise, while dialysis ensures optimal kidney function in patients who have renal failure. Vasopressors such as norepinephrine, phenylephrine, or dopamine are given to correct sepsis-induced hypotension. The indication for vasopressor therapy in sepsis is to maintain a patient's mean arterial pressure at or higher than 65 mmHg. Where enteral feeding is impossible parenteral nutrition is sometimes administered to patients. Central

venous catheter placement can also be conducted for continuous hemodynamic monitoring of patients with sepsis.

NSAIDs are used in mild sepsis to inhibit cyclooxygenase enzymes. Legras and colleagues investigated whether there was any association between NSAIDs treatment during evolving bacterial community-acquired infection in adults and development of severe sepsis or septic shock (Legras et al., 2009). They concluded that the use of NSAIDs was not associated with severe sepsis or septic shock except that NSAID users had a longer median time to prescription of effective antibiotic therapy (Legras et al., 2009). Examples of NSAIDs are aspirin, ibuprofen, celecoxib, flunixin meglumine (not currently used in humans), and others that are used as antipyretic and analgesic.

1.2.2 Specific measures

Various types of therapeutics have been used in the past to treat sepsis; some have been effective while some are not. There are some that are experimental and have not been tested in humans yet.

1.2.2.1 Antimicrobial antibiotics

Empirical antibiotics are given to patients with sepsis while awaiting the results of the microscopy, culture, and sensitivity tests. Based on these laboratory results specific antibiotics can also be given against causative organisms. Usually, combinations of two or three antibiotics are administered. Examples of antibiotics that work against Gram-negative and Gram-positive bacteria are ceftriaxone, ampicillin, piperacillin and tazobactam, levofloxacin, and others. In the case of resistance against the antibiotics, vancomycin may be given to treat methicillin-resistant *Staphylococcus aureus* (MRSA). In the case of viral-, fungal, or parasitic-mediated sepsis, therapeutics are directed against the aetiologic agents. Cutuli and colleagues conducted analysis of a multicenter registry of patients with sepsis that were treated

with polymyxin B hemoperfusion (PMX-HP) and reported that early administration of PMX-HP demonstrated improved hemodynamics and lung oxygenation and decreased mortality in a septic shock clinical trial (Cutuli et al., 2016). However, Iwagami and colleagues reported that PMX-HP failed to demonstrate any improvement in survival of patients with septic shock and reduction in mortality in a randomised controlled trial (Iwagami et al., 2014).

1.2.2.2 Corticosteroids

Use of corticosteroids in sepsis is attributed to how they attenuate the fulminant and dysfunctional pro-inflammatory response, regulate anti-inflammatory response as they ensure preservation of innate immune system (Keh et al., 2003; Marik et al., 2008). Corticosteroids mediate anti-inflammatory responses in sepsis via mitogen-activated protein kinase phosphatase-1 which inhibits the mitogen-activated protein kinase signalling pathway thus inhibiting inflammatory transcription gene target in the nucleus. Other anti-inflammatory responses include activating histone acetylation and antiprotease secretory leukoprotease inhibitor (SLPI) and inhibiting increased expression of kinins, chemokines, adhesion molecules and inducible cyclooxygenase and nitric oxide synthase (Barnes et al., 2006; Ito, Barnes & Adcock, 2000). Prednisolone modulates the immune response to ameliorate allergic, oedema, redness, and pruritus (Bunte et al., 2018). The corticosteroids that are commonly used in sepsis include hydrocortisone, prednisolone, and dexamethasone. All of these corticosteroids are known to modulate NF κ B signalling. Corticosteroids mediate induction of I κ B α inhibitory protein, which sequesters activated NF κ B in inactive cytosolic complexes thereby hindering release of a free NF κ B and preventing its translocation to nucleus where it effects transcriptional activation of inflammatory genes (Auphan et al., 1995; Verma, 2004).

1.2.2.3 PRR Antagonist

Eritoran is a potent inhibitor of TLR4 which is one of the signal transduction surface cell receptors for bacterial LPS. Eritoran is used to prevent released endotoxins from bacteria from binding to TLR4. In mice, Eritoran protected mice from lethal infection caused by influenza superimposed by bacteria (Shirey et al., 2013). However, Eritoran could not proceed beyond a clinical phase III trial for failure to improve survival of patients with sepsis (Opal et al., 2013). Resatorvid (TAK-242), a cyclohexen derivative, is a potent antagonist of TLR4 by selectively binding to the TIR domain of TLR4. In LPS-induced sepsis in mice, Resatorvid ameliorated organ dysfunction and prolonged survival. When Resatorvid was combined with imipenem, there was decreased mortality and inhibition of cytokine production in CLP-induced septic mice (Sha et al., 2011), not yet tested in humans.

1.2.2.4 HMGB-1 inhibitors

In experimental cell cultures and animal models of sepsis, HMGB-1 inhibitors especially ethyl pyruvate, chloroquine, stearyl lysophosphatidylcholine, nicotine, persicarin and isorhamnetin-3-O-galactoside demonstrated antagonism against HMGB-1 (Shukla et al., 2014). However, the efficacies of these HMGB-1 inhibitors are yet to be shown in humans.

1.2.2.5 NFκB inhibitors

Lestaurtinib, a tyrosine kinase inhibitor, is a potent NFκB inhibitor that blocks the phosphorylation of IκBα (Tickenbrock et al., 2006). Various studies with parthenolide, a sesquiterpene lactone, have shown that it induces alkylation and inactivation of a cysteine residue in the p65 subunit that is very important for DNA binding (Lyss et al., 1998). Other studies with parthenolide have shown that it can alkylate a cysteine residue in IKK, thus deterring phosphorylation and biodegradation of IκB-α and preventing availability of NFκB for translocation to nucleus and participation in the

transcription of inflammatory target genes (Hegner et al., 1999; Mazar et al., 2000). Sheehan and colleagues conducted a sepsis-induced study in rats and reported that administration of parthenolide reduced the serum levels of NF- κ B for up to 6 hours while the reduction in the serum levels of TNF and IL-6 lasted up to 18 hours (Sheehan et al., 2003). Other potential inhibitors of NF κ B are Sunitinib malate, Narasin, Sorafenib tosylate, Bithionol, Emetine, tribromsalan, fluorosalan, and lestaurtinib (Miller et al., 2010). They also prevent I κ B α phosphorylation, however, are not routinely used in humans.

1.2.2.6 Immunosuppressants

Lv and colleagues conducted a meta-analysis on seventeen studies that contained 8971 patients that investigated the efficacy of TNF antagonist treatment against placebo in patients with severe sepsis or septic shock (Lv et al., 2014). They reported that TNF antagonists significantly reduced mortality in sepsis when compared with the placebo group and improved survival in patients who had high levels of IL-6 (>1000 pg/ml) and patients with shock (Lv et al., 2014). The main TNF inhibitors are infliximab, etanercept, adalimumab, golimumab, and certolizumab pegol. Afelimomab treatment was also reported to significantly lower serum concentrations of TNF- α and IL-6 for three consecutive days, reduce mortality, and improve organ dysfunction in patients with severe sepsis (Conrad et al., 2011).

1.2.2.7 Stem cell therapy

Studies have reported the various inherent properties of stem cells such as anti-apoptotic, antimicrobial, anti-inflammatory, and cytoprotective. These properties could be very important in improving the prognosis of patients with sepsis and MODS. Mesenchymal stem cells (MSCs) have been reported to play major roles in the secretion of anti-inflammatory cytokines against TNF-stimulated genes that interact with macrophages' CD44 receptors to reduce TNF expression through down-

regulation of NF κ B signalling pathways. In response to LPS, MSCs secreted cathelicidin LL-37 peptide which exhibited antimicrobial effects by attacking bacterial membranes (Wannemuehler et al., 2012). Krasnodembskaya and colleagues administered human MSCs to septic mice and reported that MSCs decreased mortality, enhanced bacterial clearance, and improved phagocytic activity of the body defense (monocytes) (Krasnodembskaya et al., 2012).

1.2.2.8 Natural products

Pourdast and colleagues investigated the potential anti-inflammatory effects of Septimeb, a herb, in a randomised clinical trial of 51 patients with sepsis in intensive care (Pourdast et al., 2017). They reported that Septimeb treatment caused a significant reduction in sequential organ failure assessment (SOFA) score, improvement in Glasgow coma scale (GCS), and reduction in severity of sepsis in the experimental group in comparison with the control group (Pourdast et al., 2017). They also reported that the elevated concentrations of lactate, blood sugar, and white blood cells (WBC) were significantly reduced post-treatment. Although levels of ESR and CRP were reduced, they were not significantly decreased when compared with the control group. Another natural product is Chromomycin A3, an antibiotic isolated from *S. griseus* that possesses NF κ B inhibiting properties (Calabresi, 1996), has not been tested in humans. Kukoamine B, a natural alkaloid herb that inhibits LPS and CpG DNA and reduces the release of TNF and IL-6 during sepsis and improves patient survival (Liu et al., 2011). The potential use of Curcumin, an active ingredient in turmeric, in this setting is extensively discussed in chapter 6 of this thesis.

1.2.2.9 Surgery

Surgery may be required to drain abscesses, remove the source of infection, or amputate limbs to reduce bacterial load. More information on management and treatment of sepsis are available at www.nhs.uk.

1.3 Inflammatory bowel diseases

Inflammatory bowel diseases (IBD) are generally localised to the intestine, however there are similarities between IBD and the intestinal manifestations of sepsis and clues can be drawn from both conditions that will enhance scientific knowledge and research in both areas. IBD results from an immunological imbalance in response to many environmental stimuli in both genetically and non-genetically susceptible individuals (Baumgart & Carding, 2007). The postulated aetiological factors for IBD are epidemiological (diet, seasonal variation, drugs, and smoking), gut/environmental interface (gut bacteria, biofilms, epithelial barrier integrity, and immune/epithelial interactions), and inflammation (Xavier & Podolsky, 2007). There are two main subtypes of IBDs which are Crohn's disease (CD) and ulcerative colitis (UC). Prevalence and incidence of CD are 1.0% and 24.3 per 100,000 person-years respectively while in UC they are respectively 0.5% and 12.7 per 100,000 person-years in Europe (Loddo & Romano, 2015; Ventham et al., 2013).

The implicated genetic factors include mutations of NOD2/caspase recruitment domain-containing protein 15 (CARD15) or IBD protein 1 (IBD1) located on chromosome 16, organic cation transporter novel type 1/2 (OCTN1/2) on chromosome 5, discs large MAGUK scaffold protein 5 (DLG5) on chromosome 10, and IL23R (Ardizzone & Porro, 2002; Becker et al., 2003; Ogura et al., 2001). Other genes include immunity-related GTPase family M (IRGM), autophagy related 16 like 1 (ATG16L1), interleukin 23 receptor (IL23R), and protein tyrosine phosphatase non-receptor type 2 (PTPN2) (Baumgart & Sandborn, 2012; Loddo & Romano, 2015). Genetic predispositions include 15% of patients with CD have a family member who suffered from IBD, while in twin studies for CD there have been 50% concordance in monozygotic twins and less than 10% in dizygotics (Cho & Brant, 2011; Loddo & Romano, 2015). Genome-wide association (GWA) studies of over 75,000 IBD patients and controls have identified and confirmed 163 susceptibility loci for IBDs

(Baumgart & Sandborn, 2012). Shared genetic risk of IBD was confirmed based on trans-ethnic analysis of over 20,000 individuals of European and non-European ancestry of which an additional 38 new IBD loci were identified (McGovern, Kugathasan, & Cho, 2015; Liu et al., 2015). In all, contributions of identified genetic factors to pathogenesis in CD and UC are respectively 13.1% and 8.2% (Liu et al., 2015; Uhlig, 2013). Principally, CD and UC are associated respectively with type 1 helper T cells (Th-1) and Th-2 lymphocytes that are differentiated by the cytokines. The signal transduction pathways mediating IBD inflammatory processes include P38 MAPK, JNK MAPK, PI3K/Akt, NF- κ B, and TLR pathways (Wei & Feng, 2010).

1.4 Similarities between sepsis and inflammatory bowel diseases

Both sepsis and IBD have dysregulated inflammatory responses, imbalanced immunomodulation and local and systemic involvements. The signal transduction pathways via P38 MAPK, JNK MAPK, PI3K/Akt, NF- κ B, and TLR that play prominent roles in IBD are also implicated in sepsis (Kawai & Akira, 2010; Wei & Feng, 2010). The role played by the activation of proinflammatory cytokines such as TNF, IFN γ and IL-6 and in particular TNF has been associated with a damaging effect on intestinal barrier integrity. The disruption of intestinal epithelial barrier function that results in gut leakage, bacterial translocation, interstitial oedema, and loss of mucosal protection are hallmarks of local effects of the various mechanisms mediating IBD and sepsis (Kiesslich, 2012; Michielan & D'Inca, 2015; Salim & Soderholm, 2011). Poorly controlled IBD can also sometimes result in sepsis.

Colbert and colleagues analysed 92,296 visits of patients with sepsis (severe or septic) in the 2012 national inpatient sample (NIS) database in USA and adjusted for possible confounders (Colbert et al., 2016). They reported that when compared with

controls, patients with UC had markedly worsened sepsis related outcomes, including mortality (odds ratio [OR] 1.61, 95%CI 1.35-1.93) while CD had a lower mortality rate (OR 0.78, 95%CI 0.63-0.97) (Colbert et al., 2016). However, Goren and colleagues in the analysis of a nine-year observational cohort of 5522 hospitalised patients with IBD (aged 16 - 80 years) showed that 1.3% of the cases had bacteraemia and a bacteraemia-associated mortality rate of 13.7% at 30 days (Goren et al., 2020). Longer hospitalisations ($P < 0.0001$) and older age ($P < 0.0001$) were significantly associated with an increased risk of bacteraemia (Goren et al., 2020).

Antibiotics are used to treat both sepsis and IBD to mitigate bacterial load, reduce tissue invasion, and eradicate virulent bacterial species (Song et al., 2015). Other common therapeutics that are used in sepsis and IBD are corticosteroids, biologics (agents made from a living organism or its products including monoclonal or polyclonal antibodies) (such as infliximab and adalimumab), and immunomodulatory drugs (azathioprine, 6-mercaptopurine, methotrexate and cyclosporine) (Sartor, 2004; Targan et al., 1997). Immunomodulatory drugs function by modifying the response of immune system either by decreasing (immunosuppressives) or increasing (immuno-stimulators) the synthesis of serum antibodies.

1.5 Anatomy and physiology of the small intestine

The small intestine is an internal organ that is located within the gastrointestinal tract. It commences from the pylorus of the stomach to the ileocecal junction, where it meets the large intestine (Buckley & Turner, 2018). The small intestine is located around the center of the abdomen, while the large intestine is located peripherally except for the transverse colon that lies from the right colic flexure to the left colic flexure to join ascending and descending components of the colon respectively (Sinnatamby, 2013). Superiorly and laterally, the small intestine is surrounded by the

large bowel, while it is related anteriorly to the greater omentum (Driscoll, 2006). Posteriorly, the small intestine is related to the posterior wall of the peritoneal cavity. The small intestine is an intraperitoneal structure while some parts of the colon are retroperitoneal, and others are intraperitoneal. The mesentery is formed from a membranous fold (Driscoll, 2006). The intestine assists in the digestion and absorption of ingested food. In humans, the small intestine is about 6 m (20 ft) long, while the colon is about 1.5 m (5 ft) long. However, in mouse the small intestine is about 35 cm (13.8 in) long and the average length of the large bowel of C57BL/6J mice is just 10 cm (Cook, 1965).

Histologically, the small intestine consists of four layers, including the mucosa (innermost layer containing epithelium, lamina propria, and muscularis mucosae) and submucosa (connective tissue layer containing blood vessels, lymphatics, and the submucosal plexus). The remaining two layers are the muscularis externa or muscularis propria (outer longitudinal layer and inner circular layer) and the adventitia (outermost layer containing loosely arranged fibroblasts and collagen and neurovascular structures). The serosa (mesothelium) covers most of the small intestine adventitia (figure 1.2).

The superior and inferior mesenteric arteries and veins that supply the intestine are contained within the mesentery (Driscoll, 2006). The intestinal lymphatic drainage system consists of the mesenteric lymphatic vessels, gut-associated lymphoid tissue (GALT) (Peyer's patches), and the lacteals (Trevaskis et al., 2015). The intestinal nervous system terminates at the myenteric plexus (Auerbach's plexus) and submucosal plexus (Meissner's plexus) (Driscoll, 2006). The Auerbach's plexus is located between the outer longitudinal and inner circular layers of the muscularis externa (Buckley & Turner, 2018). It innervates the motor layers and provides secretomotor innervation to the mucosa (Driscoll, 2006). It possesses both sympathetic and parasympathetic fibres (Buckley & Turner, 2018). The Meissner's

plexus possesses only parasympathetic fibres and provides innervation for the smooth muscle of the muscularis mucosae (Driscoll, 2006). The gastrointestinal tract smooth muscle has interstitial cells of Cajal (ICC) within it, which act as the electrical pacemaker cells. The ICC are responsible for the basal (slow waves) rhythm necessary for peristaltic movements and contraction (Burns et al., 2009).

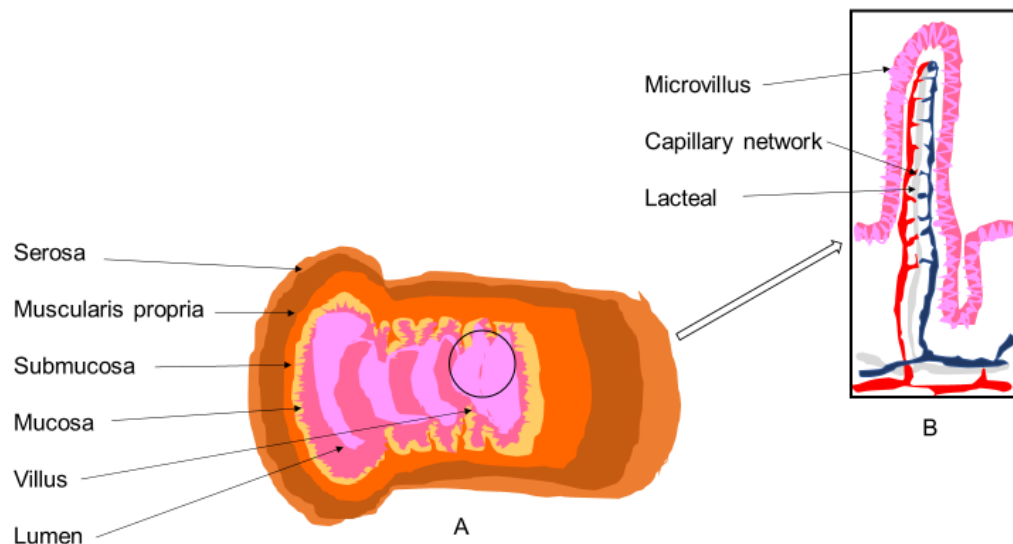


Figure 1.2 Anatomy of the small intestine showing various layers from the outer serosa to the mucosa that has an interface with the intestinal lumen and microbiota (A). The enlarged section of the small intestine depicts the structure of a villus covered in microvilli and, capillary network (B). Modified from McKinley & O'Loughlin, 2008; Mescher, 2018.

1.6 Intestinal mucosal epithelium

The intestine is lined by a single layer of columnar epithelial cells that provide a protective and functional barrier between the luminal contents and the body through the tight junction architectural structure of sealing strands (Buckley & Turner, 2018; Last & McMinn, 1994; Williams et al., 2013). It is one of the first organs to undergo pathophysiological changes during the rapid onset and progression of sepsis (Doig et al., 1998; Julian et al., 2011). LPS induces intestinal epithelial cell shedding by stimulating the release of cytokines such as tumour necrosis factor (TNF) that are known to remodel tight junctional components (Williams et al., 2013).

Functionally, the intestinal epithelium helps in nutrient absorption while structurally it provides a barrier against any invading harmful substances (Ebnet et al., 2004). It is involved in a diverse range of functions, such as providing a functional barrier between the intestinal luminal contents and underlying tissue microorganisms, nutrients' absorption regulation and waste excretion, paracrine hormonal secretion, and endocrine signalling (Furness, Kunze, & Clerc, 1999; Sato et al., 2009). Intestinal epithelial cells are polarised structures. The apical surface of epithelial cells is towards the lumen while the basal surface lies towards the basement membrane (Tsukita et al., 2008; Buckley & Turner, 2018; Williams et al., 2013). This polarity of epithelial cells determines their biochemical responses (Ebnet et al., 2004). The epithelial cells are joined by tight junction proteins which maintain the selective functional and structural barrier integrity of the epithelial surface.

1.6.1 Intestinal tight junctions

Tight junctions are one of the four junctional complexes that exist between adjacent cell plasma membranes and are commonly found in vertebrates (figure 1.3). Others junctional complexes include adherens junctions, gap junctions, and desmosomes. The role of tight junctions in regulating intestinal epithelia is unique, thus a deeper understanding of how they contribute to barrier function, epithelial structure, and regulation mechanisms might hold a key to the discovery of innovative therapeutics to prevent the breakdown of intestinal barrier function (Gasbarrini & Montalto, 1999; Zihni et al., 2016) in sepsis and IBD. The intestinal epithelial tight junction consists of strand-constituting integral membrane proteins (Schneeberger, 2004; Tsukita et al., 2008; Williams et al., 2013). The tight junction forms a continuous intercellular junctional barrier between intestinal epithelial cells and over 40 different component proteins have been identified (Schneeberger et al., 2004; Yamazaki et al., 2008). The tight junction proteins include claudins, occludin, tricellulin, junctional adhesion molecules (JAMs), endothelial cell-selective adhesion molecule (ESAM) (Nasdala et

al., 2002), coxsackie- and adenovirus receptor (CAR) (Cohen et al., 2001) and others. It is often considered that tight junctions create kissing points between adjacent plasma membranes (Van Itallie, 2006). The tight junctions are mostly found at the apical surface of the epithelium (Tsukita et al., 2008). They regulate the size of the apical intercellular spaces and are often described as the paracellular pathway “gatekeepers” (figure 1.3). Tight junctions help to regulate internal homeostasis of ions and solutes in the body and the epithelial microenvironment and they are involved in the selective permeability of solutes and solvents (Tsukita et al., 2008; Ulluwishewa et al., 2011). Activation of NF- κ B results in redistribution of tight junction proteins including an increase in the expressions of claudin-4, -6, -7, and -9 (Chavarría-Velazquez et al., 2018).

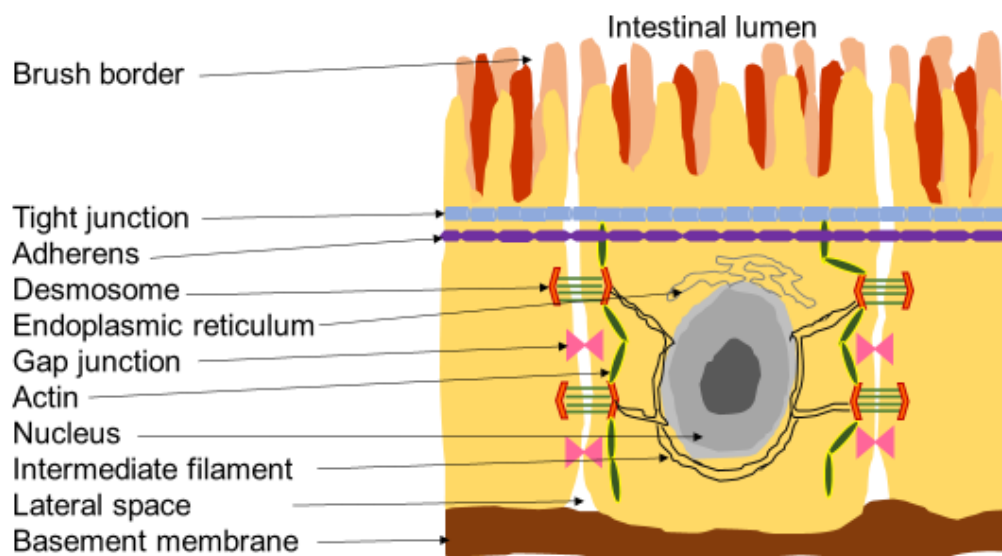


Figure 1.3 Diagram of junctional protein complexes showing different types of proteins involved in maintaining intestinal epithelial integrity including tight junctions, adherens junctions, desmosomes, and gap junctions. Tight junctions play a major prominent role in maintaining intestinal epithelial barrier function and protecting the gut against invading sepsis-inducing microbes. Modified from Williams et al., 2015.

1.6.1.1 Claudins

Claudins are tetraspan, integral membrane proteins of the tight junctional complex (Furuse et al., 1998) with small molecular masses of between 21 - 28 kDa (Van Itallie,

2006). Currently there are about 31 known members of the claudin family (Tipsmark et al., 2008). The claudin family can be broadly divided into two main classes; pore-forming claudins which include claudins 2 and 15 as the major members of this group (Furuse et al., 1998; Shinoda et al., 2016; Tamura et al., 2008; Van Itallie, 2006) and seal- or barrier-forming claudins which prominently comprise claudins 1, 4, 7, and 10 (Ding et al., 2012; Lal-Nag & Morin, 2009; Mineta et al., 2011). The seal-forming claudins are more abundant in nature than the pore-forming ones. In some layers or tissues, the pore-forming claudins may be less abundant or absent (Shinoda et al., 2016). Claudin 1 is found in most tissues (Zhu et al., 2006). Most of the claudins are charge-selective and often tend to be either up- or down-regulated during disease states (Gunzel et al., 2013). There are some claudins that can both occur as up- and down-regulated proteins in different disease states in comparison to the normal state (Amoozadeh et al., 2015; Calpado et al., 2014). Under- or overexpression of claudins has been implicated in a number of pathological conditions (appendix A). Inflammatory mediators, most especially TNF, activate transcriptional regulation, enhance endocytic trafficking, and the remodelling of claudins in epithelial tight junction (Matsuda et al., 2004). Intestinal inflammatory dysregulation induces upregulation of intestinal epithelial claudins-1, -2, and -18 and downregulation of intestinal epithelial claudins -3, -4, -5, -7, -8, and -12 (Shen, Weber, & Turner, 2008). The therapeutic target of the transcriptional regulatory effects of inflammatory mediators on the claudin family may hold a breakthrough to containing intestinal epithelial dysfunction and gut leakage. In the same vein, therapeutics that can augment the effect of intestinal epithelial integrity of the upregulated claudins may be worthy of study.

1.6.1.2 Occludin

Occludin is one of the major proteins in the tight junctions of intestinal epithelial cells and was first described in 1993. Occludin has a molecular weight of 65 kDa, is

comprised of 522 amino acids, and is encoded by the OCLN gene which is found on chromosome 5q in humans (Ando-Akatsuka et al., 1996; Furuse et al., 1993). Structurally, its C-terminal domain comprises of 257 amino acids and this is involved in ensuring the proper assembly and functional integrity of the tight junction barrier and has been reported to be a key mediator in cell survival (Chen et al., 1997). The N-terminal domain contains 66 amino acids and it promotes the adequate sealing of the tight junction barrier function (Feldman, Mullin & Ryan, 2005). Yoseph and colleagues experimented with caecal ligation and puncture (CLP), a model of polymicrobial intra-abdominal sepsis, to investigate the effects of sepsis, including intestinal barrier dysfunction on the tight junctions of mice (Yoseph et al., 2016). They reported that 12 hours after the onset of induced sepsis, occludin protein expression was statistically significantly decreased by Western blotting (Yoseph et al., 2016). On the histomicrograph, occludin expression in the lower villus was observed to be decreased (Yoseph et al., 2016). A decreased amount of occludin has also been reported to be associated with increased intestinal permeability (Li et al., 2009; Yoseph et al., 2016). Therapeutic enhancement of occludin expression may therefore potentially prevent increased intestinal permeability and a leaky gut.

1.6.1.3 Junctional adhesion molecule A (JAM-A)

Junctional adhesion molecule A (JAM-A) is a protein of the F11R gene and a member of the immunoglobulin superfamily with 299 amino acids and 32.58 kDa molecular weight that is present in many cells including epithelial cells, endothelial cells and platelets (Itoh et al., 2001). It has a PDZ (an abbreviation formed from post-synaptic density protein, Drosophila disc large tumour suppressor (Dlg1), and Zonula occludens-1 protein) binding domain that modulates common structural protein interactions of about 80-90 amino acids and targets other proteins' C-terminal short amino acids region (Izumi et al., 1998). The PDZ also coordinates the signalling functions of some proteins in organisms and enhances attachment of membranous

receptor proteins to the cytoplasmic and cytoskeletal counterparts to facilitate transduction organisation and complex formation. JAM-A forms cell-to-cell adhesions that protects and promotes tight junction barrier function in epithelial cells and, acts as a receptor for platelets and reovirus and a ligand for leucocyte ligand (Lee & Zheng, 2010; Ostermann et al., 2002). Yoseph and colleagues conducted a CLP experiment in mice and reported a significant increase in JAM-A ($p < 0.05$) by western blot 12 hours after the onset of sepsis (Yoseph et al., 2016). On the histomicrographs, the amount of JAM-A in the villus and crypt of CLP-mice was observed to be increased in comparison with the controls (Yoseph et al., 2016). Therapeutic modulation to promote the effect of JAM-A on intestinal epithelial integrity during sepsis may therefore potentially alter the sepsis-induced intestinal epithelial dysfunction that results in increased intestinal permeability, bacterial translocation, and other complications.

1.6.1.4 ZO-1

Zona occludens-1 (ZO-1) is a transmembrane protein encoded by the TJP1 gene with 1748 amino acids, 220-kDa molecular weight, and PDZ domains containing 80 - 100 amino acid residues that allow it to interact with other tight junction proteins (Balda & Matter, 2008; Willott et al., 1993). ZO-1 plays key roles in the structural and functional integrity of tight junctions, cell-to-cell transduction signalling, and regulatory transcription of the protective barrier function of tight junctions (Bauer et al., 2010). A structural complex occludin-ZO-1 regulatory protein interaction interface is usually formed between occludin and ZO-1 and this is very important in the assembly and disassembly of the tight junction (Nomme et al., 2011). ZO-1 serves as a scaffold protein with the provision of anchoring cross-links for the strand proteins of the tight junction to communicate with cytoskeletal proteins. Yoseph and colleagues in the septic mice model using CLP, reported that both western blot and histomicrographs at 12 hours following sepsis induction did not show significant

changes in the levels of ZO-1 when compared with sham mice (Yoseph et al., 2016). However, serum concentrations of ZO-1, have been demonstrated to be elevated in sepsis in other studies (Aslan et al., 2017; Zhao et al., 2016). Marchiando and colleagues reported that treatment of wild-type and transgenic mice with 7.5µg TNF intraperitoneally resulted in redistribution of intestinal epithelial tight junction including ZO-1 following TNF-induced shedding and apoptosis (Marchiando et al., 2011).

1.7 Cell dynamics of the small intestinal epithelium

1.7.1 Stem cells and epithelial cell turnover

Physiologically, intestinal homeostasis is maintained by an equilibrium between the rate of generation of the epithelia in the crypts of Lieberkühn and the rate of loss of epithelial cells from the villus tip (figure 1.4). The stem cell zone is located within the intestinal crypt and is now thought to consist of crypt base columnar cells (CBC) which express the active cycling stem cell marker leucine-rich repeat-containing G protein-coupled receptor 5 (Lgr5) (Barker et al., 2007). The CBC structures intermix among the Paneth cells at the crypt base and generate transit-amplifying (TA) daughter cells located at higher cell positions within the crypt. TA daughter cells usually differentiate into other cells such as goblet, neuroendocrine, and absorptive enterocytes as they migrate along the crypt-villus axis, thus completing the stem cell-transit cell-mature cell profile (Potten, 1990; Williams et al., 2015). At the crypt base, Lgr5-positive CBCs in the centre specifically maintain position while Lgr5-negative CBC cells at the peripheral positions of the crypt base can be displaced into the TA daughter cell population (Ritsma et al., 2014). Lgr5-positive cells possess a long survival tendency, multipotency, and self-renewal ability and usually divide once every 24 hours (Schepers et al., 2011). Lgr5 is a G-protein coupled receptor and is activated by R-spondins. Every 2-6 days, the functional epithelial villus in most adult

mammals is rapidly and almost completely renewed by the production of new cells by the stem cells within the crypt domains (Barker, 2014; Cheng & Leblond, 1974; Mayhew et al., 1999). This makes intestinal epithelial cells the cell type in the body with the highest turnover rate (Stalker, 2007). Based on mathematical mouse modelling, about 1400 mature absorptive enterocytes are thought to be shed from the extrusion zone of a single villus tip daily (Potten, 1990). Respectively, in mouse and human the rates of turnover of small intestinal epithelial cells are about 2×10^8 and 10^{11} in 24 hours (Potten & Loeffler, 1990). The intestinal stem cell population gives rise to two cell lineages which consist of five cell types. The absorptive cell lineage comprises absorptive enterocytes, while the secretory cell lineages consists of goblet, enteroendocrine, Paneth cells, and tuft cells. In certain pathological states, intestinal homeostasis could be, disrupted, leading to an intestinal disequilibrium as a result of might set in, thus resulting in greater loss of epithelial cells from the villus tip than the production of new epithelial cells in the crypts (Williams et al., 2015). This condition of intestinal homeostasis disturbance could further lead to more intestinal epithelial cell shedding and apoptosis, resulting in a dysfunctional intestinal barrier and increased intestinal permeability. If this is untreated and unabated, intestinal failure could then potentially occur. Pathologically-mediated intestinal disequilibrium could be caused by inflammatory agents (cytokines such as TNF), sepsis, trauma, and microorganisms such as Gram-negative bacteria (especially *E. coli* through increased abundance of lipopolysaccharide; LPS).

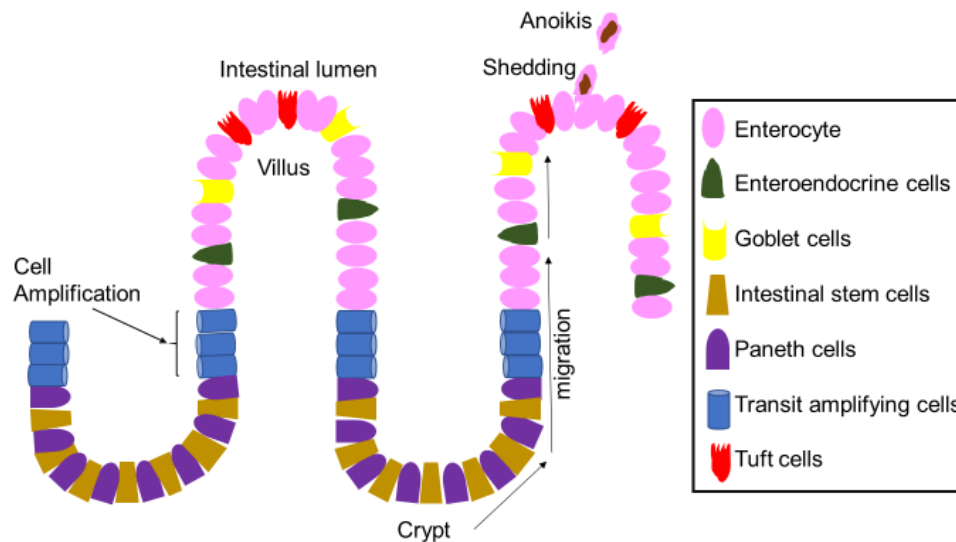


Figure 1.4 Diagrammatic representation of the small intestinal epithelium depicting the villus, crypt, intestinal stem cells, transit amplifying cells, Paneth cells, goblet, enteroendocrine cells, tuft cells, and enterocytes. The synthesised undifferentiated cells in the crypt domain migrate through the crypt-villus axis and they become differentiated, perform different cell lineage functions, and undergo shedding at the villus tip. Modified from Gerbe, Legraverend, & Jay, 2012; Gunawardene, Corfe, & Staton, 2011).

1.7.2 Enterocytes

Enterocytes are simple columnar epithelial cells saddled with specialised responsibilities of absorption, digestion, protection, and transportation of nutrient from the intestinal lumen into inner connective tissues and blood circulation (figure 1.4). Enterocytes live for about 2-6 days and can also play an endocrine role by secreting the hormone leptin (Mayhew et al., 1999). About 80% of the small intestinal mucosa consists of absorptive enterocytes in humans (Chen et al., 2018; Pearce et al., 2018). Although the intestinal lumen is internally located, it contacts directly with external environmental agents that are ingested. Apically, enterocytes are composed of microvilli that increase the absorptive surface area to facilitate movement of micro-molecules from the intestinal lumen to enterocytes (Knutson, 2017). The microvilli are like folds of finger-like projections occupying the intestinal epithelial brush border of the lumen (Crawley, Mooseker & Tyska, 2014). Basolaterally, enterocytes form cell-to-cell adhesions which allow communication with other cell types and

transportation of nutrients out of the enterocytes into blood vessels (Crawley, Mooseker & Tyska, 2014). This apical and basolateral domain polarisation of enterocytes is due to structural and architectural arrangements of their cytoskeletons, especially actin monofilaments and the proper development of vascular traffic that ensures differential distributions of molecules between the two domains (Giammanco et al., 2015; Knutson, 2017). Ultra-structurally, absorptive enterocytes consist of a supra-nuclear Golgi complex, lysosomes, ribosomes, secretory granules, rough endoplasmic reticulum, mitochondria, and heterochromatic nuclei (Sohma, 1983). The transcellular, paracellular, or endocytosis/transcytosis pathways ensure movement of small molecules from the intestinal lumen into and out of enterocytes. The transcellular pathway is coordinated by free passive diffusion, facilitated passive diffusion, or active carrier mediated transport (Collins et al., 1993). The transcellular pathway involves movement of nutrients from the intestinal lumen into the enterocytes through the cell membrane, while paracellular passage is via the intercellular space. Endocytosis or transcytosis is another form of transcellular pathway that facilitates movement of nutrients through a process by which vesicles engulf macromolecules at one end of the cell, draw it across the cell, and then eject it out at the other end (Shifrin et al., 2012). Free passive diffusion is a process of transportation of molecules across the cell membrane without any requirement for cellular energy input, whereas active mediated transport requires cellular energy input. Non-polar, small molecules such as carbon dioxide and oxygen are examples of molecules that undergo free passive diffusion. Facilitated passive diffusion is a process devoid of any need of cellular energy of ATP hydrolysis; it transports macromolecules across the cell membrane through the help of transmembrane carrier proteins such as permeases. Large molecules including glucose and amino acids and poorly soluble non-polar molecules such as fatty acids and retinol can only be transported through facilitated diffusion (Pearce et al., 2018). Active transport comprises of primary active transport and secondary active transport. Primary active

transport involves utilisation of energy provided by ATP hydrolysis to the transmembrane proteins to act like pump to transfer the molecules across the cell membrane such as in the Na⁺/K⁺-ATPase pump and H⁺/K⁺-ATPase (Snoeck, Goddeeris & Cox, 2005). The Na⁺/K⁺-ATPase pump regulates the resting potential voltage of the enterocytes while H⁺/K⁺-ATPase usually lines the stomach and regulates its acidic milieu. Secondary active transport works by the principle of electrochemical gradient of the channel proteins that acts like the co-transporters and it consists of symporters and antiporters (Lodish et al., 2000). In symporters, the ions and solute are transported in the same direction while in antiporters they are transported in opposite directions. The sodium glucose transporter (SGLT) is a symporter that actively mediates the transportation of glucose along with sodium into the apical domain of enterocytes while the sodium calcium exchanger (NCX1) mainly coordinates the exit of Ca²⁺ from enterocytes via an antiporter mechanism (Diaz de Barboza et al., 2015; Ferraris & Diamond, 1997). Calcitriol is the key regulatory hormone of intestinal Ca²⁺ transport. Basolaterally, glucose transporter 2 (GLUT2) mediates the transportation of glucose from the cytoplasm to the intercellular space, for it to move into the blood stream (Efrat et al., 1994; Navale & Paranjape, 2016). In diseases such as sepsis, cholera, and inflammatory bowel disease (IBD), the integrity of enterocytes is compromised, and invasion of the toxic agents might translocate into the blood circulation. The compromised barrier integrity resultant from excessive apoptosis and increased epithelial cell shedding in a disease state may disrupt these absorptive processes.

1.7.3 Paneth cells

Paneth cells are granulated secretory cells that constitute 5% of small intestinal epithelial cells, are usually located at the base of intestinal crypts and are the only cells that migrate downwards from the stem cell zone (Chen et al., 2018; Elphick & Mahida, 2005; Pearce et al., 2018). The secretory granules of Paneth cells are

comprised of lysozymes, antimicrobial enzymes, alpha-defensins, phospholipase A2, TNF, and others (Ayabe et al., 2000; Erlandsen, Parsons & Taylor, 1974; Wilson et al., 1999). Through the activation of myeloid differentiation primary response 88 (MYD88)-dependent Toll-like receptor (TLR), Paneth cells can detect bacterial invasion and thus trigger an antimicrobial activity against it (Vaishnava et al., 2008). Paneth cells play major roles in innate intestinal defense mechanisms by regulating microbial density and actions and by protecting and defending the viability of adjacent stem cells against any microbial invasion (Elphick & Mahida, 2005). They are very important in mediating host-microbe interactions and ensuring immune homeostasis between gut microbes and the innate immune system (Clevers & Bevins, 2013). In each small intestinal epithelial crypt, there are about 5 - 12 Paneth cells with a life span of 20 days (Bry et al., 1994; Cheng, 1974). In disease, translocation of gut microbes, invasion by gut microbes, deficiency in innate immune system protection, or dysfunction of Paneth cell immunomodulation might result in sepsis, chronic inflammatory diseases, and other immune conditions.

1.7.4 Goblet cells

Goblet cells are specialised, simple columnar epithelial cells that have a goblet-like shape with length to width ratio of about 4:1 (Knoop & Newberry, 2018). About 5-10% of small intestinal mucosal epithelial cells are goblet cells which secrete mucus, especially mucins which serve as barrier maintenance that protects and lubricates the epithelial surface (Chen et al., 2018; Pearce et al., 2018). Goblet cells have a polarised arrangement of organelles; while the nucleus and other structures are differentially located at the base, the secretory organelles especially mucins are apically concentrated (Birchenough et al., 2015). In intestinal epithelial cells, MUC2 mucin, and other carbohydrate-rich polymers are majorly secreted. Goblet cells are distributed in both intestinal villi and intestinal crypts, however while those in villi are continuously secreting mucous to ensure barrier maintenance, those residing in the

crypts only secrete mucous secondary to stimulation by either acetyl choline or after endocytosis (Birchenough et al., 2015). Goblet cells are also involved in the secretion of cytokines, anti-microbial peptides and proteins, and chemokines (Knoop & Newberry, 2018). Two postulates are thought to be responsible for the secretion of mucins, these are regulated vesicle secretion and compound exocytosis (Adler, Tuvim, & Dickey, 2013). The first process is mediated by syntaxins and other vesicle exocytosis proteins that cause adherence of single vesicles to the plasma membrane thus resulting in mucus secretion. The second process is thought to be as a result of fusion of many vesicles that constitute the goblet cell theca that later empty their mucous contents (Specian & Neutra, 1980).

1.7.5 Enteroendocrine cells

Enteroendocrine cells are usually located towards the top of the intestinal epithelial crypts of Lieberkuhn and along the villus (figure 1.4). In response to stimuli, enteroendocrine cells secrete hormones. The main types of endocrine cells are D cells, I cells, K cells, N cells, and S cells which respectively secrete somatostatin, cholecystokinin (CCK), gastric inhibitory peptide (incretin), neurotensin, and secretin hormones into the circulation. Others are enterochromaffin cells (chromaffin, serotonin), enterochromaffin-like cell (histamine), L cells (glucagon-like peptide-1), motilin, vasoactive intestinal peptide, and enteroglucagon. Release of somatostatin is mediated by low pH and inhibited by the vagus nerve. Somatostatin inhibits the releases of CCK, insulin, and glucagon, delays gastric emptying, decreases smooth muscle contractions, lowers the release of pancreatic enzymes, and reduces blood flow within the intestine (Holst et al., 1992; van der Meulen et al., 2015). In response to the presence of fatty acids and/or of amino acids in the small intestine, CCK is secreted and stimulated. The release of CCK is also mediated by acetylcholine of parasympathetic fibres of the vagus nerve. CCK elicits contraction of the gallbladder to release bile acids, increases the release of pancreatic juice -containing enzymes,

promotes relaxation of sphincter of Oddi, and inhibits of gastric emptying. Other actions of CCK are the induction of satiety and inducing an increase in anxiogenic and panicogenic activities (Zwanzger et al., 2012).

1.7.6 Tuft cells

Like enterocytes, Paneth cells, enteroendocrine cells, and goblet cells, tuft cells develop from *Lgr5*-expressing CBC stem cells (Gerbe et al., 2011). Tuft cells were previously thought to represent a quiescent stem cell pool and appeared at the +4 position of the intestinal crypt. However, they have been shown to be marked by expression of doublecortin-like kinase 1 (DCLK1) and are now considered to be distinct and unique (Gerbe et al., 2009). Tuft cells (which are also known as brush-like microvilli or caveolated cells) constitute about 0.5% of intestinal epithelial cells (McKinley et al., 2017). Tuft cell specification requires Atonal BHLH Transcription Factor 1 or Atonal homolog 1 (ATOH1), however ATOH1 is not necessary for the sustenance of mature differentiated tuft cells. Knockdown of Notch has been reported to lead to increased numbers of tuft cells (Gerbe, Legraverend, & Jay, 2012). Tuft cells function as chemosensory receptors. Other potentially implicated functions of tuft cells are their involvement in tumorigenesis, regulation of type 2 immune responses in the gut, and regulation of small intestinal lineage-specific transcription (Banerjee et al., 2018; McKinley et al., 2017).

1.7.7 Microfold cells (M cells)

Microfold cells (M cells) are unique, specialised intestinal epithelial cells that reside in Peyer's patches, gut-associated lymphoid tissue (GALT) and other gastrointestinal tract mucosa-associated lymphoid tissue (MALT) (Neutra, Mantis & Kraehenbuhl, 2001; Owen & Jones, 1974). Other GI MALT include nasopharyngeal-associated lymphoid tissues (NALT), colonic patches (CP) and isolated lymphoid follicles (ILF). Unlike enterocytes, M cells have no microvilli however similarly to enterocytes, they

have reliable junctional cellular complexes that provide a protective physical barrier. M cells have cell surface receptors such as glycoprotein-2 (GP2) and cellular prion protein (PrP) which detect, identify and bind bacteria or other antigens (Chieppa et al., 2006; Miller et al., 2007). Thus, M cells initiate responses of the mucosal immunity system (MIS) on its apical membrane and facilitate the transportation of bacteria and other injurious substances from the gut lumen via endocytosis, transcytosis or phagocytosis to the epithelial lamina propria where immune cells can bind to them and neutralise their toxic effects (Neutra et al., 2001; Owen & Jones, 1974). The M cells contain protease cathepsin and they recruit antigen-presenting cells (APC) including dendritic cell and B lymphocytes which play a major role in the immunity responses against microbes (Rescigno et al., 2001). Compromised protective M cell barriers and M cell-mediated MIS during sepsis and IBD may result in bacterial translocation from lumen to the vascular system thus further worsening patient condition.

1.8 Organoids

1.8.1 Organoid definition

Organoids are defined as three-dimensional (3D) *in vitro* tissue models or cellular clusters that are generated from embryonic stem cells (ESCs), primary tissue, or induced pluripotent stem cells (iPSCs) and which have the ability to self-propagate, auto-renew, and auto-organise and to physiologically function in a similar way to the parent tissue or tissue of origin (Fatehullah, Tan & Barker, 2016).

1.8.2 Small intestinal epithelial organoids

The first mouse model of intestinal organoids was introduced in 2009 (Sato et al., 2011). The International Stem Cell Consortium has now defined this type of small

intestinal organoid as an 'enteroid' (Stelzner et al., 2012) which is the term that will be used for the remainder of this thesis. Various growth factors are essential for survival of the enteroids. *rspondin* activates WNT signalling which regulates cell migration, cell proliferation, cell fate specification, cell survival, and cell polarity (body axis patterning) during tissue homeostasis and embryogenesis (Jin & Yoon, 2012). *Noggin* protein plays a prominent role in cell signalling, in the skeletal and nervous systems, and somite patterning (Marcelino et al., 2001). Mouse epidermal growth factor (mEGF) mediates cell differentiation, cell proliferation, cell survival, and signalling pathways (Zhang et al., 2016). The structural crypt-villus axis is clearly recapitulated in small intestinal enteroids.

1.8.3 Advantages of 3D enteroid models

The 3D model of organoids provides a near-physiological system for studies that have not previously been achievable in two dimensions with cancer-derived cell lines (Boehnke et al., 2016; Fatehullah et al., 2016). The 3D structure enables dynamics to occur within enteroid systems that similarly recapitulate those observed *in vivo*. Other advantages include the ability of organoids to expand from a limited source and with reduced probability of genomic alterations with propagation (Fatehullah et al., 2016; Middendorp et al., 2014). Three-dimensional organoids have to generate and orientate to apical-basal polarity at their own accord while 2D cell cultures have automatic and instinct apical-basal polarisation and orientation. Because of the tendency to auto-organise in 3D, cell-to-cell interactions predominate structurally, while in 2D cell-substrate interactions structurally predominate. In 3D, motility is hindered by the extracellular matrix, whereas the continuously flat surface of 2D cell cultures enhances migration and adhesion. Many 3D studies have demonstrated that enhancing the dimensional property of extracellular matrix (ECM) around cells can profoundly impact cell viability, cell proliferation, cell functionality, cell differentiation,

mechano-responses, morphology, and cell survival (Baker & Chen, 2012; Bonnier et al., 2015; Gauvin et al., 2012).

1.8.4 Disadvantages of 3D enteroid models

Absence of the native microenvironment in enteroid cultures might hinder any study that involves investigating the interaction between organoids and other cell types such as immune cells. However, reconstituted organoids can be produced by co-culture of enteroids with immune cells for example. Unfortunately, the heterogeneity of organoids in the same culture may impede any homogenous phenotypic screening studies resulting in the need for single cell or cellular population studies (Fatehullah et al., 2016; Hynds & Giangreco, 2013). Three-dimensional cultures that are thick can also potentially be challenging to microscopic analyses. Enteroid culturing is very expensive and time consuming, whereas 2D cell models are generally more simple, inexpensive, and time conserving.

1.8.5 Applications of 3D enteroids in research and medicine

Three-dimensional enteroid models afford the opportunity for phenotypic studies, especially of angiogenesis, neoplastic metastasis, amyloid accumulation, morphogenesis, organogenesis, and chondrogenesis (Sato et al., 2009). The cell-matrix interaction of 3D enteroid models provide the environment needed for phenotypic studies that resemble the dynamics of cells observed in vivo. In personalised genomic medicine, the role of 3D enteroid models are indispensable to tailoring therapeutics to individual genetic constitution (Dekkers et al., 2013). Enteroids provide possibilities to create and study cellular and molecular models of diseases, cell-cell interactions in tissues and organs, cellular interaction with the environment and their therapeutic modulations. Jones and colleagues demonstrated that TNF treatment of wild-type mouse derived enteroids induced marked rounding while there was attenuated rounding effect on *Nfkb2*^{-/-} mice enteroids (Jones et al.,

2019). Enteroids derived from patients with IBD demonstrated dysregulated endoplasmic reticulum (ER) stress that enhanced flagellin-induced IL-8 release and promoted TLR5 responses in IECs, thus resulting in increased activation of dendritic cell maturation and inflammatory responses (Rees et al., 2019).

1.9 Prominent signalling pathways involved in gut homeostasis

1.9.1 Wnt signalling

Wnt signalling is responsible for the maintenance of the stem cell niche in the intestine and modulates the rate of epithelial cell renewal. Wnt signalling consists of signal transduction pathways that are of high evolutionary conservation in animals and are known to mediate via autocrine and paracrine interaction by downstream activation of Frizzled receptors and co-receptors to regulate cell proliferation, cell fate determination, cell polarity, cell migration, embryonic development, and tissue regeneration (Wodarz & Nusse, 1998). Wnt 3A and Wnt 5a are important in the gut and regulate proliferation at the crypt base. Wnt is a coined name derived from wingless (Wg) (*Drosophila melanogaster* fruit fly) and integration 1 (Int1) (mouse mammary tumour virus) genes. Wnt contains about 350 to 400 amino acids and is a superfamily of 19 protein members in the human (Cadigan & Nusse, 1997). Wnt is secreted and composed of modified lipid (palmitoleoylation), glycoproteins, and serine residue (Hannoush, 2015). In humans, there are 10 members of the Frizzled (Fz) receptor family of G-protein coupled receptors that have an ability to span cell membranes seven times (Schulte & Bryja, 2007). The facilitating co-receptors are lipoprotein receptor-related protein (LRP)-5/6, receptor tyrosine kinase-like orphan receptor-2 (ROR-2), and receptor tyrosine kinase (RTK) (He et al., 2004; Komiya & Habas, 2008). Wnt signalling consists of canonical and non-canonical (planar cell

polarity (PCP) and Wnt/calcium) pathways. While the former is β -catenin protein-dependent, the latter is β -catenin protein-independent. Recently, it has been reported that both canonical and non-canonical Wnt signalling pathways have common, convergent, or integrated components especially when activated by the Wnt ligand (Wnt5A) (van Amerongen et al., 2012). Wnt signalling is triggered when Wnt protein binds extracellularly to the Frizzled receptor at its N-terminal cysteine-rich domain and the facilitating co-receptors stimulate the cytoplasmic phosphoprotein Dishevelled (Dsh/Dvl).

Activation of the canonical Wnt signalling pathway initiates signal transduction from cell surface receptors to the cytoplasm that results in phosphorylation of β -catenin and subsequent accumulation of phosphorylated β -catenin. In the absence of Wnt ligands, the destruction complex of axin, glycogen synthase kinase 3 (GSK3), adenomatosis polyposis coli (APC), protein phosphatase 2A (PP2A), and casein kinase 1 α (CK1 α) will make β -catenin become a target for proteasomal degradation and prevent accumulation of β -catenin in the cytoplasm (Gordon & Nusse, 2006). The interaction between Wnt and FZD and LRP co-receptors induces CK1- α and GSK3 β to phosphorylate LRP receptors and recruit DVL and axin (Janda et al., 2012). This leads to polymerisation and activation of DVL that results in inactivation of the destruction complex and prevents biodegradation of β -catenin. This allows β -catenin to stabilise and accumulate in the cytoplasm before subsequent translocation to the nucleus where it combines with lymphoid enhancer factor (LEF) and T-cell factor (TCF) proteins to initiate target gene transcription (Flanagan et al., 2018).

In the non-canonical PCP pathway, a dishevelled-associated activator of morphogenesis 1 (DAAM1) complex is formed, which modulates Rho-associated kinase (ROCK) via the activation of the guanine (G)-protein Rho which regulates the cytoskeleton and cellular shape (Gordon & Nusse, 2006; Park et al., 2006). The non-canonical Wnt/Ca²⁺ pathway involves G-protein-dependent stimulation and

regulation of intracellular Calcium release from endoplasmic reticulum (ER) (Kohn & Moon, 2005). Slusarski and colleagues reported that the frequency of Ca^{2+} signalling in the noncanonical Wnt pathway can be increased by over-expression of Wnt5a (Slusarski et al., 1997). Dysregulation of Wnt signalling has been implicated in many pathologies such as cancers, skeletal defects, spina bifida, type 2 diabetes, disruption of Wnt gradient, and intestinal damage during sepsis (Logan & Nusse, 2004).

In mammals, there are three Hedgehog (HH) homologues which include desert hedgehog (DHH), Indian hedgehog (IHH), and sonic hedgehog (SHH), however, a lot of studies have been done on sonic hedgehog. Embryologically, hedgehog (HH) signalling proteins play essential roles in foetal development including in the intestine. In adult life they are critically important in regulating tissue homeostasis, renewal, regeneration, and tumorigenesis (Yang et al., 2015). Depletion of HH signalling proteins has been implicated in defective formation of crypts and villi and lack of correct crypt polarity (Madison et al., 2004). Wnt signalling plays critical roles in intestinal homeostasis and ensures retention of stemness of the stem cells by aiding their ability to remain in an undifferentiated form and proliferate. Stem cells that are not exposed to Wnt signals differentiate into other types of intestinal epithelial cells, including mucus-secreting goblet cells, absorptive enterocytes, and chemosensory tuft cells (Pinto et al., 2003). In enteroid culture media, R-spondin is added to the media in order to activate, regulate, and amplify Wnt signalling of Wnt3A, Wnt1, and Wnt7A (Kim et al., 2008).

1.9.2 Bone morphogenic protein (BMP) signalling

Another protein that also plays a regulatory role in the crypt-villus axis is bone morphogenic protein (BMP) (figure 1.5). In the healthy gut, there are Wnt antagonists higher up the crypt, but Wnt agonists at the base, whereas BMP agonists are expressed in greater abundance higher in the villus tip with greater concentrations of

the BMP antagonists such as noggin being found at the crypt base (Qi & Chen, 2015). The Wnt gradient and BMP gradient along the crypt-villus axis are therefore in reverse directions. BMP signalling has been reported to induce terminal differentiation of cells and inhibit the auto-renewal property of intestinal stem cells. Noggin, an important additive of enteroid media, binds to BMP-2, -4, -5, -6, and -7 thus preventing the BMPs from interacting with type I and type II BMP receptors (Groppe et al., 2002).

1.9.3 Epidermal growth factor (EGF) signalling

The epithelial growth factor (EGF) signalling pathway is important in controlling intestinal stem cell proliferation and survival and coordinating the crypt transit amplifying cells. Intestinal stem cell fate specification and crypt-villus axis migration are modulated by the Wnt, Notch, BMP, and EGF that are present in the stem cell niche (Qi & Chen, 2015). Preparation of enteroid media requires the presence of EGF to facilitate budding efficiency of the developing enteroids (Wong et al., 2012).

1.9.4 Notch signalling

Notch signalling is a highly evolutionarily conserved signal transduction pathway in which receptor proteins span the cell membrane to modulate cell proliferation, cell fate specification, differentiation, cell survival, neurogenesis, embryogenic development, and cell death (Bray, 2016; Kopan, 2012). In humans, there are four notch receptor homologues, NOTCH 1-4, that consist of single-pass transmembrane proteins with longer extracellular, transmembrane, and shorter intracellular regions and five canonical ligands of Delta-Serrate-Lag (DSL) (D'Souza et al., 2010). Notch is a surface receptor protein which presents the extracellular domain for ligand binding. Ligand binding triggers the initiation of endocytosis of ligand–receptor complexes resulting in the untwisting of the Notch proteins' unique negative control region to cleave the intracellular domain (figure 1.5). The cleaved intracellular domain

then translocates into the nucleus where it attaches to the recombination signal binding protein for immunoglobulin kappa J (RBP-J) region of the DNA binding protein to activate Notch cascades of nuclear transcription target genes (Artavanis-Tsakonas et al., 1999). The transcriptional target genes include hairy and enhancer of split-related (HESR) genes, cyclin D1, c-Myc, p21, platelet-derived growth factor receptor beta (PDGFR β), and cyclin-dependent kinase 5 (CDK5) (Jin et al., 2008; Palomero et al., 2006; Rao & Kadesch, 2003). Notch receptor activation is regulated by many proteins such as endocytic adaptor protein Numb, E3 ubiquitin ligases (Nedd4, Neur, Deltex, and MIB), and α -adaptin (Furriols & Bray, 2001; Kopan 2012). Notch signalling inhibition via RBP-J deletion upregulates Math1 (proneural transcription factor) and promotes substitution of the proliferating transit amplifying region. Deficiency of Hes1 in mouse intestinal epithelial cells has been reported to be associated with a decline in the production of enterocytes whilst causing a rise in secretory cell populations including Paneth cells, goblet cells, and enteroendocrine cells) (van Es & Clevers, 2005). Dysregulation of Notch signalling has been implicated in embryonic maldevelopment (tetralogy of Fallot), cancers (T-cell acute lymphoblastic leukaemia), degenerative disease (multiple sclerosis), genetic disease (Alagille syndrome), skin disease (atopy), and Cerebral Autosomal-Dominant Arteriopathy with Sub-cortical Infarcts and Leukoencephalopathy (CADASIL) (Aster, Blacklow & Pear, 2011; de la Pompa & Epstein, 2012; Ranganathan, Weaver & Capobianco, 2011; Sharma et al., 2007). Tamoxifen was used to induce deletion of intestinal Math1 in young and adult Math1 inducible knockout mice (Durand et al., 2012). Secretory cell lineage marker genes were significantly down-regulated by 1,360-fold in Math1-deficient mice compared with those in the wild-type group (Durand et al., 2012). This strongly supports previous reports that Math1 is important for the maintenance of the intestinal secretory cell lineages.

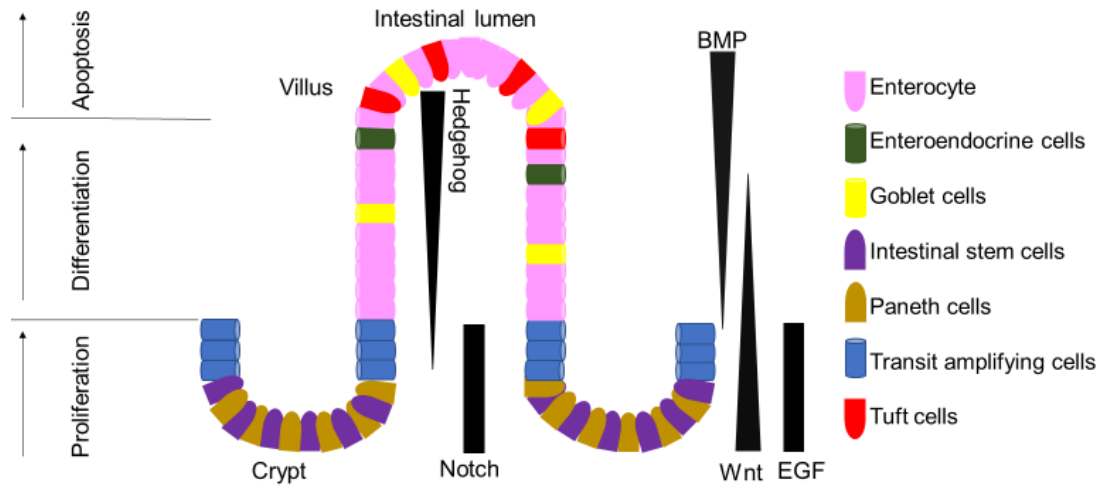


Figure 1.5 The gradients of Wnt and BMP are very important in intestinal homeostasis of which WNT signal transduction ensures the sustenance of the intestinal stem cell population in the crypts while BMP signalling maintains cell location in the crypts and prevents cell proliferation. Notch signalling enhances stem cell proliferation and aids Wnt signalling while Hedgehog promotes villus formation. Modified from Jeon et al., 2013; Spit, Koo, & Maurice, 2018.

1.10 NFκB signalling

1.10.1 Structure of the NFκB family

NFκB signalling was first reported in 1986 and was described as the κ-light chain enhancer that was discovered in B-cell tumour extracts (Sen & Baltimore, 1986). Many studies of NFκB signalling report that it is found in almost all animal cell types. The NFκB family has two classes of which class I includes NFκB1 and NFκB2 while class II contains RelA, RelB, and c-Rel. There are five NFκB subunits which are NFκB1 (p105/p50), NFκB2 (p100/p52), RelA (p65), RelB, and c-Rel. The p100 and p105 are precursors of p52 and p50 respectively. Broadly speaking, the NFκB signalling pathway comprises of classical and alternative pathways.

1.10.2 Classical NFκB signalling pathway

Activating stimuli bind to cell surface receptors and these transmembrane protein receptors trigger the recruitment of intracellular adaptor proteins, including TRAF. Basolateral and apical cell membranes of intestinal epithelial cells (IECs) express

pattern recognition receptors (PRRs) including toll-like receptors (TLRs) which become stimulated upon encountering microbial ligands (Abreu 2010; Wullaert et al., 2011). Adaptor proteins then recruit and activate the catalytic subsets of I κ B kinase (IKK) (IKK α and/or IKK β) and NF κ B essential modulator (NEMO) (non-enzymatic scaffold protein regulator) (Artis, 2008; Hayden & Ghosh, 2008). This leads to the phosphorylation of I κ B proteins and thus release of NF κ B proteins from I κ B sequestration and enables translocation of the NF κ B proteins to the nucleus for transcription of target genes. The phosphorylated I κ B proteins become a target for ubiquitination- and proteasomal biodegradation. The classical pathway is involved in inflammatory, survival, and pathogen-derived conditions. In summary, classical NF κ B pathway is NEMO-dependent, protein synthesis independent, rapid but diffuse and is activated by multiple stimuli (Chen et al., 2018; Sun, 2011).

1.10.3 Alternative NF κ B pathway

Cell surface receptors are activated by ligand binding (B cell-activating factor (BAFF), CD40L, and lymphotoxin- β (LT β)) that in turn stimulates NF κ B inducing kinase (NIK) recruitment to the intracellular domain resulting in phosphorylation and activation of the IKK α complex. Thus, BAFF binds to BAFFR, CD40L interacts with CD40, LT β binds to LT β R, RANK (receptor activator of nuclear factor κ B) combines with RANKL, and LPS interacts with TLR4 (Dejardin, 2006; Merga et al., 2016). This results in cascades of reaction that subsequently result in phosphorylation of p100 protein (p52 precursor) by IKK α , which results in processing and release of activated p52/RelB heterodimers. Thus, the liberated RelB:p52 heterodimer translocates to the nucleus to regulate the transcription of target genes (Amir et al., 2004). The alternative pathway has been implicated in developmental, organogenesis, immune cell maturation, and the immune response to sepsis (Chen et al., 2018; Cildir, Low, & Tergaonkar, 2016; Fukuyama et al., 2002; Newton & Dixit, 2012). Several mouse studies have reported that the alternative NF κ B signalling pathway plays prominent

roles in modulating susceptibility to IBD and colitis-associated cancer and mediating intestinal epithelial barrier dysfunction, apoptosis, and cell shedding (Burkitt et al., 2015; Jones et al., 2019; Watson et al., 2009; Williams et al., 2015). The alternative pathway is NEMO-independent, protein synthesis-dependent, slow but specific and only involves a subset of stimuli. More about the alternative NF κ B signalling pathway will be discussed in chapter 4 of this thesis.

1.10.4 Hybrid pathway

The hybrid pathway has some elements of both classical and alternative activation pathways. In the hybrid pathway, the alternative pathway initiates the NF κ B complex activities whilst classical pathway components stimulate the NF κ B complex (Sanz et al., 2010). The degradation process can be triggered by acetylation, sumoylation, s-nitrosylation or phosphorylation of I κ B α and other I κ B proteins (Wan & Lenardo, 2009).

1.10.5 I κ B regulation of NF κ B

NF κ B is sequestered in the cytosol and thus inactivated by the inhibitor of κ B (I κ B) proteins which combine and form complex with it. The combination of I κ B proteins with NF κ B prevents I κ B from ubiquitination and proteasomal biodegradation and makes NF κ B dimers inaccessible and unavailable for nuclear translocation and transcriptional reactions (Pahl, 1999). Thus, I κ B tightly regulates activities of the NF κ B signalling pathways. Presence of microorganisms or their component parts (such as LPS) binding to the cell surface receptor such as TLR4 rapidly leads to activation of NF κ B signalling. TLRs have been reported to play prominent roles in innate and adaptive responses to sepsis and other conditions. Other inducers of activities of NF κ B signalling pathways are reactive oxygen species (ROS), ionising radiation, tumour necrosis factor, ultraviolet radiations, interleukin 1-beta (IL-1 β), burns, cocaine, and isoproterenol (Chandel et al., 2000). Activation of NF κ B results

in phosphorylation of I κ B, which causes phosphorylated I κ B to be exposed to proteasomal biodegradation.

In a resting state, I κ B inhibits the activities of NF κ B in the cytoplasm and the nuclear translocation of NF κ B dimers. The I κ B proteins contain ankyrin repeat domains which consist of 33 amino acid residues. The interaction of I κ B proteins via their ankyrin repeat domains with the NF κ B dimers result in the covering of the nuclear localisation signals (NLS) of NF κ B proteins thus rendering the NF κ B dimers hindered and isolated and they therefore remain in a continuously inactive state in the cytosol (Jacobs & Harrison, 1998). I κ B proteins are related by having an N-terminal regulatory domain. The I κ B proteins comprises of prototypical (I κ B α , I κ B β , and I κ B ϵ) and atypical (Bcl-3 and I κ B ζ) groupings (Inoue et al., 1992). The prototypical I κ B proteins exert their inhibitory actions in the cytosol, while the atypical I κ B proteins are inhibitory in the nucleus. Because of the presence of ankyrin repeats at the halves of the C-terminal portions of p100 (I κ B γ) and p105 (I κ B δ), these also exhibit the same inhibitory properties as I κ B proteins (Basak et al., 2007; Hayden & Ghosh, 2004; Perkins, 2007).

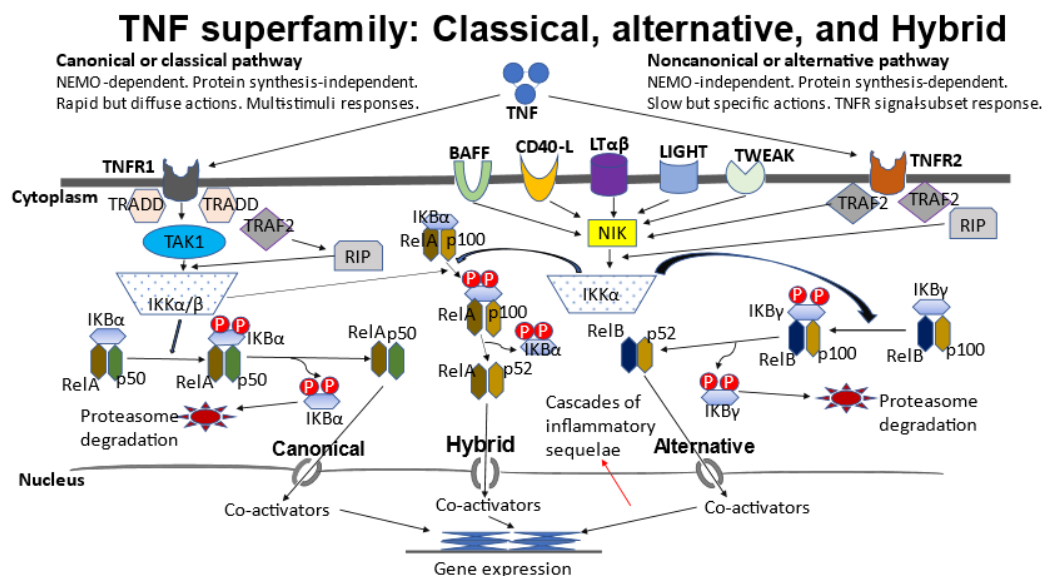


Figure 1.6 Schematic diagram summarising the NF κ B signalling pathways involving classical, alternative, and hybrid signalling pathways. In sepsis, all NF κ B signalling pathways play a major role in promoting inflammation and other cascades of reactions that result in intestinal and other organ failures. Modified from Sanz et al., 2010; Sun, 2011.

1.10.6 NFκB signalling and small intestinal homeostasis

The intestinal epithelium, mucosal immune cells, and luminal microbiota are in a state of equilibrium and any disruption of this delicate and complex homeostatic status can result in a debilitating condition. The intestinal epithelium not only provides a physical barrier to luminal microorganisms, but along with the underlying intestinal mucosa, it also protects and promotes appropriate immune responses against any bacterial mucosal translocation and pathogenic gut colonisation (Sanz et al., 2010). NFκB signalling pathways play a prominent role in the intestinal immune homeostasis of the gastrointestinal tract. The development and manifestation of inflammation and diseases resulting from dysregulated NFκB responses to stimuli cannot be over-emphasised. Increased and unregulated activation of NFκB signalling has been reported in both immune- and non-immune-related chronic inflammatory diseases (Sun, 2011). However, studies have also shown that inhibition of NFκB is associated with disruption of immune homeostasis, development of inflammation and diseases. In both chemical-induced colitis models and the colitis susceptible IL-10 knock out mouse, IKK activation was inhibited by administering antisense oligonucleotides to p65 or a peptide to bind NEMO and it was reported that the severity of colonic inflammation was ameliorated (Neurath et al., 1996). These studies demonstrated that excessive stimulation of NFκB signalling is implicated in the intestinal inflammatory responses and inhibition of NFκB signalling could have immunomodulatory therapeutic advantages in chronic inflammatory diseases including IBD (Wullaert, Bonnet, & Pasparakis, 2011). Eckmann and colleagues reported that conditional ablation of IKK in IECs inhibited NFκB but had no effect on colitis incidence or severity in the colitis-induced IL-10 knock out mouse (Eckmann et al., 2008). However, IKK ablation in myeloid cells demonstrated a reduction in colitis occurrence in colitis-induced IL-10 knock out mice (Eckmann et al., 2008; Greten et al., 2004).

Proinflammatory cytokines, cell surface receptors and PRRs play significant roles in mediating stimulation and activation of the classical NF κ B pathway. TLRs detect PAMPs and subsequently activate the NF κ B pathways. Rakoff-Nahoum and colleagues investigated the role of toll-like signalling adaptor receptors in commensal-dependent colitis and reported that development of colitis in interleukin-10-deficient mice was MyD88-dependent signalling pathway while in IL2-deficient mice it was MyD88-independent (Rakoff-Nahoum et al., 2006). Sellon and colleagues experimented with IL-10-deficient mice and kept them in germ-free, specific pathogen free (SPF) conditions, or populated them with colitis-inducing bacteria (Sellon et al., 1998). They reported that the IL-10-deficient mice that were maintained in germ-free environment did not show any evidence of colitis or an activated immune system (Sellon et al., 1998). By contrast, both the IL-10-deficient mice maintained in SPF and populated environments developed colitis and manifested activated immune system characteristics (Sellon et al., 1998).

1.10.7 NF κ B signalling in sepsis

Microbes and microbial products with host cell surface PRRs such as TLR-2 and TLR-4 trigger NF κ B signalling pathways leading to the activation of downstream gene transcription factors (Beutler et al., 2003). This results in the release and expression of mediators such as inflammatory cytokines (TNF and IL-6), chemokines, and superoxide. The released mediators induce local upregulation of adhesion molecules, enhanced vasodilation, and generation of chemotactic gradients (Faure et al., 2000). These cumulate in activation and mobilisation of neutrophils and lymphocytes and promotion of extravascular recruitment of host defence mechanisms essential for early microbial clearance. When local defences are overwhelmed, the invading microbes and microbial products including toxins are translocated to the vascular system where they induce systemic inflammatory responses such as shock, hypotension, multiple organ dysfunction and failure

(Perkins, 2007). There is a high concentration of p50/p65 heterodimer, an indication of an inflammatory process in sepsis (Li et al., 2009).

Silva and colleagues conducted bacterial challenges on mice with *Klebsiella pneumoniae* and measured TNF concentrations before and at several intervals for up to 5 hours following bacterial infusion (Silva et al., 1990). They reported that serum TNF levels rapidly increased to 153-232 ng/ml between 50 and 90 min following bacterial challenge and dropped to 10-12 ng/ml within 5 hours, probably due to effective clearance (Silva et al., 1990). They also observed that serum peak levels of TNF were LPS concentration- and animal species-dependent (Silva et al., 1990). Michie and colleagues injected 4mg/kg of *Escherichia coli* endotoxin into 21 healthy men and reported that serum levels of TNF were increased from 50 to 90 min following endotoxin administration (Michie et al., 1988). The increased TNF levels in the subjects were associated with symptoms such as headaches, chills, nausea, and myalgias and symptoms were most severe at maximal circulating circulation of TNF (Michie et al., 1988). Even when TNF concentrations were no longer detectable, the symptoms persisted for 2 hours before subsiding. Fong and colleagues and Tracey and colleagues reported that TNF was associated with induction of production of secondary mediators including IL-1 and IL-6 (Fong et al., 1989; Tracey et al., 1987). They documented that 1- and 2-hours pre-treatment with anti-TNF prior to bacterial challenge in experimental models resulted in reduction of IL-1 and IL-6 thus adding further weight of evidence that TNF is a key mediator of sepsis (Fong et al., 1989; Tracey et al., 1987). Alternative pathway NF κ B signalling in the gut has been demonstrated to be involved in sepsis, disruption of intestinal epithelial homeostasis, and inflammatory responses, so we will focus on the cytokines that have been reported to play some of these roles (Li et al., 2009). Different roles played by TWEAK, LIGHT and other alternative pathway activators in sepsis are discussed in more details in chapter 4 of this thesis.

1.11 Actions of cytokines in the small intestine

Cytokines are small proteins that are released by macrophages, lymphocytes (B and T), endothelial cells, and mast cells to effect action on these or other cells (Dinarello et al., 2000; Zhang & An, 2007). The term cytokine is a generic name that encompasses chemokine (chemotactic cytokine), lymphokine (lymphocyte-derived cytokine), interleukin (leukocyte-derived cytokine) and monokine (monocyte-generated cytokine). Cytokines have either pro-inflammatory or anti-inflammatory mechanisms of action. Tumour necrosis factor (TNF) is one of the most prominent pro-inflammatory cytokines and it has been implicated in many systemic pathological diseases including sepsis (Beutler et al., 1985). Some studies have reported that IL-6 is also often upregulated when TNF is upregulated in IBD, rheumatoid arthritis and sepsis, so this cytokine may also be worth investigating as well. Cytokines such as IL-1, IL-18, IL-33, and IL-36 play key roles in regulating small intestinal mucosal immunity and homeostasis (Bamias & Cominelli, 2016). Some cytokines including TNF, TNF-like cytokine 1A (TL1A), and IL-6 exhibit dichotomous properties, that is, they demonstrate intestinal mucosa-protective activity in acute injury, while acting as proinflammatory agents during chronic inflammation (Bamias & Cominelli, 2016).

1.11.1 Tumour necrosis factor superfamily

1.11.1.1 TNF

A trimeric form of tumour necrosis factor (TNF) protein was identified in mice in 1975 as an endotoxin-induced glycoprotein and it was later cloned in humans in 1985 (Bradley et al., 2008). It consists of membrane-associated and soluble forms with molecular weights of 26 kDa and 17 kDa respectively (Arakawa & Yphantis, 1987; Bradley et al., 2008). TNF exists in soluble and membrane bound forms and it induces signalling via NF κ B pathway activation. Sources of TNF are activated macrophages, lymphocytes, osteoclasts, fibroblasts, endothelial cells, adipose tissue, and mast

cells, and its production is upregulated by LPS stimulation (Bradley et al., 2008). In healthy humans, TNF is not usually detectable in the serum, but in diseases involving inflammation, infection, and malignancy, its circulating concentration can be elevated (Damas et al., 1989; Debets et al., 1989; Girardin et al., 1988; Spooner et al., 1992; Waage, Halstensen, & Espevik, 1987). TNF, a pro-inflammatory cytokine, has been shown to modulates intestinal tight junction permeability (Al-Sadi et al., 2016; Dinarello et al., 2000) (tables 1.1 and 1.2). It modulates signalling pathways in both physiological and pathological conditions such as cell differentiation, proliferation, migration, inflammation, immune responses, and apoptosis. TNF mediates its stimulatory actions through TNF receptor 1 (TNFR1) which is universally expressed in humans and is the key receptor for TNF, and TNF receptor 2 (TNFR2) which is commonly expressed in immune cells and has more limited biological activities (Bradley, 2008; Piguet et al., 1998; Xu & Shi, 2007). Both TNF receptors (1 and 2) are expressed in intestinal epithelial cells in both apical and basolateral compartments. However, anti-inflammatory cytokines such as IL-10 promotes intestinal barrier function by counteracting the effects of TNF (Mazzon et al., 2002). In sepsis, microbes activate the cell surface receptors including TLR and TNFR1/2, which in turn switch on the adaptor receptors such as MyD88/TRIF. This eventually leads to activation of NF κ B, ERK, JNK, and P38 signalling pathways and results in activation of macrophages to produce cytokines such as TNF, IL-6, and others (Takada et al., 2007). Conte and colleagues observed that TNF was associated with the pathological effects of LPS-TLR4 in sepsis, septic shock, and prolonged survival of macrophages (Conte et al., 2006). Waage, Halstensen and Espevik reported that all five patients diagnosed with sepsis who had circulating TNF concentrations greater than 440 units/ml (corresponding to 0.1 ng/ml recombinant TNF) did not survive (Waage et al., 1987). There are various measurements of TNF in health and diseases in serum, stool, and tissues (table 1.1). Its concentration is usually negligible

in health (0.20 ± 0.10 pg/mL in serum) (Martins et al., 2011), but can be very high in some inflammatory states (18.64 - 63.60 ng/g in stool) (Nicholls et al., 1993).

Condition	Serum	Stool (Faeces)	Tissue	References
Healthy	0.020 ng/L			Komatsu et al., 2001
Active Crohn's disease (CD)	14.0 ng/L			Komatsu et al., 2001
Active ulcerative colitis (UC)	9.46 ng/L			Komatsu et al., 2001
Active CD		994 [420-4,322] pg/g		Braegger et al., 1992
Active UC		276-5,982 pg/g		Braegger et al., 1992
Healthy children		58 pg/g		Braegger et al., 1992
Shigella flexneri infection		18,640-63,600 pg/g		Nicholls et al., 1993
Healthy children		12-130 pg/g		Nicholls et al., 1993
Sepsis	0-587.3 pg/ml			Schaumann et al., 1997
Severe sepsis and septic shock	19 (0-72) pg/ml			Gordon et al., 2004
Irritable bowel syndrom	276.23 \pm 266.40 pg/ml			Vazquez-Frias et al., 2015
Liver metastasis			2 pg/mg	Kuppen et al., 1997
Chronic wound skin tissue			6 \pm 2 ng/ml	Han et al., 2002

Table 1.1 TNF concentrations in health and diseases from the sera, stools, and tissues of patients.

Name	Gene	M. wt (kDa)	Aa length	Chr. location	Functions
TNF	TNF	17 (s) & 26 (m)	233	6 (MHC)	Regulates immune cells, inflammation, apoptosis
TWEAK	TNFSF12	17	249	17	Induces apoptosis, proliferation, migration
LIGHT	TNFSF14	26	240	19	Stimulates T cell proliferation, regulates apoptosis
CD40-L	TNFSF5	33	261	Xq26-27	Regulates adaptive immune response
LT $\alpha\beta$	LTA, LTB	25 & 33	205 & 244	6 (MHC)	Induces inflammation
BAFF	TNFSF13B	31	285	13	Activates B cell, proliferation

Table 1.2 Alternative pathway activators of TNF superfamily with their gene, molecular weights (M. wt), amino acid (Aa) lengths, chromosomal (Chr.) locations, and functions (Alexaki et al., 2009; Armitage et al., 1992; Browning et al., 1993; Granger & Rickert, 2003; Moss et al., 1997; Wiley et al., 2001). These alternative pathway activators were selected for investigation.

1.11.1.2 TWEAK

TNF-related weak inducer of apoptosis (TWEAK) is a cytokine protein of the TNF superfamily that can exist in membrane-bound and soluble isoforms. TWEAK is produced as both type I and II transmembrane proteins and is the only TNF superfamily member that binds to fibroblast growth factor-inducible 14 (Fn14) (Bossen et al., 2006; Brown et al., 2010; Meighan-Mantha et al., 1999). TWEAK binds to a surface receptor protein, which when activated induces the binding of TNFR associated factor (TRAF) to the Fn14 cytoplasmic tail that modulates downstream activation of cascades of signalling pathways including NF κ B, PI3K/Akt, and MAPK to promote cell proliferation, migration, differentiation, survival, and apoptosis (Burkly,

Michaelson & Zheng, 2011; Winkles, 2008). TWEAK is an alternative NF κ B pathway activator that binds TNF receptor-2 that in turn stimulates NIK, resulting in the translocation of p52 to the nucleus to effect the transcription of target genes. TWEAK over-expression has been reported in different types of pathological conditions including chronic inflammation, angiogenesis, and fibrosis, while under-expression has been observed in glioblastomas (Campbell et al., 2006; Jakubowski et al., 2005; Tran et al., 2003). Immunohistochemical studies of synovial tissue biopsies demonstrated over-expression of TWEAK in patients with rheumatoid arthritis in comparison with patients who had osteoarthritis or psoriatic arthritis (Park et al., 2013; van Kuijk et al., 2010). It has been observed that inhibition of TWEAK-Fn14 signalling minimises intestinal epithelial cell apoptosis and disease development (MacEwan, 2015). In γ -irradiation-induced, 2,4,6-trinitrobenzene sulfonic acid-induced, and interleukin (IL)-10 deficiency-induced colitis mouse models, inhibition of TWEAK-Fn14 signalling resulted in protection of the intestinal epithelial mucosa (Dohi et al., 2009; Kawashima et al., 2011; Son et al., 2013). Chopra and colleagues reported that inhibition of the TWEAK-Fn14 signalling pathway reduced intestinal damage in graft-versus-host disease (GVHD) and prolonged survival after allogeneic hematopoietic cell transplantation allo-(HCT) (Chopra et al., 2015). MacEwan also suggested that TWEAK inhibition could be protective in other chronic inflammatory diseases (MacEwan, 2015).

1.11.1.3 LIGHT

Light is one of the members of the TNF superfamily and derives its name from lymphotoxin-like inducible protein that competes with glycoprotein D for herpes virus entry on T cells. Light is a type II transmembrane protein and it is present in dendritic cells, activated T and B lymphocytes, macrophages, natural killer cells, and granulocytes (Mauri et al., 1998). Light has been documented to activate both classical and alternative NF κ B pathways. Many studies have reported that Light can

bind to herpes virus entry mediator (HVEM) (TNFRSF14, TR2, or LIGHTR) and lymphotoxin β receptor (LT β R) to stimulate cytokine production, whilst it can also interact with decoy receptors (DcR3) that are considered to be competitive Light inhibitors (Harrop et al., 1998; Mauri et al., 1998; Tamada et al., 2000; Lee et al., 2019; Yu et al., 1999). Activation of HVEM leads to stimulation of activator protein-1 (AP-1) and NF κ B signalling, while LT β R activation modulates lymphogenesis, cancer-related inflammation, and dendritic cell homeostasis (De Togni et al., 1994; Haybaeck et al., 2009). Light stimulates LT β R which then activates TNF receptor-associated factor 2/5 (TRAF2/5) to signal classical NF κ B pathway activation while through TRAF3 it mediates alternative NF κ B pathway activation involving P52/RelB dimers (Dejardin et al., 2002; Force et al., 2000; Ganef et al., 2011; Jang et al., 2015). It has been reported that via mitogen-activated protein kinase (MAPK), extracellular signal-regulated kinase (ERK), and phosphoinositide 3-kinase (PI3K) activation, Light induces nuclear translocation and transcription of NF κ B signalling to generate inflammatory responses (Lim, Suk, & Lee, 2013). NF κ B is activated by Light via upregulation of CD86 expression but not through p44/42 MAPK or JNK/AP-1 signalling pathways (Schwarz et al., 2007; Zou & Hu, 2005). Clayburgh and colleagues reported that administration of 5 μ g of Light by intraperitoneal injection to Na⁺/H⁺ exchanger (NHE3)^{-/-} mice caused intestinal epithelial barrier dysfunction via Myosin light-chain kinase (MLCK) activity (Clayburgh et al., 2006).

1.11.1.4 CD40-L

CD40-L (CD154, TRAP, gp39, or TBAM) is found as a surface receptor protein on both immune cells (activated CD4⁺ T cells, B cells, macrophages, monocytes, and dendritic cells) and non-immune cells (endothelial cells, epithelial cells, platelets, and mesenchymal cells such as fibroblasts, myofibroblasts, and stellate cells) and it plays a prominent role in the adaptive immune system (Michel, Zirlik & Wolf, 2017). CD40-L consists of trimeric forms that can bind to CD40, platelet integrin α IIb β 3, α 5 β 1, or

α M β 2 (Mac-1) receptors, however, the classical receptor is CD40. In most of the interactions of CD40-L with its receptors, it elicits downstream signalling patterns except in the case of Mac-1 where CD40L acted as an agonist on its own without receiving outside-in signalling (Michel et al., 2017). The interaction of CD40-L with α 5 β 1 activates MAPK - PI3K - NF κ B signalling pathways that promote translocation to the nucleus and the generation of pro-inflammatory gene expression (Michel et al., 2017). CD40L binds with CD40 receptor on B lymphocytes to activate B cell stimulation, cell proliferation, cell survival, and immunoglobulin G (IgG)-class switching to synthesise other Ig groups (Danese, Sans & Fiocchi, 2004; Lesley et al., 2006; Schönbeck & Libby, 2001). Mutational deletion of the CD40-L gene has been attributed to the malfunctioning of immunoglobulin that leads to production of the human X-linked immunodeficiency hyper IgM syndrome (XHIM) typified by deficient IgG antibody specificity and T cell humoral functionality (Notarangelo, Duse & Ugazio, 1992). CD40-L activation of endothelial cells via platelet adhesion and aggregation has been documented as one of the major factors in reactive oxygen species synthesis and inflammatory processes in the initiation, progression, and sequelae of atherosclerosis (Mach et al., 1997). Many studies have postulated that CD40-L may be a potential biomarker to determine atherosclerotic instability in the vascular system (Cipollone et al., 2002; Heeschen et al., 2003; Wang et al., 2013). Stuber and colleagues reported that CD40-CD40L signalling plays a vital role in the pathogenesis of colitis and that inhibition of the CD40-CD40L system using anti-CD40L antibodies was associated with amelioration of 2,4,6-trinitrobenzene sulfonic acid (TNBS)-induced colitis (Stuber et al., 1996). CD40 is expressed in intestinal epithelial villi, colonic surface epithelial cells, and crypts and, within these structures it is mainly located on the basolateral membrane. It was found to be highly expressed in active IBD (Borcherding et al., 2010). Gold and colleagues induced sepsis in CD40 knockout (KO) mice by caecal ligation and puncture (CLP) and observed improved survival compared with wild-type mice administered the same treatment (Gold et al.,

2003). They also reported that activation of NFκB and signal transducer and activator of transcription 3 (STAT3) signalling pathways were attenuated in both the liver and lungs of septic CD40 KO mice (Gold et al., 2003). Ischaemia-reperfusion injury was reported to cause local intestinal and distant lung tissue damage in control wild-type mice while there was significantly attenuated intestinal tissue damage and no distant lung injury in CD40 and CD154 deficient mice administered the same treatment (Lapchak et al., 2012).

1.11.1.5 Lymphotoxin alpha and beta (LTα/β)

Lymphotoxin (LT) α/β is a hematopoietic protein formed from lymphotoxin alpha combined with lymphotoxin beta on the cell surface to form heterotrimers (Nedwin et al., 1985; Ngo et al., 1999). LTα exerts its biological activities via interactions with TNF receptor 1 (TNFR1), TNF receptor 2 (TNFR2), LTβ receptor (LTβR), and HVEM (Crowe et al., 1994; Medvedev et al., 1996). The membrane LT-α1-β2 complex formation enables it to bind to and activate LT-β receptors with subsequent production of IKK-α, β, and γ, biodegradation of I-κB, and nuclear translocation of NFκB1 p50 and RelA which modulate gene expression via classical pathway NFκB signalling (Muller & Siebenlist, 2003). Lymphotoxin alpha regulates cell proliferation, cell survival, cell differentiation, innate immune responses, apoptosis, and inflammation. It also plays a prominent role in cancer prevention, cancerous cell line destruction, and secondary lymphogenesis. Over-expression of lymphotoxin alpha has been implicated in carcinogenesis and unregulated cellular growth (Bauer et al., 2012). By contrast, deletion of lymphotoxin alpha has been reported to be responsible for Peyer's patch maldevelopment, gastrointestinal developmental disruption, *Staphylococcus aureus* infections, Mycobacterium-induced granuloma formation, and splenic disorganisation (Gubernatorova & Tumanov, 2016; Roach et al., 2001). LTα and TNFα have 30% structural similarity, while LTα from human and mouse are 72% similar in primary protein sequence (Pennica et al., 1984). Wang and colleagues

demonstrated that LT β R on intestinal epithelial cells and hematopoietic-derived cells immunomodulate the host's protective response (Wang et al., 2010). In sepsis, activation of LT β R signalling recruits neutrophils via the synthesis of cytokines, especially chemokines (CXCL1, and CXCL2) (Wang et al., 2010). In *C. rodentium* infection, the LT β R signalling pathway regulates the early innate immune cell response against the infection (Wang et al., 2010).

1.11.1.6 BAFF

B-cell activating factor (BAFF) (tumour necrosis factor ligand superfamily member 13B, B Lymphocyte Stimulator (BLyS), TNF- and APOL-related leukocyte expressed ligand (TALL-1)) is a membrane-bound type II transmembrane protein (Schneider et al., 1999). It has a long peptide glycoprotein that can undergo glycosylation of its amino acid at residue 124. BAFF, which is mostly expressed on the surface of B cells, is also found in other cells such as dendritic cells, monocytes, and bone marrow-derived stromal cells. BAFF is primarily involved in the activation, proliferation, differentiation, survival, and homeostasis of B lymphocytes (Bolkun et al., 2012; Croft, 2009). BAFF interacts with BAFF receptor (BAFF-R) (BR3), transmembrane activator and calcium modulator and cyclophilin ligand interactor (TACI), and B-cell maturation antigen (BCMA) to activate classical and/or alternative NF κ B signalling pathways (Kreuzaler et al., 2012). Deficiency or dysregulation of BAFF has been implicated in immunodeficiency secondary to insufficiency of immunoglobulin, while excessive production or regulation of BAFF induces over-production of abnormal antibodies that result in autoimmune diseases including rheumatoid arthritis and systemic lupus erythematosus (Steri et al., 2017). Overexpression of BAFF has been attributed to renal transplant acute rejection, anti-malarial humoral immunity, multiple myeloma, gluten-mediated coeliac disease, non-IgE-mediated reactions, inflammation, breast cancer, and insulin resistance (Aziz, Hadjivassiliou, & Sanders, 2012; Bolkun et al., 2012; Banham et al., 2013; Fabris et al., 2007; Hamada et al., 2011; Pelekanou et

al., 2008). The luminal surface of intestinal epithelial cells expressed TLRs which become sensitised by the presence of microorganisms, especially bacteria in the gut lumen. Activation of the TLR signalling pathway stimulates intestinal epithelial cells to synthesise and secrete BAFF to promote cellular proliferation and the survival of B cell lymphocytes (Macpherson & McCoy, 2007).

1.11.2 IL-6

Interleukin-6 (IL-6) is a cytokine and myokine protein with both pro- and anti-inflammatory properties. IL-6 is expressed by smooth muscle of the tunica media, macrophages, adipocytes, and intestinal epithelial cells (Jones et al., 1993). It interacts with transmembrane protein cell-surface type I cytokine receptor complex including IL-6 receptor (IL-6R) and glycoprotein (gp130) (Kallen, zum Buschenfelde & Rose-John, 1997). In response to pathogen-associated molecular patterns (PAMPs) or microbial molecules that usually bind to pattern recognition receptors (PRRs) such as Toll-like receptors (TLRs), macrophages secrete IL-6 which interacts with surface cell receptor proteins to activate the classical NFκB signalling pathway resulting in the transcription of pro-inflammatory cytokines (Tanaka, Narazaki, & Kishimoto, 2014; Zhang et al., 2010). IL-6 induces fever, acute phase response, bone marrow synthesis of neutrophils, and B lymphocyte growth (Akira, Taga, & Kishimoto 1993). In contrast, through its inhibitory action on TNF and excitatory activities on IL-1 receptor antagonist (IL-1ra) and IL-10 via calcium/nuclear factor of activated T-cells (NFAT) and glycogen/p38 MAPK pathways, IL-6 mediates anti-inflammatory myokine effects (Brandt & Pedersen, 2010; Heinrich et al., 1998). IL-6 plays prominent roles in chronic inflammatory and auto-immune pathological conditions including rheumatoid arthritis, systemic lupus erythematosus, Behcet's disease, neoplasms (prostate cancer and multiple myeloma), diabetes, atherosclerosis, and mental health (depression and Alzheimer's Disease) (Nishimoto, 2006). Clinically, a lot of interest has been generated by studies of IL-6's mechanisms of action and by anti-IL-6

agents. Tocilizumab is an anti-IL-6 agent that is used to treat chronic inflammatory diseases such as rheumatoid arthritis, systemic juvenile idiopathic arthritis, and Castleman's disease (Ogata & Tanaka, 2012). Transgenic mice that were dominant negative for Tgfb2 expressed in T cells and IL10rb gene knock out mice models were used to determine the timing of IL-6-induced intestinal inflammation. Then researchers co-housed three-week-antibiotic pre-treated dnKO mice with non-antibiotic treated IL10rb^{+/-} littermates and serum samples were taken every three days. They observed that on the sixth day following co-housing, IL-6 was significantly increased in dnKO mice in comparison with the similarly treated IL10rb^{+/-} littermate controls (Kang et al., 2008). The dnKO mice were injected with anti-IL-6 mAb and the control dnKO mice were treated with IgG mAb at the beginning of co-housing. A statistically significant weight loss was also seen in the experimental group when compared to the control. On the ninth day following injection, the anti-IL-6-mAb treated dnKO mice demonstrated significant intestinal epithelial mucosal damage especially severe crypt loss and defective crypt regeneration in comparison with the control group (Kang et al., 2008). TNF and IL-6 are therefore acute phase protein cytokines that are found in increased amounts in the serum during sepsis, inflammatory states such as, IBD, and other infective conditions.

1.12 Intestinal cell death mechanisms

1.12.1 Apoptosis in the intestinal epithelium

Intestinal epithelial homeostasis requires a precise balance between the process of apoptosis that removes unwanted/damaged cells and the inherent ability of intestinal epithelial stem cells to regenerate and proliferate to replace the loss. Without this equilibrium, excessive activities of apoptosis will result in intestinal epithelial atrophy, while uncontrolled proliferation of intestinal epithelial stem cells may potentially lead

to neoplasia or hyperplasia that occludes the intestinal lumen. Rapid intestinal epithelial cell division that continuously replaces the apoptotic mediated cell loss usually takes place at the crypt base of the intestinal epithelium (Hall et al., 1994). By contrast the majority of the apoptotic process resulting in intestinal cell loss occurs at the villus tip of the epithelium during steady state conditions.

1.12.1.1 Crypt apoptosis

Mitotically dividing stem cells are located at the base of intestinal epithelial crypts and daughter cells differentiate and migrate from the crypt domain along the crypt-villus axis. Under normal, healthy intestinal conditions, only very few apoptotic cells can be detected in the crypt domain (Hall et al., 1994). In the crypt region, apoptosis can result from either DNA-damaged cells or excessive mitotic synthesis of intestinal epithelial cells (Potten, Wilson & Booth, 1997). The apoptosis that takes place in an intestinal epithelial cells crypt of a healthy individual is called spontaneous apoptosis. This spontaneous apoptosis assists in maintaining the homeostatic mechanism of the intestinal epithelial cell. About 1.6 cells per crypt undergo programmed cell death at any point in time (Potten & Grant, 1998). Exposure of intestinal epithelial cells to ionising radiation can induce a dramatic increase in apoptosis within 3 - 6 hours post-exposure. It has been reported that spontaneous and radiation-induced apoptosis peak at four cell positions from the intestinal crypt base (Potten, 1997). The dose-response relationship between amount of radiation exposure and the apoptotic responses of intestinal epithelial cells in the crypt has been well studied. The exposure of mouse small intestinal epithelial cells to 1 Gy and 8 Gy radiation induced maximal apoptotic activities after 3 - 6 hours (Potten & Grant, 1998). There is no cogent explanation for the variability observed in the values of some of groups of mice and among different mouse strains that are exposed to the same dose of irradiation. However, some other studies have shown that DNA damaging effects from other stimuli including chemotherapeutic drugs tend not to follow the +4-zone

positional apoptotic postulate and any cell within the transit amplifying region irrespective of position from the base of the crypt can undergo apoptosis (Ijiri & Gerbe, 1983; Ijiri & Potten, 1987). Pritchard and colleagues reported that 5-FU - induced crypt apoptosis predominantly in the transit amplifying region at cell positions 6 - 8 (Pritchard et al., 1997). The bcl-2 family of proteins plays a regulatory role in controlling spontaneous and DNA-damaging associated apoptosis in the intestinal epithelial crypt.

1.12.1.2 Villus tip apoptosis

Intestinal epithelial cell shedding is a controlled process whereby cells migrate up the crypt-villus axis and are expelled from the tip of the intestinal villus or colonic crypt table (Bullen et al., 2006). Upon expulsion of the cell from the epithelial villus tip, the structural epithelial integrity is sustained by the rapid remodelling process of cell adhesion mechanisms. This shedding and effective cell adhesion mechanism ensures that the intestinal epithelial villus integrity is efficiently coordinated and maintained (Madara, 1990). In the intestinal epithelial monolayer, major cell loss via shedding occurs at the villus tip, while cell replacement through proliferation takes place within the crypt region. In a normal physiological intestinal epithelial system, the rate of cell shedding at the villus tip equals the rate of cell proliferation in the crypt domain, thus ensuring intestinal epithelial homeostasis (Barker et al., 2007; Potten et al., 2009). However, in pathological states, this steady state equilibrium can tilt in either direction depending on the aetiological nature of the condition. Excessive pathological cell shedding at the villus tip can result in villus atrophy, villus loss, and compromised villus function. In pathological cell shedding, the rate of expulsion of the intestinal epithelial cell at the villus tip is more than the rate of proliferation of the cells in the intestinal crypt (Williams et al., 2015). In this state, the rate of replacement is lower than the rate of loss of cells. Lack of production or excessive production of cells in the crypt will alter intestinal epithelial homeostasis. All epithelial cells have

cell-to-cell and cell-matrix connections that are very important for cell growth, survival, and support; detachment of these connections particularly from the basement membrane can lead to apoptosis (Guan et al., 2011). This process of detachment-induced apoptosis is often described as anoikis, meaning “without a home” (Frisch & Francis, 1994). Williams and colleagues reported that prior to intestinal epithelial cell shedding, cells at the villus tip expressed active caspase-3 (Williams et al., 2013). This finding suggests that the initiation of apoptotic processes may precede anoikis of the expelled cells at the villus tip. Intestinal epithelial tight junction protein (especially ZO-1) remodelling ensures that intestinal integrity is maintained after cells are expelled from the villus tip (Guan et al., 2011).

1.12.2 Apoptotic mechanisms

Apoptosis is a reversible, energy-dependent biochemical process of programmed cell death that is strictly regulated by genetic mechanisms (Yuan & Horvitz, 2004). Apoptosis-mediated cell death is initiated when there is a need to remove aged, injured, malformed, or unwanted cells without causing any adverse effect on adjacent cells (Martin et al., 2012). Excessive activation of apoptosis can result in atrophy, while inadequate activation might lead to poorly regulated cell proliferation and differentiation, potentially predisposing to the development of cancer (table 1.2). The apoptosis process includes blebbing, cell shrinkage, rounding because of lamellipodia retraction and caspase-mediated cytoskeletal destruction (Bohm, 2003). This is followed by cytoplasmic changes including dense and closely arranged organelles. Nuclear changes consist of chromatin condensation, the formation of discrete chromatin bodies, chromosomal DNA fragmentation, nuclear membrane discontinuity and generalised mRNA decay (Nagata, 2000; Susin et al., 2000). About 50 - 70 billion cells undergo apoptotic forms of cell death in the adult human daily (Cole & Kramer, 2016; Reed, 1999). The unilateral migratory crypt-villus tip axis has been reported to be actively modulated by caspase-3, -6, -7, -8, and -9 (Brentnall et

al., 2013). Apoptosis is mediated by intrinsic and extrinsic caspase-dependent pathways and caspase-independent pathways. Both caspase-dependent and caspase-independent apoptosis is induced in the cell. Caspase-dependent signalling is mediated via initiator caspases such as caspases 2, 8, 9, 10, 11, and 12 and effector caspases, including caspases 3, 6, and 7 to induce proteolytic cleavage and biodegradation (Li et al., 1997). The N-terminal region of several caspases including caspase-8 contains death effector domains (DED), while in other caspases, the N-terminus contains a caspase activation and recruitment domain (CARD) such as in caspase-9 (Degterev et al., 2003; Muzio et al., 1996). The CARD region often interacts with the inflammasome. Localisations of caspase-2 in the endoplasmic reticulum and caspase-12 in the nucleus have been reported in the mediation of stress-induced apoptosis and DNA-damage-induced apoptosis respectively (Lassus et al., 2002; Nakagawa et al., 2000). In the mouse, caspase-11 has been implicated in having a regulatory role in caspase-1 induced inflammation and caspase-3 activated apoptosis (Kang et al., 2000). Pro-apoptotic proteins include Bak, Bax, Bok, Bad, Bid, Bik, Bcl-Xs, Fas receptors and caspases while anti-apoptotic proteins include Bcl-2, Bcl-xl, Bcl-w, Mcl-1, and Diva/Boo (Elmore, 2007). Over-expression of Bax/Bak has been observed to mediate mitochondrial dysfunction-programmed death in cells that do not contain apoptosome-inducing caspase signalling because of lack of caspase-3, caspase-9, or Apaf-1. In the study of Bax/Bak double knockouts, activation of the mitochondrial signalling pathway could not be induced, emphasising the importance of Bax/Bak role in mitochondrial-mediated apoptosis (Cheng et al., 2001).

1.12.2.1 Intrinsic apoptosis

Intrinsic apoptosis is a caspase-dependent process. The intrinsic pathway involves the activation of mitochondria-dependent intracellular signals that respond to stress within the cells, resulting in the release of proteins (second mitochondria-derived

activator of caspases) and cytochrome c from the mitochondrial membrane (Carmona-Gutierrez et al., 2010; Goldstein et al., 2000). Other factors that can also initiate the release of apoptogenic factors are Omi/high temperature requirement protein A2 (HtrA2), apoptosis-inducing factor (AIF), second mitochondria-derived activator of caspase/direct inhibitor of apoptosis protein (IAP)-binding protein with a low isoelectric point (pI) (Smac/DIABLO), or endonuclease G from the mitochondrial intermembrane space (Cande et al., 2002; Saelens et al., 2004). Cytochrome c that is released from mitochondria into the cytosol attaches to apoptotic protease activating factor 1 (apaf-1) to form the apoptosome (Zou et al., 1999). It also leads to triggering of caspase-3 activation through formation of the cytochrome c/Apaf-1/caspase-9-containing apoptosome complex that eventually provokes DNA fragmentation in the nucleus (Fulda & Debatin, 2006). This can also involve the activation of c-Jun N-terminal kinase (JNK), mitogen-activated protein kinase (MAPK)/extracellular signal-regulated protein kinase (ERK), and NF κ B signalling to effect apoptosis (Davis, 2000; Karin et al., 2002). The Smac/DIABLO system and Omi/HtrA2 complex promote activation of caspases by neutralising the inhibitory effects on the IAPs (Saelens et al., 2004). Intrinsic pathway can be induced by oxidative stress to mediate programmed cell death in intestinal epithelial cells (Buttke & Sandstrom, 1994).

1.12.2.2 Extrinsic apoptosis

The extrinsic apoptosis pathway of caspase-dependent apoptosis comprises type I and type II mechanisms. The type I extrinsic apoptosis pathway mediates direct caspase-8 activation through death receptors resulting in cleavage of caspases 3, 6 and 7 to effect biochemical and morphologic characteristics of apoptosis (Gunther et al., 2014; Kucuk et al., 2006). By contrast the type II pathway requires BH3 interacting-domain death (Bid), a proapoptotic agonist that facilitates cross-communication between extrinsic and intrinsic apoptotic pathways (Yang et al.,

2009). Activation of the type I pathway is sufficient to drive the apoptotic process while the type II pathway cannot induce apoptosis without amplification from Bid. The extrinsic pathway is mediated via the binding of ligands (Fas, TNF, TNF-related apoptosis-induced ligands (TRAIL)) to cell surface receptors extracellularly to form a death-inducing signalling complex (DISC) (Irmiler et al., 1997; Srinivasula et al., 1996). Other death receptors are DR3, DR4, DR5, and DR6. The attachment of FasL to Fas receptors (death receptor) on target cells can cause multiple receptors to accumulate on and around the surface of the target cell. This leads to recruitment of an adaptor protein such as Fas-associated death domain protein (FADD) on the cytoplasmic aspect of the cell surface receptors. Following this, Caspase-8, an initiator protein is recruited by FADD to form the DISC. Thus, via the recruitment of caspase-8 to DISC, caspase-8 becomes activated, resulting in subsequent direct activation of caspase-3, an effector protein which initiates biodegradation of the cell (Adrain et al., 2002). The major executioner protease is caspase-3 and minor ones are caspases-6 and 7 (Slee, Adrian & Martin, 2001). In a study of bacterial translocation and apoptosis in the small intestine during sepsis, caspases 3, 8 and 9 were observed to be activated (Mete et al., 2016).

1.12.2.3 Caspase-independent apoptosis

Caspase-independent signalling is modulated by apoptosis-inducing factor (AIF). The vital role played by Bcl-2 family proteins and mitochondria in caspase-independent apoptosis was investigated in yeast (*Schizosaccharomyces pombe*) since its genome has no caspase genes (Jurgensmeier et al., 1997). Jurgensmeier and colleagues reported that upregulation of proapoptotic Bcl-2 family members Bax and Bak was associated with programmed cell death in *S. pombe* (Jurgensmeier et al., 1997). These pro-apoptotic Bcl-2 family members are responsible for vacuolisation of the cytosol and condensation of nuclear chromatin in yeast.

Activation of the pro-apoptotic Bcl-2 family has been reported to be inhibited by anti-apoptotic Bcl-XL (Yarmolinsky, 1995).

Caspase-independent apoptosis occurs when a signal that usually induces apoptosis via caspases fails to activate it. In the absence of caspase-dependent apoptotic activity, activation of a death receptor that binds to TNF and FasL results in a series of events that induces mitochondrial outer membrane permeabilisation (MOMP) (Holler et al., 2000). This leads to the release of different types of mitochondrial intermembrane space toxic proteins such as endonuclease G, cytochrome C, AIF, Smac/Diablo, ROS, and Htr2A/Omi, thereby creating severe loss of mitochondrial structure and function (Du et al., 2000; Li et al., 2001; Suzuki et al., 2001; Verhagen et al., 2000). This mitochondrial dysregulation activates mitochondrial fission and inactivates mitochondrial fusion thus disrupting mitochondrial morphology further (Tait & Green, 2008). Collectively, cascades of mitochondrial actions and reactions contribute to caspase-independent apoptosis.

1.12.3 Necrosis

Necrosis is an uncontrolled, non-programmed, non-specific, energy-independent, irreversible cell death process resulting from microbial invasion, trauma, hypoxia, toxins or extreme environmentally induced injury (D'Arcy, 2019; Kroemer et al., 2009). Pathologically and morphologically, necrosis can be classified into coagulative necrosis, liquefactive necrosis, fibrinoid necrosis, fat necrosis, gangrenous necrosis, and caseous necrosis (table 1.2). Structurally, cells undergoing necrosis might be characterised by changes including cytoplasmic swelling, mitochondrial swelling, lysosomal rupture, nuclear membrane discontinuity, and plasma membrane blebbing and rupture (Rock, 2008). Necrosis causes inflammatory responses and severe adverse events on adjacent cells due to dissolution of cytoplasmic and organelle contents and disruption of the cell membrane (Raffray, Cohen & Cohen, 1997; Yagami, Yamamoto & Koma, 2019). The disequilibrium of ion homeostasis that

occurs in necrosis has been postulated to be mediated by calpains and lysosomal proteases such as cathepsins B and D (Yagami, Yamamoto & Koma, 2019). The necrosis process is mediated by caspase-independent proteases and has been reported to occur in ischemia-reperfusion injury.

1.12.4 Autophagy

Autophagy is the natural, regulated, self-degradative process of cell death that involves endocytosis-mediated lysosomal biodegradation (Mizushima, 2007). Autophagic mechanisms can be micro-autophagy, macro-autophagy, and chaperone-mediated autophagy (CMA) via proteases of calpain and autophagy-related genes (Yagami, Yamamoto, & Koma, 2019). Lipophagy, mitophagy, chlorophagy, pexophagy, and ribophagy are various types of selective macroautophagy. Autophagy promotes cell survival and restricts tumorigenesis by adaptively responding to stress-induced injury and starvation, while in some situations it has been reported to mediate cell death and morbidity (Cuervo, 2004; Degenhardt et al., 2006). Autophagy is involved in both selective and non-selective cell death mechanisms without any inflammatory responses (Mizushima, 2007). Internal and external stimuli secondary to injury, aged cells, or stress can induce autophagic mechanisms resulting in dephosphorylation and activation of Unc-51-like kinases (ULK) 1 and 2, with subsequent phosphorylation and activation of Beclin-1 and protein p62 (Chan, 2012). Autophagocytosed microbes, organelles and cytoplasmic contents were engulfed in autophagosomes which contain biodegrading lysosomes (table 1.3). There are about 30 autophagy genes that are involved in various types of mediation, most especially atg 1-5, 6, 8, 9, 10, 11, 13, 14, 17, and 18, (Russell et al., 2013). Yang and colleagues reported that there was alteration of autophagic flux in intestinal epithelial cells that resulted in disruption of gut microorganism composition in a gut specific Atg5 knockout mouse model (Yang et al., 2018). Other studies have shown that the Atg5-knockout mice and disruption of

Atg5, Atg7, and Atg16L1 in intestinal epithelial cells were associated with morphological abnormalities in Paneth cells, enhanced intestinal permeability, and bacterial translocation (Cadwell et al., 2009; Yang et al., 2018). Dysregulated Atg5 and Atg16L1 have been implicated in increased susceptibility to IBD and sepsis (Shao et al., 2017).

Features	Apoptosis	Necrosis	Autophagy
Energy	Dependent	Independent	Yes
Programming	Yes	No	Yes
Predictability	Yes	No	Yes
Genetic control	Yes	No	Yes
Coordination	Yes	No	Yes
Predetermined pathways	Yes	No	Selective and non-selective
Physiological	Yes	No	Yes
Pathological	Yes	Yes	Yes
Inflammatory responses	No	Yes	No
Proteases	Caspases	Calpain and cathepsin	Calpain
Adjacent cell injury	No	Yes	No
Membrane rupture	No	Yes	No
Cell size	Decrease (shrinkage)	Increase (swelling)	Increase (swelling)
Biodegradation	Apoptotic bodies	Dissolved cytoplasm	Autophagosomes
Nucleus	Nuclear fragmentation	Pyknosis, karyorrhexis	Nucleation
Activities	Atrophy	Liquefactive etc	Micro, macro, and chaperone-mediated
Reversibility	Yes	No	Yes

Table 1.3 Comparison of the features of apoptosis, necrosis, and autophagy. Activation of autophagy is aimed at saving and preserving the function of cells and cellular organelles, especially the mitochondria. Autophagy promotes recycling of the unaffected organelles. When ATP is highly consumed, apoptosis is initiated which results in programmed cell death and intestinal epithelial cell shedding. Both autophagy and apoptosis processes are reversible. However, necrosis is irreversible and involves membrane and nuclear damage.

1.13 Analysis of the intestinal proteome

Proteomics is a systematic identification, analytic quantification, and large-scale study of structure, nature, and function of a comprehensive complement of proteins of a biological system at a specific time (Anderson & Anderson, 1996; Chandramouli & Qian, 2009; Graves & Haystead, 2002; Wilkins et al., 1996). The term proteomics was coined in 1994 by Marc Wilkins (Wasinger et al., 1995) as an amalgamation of the terms protein and genomics. Proteomics essentially assists in understanding, studying, and characterising an overall protein in an organism, organ, or cell in the resting, stimulated, diseased, healthy, spatial, or dynamic state (Lindon, Tranter &

Koppelaar, 2016). Proteomics is a new field of research that combines computational algorithms and modern mass spectrometry for interrogating both dynamic and static functionality of proteins (Graves & Haystead, 2002). Translational status and post-translational modification of proteins can also be studied through proteomic analysis.

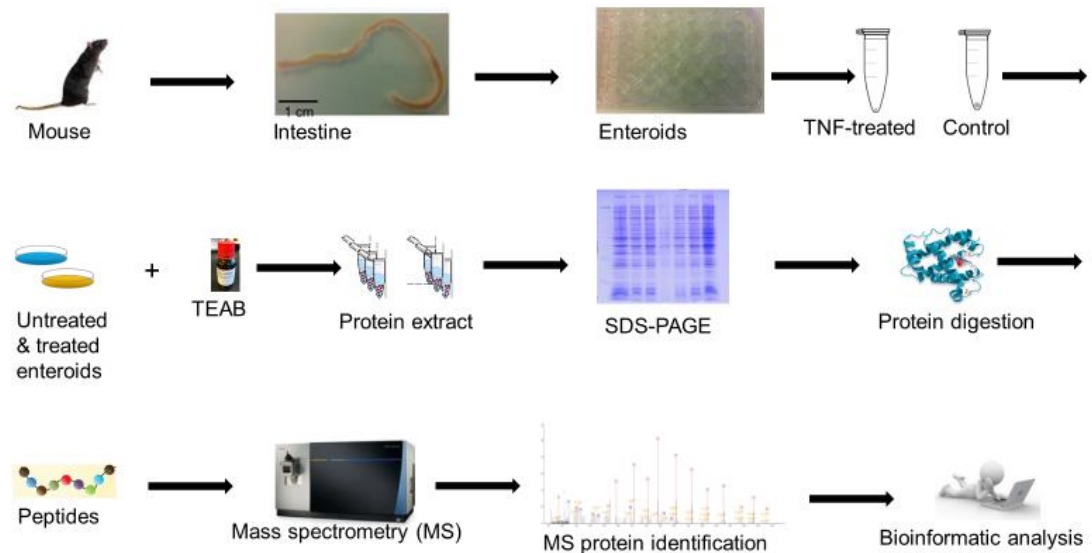


Figure 1.7 Flow chart of proteomic analysis showing harvest of enteroids from mouse through protein extraction and protein digestion to protein identification by mass spectrometry method and bioinformatic analysis. Adapted from Warwick University Proteomic Centre.

1.13.1 Proteomic technologies

Mass spectroscopy (MS) (bottom-up type) applies analytical techniques to break molecules into charged fragments or ions and determines their molecular weights and mass-to-charge ratio based on how long it takes the ions to migrate through the MS flight tube (Chandramouli & Qian, 2009; Urban, 2016). The MS is a very sensitive and specific high-throughput tool for identification, characterisation, qualification, and quantification of proteins. It can also provide information on post-translational modifications of protein (Chandramouli & Qian, 2009). However, MS limitations include an inability to identify isomers having the same mass-to-charge ratio and failure of matrix assisted laser desorption/ionisation (MALDI) and electrospray ionisation (ESI) to adequately identify basic and hydrophobic peptides (Arlinghaus,

2008). Other common proteomic technologies include bioinformatics (usually useful in all proteomic analysis), protein array, two-dimensional electrophoresis (2DE), isotope-coded affinity tag (ICAT) labelling, and fluorescence 2D difference gel electrophoresis (2D-DIGE) (Chandramouli & Qian, 2009; Graves & Haystead, 2002). Isobaric labelling including tandem mass tags (TMT) which enables multiplexed proteomic analysis is used for peptide quantification. Peptide quantification involves a fragmentation process in a tandem MS to generate reporter ions. The higher the degrees of multiplexing, the smaller the mass differences between the reporter ions, the greater the mass resolving power and the more accurate and precise the proteomic analysis (Bekker-Jensen et al., 2017; Kelstrup et al., 2018). The TMT10-plex quantification that was used in this thesis is based on sound resolution and accurate measurements of small mass differences of the reporter ions such as 0.0036 Da (Werner et al., 2014). More details about TMT10-plex are provided in chapter 2 of this thesis.

1.13.2 Proteomic analysis in the small intestine and enteroids

Based on transcriptomic and proteomic analysis, about 75% of all human protein-coding genes have been found to be expressed in the intestine (Gremel et al., 2015). The proteomic analysis of porcine small intestinal mucosa resulted in identification of 5275 quantitative proteins (Qin et al., 2016). Proteomic analysis in the small intestine and in enteroids in resting and stimulated conditions can result in reveal significantly up- and down-regulated proteins and some proteins that are statistically insignificantly regulated as a result of treatment. Proteomic analysis can be conducted on native enteroids or treated enteroids. A recent study analysed the proteome of enteroids that were skewed to specific epithelial cell lineages induced by small molecule drug treatments (Luu et al., 2018).

Through proteomic analysis, potential novel biomarker candidates such as IL-4, IL-6 precursor, desmin, fibrinogen alpha chain (FGA), and Annexin A1 have been

discovered for sepsis and local infections (Cao & Robinson, 2014; Hinkelbein et al., 2009; Sharma & Salomao, 2017; Tang et al., 2011; Zhou et al., 2011). Future studies of their molecular mechanisms of actions and signalling could therefore potentially lead to discoveries of novel therapeutics and prevention strategies against sepsis and local infection (Cao & Robinson, 2014; Malmstrom et al., 2016). Biomarkers of sepsis will be more comprehensively discussed in chapter 5 of this thesis.

1.14 Hypothesis, aims, and objectives

1.14.1 Hypothesis

Enteroids can be used to model intestinal damage observed during active IBD and sepsis to determine novel mechanisms that may be targeted therapeutically to ameliorate both diseases.

1.14.2 Aims

1.14.2.1 To determine the effects of TNF and alternative NFκB signalling pathway activators on mouse enteroid morphology and dynamics.

1.14.2.2 To assess the impact of *Nfkb2* deletion on the susceptibility of mouse enteroids to TNF-induced injury.

1.14.2.3 To investigate the consequences of deleting NFκB family members on the mouse small intestinal epithelial proteome and its response to TNF.

1.14.2.4 To develop a novel enteroid model to test potential therapeutics for IBD and sepsis.

1.14.3 Objectives

1.14.3.1 To investigate the pathological effects of TNF and a panel of alternative pathway NFκB signalling pathway activators on murine intestinal epithelia.

1.14.3.2 To use live imaging technology to capture the phenotypic responses of TNF treated wild-type and *Nfkb2*^{-/-} mouse enteroids.

1.14.3.3 To determine whether the responses of TNF-treated enteroids are different from those of forskolin-treated enteroids.

1.14.3.4 To understand the mechanisms involved in regulating morphological changes in TNF-treated mouse enteroids.

1.14.3.5 To examine the time course of events following TNF treatment of mouse enteroids.

1.14.3.6 To analyse the possible mechanism of TNF induced enteroid injury using proteomics.

1.14.3.7 To interrogate the inhibitory properties of various potential therapeutic agents against TNF-induced mouse enteroid rounding.

1.14.3.8 To understand the similarities and differences in the intestinal epithelial proteome between enteroids and epithelium-enriched extracts from *in vivo* murine small intestine.

2. Material and methods

2.1 Animals

All mice were housed in groups of 3 per cage with recommended pelleted food (standard chow diet made from ground wheat, oats, soybean, corn, alfalfa, vegetable oil, minerals, vitamins and fish) supplied by Charles River (D12450B) and water and kept under 12-hour light: dark cycle in standard specific pathogen free (SPF) conditions until they were utilized for tissues or in experiments. Animals were maintained at a temperature of $22\pm 2^{\circ}\text{C}$, $55\pm 10\%$ humidity, less than 50 dB noise, and individually ventilated cages (IVC) system with 15-20 air changes per hour and 500 square centimetres cage floor area. Environmental enrichment included wooden chew sticks, cardboard houses, plastic tubes and shredded paper. Home Office legislation was strictly followed for all procedures. The *in vivo* study was conducted under authority of project licence number 231167 held by Professor Mark Pritchard.

2.1.1 Wild type mice

C57BL/6J in-bred wild type (WT) mice were purchased from Charles River Laboratories (Margate, UK) and, were acclimatized for at least 1 week before being used in experiments.

2.1.2 Transgenic mice (*Nfkb1*^{-/-}, *Nfkb2*^{-/-}, *c-Rel*^{-/-})

Nfkb1^{-/-}, *Nfkb2*^{-/-}, and *c-Rel*^{-/-} transgenic mice were bred in the Biomedical Services Unit (BSU) of the University of Liverpool. The *Nfkb2*^{-/-} colony was established from mice by Dr Jorge Caamaño at the University of Birmingham.

2.1.2.1 Generation of *Nfkb1*^{-/-} mice

Nfkb1^{-/-} mice were generated by insertion of a phosphoglycerate kinase (PGK) neo cassette of p50 into exon 6 of *Nfkb1*^{-/-} which encodes the Rel homology domain

resulting in disruption of functioning *Nfkb1*^{-/-} (Sha et al., 1995). The targeted disruption resulted in a shortened polypeptide with an inability to bind DNA, synthesize p50 from p105 precursor, combine with itself, or dimerize with other members of the NFκB/Rel family. However, this linearized targeted disruption has no effect on IκB-γ production from internal mRNA promotion since it is located at the C-terminus of p105 (Inoue et al., 1992) and the targeted disruption took place within the N-terminus (Ghosh et al., 1990). Although *Nfkb1*^{-/-} mice did not show any developmental deficiency, defects and non-specificity was shown in their immune responses, susceptibility to infection, and inability of B cells to proliferate in response to stimulation by LPS (Sha et al., 1995).

2.1.2.2 Generation of *Nfkb2*^{-/-} mice

Nfkb2^{-/-} mice were produced in embryonic stem (ES) cells with the WT genetic background. A PGK neo cassette was inserted into exon 4 of the *Nfkb2* locus to achieve targeted disruption of the synthesis of p100 and p52 (Caamano et al., 1998). *Nfkb2*^{-/-} mice show no demonstrable developmental abnormality and upon stimulation, the thymic cells of *Nfkb2*^{-/-} mice do not express p100 or p52. This colony shows abnormalities in lymphoid organs with defective T- cell responses and low proliferative responses of B cells to LPS, CD40 and anti-IgD-dextran (Caamano et al., 1998).

2.1.2.3 Generation of *c-Rel*^{-/-} mice

c-Rel^{-/-} mice were produced on the WT genetic background. Targeted disruption of *Rel* was achieved by inserting a PGK-neo cassette to replace exons 4-9 encoding amino acid residue 145-588 of c-Rel (Kontgen et al., 1995). This disruptive technique led to truncation of c-Rel proteins that did not have the capability of promoting dimerization of protein and binding of DNA (Kontgen et al., 1995).

2.2 The 3D small intestinal enteroids

2.2.1 Organoid generation from crypt isolation

Using modifications of culturing methods first established in the Clevers laboratory (Sato & Clevers, 2013), we grew small intestinal organoids from murine small intestinal crypts. Mice used for the generation of small intestinal organoids were culled using a schedule 1 method (cervical dislocation and death confirmed by checking for heartbeat cessation, dilated pupils and lack of corneal reflex) at the BSU. The proximal 3cm of the small intestine was dissected and flushed with cold 1X PBS without Ca^{2+} and Mg^{2+} . It was longitudinally dissected and transversely cut into about 1 cm pieces and meticulously washed with cold 1X PBS to ensure cleanliness and avoid tissue disruption. The cut parts were transferred to a 30 ml 1X PBS-containing universal and transported in an ice box to the department. The dissected intestine was further washed several times before being transferred into 20 ml of 2 mmol ethylenediamine tetra-acetic acid (EDTA) in 1X PBS, chelation buffer, in a 50 ml falcon tube in a covered ice box on a shaker for 30 minutes to isolate and release villi into the solution. Then, the chelation buffer was discarded and 20 ml of shaking buffer (43.3 mmol sucrose and 59.4 mmol D-sorbitol) was added, and vigorously shaken for 2 minutes to enhance the release of stem cell-containing crypts from the intestinal basal membrane into the solution. To verify whether crypts had been released, the Falcon tube was viewed microscopically. A 70 μm cell strainer was used to filter the solution-containing crypts into a 50 ml Falcon tube kept on ice. The contents were transferred into a 15 ml Falcon tube and centrifuged at 200 *g* for 10 minutes at 4°C. Under a hood, the supernatant was discarded while the pellet was resuspended in Matrigel and 50 μl (about 500 crypts) seeded per well on a 24-well plate and placed in an incubator to polymerize. After polymerization, the 24-well plate-containing organoids was brought under the hood and 500 μl of minigut culture media was added per well. On the fourth day, minigut media was discarded and replaced with

fresh media. Enteroids were usually maintained in complete Intesticult media but switched to home-made individual growth factor media for experimental purposes as we could then be sure of all growth factor additives.

2.2.2 Organoid media

2.2.2.1 Intesticult media

Intesticult mouse basal medium is a serum-free cell organoid growth medium (OGM) made by Stem Cell Technologies. Complete Intesticult medium was made from addition of 5 ml of Intesticult mouse supplement 1, 5 ml of Intesticult mouse supplement 2, and 200 μ l of 100 μ g/ml primocin to the basal Intesticult. Intesticult was stored at 4°C and warmed to 37°C for enteroid colony maintenance.

2.2.2.2 Home-made individual growth factor media

Basal minigut medium consisted of 500 ml Dulbecco's Modified Eagle's Medium (DMEM)/Nutrient mixture F-12 ham, 1% L-Glutamine, 100 μ g/ml primocin, 10 ml B-27 supplement, 5 ml N-2 supplement, and 10mM HEPES. A complete home-made individual growth factor culture medium was made by adding 500 ng/ml R-spondin, 100 ng/ml noggin, 50 ng/ml mEGF to the basal medium. We used the home-made individual growth factor media for experimentation as Intesticult medium composition has not been released and may contain additional growth factors and inhibitors.

2.2.3 Organoid passaging

Frozen Matrigel was defrosted on ice as Matrigel solidifies at $>10^{\circ}\text{C}$. A new 24-well plate was placed in the incubator for warming to 37°C. The 24-well plate-containing organoids was brought out of the incubator, minigut culture media was discarded and organoids were washed with ice cold 1X PBS. Then 500 μ l of 1X PBS was added per well and gently pipetted up and down to break the dome shaped Matrigel that contained the organoids and the mixture was pipetted into a 5 ml Bijou. An insulin

syringe with a 27G needle was used to withdraw the mixture of organoids and Matrigel which were then transferred into a 15 ml Falcon tube. 1X PBS was added to a volume of 14 ml to the tube before being centrifuged at 200 g for 10 minutes at 4°C. Supernatant was then discarded, and the pellet was resuspended in Matrigel. The 50 µl of Matrigel-containing organoids was seeded per well on a warmed 24-well plate and placed in an incubator for the Matrigel to polymerize. After 15 minutes of polymerization, 500 µl of minigut culture media was added per well (figure 2.1). The organoid passaging procedure was conducted under sterile conditions.

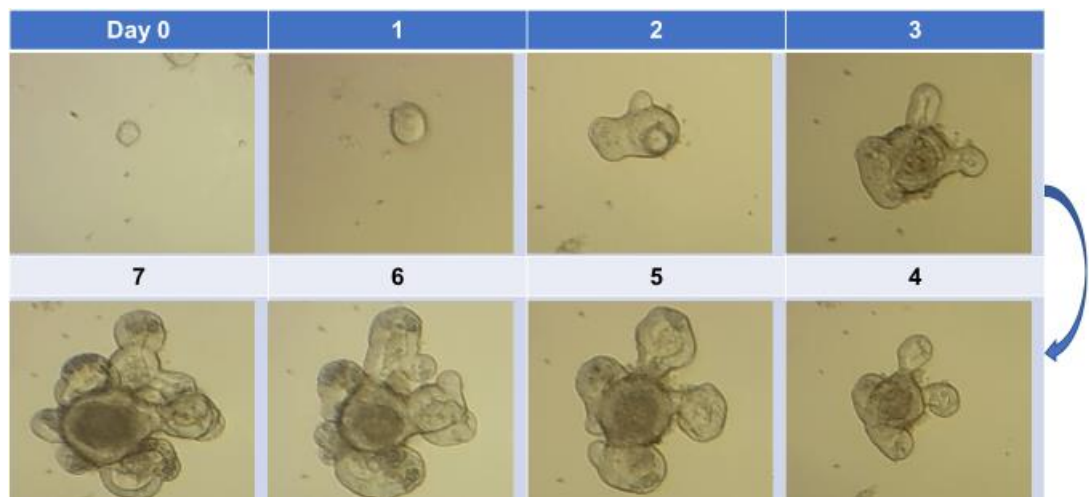


Figure 2.1 Monitoring of the growth of enteroid from embedding in Matrigel and seeding in 24-well plates with the addition of noggin, mEGF, and R-spondin containing minigut media to provide nutrition and growth factors.

2.2.4 Enteroid circularity

Increased circularity is a good indicator of altered enteroid morphology. Several enteroid treatments including cytokines and chemotherapeutic agents have previously been shown to cause increased circularity of enteroids and this positively correlated with active caspase-3 activity (Jones et al., 2019). We have therefore treated enteroids with several stimuli (treatments discussed in section 2.5 of this thesis) and assessed their changes in circularity with time and dose. Enteroid circularities were measured at 0, 24, 48, and 72 hours and bright field images of six

individual enteroids per well were captured. We used two dimensional images to quantify circularity. The freehand selection tool available in NIH ImageJ was used to measure circularity. Enteroid circularity ($[4\pi (\text{area})]/\text{perimeter}^2$) was calculated to indicate death response/health status. Values of 0 represented an infinitely elongated polygon and values of 1 indicated a perfect circle (figure 2.4). Untreated WT enteroids have circularity values of ≤ 0.4 while 50 ng/ml or 100 ng/ml TNF-treated WT enteroids were observed to have circularity values of ≥ 0.7 from 24 hours post-treatment.

2.2.5 Validation of NIH ImageJ circularity measuring technique

Determination of the reproducibility and accuracy of circularity scoring was examined first by the author by randomly scoring 10 selected enteroids on two separate days to identify any intra-scorer variability and intra-scorer reproducibility (figure 2.2). Little variation was found between two temporally spaced scoring events suggesting there was little variability within a single scorer in determining enteroid circularity. Two previously trained circularity scoring researchers (a male and a female) tested inter-scorer variability by scoring randomly the same 10 selected enteroids (figure 2.3). Little variation was observed when circularity scoring was conducted between three independent scorers, indicating that reproducibility between assessors was good, thus validating the reproducibility of the circularity scoring technique.

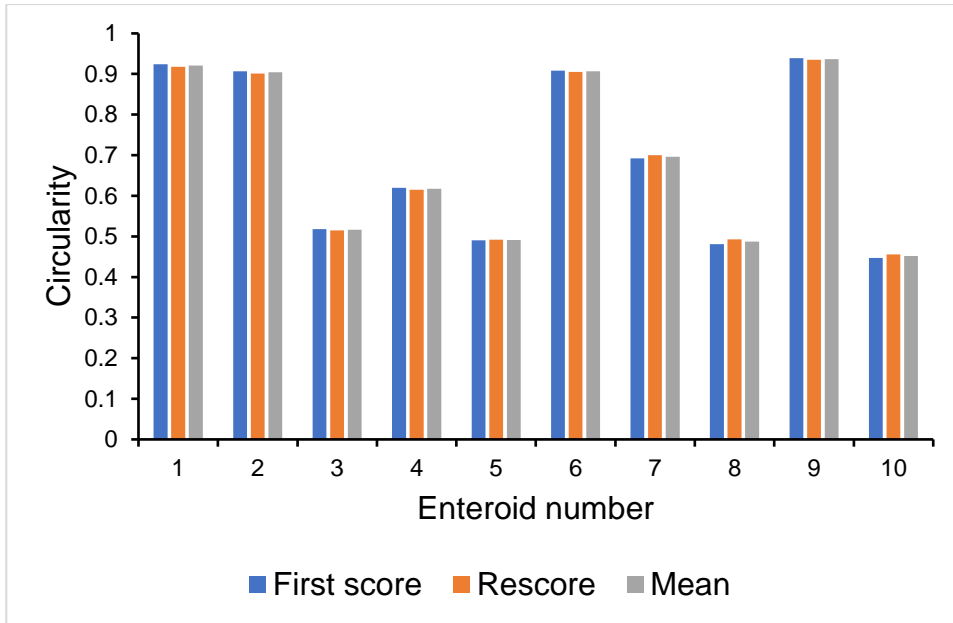


Figure 2.2 Circularity of enteroids was investigated for intra-scorer variability within the researcher. The researcher first scored 10 randomly selected enteroids from a range of enteroids given different treatments and rescored the same images on a different day.

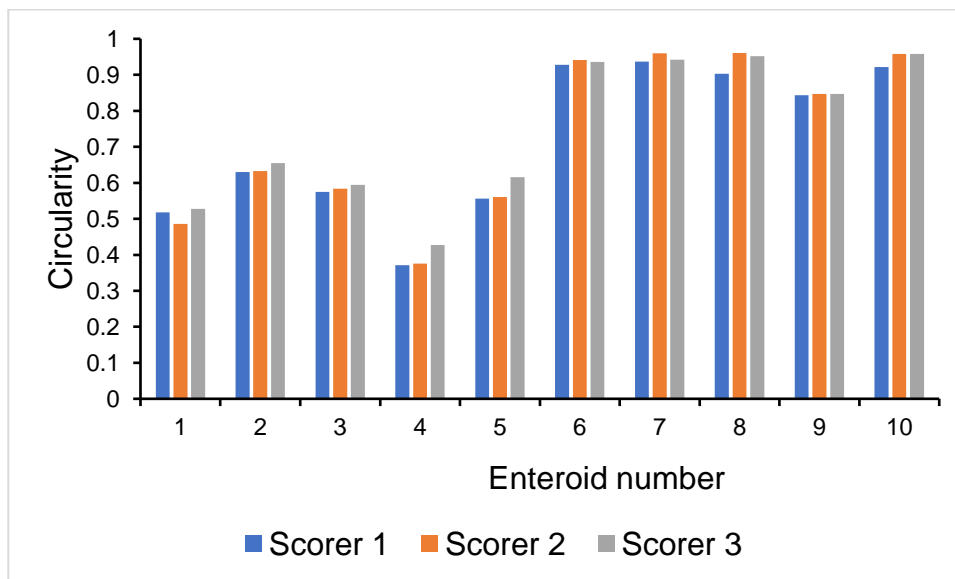


Figure 2.3 Determination of inter-scorer variability of 10 enteroids randomly selected from different treatment groups and quantified by three independent scorers. Scorer 1 was the researcher, scorer 2 was a female and scorer 3 was a male. All scorers were previously trained in assessing enteroid circularity.

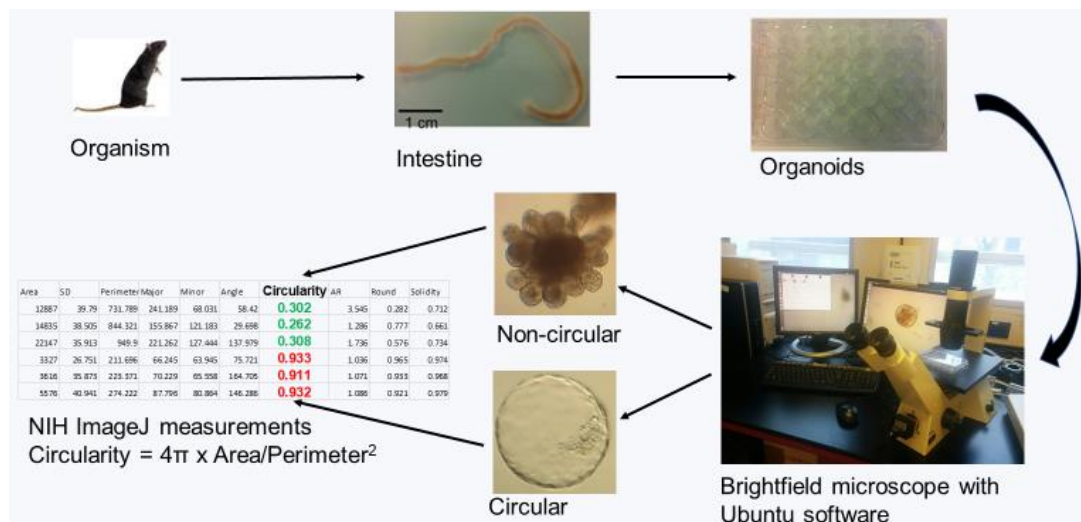


Figure 2.4 Enteroids that were generated from the mouse were cultured with growth factors and a brightfield microscope was used to capture images. Stimulation with reagents could result in a circular enteroid while resting untreated enteroids had a non-circular, morphology.

2.3 CytoSmart live cell imaging

The CytoSMART imaging system can be used for low power bright field time-lapse imaging. Enteroids were placed on the cytoSMART system (figure 2.5) and put in an incubator with 5% CO₂ and set at 37°C. The cytoSMART was focused on a field of enteroids and adjusted to obtain brightfield images. The field of view was imaged every 15 minutes for up to 4 days. Progress was also monitored remotely so that the incubator was not disturbed. Image analysis was conducted from time-lapse sequences by either tracking the motility, tracing the expansion and contraction pattern, or depicting the morphology of the enteroids. This image analysis technique was developed during this thesis project and more depth information and captured enteroid images discussed in chapter 3.

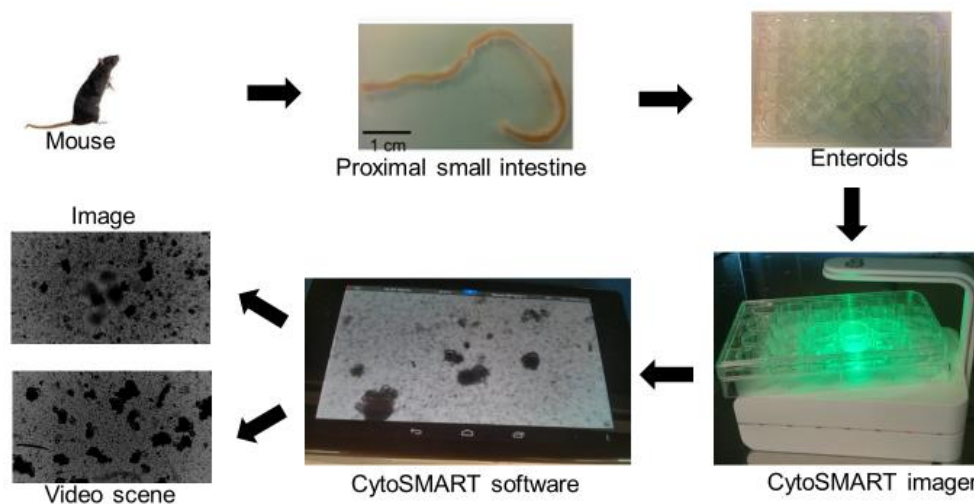


Figure 2.5 CytoSMART live cell imaging system with the 24-well plate containing enteroids placed on it to monitor behavioral patterns and morphological changes. Both images and videos could be accessed and assessed.

2.4 Alternative NF κ B signalling pathway activators

2.4.1 TNF superfamily

2.4.1.1 TNF

TNF (Pepro Tech, 315-01A-20UG) was reconstituted in sterile 0.1% bovine serum albumin (BSA) to a stock concentration of 50 μ g/ml which was immediately frozen at -80°C in aliquots. Enteroids were treated with 0, 1, 10, 50, 100 ng/ml TNF and brightfield microscopic images were captured at 0, 24, and 48 hours, $n=6$ (n represents individual enteroids), $N=3$ (N represents independent experiments conducted at different times). For CytoSMART studies, several different concentrations of TNF were selected, and imaging was conducted every 15 minutes for up to 4 days. TNF was also used as a positive control inducer of enteroid circularity in several experiments as discussed within results chapters 3-6. Enteroid samples for proteomic analysis were also treated with TNF as detailed in section 2.6 below.

2.4.1.2 TWEAK

TWEAK (R and D systems, 1237-TW) was reconstituted in sterile 0.1% bovine serum albumin (BSA) to 50 µg/ml and frozen in aliquots at -80°C. Enteroids were treated with 0, 1, 10, 50, 100 ng/ml TWEAK and brightfield microscopic images were captured at 0, 24, and 48 hours, n=6, N=3.

2.4.1.3 LIGHT

LIGHT (R and D systems, 1794-LT) was reconstituted in sterile 0.1% bovine serum albumin (BSA) to a stock concentration of 50 µg/ml and frozen in aliquots at -80°C. Enteroids were treated with 0, 1, 10, 50, 100 ng/ml LIGHT and brightfield microscopic images were captured at 0, 24, and 48 hours, n=6, N=3.

2.4.1.4 CD40-L

CD40-L (R and D systems, 8230-CL-050) was reconstituted in sterile 0.1% bovine serum albumin (BSA) to a stock concentration of 50 µg/ml, aliquoted and stored at -80°C. Enteroids were treated with 0, 1, 10, 50, 100 ng/ml CD40-L and brightfield microscopic images captured at 0, 24, and 48 hours, n=6, N=3.

2.4.1.5 LTα1/β2

LTα1/β2 (R and D systems, 8884-LY/CF) was reconstituted in sterile 0.1% bovine serum albumin (BSA) to a stock concentration of 50 µg/ml, aliquoted and frozen at -80°C. Enteroids were treated with 0, 1, 10, 50, 100 ng/ml LTα1/β2 and brightfield microscopic images captured at 0, 24, and 48 hours, n=6, N=3.

2.4.1.6 BAFF

BAFF (R and D systems, 2106-BF) was reconstituted in sterile 0.1% bovine serum albumin (BSA) to a stock concentration of 50 µg/ml and frozen in aliquots at -80°C. Enteroids were treated with 0, 1, 10, 50, 100 ng/ml BAFF and brightfield microscopic images captured at 0, 24, and 48 hours, n=6, N=3.

2.5 IL-6

IL-6 (Invitrogen, PA5-47209) is not an alternative NFκB signalling pathway activator but was selected for investigation in this study as it was produced in high quantities following LPS stimulation of bone-marrow-derived-dendritic cells in co-culture with enteroids that resulted in increased enteroid circularity which was blunted in enteroids derived from *Nfkb2*^{-/-} mice (Jones et al., 2019). IL-6 was reconstituted in sterile 0.1% bovine serum albumin (BSA) to a stock concentration of 50 µg/ml. Enteroids were treated with 0, 1, 10, 50, 100 ng/ml IL-6 and brightfield microscopic images captured at 0, 24, and 48 hours, n=6, N=3.

2.6 Organoid preparation for proteomic analysis

Four mice from each strain (WT, *Nfkb1*^{-/-}, *Nfkb2*^{-/-}, and *c-Rel*^{-/-}) were used to generate enteroids for the proteomic study. Enteroids derived from each mouse were treated for 24 hours with or without 50 ng/ml TNF (32 samples in total). Minigut culture media containing TNF was aspirated off and enteroids were washed with 500 µl of cold 1X phosphate buffer saline (PBS) (Gibco, 14190136). Then, 400 µl of gentle cell dissociation reagent was added to enteroids on ice for 45 minutes to dissolve the Matrigel (Corning, 356237) to recover the organoids. It was important to remove all residual Matrigel from the samples as Matrigel is mouse protein-rich and could have interfered with downstream processes/analyses. The dissolved Matrigel-containing enteroid solution was centrifuged at 300 g for 5 minutes at 4°C and the supernatant was discarded. About 125 µl of 0.1M Triethylammonium bicarbonate (TEAB) (Sigma-Aldrich, T7408-100ML) in 0.1 % sodium dodecyl sulphate (SDS) (Sigma-Aldrich, L3771-1KG) was added to the organoid pellet and pipetted up and down to facilitate mechanical disruption, chemical lysis, and protein solubilization. The mixture was then placed on ice on a shaker for 30 minutes. The lysed cells were centrifuged at

13,226 g for 20 minutes at 4°C and the supernatant was carefully transferred into a new 1.5 ml Eppendorf tube with murine organoid strain, number, date, and treatment or control. The Pierce bicinchoninic acid (BCA) (Thermo Fisher Scientific, 23227) protein assay reagents were used on the extracted supernatant of the organoid sample for protein quantification and the values were determined using a Tecan Sunrise absorbance microplate reader. A range of 130 - 390 µg of protein in 100 - 110 µl buffer (about 400 µg) were obtained and kept in properly labelled self-lock Eppendorf tubes at -80°C. Samples were posted in dry ice to the Proteomics Research Technology Platform at University of the Warwick for proteomic analysis for proteins identification, quantification, and comparative analyses of the effects of the TNF treatment.

Warwick Proteomic Centre used tandem mass tag (TMT) of the isobaric mass tags family, chemical labels for mass spectrometry (MS) to identify and quantify our extracted enteroid peptides solubilised by Triethylammonium bicarbonate (TEAB) digested by trypsin. Mass reporter region, mass normalization region, a cleavable linker region, and protein reactive group are the four regions of the TMT (Plubell et al., 2017). At Warwick Proteomic Centre, our peptides were diluted in 100 mM TEAB by using BCA to redetermine protein quantification following a published protocol (Plubell et al., 2017). Each sample was labelled with a different tag and then samples were pooled. The 10-plex TMT was used indicating that 10 samples could be run at the same time after being pooled together. The TMT machine detected which sample each signal came from by looking at the peptide sequence and the label. Normalisation of the pooled sample was achieved by adding 6.25 µg of peptide from each individual sample. A pooled sample was generated to run alongside 25 µg of each individual sample on the 10-plex assay. We conducted 4 x 10-plex assays with additional pools – so 32 individual samples plus 2 pools per each 10-plex ($2 \times 4 = 8$; so in total 40 samples from 32 individual samples plus 8 pooled samples) with

overlapping pools so that each 10-plex assay could be compared against each other as one experiment. Then 0.8 mg TMT 10-plex labelling reagent were dissolved in 52 μl anhydrous acetonitrile (ACN) of which 12 μl was added to each sample of 25 μg of peptide in 25 μl volume of TEAB buffer and incubated for 1 hour at room temperature. 2 μl of 5% hydroxylamine was added to the 2 μl of each reaction mixture and incubation for 15 minutes. The combined mixture was dried before being dissolved in 5% formic acid. An Orbitrap Fusion protocol was used in analysing 2 μg of peptide by a single 2-hour LC-MS/MS method. The Orbitrap Fusion protocol utilised quantification accuracy and precision of number of peptide spectrum matches (PSMs) with short transient (faster time with ion influx). The run was conducted to normalise total reporter ion intensity of each multiplexed sample and ensured label-checking and efficiency. Based on total reporter ion intensities during normalisation run, 2 μl 5% hydroxylamine were added to the remaining samples and then combined in a 1:1:1:1:1:1:1:1:1 ratio and then dried down in preparation for 2D-LC-MS/MS analysis (Plubell et al., 2017).

2.7 Organoid histology

2.7.1 Organoid preparation for histology

Culture media was aspirated from organoid cultures and each well was washed with 1X PBS. 400 μl gentle cell dissociation reagent (Stem Cell Technologies, 07190) was added to each well of a 24-well plate and the mixture was transferred to a 1.5 ml Eppendorf tube and incubated on ice for about 30 to 45 min to dissolve the Matrigel. Once Matrigel had solubilized in the gentle cell dissociation reagent, 400 μl of 4% paraformaldehyde (PFA) (Sigma Aldrich, P6148) (4% paraformaldehyde was made from 2ml of 16% stock (1:4) plus 6ml PBS or 1: 10 of 40% (37% w/v) PFA) was added to each mixture to make a final concentration of 2% paraformaldehyde and left for

30-60 min at room temperature to fix. Contents from the Eppendorf tubes were transferred to one 15 ml Falcon tube and centrifuged at 300 g for 3 minutes at room temperature. Supernatant was discarded and the pellet was re-suspended in a slightly warm 200 µl Histogel (Thermo-Fisher, HG-4000-012) and placed on top of folded 3M Micropore tape on an inverted metal lid on top of ice to rapidly polymerize the Histogel into a 'button'. The button was transferred into an embedding cassette, labelled with pencil and stored in 70% ethanol for processing.

2.7.2 Manual organoid processing

Manual processing of the 70% ethanol-stored organoids involved steps 1 to 11 (table 2.1). The cassettes-containing organoids were immersed in containers starting at step 1 in 70% ethanol and progressing to step 11 where they were immersed in wax. Forceps were used to move the cassettes-containing organoids from one container to another at the completion of each immersion time. At the completion of step 11, the fully processed cassettes-containing organoids were ready for paraffin embedding.

Step	Reagent	Temperature	Immersion time
1	70% Ethanol	Room	120 min
2	90% Ethanol	Room	120 min
3	100% Ethanol	Room	30 min
4	100% Ethanol	Room	30 min
5	100% Ethanol	Room	90 min
6	Xylene	Room	15 min
7	Xylene	Room	15 min
8	Xylene	Room	20 min
9	Xylene	Room	overnight
10	Wax	60°C	120 min
11	Wax	60°C	180 min

Table 2.1 Manual organoid processing steps, temperatures and times are shown from step 1 to step 11.

2.7.3 Organoid embedding

Processed organoids were embedded using a Histocentre 3 embedding machine. The machine was switched on for several hours to melt the wax ready for embedding.

Histogel-embedded organoids were transferred to a mould and embedded with 56°C liquid paraffin wax. Then the mould-containing-embedded organoids was transferred to the cooling plate of the Histocentre machine for about 30 minutes.

2.7.4 APES slide coating for immunohistochemistry

3-Aminopropyltriethoxysilane (APES) (Thermo Fisher Scientific, 80370) coating ensured suitably adhesive and charged slides for immunohistochemistry. Superfrost glass slides were successively dipped in glass jars respectively containing 100% acetone I, 100% acetone II, 2% APES in acetone, and 3x distilled water for 2 minutes each. Then APES-coated slides were placed in an incubator at 37°C overnight to dry before use.

2.7.5 Microtomy

Paraffin embedded organoids were mounted on the microtome for histological sectioning. The 4 µm thick sections were made and transferred to a water bath at 45°C before being mounted on APES-coated slides. The slides were incubated at 37°C overnight to allow sections to strongly adhere.

2.7.6 Immunohistochemistry

Standard dewaxing was conducted to rehydrate tissue and involved putting slides in xylene (Sigma-Aldrich, 1330-20-7) followed by a second container of xylene for 5 minutes each to remove paraffin wax. Slides were transferred to 100% ethanol 1 for 1 minute and then into 1% H₂O₂ in methanol to block endogenous peroxidase activity for 5 minutes. Thereafter, slides were placed in a second 100% ethanol bath for 1 minute, 90% ethanol for 1 minute, 70% ethanol baths for 1 minute, and distilled water for 1 minute. Slides were then placed in antigen retrieval of citrate buffer at pH6 in a microwave at 800W for 20 minutes. Slides were then cooled for 20 minutes before being washed in Tris Buffered Saline (Fisher Scientific, 77-86-1) with Tween 20

(TBST) (Thermo Fisher Scientific, 28321) on a shaker for 5 minutes. A Pap pen was used to mark around the sections to prevent loss of reagents and a block using primary antibody diluent was used for 20 minutes. Primary antibody (table 2.2) was diluted to the concentration indicated in table 2.2 and was added to the slides and placed in a dark moist chamber for 2 hours at room temperature. After washing slides with TBST on a shaker for 2 x 5 minutes each, Dako Envision polymer (secondary antibody with amplification signal) (Dako, K4003) was added and incubated for 30 minutes at room temperature. Secondary antibody was washed off with 2 x 5 minutes TBST and then a diaminobenzidine (DAB) chromogen (Sigma-Aldrich, D7304) was applied for 6 minutes at room temperature. Slides were washed in for 2 x 5 minutes in tap water. Nuclei counterstaining was conducted by putting slides in haematoxylin stain (Sigma-Aldrich, H3136) for 2 minutes. Sections were washed and blued in running tap water and then placed through standard dehydration, were mounted with DPX (Sigma-Aldrich, 06522) containing mounting media, and allowed to air dry under a fume hood.

Antibody/Reagent & Clonal class	Working concentration	Dilution	Antigen retrieval	Procedure
Alkaline phosphatase (Vector Laboratories, SK-5100)	80 µl per reagent	2 drops of each A, B, C	Citric acid or EDTA buffer	IHC
Claudin-2 (Invitrogen, 32-5600); monoclonal	3 µg/ml	1:300	Citric acid buffer	IHC
Claudin-7 (Invitrogen, 34-9100); polyclonal	2.5 µg/ml	1:300	Citric acid buffer	IHC
Claudin-15 (Invitrogen, 38-9200); polyclonal	2.5 µg/ml	1:300	Citric acid buffer	IHC
Ki-67 (Abcam, ab15580); polyclonal	1 µg/ml	1:1000	Citric acid buffer	IHC
Occludin (Abcam, ab167161); monoclonal	2 µg/ml	1:1000	Citric acid buffer	IHC
TNFAIP3 (Abcam, ab217706); polyclonal	1 µg/ml	1:100	EDTA buffer	IHC
TNFR1 (Abcam, ab19139); polyclonal	1 µg/ml	1:1000	EDTA buffer	IHC
TNFR2 (Abcam, ab109322); monoclonal	1 µg/ml	1:100	EDTA buffer	IHC
ZO-1 (Invitrogen, 61-7300); polyclonal	2.5 µg/ml	1:300	Citric acid buffer	IHC

Table 2.2 Different antibody concentrations utilized in probing for the proteins in the treated enteroids. Antigen retrieval used were citric acid and ethylenediaminetetraacetic acid (EDTA) buffers. IHC: Immunohistochemistry.

2.7.7 Alkaline phosphatase co-staining

Slides were subjected to standard dewaxing and, hydration processes as outlined above in section 2.7.6. A pap pen was used to mark the sections. Two drops of each alkaline phosphatase A, B, and C reagents (Vector Laboratories, SK-5100) was added to 5 ml of 100-200 mM Tris-HCl at pH 8.2-8.5 and incubated at room temperature for 20-30 minutes according to the Vector Laboratories manufacturer's instruction. Slides were then washed in 100-200 mM Tris-HCl buffer on a shaker for 5 minutes before being rinsed in water. Slides were bathed in 1% H₂O₂ in distilled water for 5 minutes which was followed by rinsing in distilled water for 1 minute. Antigen retrieval and subsequent IHC was conducted as detailed under immunohistochemistry (section 2.7.6) above.

2.8 Therapeutic experimentation

2.8.1 Curcumin

Curcumin (Aldi, L9108B) was reconstituted in sterile 100% DMSO to a stock concentration of 10 mM. Enteroids were treated with 0, 0.1, 1, 10 μ M curcumin. Pre-treatment with curcumin was for 1 hour. Then 50ng/ml TNF was added to the solution of the pre-treated enteroids. Brightfield microscopic images were captured at 0, 24, 48, and 72 hours, n=6, N=3.

2.8.2 Prednisolone

Prednisolone (Sigma-Aldrich, P6004-1G) was reconstituted in sterile 100% DMSO to a stock concentration of 10 mM. The same steps as in curcumin were followed.

2.8.3. Hydrocortisone

Hydrocortisone (Sigma-Aldrich, H0888-5G) was reconstituted in sterile 100% DMSO to freezing stock concentration of 10 mM. The same steps as in the above curcumin were followed.

2.8.4 Flunixin meglumine

Flunixin meglumine (Sigma-Aldrich, F0429-100MG) was reconstituted in sterile 100% DMSO to a stock concentration of 10 mM. Then same procedural steps as in the above curcumin were followed.

2.9 Reagents and solutions

Agents	Catalogue number	Vendor name	Location
3,3-Diaminobenzidine (DAB)	D7304	Sigma-Aldrich	MO, USA
3-Aminopropyltriethoxysilane (APES)	80370	Thermo Fisher Scientific	IL, USA
Alkaline Phosphatase (red AP) Substrate kit	SK-5100	Vector Laboratories Ltd,	UK

B27 supplement	0080085SA	Thermo Fisher, Life Technologies Ltd	UK
BAFF or TNFSF13B (recombinant mouse) (NSO-derived)	2106-BF	R&D systems	MN, USA
Basal minigut media (Dulbecco's Modified Eagle's Medium/Nutrient mixture F-12 ham	D8437	Sigma-Aldrich	MO, USA.
CD40 Ligand/TNFSF5 (HA-tag) (recombinant Mouse) Protein, CF	8230-CL-050	R&D systems	MN, USA
Claudin-2, mouse monoclonal antibody	32-5600	Invitrogen	IL, USA.
Claudin-7 rabbit polyclonal antibody	34-9100	Invitrogen	IL, USA.
Claudin-15 antibody	38-9200	Invitrogen	IL, USA
Complete culture medium (Basal minigut media, R-spondin, noggin, mEGF, HEPES, glutamine, B-27, and N-2, and primocin).	-	-	-
Curcumin (turmeric)	L9108B	Aldi	UK
Cystic fibrosis transmembrane regulator (CFTR) inhibitor-172	219670-5MG	Merck	UK
DPX	06522	Sigma-Aldrich	MO, USA
EGF (Recombinant mouse) protein CF	2028_EG-200	R&D Systems	MN, USA
Ethylenediaminetetraacetic acid (EDTA)	1 E5134-250G	Sigma-Aldrich	MO, USA
Flunixin meglumine	F0429-100MG	Sigma-Aldrich	MO, USA
Forskolin	F3917	Sigma-Aldrich	MO, USA
Gentle cell dissociation reagent	07190	Stem Cell Technologies	UK
Haematoxylin	H3136	Sigma-Aldrich	MO, USA
HEPES	54457	Sigma-Aldrich	MO, USA
Histogel	HG-4000-012	Thermo-Fisher	UK
Hydrocortisone	H0888-5G	Sigma-Aldrich	MO, USA
IL-6 Receptor polyclonal antibody	PA5-47209	Invitrogen	IL, USA
Intesticult mouse basal medium, catalogue number	06000	Stem Cell Technologies	UK
Intesticult mouse supplement 1	06002	Stem Cell Technologies	UK
Intesticult mouse supplement 2	06003	Stem Cell Technologies	UK
JAM-A (mouse antibody)	AF1077	R&D systems	MN, USA
Ki67, rabbit, polyclonal antibody	ab15580	Abcam	UK
LIGHT (recombinant mouse)	1794-LT	R&D systems	MN, USA

Lymphotoxin $\alpha 1/\beta 2$ (recombinant human) HEK293- derived	8884-LY/CF	R&D systems	MN, USA
Matrigel matrix basement membrane phenol red-free	356237	Corning,	NY, USA
N2 supplement	A1370701	Thermo Fisher, Life Technologies Ltd	UK
Noggin (Recombinant mouse)	Bulk 1967-NG	R&D Systems	MN, USA
Occludin, rabbit monoclonal antibody	ab167161	Abcam	UK
Paraformaldehyde	P6148	Sigma-Aldrich	MO, USA
Phosphate Buffered Saline (PBS) (1X), without Ca^{2+} and Mg^{2+}	Gibco	Gibco Life technologies Ltd	UK
Pierce bicinchoninic acid (BCA) protein assay with a BSA standard	23227	Thermo Fisher Scientific	IL, USA
Prednisolone	P6004-1G	Sigma-Aldrich	MO, USA
Primocin	NC9392943	Invivogen, Fisher Scientific	USA
R-spondin 1 (Recombinant mouse)	3474-RS-250	R&D Systems	MN, USA
Secondary antibody (Dako Envision polymer, secondary antibody with amplification signal)	K4003	Dako	CA, USA
Sorbitol	S-1876	Sigma-Aldrich	MO, USA
Sucrose	S9378-1KG	Sigma-Aldrich	MO, USA
Sodium dodecyl sulphate (SDS)	L3771-1KG	Sigma-Aldrich	MO, USA
Sodium citrate dihydrate (sodium citrate tribasic dihydrate)	S4641-1KG	Sigma-Aldrich	MO, USA
TNF α (murine)	315-01A- 20UG	PeptoTech	EC, UK
TNFAIP3 receptor, rabbit polyclonal antibody	ab217706	Abcam	UK
TNF receptor 1, Rabbit polyclonal antibody	ab19139	Abcam	UK
TNF receptor 2, Rabbit monoclonal antibody	ab109322	Abcam	UK
Triethylammonium bicarbonate	T7408-100ML	Sigma-Aldrich	MO, USA
Tris base	77-86-1	Fisher Scientific	NJ, USA
TWEAK (Recombinant mouse)	1237-TW	R&D systems	MN, USA
Tween 20	28321	Thermo Fisher Scientific	IL, USA
Xylene	1330-20-7	Sigma-Aldrich	MO, USA
ZO-1 antibody	61-7300	Invitrogen	IL, USA

Table 2.3 Reagents, antibodies and other materials utilised for the methods of the experiments performed in this thesis.

2.10 Data and Statistics

Data were analysed with analysis of variance (ANOVA) where normality ensued and Kruskal Wallis was conducted when data were not normally distributed. Multiple comparisons were performed using Dunnett's test. Statistical software used was GraphPad prism version 6. Student t-test and fold change analyses were used for proteomics. Descriptive data were presented as mean \pm standard deviation. p-values of less than 0.05 were considered statistically significant. Where applicable 95% confidence intervals were shown.

3. Characterising the actions of tumour necrosis factor (TNF) on enteroids

3.1 Introduction

Tumour necrosis factor (TNF) is a pro-inflammatory cytokine that is mainly produced by macrophages, but can also be manufactured by neutrophils, CD4+ lymphocytes, neurons, mast cells, natural killer cells and eosinophils (Wang & Lin, 2008). TNF is a cell signalling protein that is known to be involved in activation of the acute phase reaction, immune cell regulation, endogenous pyrogen generation, cell survival, proliferation, apoptosis and migration (Beutler et al., 1985; Calpado et al., 2014; Swardfager et al., 2010). TNF is a key pro-inflammatory cytokine known to be dysregulated in a wide variety of diseases including inflammatory bowel disease (IBD) and sepsis where this cytokine is massively over produced (Brynskov et al., 2002; Dowlati et al., 2010; Ferrajoli et al., 2002; Locksley, Killeen & Lenardo, 2001; Plevy et al., 1997; Victor & Gottlieb, 2002). Anti-TNF therapy with drugs such as infliximab is effective in IBD (Monaco et al., 2015; Targan et al., 1997). In sepsis, anti-TNF treatment including polyclonal anti-TNF (AZD9773), Lenercept, chimeric antibody anti-TNF and afelimomab have also been used (Aikawa et al., 2013; Butty et al., 2013; Clark et al., 1998; Gallagher et al., 2001). Some anti-TNF therapies have ameliorated sepsis and reduced 28-day mortality in patients while in other trials anti-TNF therapeutics showed no reduction in 28-day mortality in patients due to low drug potency and efficacy (Aikawa et al., 2013; Clark et al., 1998; Lv et al., 2014).

Elevated TNF concentrations in the intestine cause apoptosis and cell shedding and tight junction redistribution *in vivo* (Williams et al., 2013). TNF-induced intestinal cell shedding disturbs epithelial cell equilibrium, particularly at the villus tip and makes it difficult for the normal, tight junctional protein redistribution and zipper-like

mechanistic process between neighbouring cells to replace the shed cells effectively and promptly without breaching intestinal barrier function (Kiesslich et al., 2007; Leppkes et al., 2014). TNF-induced epithelial cell shedding can therefore promote micro-erosions or epithelial gaps that cannot be easily replaced by rearrangement of adjacent intestinal cell tight junctional proteins (Kiesslich et al., 2007; Watson & Hughes, 2012). Disruptive activities of TNF also include transepithelial impedance loss via upregulation of MLCK, downstream NF- κ B signalling pathway activation, and activation of AP-1 transcription factors (Wang et al., 2005). TNFR1 and TNFR2 are the receptors for TNF. TNFR1 which is usually stimulated by the two forms of TNF trimers is ubiquitously expressed in most cells, while TNFR2 which is activated by the membrane-bound form of the TNF homotrimer typically expressed in immune cells and intestinal epithelial cells (Leppkes et al., 2014; Theiss et al., 2005). TNFR1 is the primary effector of TNF via recruitment of TNF receptor type 1-associated DEATH domain (TRADD), TNF receptor associated factor (TRAP) and receptor interacting protein (RIP) domains and activation of NF- κ B and MAPK signalling pathways which result in apoptosis and cell shedding (Berghe et al., 2014; Hayden, West & Ghosh, 2006) (figure 1.6). However, TNFR2 via NIK stimulates phosphorylation of p100 to result in nuclear translocation of NF- κ B to induce inflammation has also been implicated in promoting cell proliferation and survival (Faustman & Davis, 2010). TNFR1, but not TNFR2 activation was shown to be important in regulating apoptosis and intestinal cell shedding in intestinal epithelia following LPS injection into mice (Williams et al., 2013).

In healthy individuals, intestinal epithelial homeostasis ensures a balance between programmed cell death and cell proliferation (Williams et al., 2013; Wullaert et al., 2011). However, in diseases such as IBD and sepsis, TNF-induced apoptosis and cell shedding may exceed the capacity of crypts to proliferate and cell-cell tight junctions are modulated; these phenomena may result in epithelia becoming more

leaky to intestinal contents and enhancing further bacterial invasion and inflammation (Salim & Soderholm, 2011; Uhlig, 2013; Williams et al., 2013). Bacterial infiltration can disrupt immune homeostasis, cause local immune responses and potentially lead to systemic immune responses in severe cases (Artis, 2008).

TNF plays significant roles in cellular and molecular mechanisms of IEC homeostasis. The protective and disruptive pathways of TNF on IECs are dose-, time point-, and context-signalling-dependent (that is, receptors and secondary signals) (Corredor et al., 2003; Guma et al., 2011; Leppkes et al., 2014). Protective activities of TNF include regulatory reconstitution of intestinal mucus by stimulating expressions of polymeric immunoglobulin receptor (pIgR) and mucin-2 (Muc2) to promote structural barrier integrity as the first line of defence of IECs (Johansson et al., 2008; Leppkes et al., 2014). Another important benefit of the protective mechanism of TNF is intestinal epithelial wound healing. Intestinal epithelial injury that is one of the pathognomonic features of IBD and sepsis results in influx of luminal content including invasive microbes into the tissue. TNF regulation of intestinal epithelial repair involves restitution and regeneration mechanisms via activation of the ErbB family of EGF receptors, lipid mediators (COX-2-derived prostaglandin E₂), PI3K/Akt and STAT3-dependent pathways (Frey et al., 2009; Hilliard et al., 2011; Leppkes et al., 2014; Pickert et al., 2009). Restitution mechanisms consist of cellular spreading, cell invasion, cell migration, transient cell dedifferentiation, and cytoskeletal reorganization whilst the regeneration mechanism involves cellular redifferentiation, proliferation, and survival (Neufert et al., 2013; Taupin & Podolsky, 2003). TNF activates a TNFR2 dependent pathway via focal adhesion kinase (FAK) to promote cell migration and survival (Corredor et al., 2003; Mizoguchi et al., 2002). TNF also stimulates TNFR2 signalling via regulation of the Wnt pathway to mediate intestinal epithelial cell proliferation (Mizoguchi et al., 2002). TNF via regulation of synthesis of cytokines and chemokines (e.g. CXCL-1, CXCL-5, and IL-8) actively

controls chemoattraction, cytokine and chemokine crosstalk and immune effector mechanisms (Lee et al., 2008). However, disruptive activities of TNF include modulation of tight-junction epithelial barrier loss, transepithelial impedance loss via upregulation of MLCK, downstream NF κ B signalling pathway activation and AP-1 transcription factors (Wang et al., 2005). Therefore, TNF concentrations need to be properly regulated to ensure the beneficial actions of TNF outweigh the negative consequences of having elevated TNF concentrations in the gut.

The physiological and pathophysiological concentrations of TNF in different body compartments are variable. However, in disease stool concentrations have been shown to be much higher, reaching around 63.6 ng/g, particularly following infection such as by *Shigella flexneri* whilst serum concentrations of active CD and active UC were respectively 14.0 ng/l and 9.46 ng/l (Komatsu et al., 2001; Nicholls et al., 1993). In sepsis, the serum concentration of TNF is also high at about 440 units/ml (corresponding to 0.1 ng/ml recombinant TNF) (Waage et al., 1987). The concentration of TNF has pathophysiological relevance to the disease course and the severity of IBD and sepsis, with increasing concentrations correlating with more severe disease.

Recent scientific advances in organoid culture have enabled enteroid studies that allow the direct study of the intestinal epithelium without the complexities of other cellular compartments found *in vivo* (Dekkers et al., 2013; Sato et al., 2009; 2011). Our lab has recently established enteroid cultures from mice and observed dose-dependent and time-dependent effects of TNF on enteroid morphology and apoptosis that aligned well with observations from intestinal tissues from TNF treated mice *in vivo* (Jones et al., 2019). Enteroids were shown to become more spherical containing an increased abundance of shed cells with increased doses of TNF and time post-treatment, suggesting that enteroids are a good model for investigating the actions of TNF on intestinal epithelia (Jones et al., 2019). The time course of these studies

was arbitrary, and the dynamic processes involved in enteroid rounding were not investigated (Jones et al., 2019). Understanding the balance between beneficial and disease-causing concentrations of TNF in IBD and sepsis and the direct actions of TNF on intestinal epithelia will guide future therapeutic approaches in IBD and sepsis. We have therefore further characterised the effects of TNF on enteroids and have investigated the consequences of elevated TNF concentrations at higher resolution using time-lapse microscopy.

In the early parts of the twenty first century, live cell imaging system with an in-built time lapse microscopy device to monitor the dynamics of cells started to come into the limelight (Baker, 2010). The CytoSMART Lux is a live cell imaging system built with a phase contrast microscope innovative development and works within a tissue culturing incubator. It is user friendly and can monitor and capture cell culture, growth, treatment, and migration using time-lapse microscopy. Morphological changes that take place in enteroids after being treated with TNF could therefore be monitored at short time intervals over several days. Remotely, images and videos of cell culture can be viewed and warning messages in the case of something going wrong with the system can also be received. We therefore used CytoSMART Lux to monitor the behavioural patterns and morphological changes of enteroids after treatment with TNF.

3.2 Results

3.2.1 TNF induces rounding in WT enteroids

Jones and colleagues previously investigated the effects of TNF on WT enteroids using TNF doses of 0, 1, 10, 100, and 1000 ng/ml. TNF induced enteroid rounding reliably and reproducibly following 100 ng/ml by 24 hours post-treatment (Jones et al., 2019). However, maximal stool concentrations of TNF in humans infected by

Shigella flexneri were approximately 63.6 ng/g (Nicholls et al., 1993) and so we wanted to investigate whether doses of TNF applied to enteroids between 10 and 100 ng/ml caused altered enteroid morphology to align with previously recorded pathologically relevant doses in humans.

Different concentrations of TNF (0, 1, 10, 50, and 100 ng/ml) were used to treat enteroids and images were recorded at time intervals of 0, 24, and 48 hours post-treatment (figure 3.1). We observed that 50 and 100 ng/ml TNF induced statistically significantly increased the rounding of enteroids while 1 ng/ml, and 10 ng/ml did not (figure 3.2).

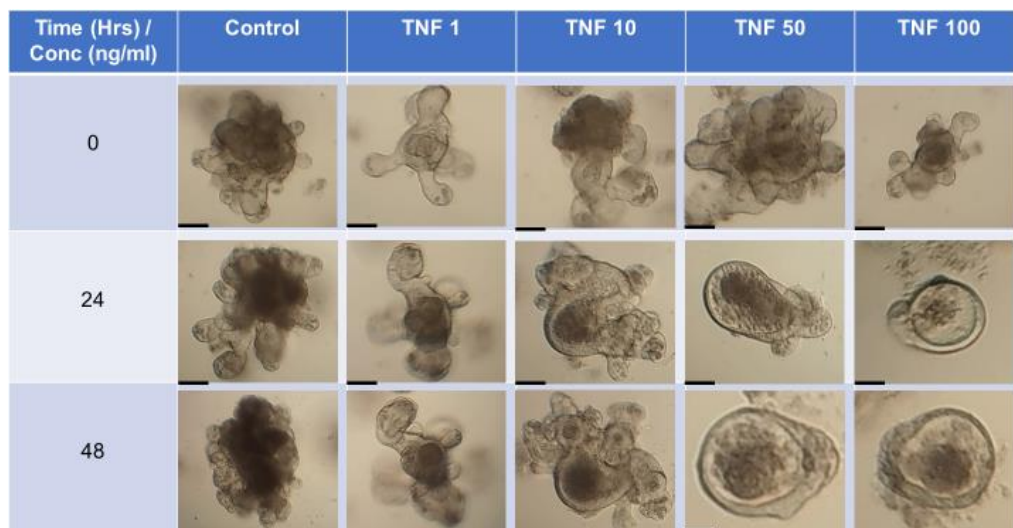


Figure 3.1 Bright field images of TNF-treated WT enteroids. A dose-dependent and time-dependent increase in TNF-treated WT enteroid circularity was observed. Images were taken with x10 original magnification and scale bars = 100 μ m.

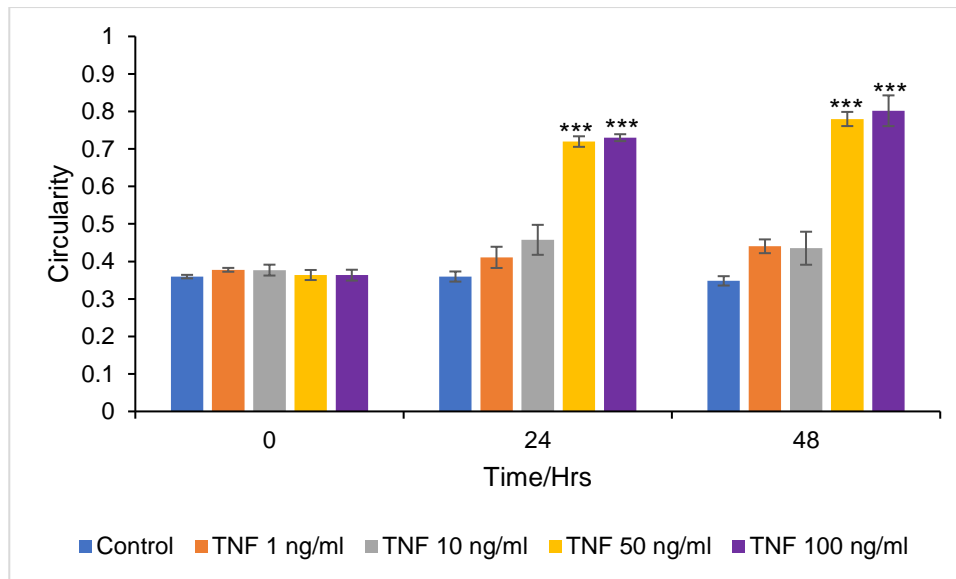


Figure 3.2 TNF caused a dose-dependent increase in WT-derived enteroid circularity. TNF was applied to enteroids at concentrations of 0 (purple), 1 (orange), 10 (grey), 50 (yellow) and 100 (purple) ng/ml and circularity was assessed at 0, 24 and 48 hrs; ($P = * \leq 0.05$, $*** \leq 0.001$ by one-way ANOVA), error bars represent SEM, $n=6$, $N=3$.

3.2.2 TNF-treated WT-derived enteroids show reduced epithelial thickness

As intestinal epithelial cells in enteroids have been shown to undergo TNF-induced apoptosis and cell shedding similarly to that observed in TNF treated small intestinal epithelia *in vivo* (Jones et al., 2019), we wanted to determine whether any other histological features present in the small intestine *in vivo* in response to TNF were also present in organoids *in vitro* in the absence of lamina propria. Enteroids were treated with 50 ng/ml TNF and collected for histology at time intervals of 0, 6, and 24 hours. Alkaline phosphatase stained enteroids counterstained with haematoxylin demonstrated there was a gradual loss of epithelial thickness from 0-24 hours following TNF addition (figure 3.3 and appendix B). Epithelial thickness was quantified and untreated enteroids had a relative thickness of 153.62 ± 27 units that significantly decreased to 105.69 ± 5.90 units after 6 hours and 66.46 ± 12.99 units by

24 hours thus demonstrating a reduction in epithelial thickness of around 56.74% over a 24-hour period in response to 50 ng/ml TNF (figure 3.4).

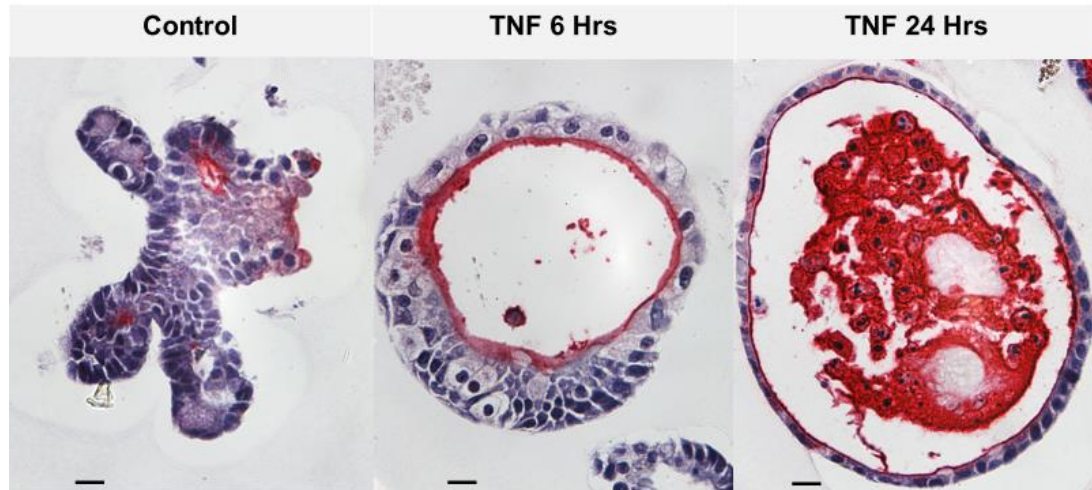


Figure 3.3 Alkaline phosphatase counterstained with haematoxylin micrographs of 50 ng/ml TNF-treated enteroids at 0, 6, and 24 hours. Epithelial thinning over time from 0 to 24 hours is indicated. Original magnification, x63 and scale bar = 100 μ m.

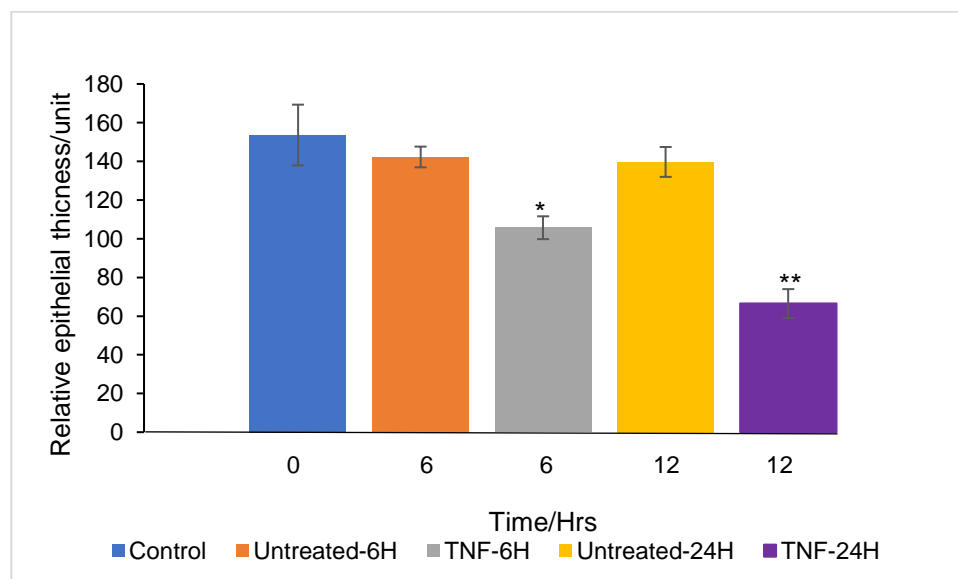


Figure 3.4 Relative epithelial thickness of untreated and 50 ng/ml TNF-treated WT enteroids were compared over a time course of 0 (blue), untreated 6 hours (brown), TNF-6 hours (grey), untreated 24 hours (orange) and TNF-24 hours (grey) hours, ($P = * \leq 0.05$, $** \leq 0.01$), error bars with SEM, $n=6$, $N=3$.

3.2.3 TNF treatment induces claudin-7 remodelling in WT enteroids

The claudin family are major proteins forming the tight junctional complexes of intestinal epithelial cells. Regulation of intestinal barrier function is managed by the integrity of junctional complexes. TNF has been shown previously to modulate the porosity of these junctional complexes (Marchiando et al., 2011) and redistribution of claudin family members may potentially contribute to IBD and sepsis pathogenesis. We therefore selected a panel of claudin family members and JAM-A known to be expressed in intestinal epithelia to determine whether they were remodelled in the enteroid system over the time-course of TNF treatment.

Claudins that were selected for analysis included claudins -2, -7, 15, and JAM-A. Several of these proteins did not show redistribution or selected antibodies were not convincingly reliable (appendix B). However, TNF treatment of WT enteroids resulted in prominent claudin-7 redistribution. Immunohistochemistry demonstrated claudin-7 expression along the epithelial junctions between neighbouring cells of untreated enteroids and this progressively decreased in intensity from untreated to 24 hours post-treatment with TNF. Claudin-7 staining gradually became more punctate and redistributed away from cell-cell junctions, suggesting that TNF treated enteroids may start to show differences in the regulation of the paracellular space between neighbouring epithelial cells (figures 3.5A and B).

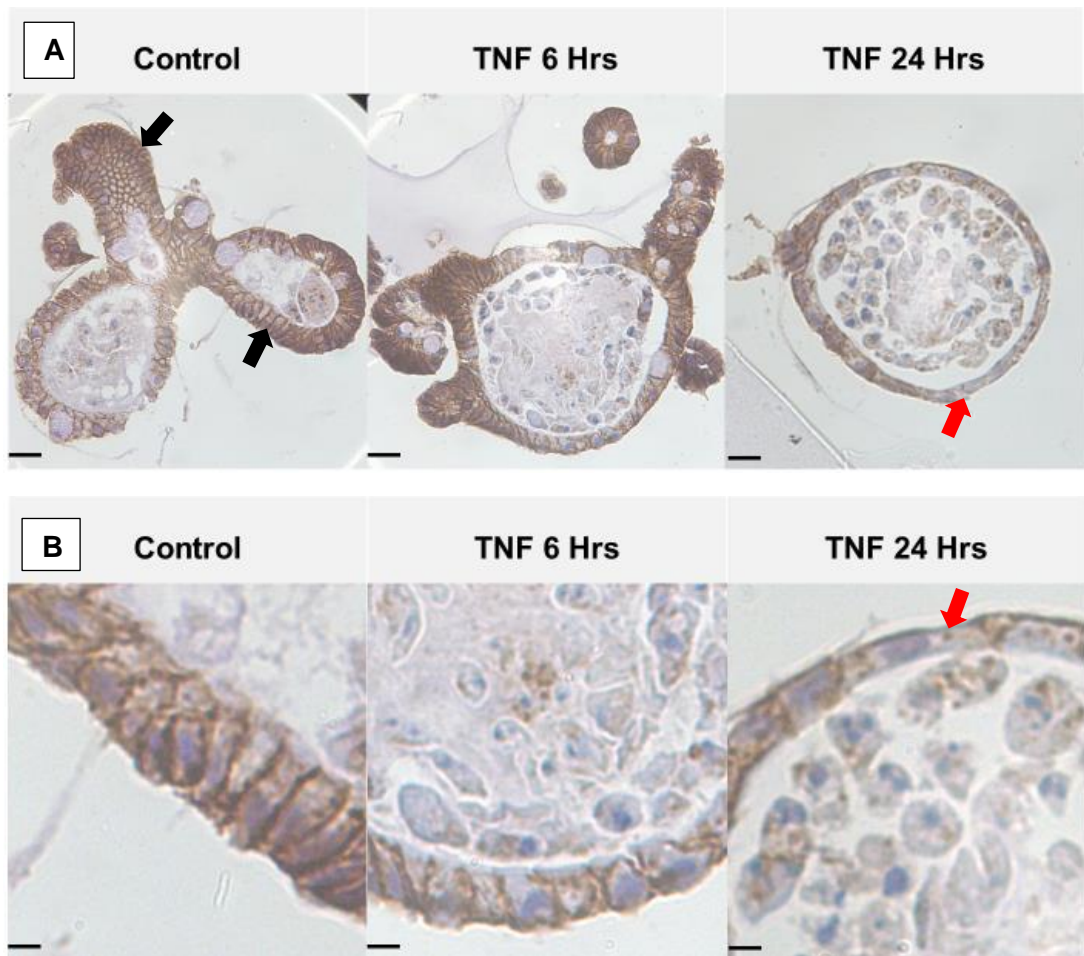


Figure 3.5 Immunohistochemical images of untreated and 6-hour and 24-hour post-treatment of 50 ng/ml TNF-induced enteroids stained for claudin-7. Untreated enteroids displayed intact tight junction structural architecture (black arrows) whilst TNF-treated enteroids depicted remodelled junctions and punctate characterisations (red arrows), N=3. Original image (A) and enlarged (B) section. Original magnification, x63 and scale bars, A (100 μ m) and B (20 μ m).

3.2.4 TNF-treated WT enteroids show asynchronous expansions and contractions

TNF-induced behavioural patterns and morphological changes have not been monitored under dynamic conditions in enteroids. Additionally, current studies have not investigated the process of TNF-induced enteroid rounding and how this may relate to *in vivo* activity. TNF concentrations of 0 ng/ml, 50 ng/ml, 100 ng/ml, and 200 ng/ml were used to treat WT murine proximal enteroids and were imaged every 15 minutes for 72 hours. Surface area was assessed for 9 individual organoids over the

time course. There were no overt expansions and contractions in the untreated enteroids (figure 3.6). However, TNF treatment caused expansions and contractions of enteroids that were asynchronous between different enteroids. Each enteroid had different times of onset and duration of expansions and contractions (figure 3.7). In general, the expansion phase was longer than the contraction phase in TNF-treated enteroids.

The earliest phenotypic behaviours of asynchronous expansions and contractions following 50, 100, and 200 ng/ml TNF started at 6 hours and 15 minutes, 6 hours and 30 minutes, and 6 hours and 15 minutes for each dose respectively suggesting that expansions and contraction initiation in enteroids is not TNF dose-dependent. The last expansions and contractions following 50, 100, and 200 ng/ml TNF were observed at 61, 69, and 67 hours for each dose respectively, suggesting that it is only necessary for TNF to reach a threshold concentration to initiate these effects (figures 3.7B-D). The mean duration of expansions and contractions of 50, 100, and 200 ng/ml TNF-treated WT enteroids were respectively 34 ± 0.49 hours, 47 ± 3.64 hours, and $44 \text{ hours} \pm 7.39$ hours. We observed that the majority of TNF-treated enteroids became auto-punctured before 50 hours, however this required timelapse visualisation to confirm so we could not determine whether enteroids that were not subjected to time lapse imaging got punctured. There was inconsistency of expansion and contraction among the TNF-treated enteroids which could be due to differences in the sizes and extent of responses of enteroids to TNF treatment.

Hours	0	22.8	23.0	29.3	29.5	34.5	34.8	42.0	42.3
TNF Treated	Start	Expand	Contract	Expand	Contract	Expand	Contract	Expand	Puncture
Control	Start	Growth	No Cont.	Growth	No Cont.	Growth	No Cont.	Growth	No Pun.

Figure 3.6 The 50 ng/ml TNF treatment induced periodic, asynchronous expansions and contractions of WT murine enteroids. Untreated WT mouse enteroids did not demonstrate this behavioural pattern. Under the dynamic monitoring by CytoSMART, live cell imaging, the asynchronous expansions and contractions of TNF-treated enteroids were captured. During the expansion phase, the enteroids continued to expand until at a certain point they abruptly contracted and resumed the expansion phase and the expanding surface area seemed to be larger than the previous phase and suddenly contracted again. These interrupting cycles of expansions and contractions continued until the enteroid finally ruptured or leaked. Even though alternating expansion and contraction phases were not observed in untreated enteroids, these continued to grow and increase in surface area. Brightfield images were taken with 10x original magnification.

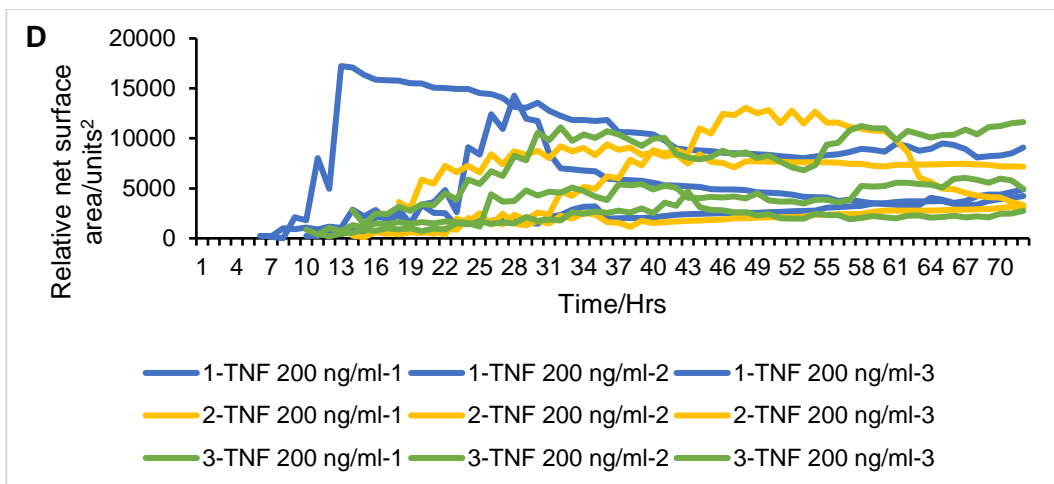
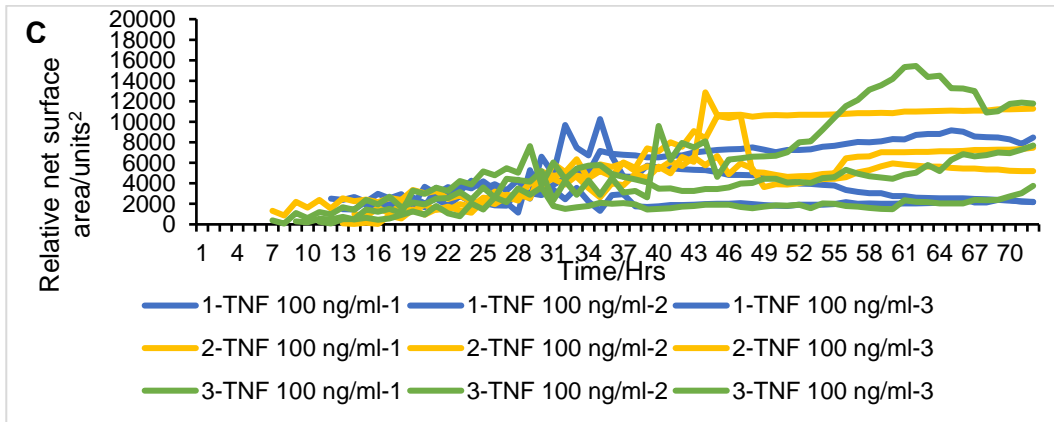
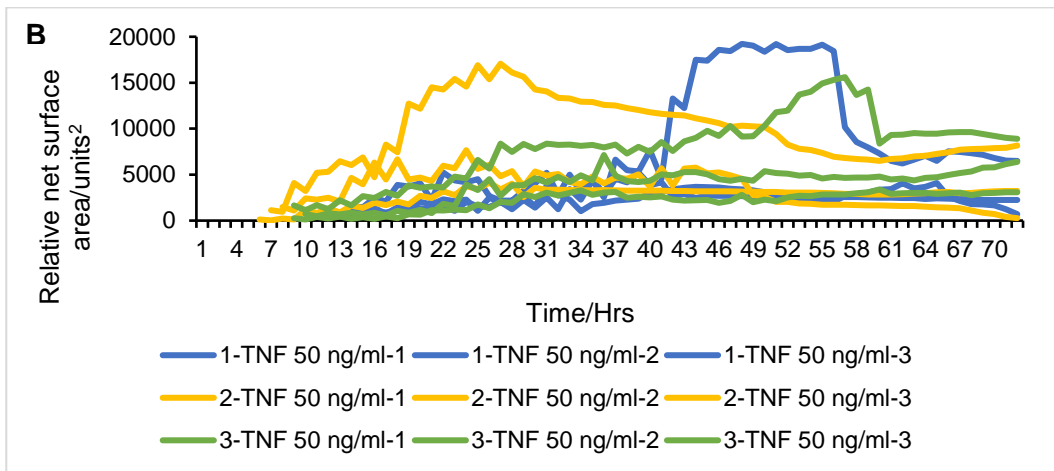
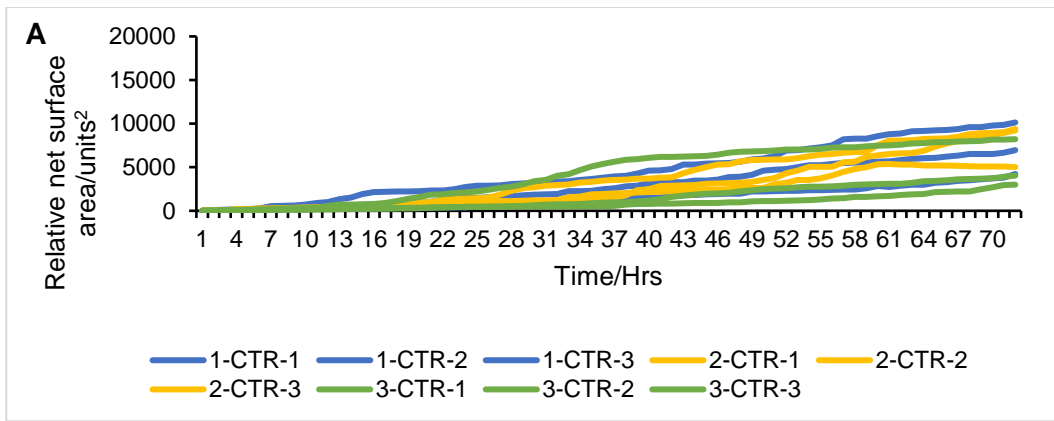


Figure 3.7 WT enteroids were treated with 0 (A), 50 (B), 100 (C), and 200 (D) ng/ml TNF and the CytoSMART imager collected images of nine individual enteroids per treatment every 15 minutes to monitor behavioural and morphological patterns over 72 hours. The TNF-treated enteroids demonstrated periodic, asynchronous expansions and contractions while untreated enteroids did not. Enteroids showed differential onsets of expansion and contraction. In the graphs, experiments 1 (blue), 2 (yellow) and green (3), n=3, N=3

3.2.5 TNF treatment is associated with increased motility of enteroids

Enteroids were observed to move within the Matrigel (a source of extracellular matrix ECM). We used the CytoSMART live cell imaging system to capture and monitor the migration of both untreated and treated WT-derived enteroids for 72 hours. WT-derived enteroids migrated in unpredictable patterns within the ECM (figure 3.8). TNF treatment induced increased migratory distance and erratic patterns of motility in WT-derived enteroids (figures 3.8B-D). The distance covered by untreated enteroids ranged from 200 to 300 μm with a mean distance of $260 \pm 18.56 \mu\text{m}$ (figure 3.8A). Enteroids treated with 50 ng/ml TNF covered distances ranging from 240 to 580 μm with a mean distance of $415.56 \pm 50.48 \mu\text{m}$. Similarly, enteroids treated with 100 ng/ml TNF covered distances ranging from 270 to 680 μm with a mean distance of $453.33 \pm 60.00 \mu\text{m}$ and enteroids treated with 200 ng/ml TNF covered distances ranging from 290 to 660 μm with a mean distance of $398.89 \pm 50.48 \mu\text{m}$. Within the first 12 hours post-treatment with TNF, the cumulative distance covered by TNF treated enteroids was not statistically significantly different compared with untreated enteroids. However, by 24 hours post-TNF treatment, enteroids treated with 200 ng/ml TNF were statistically significantly more motile than untreated enteroids ($P=0.0075$; 95% confidence interval (CI) = +12.36 to +43.20) and at 36 hours post-TNF treatment, only enteroids treated with 100 ng/ml TNF had statistically significantly increased motility ($P=0.0295$; 95%CI +18.74 to +212.4). By 48 hours, all concentrations of TNF-treated enteroids exhibited migrations that were statistically significantly increased compared to untreated enteroids (figure 3.9).

TNF-treated WT-derived enteroids also demonstrated increased velocity in comparison to untreated enteroids (figure 3.10). All the different concentrations of TNF caused increased enteroid velocity between 36- and 60-hours post-treatment. 100 ng/ml TNF resulted in the highest enteroid velocity ($10.00 \pm 5.30 \mu\text{m/hr}$) at 36 hours post-treatment. This was almost triple the velocity ($3.52 \pm 0.58 \mu\text{m/hr}$) of untreated enteroids at the same time.

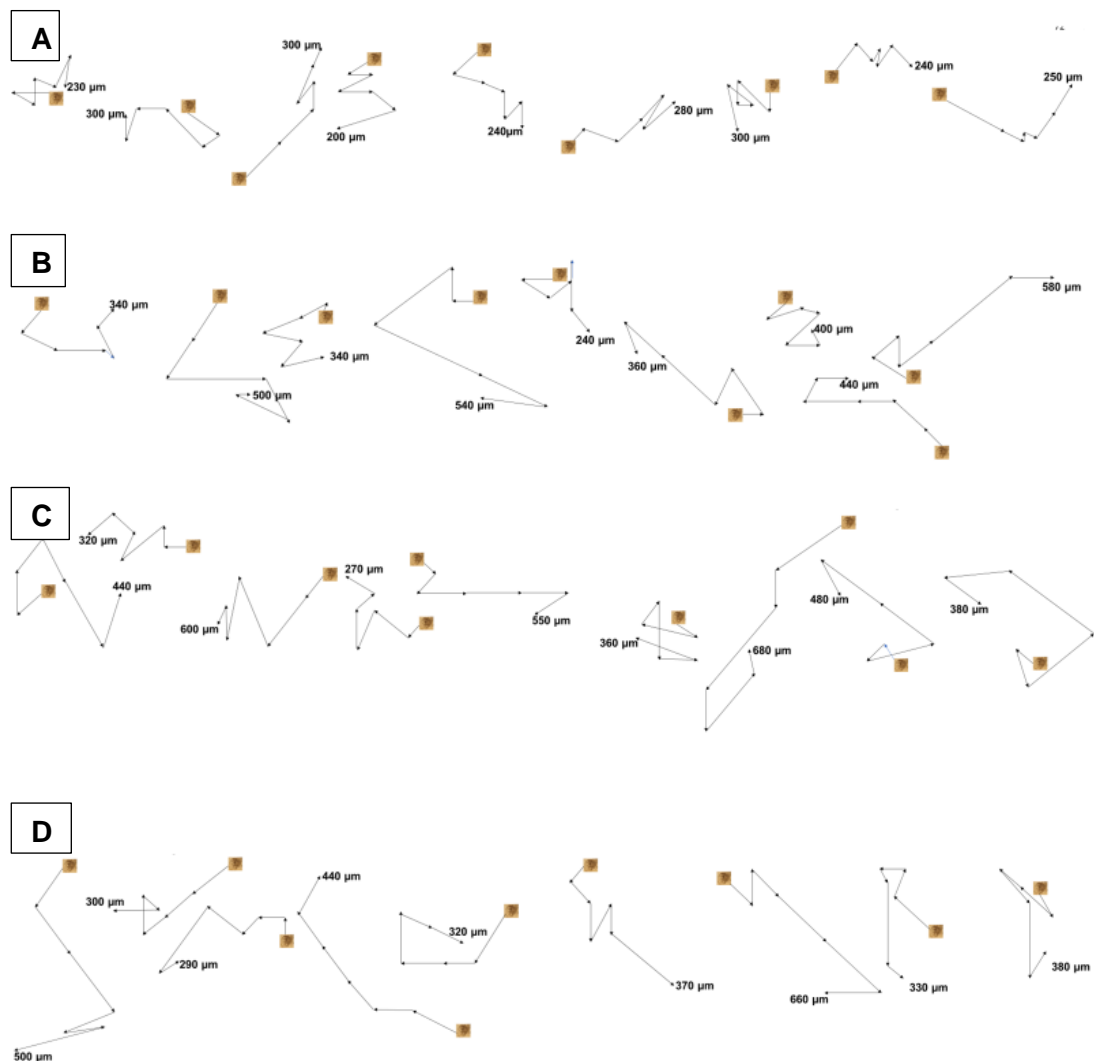


Figure 3.8 Each enteroid migrated independently and without a defined direction. The motility of enteroids was captured by CytoSMART live cell imaging and motility patterns are presented. Untreated WT enteroids migrated through the ECM in multi-directional patterns and covered distances of 200-300 μm (A). TNF-treated WT enteroids covered distances of 240-580 μm following 50 ng/ml (B), 270-680 μm following 100 ng/ml (C), and 270-660 μm following 200 ng/ml (D). Both untreated and TNF-treated WT enteroids covered different distances at different paces. Motility patterns are not to scale, $n=3$, $N=3$.

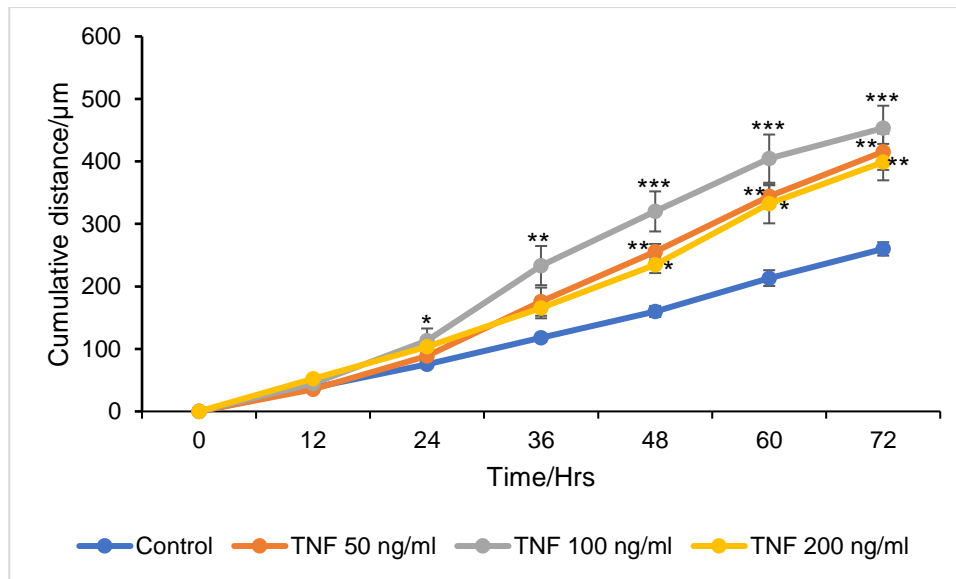


Figure 3.9 Cumulative distances covered by untreated WT control enteroids (blue) in 72 hours was $260 \pm 18.56 \mu\text{m}$ while that of 50 (orange), 100 (grey) and 200 (yellow) ng/ml, TNF were respectively $415.56 \pm 50.48 \mu\text{m}$, $453.33 \pm 60.00 \mu\text{m}$, and $398.89 \pm 50.48 \mu\text{m}$. * $P \leq 0.05$, ** ≤ 0.01 , *** ≤ 0.001 , $n=3$, $N=3$, error bars = SEM.

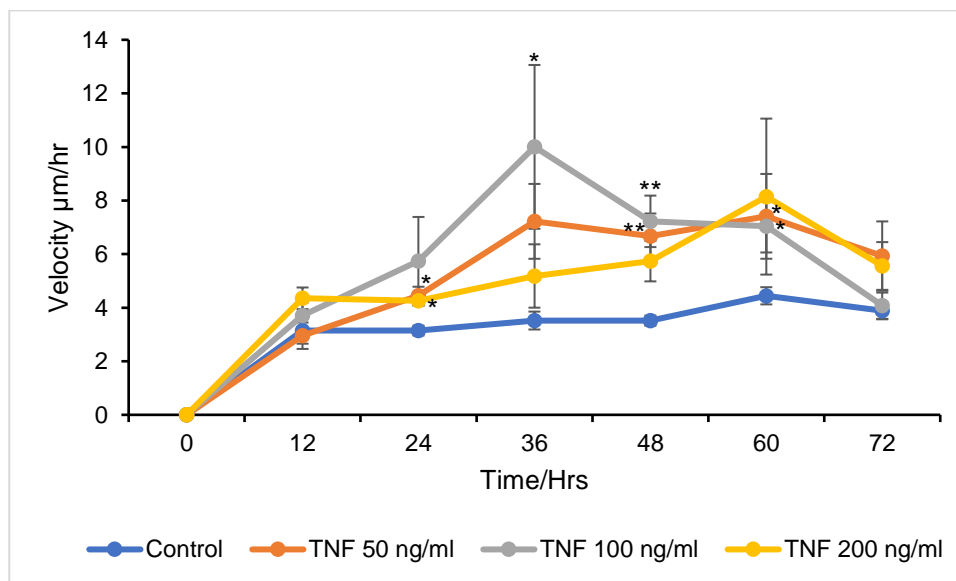


Figure 3.10 The velocity pattern of untreated WT enteroids (blue) was steady without any sudden increases. 50 (orange), 100 (grey), and 200 (yellow) ng/ml TNF-treated WT enteroids showed marked accelerations and decelerations at different times. * $P \leq 0.05$, ** ≤ 0.01 , $n=3$, $N=3$, error bars = SEM.

3.2.6 TNF-treated enteroids showed early increases in surface area

Normally, growing enteroids continue to increase in surface area as stem cell division is supported by their culture media. However, TNF-treated enteroids responded to stimulation and deviated from this normal growth pattern. The CytoSMART live cell

imaging system was used to capture the growth patterns of both resting and TNF-stimulated enteroids. At 24 hours post-treatment, TNF-treated enteroids were about three times larger in relative net surface area (TNF 50 ng/ml [3183.78±1123.61 units²], TNF 100 ng/ml [2748±722.62 units²], and TNF 200 ng/ml [2849.65±1051.10 units²]) than control enteroids (1085.44±76.05 units²) (figure 3.11). Untreated enteroids did not demonstrate interrupted growth patterns as seen in the TNF-treated enteroids. The growth patterns of TNF-treated enteroids were perturbed by an abrupt increase in relative net surface area followed by a sudden decrease in their relative net surface area. All TNF doses resulted in increased surface area from 24 - 36 hrs. This then plateaued or enteroids even showed decreased surface area to lower values than that of the control.

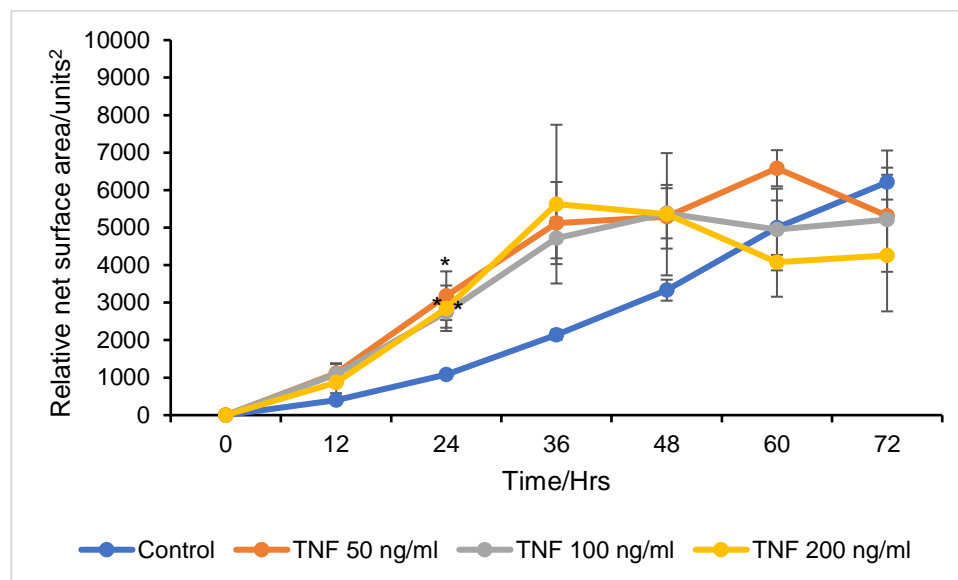


Figure 3.11 TNF induced early and sudden increases in the relative net surface area of enteroids while untreated enteroids (blue) progressively increased in the net surface area. Control (blue), TNF 50 ng/ml (orange), TNF 100 ng/ml (grey), and TNF 200 ng/ml (yellow), *P≤0.05, n=3, N=3, error bars = SEM.

3.2.7 Rescued TNF-treated enteroids demonstrated no rhythmic contractions and expansions

TNF caused extensive damage to enteroids over 72 hours of treatment. We have previously shown Paneth cell depletion within this system suggesting that the

enteroid stem cell niche may be negatively affected by TNF (Jones et al., 2019). Due to extensive apoptosis caused by TNF in this system, we wanted to address whether enteroid stem cells were capable of surviving and replicating upon TNF stimulation and subsequent removal. TNF was added to cultures for 72 hours and then the culture media was discarded, enteroids were washed to remove residual TNF, fresh, culture media was added to the 24-well plates, and cultures were monitored for an additional 72 hours via CytoSMART live cell imaging. There were no periodic, asynchronous expansion and contraction patterns observed in the rescued enteroids following previous TNF treatment. The growth dynamics were similar to control enteroids and no sudden increases in enteroid area or abrupt decreases in area as a result of contractions were observed. The growth rate of rescued enteroids was however faster than that observed in untreated enteroids (although there was enteroid-enteroid variation), suggesting that stem cells remained active post-TNF treatment and signals were present to recover the damaged epithelium (figures 3.12B-D).

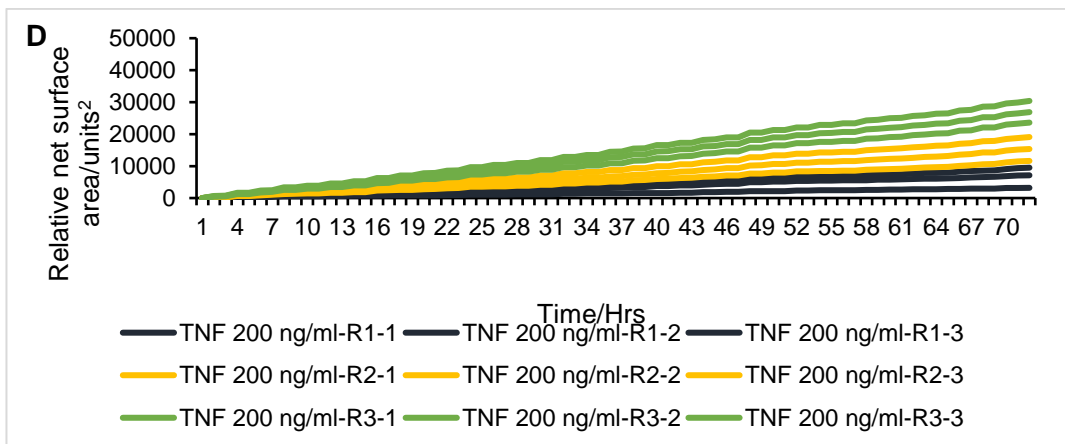
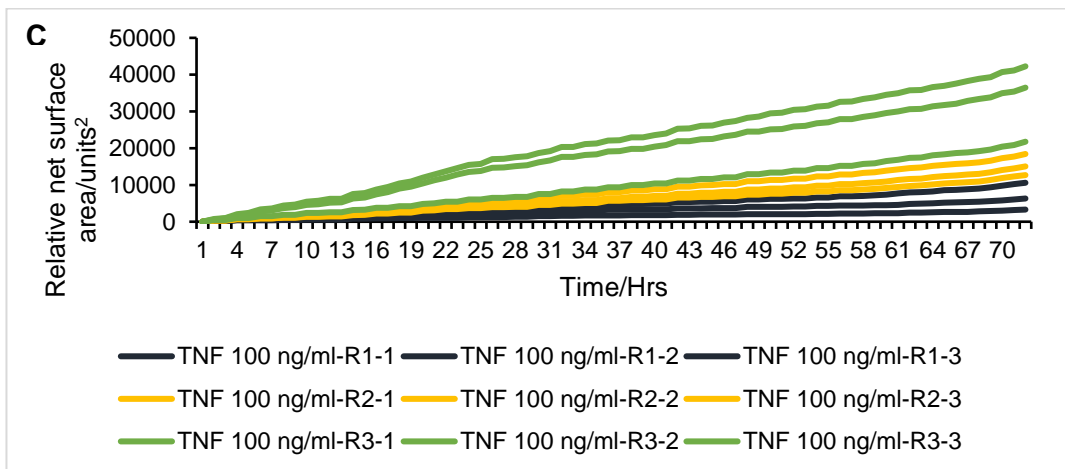
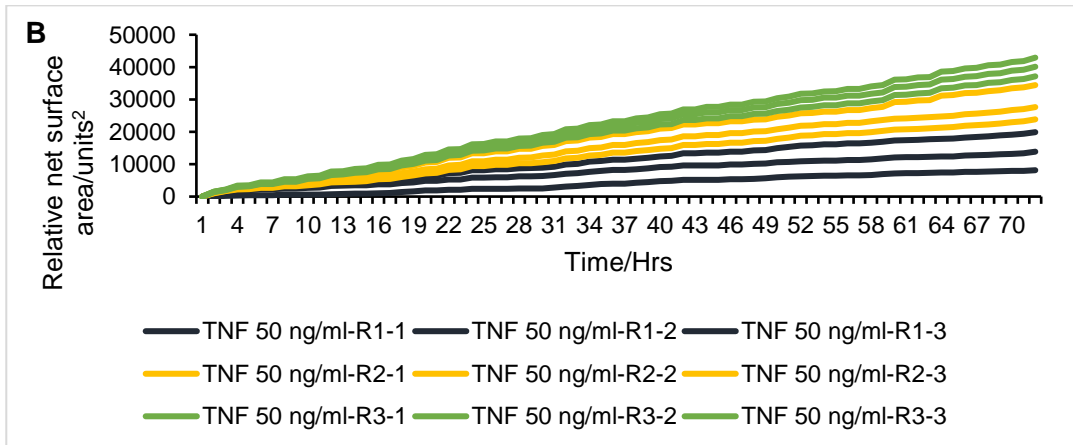
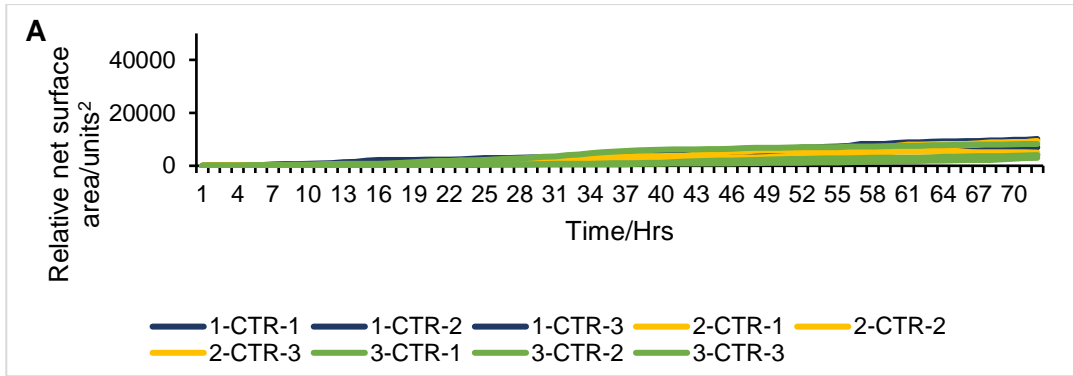


Figure 3.12 Rescued enteroids from the previously 50, 100, and 200 ng/ml TNF treated enteroids did not show the spikes of asynchronous expansions and contractions that they showed while in the presence of the stimulant (B-D). In comparison with untreated enteroids (A) their growth patterns were similar. The rescued enteroids showed progressive, uninterrupted growth patterns as captured by CytoSMART live cell imaging. Over 72 hours continuous monitoring, the rescued enteroids progressively increased in surface area. In the graphs, experiments 1 (blue), 2 (yellow) and green (3), n=3, N=3.

3.2.8 Rescued TNF-treated enteroids show reduced motility

TNF treatment was applied to WT-derived enteroids for 72 hours, after which the treated culture media were discarded, enteroids were washed and the media was replaced. CytoSMART live cell imaging was used to capture the movement of rescued enteroids. The motility patterns of rescued WT enteroids were similar to those of untreated WT enteroids. There was no greatly accelerated motility in the rescued enteroids unlike during the previous 72 hours when TNF was applied. The cumulative distance covered within 72 hours by untreated WT enteroids was $260 \pm 18.56 \mu\text{m}$ (figures 3.13 and 14). The cumulative distance covered within 72 hours following the removal of 50 ng/ml TNF was $246.67 \pm 14.53 \mu\text{m}$, following the removal of 100 ng/ml TNF was $181.11 \pm 44.39 \mu\text{m}$ and following removal of 200 ng/ml TNF was $198.89 \pm 45.01 \mu\text{m}$.

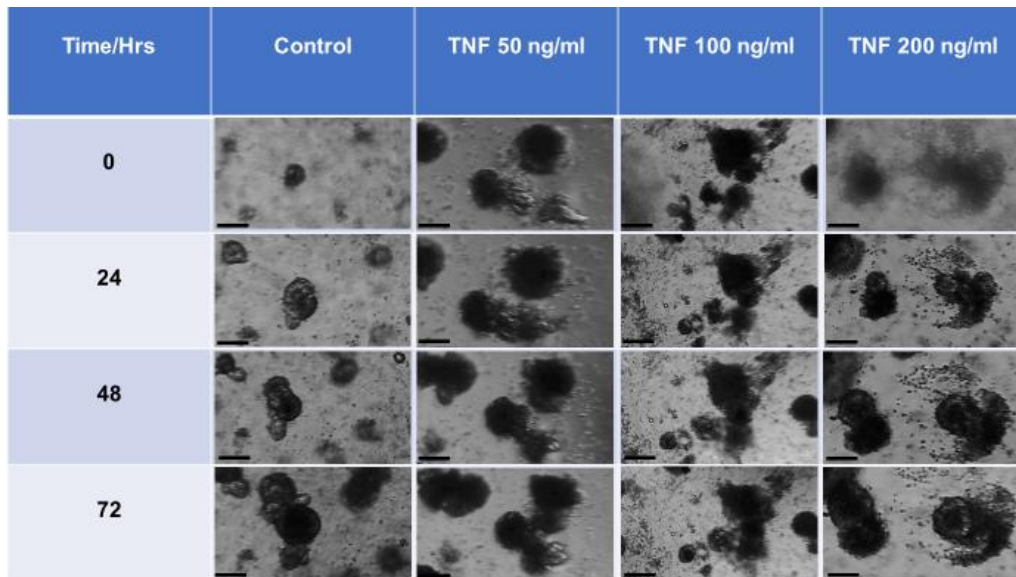


Figure 3.13 Micrographs of rescued enteroids that were previously treated with 50 ng/ml, 100 ng/ml and 200 ng/ml TNF against untreated control. Rescued enteroids did not exhibit asynchronous expansions and contractions or increased motility. Magnification, x10 and scale bars, 100 μ m.

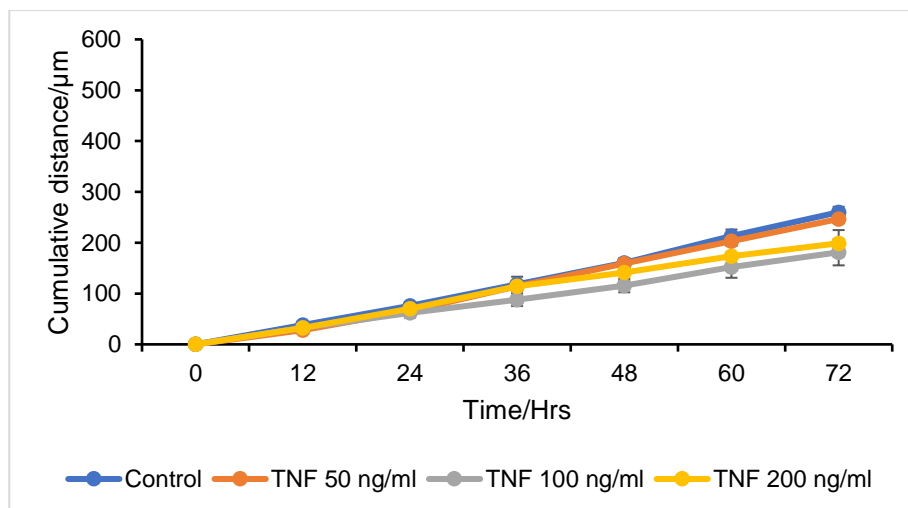


Figure 3.14 Cumulative distance (μ m) travelled by control (blue), 50 (orange), 100 (grey), and 200 (yellow) ng/ml TNF rescued enteroids over a 72-hour period following TNF washout. No statistically significant difference was observed between untreated and TNF rescued enteroids, $n=3$, $N=3$, error bars = SEM.

3.2.9 Forskolin-treated enteroids are associated with asynchronous expansions and contractions

Forskolin is an adenylyl cyclase activator and as such can be used to stimulate chloride secretion in intestinal epithelial cells (De Wolf, Van Driessche & Nagel, 1989;

Niisato & Marunaka, 2001). Boj and colleagues developed organoids from rectal biopsies containing either wild type or mutant cystic fibrosis transmembrane conductance regulator (CFTR) and showed that wild-type colonoids swelled in response to forskolin whereas CFTR mutant colonoids did not respond, showing the specificity of forskolin for CFTR-induced chloride secretion (Boj et al., 2017).

We used forskolin in this study as a positive control for enteroid expansion to determine whether increased enteroid expansion was responsible for our observed increased enteroid motility in response to TNF. CytoSMART live cell imaging was used to capture the behavioural patterns and morphological changes of forskolin-treated enteroids. The earliest observations of asynchronous expansions and contractions of forskolin-treated enteroids started at 2 hours and 15 minutes post-treatment and lasted for 70 hours (figure 3.14). The mean duration of expansions and contractions of forskolin treated WT enteroids was 52 ± 0.27 hours. The expansion phase ranged from 15 minutes to 8 hours while the contraction phase was shorter, usually up to 15 minutes. The expansion and contraction phases of forskolin-treated enteroids started earlier than those observed post-TNF treatment. During live cell imaging, the mean frequency of expansions and contractions of forskolin-treated enteroids was almost double that of TNF-treated enteroid (figure 3.15). However, the lengths of the contraction phases of forskolin-treated and TNF-treated enteroids were similar (figure 3.15).

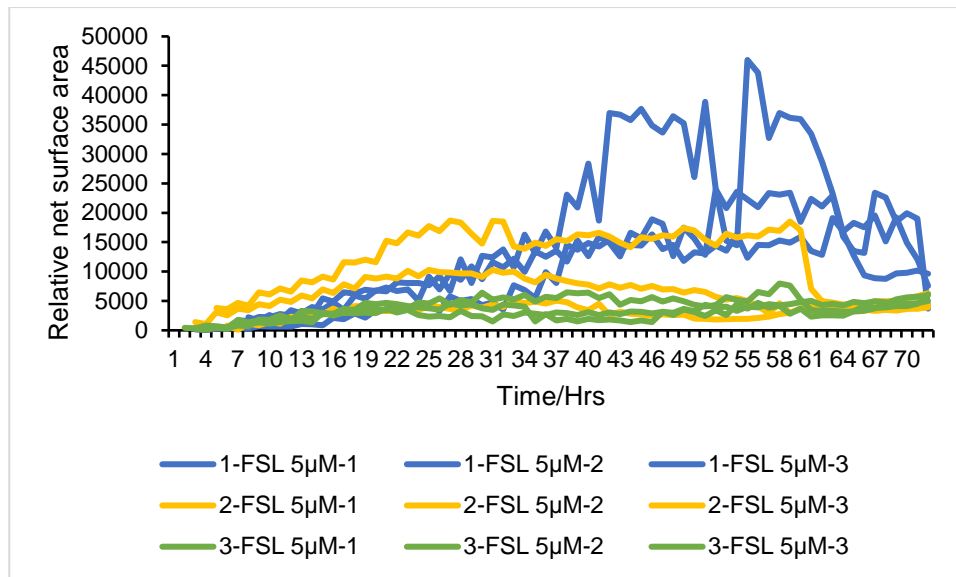


Figure 3.15 The 5 µM Forskolin was added to WT-derived enteroids for 72 hours. CytoSMART images were captured every 15 minutes to monitor the behavioural and morphological patterns of forskolin-treated enteroids. In the graphs, experiments 1 (blue), 2 (yellow) and green (3), n=3, N=3.

3.2.10 Forskolin-treated enteroids demonstrated reduced motility

As previously stated, we used forskolin in this study as a positive control for enteroid expansion. We treated enteroids with 5 µM forskolin and monitored them using time-lapse imaging to capture behavioural and morphological changes. Forskolin-treated WT enteroids showed reduced motility compared with untreated and TNF -treated enteroids, but exhibited multi-directional patterns similarly to untreated and TNF treated enteroids (figures 3.8 & 3.16). The cumulative distance covered by forskolin-treated WT enteroids in 72 hours ranged from 130 to 320 µm with a mean distance of 196.67 ± 31.80 µm (figure 3.17). Patterns of velocity are shown in figure 3.18. We statistically compared the motility of forskolin treated enteroids to untreated control enteroids at various intervals and no statistically significant differences were observed.

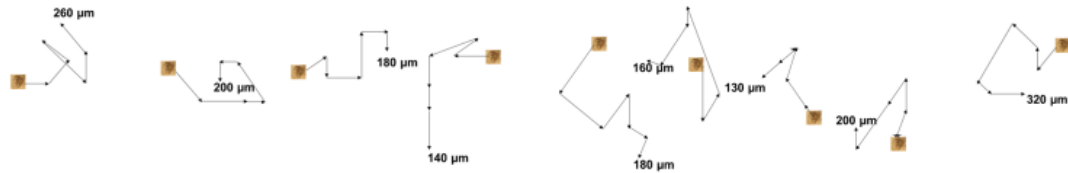


Figure 3.16 Forskolin (5 μM)-treated WT enteroids migrated through the ECM in multi-directional patterns slowly and covered different distances. The shortest distance covered was 130 μm while the longest was 320 μm in 72 hours. Each enteroid migrated independently without a common direction. The motility of forskolin-treated enteroids was captured by CytoSMART live cell imaging (n=3, N=3).

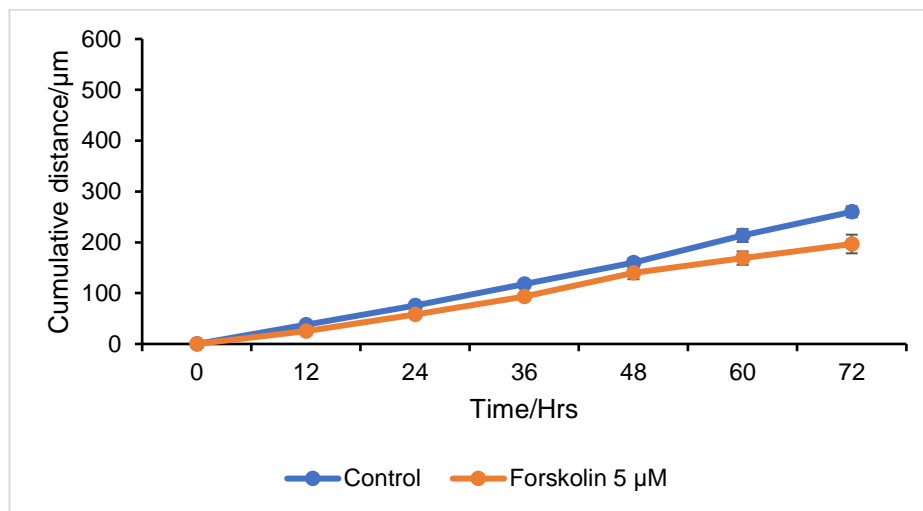


Figure 3.17 Cumulative distances covered by untreated WT enteroids (blue) in 72 hours was $260 \pm 18.56 \mu\text{m}$ while that of forskolin-treated enteroids (orange) was $196.67 \pm 31.80 \mu\text{m}$. There was no statistically significant difference between the distance covered by untreated WT and forskolin-treated enteroids by one-way ANOVA, n=3, N=3, error bars = SEM.

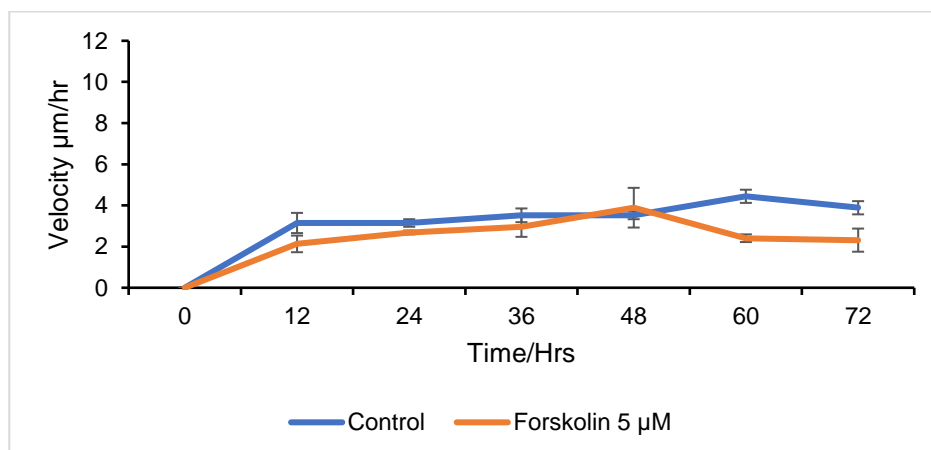


Figure 3.18 The velocity of both untreated (blue) and forskolin (5 μM)-treated (orange) WT enteroids were constant without any sudden increases or decreases in the first 48 hours of observation. Whilst the velocity of untreated enteroids continued to be constant throughout, that of forskolin-treated enteroids reduced at 48-72 hours post-treatment, n=3, N=3, error bars = SEM

3.2.11 Forskolin stimulates increased enteroid surface area

Forskolin-treated enteroids did not grow and show a steady increase in area like untreated enteroids (figure 3.19), but followed a similar trajectory to those treated with TNF. At 24 hours following forskolin treatment, the relative net surface area was doubled from 4052.11 ± 1679.14 units² to 8014.78 ± 3221.73 units². The maximal relative net surface areas of forskolin-induced swelling were observed at 36 hours (10427.89 ± 6961.87) units² and 48 hours (10517.89 ± 11386.20) units² following forskolin treatment (figure 3.20). The growth patterns of forskolin-treated enteroids were perturbed by abrupt increases in the net surface areas followed by sudden decreases in the net surface areas.

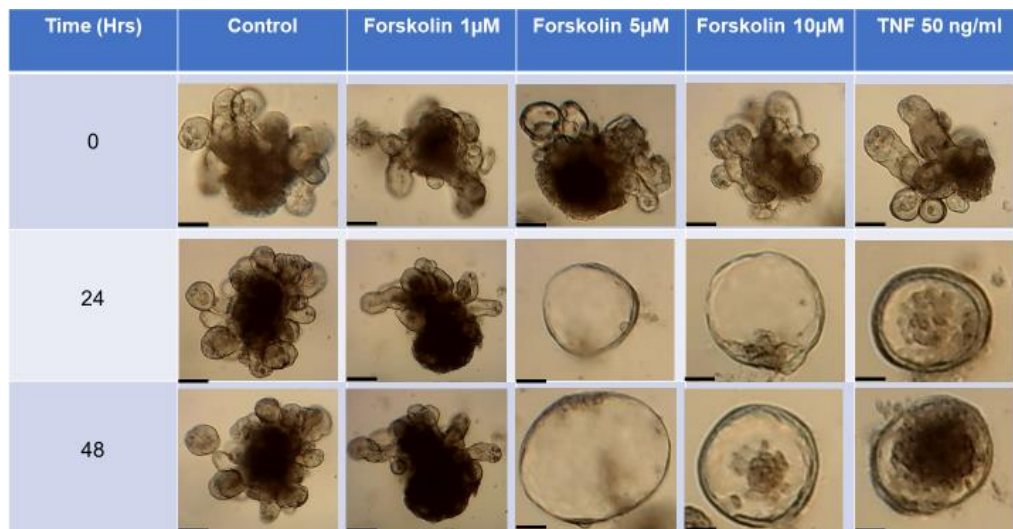


Figure 3.19 Bright field images of forskolin and TNF-treated WT enteroids. Dose-dependent and time-dependent increases were observed in the circularity of forskolin-treated WT enteroids. Forskolin and TNF induced the highest degree of circularity on the treated WT enteroids at 48 hours while untreated WT enteroids had the lowest circularity measurement. Micrograph x10 magnification and scale bar, 100 μ m.

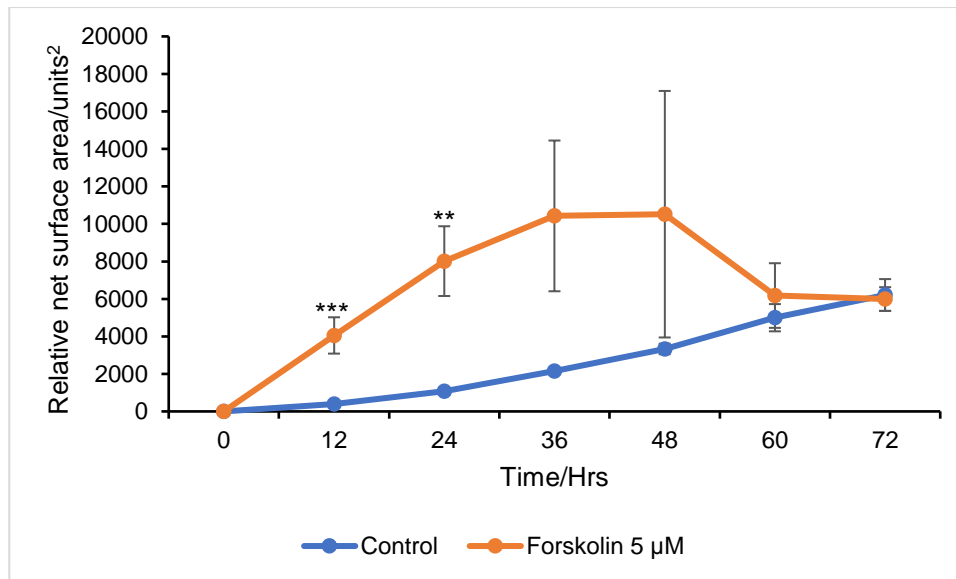


Figure 3.20 Forskolin (5 µM) induced an early and sudden increase in the net surface area of enteroids (orange) while untreated enteroids progressively increased in the net surface area at a slower rate (blue). Forskolin (5 µM) stimulated the largest net surface area (10517.89±11386.20) units² at 48 hours post-treatment while the largest net surface area in untreated enteroids (6208.89±1468.32) units² was at 72 hours. (P = **≤0.01, ***≤0.001), ANOVA, n=3, N=3, error bars = SEM.

3.2.12 CFTR inhibition does not prevent TNF-induced rounding, expansion, and contraction in enteroids

We observed that both TNF- and forskolin-treated enteroids demonstrated increased circularity. Previous studies have reported that forskolin-induced swelling was cystic fibrosis transmembrane conductance regulator (CFTR)-dependent (Boj et al., 2017; De Wolf et al., 1989). We therefore wanted to determine the mechanism responsible for TNF-induced enteroid expansions and contractions so utilised a specific CFTR inhibitor to determine whether chloride secretion was responsible for the altered enteroid morphology observed following TNF treatment.

We treated WT enteroids with 0, 5, 20, and 50 µM CFTRinh-172 (CFTR inhibitor) and assessed enteroids for circularity at 0, 24 and 48 hours. The CFTRinh-172 did not induce any increase in circularity or cause pronounced cell apoptosis when administered alone at the doses and time points tested (figures 3.21 and 3.23A). We

then proceeded to first pre-treat WT enteroids with different concentrations of CFTRinh-172 for one hour, after which we exposed them to 50 ng/ml TNF and obtained brightfield images at 0, 24, and 48 hours. We noticed that the actions of TNF on WT enteroids were not CFTR-dependent, since pre-treatment with the CFTR-inhibitor failed to block TNF-induced increases in circularity (figures 3.22 and 3.23B). However, pre-treatment with 50 μ M CFTRinh-172 has been shown the ability to inhibit forskolin-induced swelling and completely suppress an α -gliadin derived peptide-induced swelling in our laboratory under the same treatment conditions (Thompson and Duckworth unpublished observations, data not shown).

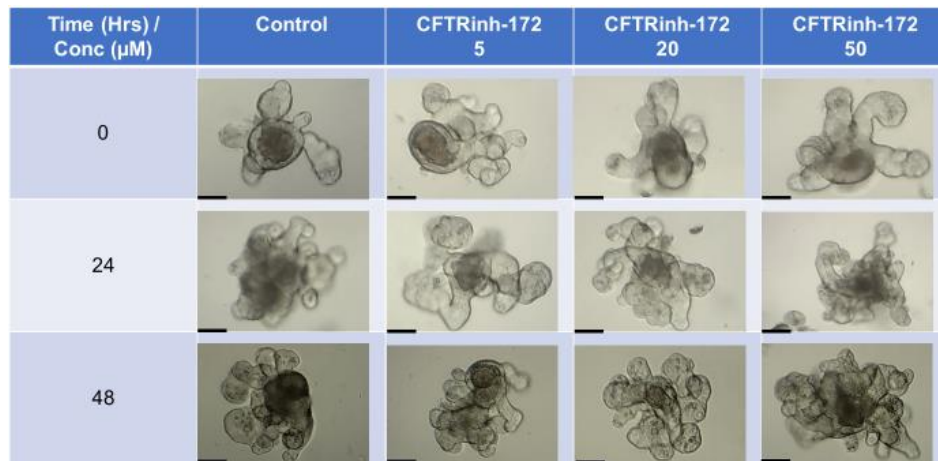


Figure 3.21 Bright field images of CFTRinh-172-treated WT enteroids. There was no observed increase in circularity at 0, 24, and 48 hours following treatment with CFTR inhibitor at 0, 5, 20 and 50 μ M. x10 original magnification and scale bars represent, 100 μ m.

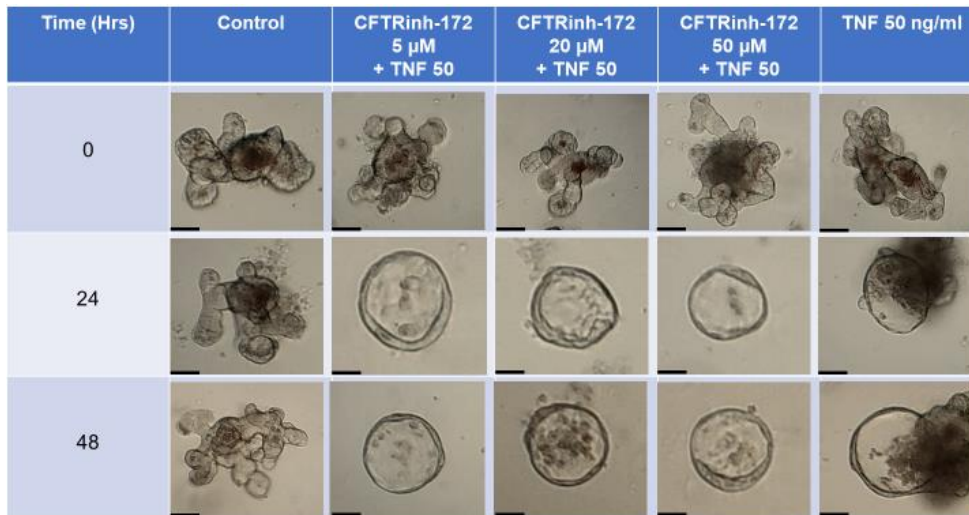


Figure 3.22 Bright field images of TNF treated enteroids following one-hour pre-treatment with CFTRinh-172 at indicated concentrations. Circularity increased in response to TNF following CFTR inhibition. However, there was no increase in circularity of untreated enteroids. Micrograph x10 magnification and scale bar = 100 μ m.

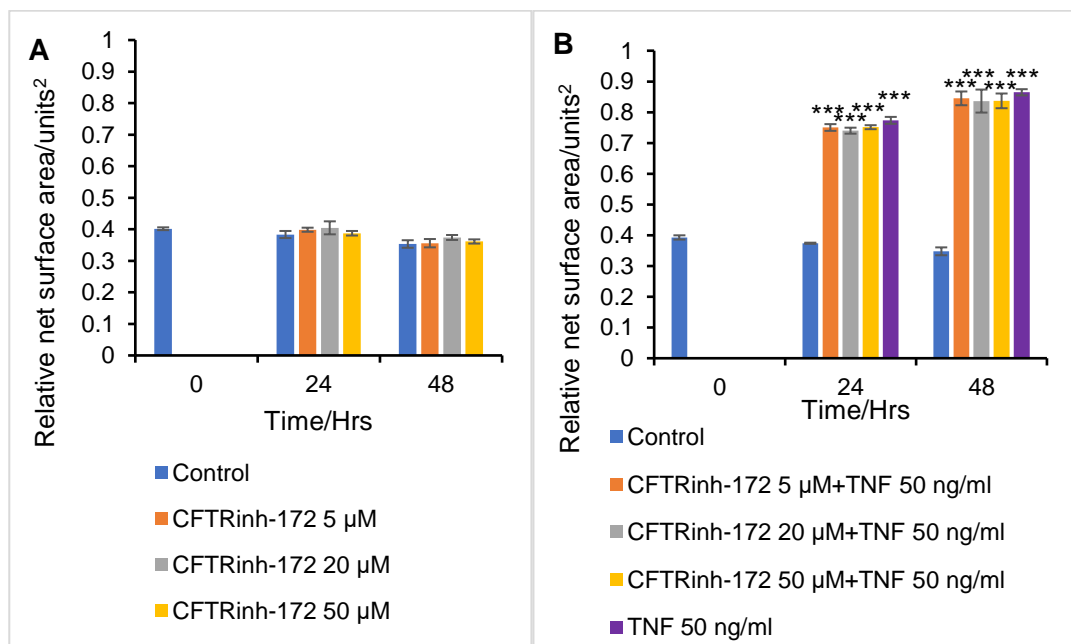


Figure 3.23 TNF causes increased enteroid circularity following CFTR inhibition. Circularity analysis at 0, 24 and 48 hrs following 0, 5, 20 and 50 μ M CFTRinh-172 pre-treatment (A). Circularity analysis following 1hr CFTRinh-172 pre-treatment followed by 50 ng/ml TNF at 0, 24 and 48 hrs (B). ($P = ***\leq 0.001$), one-way ANOVA, mean of mean from three experiments, $n=6$, $N=3$, and error bars with SEM.

3.2.13 Summary table of the characteristics of actions of TNF on WT enteroids

Several parameters were investigated following treatment of WT-derived enteroids with TNF. Our observations are summarised in the table below.

Differences between untreated and treated WT enteroids		
Features	Untreated	TNF-treated
Growth pattern	Normal	Abnormal and interrupted
Asynchronous expansions and contractions	Absent	Present
Growth predictability	Almost steadily progressive	Unpredictable with spikes
Relative surface areas	Progressively increasing	Larger with expansions; smaller with contractions
Motility	Normal	Increased
Morphological shape	Increasing irregularity	Increasing rounding
Epithelial thinning	Normal	Present
Claudin-7 redistribution	Normal	Present
Permeability	Normal	Increased
CFTR inhibitor	No rounding	Does not prevent rounding

Table 3.1 Phenotypic differences between untreated and TNF-treated enteroids. The growth patterns of untreated enteroids were not interrupted with asynchronous expansions and contractions as seen in TNF treated enteroids. Untreated enteroids showed a steady increase in relative surface areas, while TNF treated enteroids demonstrated frequent increases and decreases in relative surface areas. Untreated enteroids did not show any increase in motility or migratory trends as seen in TNF-treated enteroids.

3.3 Discussion

In this study, we characterised several novel actions of the pro-inflammatory cytokine TNF on enteroid cultures to further understand how TNF interacts with the intestinal epithelium to cause local and systemic disease. Previous studies have investigated the actions of TNF on cell populations along the crypt-villus axis *in vivo* and several of these studies have characterised the dynamic nature of villus tip epithelial cells using time-lapse microscopy over 1-4 hours (Kiesslich et al., 2007; Marchiando et al., 2011; Duckworth & Watson, 2011). However, to date, to the best of our knowledge,

whilst cellular dynamics in response to TNF have been explored, tissue level dynamics have not. Therefore, we investigated whether we could dynamically via CytoSMART live cell imaging monitor the pathological responses of enteroids derived from the proximal small intestinal epithelia of WT mice to different concentrations (0, 50, 100 and 200 ng/ml) of TNF treatment.

The intraperitoneal injection of TNF into mice *in vivo* results in a rapid onset of small intestinal apoptosis and cell shedding that peaks around 90 minutes following administration (Duckworth & Watson, 2011; Watson et al., 2009). The administration of lipopolysaccharide (LPS) intraperitoneally to WT mice also resulted in intestinal mucosal cell shedding and apoptosis that was likely mediated by the actions of LPS on monocytes and macrophages to produce TNF (Williams et al., 2013). It has been widely reported in the literature that LPS treatment stimulates abundant cytokine production, most notably TNF as a major mediator of sepsis (Amiot et al., 1997; Amura et al., 1998; Hesse et al., 1988; Werner, Barken & Hoffmann, 2005). The intestinal epithelium is one of the first tissues to be damaged during the first 1-2 hours of sepsis and mechanistically there are many similarities with hyper-inflammation and mucosal damage observed during active inflammatory bowel disease where anti-TNF therapy shows efficacy (Doig et al., 1998; Julian et al., 2011; Monaco et al., 2015). Until recently, *in vitro* studies of tissue level dynamics have not been possible, as the majority of studies relied on standard two-dimensional tissue culture of cancer-derived cell lines. It is now possible to reproduce the epithelial structure of the intestinal epithelium in enteroid cultures that display similar crypt-villus orientation and dynamics to that observed *in vivo* (Middendorp et al., 2014; Wallach & Bayrer, 2017). The current study firstly corroborated our previous work (Jones et al., 2019) and demonstrated that TNF treatment caused dose-dependent and time-dependent enteroid rounding consistent with an increase in epithelial cell shedding and apoptosis. Building on these studies, we observed histologically that TNF treated

enteroids showed a time-dependent reduction in epithelial thickness – a phenomenon observed following TNF administration in experimental *in vivo* models and in recovery from active intestinal disease in humans (Dotti et al., 2017; Yoo & Donowitz, 2019). This suggests that intestinal enteroids are a good *in vitro* model that accurately replicates *in vivo* intestinal epithelial dynamics.

We have previously investigated the actions of TNF in static conditions by bright field microscopy and by histology which have only allowed the analysis of a snapshot in time. In this chapter we dynamically monitored behavioural patterns and morphological changes in TNF-treated enteroids using CytoSMART time-lapse imaging and observed several surprising and unexpected phenomena. Though previous studies have reported the secretion of MMP from TNF-treatment (Yan et al., 2001), we are not sure whether digestive effect of MMP might contribute to the increased motility of TNF-treated enteroids within the Matrigel. However, our proteomic results (chapter 5) shows that MMP7 proteins were upregulated in all the four strains. More investigations are warranted to understand the plausible mechanisms that might be responsible for the TNF-induced motility.

Our results showed that different concentrations (50, 100, and 200 ng/ml) of TNF administered to WT enteroids were associated with periodic, expansions and contractions of whole enteroids that were asynchronous between enteroids within the same Matrigel support matrix. Previous studies have investigated TNF-induced oscillations of NFκB subunits (especially p65) between the cytosol and the nucleus in individual cells in two-dimensional tissue culture and observed a frequency of around 0.5 oscillations per hour (Dorrington & Fraser, 2019; Lane et al., 2017; Lee et al., 2014; Pekalski et al., 2013; Zambrano et al., 2016). It warrants more investigations to elicit what might be the driving mechanisms behind asynchronous expansions and contractions of TNF-treated enteroids. Further work is needed to determine whether this is related to NFκB signalling activation.

The CytoSMART live cell imaging system that we used to monitor the behavioural patterns of TNF-treated enteroids captured increased motility and multi-directional migration of enteroids. Different concentrations of TNF were associated with changes in velocities, acceleration, deceleration, and overall distance migrated. TNF has been widely reported in many studies to play a key role in promoting cell motility. Wolczyk and colleagues reported that the cell migration induced by TNF treatment of MCF7 and MDA-MB-231 cell lines was due to an increase in matrix metalloprotease 9 (MMP9) (Wolczyk et al., 2016). Boecke and colleagues in a B16 mouse melanoma cell line study reported that TNF induced motility and invasion occurred via TNF-receptor-1 adaptor protein FAN (factor associated with neutral sphingomyelinase activation) (Boecke et al., 2013). TNF and transforming growth factor- β (TGF- β) synergistically stimulated epithelial-mesenchymal transition (EMT) to promote cell motility, cell-cell adhesion dissociation, and spindle-cell shape reorganization (Saito et al., 2013; Zhang et al., 2015). Pathologically, TNF-mediated motility contributes in no small measure to cancer migration, invasion, and metastasis and physiologically it is very relevant in wound healing and repair (Bingle, Brown & Lewis, 2002; Waters, Pober & Bradley, 2013; Yu et al., 2010). The biological significance of the expansions and contractions and enhanced motility observed in TNF treated enteroids is currently unclear. However, migration of stem cell containing crypts at the tissue level within intestinal epithelia could help to distribute stem cells around the mucosa efficiently to stimulate and enhance the production of new crypts, thus aiding greatly in tissue restitution following injury. We hypothesise that intestinal stem cells had the capacity to resist cell death and apoptosis by demonstrating the capacity of enteroids to continue to grow following TNF removal. This ability to regenerate persisted at all TNF concentrations tested including 200 ng/ml, which is a supra-pathophysiological concentration. To date, tissue-level dynamics in the intestinal mucosa have not been extensively investigated in real-time and in 3 dimensions, and so the enteroid platform may provide a novel approach to study this area.

We demonstrated that TNF treatment caused rapid swelling of WT murine enteroids by using NIH ImageJ to quantify the net surface areas and wanted to understand the responsible mechanism, as fluid infiltrate is also observed within the intestinal luminal compartment following TNF or LPS injection into mice (Williams et al., 2013) and diarrhoea is associated with human IBD and sepsis (Anbazhagan et al., 2018; Larmonier et al., 2011; Laubitz et al., 2016). It is possible that TNF mediates these biological activities of fluid effusion into the lumen via ion channels opening and dysfunction of cell-cell junctions leading to increased epithelial barrier porosity (Ma et al., 2005; Schmitz et al., 1996; Ye et al., 2006). We observed an accumulation of fluid in the enteroid lumen following TNF administration and reported a decrease in epithelial thickness which may have caused a similar phenotypic response as to that shown in *in vivo* intestinal epithelia following TNF or LPS administration and also in humans with resultant fluid accumulation in the gut prior to diarrhoea. We therefore sought to investigate potential mechanisms. Several protein components make up intestinal tight junctions which modulate the paracellular space and are the components that modulate the leakiness of the epithelial barrier. We identified several claudins and junctional adhesion molecules that are known to be important in maintaining gut barrier function and investigated their expression in enteroids over the time-course of TNF treatment. Claudin-7 knockout and intestinal-specific claudin-7 knockout mice die soon after birth due to a lack of intestinal crypt and villus formation, connective tissue hyperplasia and excessive inflammatory infiltrate (Xu et al., 2019). Claudin-7 showed significant remodelling following the application of TNF to enteroids suggesting that this claudin is important in regulating the epithelial cell response to TNF and may be at least partially responsible for enhanced permeability leading to fluid accumulation. Tanaka and colleagues investigated the role claudin-7 played in initiating inflammation via paracellular-barrier change by conducting an experiment on intestine-specific conditional knockout mice of claudin-7 (Tanaka et al., 2015). Claudin-7 deficiency increased paracellular permeability across the

colonic epithelium (paracellular flux (pFlux). They observed passage of the small organic solute Lucifer Yellow (457 Da) across the intestinal epithelium due to enhanced paracellular permeability whilst larger organic solute such as FITC-Dextran (4400 Da) could not pass through (Tanaka et al., 2015).

To address further potential mechanisms responsible for fluid accumulation in TNF treated enteroids and to determine whether the act of expansion was responsible for enhanced enteroid motility, we explored whether forskolin (Sigma-Aldrich, F3917) treatment had similar phenotypic consequences when applied to enteroids. Forskolin is an adenylate cyclase activator that has previously been used to stimulate chloride ion secretion in enteroids resulting in enteroid expansion. Forskolin-mediated chloride secretion was shown to be mainly mediated by CFTR as cystic fibrosis patient-derived or CFTR mutant mouse enteroids were resistant to forskolin-induced swelling (Dekkers et al., 2013). Forskolin-treated enteroids demonstrated early rapid swelling and reduced motility compared with untreated enteroids as previously reported in other studies (Dekkers et al., 2013). The observation that forskolin treated enteroids did not migrate to the magnitude observed in TNF-treated enteroids suggests that the act of expansion itself is not responsible for stimulating this enhanced motility and that other as yet unknown mechanisms are therefore likely to be responsible. Enteroids migrated in seemingly random directions and no obvious chemotactic gradient in the surrounding matrix was observed. We cannot rule out the production of TNF-induced secretions from neighbouring enteroids that would have influenced the direction of migration depending on each individual enteroid's local environment.

We further explored whether the swelling observed in TNF treated enteroids was CFTR-dependent. We first treated enteroids with CFTR inhibitor-172 (Merck, 219670-5MG) to observe whether it would have any lethal effect and/or morphological changes on the enteroids. We did not observe any CFTR inhibitor-

172-lethal effects or induced morphological changes. We blocked CFTR in TNF-treated enteroids using a CFTR-specific inhibitor at concentrations previously shown in our lab to block forskolin-induced enteroid swelling. CFTR inhibition did not however prevent the expansion, contraction or motility changes observed in TNF treated enteroids, so we can conclude that the mechanisms of TNF and forskolin-induced expansions are likely to be different. CFTR inhibitor-172 was applied prior to forskolin in a separate study at the same concentration and was shown to block forskolin-induced enteroid expansion. Unfortunately, this combination of treatments was not conducted at the same time as other treatments in the current study.

We have therefore demonstrated under static and dynamic conditions that TNF treatment of enteroids induces various types of pathological actions which might have significant importance in the dysregulation of intestinal barrier function that is present during active IBD and sepsis. The enteroid model shows features of intestinal damage that are consistent with damage in inflammatory disease conditions of the gut and in isolation will be important in the exploration of tissue level dynamics within the intestinal epithelium that are difficult to conduct *in vivo*. Future studies of pro-inflammatory cytokines and their mechanisms of action both at the cellular and tissue levels will enable far greater understanding of the processes of IBD and sepsis pathogenesis, but will also shed light into future novel therapeutic approaches to ameliorate these conditions.

4. The effect of alternative pathway NFκB activation on enteroids

4.1 Introduction

Intestinal epithelial cells provide physical (mucus layer, glycocalyx and cell junctional complexes) and chemical barriers (antimicrobial peptides, lysozyme and immune cell-derived cytokines) to protect the gut against any invading microorganisms and maintain intestinal homeostasis between the luminal commensal microbiota and the body (Liang et al., 2006; Okumura & Takeda, 2017). Any disruption of this delicate equilibrium can result in compromised intestinal epithelial barrier function. Kiesslich and colleagues reported that the defective intestinal barrier integrity that resulted from cell shedding in the terminal ileum played a major role in the prediction of relapse of IBD in humans (Kiesslich et al., 2012). Additionally, Cani and colleagues and Piton and colleagues postulated that a dysfunctional intestinal barrier is a critical component of the pathogenesis of acute intestinal failure due to sepsis and metabolic endotoxemia-induced inflammation (Cani et al., 2008; Piton et al., 2011).

Activation of NFκB signalling pathways is involved in the regulation of various cellular processes. The alternative NFκB signalling pathway has been implicated in modulating disease susceptibility in sepsis and IBD and has also been demonstrated to regulate intestinal epithelial cell-specific apoptosis and cell shedding in mice and in enteroid cultures (Williams et al., 2013, Jones et al., 2019). In particular, NFκB2 was shown to be an important NFκB family member in regulating the epithelial damage response to TNF and IFNγ (Jones et al., 2019, chapter 4 of this thesis). However, these previous studies did not investigate how extensive the protective response conferred by alternative NFκB pathway inhibition (by deletion of NFκB2) was to other stimuli and whether the response was fully mediated via alternative

NFκB signalling pathway activation or whether complex links with classical pathway NFκB signalling were also implicated. Alternative pathway NFκB signalling can be activated by the interaction of a ligand (LPS, virus, BAFF, CD40L and others) with intestinal cell surface receptors such as TLR4 and LTβR (Dejardin, 2006; Luftig et al., 2004). The ligand triggers recruitment of TRAFs especially TRAF3, which only regulates the alternative NFκB signalling pathway (Greten et al., 2004). This results in activation of NIK and IKKα that stimulate the processing of p100 into p52, which dimerizes with RelB. The p52/RelB heterodimers translocates from the cytoplasm to the nucleus resulting in the transcription of inflammatory target genes (Merga et al., 2016; Nishikori et al., 2005). Several members of the TNF superfamily are thought to exclusively regulate alternative pathway NFκB signalling.

The TNF superfamily is a group of cytokines with common features and currently consists of 19 TNF superfamily (TNFSF) ligands and 29 TNF receptor superfamily (TNFRSF) receptors in humans (Lang et al., 2016) (table 1). The majority of TNFSF ligands are type II transmembrane proteins (single pass molecules that anchored with a signal-anchor sequence with its C-terminal (not N-terminal) directed toward the endoplasmic reticulum) with polytopic proteins that readily aggregate and easily precipitate in water (Qu, Zhao, & Li, 2017). By contrast, the TNFRSF receptors are derived from oligomeric, type I, or type III transmembrane proteins (Smulski et al., 2017; Ward-Kavanagh et al., 2016). Ligands of TNFSF interact with TNFRSF to generate intracellular signals on target cells such as the intestinal epithelium.

The TNFSF ligands and TNFRSF receptors play regulatory and signalling roles in inflammation, proliferation, apoptosis, immune cells, cell functions, embryogenesis cell differentiation and tissue homeostasis (Bodmer et al., 2002; Locksley, Killeen, & Lenardo, 2001). From 19 TNFSF ligands, we selected 6 for evaluation based on their ability to strongly activate alternative pathway NFκB signalling (table 4.1). The selected family members were TNF, TNF-related weak inducer of apoptosis

(TWEAK), lymphotoxin-like, exhibits inducible expression and competes with HSV glycoprotein D for herpesvirus entry mediator [HVEM] receptor, expressed by T lymphocytes (LIGHT), cluster of differentiation 40-L (CD 40-L), lymphotoxin α/β (LT α/β), and B-cell activating factor (BAFF). Expression of these TNFSF members has previously been detected in humans and is upregulated in inflammatory conditions, however, most studies report serum concentrations and not local tissue or stool concentrations which may be further elevated beyond those found in serum similarly to TNF (Komatsu et al., 2001; Nicholls et al., 1993, table 4.2).

TWEAK is associated with cell apoptosis, proliferation and survival via activation of TNF receptor-2 followed by stimulation of NIK to effect transcriptional inflammatory genes (Burkly et al., 2011). Activation of TWEAK signalling via Fn14 induces a dysfunctional intestinal epithelial cell barrier and promotes recruitment of inflammatory cells and enhanced synthesis of inflammatory mediators, especially in IBD and sepsis (Chicheportiche et al., 1997; Dohi & Burkly, 2012; Winkles, 2008). Upregulation of the TWEAK signalling pathway disrupts intestinal epithelial homeostasis and encourages translocation of commensal and invading microbes. Chopra and colleagues reported that inhibition of TWEAK-Fn14 signalling resulted in reduction of intestinal cell apoptosis and development of disease (Chopra et al., 2015). As previous studies have been performed to evaluate whole organ pathophysiology, we wanted to determine whether the actions of TWEAK were important specifically by direct interaction with intestinal epithelial cells.

LIGHT, through activation of HVEM, TNFRSF14 (TR2 or LIGHTR), and lymphotoxin β receptor (LT β R) modulates T cell proliferation, cell survival and apoptotic regulation (Clayburgh et al., 2006; Granger & Rickert, 2003). Krause and colleagues administered dextran sulphate sodium (DSS) to TNFSF14 (LIGHT) KO mice and reported that they had lower survival rates, higher loss of body weight, and developed more severe colitis in comparison with WT mice (Krause et al., 2014). Activation of

LIGHT via MLCK causes compromised intestinal epithelial integrity (Clayburgh et al., 2006). We therefore assessed the direct effects of LIGHT on the intestinal epithelium in the context of *Nfkb2* deletion.

CD40-L interacts with CD40 cell-surface glycoprotein to modulate adaptive immune responses by upregulating MHC and co-stimulatory mediators including CD80 or CD86. CD40 can be found in various cells including intestinal epithelial cells, antigen presenting cells (APCs), B cells, endothelial cells, and epithelial cells of other organs (Gelbmann et al., 2003). Activation of CD40-L and its interaction with the CD40 cell surface of intestinal epithelial cells (IECs) stimulates effector T cells and inflammatory processes in IBD (van Kooten & Banchereau, 2000). Borchering and colleagues obtained biopsies from 112 patients with Crohn's disease and 67 patients with ulcerative colitis and reported that patients with active IBD showed immunofluorescence staining for CD40 in IECs within inflamed mucosae (Borchering et al., 2010). However, biopsies from 38 healthy controls, patients with IBD in remission, and the non-involved mucosa of patients with active IBD consistently showed lack of CD40 immunofluorescence staining in IECs (Borchering et al., 2010). We therefore wanted to assess the epithelial cell-specific effects of CD40 binding to CD40-L.

Lymphotoxin plays an important role in the regulation of intestinal mucosal immune responses (Wang et al., 2010). Activation of $LT\beta$ receptor ($LT\beta R$) signalling has been reported to mediate both protective and pathogenic responses during intestinal inflammation (Upadhyay & Fu, 2013). Several studies using sepsis-induced models have demonstrated that lymphotoxin had protective properties against intestinal injury (Jungbeck et al., 2008; Tumanov et al., 2011) while inhibition of the $LT\beta R$ signalling pathway has been observed to decrease intestinal damage in a T-cell-mediated colitis model (Mackay et al., 1998).

BAFF through high affinity receptors such as BAFFR and transmembrane activator-calcium modulator and cyclophilin ligand interactor (TACI) mediates cell proliferation, differentiation and survival of B cells, while through low affinity receptors such as B cell maturation antigen (BCMA) it coordinates immunoglobulin class-switch recombination (Mackay & Leung, 2006; Ng, Mackay, & Mackay, 2005). BAFF promotes intestinal epithelial cell proliferation by activating the TLR signalling pathway (Macpherson & McCoy, 2007). Zhang and colleagues conducted a study on 44 healthy controls, 78 patients with UC, and 37 patients with CD and reported that serum BAFF concentrations (pg/ml) were 977 (482-1345) in healthy, 1430 (1105-1624) in CD and 1472 (1018-1772) in CD subjects (Zhang et al., 2016). The sensitivity and specificity of serum BAFF concentration in identifying active IBD from healthy controls was 64% and 93% respectively (Zhang et al., 2016). Previous studies in our laboratory have demonstrated that *Nfkb2*^{-/-} enteroids were protected against damage caused by IFN γ , which is not known to directly stimulate alternative pathway NF κ B signalling (Jones et al., 2019). Several studies in lung epithelia have suggested that IFN γ can upregulate BAFF which is known to activate the alternative NF κ B signalling cascade hence we sought to address whether BAFF can cause direct epithelial cell damage in an enteroid model.

One of the aims of this study was to understand how activation of alternative pathway NF κ B signalling by members of the TNFSF superfamily regulates epithelial cell survival and contributes to the disease processes of IBD and sepsis. Many previous studies that have been conducted in our laboratory have demonstrated rounding effects of TNF in WT enteroids and a blunted effect of TNF on rounding in *Nfkb2*^{-/-} enteroids. Therefore, we were interested in investigating the actions of other members of the TNF superfamily and to find out how this family of cytokines modulates the development of intestinal and systemic diseases.

Name	Gene	Molecular weight (kDa)	Amino acids length	Chromosomal location	Functions
TNF	TNF	17 (s) & 26 (m)	233	6 (MHC)	Regulates immune cells, induces fever, cachexia, inflammation, apoptosis; inhibits tumorigenesis, viral replication, response to sepsis
TWEAK	TNFSF12	17	249	17	Induces apoptosis, proliferation, migration, regulates angiogenesis
LIGHT	TNFSF14	26	240	19	Stimulates T cell proliferation, regulates apoptosis
CD40-L	TNFSF5	33	261	Xq26-27	Regulates adaptive immune response, activates antigen-presenting cell
LT $\alpha\beta$	LTA, LTB	25 & 33	205 & 244	6 (MHC)	Induces inflammation, antiviral response, tumorigenesis, secondary lymphoid organs development
BAFF	TNFSF13B	31	285	13	Activates B cell, proliferation and differentiation of B cells

Table 4.1 Alternative pathway activators with their gene, molecular weights, amino acid lengths, chromosomal locations, and functions (Alexaki et al., 2009; Armitage et al., 1992; Browning et al., 1993; Granger & Rickert, 2003; Moss et al., 1997; Wiley et al., 2001). These alternative pathway activators were selected for investigation.

TNF superfamily	Health	Disease
TNF	Serum: 0.020 ng/ml; Faecal: undetectable	Serum: 44 ng/ml (sepsis); Faecal: 18.64-63.6 ng/g (Shigellosis)
TWEAK	Plasma: 307 (63-3492) pg/ml	Plasma: 352 (101–9179) pg/ml (CD); 502 (109–4547) ng/ml (UC)
LIGHT	Serum: 26.4±24.6 pg/ml	Serum: 79.1±53.49 pg/ml (non-alcohol fatty liver disease)
CD40-L	Plasma: 1.10±0.07 ng/ml	Plasma: 3.55±0.67 ng/ml (CD); 2.71±0.37 ng/ml (UC)
LTαβ	Serum: 102.9 (20–261.1) pg/ml	Serum: 91.5 (20.0–581.0) pg/ml (rheumatoid arthritis)
BAFF	Serum: 977 (482-1345) pg/ml; Faecal: 295 (284-309) pg/ml	Serum: 1472 (1018-1772) pg/ml (CD), 1430 (1105-1624) pg/ml (UC); Faecal: 369 (326-493) pg/ml (CD), 542 (358-1758) pg/ml (UC)

Table 4.2 The TNF superfamily, alternative pathway activators with their concentrations in health and disease (Arican et al., 2005; Damas et al., 1992; Grimstad et al., 2017; Komatsu et al., 2001; Ludwiczek et al., 2003; Nicholls et al., 1993; Otterdal et al., 2015; Schwartz et al., 2009; Waage et al., 1987; Young et al., 2010; Zhang et al., 2016).

4.2 Results

4.2.1 TNF-induced phenotypic changes in enteroids is blunted following

Nfkb2 deletion

WT mouse intestinal epithelial enteroids were treated with different TNF concentrations (0, 1, 10, 50, and 100 ng/ml) for 48 hours. Under static conditions, bright field images were taken at 0, 24, and 48 hours from six individual enteroids for each of 3 independent experiments (n=6, N=3). TNF caused a dose-dependent

increase in enteroid rounding (figures 4.1 and 4.3a) which has previously been linearly correlated with enteroid cell death (Jones et al., 2019). Baseline circularity in untreated WT enteroids was 0.36 ± 0.01 and 24 hours post-TNF, circularity values increased to 0.41 ± 0.05 following 1 ng/ml TNF up to 0.73 ± 0.02 following 100 ng/ml TNF and reaching statistical significance versus control by 10 ng/ml. Similar significantly increased TNF-induced circularity values were obtained up to 48 hours post treatment (figure 4.3a). *Nfkb2*^{-/-} enteroids proliferated at similar rates to WT enteroids and displayed morphologically identical features at baseline. Baseline circularity of *Nfkb2*^{-/-} enteroids was 0.35 ± 0.02 and was not statistically significantly different from baseline WT enteroid circularity. However, TNF-treated *Nfkb2*^{-/-} enteroids did not respond with the same degree of rounding observed in TNF-treated WT enteroids at the same TNF doses and time points (figures 4.2 and 4.3b). *Nfkb2*^{-/-} enteroids achieved maximal circularity across all doses and time-points of only 0.58 ± 0.03 at 48 hours post 100 ng/ml TNF suggesting that they were more resistant than WT enteroids to the effects of TNF (figure 4.3b). Comparison of TNF-treated WT with TNF-treated *Nfkb2*^{-/-} enteroids demonstrated that there were statistically significant differences between them at 24- and 48-hours following treatment. Morphologically, there were no differences between untreated WT and untreated *Nfkb2*^{-/-} enteroids.

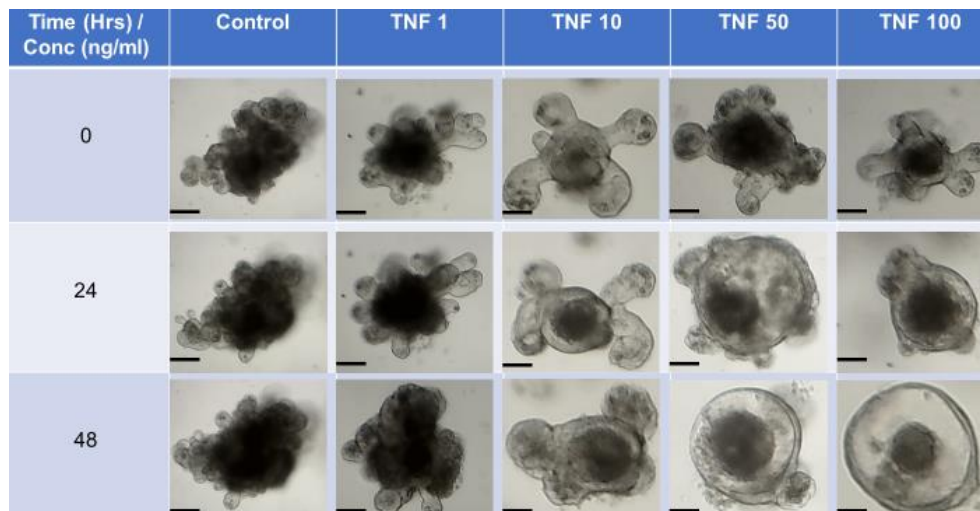


Figure 4.1 Bright field images of TNF-treated WT enteroids. Enteroids were treated with 0, 1, 10, 50 and 100 ng/ml TNF and images were collected at 0, 24, and 48 hours post treatment as indicated. Marked dose-dependent and time-dependent increases in enteroid circularity were observed. Images were taken at 10x original magnification; scale bars, 100 μ m.

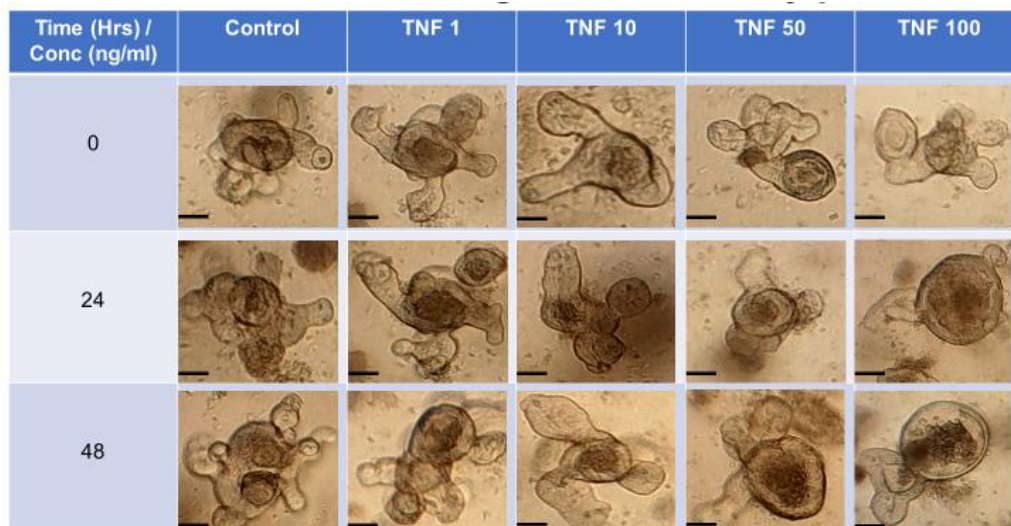


Figure 4.2 Bright field images of TNF-treated *Nfkb2*^{-/-} enteroids. Enteroids were treated with 0, 1, 10, 50 and 100 ng/ml TNF and images were collected at 0, 24, and 48 hours post treatment as indicated. Subtle dose-dependent and time-dependent increases in TNF-treated *Nfkb2*^{-/-} enteroid circularity can be discerned. Images were taken at 10x original magnification; scale bars, 100 μ m.

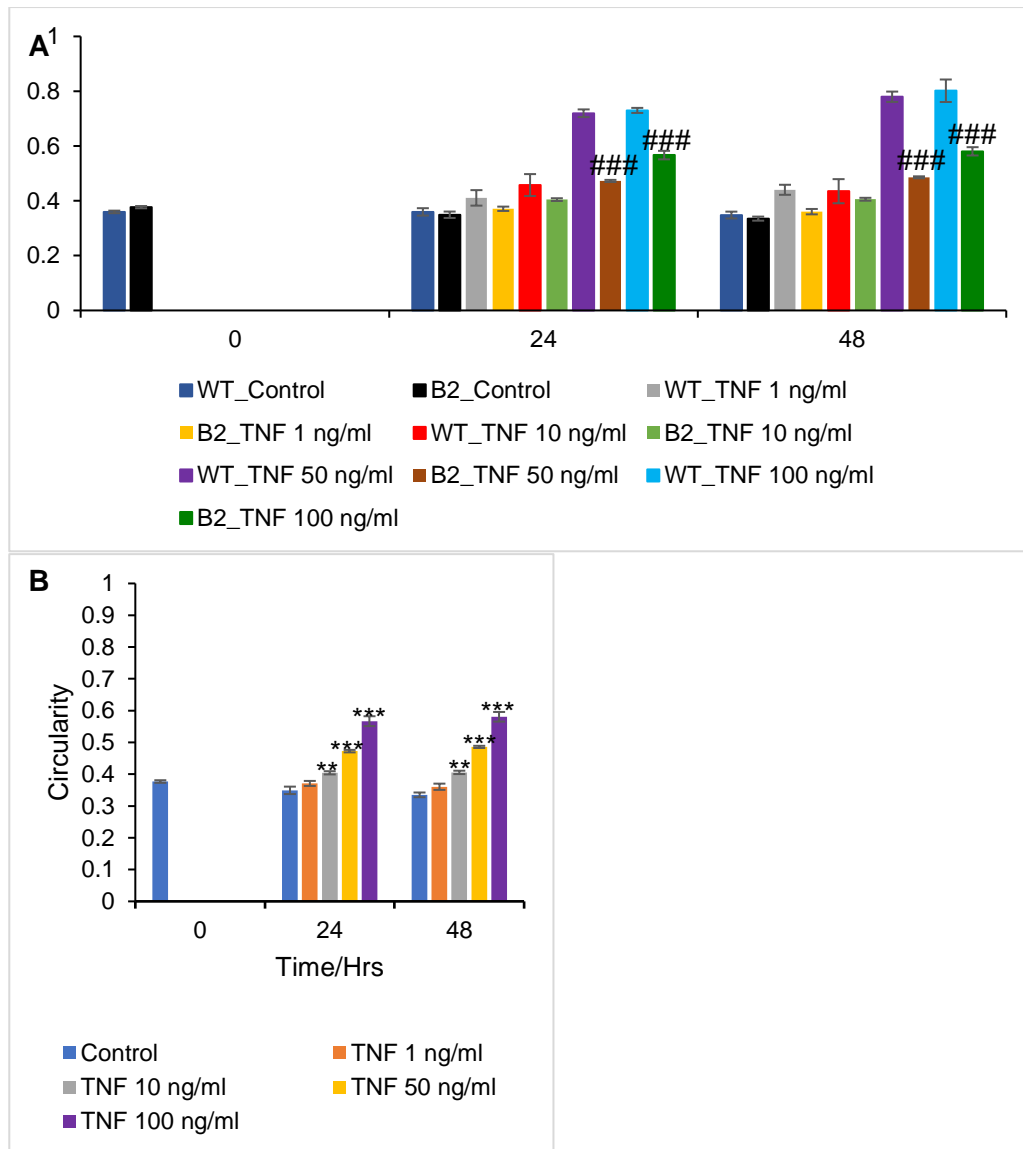


Figure 4.3 WT and *Nfkb2*^{-/-} enteroids treated with TNF (A). TNF causes a dose-dependent and time-dependent increase in WT-derived enteroid circularity (A) but a blunted increase in circularity in *Nfkb2*^{-/-} enteroids (B). Statistical differences were identified by ANOVA vs control at same time point, $P = (*\leq 0.05, **\leq 0.01, ***\leq 0.001)$, and statistically significant differences between WT + TNF vs *Nfkb2*^{-/-} + TNF at the same concentration and time point are shown by ($###p\leq 0.001$), $n=6$ organoids per treatment group, $N=3$ independent experiments, error bars with SEM.

4.2.2 TWEAK requires *Nfkb2* signalling to cause morphological changes of enteroids

Differential doses of TWEAK ranging from 0, 1, 10, 50, and 100 ng/ml were used to treat WT mouse intestinal epithelial enteroids for 48 hours. At 0, 24, and 48 hours, bright field images were captured from six individual enteroids for each of 3

independent experiments (n=6, N=3). TWEAK induced a dose-dependent increase in enteroid rounding (figures 4.4 and 4.6a). Untreated WT enteroid circularity at the outset was 0.37 ± 0.03 and at 24 hours post-treatment with TWEAK, circularity increased from 0.44 ± 0.03 following 1 ng/ml TWEAK to 0.66 ± 0.07 following 100 ng/ml TWEAK. TWEAK treatment versus control became statistically significant at doses at and greater than 10 ng/ml TWEAK. At 48 hours post-TWEAK treatment, similar significantly increased TWEAK-associated circularity was observed. Baseline morphological characteristics of WT and *Nfkb2*^{-/-} enteroids were similar. There was no statistically significant difference between baseline WT enteroid circularity and baseline *Nfkb2*^{-/-} enteroid circularity (0.39 ± 0.01) (figures 4.4 and 4.5). However, there was a stark difference in the degree of rounding in TWEAK-treated WT enteroids in contrast with TWEAK treated *Nfkb2*^{-/-} enteroids. TWEAK-treated WT enteroids demonstrated higher circularity values than *Nfkb2*^{-/-} enteroids at the same doses and time points (figure 4.6). At 48 hours following TWEAK administration, *Nfkb2*^{-/-} enteroids attained maximal circularity of 0.49 ± 0.01 following 100 ng/ml TWEAK suggesting that they exhibited more attenuated effects than WT enteroid responses to actions of TWEAK (figure 4.6b). At 24- and 48- hours following treatment, we compared TWEAK-treated WT with TWEAK-treated *Nfkb2*^{-/-} enteroids and observed that there were statistically significant differences.

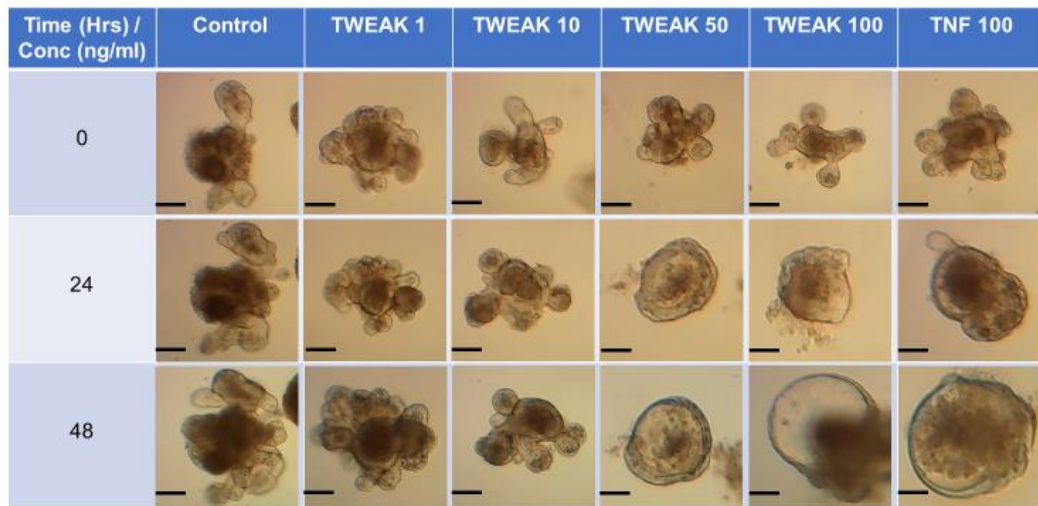


Figure 4.4 Bright field micrographs of TWEAK-treated WT enteroids. Enteroids were treated with different concentrations of TWEAK from 0, 1, 10, 50 to 100 ng/ml. Their images were collected at 0, 24 and 48 hours post-treatment. Apparent dose-dependent and time-dependent increases in enteroid circularity were noticed. Images were taken at 10x original magnification; scale bars, 100 μ m.



Figure 4.5 Bright field images of TWEAK-treated *Nfkb2*^{-/-} enteroids. Enteroids were treated with 0, 1, 10, 50 and 100 ng/ml TWEAKF and images were captured at 0, 24 and 48 hours following TWEAK treatment. Blunted dose-dependent and time-dependent increases in TWEAK-treated *Nfkb2*^{-/-} enteroid circularity were observed. Images were taken at 10x original magnification; scale bars, 100 μ m.

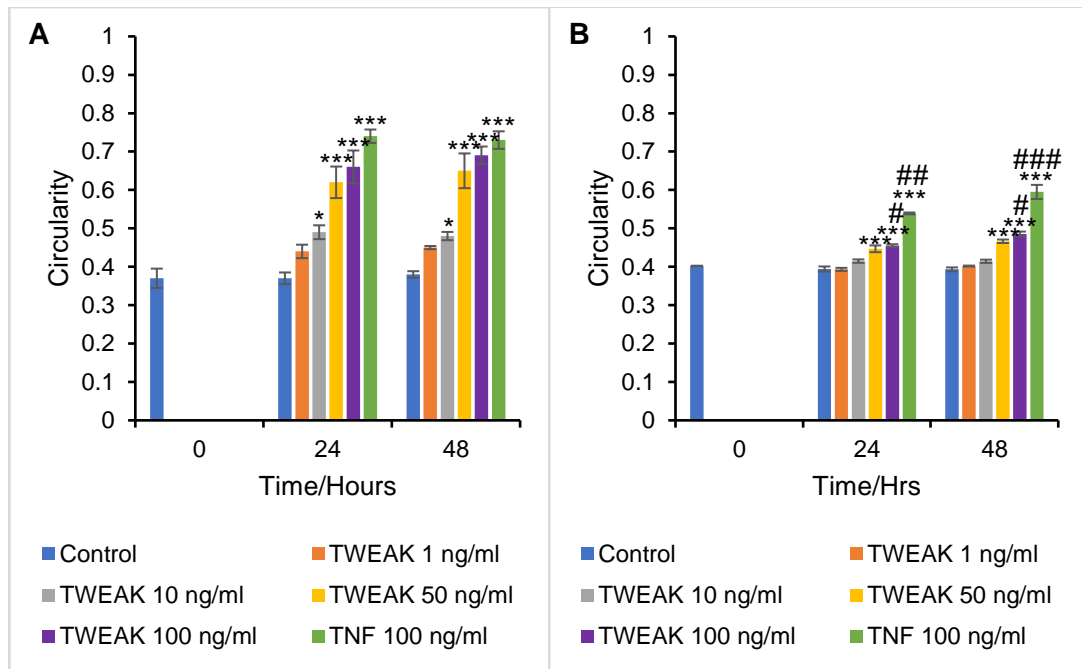


Figure 4.6 TWEAK induced a dose-dependent and time-dependent increase in WT-derived enteroid circularity (A) but attenuated increase in circularity in *Nfkb2*^{-/-} enteroids [Control (blue), 1 ng/ml TWEAK (orange), 10 ng/ml TWEAK (grey), 50 ng/ml TWEAK (yellow), 100 ng/ml TWEAK (purple) and 100 ng/ml TNF (green)]. Statistical differences were identified by ANOVA vs control at same time point, P = (* ≤ 0.05 , ** ≤ 0.01 , *** ≤ 0.001), and statistically significant differences between WT + TWEAK vs *Nfkb2*^{-/-} + TWEAK at the same concentration and time point are shown by (# ≤ 0.05 , ## ≤ 0.01 , ### $p \leq 0.001$), n=6 organoids per treatment group, N=3 independent experiments, error bars with SEM.

4.2.3 LIGHT causes increased WT enteroid circularity which is blunted following *Nfkb2* deletion

We treated WT mouse enteroids with different LIGHT concentrations (0, 1, 10, 50, and 100 ng/ml) for 48 hours. Bright field images were captured at 0, 24, and 48 hours from six individual enteroids for each of 3 independent experiments (n=6, N=3). LIGHT stimulated a dose-dependent increase in enteroid rounding (figures 4.7 and 4.9a). Untreated WT enteroid circularity at baseline was 0.36 ± 0.01 , but at 24 hours following treatment with LIGHT, circularity values increased dose-dependently from 0.41 ± 0.02 following 1 ng/ml LIGHT to 0.55 ± 0.03 following 100 ng/ml LIGHT. LIGHT-induced circularity showed a significant increase following 50 ng/ml. Similarly, LIGHT-treated enteroids demonstrated significantly increased LIGHT-induced circularity

values at 48 hours following treatment (4.9a). LIGHT-treated *Nfkb2*^{-/-} enteroids demonstrated a blunted rounding response compared to LIGHT-treated WT enteroids at similar LIGHT concentrations and time points (4.8 and 4.9b). Across all doses and time courses, the maximal LIGHT-induced circularity obtained in *Nfkb2*^{-/-} enteroids was only 0.41±0.04 at 48 hours following 100 ng/ml LIGHT. This suggests that *Nfkb2*^{-/-} enteroids are more resistant to LIGHT treatment than WT enteroids exposed to the same treatment (figure 4.9b). Comparison of LIGHT-treated WT with LIGHT-treated *Nfkb2*^{-/-} enteroids demonstrated that there were statistically significant differences at 24- and 48-hours following treatment.

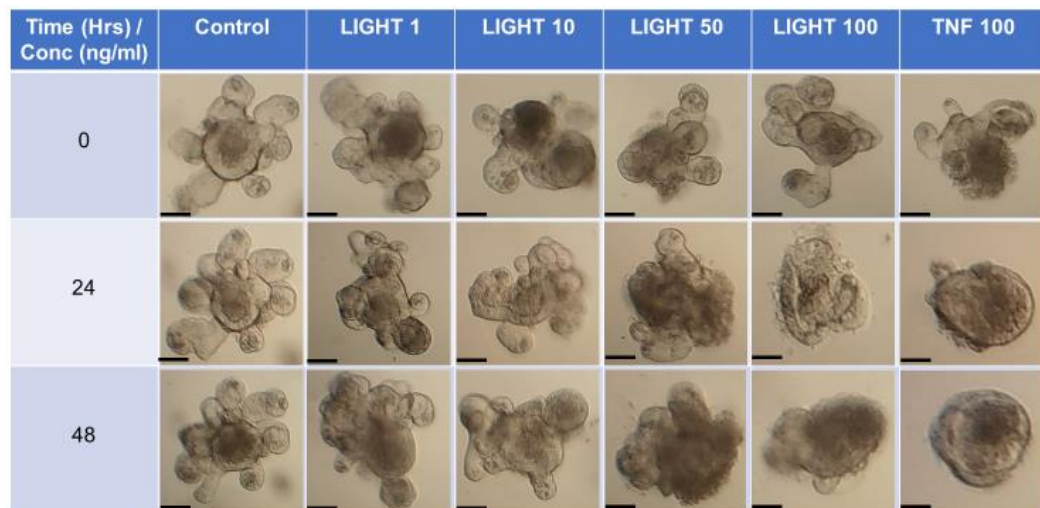


Figure 4.7 LIGHT-treated WT enteroid bright field micrographs. Enteroids were treated with 0, 1, 10, 50 and 100 ng/ml LIGHT. At 0, 24 and 48 hours post-treatment images were recorded. Relative dose-dependent and time-dependent increases in enteroid circularity were noticed. Images were taken at 10x original magnification; scale bars, 100 μ m.

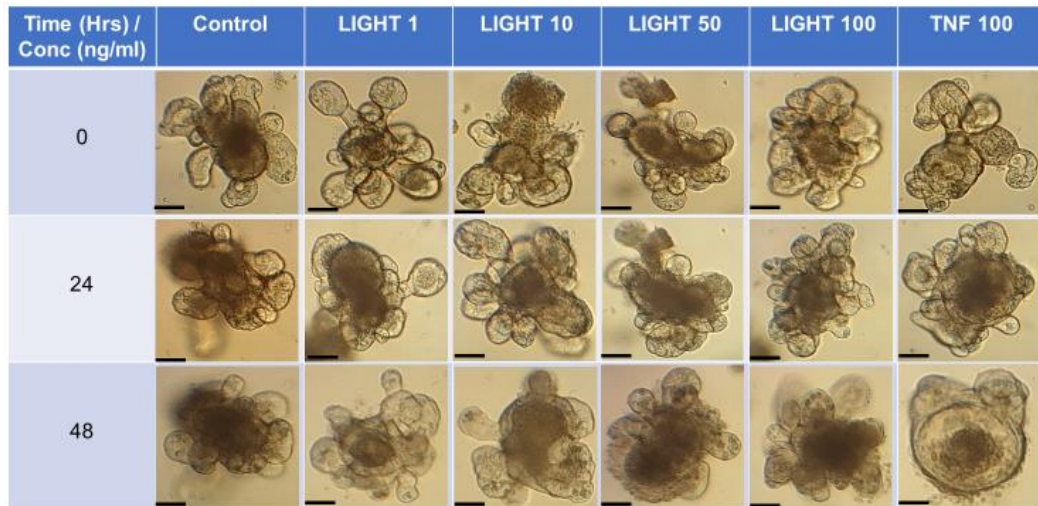


Figure 4.8 Bright field images of LIGHT-treated *Nfkb2*^{-/-} enteroids. LIGHT concentrations of 0, 1, 10, 50 and 100 ng/ml were used to treat *Nfkb2*^{-/-} enteroids and images were captured at 0, 24 and 48 hours following treatment. Diminished dose-dependent and time-dependent increases in LIGHT-treated *Nfkb2*^{-/-} enteroid circularity can be observed. Images were taken at 10x original magnification; scale bars, 100 μ m.

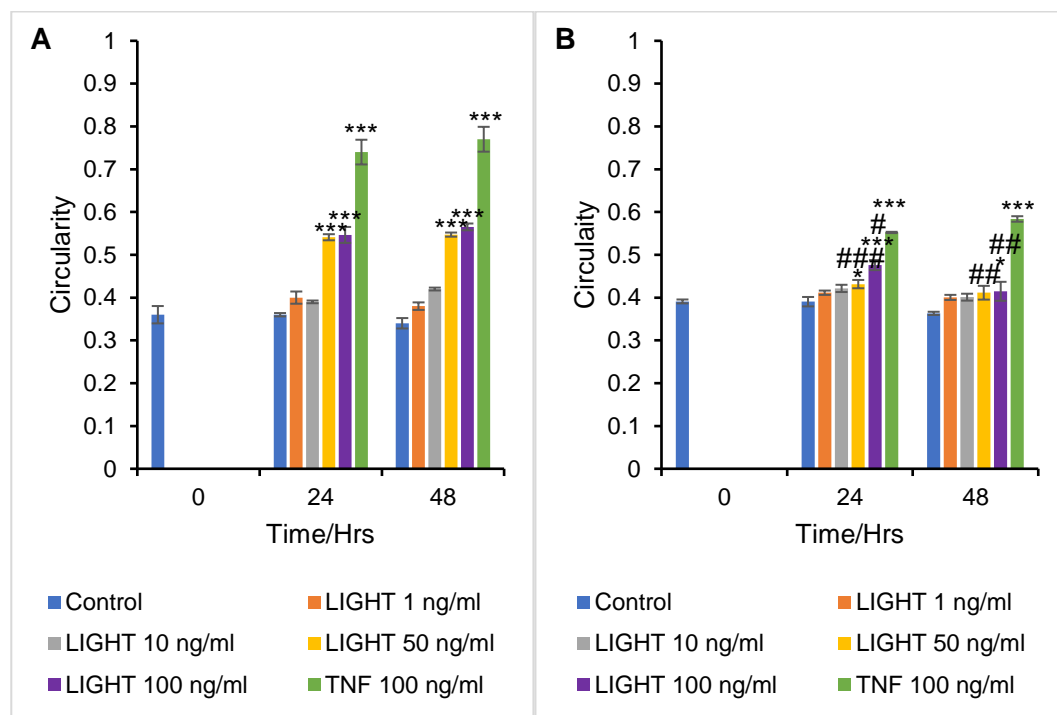


Figure 4.9 LIGHT induced a dose-dependent and time-dependent increase in WT-derived enteroid circularity (A) but diminished responses in circularity in *Nfkb2*^{-/-} enteroids (B) [Control (blue), 1 ng/ml LIGHT (orange), 10 ng/ml LIGHT (grey), 50 ng/ml LIGHT (yellow), 100 ng/ml LIGHT (purple) and 100 ng/ml TNF (green)]. Statistical differences were identified by ANOVA vs control at same time point, P = (* \leq 0.05, ** \leq 0.01, *** \leq 0.001), and statistically significant differences between WT + LIGHT vs *Nfkb2*^{-/-} + LIGHT at the same concentration and time point are shown by (# \leq 0.05, ## \leq 0.01, ### p \leq 0.001), n=6 organoids per treatment group, N=3 independent experiments, error bars with

4.2.4 CD40-L induces moderate morphological changes in WT enteroids but less in *Nfkb2*^{-/-} enteroids

A range of CD40-L concentrations (0, 1, 10, 50, and 100 ng/ml) were similarly used to treat WT mouse intestinal epithelial enteroids for 48 hours. Under static conditions, bright field images were taken at 0, 24, and 48 hours of six individual enteroids in each of 3 independent experiments (n=6, N=3). Dose-dependent and time-dependent increases in rounding in the CD40-L-treated WT enteroid were observed (figures 4.10 and 4.12a). Baseline circularity in untreated WT enteroids was 0.36 ± 0.01 , while at 24 hours following CD40-L treatment, the circularity increased from 0.40 ± 0.03 following 1 ng/ml to 0.55 ± 0.02 following 100 ng/ml CD40-L. There was a similar trend of increased CD40-L-induced circularity values observed 48 hours following CD40-L treatment (4.12a). The degree of rounding caused by CD40-L-treatment of *Nfkb2*^{-/-} enteroids differed from the response observed in CD40-L-treated WT enteroids at the same CD40-L doses and time points (figures 4.11 and 4.12b). *Nfkb2*^{-/-} enteroids reached maximal circularity values across all concentrations and time course of 0.45 ± 0.03 at 48 hours post 100 ng/ml indicating that they were less susceptible than WT enteroids to the effects of CD40-L (figure 4.12b). At 24- and 48-hours following treatment, comparison of CD40-L-treated WT with CD40-L-treated *Nfkb2*^{-/-} enteroids showed that there were statistically significant differences.

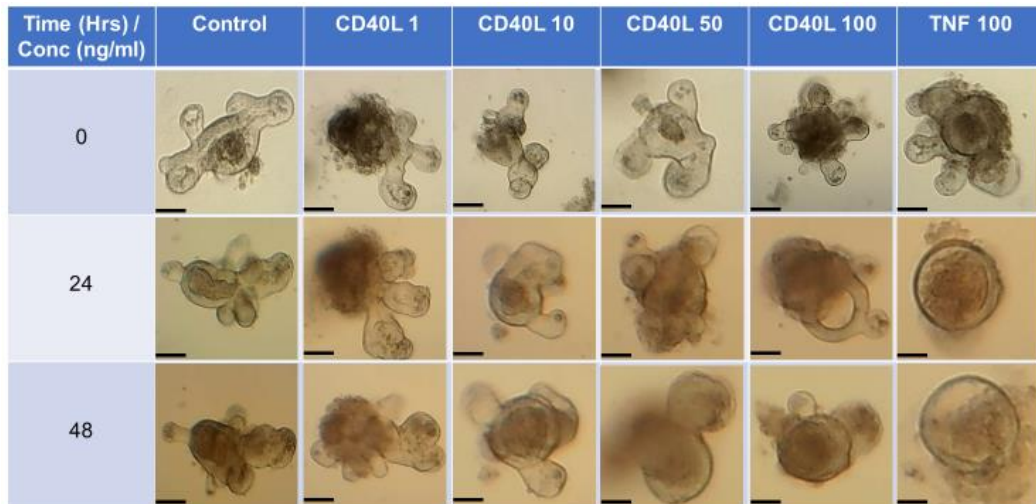


Figure 4.10 Bright field micrographs of CD40L-treated WT enteroids. CD40-L concentrations (0, 1, 10, 50 and 100 ng/ml) were utilised to treat WT enteroids and images were taken at 0, 24 and 48 hours post-treatment. Subtle dose-dependent and time-dependent increases in enteroid circularity were demonstrated. Images were taken at 10x original magnification; scale bars, 100 μ m.

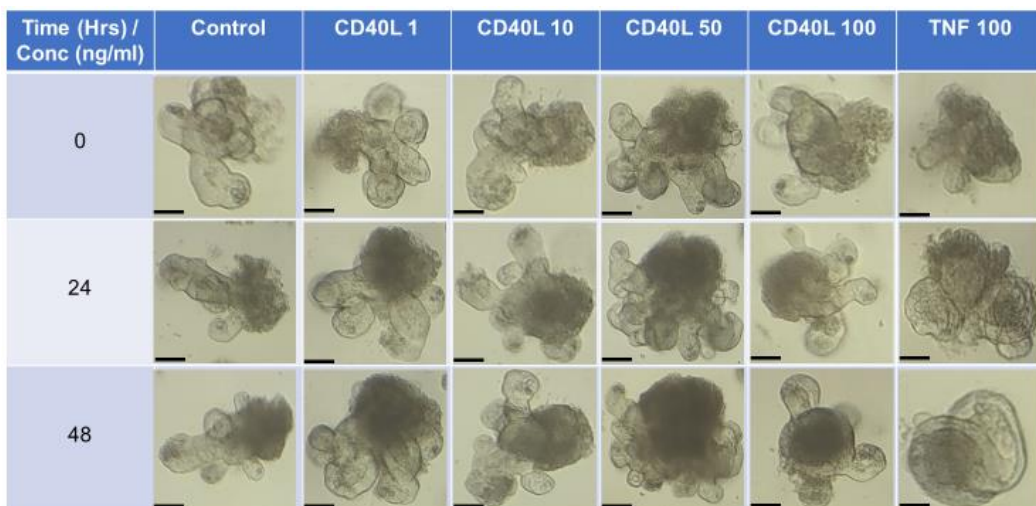


Figure 4.11 Bright field images of CD40-L-treated *Nfkb2*^{-/-} enteroids. Enteroids were treated with 0, 1, 10, 50 and 100 ng/ml CD40-L. At 0, 24 and 48 hours following treatment with CD40-L images were captured. No significant dose-dependent and time-dependent increases in CD40-L-treated *Nfkb2*^{-/-} enteroid circularity can be discerned. Images were taken at 10x original magnification; scale bars, 100 μ m.

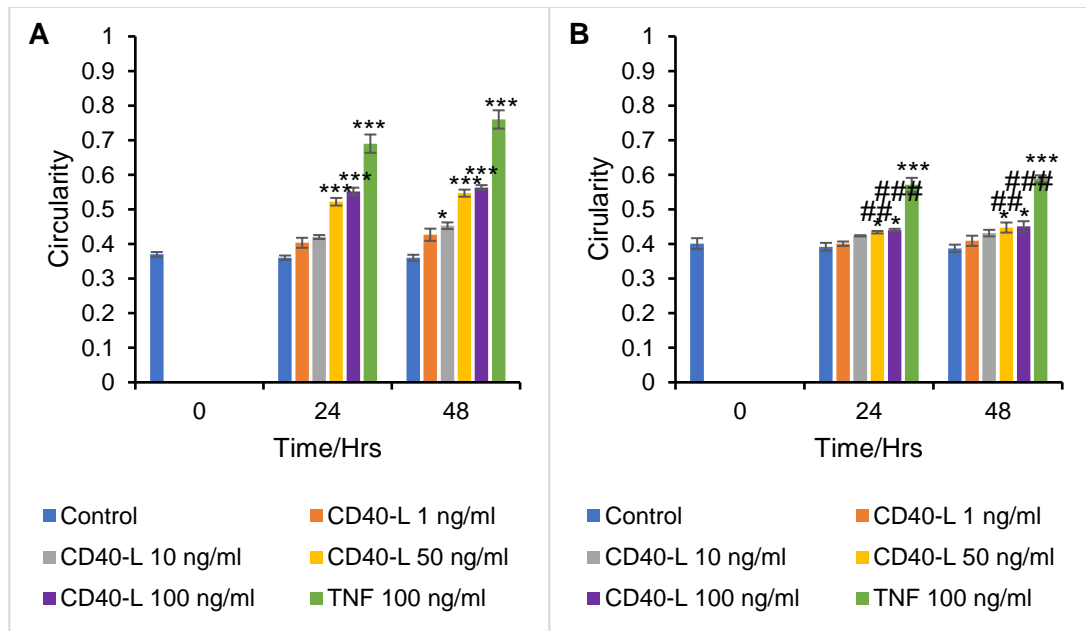


Figure 4.12 CD40-L triggered a dose-dependent and time-dependent increase in WT enteroid circularity (A) more reduced responses in circularity in *Nfkb2*^{-/-} enteroids (B) [Control (blue), 1 ng/ml CD40-L (orange), 10 ng/ml CD40-L (grey), 50 ng/ml CD40-L (yellow), 100 ng/ml CD40-L (purple) and 100 ng/ml TNF (green)]. Statistical differences were identified by ANOVA vs control at same time point, P = (*≤0.05, **≤0.01, ***≤0.001), and statistically significant differences between WT + CD40-L vs *Nfkb2*^{-/-} + CD40-L at the same concentration and time point are shown by (##≤0.01, ###p≤0.001), n=6 organoids per treatment group, N=3 independent experiments, error bars with SEM.

4.2.5 LTα/β slightly regulates WT and *Nfkb2*^{-/-} enteroid phenotype

WT mouse intestinal epithelial enteroids were treated with different LTα/β concentrations (0, 1, 10, 50, and 100 ng/ml) for 48 hours. Using a microscope, bright field images were captured at 0, 24, and 48 hours from six individual enteroids for each of 3 independent experiments (n=6, N=3). LTα/β slightly caused a dose-dependent increase in enteroid rounding (figures 4.13 and 4.15a). Baseline circularity in untreated WT enteroids was (0.40±0.03) and 24 hours following treatment with LTα/β, circularity values gradually increased from 0.43±0.04 following 1 ng/ml LTα/β to 0.48±0.04 following 100 ng/ml LTα/β. In comparison with the control, LTα/β treatment did not induce any statistically significant circularity at 24 hours post-treatment. However, at 48 hours post-LTα/β treatment there was statistically

increased circularity only at the highest concentrations of 50 and 100 ng/ml LT α / β (figure 4.15a). Although LT α / β -treated *Nfkb2*^{-/-} enteroids slightly responded with minimal rounding at 24 hours following treatment, there was no statistically significant difference between the LT α / β -induced responses at 48 hours compared to controls (figures 4.14 and 4.15b). Maximal LT α / β -induced *Nfkb2*^{-/-} enteroid circularity achieved across all doses and time-points was only 0.40 \pm 0.02 at 48 hours post 100 ng/ml LT α / β (figure 4.15) suggesting that this stimulus has little direct impact on damage to the intestinal epithelium. Comparison of LT α / β -treated WT with LT α / β -treated *Nfkb2*^{-/-} enteroids demonstrated that there was significant difference at 48 hours.

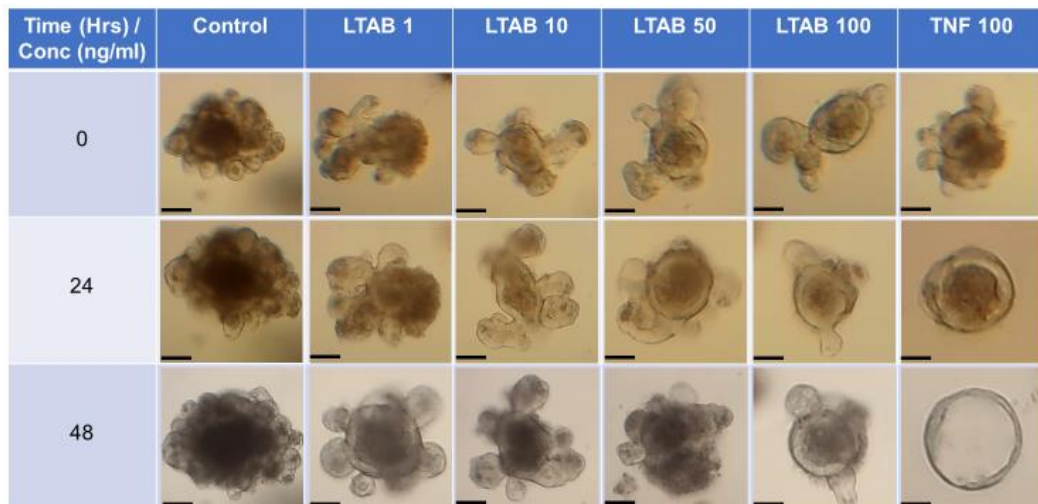


Figure 4.13 Bright field micrographs of LT α / β -treated WT enteroids. Enteroids were treated with 0, 1, 10, 50 and 100 ng/ml LT α / β . At 0, 24, and 48 hours post-treatment various images of the enteroids were recorded. No major dose-dependent and time-dependent increases in enteroid circularity were observed. Images were taken at 10x original magnification; scale bars, 100 μ m.

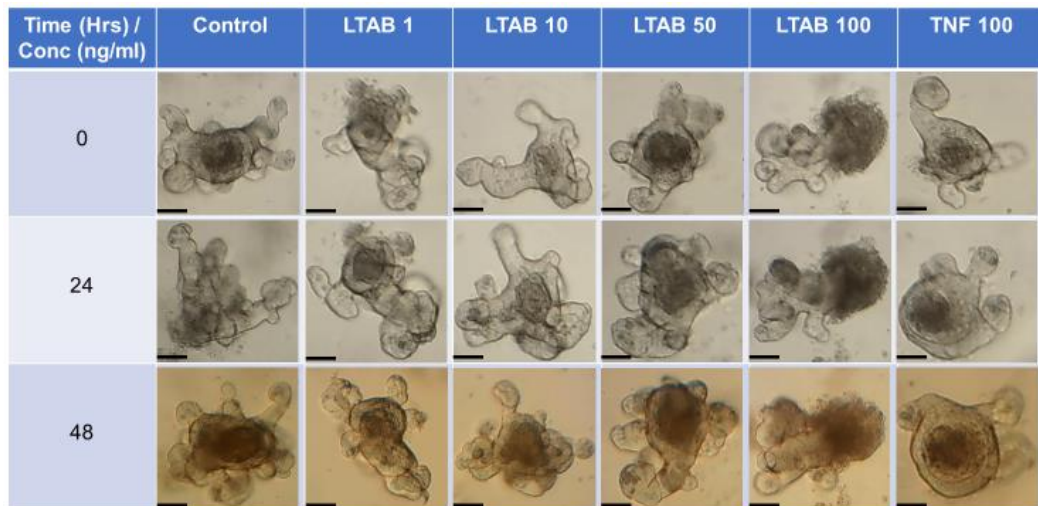


Figure 4.14 Bright field images of LT α / β -treated *Nfkb2*^{-/-} enteroids. Enteroids were treated with 0, 1, 10, 50 and 100 ng/ml LT α / β . At 0, 24, and 48 hours following treatment with LT α / β images were captured. No major significant dose-dependent and time-dependent increases in LT α / β -treated *Nfkb2*^{-/-} enteroid circularity can be discerned. Images were taken at 10x original magnification; scale bars, 100 μ m.

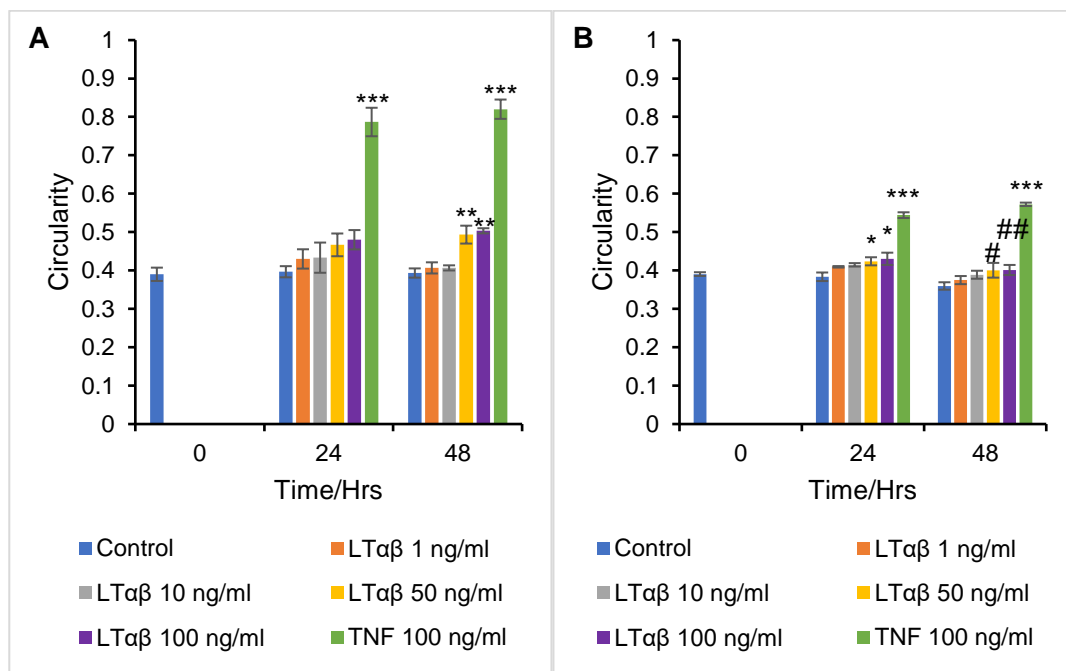


Figure 4.15 LT α / β induces a minor dose-dependent and time-dependent increase in WT-derived enteroids circularity (A) and slightly appreciable responses in circularity in *Nfkb2*^{-/-} enteroids (B) [Control (blue), 1 ng/ml LT α / β (orange), 10 ng/ml LT α / β (grey), 50 ng/ml LT α / β (yellow), 100 ng/ml LT α / β (purple) and 100 ng/ml TNF (green)]. Statistical differences were identified by ANOVA vs control at same time point, P = (* \leq 0.05, ** \leq 0.01, *** \leq 0.001), and statistically significant differences between WT + LT α / β vs *Nfkb2*^{-/-} + LT α / β at the same concentration and time point are shown by (ns = not significant, # \leq 0.05, ## p \leq 0.01), n=6 organoids per treatment group, N=3 independent experiments, error bars with SEM.

4.2.6 BAFF does not modulate a major WT or *Nfkb2^{-/-}* enteroid morphology

In our previous study (Jones et al 2019), IFN γ stimulated enteroid rounding that was blunted in *Nfkb2^{-/-}* enteroids but the mechanism responsible for this remains intriguing and elusive. As IFN γ is known to stimulate BAFF production (Lundell et al., 2017) and BAFF is a known NF κ B alternative pathway activator, we wanted to determine whether BAFF had a direct effect on enteroids that may partially explain the protection of *Nfkb2^{-/-}* enteroids from IFN γ . BAFFR is normally expressed on immune cell populations and less is known about its expression/potential to be expressed following stimulation on intestinal enterocytes. Our broad-spectrum proteomic analysis (Chapter 5) did not enrich for cell surface receptors and BAFFR was not detected, however, this may have been due to assay sensitivity. We therefore treated WT mouse intestinal epithelial enteroids with different BAFF concentrations (0, 1, 10, 50, to 100 ng/ml) for 48 hours to determine whether BAFF caused any morphological effects on WT enteroids. Bright field micrographs were obtained at 0, 24, and 48 hours from six individual enteroids for each of 3 independent experiments (n=6, N=3). BAFF induced a minor dose-dependent increase in enteroid rounding (figures 4.16 and 4.18a). The baseline circularity value in untreated WT enteroids was 0.36 ± 0.00 and 24 hours following BAFF treatment when compared with control, there was no remarkable increase in circularity values from the lowest concentration of 1 ng/ml BAFF (0.41 ± 0.02) to the highest concentration of 100 ng/ml BAFF (0.49 ± 0.05). Similarly, there was no significant increase in BAFF-induced circularity values at 48 hours post-treatment (Figure 4.18a). There were minor significant differences in circularity between WT and BAFF-treated *Nfkb2^{-/-}* enteroids. BAFF doses and time points tested (figure 4.17 and 4.18b). *Nfkb2^{-/-}* enteroids achieved maximal circularity across all doses and time-points of only 0.45 ± 0.01 at 48 hours following 100 ng/ml BAFF suggesting that BAFF has a minimal effect on the rounding of WT or *Nfkb2^{-/-}*

enteroids at the doses and time-points tested (figure 4.18b). At 24- and 48- hours following treatment, comparison of BAFF-treated WT with BAFF-treated *Nfkb2*^{-/-} enteroids did not demonstrate any statistical significance.

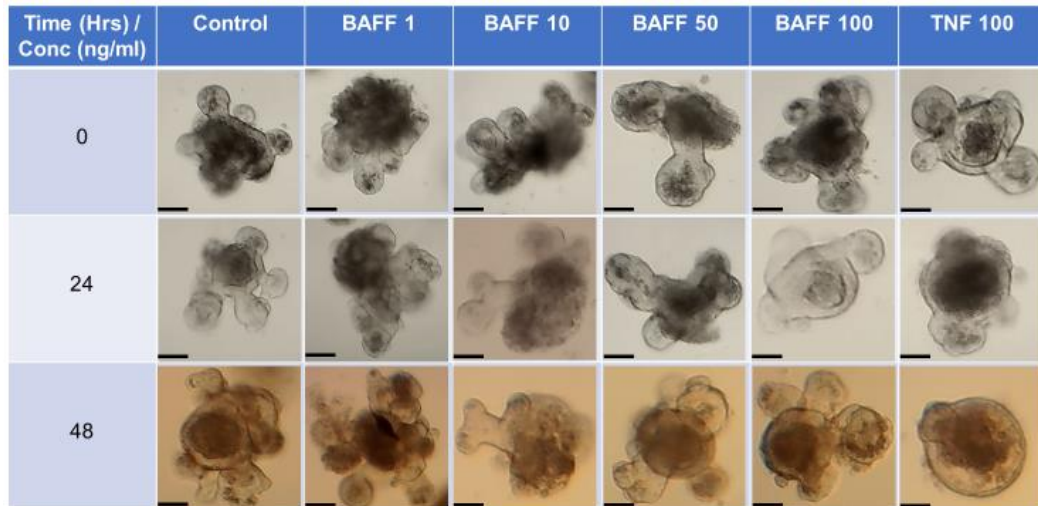


Figure 4.16 Bright field images of BAFF-treated WT enteroids. Enteroids were treated with 0, 1, 10, 50 and 100 ng/ml BAFF. At 0, 24, and 48 hours following treatment several images of the enteroids were captured. BAFF induced minor dose-dependent and time-dependent increases in enteroid circularity. Images were taken at 10x original magnification; scale bars, 100 μ m.

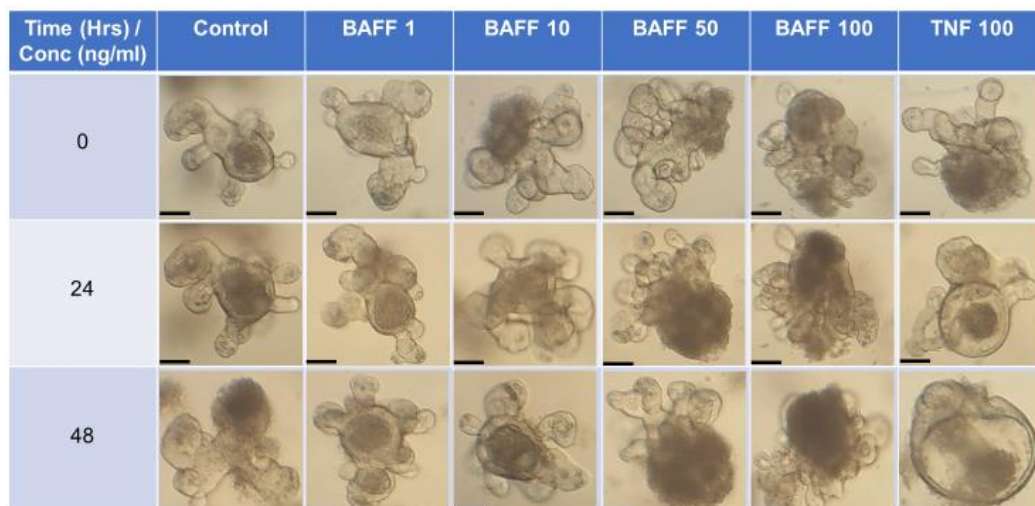


Figure 4.17 Bright field micrographs of BAFF-treated *Nfkb2*^{-/-} enteroids. Enteroids were treated with 0, 1, 10, 50 and 100 ng/ml BAFF. At 0, 24, and 48 hours following treatment with BAFF images were taken. No major significant dose-dependent and time-dependent increases in BAFF-treated *Nfkb2*^{-/-} enteroid circularity were observed. Images were taken at 10x original magnification; scale bars, 100 μ m.

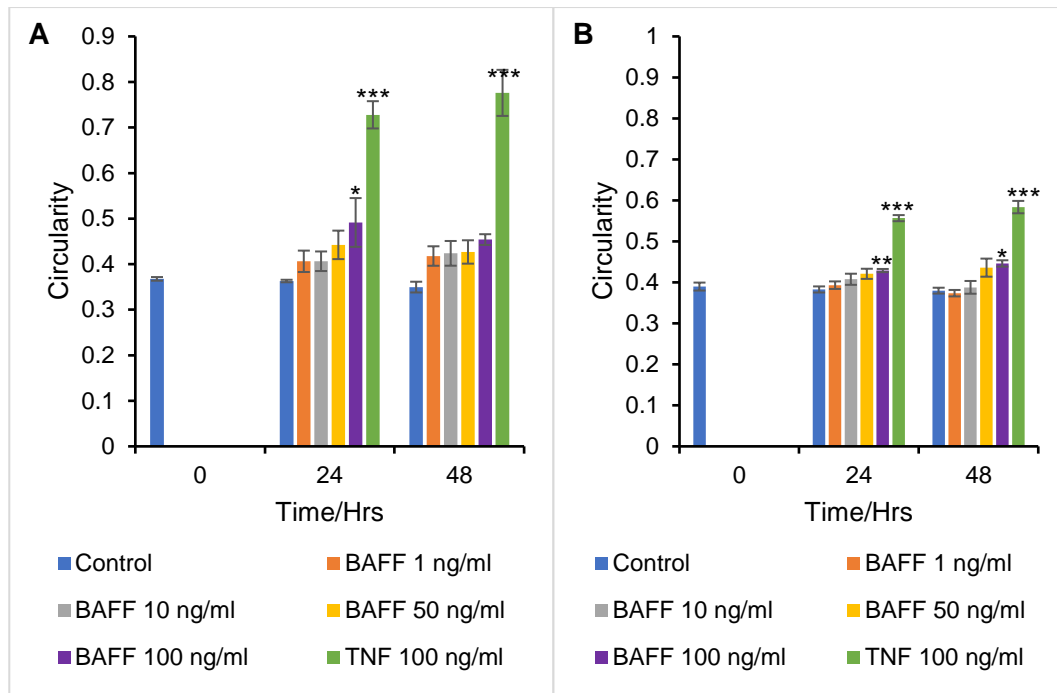


Figure 4.18 BAFF caused a minimal dose-dependent increase in WT-derived (A) and *Nfkb2*^{-/-} (B) enteroid circularity [Control (blue), 1 ng/ml BAFF (orange), 10 ng/ml BAFF (grey), 50 ng/ml BAFF (yellow), 100 ng/ml BAFF (purple) and 100 ng/ml TNF (green)]. Statistical differences were identified by ANOVA vs control at same time point, P = (* \leq 0.05, ** \leq 0.01, *** \leq 0.001), and statistically significant differences between WT + LT α / β vs *Nfkb2*^{-/-} + LT α / β at the same concentration and time point are not significant, n=6 organoids per treatment group, N=3 independent experiments, error bars with SEM.

4.2.7 TNF and TWEAK have additive effects on WT enteroid morphology

As TNF and TWEAK both independently stimulated increased enteroid circularity, but mostly at concentrations at the higher end of the pathological concentrations observed in humans, we wanted to determine whether reduced amounts of these cytokines in combination would have an additive effect on inducing enteroid circularity. WT mouse enteroids were therefore treated with various concentrations of both TNF and TWEAK in combination (0, 1, 10, 50, and 100 ng/ml) for 48 hours. Under static conditions, bright field images were taken at 0, 24 and 48 hours of six individual enteroids from each of 3 independent experiments (n = 6, N = 3). WT enteroids showed dose- and time-dependent increases in circularity with various combinations of TWEAK and TNF, some of which were at lower concentrations than

those observed in experiments where the cytokines were added alone (figures 4.19 and 4.20). Untreated WT enteroids had a baseline circularity of 0.37 ± 0.00 which was similar to all previous studies above. Following 24 hours of treatment with each cytokine in equal quantities measured in ng/ml, circularity values were 0.39 ± 0.02 (1 ng/ml), 0.54 ± 0.00 (10 ng/ml), 0.72 ± 0.01 (50 ng/ml) and 0.77 ± 0.02 (100 ng/ml). A similar trend was observed at 48 hours post treatment (figure 4.2). Enteroids treated with 10 ng/ml TNF and 10 ng/ml TWEAK had statistically significantly increased circularity compared to enteroids treated with 10 ng/ml of each cytokine alone. The mean difference in circularity between 10 ng/ml each of TWEAK and TNF compared to 10 ng/ml TWEAK was 0.05 ± 0.04 ($p = 0.05$) at 24 hours post treatment and 0.12 ± 0.05 ($p = 4.9 \times 10^{-3}$) at 48 hours post-treatment. Similarly, the mean difference in circularity between 10 ng/ml each of TWEAK and TNF and 10 ng/ml TNF alone were 0.08 ± 0.08 ($p = 0.11$) at 24 hours and 0.17 ± 0.06 ($p = 0.02$) at 48 hours post-treatment.

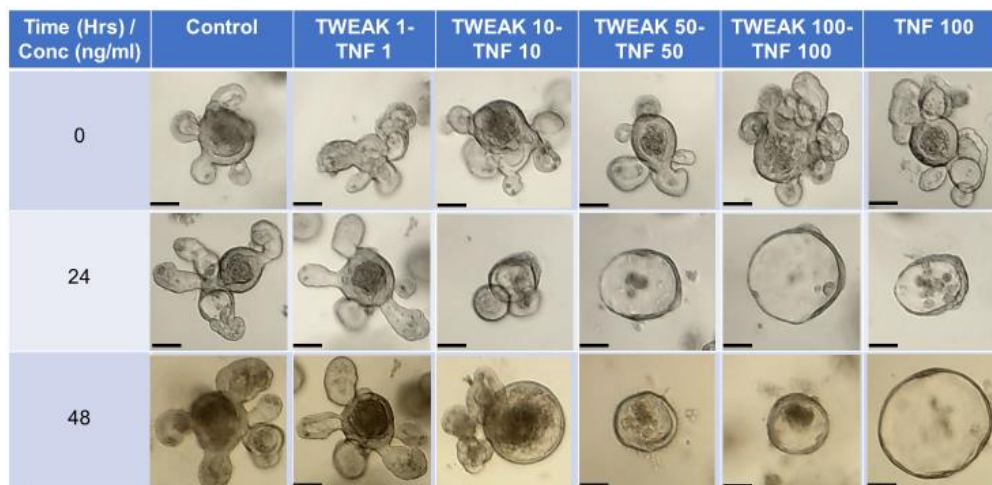


Figure 4.19 Bright field images of TWEAK-TNF-treated WT enteroids. Enteroids were treated with 0, 1, 10, 50 and 100 ng/ml each of TWEAK and TNF. At 0, 24, and 48 hours following treatment several images of the enteroids were obtained. TWEAK-TNF induces marked increase in dose-dependent and time-dependent increases in enteroid circularity values. Images were taken at 10x original magnification; scale bars, 100 μ m.

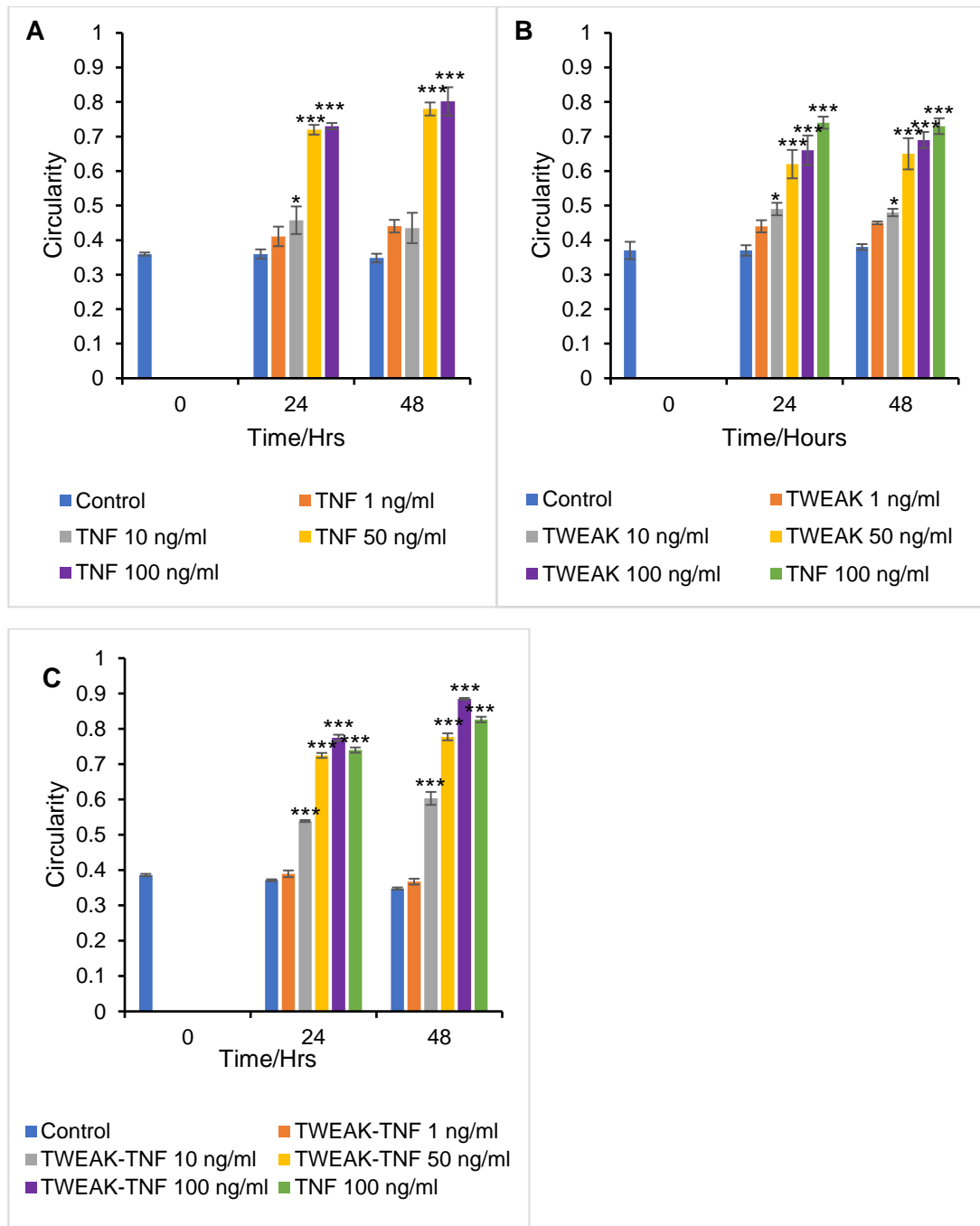


Figure 4.20 TWEAK-TNF causes a dose-dependent increase in WT enteroids circularity. The dose of combined 10 ng/ml each of TWEAK and TNF (C) induced a significant increase in circularity compared to individual TNF (A) or TWEAK (B) doses of the same concentration at 48 hours post-treatment. Statistical differences were identified by ANOVA vs control at same time point, $P = (*\leq 0.05, **\leq 0.01, ***\leq 0.001)$, $n=6$ organoids per treatment group, $N=3$ independent experiments, error bars with SEM.

4.2.8 Other cytokines: IL-6 induced major increase in circularity of WT but reduced in *Nfkb2*^{-/-} enteroids

When WT enteroids were reconstituted with LPS-activated bone-marrow-derived-dendritic cells, enteroids underwent circularity changes similarly to enteroids treated with 100 ng/ml (Jones et al., 2019). However, when a panel of cytokines were assayed from the enteroid media, the concentration of TNF was lower than that necessary to induce the observed circularity changes suggesting that another cytokine may contribute to enteroid damage. IL-6 was the most abundant cytokine detected (Jones et al., 2019). We therefore assessed the effects of IL-6 on enteroid circularity in addition to the panel of alternative pathway NFκB activators, as increased concentrations of this cytokine are often found in conditions that cause elevated circulating TNF concentrations. WT enteroids were therefore treated with different IL-6 concentrations (0, 1, 10, 50 and 100 ng/ml) for 48 hours. Under static conditions, bright field images were taken at 0, 24, and 48 hours of six individual enteroids each of from 3 independent experiments (n=6, N=3). A dose-dependent and time-dependent increase in circularity was quantified in IL-6-treated WT enteroids (figures 4.21 and 4.23a). Untreated WT enteroids displayed a baseline circularity of 0.39 ± 0.03 . Enteroids treated with IL-6 showed dose-dependent increases in circularity by 24 hours post-treatment which were 0.42 ± 0.03 (1 ng/ml), 0.43 ± 0.05 (10 ng/ml), 0.57 ± 0.05 (50 ng/ml), and 0.63 ± 0.04 (100 ng/ml). TNF (100 ng/ml) was used as a positive rounding control and showed a circularity of 0.72 ± 0.01 at 24 hours which was greater than the degree of circularity generated by IL-6 at the same dose and time-point. Similar trends continued to be observed in enteroids at the 48-hour time point. IL-6-treated *Nfkb2*^{-/-} enteroids did not respond with the same degree of rounding that was observed in IL-6-treated WT enteroids (figure 4.22). They exhibited a blunted response to IL-6 treatment (figure 4.23b). Untreated *Nfkb2*^{-/-} enteroids had a baseline circularity of 0.40 ± 0.01 and at 24 hours post-treatment

showed a maximum circularity of 0.49 ± 0.01 following 100 ng/ml which was significantly lower than the circularity observed in WT enteroids given the same dose of IL-6 (0.63 ± 0.04) and time. The blunted circularity response of *Nfkb2*^{-/-} enteroids to IL-6 continued at 48 hours post-treatment. Comparison between IL-6-treated WT with IL-6-treated *Nfkb2*^{-/-} enteroids demonstrated that there were statistically significant differences at 24- and 48-hours following treatment.

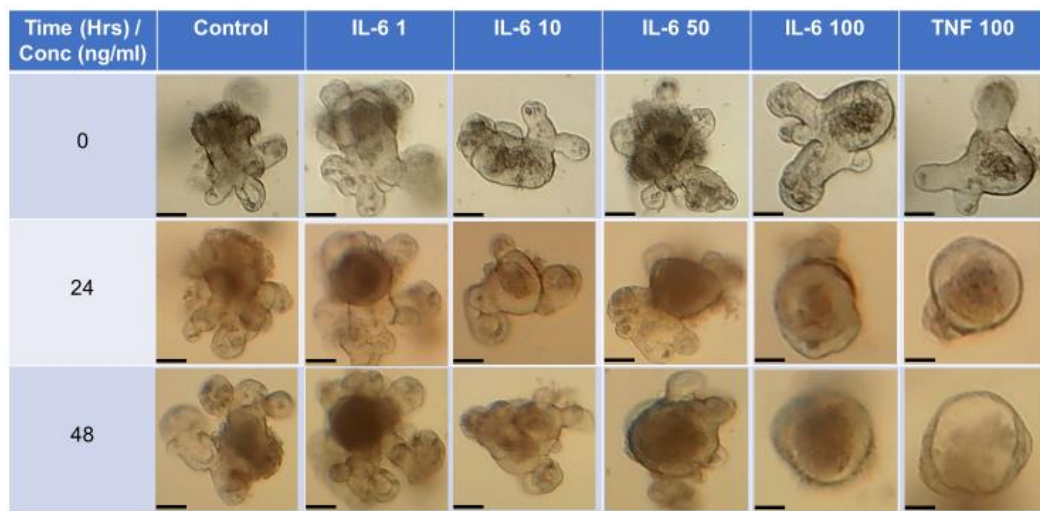


Figure 4.21 Bright field images of IL-6-treated WT enteroids. Enteroids were treated with 0, 1, 10, 50 and 100 ng/ml IL-6. Images were taken at 0, 24, and 48 hours post-IL-6 treatment. Marked dose-dependent and time-dependent increases in enteroid circularity were demonstrated. Images were taken at 10x original magnification; scale bars, 100 μ m.

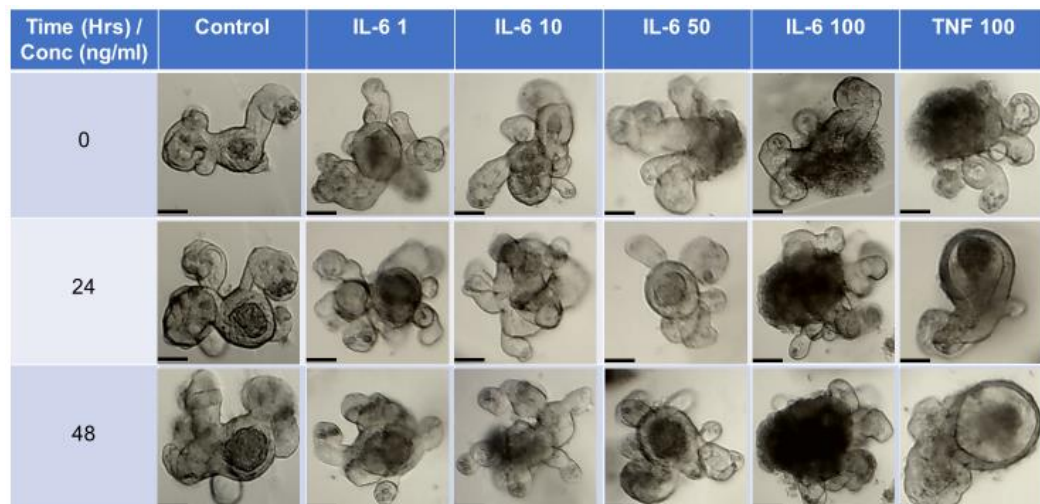


Figure 4.22 Bright field micrographs of IL-6-treated *Nfkb2*^{-/-} enteroids. Enteroids were treated with 0, 1, 10, 50 and 100 ng/ml TNF and images were collected at 0, 24, and 48 hours following treatment as indicated. Blunted dose-dependent and time-dependent increases in TNF-treated *Nfkb2*^{-/-} enteroid circularity can be discerned. Images were taken at 10x original magnification; scale bars, 100 μ m.

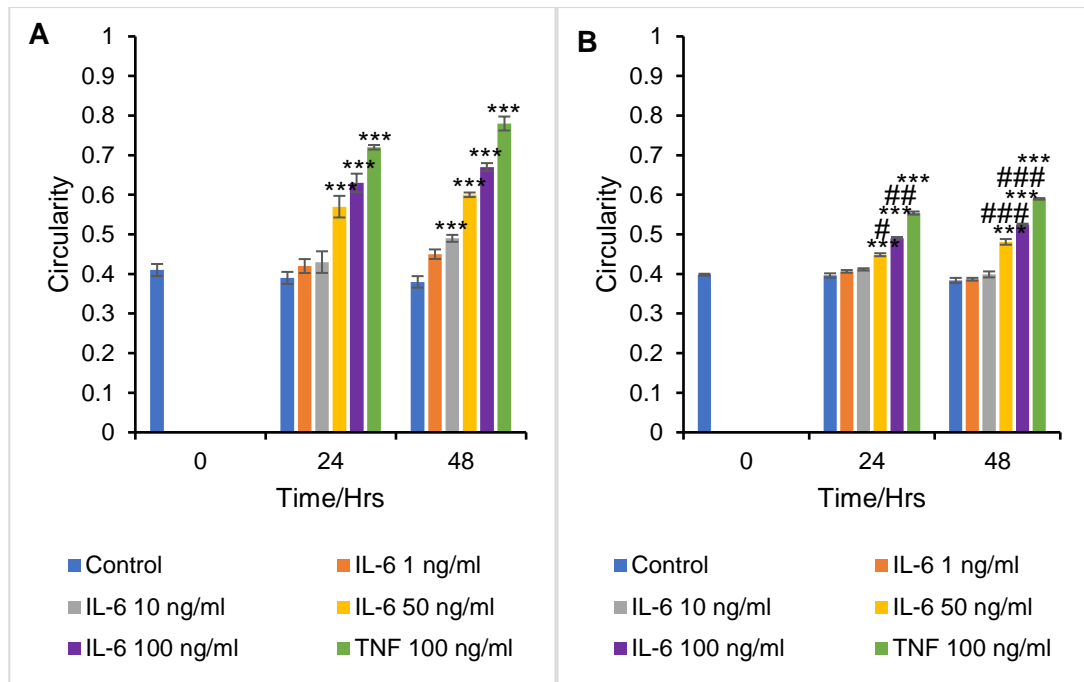


Figure 4.23 IL-6 caused a dose-dependent and time-dependent increase in WT-derived enteroid circularity (A) which was suppressed in *Nfkb2*^{-/-} enteroids (B) [Control (blue), 1 ng/ml IL-6 (orange), 10 ng/ml IL-6 (grey), 50 ng/ml IL-6 (yellow), IL-6 (purple), and 100 ng/ml TNF (green)]. Statistical differences were identified by ANOVA vs control at same time point, P = (*≤0.05, **≤0.01, ***≤0.001), and statistically significant differences between WT + IL-6 vs *Nfkb2*^{-/-} + IL-6 at the same concentration and time point are shown by (#≤0.05, ##≤0.01, ###≤0.001), n=6 organoids per treatment group, N=3 independent experiments, error bars with SEM.

4.2.9 Summary of action of alternative pathway activators

Different actions of the alternative pathway activators on WT and *Nfkb2*^{-/-} enteroids are tabulated below (table 4.3).

Cytokines	WT enteroids	<i>Nfkb2</i> ^{-/-} enteroids
TNF	↑↑↑↑	↑
TWEAK	↑↑	↑
LIGHT	↑↑	↑
CD40-L	↑	↑
LTαβ	↑	-
BAFF	↑	-
IL-6	↑↑↑↑	↑

Table 4.3 A summarise table of different rounding responses of WT and *Nfkb2*^{-/-} enteroids to treatment of various cytokines. TNF induces the highest rounding while LTαβ and BAFF stimulated the least in enteroids at both 24 and 48 hours.

4.3 Discussion

TNF, TWEAK, LIGHT, CD40-L, LT $\alpha\beta$, and BAFF are TNF superfamily members with alternative pathway NF κ B activation properties. Members of the TNF superfamily and IL-6 are proinflammatory cytokines. Most of the alternative pathway activators in our study induced rounding in WT intestinal epithelial enteroids derived from the proximal small intestine of mice, while none of them exerted the same degree of rounding in *Nfkb2*^{-/-} enteroids. We showed a hierarchical effect of the TNF superfamily on circularity of WT enteroids with TNF having the greatest and BAFF the least effect. The extent of TNF superfamily-induced circularity of WT enteroids decreased in the order TNF, TWEAK, LIGHT, CD40-L, LT $\alpha\beta$ and BAFF. By contrast, in the *Nfkb2*^{-/-} enteroids the hierarchical effects of TNF superfamily-induced circularity were not applicable as a blunted response to enteroid rounding in *Nfkb2*^{-/-} enteroids compared to WT enteroids administered the same treatment was observed. This finding of relative resistance to morphological changes caused by *Nfkb2* deletion was previously reported in enteroids treated with TNF and IFN γ (Jones et al., 2019 and in chapter 3 of this thesis) and in dextran sulphate sodium (DSS) treated *Nfkb2*^{-/-} mice in our lab (Burkitt et al., 2015).

Enteroid rounding is associated with apoptosis, cell shedding, cell death, loss of villus domains and loss of epithelial thickness (Jones et al., 2019 and Duckworth et al. unpublished). Enteroid rounding results from the accumulation of fluid in the enteroid lumen; this may correspond to a clinical feature often seen prior to diarrhoea or increased intestinal motility. Increased fluid accumulation in the small intestine has also been observed following systemic LPS injection into mice (Williams et al., 2013) suggesting that similar mechanisms are observed *in vivo* and in enteroids *in vitro*. TWEAK was previously thought to exclusively activate the alternative NF κ B signalling pathway (Armstrong et al., 2016) however in renal epithelial junctional protein expression perturbation, TWEAK has been implicated in the activation of canonical

NF κ B pathway (Berzal et al., 2015). Previous studies reported that TWEAK was up-regulated in Crohn's disease and played a major role in mediating Crohn's-like ileitis and intestinal inflammation via multiple innate and adaptive cellular pathways in experimental animals (Di Martino et al., 2019). The elevated concentration of TWEAK detected in serum during traumatic brain injury has also been associated with the severity of inflammatory response, morbidity, mortality, and clinical outcome index (Tang et al., 2019). It is not clear from previous whole organism studies however whether TWEAK has a direct effect on the intestinal epithelium to modulate cellular dynamics. We were able to isolate the epithelium from other cellular compartments using enteroids to address the direct impact of TWEAK on epithelial cells alone. Similarly, to the increased circularity induced by TNF, TWEAK induced rounding of WT murine enteroids, but with a lesser degree of potency than that caused by TNF, suggesting that TWEAK has a direct effect on the intestinal epithelium. The combination of TWEAK and TNF treatment in WT enteroids induced more rounding following 10 ng/ml each of TNF and TWEAK and was greater than the circularity induced by either TNF or TWEAK alone. This finding demonstrates that *in vivo* there may be a complex milieu of cytokines that regulate the damage response of the intestinal epithelium and the tissue concentration of individual cytokines may exert damaging effects at significantly lower concentrations than single cytokines or combinations of a small number of cytokines *in vitro*.

LIGHT signals lymphotoxin beta receptor (LT β R) to mediate many proinflammatory responses, progression of DSS-induced colitis, autoimmune encephalomyelitis, systemic sclerosis, multiple myeloma, and severity of inflammation-related diseases (Brunetti et al., 2018; Gindzienska-Sieskiewicz et al., 2019; Mana et al., 2103). However, LIGHT signalling through the receptor of herpes virus entry mediator (HVEM) had a protective effect against DSS-induced colitis in mouse models (Giles et al., 2018). LIGHT signalling is therefore context and tissue dependent. Our results

showed that LIGHT induced rounding of WT enteroids, though this was greatly blunted in *Nfkb2*^{-/-} enteroids suggesting that LIGHT damages the intestinal epithelium and that alternative pathway NF-κB signalling is important for LIGHT-induced pathology in this tissue. CD40 is present on the surfaces of non-immune (epithelial, platelets, endothelial and mesenchymal) and immune (B cells, monocytes, macrophages and dendritic cells) cells (Schonbeck & Libby, 2001). CD40 combines with CD40L to trigger a complex signalling pathway that involve activation of TNF receptors and stimulation of ERK-1/2, p38 and JNK resulting in activation and translocation of transcription factors (NFκB, activator protein 1 (AP-1) and nuclear factor of activated T-cells (NFAT)) to induce inflammatory conditions including IBD (Danese, Sans & Fiocchi, 2004; Grammer & Lipsky, 2001). Many studies have reported that CD40-L is expressed by activated T-cells and via CD40 acts on B cells to mediate cell proliferation, survival, inflammation, thrombosis, oxidative stress, and differentiation (Jabati et al., 2018; Lai et al., 2019; Rizvi et al., 2008). Sathawane and colleagues in their mouse tumour model reported that CD40 had a dual functionality because they observed that lower expression levels of CD40/CD40-L promoted tumour growth while higher expression levels of CD40/CD40-L were associated with tumour regression (2013). In our study, CD40-L induced a moderate rounding response in treated WT mouse enteroids and this may suggest that interaction of CD40 with CD40-L plays an important role in the epithelial cell-specific immunomodulation. Portillo and colleagues reported the functional importance of how simultaneous stimulation of mouse macrophages via CD40 and TNF activation resulted in up-regulation of inducible nitric oxide synthase (NOS2) and nitric oxide production which play prominent roles in proinflammatory production and hyperinflammatory response (Portillo et al., 2012).

LTαβ did not induce any rounding effect on the WT enteroids at 24 hours post-treatment, the minimal rounding response it induced on WT enteroids was only

observed at 48 hours post-treatment. Previous studies have shown that $LT\alpha\beta$ signalling through $LT\beta$ receptor mediated regulatory control of inflammation, cell proliferation, survival, immune response, apoptosis, and differentiation (Bauer et al., 2012; Shen et al., 2017). $LT\alpha\beta$ therefore has little direct impact on the intestinal epithelium, but its effects could be exerted indirectly by modulating intestinal immune responses. Clinically, BAFF plays a significant role in immunostimulatory modulation and deficiency or impairment of BAFF function has been associated with reduced immunoglobulin production and development of immunodeficiencies (Sakai & Akkoyunlu, 2017; Vincent et al., 2013). Damage to lung epithelia has been demonstrated by the $IFN\gamma$ induction of BAFF (Kato et al., 2006) and we therefore wanted to address whether this alternative pathway NF κ B activator was important in directly regulating intestinal epithelial damage. BAFF induced minimal rounding of WT or *Nfkb2*^{-/-} enteroids during the experimental time course at all doses investigate suggesting that BAFF is not an important direct regulator of the intestinal epithelial damage response. In a previous study using a co-culture of bone marrow-derived dendritic cells with enteroids, we determined that secreted factors from LPS activated dendritic cells induced increased enteroid circularity. Interestingly, the concentration of TNF produced from activated dendritic cells was not high enough to generate the observed circularity increases alone, but we identified that IL-6 in the supernatant of LPS activated dendritic cells was in great abundance (43967.35 ± 4220.72 pg/ml) (Jones et al., 2019). We therefore conducted IL-6 dose-response and time-course studies on enteroids. IL-6 induced enteroid circularity, but to a lesser extent than that observed following TNF treatment and this effect was blunted following *Nfkb2* deletion. This suggests that the combination of TNF and IL-6 may have caused increased enteroid circularity when LPS activated bone marrow-derived dendritic cells were previously co-cultured with enteroids. These two cytokines are also major players in the pathogenesis of IBD, rheumatoid arthritis, sepsis and other inflammatory diseases (Koss et al., 2000; Matsumoto et al., 2018). Various studies

have reported that patients with active IBD presented with highly increased serum concentrations of IL-6 and inflamed intestinal mucosa exhibited several IL-6-positive mesenchymal cells on tissue biopsies (Mudter & Neurath, 2007; Reinisch et al., 1999). The combined inhibition of TNF, IL-6 and NF κ B2 signalling may therefore show added efficacy in IBD and sepsis therapy and warrants further investigation.

The results presented in this chapter indicate the important role alternative NF κ B pathway activators play in health and disease especially during sepsis and IBD (Tak & Firestein, 2001). Further interrogation of the mechanisms involved in the susceptibility of WT enteroids to the effects of alternative pathway activators and resistance of *Nfkb2*^{-/-} enteroids to the alternative NF κ B pathway activators maybe a gateway to understanding the pathogenesis, progression, and prognosis of sepsis and the development of directed therapeutics against it. Various receptors (BAFFR, LT β r and others) play prominent roles in binding with the alternative NF κ B pathway activators (Vincent et al., 2013; Shen et al., 2017) but the degree of accessibility and activation by ligands warrant further investigations.

5 Mechanisms by which TNF may modulate enteroid morphology and dynamics

5.1 Introduction

In studies presented in chapters 3 and 4 under both dynamic and static conditions, we reported morphological changes and behavioural patterns of enteroids induced by NFκB signalling pathway activators. We also previously reported in chapter 3 that TNF treated WT and TNF treated *Nfkb2*^{-/-} enteroids demonstrated different morphological responses. WT enteroids rounded in the presence of TNF whereas this response was blunted in *Nfkb2*^{-/-} enteroids, suggesting that the deletion of *Nfkb2* in mice confers protectivity against TNF-induced injury in the small intestinal epithelium. Several additional TNF superfamily members were also shown to alter enteroid morphology, indicating that this phenotype is not unique to TNF and suggesting that some of the downstream signalling that occurs following receptor ligation and NFκB activation may be similar.

TNF is widely recognised to activate both classical and alternative NFκB signalling pathways to perpetuate or inhibit inflammation. Several publications have utilised animal models to demonstrate that perturbation of the classical NFκB signalling pathway specifically in the intestinal epithelium modulates the response to inflammatory stimuli (Gebert et al., 2020; Han et al., 2018; Mikuda et al., 2020). We have also demonstrated that signalling via alternative NFκB pathway activation is important in regulating the intestinal epithelial response to injury (chapters 3 and 4 and Jones et al., 2019). TNF stimulation of *Nfkb1*^{-/-} enteroids resulted in a similar degree of rounding compared to enteroids derived from WT jejunum (Jones et al., 2019), suggesting that *Nfkb1* itself either confers protectivity that could not be demonstrated at the time points and doses of TNF selected or that there is functional

redundancy with other classical NFκB signalling pathway members within intestinal epithelial cells (Jones et al., 2019). However, global knockout of *Nfkb1* increased the susceptibility of *Nfkb1*^{-/-} mice to experimental colitis (Burkitt et al., 2015; Williams et al., 2013) and radiation-induced intestinal mucositis (Burkitt et al., 2017; Wang et al., 2004), suggesting that there is a complex interplay between different tissue compartments such as intestinal immune cells and the intestinal epithelium.

We therefore wanted to interrogate the possible mechanisms responsible for the blunted effects of TNF on *Nfkb2*^{-/-} enteroids and the potential alterations in the intestinal epithelial-specific proteome that occur when various different NFκB family members have been deleted. This will allow an increased understanding of how the NFκB family of transcription factors modulates the intestinal epithelium under homeostatic conditions and under inflammatory stress present during IBD and sepsis.

Proteomics is a vast field and it combines computational algorithms and modern mass spectrometry to study the dynamics of functional and static proteins (Graves & Haystead, 2002). It enables a thorough study of proteins in a system at the translational level. To date, no studies have been conducted to determine how TNF impacts the enteroid proteome, however, several broad-spectrum proteomic analyses of the intestinal mucosa under inflammatory conditions have been described (Han et al., 2013). These studies have used either human intestinal mucosa from pinch biopsies, resected intestinal tissue (M'Koma et al., 2011; Starr et al., 2017) or mucosal scrapes from the murine intestine (Jensen et al., 2017; Sotillo et al., 2017) which all contain multiple cell types in addition to epithelial cells. Mixed cell populations can make proteomic analysis difficult to interpret, as it is unclear as to whether inflammatory mediators modulate the proteome of immune, mesenchymal stromal cells or epithelial cells and whether changes in the proteome of specific cell types are direct or indirect consequences of interaction with these mediators. The

intestinal enteroid system is a culture system that contains purely epithelial cells and has been shown to have consistent cellular dynamics and degrees of differentiation with the intestine *in vivo*. We have therefore determined the direct impact of a defined cytokine specifically on the epithelium using enteroids and a broad-spectrum proteome analysis approach.

5. 2 Results

5.2.1 There are differences in the intestinal epithelial proteome following *Nfkb* modulation

Intestinal epithelial enteroids were cultured from *Nfkb1*^{-/-}, *Nfkb2*^{-/-} and *c-Rel*^{-/-} transgenic and wild type mice. Due to anticipated baseline differences in epithelial protein expression between different transgenic enteroid lines, comparative analyses of protein profiles for the resting murine transgenic enteroids against the proteome of resting WT enteroids was first conducted (Figures 5.1). We identified around 5000-6000 different proteins from each enteroid sample. From comparison of the untreated WT enteroids against untreated *Nfkb1*^{-/-} enteroids, there were only 3 (43%) proteins that were significantly up-regulated and 4 (57%) that were significantly down-regulated. We are not sure what could be responsible for the small difference we observed between untreated WT and *Nfkb1*^{-/-} enteroids, probably due to redundancy, variability in sample preparation for proteomic analysis or limitation of the lysing buffer we used. The comparison of untreated *Nfkb2*^{-/-} with untreated WT-derived enteroids yielded 52 significantly differentially regulated proteins of which 27 (52%) were upregulated and 25 (48%) were down-regulated. When untreated *c-Rel*^{-/-} enteroids were compared against WT enteroids, 36 significantly differentially regulated proteins were detected, of which 14 (39%) were up-regulated and 22 (61%) were down-regulated (figure 5.1). These data indicate that whilst enteroids derived from *Nfkb1*^{-/-}

, *Nfkb2*^{-/-} and *c-Rel*^{-/-} proximal small intestine look morphologically alike at baseline (chapter 4 and Duckworth unpublished), subtle changes in their proteome can be identified using our broad-spectrum proteomic approach.

Several of these differentially regulated proteins may contribute to the background susceptibility of the intestinal epithelium to cytokine induced damage and therefore contribute to IBD and sepsis severity. For example, Regenerating islet-derived protein 4 (Reg4) was up-regulated in *Nfkb1*^{-/-}, *Nfkb2*^{-/-} and *c-Rel*^{-/-} enteroids. Reg4 is known to be epithelial cell-derived and is upregulated in the human intestinal mucosa during active ulcerative colitis and following remission (Planell et al., 2013). ATP-binding cassette sub-family G member 5 (*Abcg5*) and *H2-m2* were both down-regulated in *Nfkb1*^{-/-}, *Nfkb2*^{-/-} and *c-Rel*^{-/-} enteroids. *Abcg5* is an intestinal transporter implicated in the regulation of fat digestion and absorption and may therefore modulate the intestinal luminal environment resulting in different susceptibilities of the intestinal epithelium to damage. A protein that was exclusively up-regulated in *Nfkb1*^{-/-} enteroids was alcohol dehydrogenase 4 (*Aldh4*) which is implicated in the formation of retinoic acid from retinol and contributes to maintaining normal morphology. Down-regulated proteins found exclusively in *Nfkb1*^{-/-} enteroids were cytochrome b-245 light chain, which is required for efficient microbicidal activity and alcohol dehydrogenase 6 (*Adh6a*). H-2 class II histocompatibility antigen and transcription factor RelB, and ubiquitin-like protein *Isg15* proteins were commonly up-regulated in *Nfkb2*^{-/-} and *c-Rel*^{-/-} enteroids, suggesting that these enteroids have altered immune regulation and show potential compensatory increases in other major NFkB family members. Regenerating islet-derived protein 3-gamma (Reg3) protein was over-expressed in *Nfkb2*^{-/-} but under-expressed in *c-Rel*^{-/-} enteroids, which could potentially account for some of the protectivity against epithelial injury observed in *Nfkb2*^{-/-} enteroids, but not in other transgenic enteroid lines. Reg3 is a protective factor in experimental colitis and is induced by propionate (shown to confer

protectivity in inflammatory GI experimental models) in intestinal organoids (Bajic et al., 2020; Shin et al., 2019). Therefore, at baseline there are several proteins that are known to be expressed in intestinal epithelia that may regulate the response of the epithelium to damage-inducing stimuli via direct or indirect mechanisms.

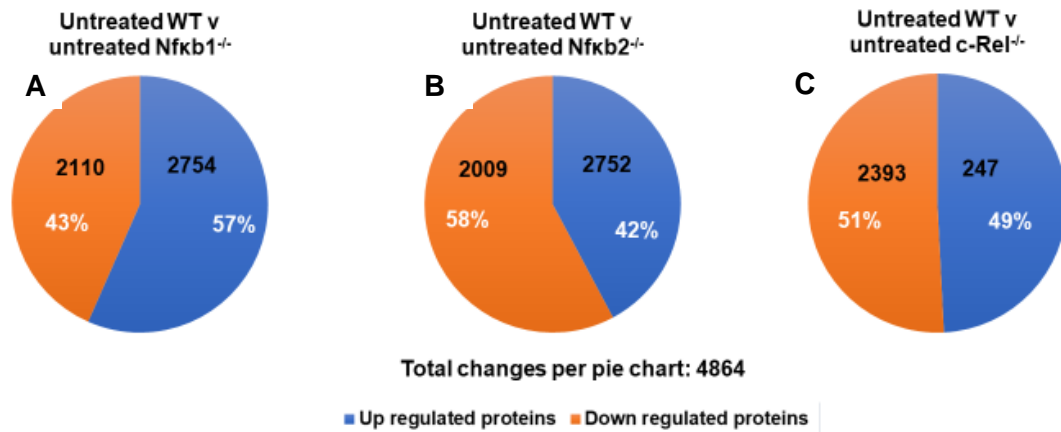


Figure 5.1 Pie charts representing the total number of quantified proteins that were up- (blue) and down- (orange) regulated in untreated *Nfkb1*^{-/-}, *Nfkb2*^{-/-} and *c-Rel*^{-/-} enteroids when compared with untreated WT enteroids. The comparison of multiple means was tested by student t-test, N = 4.

5.2.2 There are changes in the enteroid proteome following TNF treatment

Resting murine WT enteroids had total number of 5770 quantified proteins and following treatment with TNF 50 ng/ml for 24 hours, we demonstrated that 173 of these proteins were significantly up-regulated and 117 were significantly down-regulated (figure 5.2A). We detected 5646 proteins in untreated murine *Nfkb1*^{-/-} enteroids. Twenty-four hours post-treatment with 50 ng/ml TNF, we detected 55 proteins that were significantly upregulated and 73 that were significantly down regulated (figure 5.2B). Untreated *Nfkb2*^{-/-} proximal small intestinal-derived enteroids showed a total number of 5951 detected proteins. Following 24 hours treatment with 50 ng/ml TNF, 266 proteins were significantly up-regulated and 91 were significantly down-regulated (figure 5.2C). The total number of proteins detected in unstimulated *c-Rel*^{-/-} enteroids was 5411. Following 24 hours of treatment with 50 ng/ml TNF, 28

proteins were significantly up-regulated and 26 were significantly down-regulated (figure 5.2D). Ubiquitin-like protein (interferon-stimulated gene 15 ubiquitin-like modifier, (ISG15)) protein was the most significantly upregulated protein in TNF treated WT vs untreated WT enteroids (3.23-fold change and p-value 5.89×10^{-4}), *Nfkb1*^{-/-} (1.24 and 1.99×10^{-3}) *Nfkb2*^{-/-} (1.97 and 0.03) and *c-Rel*^{-/-} (1.61 and 0.02). Isg15 has been implicated in IBD and colon cancer and it is also responsible for chemotaxis of neutrophils (Zuo et al., 2016). Isg15 up-regulation by TNF could therefore potentially contribute to the enhanced motility we observed in TNF-treated enteroids (chapter 3) and is worth further exploration. Our findings of upregulated Isg15 were supported by the previously reported by Isg15 signature and upregulation in the proteome-wide mass spectrometry of mouse experiment (Ballegeer et al., 2018).

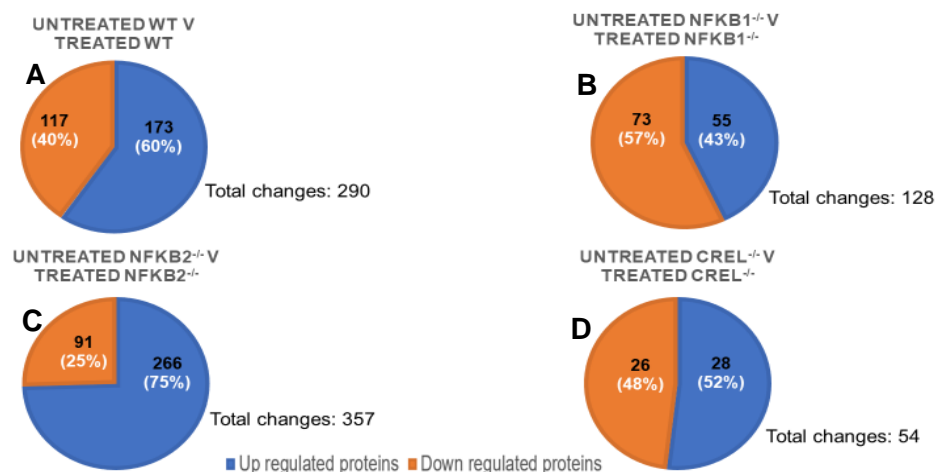


Figure 5.2 Pie charts showing that the total significantly up-regulated and down-regulated proteins in murine WT, *Nfkb1*^{-/-}, *Nfkb2*^{-/-} and *c-Rel*^{-/-} enteroids following 24 hours treatment with TNF 50 ng/ml in comparison respectively with untreated WT, *Nfkb1*^{-/-}, *Nfkb2*^{-/-} and *c-Rel*^{-/-} enteroids of the same strains were 290, 128, 357 and 54 respectively. The comparison of multiple means was tested by student t-test, N = 4.

5.2.3 TNF alters the abundance of NF-κB signalling pathway components in enteroids

Alternative NFκB signalling pathway protein markers were identified in WT enteroids and we were interested in knowing whether they were also expressed in enteroids

derived from the other transgenic mouse strains (figure 5.3). Transcription factor RelB expression was significantly increased in all the four strains of enteroids following TNF treatment, suggesting that this alternative NFκB pathway regulator is important in regulating the intestinal epithelial response to TNF. Reassuringly, NF-κB2 p100 and p52 subunits were significantly up-regulated in WT, *Nfkb1*^{-/-} and *c-Rel*^{-/-} enteroids following TNF treatment, but were not detected in *Nfkb2*^{-/-} enteroids. There was no detection of inhibitor of nuclear factor kappa-B kinase subunit epsilon (*Ikbke*) in *c-Rel*^{-/-} or *Nfkb1*^{-/-} enteroids, however, it was significantly up-regulated in *Nfkb2*^{-/-} and WT enteroids. *Ikbke* regulates inflammatory processes, immune system, cell proliferation, growth and cancer progression and invasion (Boehm et al., 2007; Lu et al., 2017). Therefore, we hypothesise that *Ikbke* regulation could play a major role in the restrictive activity of TNF-treated *Nfkb2*^{-/-} enteroids.

Strains	FC_A	PV_A(-log10)	FC_B	PV_B(-log10)	FC_C	PV_C(-log10)
WT	Green	Green	Orange	Green	Orange	Green
<i>Nfkb1</i> ^{-/-}	Green	Green	Orange	Green	Red	Red
<i>Nfkb2</i> ^{-/-}	Orange	Green	Red	Red	Orange	Green
<i>c-Rel</i> ^{-/-}	Yellow	Green	Orange	Green	Red	Red
Genes	RelB	RelB	Nfκb2	Nfκb2	Ikbke	Ikbke

Figure 5.3 Heat map of alternative pathway protein markers of untreated versus 24-hour 50 ng/ml TNF-treated *Nfkb1*^{-/-}, *Nfkb2*^{-/-} and *c-Rel*^{-/-} intestinal epithelial enteroids. Fold change (FC) and p-value (PV) of various detected proteins were analysed; green colour highest and red indicated lowest value, t-test, upregulated protein values ranged from $p \leq 1.0 \times 10^{-7}$ - $\leq 1.0 \times 10^{-5}$, (N = 4).

5.2.4 TNF modulates the crypt and villus proteome

TNF treatment *in vivo* causes a biphasic apoptotic response with structural changes and increased apoptosis occurring at the small intestinal villus tip within hours and later onset apoptosis being observed in the crypt at around 24 hours. We therefore wanted to assess whether there were any differences in the profile of proteins normally associated with the crypt and villus domains in enteroids following TNF treatment. Crypt domain protein markers were identified in TNF treated WT enteroids

and their fold change was determined compared to untreated enteroids (table 5.1 and appendix C). We also determined whether there were any expression changes within these crypt domain proteins in *Nfkb1*^{-/-}, *Nfkb2*^{-/-} and *c-Rel*^{-/-} enteroids treated with TNF versus untreated enteroids of the same genotype. Telomerase protein component 1 (Tep1), integrin beta-1, group XIIB secretory phospholipase A2-like protein, and cytosolic phospholipase A2 proteins were all significantly up-regulated by TNF in the four (WT, *Nfkb1*^{-/-}, *Nfkb2*^{-/-}, and *c-Rel*^{-/-}) enteroid genotypes, suggesting that TNF is important for their up-regulation, but deletion of components of the NF-κB signalling pathways did not modulate their expression. Bone morphogenetic protein 3 (Bmp3), calcium-independent phospholipase A2-gamma, RNA-binding protein Musashi homolog 2, and olfactomedin-4 were upregulated in WT, *Nfkb1*^{-/-}, and *Nfkb2*^{-/-} but down-regulated in *c-Rel*^{-/-} enteroids following TNF treatment. These differences in protein regulation suggests that there may be an altered stem cell niche within the *c-Rel*^{-/-} intestinal epithelium, as these proteins are all differentially expressed in crypt stem cells. BMP3 down-regulation is observed in 89% of human colon cancers (Loh et al., 2008) and *c-Rel*^{-/-} mice are more susceptible to the experimental induction of colon tumours (Burkitt et al., 2015). Group XIA secretory phospholipase A2 (Pla2g12a) was not expressed in WT but was over-expressed in *Nfkb1*^{-/-} and *c-Rel*^{-/-} and down-regulated in *Nfkb2*^{-/-} enteroids following TNF treatment. Phospholipase is involved in the breakdown of arachidonic acid into fatty acid and the mediation of inflammation (Rouault et al., 2003). The downregulation of Pla2g12a in *Nfkb2*^{-/-} enteroids may therefore partly explain why the response to TNF treatment in *Nfkb2*^{-/-} enteroids and mice is attenuated.

WT (treated v untreated)				Expressions in genotypes (treated vs untreated)		
Protein names	Gene names	Fold change	p-value	<i>Nfkb1</i> ^{-/-}	<i>Nfkb2</i> ^{-/-}	<i>c-Rel</i> ^{-/-}
Telomerase protein component 1	Tep1	1.18	2.27 x 10⁻⁴	↑	↑	↑
Integrin beta-1	Itgb1	1.15	4.01 x 10⁻⁴	↑	↑	↑
Group XIIB secretory phospholipase A2-like protein	Pla2g12b	1.25	1.14 x 10⁻³	↑	↑	↑
Bone morphogenetic protein 3	Bmp3	1.11	0.01	↑	↑	↓
Calcium-independent phospholipase A2-gamma	Pnpla8	1.09	0.06	↑	↑	↓
RNA-binding protein Musashi homolog 2	Msi2	1.04	0.16	↑	↑	↓
Cytosolic phospholipase A2	Pla2g4a	1.04	0.43	↑	↑	↑
Olfactomedin-4	Olfm4	1.04	0.88	↑	↑	↓
Ephrin type-B receptor 2	Ephb2	-1.08	0.19	↑	↓	↑
RNA-binding protein Musashi homolog 1	MSi1	-	-	↑	↑	-
Group XIIA secretory phospholipase A2	Pla2g12a	-	-	↑	↓	↑

Table 5.1 Crypt domain protein markers from untreated versus 24-hour 50 ng/ml TNF-treated WT, *Nfkb1*^{-/-}, *Nfkb2*^{-/-} and *c-Rel*^{-/-} enteroids. Proteins detected are indicated by none (-), upregulated (↑), downregulated (↓) and statistically significantly upregulated (↑) or down-regulated (↓) t-test, $p \leq 1.0 \times 10^{-4} - 0.05$, (N = 4).

In addition to crypt domain-associated proteins, villus domain protein markers were also identified in WT enteroids at baseline and following TNF treatment. We also wanted to determine whether there were any differences in expression between WT and *Nfkb1*^{-/-}, *Nfkb2*^{-/-} and *c-Rel*^{-/-} enteroids (table 5.3). Guanylate cyclase activator

2B (Guca2b) was upregulated in all four enteroid genotypes and is known to regulate proliferation, metabolism, barrier function and intestinal tumourigenesis via its interaction with Gucy2c. This interaction now warrants further exploration in inflammation-driven colon cancers (Pattison et al., 2016; 2020). The most abundant protein expressed in intestinal villi is villin-1 (Vil1) and we determined that Vil1 was significantly down-regulated following TNF treatment in enteroids derived from WT, *Nfkb1*^{-/-} and *c-Rel*^{-/-} jejunum, but reassuringly, Vil1 was up-regulated although not significantly in *Nfkb2*^{-/-} enteroids, which corroborates our previous findings that *Nfkb2*^{-/-} enteroids are less susceptible to the effects of TNF than other enteroid lines (table 5.2).

WT (treated v untreated)				Expressions in genotypes (treated v untreated)		
Protein names	Gene names	Fold change	p-value	<i>Nfkb1</i> ^{-/-}	<i>Nfkb2</i> ^{-/-}	<i>c-Rel</i> ^{-/-}
Guanylate cyclase activator 2B	Guca2b	3.50	5.90 x 10⁻⁸	↑	↑	↑
Alkaline phosphatase, placental-like	Alpl2	1.26	0.04	↑	↓	-
Alpha-actinin-1	Actn1	1.03	0.47	↑	↑	↓
Alpha-actinin-4	Actn4	1.04	0.52	↓	↑	↓
Acid trehalase-like protein 1	Ath1	1.05	0.58	-	↑	-
Supervillin	Svil	1.02	0.64	↓	↑	↑
Alkaline phosphatase	Alpi	1.05	0.72	↓	↓	↑
Alkaline phosphatase	Akp3	1.06	0.76	↑	↓	↑
Villin-1	Vil1	-1.10	1.70 x 10⁻⁵	↓	↑	↓
Trehalase	Treh	-1.12	0.03	↓	↑	↓
Advillin-1	Avil	-	-	↑	↓	-

Table 5.2 Villi domain protein markers from untreated versus 24-hour 50 ng/ml TNF-treated WT, *Nfkb1*^{-/-}, *Nfkb2*^{-/-} and *c-Rel*^{-/-} enteroids. Proteins detected are indicated by none (-), upregulated (↑), downregulated (↓) and statistically significantly up-regulated (↑) or down-regulated (↓) t-test, p ≤ 1.0 x 10⁻⁸ - 0.05, (N = 4).

5.2.5 TNF treatment of enteroids modulates autophagy and apoptosis

Autophagy protein markers were identified in WT intestinal enteroids and we wanted to understand whether they were also expressed by other enteroids that were deficient in NF κ B signalling components (table 5.3). Lysosome-associated membrane glycoprotein 2 (Lamp2) and microtubule-associated proteins 1A/1B light chain 3B (Map1lc3b) were upregulated in all four enteroid lines in response to TNF, suggesting that the degree of autophagy is increased in enteroids following TNF treatment. Map1lc3b (Lc3b-II) has also been shown to be increased in cell line culture and the resultant increase in epithelial monolayer permeability was attributed to the inhibition of autophagic degradation (Zhang et al., 2017). LC3B and LAMP2 are also upregulated in human colonic tumours (Furuta et al., 2001; Niklaus et al., 2017) again suggesting that TNF may induce an intestinal tumour-like phenotype. Bcl-2-like protein 15 (Bcl2l15) is an intestinal-specific pro-apoptotic protein (Coultas et al., 2003; Ozoren et al., 2009) that was down-regulated by TNF in all enteroid strains. This protein also shows reduced expression during malignant transformation in the human gastrointestinal tract (Dempsey et al., 2005). However, small intestinal tumours are rare and constitute only 5% of the GI tumours and about 0.6% of all cancers whilst colonic tumours make up about 95% of GI tumours and about 11% of all cancers (Bray et al., 2018; Neugut et al., 1998). Enteroids are therefore not the best model to investigate intestinal tumourigenesis, nonetheless, several mechanisms that drive epithelial regeneration in homeostasis and in pathogenic conditions are similar in the colon and small intestine and several findings from our enteroid proteome analysis warrant further investigation in colonoid models.

WT (treated v untreated)				Expressions in genotypes (treated v untreated)		
Protein names	Gene names	Fold change	p-value	<i>Nfkb1</i> ^{-/-}	<i>Nfkb2</i> ^{-/-}	<i>c-Rel</i> ^{-/-}
Lysosome-associated membrane glycoprotein 2	Lamp2	1.31	7.14 x 10 ⁻³	↑	↑	↑
Microtubule-associated proteins 1A/1B light chain 3B	Map1lc3b	1.21	0.05	↑	↑	↑
Autophagy-related protein 16-1	Atg16l1	1.03	0.06	↑	↑	↓
Beclin-1	Becn1	1.15	0.05	↑	↑	↓
Bcl-2-like protein 15	Bcl2l15	-1.27	0.02	↓	↓	↓
DNA damage-regulated autophagy modulator protein 2	Dram2	1.16	0.01	↓	↑	↑
Beclin 1-associated autophagy-related key regulator	Atg14	-	-	↓	-	-
Autophagy protein 5	Atg5	-1.03	0.07	↓	↑	↓
Autophagy-related protein 2 homolog B	Atg2b	1.17	0.03	↓	↑	↑
Autophagy-related protein 9A	Atg9a	-	-	↓	↓	↓

Table 5.3 Autophagy protein markers of untreated versus 24-hour 50 ng/ml TNF-treated WT, *Nfkb1*^{-/-}, *Nfkb2*^{-/-} and *c-Rel*^{-/-} enteroids. Proteins detected are indicated by none (-), up-regulated (↑), down-regulated (↓) and statistically significantly upregulated (↑) or down-regulated (↓) t-test, $p \leq 1.0 \times 10^{-3} - 0.05$, (N = 4).

Apoptosis-related proteins were identified in WT enteroids and we wanted to understand whether they were also expressed by enteroids derived from other transgenic mouse strains (table 5.4). Interleukin-1 receptor antagonist protein (Il1rn) was significantly up-regulated in *c-Rel*^{-/-} enteroids and non-significantly up-regulated

in all other enteroid strains treated with TNF. The deletion of *Ii1rn* in mice has previously been shown to result in a reduction of villus height and width and the development of spontaneous IBD (Dosh et al., 2019). Bcl-2-like protein 15 was significantly downregulated in WT, *Nfkb1*^{-/-} and *Nfkb2*^{-/-} enteroids. E3 ubiquitin-protein ligase (XIAP) was downregulated in *Nfkb1*^{-/-} enteroids. Bcl-2-like protein 1 was significantly upregulated in WT and *Nfkb2*^{-/-} enteroids. Bcl-2-associated transcription factor 1 was under-expressed in all the enteroids tested except in WT, where it was overexpressed. Tumour necrosis factor alpha-induced protein 3 (*Tnfaip3*), fas-associated death domain protein (*Fadd*), tumour necrosis factor receptor superfamily member 6 (*Fas*) and caspase-8 (*Casp8*) were significantly upregulated only in *Nfkb2*^{-/-} enteroids. *Tnfaip3* is a regulator of immune cell homeostasis, apoptosis and NFκB activation (Jung et al., 2019; Serramito et al., 2019). Its upregulation in TNF-treated *Nfkb2*^{-/-} enteroids may play a key role in dampening TNF-induced injury observed in this enteroid and murine strain. *Fas* plays a prominent function in regulating cell apoptosis, survival, proliferation and immune response (Siegel et al., 2000). Increased *Fas* expression has been shown previously in murine embryonic fibroblasts (MEFs) deficient in p52 and increased *Fas* expression is thought to protect against spontaneous colon carcinoma development (Liu et al., 2012). These findings could partially explain why *Nfkb2*^{-/-} mice are less susceptible to the induction of colonic tumours by AOM/DSS (Burkitt et al., 2015).

WT (treated v untreated)				Expressions in genotypes (treated v untreated)		
Protein names	Gene names	Fold change	p-value	<i>Nfkb1</i> ^{-/-}	<i>Nfkb2</i> ^{-/-}	<i>c-Rel</i> ^{-/-}
Bcl-2-like protein 1	Bcl2l1	1.16	5.16 x 10⁻³	↓	↑	↑
Caspase-8	Casp8	1.07	0.21	↑	↑	↑
Interleukin-1 receptor-associated kinase 4	Irak4	-1.04	0.10	↓	↑	↑
Bcl-2-like protein 15	Bcl2l15	-1.27	0.02	↓	↓	↓
Apoptosis facilitator Bcl-2-like protein 14	Bcl2l14	-1.02	0.35	↓	↓	↓
Bcl-2-associated transcription factor 1	Bclaf1	1.01	0.82	↓	↓	↓
Bcl-2 homologous antagonist/killer	Bak1	-1.08	0.30	↓	↓	↓
E3 ubiquitin-protein ligase XIAP	Xiap	-1.09	0.18	↓	↓	↓
Bcl-2-like protein 13	Bcl2l13	-1.03	0.46	↓	↓	↓
Interleukin-1 receptor antagonist protein	Il1rn	1.50	0.08	↑	↑	↑
FAS-associated death domain protein	Fadd	-1.09	0.12	↓	↑	↓
Caspase-3	Casp3	-1.07	5.16 x 10⁻³	↓	↑	↓
Caspase-9	Casp9	-1.06	0.07	↓	↑	↓
Bax inhibitor 1	Tmbim6	1.21	0.01	↑	↑	↑
Tumor necrosis factor alpha-induced protein 3	Tnfaip3	-	-	-	↑	-
Tumor necrosis factor receptor superfamily member 6	Fas	-	-	-	↑	-

Table 5.4 Apoptosis-related protein markers of untreated versus 24-hour 50 ng/ml TNF-treated WT, *Nfkb1*^{-/-}, *Nfkb2*^{-/-} and *c-Rel*^{-/-} enteroids. Proteins detected are indicated by none (-), upregulated (↑), downregulated (↓) and statistically significantly upregulated (↑) or down-regulated (↓) t-test, $p \leq 1.0 \times 10^{-3} - 0.05$, (N = 4).

5.2.6 TNF treatment causes perturbations in small intestinal secretory cell populations

Goblet cell protein markers were identified in all enteroid strains and we were interested in knowing if there were any alterations in goblet cell-associated protein abundance with TNF treatment and also as a result of NFκB perturbation. (table 5.5). Endoplasmic reticulum lectin 1 (Erlec1) was significantly up-regulated in *Nfkb1*^{-/-} enteroids with insignificant up-regulations also being observed in *Nfkb2*^{-/-} and *c-Rel*^{-/-} enteroids. Trefoil factor 3 (Tff3) was upregulated in all groups of enteroid following TNF treatment and Mucin-2 (Muc2) was insignificantly upregulated in WT, *Nfkb1*^{-/-} and *C-rel*^{-/-}, but down-regulated in *Nfkb2*^{-/-} enteroids, although these changes did not reach statistical significance. These data suggest that TNF may stimulate goblet cell differentiation in general and the mucous composition in *Nfkb2*^{-/-} enteroids.

WT (treated v untreated)				Expressions in genotypes (treated v untreated)		
Protein names	Gene names	Fold change	p-value	<i>Nfkb1</i> ^{-/-}	<i>Nfkb2</i> ^{-/-}	<i>c-Rel</i> ^{-/-}
Endoplasmic reticulum lectin 1	Erlec1	1.02	0.53	↑	↑	↑
Homeobox protein CDX-2	Cdx2	-1.05	0.39	↑	↑	↑
Trefoil factor 3	Tff3	1.27	0.21	↑	↑	↑
Muc5ac	Muc5ac	-1.31	0.12	↓	↓	↓
Mucin-2	Muc2	1.16	0.30	↑	↓	↑

Table 5.5 Goblet cell protein markers of untreated versus 24-hour 50 ng/ml TNF-treated WT, *Nfkb1*^{-/-}, *Nfkb2*^{-/-} and *c-Rel*^{-/-} enteroids. Proteins detected are indicated by none (-), upregulated (↑), downregulated (↓) t-test and statistically significantly upregulated (↑), p ≤ 0.05, (N = 4).

Paneth cell protein markers were identified in the profiled enteroid proteome and we were interested in determining whether they were modulated by TNF or NFκB perturbation (table 5.6). Matrilysin (Mmp7) was significantly upregulated in the WT, *Nfkb1*^{-/-}, *Nfkb2*^{-/-} and *c-Rel*^{-/-} enteroids suggesting that Paneth cell composition may

be altered following TNF stimulation. Mmp7 has several biological roles, however, it has been implicated in defensin regulation and defensins are abundantly produced by Paneth cells. Tumour necrosis factor receptor type 1-associated DEATH domain protein (Tradd) and alpha-defensin 20 (Defa20) were down-regulated in all the four enteroid genotypes whilst tuftelin-interacting protein 11 (Tfip11) was upregulated in *Nfkb2*^{-/-} but down-regulated in the others; although these changes did not reach statistical significance.

WT (treated v untreated)				Expressions in genotypes (treated v untreated)		
Protein names	Gene names	Fold change	p-value	<i>Nfkb1</i> ^{-/-}	<i>Nfkb2</i> ^{-/-}	<i>c-Rel</i> ^{-/-}
Alpha-defensin 20	Defcr20; Defa20	-1.20	0.51	↓	↓	↓
Alpha-defensin 23	Akp3	-1.21	0.39	↑	↓	↑
Lipopolysaccharide-induced tumor necrosis factor-alpha factor homolog	Litaf	-1.02	0.70	-	↑	-
Matrilysin	Mmp7	1.33	0.17	↑	↑	↑
Angiogenin-4	Ang4	1.56	1.22 x 10 ⁻³	↑	↓	↑
Lysozyme C-1	Lyz1	-1.18	0.09	↑	↓	↓
Serine/threonine-protein kinase	DCLK1	1.10	0.42	-	↓	-
Tumor necrosis factor receptor type 1-associated DEATH domain protein	Tradd	-1.12	0.10	↓	↓	↓
Tuftelin-interacting protein 11	Tfip11	-1.01	0.78	↓	↑	↓

Table 5.6 Paneth cell protein markers of untreated versus 24-hour 50 ng/ml TNF-treated WT, *Nfkb1*^{-/-}, *Nfkb2*^{-/-} and *c-Rel*^{-/-} enteroids. Proteins detected are indicated by none (-), upregulated (↑), downregulated (↓) and statistically significantly upregulated (↑) t-test, $p \leq 1.0 \times 10^{-3}$, (N = 4).

5.2.7 Mechanisms by which TNF may modulate intestinal barrier function

Barrier function and tight junction protein markers were identified in WT intestinal enteroids and we wanted to understand whether they were also expressed by other transgenic enteroid lines (table 5.7). Integrin alpha-2 (Itga2), junctional adhesion molecule A (F11r), claudin-4 (Cldn4), integrin beta-6 (Itgb6), integrin alpha-V (Itgbv), claudin-3 (Cldn3), and neural cell adhesion molecule L1 (L1cam) were upregulated in all the four enteroid genotypes, suggesting that these components are regulated by TNF, but may not require the NfκB signalling components that were deleted in our enteroids for transcription/translation. Interestingly, some of these components not only regulate intestinal tight junctions, but can contribute to the regulation of the intestinal barrier in other ways, such as by modulating the immune function of intestinal epithelial cells (Holmes et al., 2006; Lee & Juliano, 2000). Intercellular adhesion molecule 1 was significantly overexpressed in all enteroid lines except in *Nfkb1*^{-/-} where it was not detected, suggesting that NF-κB1 is required for its transcription/translation. *Nfkb1*^{-/-} enteroids showed reduced expression of cadherin-related family member 5 (Cdhr5) while it was upregulated in all other enteroid lines. Cdhr5 (also known as μ-protocadherin) has a role in regulating osmotic diarrhoea due to microvillus modulation and is down-regulated in human colon cancers (Moulton et al., 2004; Crawley et al., 2014).

WT (treated v untreated)				Expressions in genotypes (treated v untreated)		
Protein names	Gene names	Fold change	p-value	<i>Nfkb1</i> ^{-/-}	<i>Nfkb2</i> ^{-/-}	<i>c-Rel</i> ^{-/-}
Intercellular adhesion molecule 1	Icam1	3.47	1.07 x 10 ⁻⁵	-	↑	↑
Claudin-7	Cldn7	1.04	0.26	↓	↓	↑
Integrin alpha-2	Itga2	1.30	1.03 x 10 ⁻⁴	↑	↑	↑
Junctional adhesion molecule A	F11r	1.43	4.80 x 10 ⁻⁴	↑	↑	↑
Claudin-4	Cldn4	1.76	7.67 x 10 ⁻⁴	↑	↑	↑
Integrin beta-6	Itgb6	1.14	0.03	↑	↑	↑
Integrin alpha-V	Itgav	1.21	8.55 x 10 ⁻⁴	↑	↑	↑
Claudin-3	Cldn3	1.29	9.83 x 10 ⁻⁵	↑	↑	↑
Cadherin-related family member 5	Cdhr5	1.28	1.78 x 10 ⁻³	↓	↑	↑
Claudin-2	Cldn2	1.02	0.85	↑	↓	↑
Claudin-23	Cldn23	1.16	0.04	↑	↓	-

Table 5.7 Barrier function and tight junction protein markers of untreated versus 24-hour 50 ng/ml TNF-treated *c-Rel*^{-/-} intestinal epithelial enteroids. Proteins detected are indicated by none (-), upregulated (↑), downregulated (↓) and statistically significantly upregulated (↑) t-test, $p \leq 1.0 \times 10^{-5} - 0.05$, (N = 4).

5.2.8 Determining the effects of NFκB modulation on the intestinal epithelial response to TNF-induced injury

The proteomes of TNF treated murine WT enteroids were compared with TNF treated *Nfkb1*^{-/-}, *Nfkb2*^{-/-} and *c-Rel*^{-/-} enteroids following the elimination of proteins which showed altered expressions between all enteroid lines at baseline to determine how downstream signalling following TNF is affected by the deletion of individual NF-κB family members. A total of 1239 proteins were significantly differentially regulated across TNF treated *Nfkb2*^{-/-}, *Nfkb1*^{-/-} and *c-Rel*^{-/-} enteroids of which 791 were identified in *Nfkb2*^{-/-}, 464 in *Nfkb1*^{-/-} and 56 in *c-Rel*^{-/-} enteroids (figure 5.4). There were only 8 significantly up-regulated proteins and 4 significantly down-regulated

proteins that were common to all three transgenic enteroid lines. Regenerating islet-derived family member 4 (Reg4) is known to be upregulated in epithelial cells during intestinal inflammation, its deletion confers protectivity against mucosal injury, however, Reg4 also drives the growth of colonic organoids via STAT3 signalling *in vitro* and is thought to regulate the Lgr5+ stem cell niche (Sasaki et al., 2016; Xiao et al., 2019). Different expression levels of Reg4 across different NFκB deficient enteroid lines in response to TNF may potentially regulate their susceptibility to TNF-induced injury. Little is known about B box and SPRY domain-containing protein (Bspry), myoferlin (Myof), Mitochondrial tRNA-specific 2-thiouridylase 1 (Trmu) and Cytoskeleton-associated protein 4 (Ckap4) in the intestinal epithelium, although nuclear expression of Ckap4 is found in most rectal squamous cell carcinomas (Long et al., 2009) and this protein may therefore be implicated in tumourigenesis. *Nfkb2*^{-/-}, *Nfkb1*^{-/-} and *c-Rel*^{-/-} enteroids all demonstrated reduced expression of lithostathine-1 (Reg1) (table 5.8). Reg1 is protective against nonsteroidal anti-inflammatory drug-induced gastrointestinal toxicity and is thought to protect the intestinal epithelial barrier by regulating claudin-3 and -4 expression (Kitayama et al., 2016).

Proteins	Genes	<i>Nfkb1</i> ^{-/-}		<i>Nfkb2</i> ^{-/-}		<i>c-Rel</i> ^{-/-}	
		Fold change	p-value	Fold change	p-value	Fold change	p-value
Regenerating islet-derived protein 4	Reg4	2.40	5.30 x 10⁻⁸	1.87	1.19 x 10⁻³	2.02	5.63 x 10⁻⁴
B box and SPRY domain-containing protein	Bspry	1.31	3.82 x 10⁻⁶	1.28	1.19 x 10⁻⁴	1.27	2.21 x 10⁻⁴
Cytoskeleton-associated protein 4	Ckap4	1.71	9.68 x 10⁻⁵	1.32	5.93 x 10⁻³	1.45	5.82 x 10⁻³
Myoferlin	Myof	2.58	2.82 x 10⁻³	1.82	0.05	1.92	6.89 x 10⁻³
Mitochondrial tRNA-specific 2-thiouridylase 1	Trmu	1.40	8.76 x 10⁻³	1.30	8.70 x 10⁻³	1.42	3.43 x 10⁻³
Arylamine N-acetyltransferase 2	Nat2	1.38	8.93 x 10⁻³	1.38	7.04 x 10⁻⁴	1.39	1.02 x 10⁻³
Ribonuclease pancreatic	Rnase 1	-1.70	6.01 x 10⁻⁵	-1.50	1.73 x 10⁻³	-1.45	1.29 x 10⁻³
Transcription factor RelB	Relb	-1.91	2.08 x 10⁻⁴	-2.08	7.35 x 10⁻⁶	-1.70	2.41 x 10⁻³
Lithostathine-1	Reg1	-3.02	1.36 x 10⁻³	-1.43	3.91 x 10⁻²	-2.33	2.15 x 10⁻²
N-alpha-acetyltransferase 30	Naa30	-1.38	1.22 x 10⁻²	-1.60	5.35 x 10⁻⁵	-1.38	3.98 x 10⁻⁴

Table 5.8 Commonly under- and over-expressed proteins in *Nfkb2*^{-/-}, *Nfkb1*^{-/-}, and *c-Rel*^{-/-} all the three transgenics compared to WT after 24 hours of 50 ng/ml TNF treatment and were individually compared with the 24 hours TNF-treated WT; up-regulated (bold black), down-regulated (bold red), t-test, $p \leq 1.0 \times 10^{-8} - 0.05$.

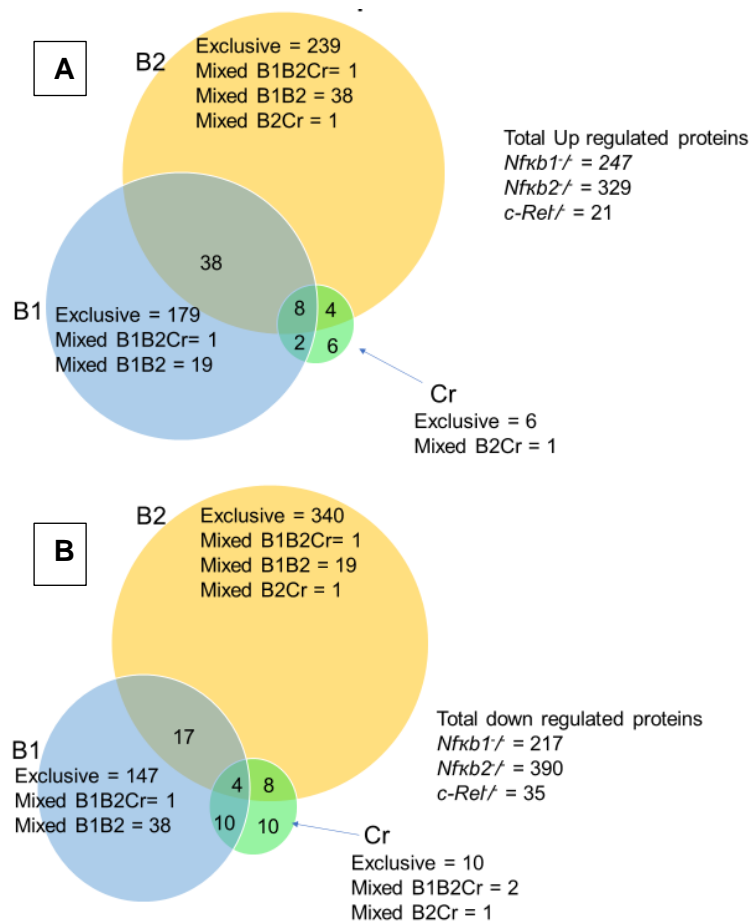


Figure 5.4 Venn diagrams depicting comparisons of significant proteomic changes (up-regulated proteins [A] and down-regulated proteins [B]) between WT and *Nfkb1*^{-/-}, WT and *Nfkb2*^{-/-}, and WT and *c-Rel*^{-/-} enteroids 24 hours following 50 ng/ml TNF treatment. Exclusive indicates proteins only found in that strain while mixed indicates that the same proteins are upregulated in one strain but are downregulated in another strain. B1, B2, and Cr indicate *Nfkb1*^{-/-}, *Nfkb2*^{-/-}, and *c-Rel*^{-/-} respectively. Of the up-regulated proteins, 8 were common among the three transgenic lines while 4 were commonly downregulated among the three transgenic lines, N=4.

5.2.9 Similarities and differences between proteomes of TNF treated enteroids and LPS-treated intestinal mucosa

WT, *Nfkb2*^{-/-}, *Nfkb1*^{-/-} and *c-Rel*^{-/-} murine strains were treated with 0.125 mg/kg LPS for 1.5 hours to induce small intestinal epithelial apoptosis and shedding before being culled (with help from PhD student Ahmed Elramli). The small intestine was opened longitudinally, and the mucosa was isolated from the proximal small intestine for protein extraction and proteomic analysis. This was performed using the same method as for murine enteroid cultures generated from the same small intestinal

region from the same murine strain and were these were either untreated or TNF treated (methods described in chapter 2.6). The proteomes generated from both LPS treated murine small intestinal crypts and villi and TNF-treated murine organoids were comparatively analysed to determine their similarities and differences. The total number of proteins detected in untreated WT mice was 5770 in enteroids and 5845 in small intestinal mucosal scrapes, for *Nfkb1*^{-/-} the number of proteins was 5646 in enteroids and 5678 in small intestinal mucosa, for *Nfkb2*^{-/-}, 5951 in enteroids and 5686 in small intestinal mucosa, and for *c-Rel*^{-/-}, 5411 in enteroids and 5750 in intestinal mucosa suggesting that protein extractions, processing and detection were similar across the *in vitro* and *in vivo* model systems (table 5.9).

We first wanted to determine whether different transgenic and treatment conditions resulted in similar numbers of up-regulated and down-regulated proteins across the enteroids and small intestinal crypts/villi (table 5.10). For the majority of comparisons, there were more up- and down- regulated proteins detected within the small intestinal isolates compared to the enteroid cultures. Of note, there were few up- and down-regulated proteins detected in the small intestinal mucosa of *Nfkb2*^{-/-} mice following treatment compared to untreated mice of the same genotype (14 changes) and many more changes were detected in enteroids following TNF treatment (357 changes). This may be a result of direct tissue crypt/villus isolates containing several different cell populations in addition to epithelial cells which could potentially dilute epithelial cell-specific proteins, whereas enteroids are purely epithelial cells and may be more sensitive for the detection of lower abundant proteins. These data may also demonstrate the importance of NFκB2 signalling within the epithelial cell compartment.

We also wanted to explore the percentages of similarities and differences across all proteins with significant up- or down-regulations between murine enteroids and small intestinal mucosa at baseline and following treatment (table 5.11). The percentage

similarity between murine enteroids and small intestinal crypt/villus isolates for significantly down-regulated proteins ranged from 0% in untreated WT versus untreated *Nfkb1*^{-/-} to 37% in untreated WT v untreated *Nfkb2*^{-/-} suggesting that interpretation of specific protein regulations at the epithelial level in enteroids may untangle part of the epithelial cell-specific mechanisms responsible for *Nfkb2*^{-/-}-induced protectivity against epithelial damage. However additional information may be yielded from the interaction of complex cellular systems by further assessment *in vivo*.

Many significantly regulated proteins were expressed in enteroids (appendices D – J) and small intestinal mucosae. Additionally, several proteins were detected in enteroids that fell below the limit of detection in small intestinal crypt/villus isolates and vice versa (table 5.12). Guanylate cyclase activator 2B (*Guca2b*) was upregulated in both WT enteroids and small intestinal crypt/villus isolates following treatment, suggesting that this protein demonstrates similarity between *in vitro* and *in vivo* model systems. Isocitrate dehydrogenase [NADP] cytoplasmic (*Idh1*) was downregulated in enteroids, but upregulated in mucosae. Acyl-CoA dehydrogenase family member 11 (*Acad11*) was down-regulated in TNF treated *c-Rel*^{-/-} enteroids, but was not detected in *c-Rel*^{-/-} small intestinal crypt/villus isolates. By contrast, splicing regulatory glutamine/lysine-rich protein 1 (*Srek1*) was downregulated following LPS treatment in *c-Rel*^{-/-} small intestinal crypt/villus isolates but was not detected in *c-Rel*^{-/-} enteroids.

Strains	Enteroids	Mucosae
WT	5570	5845
<i>Nfkb1</i> ^{-/-}	5646	5678
<i>Nfkb2</i> ^{-/-}	5951	5686
<i>c-Rel</i> ^{-/-}	5411	5750

Table 5.9 Total number of different proteins identified in untreated mouse enteroids and small intestinal mucosae with about 9 – 37% similarity.

Features	Enteroids		Mucosae	
Samples	Up	Down	Up	Down
Untreated WT v treated WT	173	117	255	579
Untreated WT v untreated <i>Nfkb1</i> ^{-/-}	3	4	250	251
Untreated <i>Nfkb1</i> ^{-/-} v treated <i>Nfkb1</i> ^{-/-}	55	73	59	43
Treated WT v treated <i>Nfkb1</i> ^{-/-}	247	217	144	154
Untreated WT v untreated <i>Nfkb2</i> ^{-/-}	27	25	1036	1237
Untreated <i>Nfkb2</i> ^{-/-} v treated <i>Nfkb2</i> ^{-/-}	266	91	7	7
Treated WT v treated <i>Nfkb2</i> ^{-/-}	329	390	419	496
Untreated WT v untreated <i>c-Rel</i> ^{-/-}	14	22	220	143
Untreated <i>c-Rel</i> ^{-/-} v treated <i>c-Rel</i> ^{-/-}	28	26	87	114
Treated WT v treated <i>c-Rel</i> ^{-/-}	21	35	83	93

Table 5.10 Significantly over- and under-expressed proteins in enteroids and small intestinal mucosae in WT, *Nfkb1*^{-/-}, *Nfkb2*^{-/-} and *c-Rel*^{-/-}.

Enteroids	Differences		Similarities	
Samples	Up	Down	Up	Down
Untreated WT v treated WT	154 (89.0%)	96 (82.1%)	9+10=19 (11.0%)	5+16=23 (17.9%)
Untreated WT v untreated <i>Nfkb1</i> ^{-/-}	3 (100%)	4 (100%)	0	0
Untreated <i>Nfkb1</i> ^{-/-} v treated <i>Nfkb1</i> ^{-/-}	55 (100%)	73 (96.1%)	0	0+3 (3.9%)
Treated WT v treated <i>Nfkb1</i> ^{-/-}	225 (91.1%)	194 (89.4%)	12+10=22 (8.9%)	17+6=23 (10.6%)
Untreated WT v untreated <i>Nfkb2</i> ^{-/-}	17 (63.0%)	17 (68%)	7+3=10 (37.0%)	6+2=8 (32.0%)
Untreated <i>Nfkb2</i> ^{-/-} v treated <i>Nfkb2</i> ^{-/-}	266 (100%)	91 (100%)	0	0
Treated WT v treated <i>Nfkb2</i> ^{-/-}	271 (82.4%)	332 (85.1%)	32+26 =58 (17.6%)	40+18=58 (14.9%)
Untreated WT v untreated <i>c-Rel</i> ^{-/-}	12 (85.7%)	17 (77.3%)	2 (14.3%)	3+2=5 (22.7%)
Untreated <i>c-Rel</i> ^{-/-} v treated <i>c-Rel</i> ^{-/-}	28 (100%)	26 (100%)	0	0
Treated WT v treated <i>c-Rel</i> ^{-/-}	18 (85.7%)	28 (80.0%)	3 (14.3%)	7 (20.0%)

Table 5.11 Similarities and differences between murine intestinal epithelial organoids and murine intestinal mucosa. Bold black fonts represent commonly expressed proteins between enteroids and mucosa while bold brown fonts represent proteins that were expressed as both up- and down-regulated.

Enteroids					Mucosae
Strains	Protein names	Gene names	Fold change	p-value	Expressions
WT	Guanylate cyclase activator 2B;Uroguanylin	Guca2b	3.50	5.90 x 10 ⁻⁸	↑
	Complement C3;Complement C3 beta chain	C3	2.70	1.20 x 10 ⁻⁵	↓
	Isocitrate dehydrogenase [NADP] cytoplasmic	Idh1	-1.19	3.69 x 10 ⁻⁴	↑
	Thymidine kinase, cytosolic	Tk1	-1.19	6.94 x 10 ⁻⁴	↓
NFκB1 ^{-/-}	BTB/POZ domain-containing protein KCTD5	Kctd5	1.45	8.59 x 10 ⁻⁴	↓
	Sodium/nucleoside cotransporter	Slc28a1	1.48	3.38 x 10 ⁻³	↓
	BCL2/adenovirus E1B 19 kDa protein-interacting protein 3	Bnip3	-1.86	1.84 x 10 ⁻⁴	-
	Glutaredoxin-1	Glrx	-1.47	6.46 x 10 ⁻⁴	↓
NFκB2 ^{-/-}	Intercellular adhesion molecule 1	Icam1	3.75	2.39 x 10 ⁻⁸	-
	Receptor-type tyrosine-protein phosphatase F	Ptprf	-1.47	5.06 x 10 ⁻⁸	-
	Pre-B-cell leukemia transcription factor 1	Pbx1;Pbx2	-	-	↑
	F-box only protein 25	Fbxo25	-	-	↓
C-rel ^{-/-}	Kunitz-type protease inhibitor 2	Spint2	1.46	2.07 x 10 ⁻⁵	-
	Acyl-CoA dehydrogenase family member 11	Acad11	-1.46	1.06 x 10 ⁻⁴	-
	Splicing regulatory glutamine/lysine-rich protein 1	Srek1	-	-	↓
	Nuclear prelamin A recognition factor	Narf	-	-	↓

Table 5.12 Significantly up-and down-regulated proteins in TNF-treated enteroids and their corresponding proteins in murine small intestinal mucosa treated with LPS. Changes in regulation are shown as, none (-), upregulation (↑), downregulation (↓) and statistically significant (↑ or ↓), in the small intestinal mucosae, t-test, $p \leq 1.0 \times 10^{-8} - 0.05$, $N = 4$.

5.2.10 Integration of proteomic analyses with known sepsis biomarkers

We further analysed the proteomic data from TNF treated WT, *Nfkb1*^{-/-}, *Nfkb2*^{-/-} and *c-Rel*^{-/-} enteroids and identified protein biomarkers that have previously been implicated in contributing to sepsis (table 5.14). Serum amyloid A-3 protein (Saa3) is an acute phase protein biomarker that was significantly upregulated in *Nfkb2*^{-/-} without any detection in the enteroids from the other mouse strains. Fan and colleagues reported that serum Amyloid A3 protected against acute lung injury in *Pseudomonas aeruginosa*-infected mice (Fan et al., 2020). Saa3 also plays a prominent role in protecting epithelial cells against sepsis (Ather et al, 2018). This suggests that protectivity against TNF-induced enteroid death following *Nfkb2* deletion may be partially a result of TNF-induced Saa3 production. We identified peptidoglycan recognition protein 1 (Pglyrp1), which is implicated in host defence and it showed the highest significant upregulation following TNF treatment compared to all the other enteroid strains. Pglyrp1 has been reported to demonstrate protective effects against sepsis during experimental colitis in mice (Saha et al., 2010). Pglyrp1 may also therefore contribute to *Nfkb2*^{-/-} enteroid resistance to TNF-induced morphological changes. Protein S100a11 (S100a11) is an organ dysfunction biomarker and was observed to be insignificantly upregulated in *Nfkb2*^{-/-}, but significantly upregulated in the WT and all other transgenic enteroid lines. S100a11 has been reported to play a major role in cell proliferation, apoptosis, migration and chemotaxis (Donato et al., 2013). In critically ill patients, serum S100a11 has been reported to be increased in Staphylococcal infection (Thuny et al., 2012). The attenuated effect of TNF on *Nfkb2*^{-/-} enteroids could therefore partly be due to reduced expression of S100a11. Laminin subunit gamma-1 (Lamc1) is a vascular endothelial damage biomarker and was observed to be downregulated in *Nfkb2*^{-/-} enteroids, but was upregulated in all other enteroid lines. In critically ill patients, serum laminin has been reported to be increased in Candida-induced sepsis (Presterl et al., 2012). One of the receptor biomarkers identified from our proteomic analysis

was TNF receptor-associated factor 4 (Traf4). Traf4 is an adapter and signal-transducing protein and has been implicated in regulation of cell apoptosis and survival and modulation of Traf6 and NFκB inflammatory responses (Ayala et al., 1996; Shiels et al., 2000). Traf4 was downregulated in *Nfkb2*^{-/-}, but up-regulated in *Nfkb1*^{-/-} and *c-Rel*^{-/-} enteroids, but was not detected in WT enteroids. Traf4 was not significantly expressed, however, its downregulation in only *Nfkb2*^{-/-} enteroids could have a protective effect and could potentially contribute to why *Nfkb2*^{-/-} enteroids exhibit different TNF-induced behaviours compared with other TNF treated enteroid strains.

Groups	Strains	Proteins	Genes	FC	P-value	Comments
Acute phase protein biomarker	WT	Serum amyloid A-3 protein	Saa3	-	-	Protectives against sepsis
	<i>Nfkb1</i> ^{-/-}	Serum amyloid A-3 protein	Saa3	-	-	
	<i>Nfkb2</i> ^{-/-}	Serum amyloid A-3 protein	Saa3	2.24	0.01	
	<i>c-Rel</i> ^{-/-}	Serum amyloid A-3 protein	Saa3	-	-	
Host defence proteins biomarker	WT	Peptidoglycan recognition protein 1	Pglyrp1	1.54	2.55 x 10⁻⁴	Protectives against sepsis
	<i>Nfkb1</i> ^{-/-}	Peptidoglycan recognition protein 1	Pglyrp1	1.36	0.03	
	<i>Nfkb2</i> ^{-/-}	Peptidoglycan recognition protein 1	Pglyrp1	2.03	5.35 x 10⁻⁶	
	<i>c-Rel</i> ^{-/-}	Peptidoglycan recognition protein 1	Pglyrp1	1.38	0.05	
Organ dysfunction biomarker	WT	Protein S100-A11	S100a11	2.12	5.97 x 10⁻⁴	Increases in sepsis
	<i>Nfb1</i> ^{-/-}	Protein S100-A11	S100a11	2.41	4.17 x 10⁻³	
	<i>Nfb2</i> ^{-/-}	Protein S100-A11	S100a11	1.62	0.15	
	<i>c-Rel</i> ^{-/-}	Protein S100-A11	S100a11	2.02	1.88 x 10⁻³	
Vascular endothelial damage biomarker	WT	Laminin subunit gamma-1	Lamc1	1.06	0.59	Increases in sepsis
	<i>Nfkb1</i> ^{-/-}	Laminin subunit gamma-1	Lamc1	1.13	0.33	
	<i>Nfkb2</i> ^{-/-}	Laminin subunit gamma-1	Lamc1	-1.02	0.93	
	<i>c-Rel</i> ^{-/-}	Laminin subunit gamma-1	Lamc1	1.16	0.60	
Receptor biomarker	WT	TNF receptor-associated factor 4	Traf4	-	-	Regulates cell survival and apoptosis
	<i>Nfkb1</i> ^{-/-}	TNF receptor-associated factor 4	Traf4	1.14	0.14	
	<i>Nfkb2</i> ^{-/-}	TNF receptor-associated factor 4	Traf4	-1.07	0.28	
	<i>c-Rel</i> ^{-/-}	TNF receptor-associated factor 4	Traf4	1.03	0.75	

Table 5.13 Protein biomarkers of sepsis detected in WT, *Nfkb1*^{-/-}, *Nfkb2*^{-/-} and *c-Rel*^{-/-} enteroids following 24 hours treatment with TNF (50 ng/ml); Fold change (FC).

5.2.11 Hallmark analysis of TNF-treated enteroid proteomes

The total number of significant proteomic changes with \log_2 fold ≥ -0.5 and $\leq +0.5$ in WT and *Nfkb2*^{-/-} intestinal epithelial enteroids that were treated with 50 ng/ml TNF were 141 and 276 respectively. Gene ontology (GO) analysis, functional annotation and pathway analysis of these significant changes was performed with the NIH Database for Annotation, Visualization and Integrated Discovery (DAVID) software to determine gene count, percentage of categorised gene count (GC), fold enrichment (FE) and false discovery rate (FDR) (table 5.14). The higher the enrichment the more significant the annotation group and the lower the p-values of the hits. The lower the false discovery rate (<0.05) the more positive the annotation group. The functional annotation clustering describes various components including protein domains, Kyoto Encyclopedia of Genes and Genomes (KEGG) pathway and GO. In order to determine whether there was any TNF-mediated effect on the strains, the baseline characteristics were first observed (table 5.14A). The enrichment score (ES) of immune response in WT enteroids treated with TNF (5.3) was observed to be higher than in *Nfkb2*^{-/-} enteroids treated with TNF (4.7). In the functional annotation clustering analysis, serpin signalling was observed in the annotation cluster of TNF-treated *Nfkb2*^{-/-} enteroids which was not present in WT enteroids. Previous studies have reported the protective property of *Nfkb2*^{-/-} against chemical carcinogenesis in AOM/DSS-induced colon cancer model (Burkitts et al., 2015). ISG15-protein conjugation was not detected under the GO process category at baseline, however, when enteroids were treated with TNF, fold enrichment was 55.2 in WT and 42.5 in *Nfkb2*^{-/-}. ISG15 has been previously reported to demonstrate both innate and adaptive immune responses against viral and other microbial infections.

A. GO process category	Untreated WT v untreated Nfkb2^{-/-}			
Features	GC	%	FE	FDR
NIK/NF-kappa B signalling	-	-	-	-
Protection from natural killer cell mediated cytotoxicity	-	-	-	-
Antigen processing and presentation	4	2.9	11	0.5300
ISG15-protein conjugation	-	-	-	-
Negative regulation of mature B cell apoptotic process	-	-	-	-
KEGG Pathway	GC	%	FE	FDR
Complement and coagulation cascades	-	-	-	-
TNF signalling pathway	-	-	-	-
Chemical carcinogenesis	5	3.6	5.6	0.2300
PPAR signalling pathway	-	-	-	-
Cell adhesion molecules (CAMs)	-	-	-	-
Functional annotation cluster	GC	FC	ES	FDR
Immune system process	7	2.7	1.11	1.0000
Innate immunity	-	-	-	-
Innate immune response	4	1.5	1.11	1.0000
Serpin	3	5.8	1.5	0.8100
Acute-phase response	-	-	-	-

B. GO process category	Treated WT				Treated Nfkb2^{-/-}			
	GC	%	FE	FDR	GC	%	FE	FDR
NIK/NF-kappa B signalling	2	1.4	55.2	0.7800	-	-	-	-
Antigen processing and presentation	2	1.4	55.2	0.0190	4	1.4	56.7	0.0190
ISG15-protein conjugation	2	1.4	55.2	0.7800	3	1.1	42.5	0.1800
Negative regulation of mature B cell apoptotic process	2	1.4	55.2	0.7800	3	1.1	42.5	0.1800
Protection from natural killer cell mediated cytotoxicity	-	-	-	-	3	1.1	35.5	0.2000
KEGG Pathway	GC	%	FE	FDR	GC	%	FE	FDR
Complement and coagulation cascades	-	-	-	-	8	2.9	5.3	0.0270
TNF signalling pathway	-	-	-	-	9	3.3	4.2	0.0380
Chemical carcinogenesis	12	8.5	12.1	3.3x10 ⁻⁷	7	2.5	3.8	0.1800
PPAR signalling pathway	8	5.7	9.3	4.9x10 ⁻⁴	5	1.8	3.1	0.5600
Cell adhesion molecules (CAMs)	8	5.7	4.6	0.0220	8	2.9	2.5	0.4600
Functional annotation cluster	GC	FC	ES	FDR	GC	FC	ES	FDR
Immune system process	15	5.4	5.3	0.0006	22	4.1	4.7	0.0002
Innate immunity	14	4.8	5.3	0.0019	10	3.4	4.7	0.0300
Innate immune response	8	5.3	5.3	0.0130	14	2.5	4.7	0.2400
Serpin	-	-	-	-	9	8.2	3.6	0.0005
Acute-phase response	-	-	-	-	6	12.0	3.6	0.0250

Table 5.14 Summary of the hallmark analysis showing the name process category, pathway description, gene count (GC, percentage (%), fold enrichment (FE), fold change (FC), enrichment score (ES) and false discovery rate (FDR) of some significant functional annotation cluster, gene ontology and Kyoto Encyclopedia of Genes and Genomes (KEGG) pathway of baseline (A) and 50 ng/ml TNF-treated WT vs untreated WT and 50 ng/ml TNF-treated Nfkb2^{-/-} vs untreated Nfkb2^{-/-} (B). Yellow highlights indicate higher values whilst grey highlights indicate lower values.

5.3 Discussion

We investigated the proximal small intestinal epithelial cell-specific proteome of WT mice and changes in the proteome secondary to germline deletion of *Nfkb1*^{-/-}, *Nfkb2*^{-/-} and *c-Rel*^{-/-} in enteroids (appendices D – J). This study also determined the impacts of TNF treatment on the proximal small intestinal epithelial proteome of WT enteroids and in the context of NFκB signalling perturbation. From the changes anticipated in protein expression and abundance, we wanted to understand the mechanisms that could potentially be responsible for the TNF-induced enteroid rounding, expansion, contraction and enhanced motility that have been described in chapter 3. Furthermore, a deeper investigation of how the intestinal epithelial proteome changes in response to the disturbance of NFκB signalling could elucidate potential mechanisms by which *Nfkb2*^{-/-} enteroids are more resistant to TNF treatment than all other NFκB deficient enteroids.

We initially showed that a range of epithelial cell specific proteins were expressed by enteroids, thus validating their epithelial nature in culture and reliability to represent the intestinal epithelium in subsequent proteomic analyses. At baseline, *Nfkb2*^{-/-} enteroids exhibited more Reg3 than WT-derived, *Nfkb1*^{-/-} and *c-Rel*^{-/-} enteroids which may have conferred protectivity from TNF-induced damage prior to the application of TNF (Dessein et al., 2009). Villin (Vil1) is the most abundant protein produced in small intestinal villi and as such is often the gene promoter of choice to generate intestinal-specific and conditional knockout animals. Reassuringly, Vil1 was detected by our proteomic analyses in all enteroid genotypes and was shown to be depleted following TNF treatment in all enteroids except *Nfkb2*^{-/-} in which its abundance was insignificantly elevated following TNF treatment. This finding demonstrates at the molecular level that *Nfkb2*^{-/-} enteroids maintain a consistent proportion of villus domains after TNF administration (Vlantis et al., 2016), whereas the other strains are depleted similarly to histological observations of villus blunting following excessive

apoptosis and cell shedding *in vivo* and increased circularity in enteroids *in vitro*. *Nfkb2*^{-/-} enteroids also demonstrated increased expression of RelB compared to WT enteroids, suggesting that enteroids were attempting to activate alternative NFκB pathway signalling and there was no feedback inhibition for this pathway. RelB was up-regulated in all enteroid lines following TNF stimulation, demonstrating activation of the alternative NFκB signalling pathway by this stimulus. Reassuringly, no *Nfkb2* was detected in *Nfkb2*^{-/-} enteroids, whereas it was detected in all the other enteroid lines, validating that these enteroids were devoid of *Nfkb2*. *RelB*^{-/-} mice have been shown to exhibit similar pathologic and histological changes to WT mice following stimulating with LPS (unpublished observations by Ahmed Elramli in our laboratory) and *RelB*^{-/-} enteroids (unpublished observations by Steph James in our laboratory) also responded similarly to WT enteroids, suggesting that its binding partner NFκB2 p52 is more important in regulating this response.

Several proteins were upregulated in all enteroid lines following TNF treatment. Whilst this does not demonstrate the importance of the specific contributions of *Nfkb1*^{-/-}, *Nfkb2*^{-/-} and *c-Rel*^{-/-} in regulating the epithelial damage response, the contribution of these elucidated proteins to the induction of TNF-induced pathology should be further explored. Whilst small intestinal pathology is ameliorated following TNF treatment of *Nfkb2*^{-/-} enteroids and in mice *in vivo*, pathology is not completely inhibited and there is likely a complex set of proteins and signalling cascades involved in generating the morphological and histological response that is observed. *Guca2b* was identified as being upregulated in all enteroid strains in response to TNF and is known to regulate proliferation, metabolism, barrier function and intestinal tumourigenesis via its interaction with *Gucy2c* (Lorenz et al., 2003; Yoshikawa et al., 2007). This was one of the most up-regulated proteins detected. Interestingly, a SNP was recently detected in *Gucy2c* in colonic tumouroids versus normal colonoids generated from azoxymethane/dextran sulphate colitis treated WT mice by another

PhD student (Harvey Fowler-Williams) in our laboratory (unpublished observations). This interaction now warrants further exploration in inflammation-driven colon cancers and also in its potential contribution to IBD and sepsis pathogenesis.

We observed an increase in Tnfaip3 (also well known as A20) following TNF treatment of *Nfkb2*^{-/-} enteroids, but we did not observe any such increase in all other enteroid lines. Tnfaip3 is a well characterised inhibitor of NFκB activity; it regulates the response to TNF-induced apoptosis (Jung et al., 2019; Lerebours et al., 2008; Serramito et al., 2019) and may contribute to the resistance of *Nfkb2*^{-/-} enteroids to TNF-induced pathology. Alternative pathway NF-κB signalling is predominantly activated by the processing of inactive p100 to transcriptionally active p52. This process occurs by the kinase activity of NIK and IKKα which are directly inhibited by Tnfaip3 (A20), resulting in reduced p100 processing and therefore reduced alternative pathway NF-κB signalling activation (Jung et al., 2019; Serramito et al., 2019; Verhelst et al., 2015). *Nfkb2*^{-/-} mice have been shown to be resistant to the induction of experimental colitis and colitis-associated colon cancer (Burkitt et al., 2015), however, the mechanisms responsible for this have not been extensively explored. From our studies, Tnfaip3 is an attractive candidate that could be an important regulator of colonic tumour development as its expression has been shown to be reduced in human colonic adenomas and carcinomas (Perrot-Appianat et al., 2011; Shao et al., 2013; Wang et al., 2016). We conducted a preliminary test to confirm our proteomics data using a Tnfaip3 antibody via IHC on enteroids, but did not observe any obvious differences in Tnfaip3 expression between NFκB genotypes with or without TNF treatment (data not shown). Further work is now warranted to conduct an antibody titration and explore different antigen retrieval methods and antibodies to validate this finding. Kattah and colleagues reported that Tnfaip3 (A20) and A20 Binding and Inhibitor of NFκB (ABIN-1) were protective against autoimmune and inflammatory diseases including IBD (Kattah et al., 2018). They showed that the

mechanism was via *Tnfrsf25* and ABIN-1 mediated restriction of NFκB signalling and cell death via caspase-8 and RIPK1 activation (Kattah et al., 2018). However, they also reported that IEC-specific deletion of either A20 or ABIN-1 did not induce rapid and severe death of intestinal epithelial enteroids and that down regulation of both A20 and ABIN-1 was required (Kattah et al., 2018). We interrogated the epithelial proteome for Abin-1 with and without TNF treatment and in WT and NFκB-deficient lines and this protein was not detected. *Tnfrsf25* tends to regulate intestinal homeostasis, autophagic response and NFκB activation (Jung et al., 2019; Serramito et al., 2019).

One of the acute phase protein biomarkers we identified in enteroids was *Saa3* which was significantly upregulated in *Nfkb2^{-/-}* enteroids only. It was not detected in the enteroids derived from the other transgenic mouse lines. It has been reported that *Saa3* has a protective property against *Pseudomonas aeruginosa*-induced acute lung injury mice (Fan et al., 2020). *Pglyrp1* is a host defence protein marker and was observed to be most significantly upregulated in *Nfkb2^{-/-}* compared to the other enteroids tested. *Pglyrp1* protected the intestine against experimental colitis in mice (Saha et al., 2010).

There are several advantages and limitations to studies using enteroids in order to investigate the intestinal epithelial proteome. A clear advantage of these *in vitro* studies compared to *in vivo* investigations is the absence of other cellular compartments that could complicate the interpretation of direct epithelial cell-specific effects in response to treatment with cytokines such as TNF (and others presented in chapter 4 of this thesis). However, whilst enteroids have been demonstrated to consistently recapitulate the cellular dynamics and constitution of intestinal epithelia, we cannot ignore the impact of culture conditions and indirect effects of other cellular compartments on the intestinal proteome. We therefore injected LPS into WT, *Nfkb1^{-/-}*, *Nfkb2^{-/-}* and *c-Rel^{-/-}* mice from the same sex and inbred mouse colony from which

the enteroids were derived to elicit a TNF response that caused cell shedding and apoptosis (Beutler & Grau, 1993; van der Bruggen, 1999; Williams et al., 2013; Yao et al., 1997). We harvested proximal small intestinal crypts and villi from the same location from which the enteroids were derived and conducted comparative proteomic analyses to determine similarities and differences between enteroid cultures and *in vivo* tissues. We observed several similarities between the protein profiles of enteroids and crypt/villus isolates at baseline and following treatment, but these only reached a maximal percentage of 37% similarity. Small intestinal crypt/villus isolates contained several different cell populations including epithelial cells, immune cells, mesenchymal stromal cells and supporting extracellular matrices that are likely responsible for the majority of these differences and from *in vivo* studies, it is difficult to interpret which compartment specific proteins are derived from. Care was taken to remove the Matrigel matrix very thoroughly prior to protein extraction from enteroids as Matrigel is derived from a mouse sarcoma and is heavily enriched for murine laminin and fibronectin extracellular matrix components that could have interfered with downstream proteomic analyses. Growth factors used to maintain enteroids in culture could also impact on protein expression within enteroids (for instance, high concentrations of Wnt activators would enhance the detection of proteins that are associated with proliferation). Culture conditions were however kept constant between different enteroid strains and treatments. Though we did not perform proteomic analysis on rescued enteroids following TNF treatment, their proteome would be interesting to analyse in the future to determine any potential longterm differences induced by prior TNF treatment. The proteomic analyses conducted were undertaken at 24 hours post treatment. The time selection was arbitrary and based on the start of morphological changes being observed via bright field microscopy at this time point. Time course studies of the proteome at earlier time points from at 0, 3, 6, 9, 12 and 24 hour time points may yield further information

about the time course of protein activation but also may have identified different proteins whose production and utility is short lived.

Broad-spectrum proteomic analyses were selected for this study, but future studies could focus on specific protein populations such as membrane-enriched or nuclear protein extracts to further define intestinal epithelial proteome differences induced by TNF or NFκB modulation that may elucidate further potential targets for IBD and sepsis. However, several proteins have been elucidated in this study that may contribute towards the observed protectivity from TNF-induced small intestinal epithelial cell damage that is conferred by *Nfkb2* deletion. Several additional proteins have also been identified that may be modulate TNF-induced damage independent of NFκB2 signalling. Further work is now warranted to understand the importance of the contributions of these proteins and the pathways they regulate to the development of epithelial cell damage in the intestine and how this relates to damage responses in the local mucosal and systemic immune system responses to modulate the susceptibility to sepsis and IBD.

In summary, we postulated that *Tnfaip3* which has been previously reported in many studies (Jung et al., 2019; Katta et al., 2018; Lerebours et al., 2008; Serramito et al., 2019) as having inhibitory actions on inflammation, apoptosis and autoimmune responses might play a significant role in blunting the *Nfkb2*^{-/-} enteroid response to TNF treatment. TNF treated WT, *Nfkb1*^{-/-} and *c-Rel*^{-/-} enteroids demonstrated reduced *vil1*, however TNF treatment of *Nfkb2*^{-/-} enteroids led to reduced *Vil1* depletion suggesting that there was a better retention of absorptive villus enterocytes and less intestinal cell shedding from the villus domains). The upregulation of *Saa3* and *Pglyrp1* in *Nfkb2*^{-/-} enteroids could also contribute to the blunted response of these enteroids to TNF treatment.

We utilised the NIH Database for Annotation, Visualization and Integrated Discovery (DAVID) software to determine the hallmark analysis of the significant proteins of the

proteomic results. Uchiyama and colleagues reported the protective property of serpin B1 in colonic epithelial cells to inflammation-induced damage via blockage of neutrophil elastase activity (Uchiyama et al., 2012). Serpin has also been shown to play a regulatory role in cellular proliferation and cell death via modulation of apoptosis and perturbation of proteasome activity (Gatto et al., 2013; Van Gent et al., 2003). We hypothesise that the protective actions of serpin signalling against pro-inflammatory responses contribute to the blunted response of *Nfkb2*^{-/-} enteroids against to TNF treatment. This now warrants further interrogation. We also observed in hallmark analysis of Kyoto Encyclopedia of Genes and Genomes (KEGG) pathway that chemical carcinogenesis, PPAR signalling pathway and cell adhesion molecules (CAMs) were notably higher in WT than the corresponding expressions in *Nfkb2*^{-/-} enteroids. ISG15 is a posttranslational modifier and protein ISGylation via activation of IFN- α/β signalling at the interferon receptor can attenuate IFN responses and through stimulation of natural killer cells promote type 2 interferon (IFN- γ) secretion (Ballegeer et al., 2018). An ISG proteome signature has been implicated in the regulation of intestinal STAT1 and TNF-induced intestinal inflammation in mice *in vivo* (Ballegeer et al., 2018), we determined that *Isg15* was upregulated following TNF treatment of enteroids suggested that ISG might be very important in characterising actions of TNF and that this may be driven by the intestinal epithelium in terms of helping the recruitment of immune cells and in the motility of epithelial cells within the mucosa. The differential regulation of these proteins may modulate IBD and sepsis clinically and are worth interrogating to determine the potential role they play in modulating the response to TNF-induced sepsis. The possibly attenuating effects of ISG15 in *Nfkb2*^{-/-} enteroids now warrant further investigation.

6 Development of an enteroid model to test potential sepsis and inflammatory bowel disease therapeutics

6.1 Introduction

Currently, the only form of treatment for critically ill patients with sepsis is supportive or symptomatic relief. There is no cellular or molecularly directed specific therapeutic intervention. Highly specific and sensitive diagnostics for sepsis are also yet to be optimally developed. Clinically, goal-oriented approaches for ameliorating sepsis include early recognition and commencement of supportive treatment within 6 hours of onset in order to improve a patient's condition, prevent deterioration and prevent the development of multiple organ dysfunction syndrome (MODS) or organ failure. The four major elements of this goal-targeted approach are supportive care, monitoring, anti-inflammatory therapy and antibiotic administration.

Key players driving sepsis pathogenesis systemically are similar to those that drive inflammatory bowel disease (IBD) pathogenesis at a local level in the intestinal mucosa and are characterised by a hyperactive immune response containing high concentrations of TNF and IL-6 (Murch et al., 1993; Remick et al., 2005). Similar pathologies resulting from excessive cytokine stimulation in the lungs and intestine are observed in patients with sepsis prior to the onset of MODS and also early in sepsis pathogenesis. Therefore, if molecular mechanisms can be targeted at the earlier stages of onset of sepsis, early onset pathologies such as in the intestine and lung may be ameliorated, thus preventing the perpetual positive feedback systemic inflammatory response syndrome that results partially from the cytokine storm, but also from increased bacterial invasion across these mucosal surfaces due to the breakdown of barrier function. Such an approach could greatly enhance the opportunity for life saving antibiotic therapy to be efficacious.

Over recent years, enteroids and colonoids have been generated from patients with inflammatory diseases of the gut. A recent study has identified differences in the expression of antigen presentation genes within enteroids and colonoids from IBD patients, suggesting that there are epithelial cell-intrinsic differences that contribute to IBD susceptibility and that these are retained in culture (Kelsen et al., 2020). Enteroids derived from an inflammatory environment in either SAMP1/YitFc or TNF^{ΔARE/+} murine intestine (murine models of Crohn's disease-like ileitis) have also been demonstrated to have an impaired intestinal stem cell niche and have a reduced capacity to grow. However, treatment with the corticosteroid dexamethasone partially rescued this altered enteroid phenotype (Butto et al., 2020). Dexamethasone is also known to downregulate pro-inflammatory NF-κB signals and has been shown to reduce *Nfkb1*, *Jak1* and *Mmp9* expression in SAMP-derived enteroids (Butto et al., 2020). We have identified different susceptibilities of Nfkb-deficient murine-derived enteroids to the damaging effects of TNF (chapter 3 and in Jones et al., 2019), also demonstrating the epithelial cell-intrinsic differences that can contribute to different phenotypic responses in different environments known to modulate NF-κB signalling. We therefore wanted to investigate whether the phenotypic responses that we have previously robustly observed in enteroids in response to TNF (and recently corroborated by Butto et al., 2020) could be ameliorated by the direct application of potential therapeutic agents that modulate the epithelial cell intrinsic environment prior to the addition of TNF. This would enable the generation of an *in vitro* assay to test novel therapeutics for both sepsis and IBD without the initial need for co-culture of enteroids with immune cells.

TNF is a cytokine that robustly causes dose- and time-dependent damage to enteroid cultures (Butto et al., 2020; Jones et al., 2019). Anti-TNF therapy has shown efficacy in inflammatory conditions such as IBD and rheumatoid arthritis (Monaco et al., 2015) and there are also limited studies of its use to treat sepsis. This cytokine is therefore

highly relevant to the pathogenesis of sepsis and IBD and we wanted to determine whether there were any pharmacological ways of blocking its effects other than direct receptor or cytokine blockade, as these approaches are known to cause potentially severe side effects (Abraham et al., 1998; Murch et al., 1993; Remick et al., 2005). Corticosteroids are known to mediate immune dampening effects by modulating NF κ B signalling. There has been more focus on the actions of classical NF κ B pathway components than alternative pathway NF κ B components in response to corticosteroids, however it is also possible that corticosteroids could modulate alternative NF κ B pathway signalling to exert their protective effects (Inoue et al., 1992).

We therefore investigated the potential therapeutic properties of several different classes of agent including corticosteroids (prednisolone and hydrocortisone), a non-steroidal anti-inflammatory drug (flunixin meglumine), and a natural agent (curcumin) that have shown efficacy in murine IBD models to determine whether the damage caused by TNF could be ameliorated *in vitro*. Several of these agents have shown efficacy in humans and/or murine and rat IBD models and have proven anti-inflammatory properties (Berg et al., 2002; Clarke et al., 2019; Herfarth et al., 1998).

Prednisolone and hydrocortisone are corticosteroids that are administered to IBD patients who have a moderate to severe disease flare up to suppress intestinal inflammation and allow their intestinal mucosa to heal. These corticosteroids are known to suppress NF κ B signalling and thus dampen the production of, and signalling mediated by, TNF (Ardite et al., 1998; Schreiber, Nikolaus & Hampe, 1998; Quaglio et al., 2015). Both of these corticosteroids have also shown efficacy in the DSS and TNBS experimental models of colitis (Zhang et al., 2019), but it is currently not clear whether they will also show efficacy in an enteroid model. We wanted to determine whether the intestinal epithelium is an important regulator of the anti-inflammatory effects of prednisolone and hydrocortisone in the absence of the

intestinal immune system. The demonstration that epithelial cells themselves could respond to corticosteroids and prevent the break down in intestinal barrier function caused by TNF would pave the way for novel therapeutics that target the epithelial cellular compartment to prevent the breakdown of barrier function by pro-inflammatory cytokines rather than causing overt immune suppression to the patient.

Flunixin meglumine is a potent, analgesic, anti-pyretic, non-narcotic, and nonsteroidal anti-inflammatory drug (NSAID) that is currently licensed for use in horses, pigs, and cattle (Anderson, Hunt, & Davis, 1991). Flunixin meglumine inhibits cyclooxygenase (COX) to prevent arachidonic acid from synthesizing prostaglandins (Vane & Botting, 1996). Flunixin meglumine is a nonselective COX inhibitor that is known to inhibit the activation of NF κ B (Bryant et al., 2003). A dose of 2.2 mg/kg has been administered in horses with 0.1 to 0.3 L/kg volume of distribution and plasma elimination half-life of 1 to 2 hours (Konigsson et al., 2003). A low dose of 0.25 mg/kg Flunixin meglumine was given as an adjunctive treatment for sepsis in horses (Papich, 2016). However, this low dose had no anti-endotoxin effect, but was efficacious enough to inhibit the prostaglandin that mediates sepsis-induced haemodynamic derangement in horses (Papich, 2016). The inhibition of LPS-induction of iNOS by flunixin meglumine has been demonstrated, suggesting that this drug may modulate mechanisms other than COX metabolism (Bryant et al., 2003) and is worth investigating to determine whether it has any direct protective effects on the intestinal epithelium. We therefore wanted to determine whether another class of drug (non-steroidal anti-inflammatory drug) known to show efficacy in sepsis would also demonstrate protectivity against TNF in an enteroid culture model.

Curcumin (also known as diferuloylmethane), is a non-steroidal anti-inflammatory agent found in the diet (Srimal & Dhawan, 1973). The anti-inflammatory effect of curcumin has been reported to be mediated by several mechanisms including via upregulation of peroxisome proliferator-activated receptor gamma (PPAR- γ)

activation, and by inhibition of NFκB signalling (Jacob et al., 2007; Siddiqui et al., 2006; Song et al., 2010). In a caecal ligation and puncture (CLP) model of sepsis, curcumin was shown to be protective against pulmonary oedema and chronic lung injury (Liu et al., 2017). Pre- or post-treatment with curcumin in the CLP model also decreased tissue injury, reduced mortality, and lowered TNF expression in septic animals (Siddiqui et al., 2006). Curcumin has also shown efficacy in dextran sulphate-sodium (DSS) and trinitrobenzene sulphonic acid (TNBS)-induced colitis models and suppresses the LPS-induced NFκB p65 nuclear translocation that is associated with immune cell activation and small intestinal epithelial cell shedding (Burge et al., 2013; Toden et al., 2017; Zhang et al., 2016). Curcumin is thought to block TNF production and TNF-induced signalling pathways to exert its protective effects. We therefore wanted to determine whether curcumin had protective effects against the damaging effects of TNF on the epithelium in an enteroid model in the absence of the intestinal immune system. Curcumin was chosen because of reports from previous studies in cell lines that it has anti-inflammatory properties (Edwards et al., 2017) and we wanted to know whether the anti-inflammatory action could be reproduced in enteroids.

6.2 Results

6.2.1 Prednisolone delays TNF-induced enteroid rounding

WT enteroids were treated with prednisolone alone to determine whether this drug caused any adverse morphological effects. Prednisolone treatment did not induce any significant changes in enteroid circularity vs untreated enteroids for 0-72 hours post-treatment, with all enteroids consistently showing circularity values of around 0.4 throughout the time course (figures 6.1 and 6.3A). This demonstrated that enteroid treatment with prednisolone did not show any obvious deviation from the

growth patterns of untreated enteroids. We therefore wanted to determine whether prednisolone protected enteroids from the damaging effects of TNF. Enteroids were pre-treated with 0.1, 1 or 10 $\mu\text{mol/l}$ prednisolone for 1 hour prior to the addition of 50 ng/ml TNF. Enteroid circularity was measured at 0, 24, 48, and 72 hours post-TNF treatment. At 24 hours post-treatment, 10 $\mu\text{mol/l}$ prednisolone exhibited statistically significant inhibitory effects against TNF-induced rounding in WT enteroids. Prednisolone at this dose almost completely suppressed the morphological changes associated with TNF treatment. There was no statistically significant difference in the measurement of enteroid circularity between untreated and 10 $\mu\text{mol/l}$ prednisolone-treated enteroids at 24 hours following TNF treatment. However, at 48 hours and 72 hours post-treatment the protective effects of prednisolone were abrogated, and circularity values were not statistically different from TNF alone treated enteroids, suggesting that the effects of a single treatment of prednisolone may be shorter lived than a single treatment of TNF (figures 6.2 and 6.3B). Alternatively, it could mean that prednisolone delays the onset of TNF-induced effects.

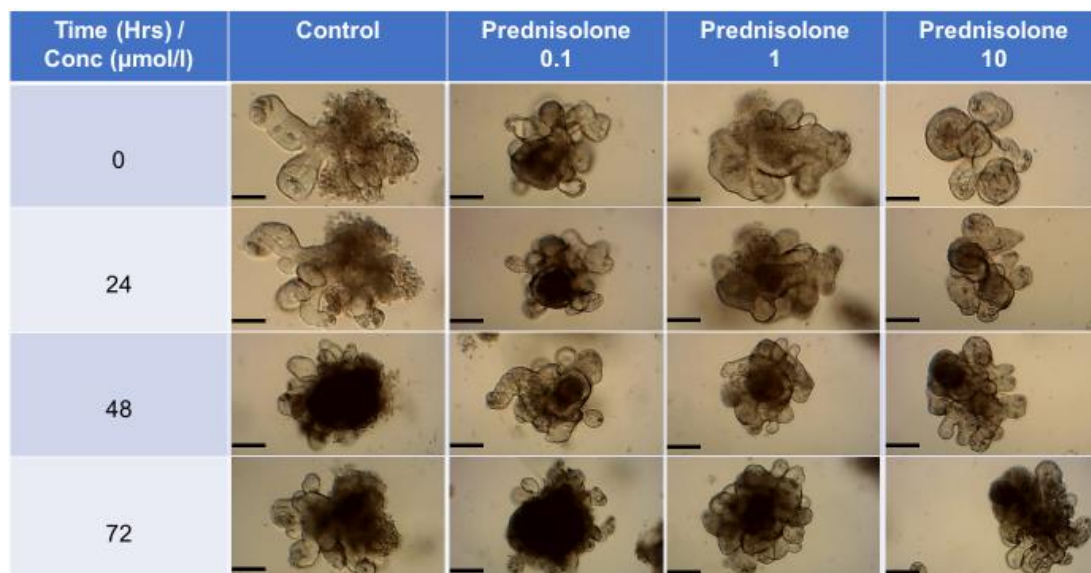


Figure 6.1 Bright field micrographs of untreated, 0.1, 1 and, 10 $\mu\text{mol/l}$ prednisolone treated WT enteroids at 0, 24, 48, and 72 hours post-treatment. Both untreated (DMSO control) and prednisolone treated enteroids have phenotypically irregular shapes. Prednisolone treatment did not induce any injury or death of the enteroids. Original magnification x10, scale bars, 100 μm .

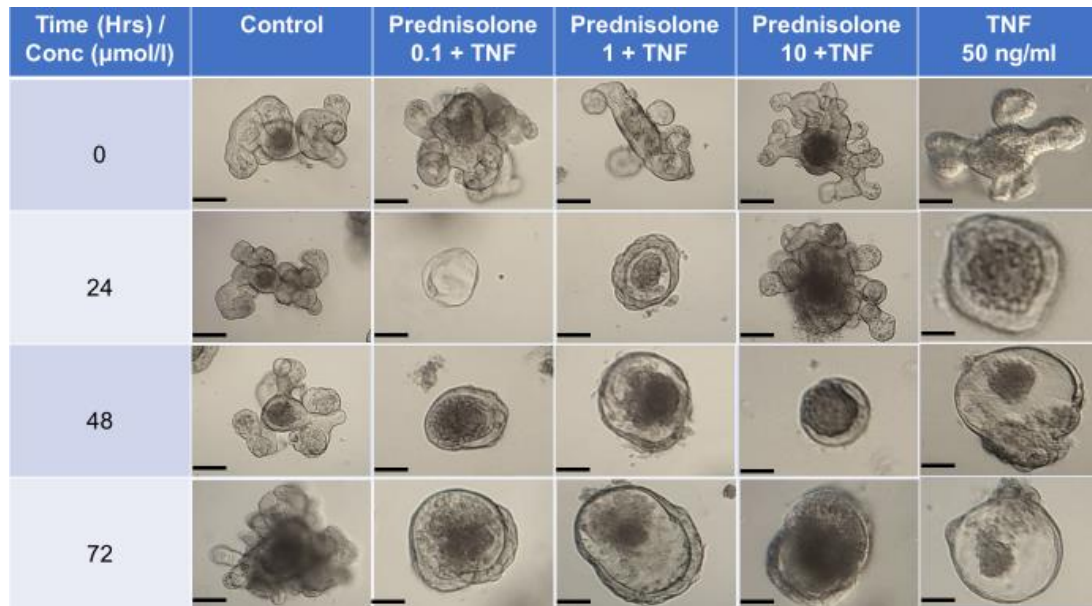


Figure 6.2 Bright field images of untreated, 0.1, 1, 10 µmol/l prednisolone 1-hour pre-treated WT enteroids stimulated by 50 ng/ml TNF for 0, 24, 48, and 72 hours. Untreated enteroids (DMSO control) showed phenotypically normal structures while all TNF treated enteroids displayed rounding morphology. Original magnification x10, scale bars, 100 µm.

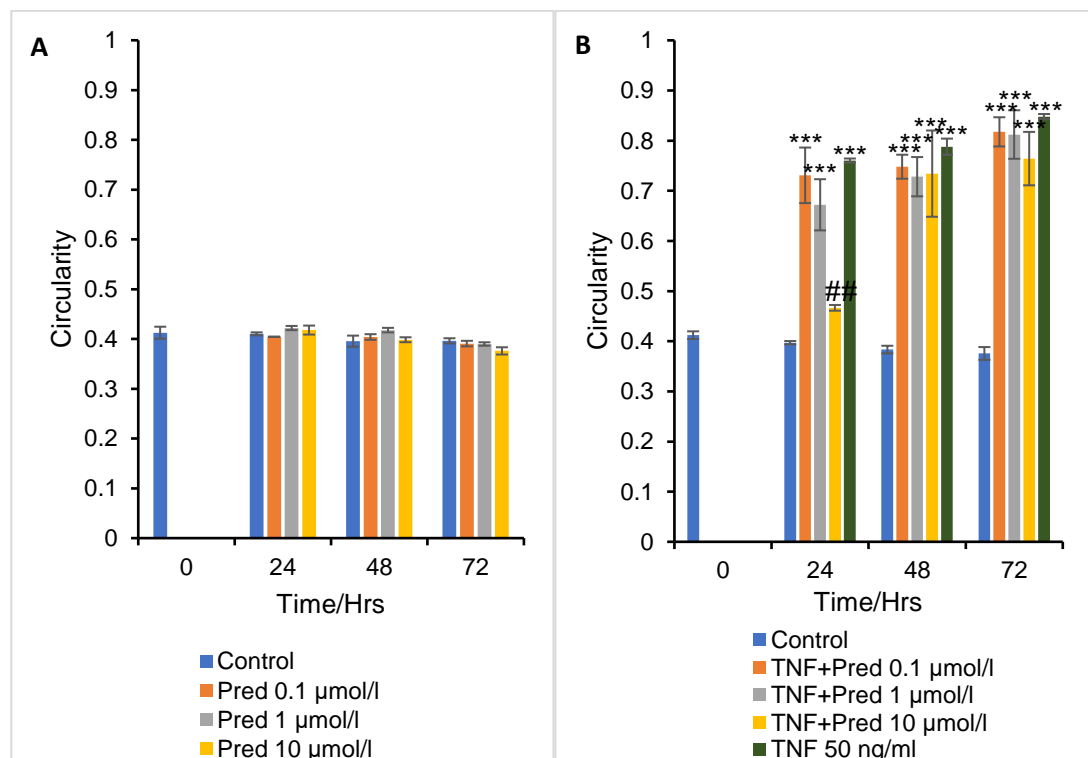


Figure 6.3 WT enteroids were treated with 0, 0.1, 1, and 10 µmol/l prednisolone alone for 0, 24, 48, and 72 hours (A). Pre-treatment of WT enteroids with 0.1, 1, and 10 µmol/l prednisolone for 1 hour before 50 ng/ml TNF was added (B). Statistically significant differences vs untreated (DMSO control) at the same time point are indicated *** $p \leq 0.001$, and statistically significant differences between prednisolone + TNF vs TNF are depicted by ## $p \leq 0.01$; $n=6$, $N=3$, SEM = error bars, 2-way ANOVA.

6.2.2 Hydrocortisone delays TNF-induced enteroid injury

In order to determine whether hydrocortisone caused any adverse morphological effects, we treated WT enteroids with hydrocortisone alone. Hydrocortisone treatment was not associated with any significant changes in enteroid circularity vs untreated enteroids for 0-72 hours and all enteroids consistently showed circularity values of around 0.4 throughout the time course (figures 6.4 and 6.6A). This demonstrated that enteroid treatment with hydrocortisone followed similar growth patterns to untreated enteroids. We then wanted to determine whether hydrocortisone pre-treatment protected enteroids from the TNF-induced damaging effects. Enteroids were first pre-treated with 0.1, 1 or 10 $\mu\text{mol/l}$ hydrocortisone for 1 hour before the addition of 50 ng/ml TNF. Enteroid circularity was measured at 0, 24, 48, and 72 hours following treatment with TNF. At 24 hours post-treatment, 10 $\mu\text{mol/l}$ hydrocortisone caused statistically significant inhibitory effects against TNF-induced rounding in WT enteroids. At this dose (10 $\mu\text{mol/l}$), hydrocortisone almost completely suppressed the rounding changes that were induced by TNF. At 24 hours following treatment with 10 $\mu\text{mol/l}$ hydrocortisone, there was no statistically significant difference in the measurement of enteroid circularity between untreated enteroids and enteroids treated with 10 $\mu\text{mol/l}$ hydrocortisone. By 48 hours following a single treatment with hydrocortisone, we did not observe the protective actions of hydrocortisone any longer and the morphological changes and circularity values of hydrocortisone-treated enteroids were not statistically different from TNF treated enteroids suggesting that a single treatment of hydrocortisone seemed to have a shorter effect than a single treatment of TNF (figure 6.6B).

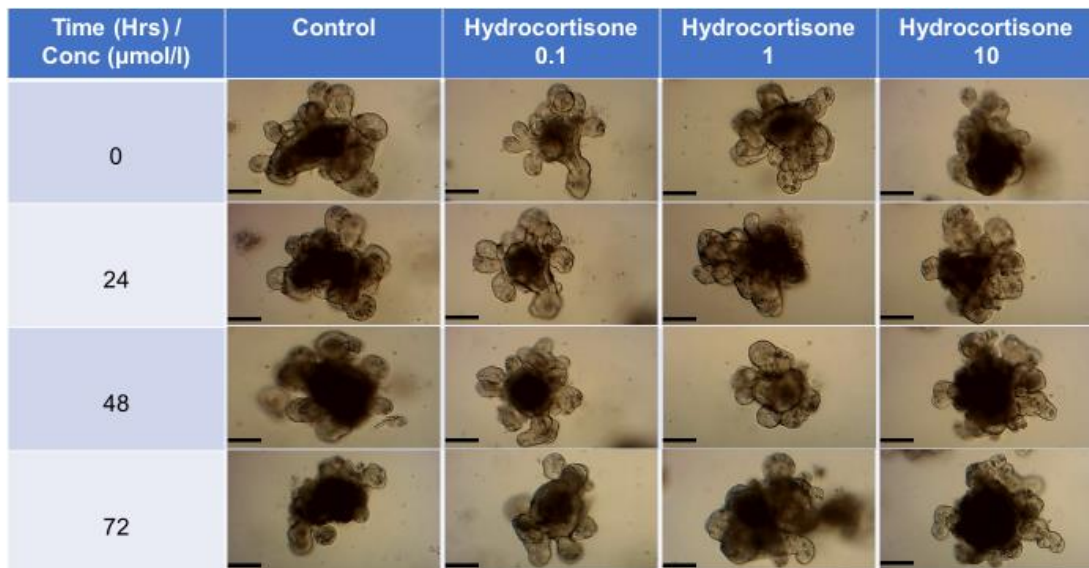


Figure 6.4 Bright field micrographs of untreated, 0.1, 1, 10 μmol/l hydrocortisone treated WT enteroids at 0, 24, 48, and 72 hours. Both untreated (DMSO control) and hydrocortisone treated enteroids have phenotypically irregular shapes. Hydrocortisone treatment did not induce any morphologically demonstrated injury or death on the enteroids. Magnification x10, scale bar, 80 μm.

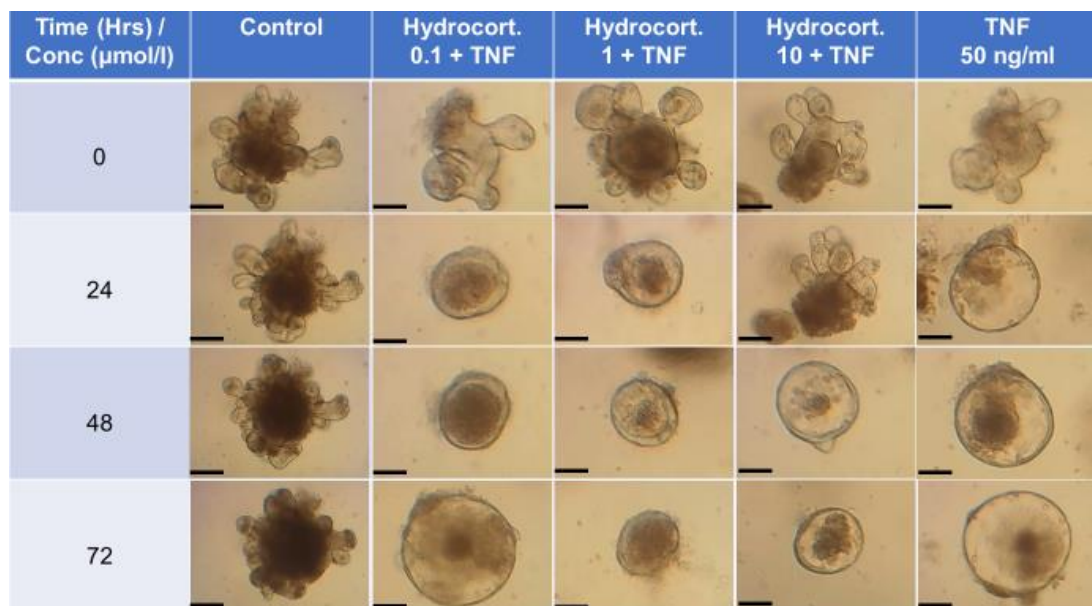


Figure 6.5 Bright field images of untreated, 0.1, 1, 10 μmol/l hydrocortisone- and 50 ng/ml TNF-treated WT enteroids at 0, 24, 48, and 72 hours. Untreated enteroids (DMSO control) had phenotypically irregular structures while TNF treated enteroids had a rounded appearance at 24, 48, and 72 hours post-treatment 10 μmol/l hydrocortisone protected against TNF-induced rounding at 24 hours post-treatment. Magnification x10, scale bar, 80 μm.

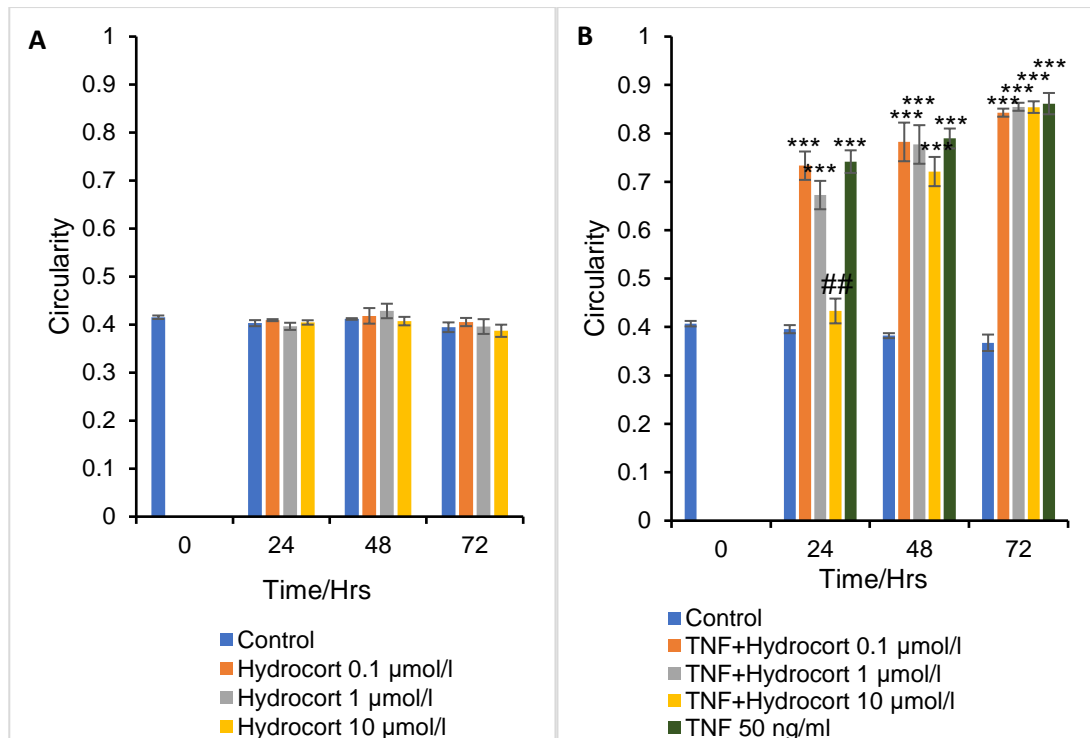


Figure 6.6 Measurement of WT enteroid circularity was performed following treatment with 0, 0.1, 1, and 10 µmol/l hydrocortisone for 0, 24, 48, and 72 hours (A). WT-enteroids were pre-treated with 0.1, 1, and 10 µmol/l hydrocortisone for 1 hour prior to addition of 50 ng/ml TNF and circularity was analysed at 0, 24, 48, 72 hours (B). Statistically significant differences vs untreated (DMSO control) at the same time point are indicated *** $p \leq 0.001$, and statistically significant differences between hydrocortisone + TNF vs TNF alone at the same time point are shown by ### $p \leq 0.01$, $n=6$, $N=3$, $n=6$, SEM = error bars, 2-way ANOVA.

6.2.3 Flunixin meglumine transiently protects enteroids against TNF-treated induced injury

Flunixin meglumine alone was administered to WT enteroids in order to determine whether flunixin meglumine induced any adverse morphological effects. When we compared flunixin meglumine-treated enteroids with non-flunixin meglumine-treated enteroids, there were no significant changes in enteroid circularity for 0-72 hours post-treatment and all enteroids consistently showed circularity values of around 0.4 throughout the time course (figures 6.7 and 6.9A). This showed that flunixin meglumine treatment of enteroids did not cause any obvious deviation from the growth patterns of untreated enteroids. We subsequently investigated whether

flunixin meglumine would protect enteroids from the injurious effects of TNF. Prior to addition of 50 ng/ml TNF to enteroids, we first pre-treated enteroids with 0.1, 1 or 10 $\mu\text{mol/l}$ flunixin meglumine for 1 hour. Following TNF treatment, we measured enteroid circularity at 0, 24, 48, and 72 hours. At 24 hours post-treatment, 10 $\mu\text{mol/l}$ flunixin meglumine demonstrated statistically significant inhibitory effects against TNF-associated rounding in WT enteroids. Flunixin meglumine at this dose almost completely attenuated the morphological changes induced by TNF. There was no statistically significant difference in the phenotypic appearance and measurement of enteroid circularity between untreated and 10 $\mu\text{mol/l}$ flunixin meglumine-treated enteroids at 24 hours post-treatment. At 48- and 72-hours following treatment, flunixin meglumine did not continue to exert protective effects. At 48- and 72-hours following treatment, circularity values were not statistically different from TNF-treated enteroids suggesting that a single treatment of flunixin meglumine may not provide long-lasting protection from TNF and repeat doses may be needed (figures 6.8 and 6.9B).

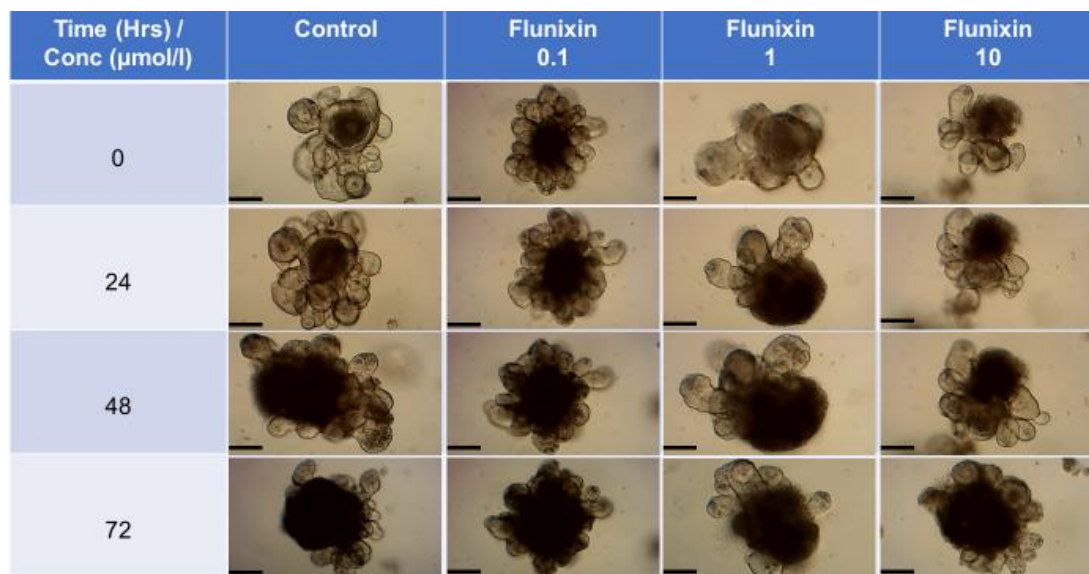


Figure 6.7 Bright field micrographs of untreated, 0.1, 1, 10 $\mu\text{mol/l}$ flunixin meglumine treated WT enteroids at 0, 24, 48, and 72 hours. Both untreated enteroids (DMSO control) and flunixin meglumine treated have phenotypically irregular shapes. Flunixin meglumine treatment did not induce any morphological changes. Magnification x10, scale bar, 100 μm .

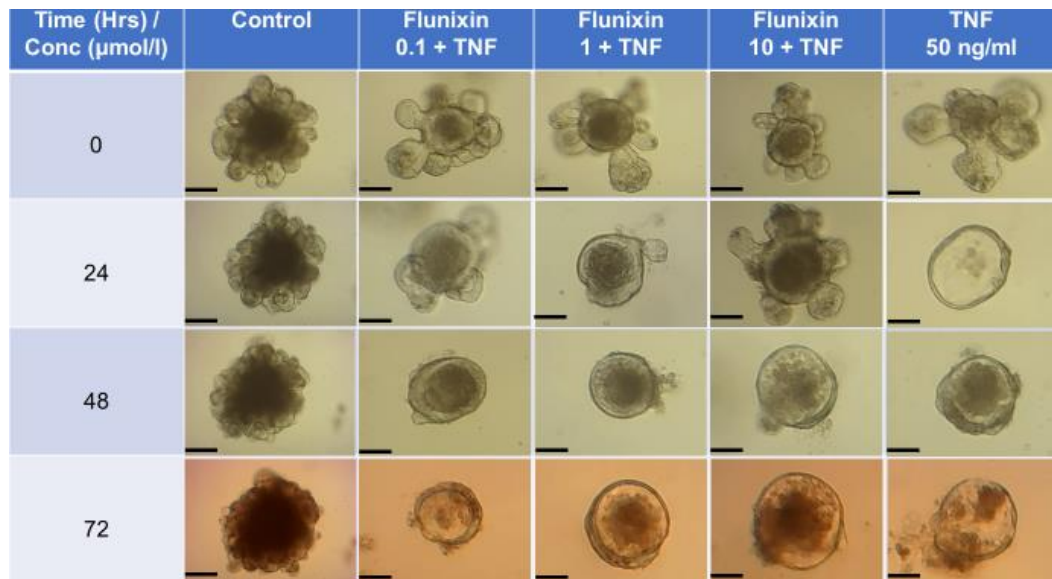


Figure 6.8 Bright field images of untreated, 0.1, 1, 10 µmol/l flunixin meglumine and 50 ng/ml TNF-treated WT enteroids at 0, 24, 48, and 72 hours. Untreated enteroids (DMSO (0.1%) control) have phenotypically irregular structures while TNF treated enteroids showed rounding at 24, 48, and 72 hours post-treatment; 10 µmol/l flunixin prevented TNF-induced enteroid at 24 hours post-treatment. Magnification x10, scale bar, 100 µm.

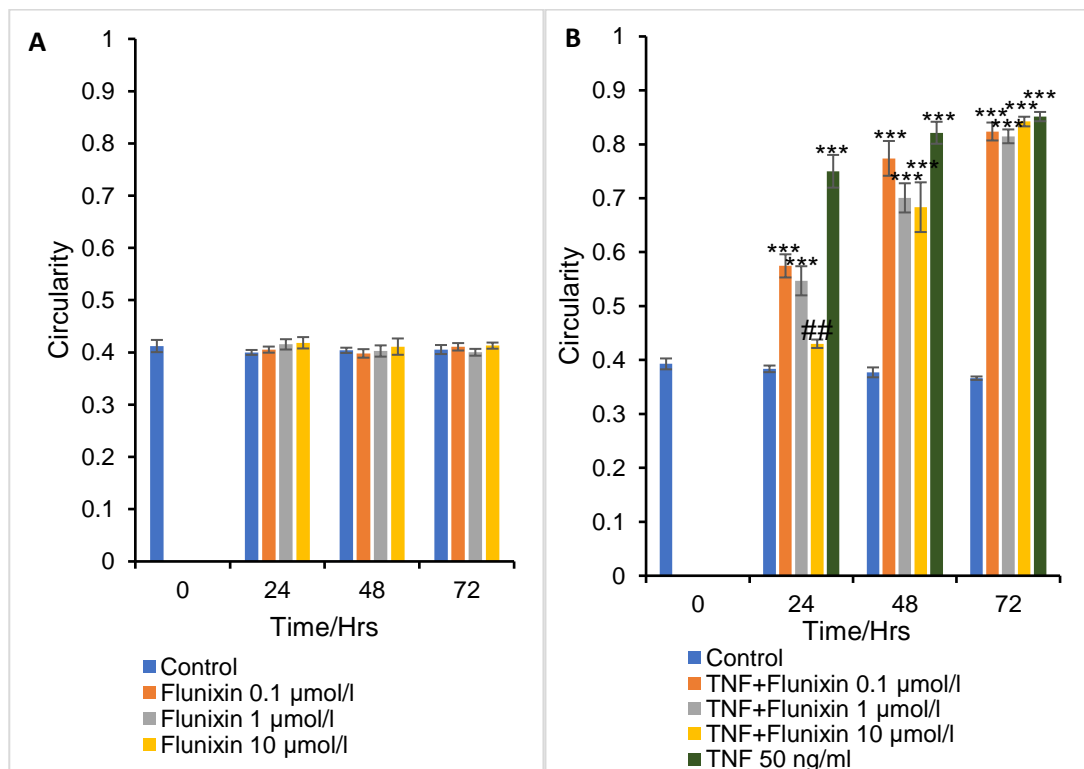


Figure 6.9 WT enteroids were treated with 0, 0.1, 1 and 10 µmol/l flunixin meglumine alone for 0, 24, 48, and 72 hours (A). Prior to addition of 50 ng/ml TNF, WT enteroids were pre-treated with 0.1, 1, and 10 µmol/l flunixin meglumine for 1 hour (B). Statistically significant differences vs untreated (DMSO (0.1%) control) at the same time point are indicated *** $p \leq 0.001$, statistically significant differences between flunixin meglumine + TNF vs TNF alone are depicted by ### $p \leq 0.01$, $n=6$, $N=3$, SEM = error bars, 2-way ANOVA.

6.2.4 Curcumin does not protect against TNF-induced enteroid damages

We first treated WT enteroids with curcumin alone to determine if there were any adverse morphological effects such as cell death caused by curcumin treatment. None of the curcumin doses selected caused increased cell death or enteroid rounding beyond that observed in untreated control enteroids. Baseline circularities of all treatment groups were similar to those presented in chapters 3 and 4 and were all less than 0.44 ± 0.01 (Fig 6.10). Observations of curcumin-treated enteroids at 24, 48, and 72 hours demonstrated continuous normal, polygonal growths without any morphological signs of rounding suggestive of apoptosis with consistent circularity values of less than 0.44 ± 0.10 that were not statistically significant from baseline values or untreated enteroid circularity values at the same time point (figure 6.12A).

Based on the above results, we proceeded to phase two of the study by pre-treating enteroids with curcumin prior to the addition of TNF to determine whether curcumin protected enteroids against TNF-induced enteroid cell death and consequent increased circularity. WT enteroids were pre-treated with 0-10 $\mu\text{mol/l}$ curcumin for 1 hour prior to the addition of 50 ng/ml TNF and circularity was measured at 0, 24, 48, and 72 hours post-TNF treatment. As expected, and in line with data presented in chapters 3 and 4, TNF induced a significant increase in enteroid circularity from baseline by 24 hours reaching 0.79 ± 0.05 . However, there was no statistical significance between curcumin pre-treated enteroids and TNF treated enteroids at any dose or time point tested, suggesting that curcumin is unable to protect enteroids from damage caused by TNF (figures 11 and 12B).

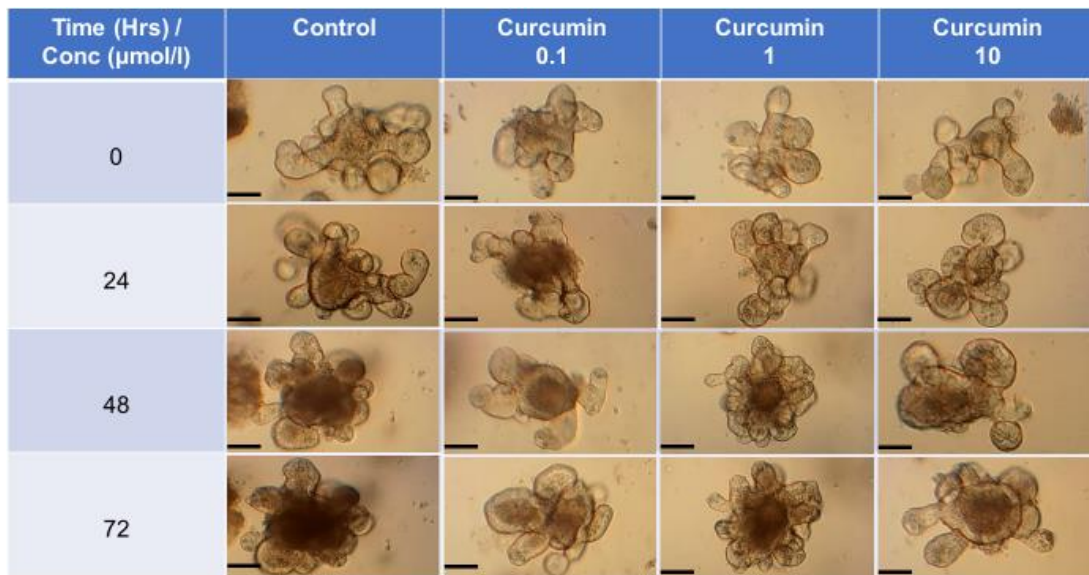


Figure 6.10 Bright field micrographs of untreated, 0.1, 1 and, 10 µmol/l curcumin treated WT enteroids at 0, 24, 48, and 72 hours post-treatment. Both untreated enteroids (DMSO control) and curcumin treated have phenotypically irregular shapes. Curcumin treatment did not induce any morphological changes. Original magnification x10, scale bars, 100 µm.

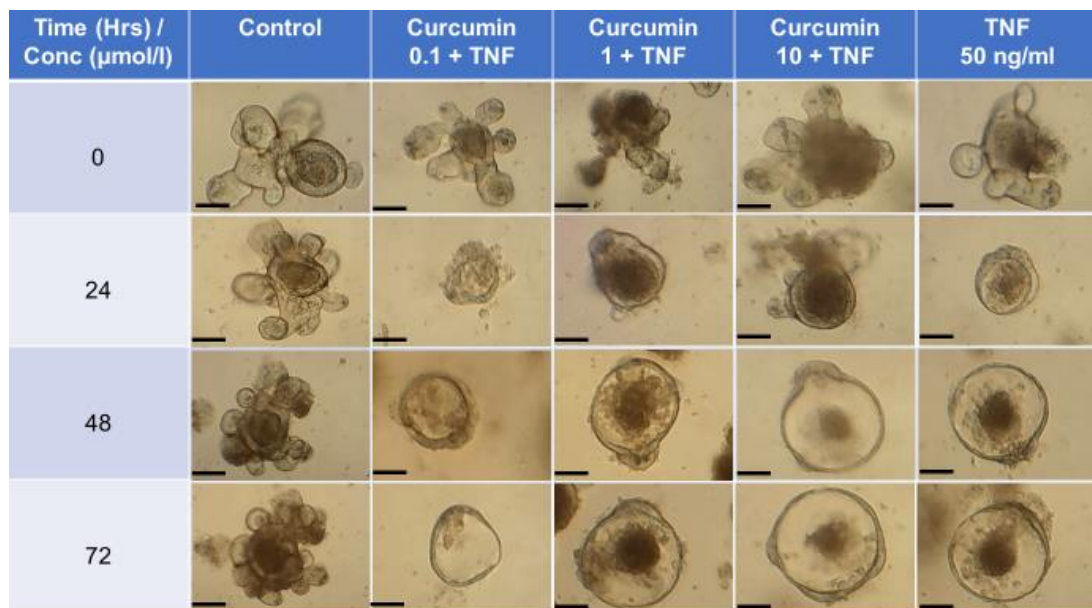
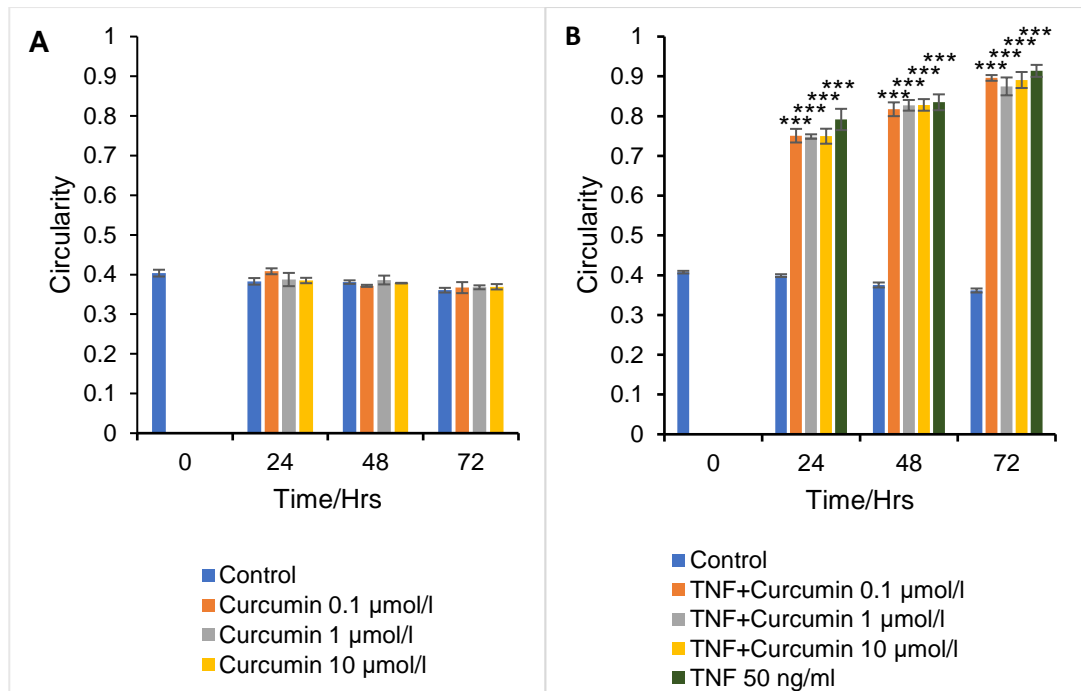


Figure 6.11 Bright field images of untreated WT enteroids and enteroids pre-treated with 0.1, 1, 10 µmol/l curcumin for 1 hr prior to the addition of 50 ng/ml TNF. Enteroids were imaged at 0, 24, 48, and 72 hours post-TNF treatment. Untreated enteroids (DMSO control) had phenotypically irregular structures whilst all TNF treated enteroids displayed a rounding morphology. Original magnification x10, scale bars, 100 µm.



6.2.5 Summary of the actions of therapeutics on TNF-treated enteroids

Below is a summary table of the biological actions of therapeutics on TNF-treated enteroids over the course of 72 hours.

Therapeutic agents	24 hours post-treatment inhibitory effect (10 $\mu\text{mol/l}$ only)	48- & 72-hours post-treatment inhibitory effect
Prednisolone	↑↑↑	-
Hydrocortisone	↑↑↑	-
Flunixin meglumine	↑↑↑	-
Curcumin	-	-

Table 6.1 Prednisolone, hydrocortisone, and flunixin meglumine ameliorated TNF-induced rounding in WT enteroids at 24 hours following treatment, but curcumin did not exert any inhibitory effect at the same time point. However, at 48- and 72- hours following treatment, none of the therapeutics exhibited any inhibitory properties against TNF-induced rounding in WT enteroids.

6.3 Discussion

In this study we investigated whether prednisolone, hydrocortisone, flunixin meglumine and curcumin had abilities to inhibit TNF-induced enteroid rounding. Our data indicate that several agents known to have therapeutic actions against inflammation-induced injury in the gut also show some efficacy in an *in vitro* intestinal epithelial cell model in the absence of other cellular compartments such as immune cells. The 3D enteroid model may therefore provide great future opportunities to study whether repurposed and novel therapeutics are potential candidates for attenuating inflammatory bowel disease (IBD) and sepsis-mediated adverse effects. This needs to be interrogated; whether the results we observed in *in vitro* can be reproduced in *in vivo* and species-specificity and species-sensitivity and metabolism will also need to be taken into consideration.

Corticosteroids are drugs administered to dampen inflammation in a variety of disease conditions including IBD (Ardite et al., 1998). Efficacy of corticosteroid use has also been demonstrated in the prevention of death in sepsis (Marik et al., 2017). A Cochrane review including 61 human trials and 12,192 patients was published in 2019 suggesting that corticosteroids (including prednisolone and hydrocortisone) reduce the 28-day mortality risk in sepsis (Annane et al., 2019) and a recent meta-analysis indicated that hydrocortisone showed greater efficacy than prednisolone in reversing septic shock (Gibbison et al., 2017). *In vivo* studies also support these observations and suggest that rodent tissues respond similarly to humans. For instance, in a CLP-induced abdominal sepsis model in rats, a methylprednisolone (2 mg/kg) peritoneal lavage improved survival rates in abdominal sepsis (Tetikcok et al., 2016). Corticosteroids are also known to mediate their anti-inflammatory properties by modulating NF κ B signalling and I have shown in chapters 3, 4 and 5 of this thesis that perturbation of NF κ B signalling specifically in the intestinal epithelium modulates the epithelial response to TNF and other TNFSF members, so it is not unreasonable

to speculate that corticosteroids could have a direct effect on the intestinal epithelium to desensitise this tissue to the actions of pro-inflammatory cytokines. We identified that at a concentration of 10 $\mu\text{mol/l}$ of either prednisolone or hydrocortisone prevented intestinal epithelial cell-specific damage mediated by TNF over a 24-hour period. However, this protectivity did not persist beyond 24 hours. This is likely to be due to the experimental approach taken and future studies should consider the re-administration of corticosteroid at 12- or 24-hour intervals. The plasma half-life of prednisolone is 2-3 hours in human adults (Bennett et al., 1994; Schijvens et al., 2018), although the biological half-life is around 24 hours allowing for a single daily dose (Cronin et al., 2012). The plasma half-life of hydrocortisone is around 1.5 hours in human plasma (Lennernas, Skrtic & Johannsson, 2008), with a biological half-life of 8-12 hours (Yasir et al., 2020). It is difficult to extrapolate half-lives into the enteroid culture system, however, enteroids express cytochrome P450 enzymes which are responsible for corticosteroid metabolism (Parween et al., 2019) and regular replenishment of the corticosteroids may therefore be needed to confer continued protectivity from TNF-induced pathology. Whilst our study was aimed at assessing the capacity of corticosteroids to desensitise the intestinal epithelium to TNF, they may also protect against further TNF-mediated production of TNF that has been observed in enteroid culture (Bradford et al., 2017). Barber and colleagues reported that administration of hydrocortisone in healthy subjects reduced the concentration of plasma TNF (Barber et al., 1993). Hydrocortisone has been documented to improve survival and haemodynamic response, lower plasma IL-6 concentrations and decrease the levels of phospholipase A2 and E-selectin (Briegel et al., 1994; Heming et al., 2018; Keh et al., 2003; White et al., 1978). The assay of TNF concentration in enteroid culture media should therefore be considered in future experiments to determine whether the observed protectivity in TNF-induced enteroid injury conferred by corticosteroids may in part result from inhibition of TNF production from intestinal epithelial cells. We observed that 1 $\mu\text{mol/l}$ of hydrocortisone or

prednisolone did not show any statistically significant response, whereas 10 $\mu\text{mol/l}$ was protective at 24 hours, so further investigation of doses between 1 and 10 $\mu\text{mol/l}$ will now be required to investigate this dose response relationship in more detail.

Our findings also demonstrated that flunixin meglumine attenuated the effects of TNF-induced rounding at 24 hours post-treatment with TNF in WT enteroids. Flunixin meglumine is a non-steroidal anti-inflammatory drug (NSAID) that has shown efficacy in treating sepsis in horses and dogs and is known to modulate NF- κ B activity (Konigsson et al., 2003; Hardie et al., 1983). The plasma half-life of flunixin meglumine is 1.6 - 2.5 hours, but it has been reported that its effects can last up to 30 hours as a result of the drug accumulation in an inflammatory environment (May & Lees, 1996). The degradation and uptake of flunixin meglumine in enteroid cultures has not been measured. However, in our study at 48 and 72 hours we did not observe any ameliorating effects of flunixin meglumine on TNF-induced rounding and re-application of the drug may therefore be necessary every 12-24 hours to observe continued protectivity due to reduced potency of flunixin meglumine following drug metabolism.

Unlike the previously reported therapeutics, we observed that curcumin had no inhibitory activity on TNF-induced enteroid rounding despite it showing efficacy in *in vivo* CLP sepsis and IBD models (Anand et al., 2007; Da Silva et al., 2017; Nelson et al., 2017). Curcumin significantly lowered levels of sepsis-induced proinflammatory cytokines (IL-1 β and IL-6) in the plasma and peritoneal lavage fluid following CLP. However, plasma curcumin levels were shown to decrease from 2.5 ng/mL at 4 hours, to being undetectable by 24 hours (Da Silva et al., 2017). Curcumin is relatively insoluble in water with unstable, poor bioavailability and rapid metabolism (Anand et al., 2007; Nelson et al., 2017). The half-life of curcumin is between 6 and 7 hours (Jager et al., 2014). So, our lack of curcumin inhibitory findings against TNF-induced rounding at 24, 48, and 72 hours could be due to its shorter half-life and poor solubility

which might affect its absorption. The protective effects of curcumin against IBD and sepsis may also be a result of the inhibition of TNF (and other cytokine inhibition) rather than reducing the sensitivity of the intestinal epithelium to the effects of TNF as we have demonstrated with prednisolone, hydrocortisone and flunixin meglumine. All of the drugs tested above for their ability to ameliorate TNF-induced enteroid pathology are known to modulate NF κ B signalling. The true nature of how NF κ B signalling is modulated specifically in intestinal epithelial cells by these agents is however still to be elucidated. Two broad mechanisms by which these drugs modulate the epithelial damage response have been proposed. The first is by means of reducing the sensitivity of enteroids to TNF by blunting downstream signalling following TNF binding to TNFR1 or TNFR2 and this is the component that the assays in this chapter were designed to assess. The second mechanism is likely to involve inhibition of cytokine production from immune cells and to a lesser extent by intestinal epithelial cells themselves. NF κ B signalling is likely to be implicated in both of these proposed processes. Work has been carried out *in vivo* demonstrating the suppression of classical pathway NF κ B signalling by means of dampening p50 or p65 by these agents (Sanz et al., 2010; Sun, 2011), but little attention has been directed towards their impact on alternative pathway NF κ B signalling, which we have demonstrated as being important in regulating the epithelial-specific damage response (chapters 3 and 4, Jones et al., 2019). Auphan and colleagues and Haskill and colleagues documented that corticosteroid treatment enhances cytoplasmic I κ B sequestering of NF κ B, thus preventing it from being translocated to the nucleus to induce inflammatory gene transcription (Auphan et al., 1995; Haskill et al., 1991). They also reported that corticosteroid, through MAD-3, induces production of I κ B α to prevent activation of the NF κ B signalling pathway (Auphan et al., 1995; Haskill et al., 1991).

In summary, we have developed and tested a 3D enteroid model of intestinal inflammation that can potentially be used in future to assess repurposed and novel therapeutic agents for IBD and sepsis. The model provides structures that accurately recapitulate the intestinal epithelium and isolates this cellular compartment from others in order to address epithelial cell-specific responses without the complex signalling between the epithelium and other mucosal compartments. Future adaptations of the enteroid model to include multiple cell populations (termed reconstituted organoids) are possible to assess specific cell-cell interactions. We have demonstrated the importance of therapeutic approaches to inhibit the actions of TNF specifically on the intestinal epithelium and how targeting this component of the mucosa may ameliorate local and systemic inflammation by promoting the maintenance of intestinal barrier function, thus preventing the perpetuation of inflammation. We would in future like to use this enteroid model to investigate the consequences of 5-aminosalicylic acid (5-ASA) treatment, an anti-inflammatory agent that interferes with the synthesis of prostaglandin from arachidonic acid, and which is widely used to treat IBD (Punchard, Greenfield & Thompson, 1992). We would like to investigate concentrations of tested agents between 1 $\mu\text{mol/l}$ and 10 $\mu\text{mol/l}$ for possible inhibitory effects on induced circularity in enteroids. We demonstrated in chapter 3 (forskolin) and chapter 4 (alternative pathway activators such as TWEAK, LIGHT, CD40-L and another cytokine IL-6) that various other stimuli also induced the rounding of enteroids, so we would like to investigate whether the therapeutic agents that we tested in this chapter also delay, ameliorate or annul the circularity changes that are induced by these stimuli. We would also like to explore the extent to which NF- κ B signalling modulates these drug responses. Whilst inflammatory bowel disease can affect the small intestine, there are many more cases where the colon is inflamed, and the small intestine is not involved. Enteroids are quicker to grow and are more abundant in culture and were chosen to represent both IBD and sepsis where quantification of epithelial dynamics normally yields

greater differences in response to drug treatment compared to the colon. We are currently not certain whether similar findings would have been demonstrated in colonoid culture but studies using colonoids are warranted. Quantification of circularity is less robust in colonoid culture compared with enteroid culture and other analysis methods will be needed to assess changes in morphology. Histological quantification of active caspase 3 and Ki67 would be achievable to assess the impact of TNF and drug treatment on apoptosis and proliferation.

7 General discussion

Sepsis and inflammatory bowel disease (IBD) have several common features and mechanisms. One of the first organs to be damaged in sepsis is the intestine whilst this is also the main location of IBD manifestation. Both conditions are perpetuated by uncontrolled inflammation. Both sepsis and IBD have local and systemic sequelae resulting in dysregulated inflammatory responses. They are both characterised by the hyperproduction of TNF, IFN γ , IL-6 and other pro-inflammatory cytokines, a hyper-inflammatory response to inflammation-inducing agents and intestinal epithelial barrier dysfunction, leading to compromised mucosal protection, microbe translocation, gut leakage, interstitial oedema, apoptosis and intestinal epithelial cell shedding (Kiesslich, 2012; Michielan & D'Inca, 2015; Salim & Soderholm, 2011). Poorly managed IBD can also eventually lead to sepsis. Currently, antibiotics, corticosteroids, biologics and immunomodulatory drugs are the main components of clinical treatment of both sepsis and IBD (Sartor, 2004; Song et al., 2015; Targan et al., 1997). Therefore, in order to effectively generate efficient and efficacious novel therapeutics against both diseases, the importance of in-depth understanding of these conditions at both the cellular and molecular levels cannot be over-emphasised and lessons from one condition may inform the other. It has historically been difficult to develop models of these conditions *in vitro* due to the need for interaction of epithelia with the immune system, the limitation of generating exact culture media to mimic that of the diseased state in humans and an inability to replicate the environmental factors encountered by humans. As a result, new higher throughput reliable *in vitro* models to generate a more physiological environment are needed to complement *in vivo* and clinical studies. The generation of enteroid cultures leading to the data presented in this thesis have addressed some of the limitations previously encountered in model development and have allowed novel studies of NF κ B signalling in the intestinal epithelium.

As previously stated in chapter 1.9.6 and 1.9.7, both classical and alternative NFκB signalling pathways play key roles in gut immune homeostasis. NFκB signal transduction plays major regulatory roles in DNA transcription, intestinal epithelial homeostasis, cytokine production and cell proliferation (Brasier, 2006; Gilmore, 2006; Perkins, 2007). In sepsis, microbes and microbial products interact with host intestinal cell surface pattern recognition receptors (PRRs) such as TLR-2 and TLR-4 to trigger activation of NFκB signalling pathways that result in a cascade of reactions leading to downstream gene transcription of pro-inflammatory cytokines (Beutler et al., 2003). In IBD, dysregulation of the immune system results in the production of pro-inflammatory cytokines that interact with gut epithelial cell surface receptors such as TLR4 to trigger activation of NFκB signalling pathways and subsequent inflammatory reactions (Isaacs et al., 1992; Reinecker et al., 1993). Previous studies have documented TNF as a major activator of the classical and alternative NFκB signalling pathways and have characterised the key role it plays in inducing intestinal damage during IBD and sepsis (Gutierrez et al., 2008; Jones et al., 2019; Kelliher et al., 1998). This is why it was selected as the predominant cytokine for investigation in this thesis. NFκB signalling is important in maintaining epithelial integrity, normal antimicrobial peptide expression, intestinal immune homeostasis, and prevention of translocation of bacteria into the intestinal mucosa (Nenci et al., 2007). However, extensive studies have not been conducted of the importance of alternative NFκB pathway signalling compared with classical NFκB pathway signalling in the intestine.

RelB and NFκB2 mediate alternative NFκB pathway signalling via NEMO-independent signalling to activate alternative activator inducing hyperinflammatory responses including intestinal apoptosis (Moore et al., 2007). Williams and colleagues reported that classical NFκB signalling via NFκB1 (p105/p50) and c-Rel mediated cell survival, whilst alternative pathway signalling via NFκB2 (p100/p52)

coordinated intestinal cell apoptosis (Williams et al., 2013). Burkitt and colleagues additionally demonstrated that that *Nfkb2*^{-/-} mice were protected from DSS-induced experimental colitis, suggesting that alternative pathway NFκB signalling is important in regulating the intestinal damage response (Burkitt et al., 2017). *Nfkb2*^{-/-} mice also showed reduced inflammation in their stomachs compared to WT and *Nfkb1*^{-/-} mice when infected with *Helicobacter felis* (Burkitt et al., 2013). From these studies, the importance of intestinal epithelial cell-specific NFκB signalling was not discernible as global *Nfkb* knockout mouse strains also have defective immune systems and altered damage responses in *Nfkb2*^{-/-} mice could have been a result of perturbed inflammation. Jones and colleagues addressed the importance of epithelial-specific NF-κB2 signalling using enteroids (Jones et al., 2019). *Nfkb2*^{-/-} enteroids were less susceptible to the damaging effects of TNF compared with WT enteroids and other *Nfkb*^{-/-} enteroid lines, suggesting that alternative pathway NFκB signalling specifically in the intestinal epithelium regulates the epithelial damage response and consequently regulates the intestinal barrier (Jones et al., 2019).

This thesis builds on previous findings that the intestinal epithelial damage response is regulated by alternative pathway NFκB signalling. Reports from previous enteroid studies were only based on static conditions and arbitrarily defined time-points. We wanted to extend these findings by determining the range of actions of TNF stimulation and NFκB modulation in enteroids at higher resolution by assessment of enteroids under dynamic conditions using live cell time-lapse imaging technology. We further wanted to determine the mechanistic nature of the resistance to TNF-induced intestinal epithelial damage, so we conducted broad spectrum proteomic analyses of WT, *Nfkb1*^{-/-}, *Nfkb2*^{-/-} and *c-Rel*^{-/-} enteroids with and without TNF to determine factors that may be responsible for modulating the intestinal damage response. Our studies also identified that other stimuli which are known to stimulate alternative pathway NFκB signalling also affect the enteroid damage response

suggesting that the epithelial damage response is not solely regulated by TNF, but also by other cytokines that are known to be upregulated during IBD and sepsis. We were also interested in developing an enteroid model to test potential therapeutics against sepsis and IBD and through interrogation of the enteroid proteome wanted to discover proteins that might be responsible for the protective effects demonstrated by *Nfkb2* null enteroids to the damage caused by TNF to determine potential new therapeutic targets for sepsis and IBD.

7. 1 Main findings

7.1.1 TNF causes altered enteroid morphology

TNF caused enteroids to undergo a rounding morphology which we have shown previously to be associated with increased apoptosis (Jones et al., 2019). The actions of TNF were associated with shortening of the crypt and villus domains and immunohistochemistry demonstrated a significant reduction in proliferation (by Ki67 quantification) (appendix C) and a dose and time-dependent decline in the epithelial thickness of TNF treated enteroids (chapter 3, figures 3.3, 3.4). Through co-staining immunohistochemical techniques developed in this thesis, we were able to identify enteroid villus domains using alkaline phosphatase and crypt domains using Ki67 staining within the same enteroid which may be useful in future studies to understand the differences in sensitivity to different damaging stimuli between these crypt-villus axis regions. We demonstrated villus atrophy as a result of cell shedding in TNF treated enteroids (figure 3.3) and this supported previously reported studies of TNF induced small intestinal epithelial apoptosis and cell shedding following administration to WT mice (Williams et al., 2013). TNF treatment has previously been reported to play key roles in the dysregulation of the integrity of intestinal epithelial tight junction function and structure *in vivo* (Al-Sadi et al., 2013; Arrieta et al., 2009;

Hollander, 1999; Mayhew et al., 1999; Turner, 2009). We also demonstrated a redistribution of claudin-7 in enteroids in response to TNF treatment which suggests that the permeability of the intestinal barrier is altered in enteroids by the actions of TNF (figure 3.5). Clinically, loss of villi and epithelial integrity have been reported to be responsible for malabsorption, increased intestinal permeability, and diarrhoea (Blander, 2016; Mankertz & Schulzke, 2007; Schulzke et al., 2009; Watson & Hughes, 2012).

7.1.2 TNF alters tissue dynamics of enteroids

Live cell imaging of TNF-treated WT intestinal epithelial enteroids demonstrated several behavioural patterns that could not be observed by static bright field imaging. TNF treated enteroids underwent periodic expansions and contractions that were nonsynchronous between enteroids, whereas untreated enteroids did not undergo the same degree of expansion and contraction. TNF treated enteroids were also observed to migrate erratically with a greater cumulative distance of migration and greater speed compared to untreated enteroids. These observations suggest that TNF not only regulates cellular dynamics (a widely reported phenomenon) (Middendorp et al., 2014; Wallach & Bayrer, 2017), but also regulates tissue level dynamics within the intestinal epithelium (a process that is not currently well understood). We were able to show that WT enteroids treated with high doses of TNF regained proliferative capacity once TNF was removed, suggesting that intestinal stem cells are resistant to long-lasting TNF-induced damage compared to other epithelial cell populations. TNF may therefore contribute to the distribution of intestinal stem cells laterally within the intestinal mucosa to aid in healing. There is likely a fine balance between the impact of TNF on cell death and cell shedding (the increased rate of cell shedding induced by TNF could partially be a result of enhanced TNF-induced cellular migration along the crypt-villus axis) with the protective effects that we have potentially demonstrated at the tissue level using enteroids.

7.1.3 NFκB2 signalling is important in regulating the actions of TNF in intestinal epithelia

Enteroids generated from *Nfkb2*^{-/-} mice showed blunted responses to TNF treatment compared with WT enteroids (Chapters 3 and 4; Jones et al., 2019). Whilst TNF-treated WT enteroids became more spherical in appearance and demonstrated increased cell death and cell shedding, *Nfkb2*^{-/-} enteroids showed resistance to the effects of TNF displaying a significantly blunted rounding response. Furthermore, *Nfkb2*^{-/-} enteroids did not expand and contract or migrate to the extent observed in WT enteroids treated with TNF. NF-κB2 signalling is therefore an important regulator of TNF-induced injury specifically in intestinal epithelial cells and may also contribute to the regulation of tissue restitution following mucosal damage.

7.1.4 The intestinal epithelial proteome is modulated by TNF and NFκB perturbations

Several proteins were identified from proteomic analyses that may contribute to the actions of TNF on the intestinal epithelium and the resistance to TNF-induced damage observed in *Nfkb2*^{-/-} enteroids. Ubiquitin-like protein (interferon-stimulated gene 15 ubiquitin-like modifier, (ISG15)), cytoskeleton-associated protein 4 (Ckap4), myoferlin (Myof), and N-alpha-acetyltransferase 30 (Naa30) proteins from our proteomic analysis were upregulated following TNF and have been reported in previous studies to play important roles in cell migration or motility. Isg15 has been implicated to be responsible for chemotaxis of neutrophils in IBD and colon cancer (Zuo et al., 2016). Cytoskeleton-associated protein 4 (Ckap4), N-alpha-acetyltransferase 30 (Naa30) and ribonuclease pancreatic (Rnase1) were upregulated cytoskeletal proteins which play key role in cell dynamics. Ckap4 modulation of actin dynamics via the Abelson interactor 1 (Abi-1) pathway and other intracellular trafficking and signalling coordinated cell contraction, retraction,

migration, focal adhesions, and other cell mechanics (Cleary et al., 2014; Gerthoffer, 2008; Tang & Gerlach, 2017). Intestinal tight junction proteins such as integrin alpha-2 (Itga2), junctional adhesion molecule A (F11r), claudin-4 (Cldn4), integrin beta-6 (Itgb6), integrin alpha-V (Itgbv), claudin-3 (Cldn3), and neural cell adhesion molecule L1 (L1cam) were upregulated following treatment with TNF. They are also involved in regulation of the intestinal barrier and the immunomodulating function of intestinal epithelial cells (Holmes et al., 2006; Lee & Juliano, 2000).

Serum amyloid A-3 protein (Saa3) was significantly upregulated in *Nfkb2*^{-/-} enteroids following TNF treatment and *saa3* has previously been reported to protect against acute lung injury in *Pseudomonas aeruginosa*-infected mice (Fan et al., 2020) and against sepsis (Ather et al., 2018). *Saa3* also plays a prominent role in protecting epithelial cells against sepsis (Ather et al., 2018). Peptidoglycan recognition protein 1 (Pglyrp1) was most significantly up-regulated in *Nfkb2*^{-/-} enteroids and Pglyrp1 demonstrated protection against sepsis during experimental colitis in mice (Saha et al., 2010). *Traf4* was downregulated in *Nfkb2*^{-/-} enteroids and is involved in the protective modulation of cell apoptosis and survival and regulation of *Traf6* and NFκB inflammatory responses (Ayala et al., 1996; Shiels et al., 2000). Downregulation of *traf4* in *Nfkb2*^{-/-} enteroids might be one of the factors responsible for the attenuating effects observed in this transgenic mouse strain. *Tnfaip3* was significantly upregulated in *Nfkb2*^{-/-} enteroids and it has been well documented that *Tnfaip3* exhibits inhibitory activity on NF-κB pathway signalling and regulation of TNF-induced apoptosis (Jung et al., 2019; Lerebours et al., 2008; Serramito et al., 2019). Some interesting proteins were therefore identified that warrant further exploration as targets for modulating the severity of TNF-induced damage in the gut during IBD and sepsis to generate novel therapeutic strategies.

7.1.5 Alternative pathway NFκB2 activators regulate intestinal epithelial survival

We demonstrated in Chapter 3 that alternative pathway NFκB signalling was important in regulating the intestinal epithelial response to TNF. However, we wanted to determine whether this protective effect of *Nfkb2* deletion was unique to TNF or whether *Nfkb2* deletion would confer a similar resistance to other TNF superfamily members that are known to modulate alternative pathway NFκB signalling. We found that there were differential responses to treatment with several TNF superfamily members in WT and *Nfkb2*^{-/-} enteroids. Four out of six members of the TNFSF (TNF, TWEAK, LIGHT and CD40-L with decreasing induced-circularity hierarchy) investigated in this thesis demonstrated different degrees of damage to WT enteroids whilst *Nfkb2*^{-/-} enteroids showed reduced responses to some of these stimuli. Several stimuli however did not induce major rounding in both WT and *Nfkb2*^{-/-} enteroids (CD40-L, LTα/β and BAFF) and no stimulus tested induced greater rounding effects in *Nfkb2*^{-/-} enteroids than in WT. NFκB2 signalling specifically in intestinal epithelial cells is therefore important in regulating the damage response to several cytokines and is not restricted to TNF.

7.1.6 Development of an *in vitro* enteroid model to investigate potential sepsis and IBD therapeutics known to modulate intestinal epithelial cell-specific NFκB signalling

As previous studies have consistently shown, the intestine is one of the first tissues to be damaged during sepsis. So, a reliable *in vitro* model of the GI epithelium would be good to model sepsis and IBD-induced intestinal epithelial effects and thus the potential development of novel therapeutics. TNF is a major cytokine responsible for sepsis and IBD severity and its effects on enteroids were extensively studied in chapters 3-5. We therefore used TNF as an inflammatory stimulus in the enteroid

model to assess various different treatment approaches. Different drug classes such as corticosteroids, an NSAID and a natural anti-inflammatory herb were selected and showed different responses in the model. Corticosteroids tested included prednisolone and hydrocortisone, flunixin meglumine was the NSAID and curcumin was the natural anti-inflammatory herb. Previous studies demonstrated the major roles NF κ B signalling pathways play in initiation, propagation, and progression of both IBD and sepsis with resultant hyper-production of cytokines, dysregulation of hyper-inflammatory responses and disruption of intestinal barrier function and immune system (Beutler et al., 2003; Burkitt et al., 2015; Ghosh et al., 1998). The drugs that were selected to test potential *in vitro* therapeutic approaches in this thesis are already known to modulate NF κ B signalling. We observed that corticosteroids and the NSAID were partially protective against TNF-induced enteroid damage 24-hour following treatment (chapters 4 and 5). NF κ B signalling modulation following treatment still remains to be explored. Many therapeutics are well known to modulate classical pathway NF κ B signalling, but the alternative pathway is relatively under-explored. Future studies will determine whether some of the therapeutic effects observed specifically on the intestinal epithelium may be modulated by suppression of alternative pathway NF κ B signalling.

In this thesis, we therefore demonstrated the reliability of our enteroid model in providing a near-physiological microenvironment of the intestinal epithelium and how it was used as a good model for investigating different classes of agents for potential development of novel therapeutics for the amelioration of sepsis and IBD. At 24 hours following putative therapeutic agent treatment, only prednisolone, hydrocortisone and flunixin meglumine exhibited inhibitory effects against TNF-induced rounding in our enteroid model, whilst curcumin did not demonstrate any inhibition. Further investigation of these promising therapeutic candidates is now needed and approaches to test repurposed and novel IBD and sepsis therapeutics in human

enteroid models would also be useful to determine whether the results in mouse enteroids translate into human enteroids and ultimately humans.

7.2 Implications for sepsis and IBD research and therapeutic intervention

Sepsis and IBD have related pathophysiological mechanisms. Lessons about sepsis management including intestinal epithelial repair and restoration can be learned from IBD research owing to this tissue being one of the first damaged tissues in sepsis. Other tissues particularly epithelial-derived ones such as the lung may undergo similar damage responses to cytokines such as TNF and management of intestinal epithelial-specific signalling pathway derangement may be applicable to cytokine-induced lung hyper-inflammatory responses. Tissue-level dynamic alterations observed in this thesis may also not be exclusive to TNF, as other TNFSF members also induce enteroid morphological changes. It is now timely to investigate whether other pro-inflammatory cytokines also induce expansions/contractions/enhanced motility and other behavioural patterns in enteroids.

We observed that Ckap4, Naa30 and Rnase1 are altered in the intestinal epithelial proteome following TNF treatment, suggesting that these proteins may be responsible for intracellular trafficking and cell mechanics including enhanced motility. We reported that TNF-induced damage in *Nfkb2*^{-/-} enteroids was milder than that observed in WT enteroids and from our proteomic analysis we found that Tnfaip3 protein was upregulated in *Nfkb2*^{-/-} enteroids. Many studies have reported the protective effects of TNFAIP3 protein in *Nfkb2*^{-/-} mice (Kovalenko et al., 2003; Mauro et al., 2006; Nijman et al., 2005; Stilo et al., 2008). This might warrant further investigations in order to understand mechanisms and any plausible inherent therapeutic advantages against sepsis in Tnfaip3 protein signalling.

We demonstrated that some TNF-treated enteroids were rescued after we discarded the TNF-treated media and replaced it with fresh culture media. Results from our therapeutic experiments also demonstrated that pre-treatment with corticosteroids and NSAID attenuated the effects of TNF in the 24-hours following treatment. Thus, we suggest that focusing on nutritional support, cell growth-enhancers, and antagonising sepsis-induced hyper-production of cytokines might be important in treating sepsis. Translationally, this could lead to studies of samples obtained from patients with sepsis and IBD who have been treated with these therapeutics.

We demonstrated that live cell imaging technology provides additional information about morphological changes and behavioural responses to pro-inflammatory cytokines that are easily missed using static bright field microscopy. The importance of these observations is not currently clear, but is likely to present a method of investigating tissue-level dynamics *in vitro* which may greatly enhance the field by providing mechanistic understanding of intestinal tissue restitution following injury such as that observed in IBD and sepsis. Many studies currently use time-lapse confocal imaging, but over short time courses of minutes to several hours. However, imaging multiple enteroids at low power bright-field magnification over a time course of several days was more effective at demonstrating the full extent of tissue-level dynamics. TNF is a major cytokine that contributes to the intestinal pathologies observed in IBD and sepsis. TNF induces apoptosis and in our enteroid model, promising therapeutic agents (prednisolone, hydrocortisone and flunixin meglumine) might have potentially inhibited inflammatory and apoptotic mediated signalling pathways (for an example, NFκB) in the 24-hour period following treatment during which we observed less enteroid rounding.

7.3 Strengths of the study

Enteroids were grown in a 3D microenvironment that is widely demonstrated to be a near-physiological model system for the study of the intestinal epithelium. Enteroids self-propagate, self-organize, undergo self-renewal, and differentiate with little genomic variation for many passages allowing reproducible studies and many more doses and time points to be tested compared to *in vivo* analyses (Fatehullah et al., 2016; Lancaster & Knoblich, 2014). Enteroids contain solely intestinal epithelial cells and therefore allow investigation of the direct impact of factors such as pro-inflammatory cytokines on the epithelium without the complex interplay of signalling networks present between different cellular compartments *in vivo*. This has allowed us to demonstrate the direct impact of TNF and other TNFSF members on the epithelium to address the importance of this tissue compartment in regulating its response to pro-inflammatory cytokines. We have shown that alternative pathway NFκB signalling in this tissue is an important regulator of the damage response and that differences in NFκB2 transcription factor signalling between patients may therefore modulate patients' responses to the development of IBD and sepsis. The live cell imaging technology system provided a real-time and time course video and image capturing of the behavioural responses and morphological changes of the organoids to various treatments. Both static and dynamic images showed cytokine-induced circularity and TNF-induced enteroid circularity has previously been correlated with degree of apoptosis and cell shedding (Jones et al., 2019). The comparison of the proteomic data from intestinal epithelium following administration of LPS to mice and treatment of organoids generated from the same strains of mice with TNF is novel and adds to the generalisable knowledge of pathways that are activated by LPS and TNF and highlights similarities and differences between *in vivo* and *in vitro* approaches at the proteome level.

Crypt and villus compartments of intestinal epithelia demonstrate different functions. Whilst self-propagation and auto-renewal of cells take place in the crypt domain, apoptosis, shedding and expulsion predominantly take place in villus domain. These crypt/villus compartments also exhibit different resistances and responses to cytokine treatment. We developed a co-staining immunohistochemical technique which made it possible to simultaneously investigate crypt/villus domains of interest in enteroids. Our enteroid model has now been developed to test repurposed drugs and novel therapeutics. This will also aid in investigating the alternative pathway NF- κ B signalling pathway more mechanistically and may potentially facilitate the development of drugs that may target this pathway.

7.4 Limitations of the study

Enteroids within a single culture have a range of different sizes, shapes and number of cells. The heterogeneity of organoids might cause clonal drift and slight variation in reproducibility and responses to stimulation and treatment (Fatehullah et al., 2016; Huch et al., 2017). In this study we used a Lonza cytoSMART live cell imaging system which only had 10x magnification to capture enteroid morphological changes and behavioural patterns. The resolution of video-microscopy used could not capture all the detailed information. Confocal imaging would be necessary in enteroids that are several 100 μ m thick to generate high quality cellular resolution. However, low power imaging did allow us to capture many enteroids per field of view that would not be possible by standard confocal microscopy. High throughput 96-well plate confocal imaging is now possible, but unfortunately the equipment is expensive and very specialized. We observed during treatment with TNF that some enteroids migrated away from the microscopic field of view thereby making them lost to follow up. There were also several enteroids that migrated into the microscopic field without us having

prior knowledge of their motility at the beginning of the experiment. These are some of the limitations of the image capture system that we used.

In our proteomic study, we opted for a broad-spectrum proteomic analysis. The proteomic buffer we used was not strong enough to efficiently lyse the membrane and nuclear proteins. According to Wallin and von Heijne, about 30% of genes in the majority of organisms encode membrane proteins (Wallin & von Heijne, 1998). Moreover, membrane proteins have amphipathic biomacromolecules which comprises of central hydrophobic entity and the two hydrophilic ends, thus making it challenging to solubilize membrane proteins for proteomic study (Vit & Petrak, 2017). Future investigation of membrane proteins in the enteroid system with and without TNF might be helpful in determining their roles in tight junction regulation, cell migration, and integrity of the mechanical protective function against bacterial invasion and translocation. Further investigation of nuclear proteins might also be helpful in analysing transcription factors such as NFκB and post-translational modification, acylation and methylation analysis would enable us to determine the activation states of some protein families.

7.5 Future directions

Several potential future directions have already been discussed in this thesis and conducting these studies could help to provide deeper insights into our understanding of the molecular mechanisms that are associated with sepsis and IBD pathogenesis, altered intestinal epithelial cell mechanics, morphological changes, perturbed intestinal tissue level dynamics and regulation of gut barrier function integrity. We have comprehensively demonstrated the prominent roles NFκB signalling pathways in the activation, modulation and propagation of pathological intestinal epithelial responses including rounding, apoptosis and tight junction redistribution subsequent

to various damage-inducing stimuli. From our proteomic analysis, we have also identified many up- and down-regulated proteins following *Nfkb* subunit deletion. It would now be interesting to discover which proteins play passenger or driver roles in intestinal epithelial hyper-inflammatory responses. It would be fascinating to know the biological relevance of the TNF phenotype in WT enteroids and fully understand how TNF affects the intestinal epithelium and other tissues (especially the epithelia lining other organ systems such as the lung) during sepsis. Furthermore, we would like to understand whether sepsis-induced intestinal epithelial dysregulation may mimic similar processes in other tissues or whether it is unique to the intestine, so it would be interesting to analyse other tissues including lung.

Performance of further experiments on the identified proteins for pathway analysis, proteomic signatures, nuclear transcriptional analysis, trans-membrane specific analysis and the roles they play in sepsis and IBD would be of great importance in further understanding the mechanism of sepsis and IBD pathogenesis. Some of these identified proteins could then be selected for location identification by immunohistochemistry and quantification by western blotting experiments.

Various members of the TNFSF have been investigated in this thesis. It would be of scientific and translational importance to further investigate their roles in intestinal epithelial specific NF κ B signalling as well as in other tissues such as lungs that are affected during sepsis. It would also be fascinating to understand how specific inhibitors of the alternative NF κ B pathway signalling (eg IKK α , NIK) modulate and regulate the protective response in WT epithelia as the responses may be similar to those which we observed in *Nfkb2*^{-/-} enteroids and mice with experimentally induced gastrointestinal damage. Therapeutics for sepsis and IBD may therefore also be elucidated based by modulation of this pathway.

We would like to use our enteroid model to test 5-ASA and derivatives (therapeutics commonly used to treat human IBD in the clinic) to determine any possible regulating

and attenuating roles they might have on NFκB signalling pathway and ameliorating effects on sepsis and IBD *in vitro*. Studies of therapeutic combinations on our enteroid model for potential synergistic, additive or antagonistic action might also shed more light on the NFκB signalling pathway, sepsis and IBD.

One of the limitations of the enteroid model is that it has an immune deficit, so we would like to develop enteroid co-cultures with immune cells, mesenchymal cells and other cell populations and then study the interactions between different cellular compartments and test therapeutic agents on induced sepsis and observe how they affect sepsis and NFκB signalling pathway activation. Based on our proteomic results we observed that intestinal epithelial enteroids and mucosa from the same mouse strain had some differences in expressed proteins so we would like to perform animal studies and observe their differences and similarities in term of refining doses, time points and pre-treatment of the investigated therapeutics.

The ultimate aim of this study was to characterise the actions of TNF in dynamic and static states, understand the roles played by the NFκB signalling pathway in intestinal epithelia and to develop potential novel *in vitro* models of IBD and sepsis in which therapeutic approaches could be tested. Future studies of epithelial ultrastructure using transmission electron microscopy and 3D scanning electron microscopy would enable detailed mapping of tight junction and sub-cellular responses to cytokine treatment and NFκB signal transduction modulation. Advanced real-time and quantitative fluorescent live-cell imaging to spatiotemporally monitor complex cell biology would further elucidate cellular and sub-cellular dynamic changes. Development of real-time software to capture, collate, and analyse circularity data would not only minimize manual errors, but would also reduce the screening time for enteroid analysis thus making experiments more efficient.

7.6 Overall conclusions

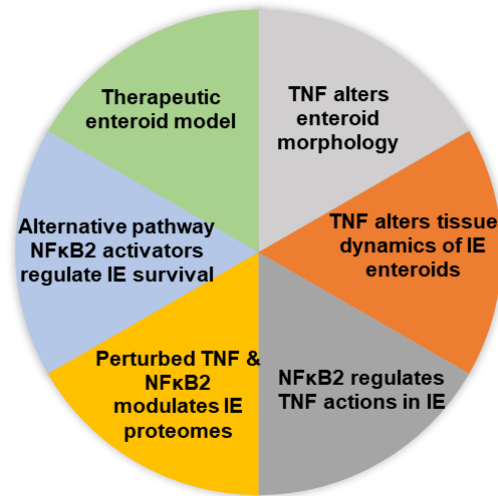


Figure 7.1 A graphical representation of the main findings of the actions of TNF on WT and *Nfkb2*^{-/-} intestinal epithelial (IE) enteroids and quantified proteomes.

This thesis project has identified and described in detail the roles that some members of the TNF superfamily play in modulating susceptibility to developing IBD and sepsis and how NFκB2 contributes to regulating the susceptibility of the intestinal epithelium to cytokine-induced damage (figure 7.1). We have also identified through proteomic analysis several interesting protein targets that warrant further investigation. We have extensively discussed the role of the alternative NFκB signalling pathway activators in inducing pathological morphological changes. The dose- and time-dependent inhibitory roles of several corticosteroids and an NSAID in modulating TNF-induced rounding in enteroids have also been studied. Intestinal epithelial susceptibility to injury caused by TNF superfamily members is modulated by intestinal epithelial cell-specific expression of *Nfkb2*. Interrogation of this signalling pathway is now warranted to further explore whether it can be manipulated to reduce sepsis/IBD severity.

8 Bibliography

- Abraham, E., Anzueto, A., Gutierrez, G., Tessler, S., San Pedro, G., Wunderink, R., . . . Porter, S. (1998). Double-blind randomised controlled trial of monoclonal antibody to human tumour necrosis factor in treatment of septic shock. NORASEPT II Study Group. *Lancet*, *351*(9107), 929-933.
- Abreu, M. T. (2010). Toll-like receptor signalling in the intestinal epithelium: how bacterial recognition shapes intestinal function. *Nat Rev Immunol*, *10*(2), 131-144. doi:10.1038/nri2707
- Adler, K. B., Tuvim, M. J., & Dickey, B. F. (2013). Regulated mucin secretion from airway epithelial cells. *Front Endocrinol (Lausanne)*, *4*, 129. doi:10.3389/fendo.2013.00129
- Adrain, C., Creagh, E. M., Cullen, S. P., & Martin, S. J. (2004). Caspase-dependent inactivation of proteasome function during programmed cell death in *Drosophila* and man. *J Biol Chem*, *279*(35), 36923-36930. doi:10.1074/jbc.M402638200
- Aikawa, N., Takahashi, T., Fujimi, S., Yokoyama, T., Yoshihara, K., Ikeda, T., . . . Maruyama, T. (2013). A Phase II study of polyclonal anti-TNF-alpha (AZD9773) in Japanese patients with severe sepsis and/or septic shock. *J Infect Chemother*, *19*(5), 931-940. doi:10.1007/s10156-013-0612-y
- Akira, S., Taga, T., & Kishimoto, T. (1993). Interleukin-6 in biology and medicine. *Adv Immunol*, *54*, 1-78. doi:10.1016/s0065-2776(08)60532-5
- Alexaki, V. I., Notas, G., Pelekanou, V., Kampa, M., Valkanou, M., Theodoropoulos, P., . . . Castanas, E. (2009). Adipocytes as immune cells: differential expression of TWEAK, BAFF, and APRIL and their receptors (Fn14, BAFF-R, TACI, and BCMA) at different stages of normal and pathological adipose tissue development. *J Immunol*, *183*(9), 5948-5956. doi:10.4049/jimmunol.0901186
- Al-Sadi, R., Guo, S., Ye, D., & Ma, T. Y. (2013). TNF-alpha modulation of intestinal epithelial tight junction barrier is regulated by ERK1/2 activation of Elk-1. *Am J Pathol*, *183*(6), 1871-1884. doi:10.1016/j.ajpath.2013.09.001
- Al-Sadi, R., Guo, S., Ye, D., Rawat, M., & Ma, T. Y. (2016). TNF-alpha Modulation of Intestinal Tight Junction Permeability Is Mediated by NIK/IKK-alpha Axis Activation of the Canonical NF-kappaB Pathway. *Am J Pathol*, *186*(5), 1151-1165. doi:10.1016/j.ajpath.2015.12.016
- Amalakuhan, B., Habib, S. A., Mangat, M., Reyes, L. F., Rodriguez, A. H., Hinojosa, C. A., . . . Restrepo, M. I. (2016). Endothelial adhesion molecules and multiple organ failure in patients with severe sepsis. *Cytokine*, *88*, 267-273. doi:10.1016/j.cyto.2016.08.028
- Amiot, F., Fitting, C., Tracey, K. J., Cavaillon, J. M., & Dautry, F. (1997). Lipopolysaccharide-induced cytokine cascade and lethality in LT alpha/TNF alpha-deficient mice. *Mol Med*, *3*(12), 864-875.
- Amir, R. E., Haecker, H., Karin, M., & Ciechanover, A. (2004). Mechanism of processing of the NF-kappa B2 p100 precursor: identification of the specific polyubiquitin chain-anchoring lysine residue and analysis of the role of NEDD8-modification on the SCF(beta-TrCP) ubiquitin ligase. *Oncogene*, *23*(14), 2540-2547. doi:10.1038/sj.onc.1207366
- Amoozadeh, Y., Dan, Q., Xiao, J., Waheed, F., & Szaszi, K. (2015). Tumor necrosis factor-alpha induces a biphasic change in claudin-2 expression in tubular epithelial cells: role in barrier functions. *Am J Physiol Cell Physiol*, *309*(1), C38-50. doi:10.1152/ajpcell.00388.2014
- Amura, C. R., Silverstein, R., & Morrison, D. C. (1998). Mechanisms involved in the pathogenesis of sepsis are not necessarily reflected by in vitro cell activation

- studies. *Infect Immun*, 66(11), 5372-5378. doi:10.1128/IAI.66.11.5372-5378.1998
- Anbazhagan, A. N., Priyamvada, S., Alrefai, W. A., & Dudeja, P. K. (2018). Pathophysiology of IBD associated diarrhea. *Tissue Barriers*, 6(2), e1463897. doi:10.1080/21688370.2018.1463897
- Anderson, K. L., Hunt, E., & Davis, B. J. (1991). The influence of anti-inflammatory therapy on bacterial clearance following intramammary *Escherichia coli* challenge in goats. *Vet Res Commun*, 15(2), 147-161. doi:10.1007/BF00405146
- Anderson, N. G., & Anderson, N. L. (1996). Twenty years of two-dimensional electrophoresis: past, present and future. *Electrophoresis*, 17(3), 443-453. doi:10.1002/elps.1150170303
- Ando-Akatsuka, Y., Saitou, M., Hirase, T., Kishi, M., Sakakibara, A., Itoh, M., . . . Tsukita, S. (1996). Interspecies diversity of the occludin sequence: cDNA cloning of human, mouse, dog, and rat-kangaroo homologues. *J Cell Biol*, 133(1), 43-47. doi:10.1083/jcb.133.1.43
- Annane, D., Bellissant, E., Bollaert, P. E., Briegel, J., Keh, D., Kupfer, Y., . . . Rochweg, B. (2019). Corticosteroids for treating sepsis in children and adults. *Cochrane Database Syst Rev*, 12, CD002243. doi:10.1002/14651858.CD002243.pub4
- Arakawa, T., & Yphantis, D. A. (1987). Molecular weight of recombinant human tumor necrosis factor-alpha. *J Biol Chem*, 262(16), 7484-7485.
- Ardite, E., Panes, J., Miranda, M., Salas, A., Elizalde, J. I., Sans, M., . . . Pique, J. M. (1998). Effects of steroid treatment on activation of nuclear factor kappaB in patients with inflammatory bowel disease. *Br J Pharmacol*, 124(3), 431-433. doi:10.1038/sj.bjp.0701887
- Ardizzone, S., & Bianchi Porro, G. (2002). Inflammatory bowel disease: new insights into pathogenesis and treatment. *J Intern Med*, 252(6), 475-496. doi:10.1046/j.1365-2796.2002.01067.x
- Arens, C., Bajwa, S. A., Koch, C., Siegler, B. H., Schneck, E., Hecker, A., . . . Uhle, F. (2016). Sepsis-induced long-term immune paralysis--results of a descriptive, explorative study. *Crit Care*, 20, 93. doi:10.1186/s13054-016-1233-5
- Arican, O., Aral, M., Sasmaz, S., & Ciragil, P. (2005). Serum levels of TNF-alpha, IFN-gamma, IL-6, IL-8, IL-12, IL-17, and IL-18 in patients with active psoriasis and correlation with disease severity. *Mediators Inflamm*, 2005(5), 273-279. doi:10.1155/MI.2005.273
- Armitage, R. J., Fanslow, W. C., Strockbine, L., Sato, T. A., Clifford, K. N., Macduff, B. M., . . . et al. (1992). Molecular and biological characterization of a murine ligand for CD40. *Nature*, 357(6373), 80-82. doi:10.1038/357080a0
- Armstrong, C. L., Galisteo, R., Brown, S. A., & Winkles, J. A. (2016). TWEAK activation of the non-canonical NF-kappaB signaling pathway differentially regulates melanoma and prostate cancer cell invasion. *Oncotarget*, 7(49), 81474-81492. doi:10.18632/oncotarget.13034
- Armstrong, R. (2000). *The Gray's anatomy* (1st ed.). London: Serpent's Tail.
- Arrieta, M. C., Madsen, K., Doyle, J., & Meddings, J. (2009). Reducing small intestinal permeability attenuates colitis in the IL10 gene-deficient mouse. *Gut*, 58(1), 41-48. doi:10.1136/gut.2008.150888
- Artavanis-Tsakonas, S., Rand, M. D., & Lake, R. J. (1999). Notch signaling: cell fate control and signal integration in development. *Science*, 284(5415), 770-776. doi:10.1126/science.284.5415.770
- Artis, D. (2008). Epithelial-cell recognition of commensal bacteria and maintenance of immune homeostasis in the gut. *Nat Rev Immunol*, 8(6), 411-420. doi:10.1038/nri2316

- Aslan, A., van Meurs, M., Moser, J., Popa, E. R., Jongman, R. M., Zwiers, P. J., . . . Zijlstra, J. G. (2017). Organ-Specific Differences in Endothelial Permeability-Regulating Molecular Responses in Mouse and Human Sepsis. *Shock*, *48*(1), 69-77. doi:10.1097/SHK.0000000000000841
- Aster, J. C., Blacklow, S. C., & Pear, W. S. (2011). Notch signalling in T-cell lymphoblastic leukaemia/lymphoma and other haematological malignancies. *J Pathol*, *223*(2), 262-273. doi:10.1002/path.2789
- Ather, J. L., Dienz, O., Boyson, J. E., Anathy, V., Amiel, E., & Poynter, M. E. (2018). Serum Amyloid A3 is required for normal lung development and survival following influenza infection. *Sci Rep*, *8*(1), 16571. doi:10.1038/s41598-018-34901-x
- Auphan, N., DiDonato, J. A., Rosette, C., Helmborg, A., & Karin, M. (1995). Immunosuppression by glucocorticoids: inhibition of NF-kappa B activity through induction of I kappa B synthesis. *Science*, *270*(5234), 286-290. doi:10.1126/science.270.5234.286
- Ayabe, T., Satchell, D. P., Wilson, C. L., Parks, W. C., Selsted, M. E., & Ouellette, A. J. (2000). Secretion of microbicidal alpha-defensins by intestinal Paneth cells in response to bacteria. *Nat Immunol*, *1*(2), 113-118. doi:10.1038/77783
- Ayala, A., Herdon, C. D., Lehman, D. L., Ayala, C. A., & Chaudry, I. H. (1996). Differential induction of apoptosis in lymphoid tissues during sepsis: variation in onset, frequency, and the nature of the mediators. *Blood*, *87*(10), 4261-4275.
- Aziz, I., Hadjivassiliou, M., & Sanders, D. S. (2012). Does gluten sensitivity in the absence of coeliac disease exist? *BMJ*, *345*, e7907. doi:10.1136/bmj.e7907
- Bajic, D., Niemann, A., Hillmer, A. K., Mejias-Luque, R., Bluemel, S., Docampo, M., . . . Stein-Thoeringer, C. K. (2020). Gut microbiota derived propionate regulates the expression of Reg3 mucosal lectins and ameliorates experimental colitis in mice. *J Crohns Colitis*. doi:10.1093/ecco-jcc/jjaa065
- Baker, B. M., & Chen, C. S. (2012). Deconstructing the third dimension: how 3D culture microenvironments alter cellular cues. *J Cell Sci*, *125*(Pt 13), 3015-3024. doi:10.1242/jcs.079509
- Baker, M. (2010). Cellular imaging: Taking a long, hard look. *Nature*, *466*(7310), 1137-1140. doi:10.1038/4661137a
- Balda, M. S., & Matter, K. (2008). Tight junctions at a glance. *J Cell Sci*, *121*(Pt 22), 3677-3682. doi:10.1242/jcs.023887
- Ballegeer, M., Van Looveren, K., Timmermans, S., Eggermont, M., Vandevyver, S., Thery, F., . . . Libert, C. (2018). Glucocorticoid receptor dimers control intestinal STAT1 and TNF-induced inflammation in mice. *J Clin Invest*, *128*(8), 3265-3279. doi:10.1172/JCI96636
- Bamias, G., & Cominelli, F. (2016). Cytokines and intestinal inflammation. *Curr Opin Gastroenterol*, *32*(6), 437-442. doi:10.1097/MOG.0000000000000315
- Banerjee, A., McKinley, E. T., von Moltke, J., Coffey, R. J., & Lau, K. S. (2018). Interpreting heterogeneity in intestinal tuft cell structure and function. *J Clin Invest*, *128*(5), 1711-1719. doi:10.1172/JCI120330
- Banham, G., Prezzi, D., Harford, S., Taylor, C. J., Hamer, R., Higgins, R., . . . Clatworthy, M. R. (2013). Elevated pretransplantation soluble BAFF is associated with an increased risk of acute antibody-mediated rejection. *Transplantation*, *96*(4), 413-420. doi:10.1097/TP.0b013e318298dd65
- Barber, A. E., Coyle, S. M., Marano, M. A., Fischer, E., Calvano, S. E., Fong, Y., . . . Lowry, S. F. (1993). Glucocorticoid therapy alters hormonal and cytokine responses to endotoxin in man. *J Immunol*, *150*(5), 1999-2006.
- Barker, N. (2014). Adult intestinal stem cells: critical drivers of epithelial homeostasis and regeneration. *Nat Rev Mol Cell Biol*, *15*(1), 19-33. doi:10.1038/nrm3721

- Barker, N., van Es, J. H., Kuipers, J., Kujala, P., van den Born, M., Cozijnsen, M., . . . Clevers, H. (2007). Identification of stem cells in small intestine and colon by marker gene *Lgr5*. *Nature*, *449*(7165), 1003-1007. doi:10.1038/nature06196
- Barker, N., van Es, J. H., Kuipers, J., Kujala, P., van den Born, M., Cozijnsen, M., . . . Clevers, H. (2007). Identification of stem cells in small intestine and colon by marker gene *Lgr5*. *Nature*, *449*(7165), 1003-1007. doi:10.1038/nature06196
- Barnes, P. J. (2006). How corticosteroids control inflammation: Quintiles Prize Lecture 2005. *Br J Pharmacol*, *148*(3), 245-254. doi:10.1038/sj.bjp.0706736
- Basak, S., Kim, H., Kearns, J. D., Tergaonkar, V., O'Dea, E., Werner, S. L., . . . Hoffmann, A. (2007). A fourth I κ B protein within the NF- κ B signaling module. *Cell*, *128*(2), 369-381. doi:10.1016/j.cell.2006.12.033
- Bauer, H., Zweimueller-Mayer, J., Steinbacher, P., Lametschwandtner, A., & Bauer, H. C. (2010). The dual role of zonula occludens (ZO) proteins. *J Biomed Biotechnol*, *2010*, 402593. doi:10.1155/2010/402593
- Bauer, J., Namineni, S., Reisinger, F., Zoller, J., Yuan, D., & Heikenwalder, M. (2012). Lymphotoxin, NF- κ B, and cancer: the dark side of cytokines. *Dig Dis*, *30*(5), 453-468. doi:10.1159/000341690
- Baumgart, D. C., & Sandborn, W. J. (2012). Crohn's disease. *Lancet*, *380*(9853), 1590-1605. doi:10.1016/S0140-6736(12)60026-9
- Becker, C., Wirtz, S., Blessing, M., Pirhonen, J., Strand, D., Bechthold, O., . . . Neurath, M. F. (2003). Constitutive p40 promoter activation and IL-23 production in the terminal ileum mediated by dendritic cells. *J Clin Invest*, *112*(5), 693-706. doi:10.1172/JCI17464
- Bekker-Jensen, D. B., Kelstrup, C. D., Batth, T. S., Larsen, S. C., Haldrup, C., Bramsen, J. B., . . . Olsen, J. V. (2017). An Optimized Shotgun Strategy for the Rapid Generation of Comprehensive Human Proteomes. *Cell Syst*, *4*(6), 587-599 e584. doi:10.1016/j.cels.2017.05.009
- Bennett, W. M., Aronoff, G. R., Morrison, G., Golper, T. A., Pulliam, J., Wolfson, M., & Singer, I. (1983). Drug prescribing in renal failure: dosing guidelines for adults. *Am J Kidney Dis*, *3*(3), 155-193. doi:10.1016/s0272-6386(83)80060-2
- Berg, D. J., Zhang, J., Weinstock, J. V., Ismail, H. F., Earle, K. A., Alila, H., . . . Lynch, R. G. (2002). Rapid development of colitis in NSAID-treated IL-10-deficient mice. *Gastroenterology*, *123*(5), 1527-1542. doi:10.1053/gast.2002.1231527
- Berzal, S., Gonzalez-Guerrero, C., Rayego-Mateos, S., Uceros, A., Ocana-Salceda, C., Egido, J., . . . Ramos, A. M. (2015). TNF-related weak inducer of apoptosis (TWEAK) regulates junctional proteins in tubular epithelial cells via canonical NF- κ B pathway and ERK activation. *J Cell Physiol*, *230*(7), 1580-1593. doi:10.1002/jcp.24905
- Beutler, B., Greenwald, D., Hulmes, J. D., Chang, M., Pan, Y. C., Mathison, J., . . . Cerami, A. (1985). Identity of tumour necrosis factor and the macrophage-secreted factor cachectin. *Nature*, *316*(6028), 552-554. doi:10.1038/316552a0
- Beutler, B., Hoebe, K., Du, X., & Ulevitch, R. J. (2003). How we detect microbes and respond to them: the Toll-like receptors and their transducers. *J Leukoc Biol*, *74*(4), 479-485. doi:10.1189/jlb.0203082
- Bingle, L., Brown, N. J., & Lewis, C. E. (2002). The role of tumour-associated macrophages in tumour progression: implications for new anticancer therapies. *J Pathol*, *196*(3), 254-265. doi:10.1002/path.1027
- Birchenough, G. M., Johansson, M. E., Gustafsson, J. K., Bergstrom, J. H., & Hansson, G. C. (2015). New developments in goblet cell mucus secretion and function. *Mucosal Immunol*, *8*(4), 712-719. doi:10.1038/mi.2015.32

- Blander, J. M. (2016). Death in the intestinal epithelium-basic biology and implications for inflammatory bowel disease. *FEBS J*, 283(14), 2720-2730. doi:10.1111/febs.13771
- Blikslager, A. T., Moeser, A. J., Gookin, J. L., Jones, S. L., & Odle, J. (2007). Restoration of barrier function in injured intestinal mucosa. *Physiol Rev*, 87(2), 545-564. doi:10.1152/physrev.00012.2006
- Boecke, A., Carstens, A. C., Neacsu, C. D., Baschuk, N., Haubert, D., Kashkar, H., . . . Kronke, M. (2013). TNF-receptor-1 adaptor protein FAN mediates TNF-induced B16 melanoma motility and invasion. *Br J Cancer*, 109(2), 422-432. doi:10.1038/bjc.2013.242
- Boehm, J. S., Zhao, J. J., Yao, J., Kim, S. Y., Firestein, R., Dunn, I. F., . . . Hahn, W. C. (2007). Integrative genomic approaches identify IKBKE as a breast cancer oncogene. *Cell*, 129(6), 1065-1079. doi:10.1016/j.cell.2007.03.052
- Boehnke, K., Iversen, P. W., Schumacher, D., Lallena, M. J., Haro, R., Amat, J., . . . Velasco, J. A. (2016). Assay Establishment and Validation of a High-Throughput Screening Platform for Three-Dimensional Patient-Derived Colon Cancer Organoid Cultures. *J Biomol Screen*, 21(9), 931-941. doi:10.1177/1087057116650965
- Bohm, I. (2003). Disruption of the cytoskeleton after apoptosis induction with autoantibodies. *Autoimmunity*, 36(3), 183-189. doi:10.1080/0891693031000105617
- Boj, S. F., Vonk, A. M., Statia, M., Su, J., Vries, R. R., Beekman, J. M., & Clevers, H. (2017). Forskolin-induced Swelling in Intestinal Organoids: An In Vitro Assay for Assessing Drug Response in Cystic Fibrosis Patients. *J Vis Exp*(120). doi:10.3791/55159
- Bolkun, L., Lemancewicz, D., Jablonska, E., Kulczynska, A., Bolkun-Skornicka, U., Kloczko, J., & Dzieciol, J. (2014). BAFF and APRIL as TNF superfamily molecules and angiogenesis parallel progression of human multiple myeloma. *Ann Hematol*, 93(4), 635-644. doi:10.1007/s00277-013-1924-9
- Bonnier, F., Keating, M. E., Wrobel, T. P., Majzner, K., Baranska, M., Garcia-Munoz, A., . . . Byrne, H. J. (2015). Cell viability assessment using the Alamar blue assay: a comparison of 2D and 3D cell culture models. *Toxicol In Vitro*, 29(1), 124-131. doi:10.1016/j.tiv.2014.09.014
- Borcherding, F., Nitschke, M., Hundorfean, G., Rupp, J., von Smolinski, D., Bieber, K., . . . Buning, J. (2010). The CD40-CD40L pathway contributes to the proinflammatory function of intestinal epithelial cells in inflammatory bowel disease. *Am J Pathol*, 176(4), 1816-1827. doi:10.2353/ajpath.2010.090461
- Bossen, C., Ingold, K., Tardivel, A., Bodmer, J. L., Gaide, O., Hertig, S., . . . Schneider, P. (2006). Interactions of tumor necrosis factor (TNF) and TNF receptor family members in the mouse and human. *J Biol Chem*, 281(20), 13964-13971. doi:10.1074/jbc.M601553200
- Bradford, E. M., Ryu, S. H., Singh, A. P., Lee, G., Goretsky, T., Sinh, P., . . . Barrett, T. A. (2017). Epithelial TNF Receptor Signaling Promotes Mucosal Repair in Inflammatory Bowel Disease. *J Immunol*, 199(5), 1886-1897. doi:10.4049/jimmunol.1601066
- Bradley, J. R. (2008). TNF-mediated inflammatory disease. *J Pathol*, 214(2), 149-160. doi:10.1002/path.2287
- Braegger, C. P., Nicholls, S., Murch, S. H., Stephens, S., & MacDonald, T. T. (1992). Tumour necrosis factor alpha in stool as a marker of intestinal inflammation. *Lancet*, 339(8785), 89-91. doi:10.1016/0140-6736(92)90999-j
- Brandt, C., & Pedersen, B. K. (2010). The role of exercise-induced myokines in muscle homeostasis and the defense against chronic diseases. *J Biomed Biotechnol*, 2010, 520258. doi:10.1155/2010/520258
- Brasier, A. R. (2006). The NF-kappaB regulatory network. *Cardiovasc Toxicol*, 6(2), 111-130. doi:10.1385/ct.6:2:111

- Bray, F., Ferlay, J., Soerjomataram, I., Siegel, R. L., Torre, L. A., & Jemal, A. (2018). Global cancer statistics 2018: GLOBOCAN estimates of incidence and mortality worldwide for 36 cancers in 185 countries. *CA Cancer J Clin*, *68*(6), 394-424. doi:10.3322/caac.21492
- Bray, S. J. (2016). Notch signalling in context. *Nat Rev Mol Cell Biol*, *17*(11), 722-735. doi:10.1038/nrm.2016.94
- Brentnall, M., Rodriguez-Menocal, L., De Guevara, R. L., Cepero, E., & Boise, L. H. (2013). Caspase-9, caspase-3 and caspase-7 have distinct roles during intrinsic apoptosis. *BMC Cell Biol*, *14*, 32. doi:10.1186/1471-2121-14-32
- Briegel, J., Kellermann, W., Forst, H., Haller, M., Bittl, M., Hoffmann, G. E., . . . Peter, K. (1994). Low-dose hydrocortisone infusion attenuates the systemic inflammatory response syndrome. The Phospholipase A2 Study Group. *Clin Investig*, *72*(10), 782-787. doi:10.1007/BF00180547
- Brown, S. A., Ghosh, A., & Winkles, J. A. (2010). Full-length, membrane-anchored TWEAK can function as a juxtacrine signaling molecule and activate the NF-kappaB pathway. *J Biol Chem*, *285*(23), 17432-17441. doi:10.1074/jbc.M110.131979
- Browning, J. L., Ngam-ek, A., Lawton, P., DeMarinis, J., Tizard, R., Chow, E. P., . . . Ware, C. F. (1993). Lymphotoxin beta, a novel member of the TNF family that forms a heteromeric complex with lymphotoxin on the cell surface. *Cell*, *72*(6), 847-856. doi:10.1016/0092-8674(93)90574-a
- Brunetti, G., Rizzi, R., Storlino, G., Bortolotti, S., Colaianni, G., Sanesi, L., . . . Colucci, S. (2018). LIGHT/TNFSF14 as a New Biomarker of Bone Disease in Multiple Myeloma Patients Experiencing Therapeutic Regimens. *Front Immunol*, *9*, 2459. doi:10.3389/fimmu.2018.02459
- Bry, L., Falk, P., Huttner, K., Ouellette, A., Midtvedt, T., & Gordon, J. I. (1994). Paneth cell differentiation in the developing intestine of normal and transgenic mice. *Proc Natl Acad Sci U S A*, *91*(22), 10335-10339. doi:10.1073/pnas.91.22.10335
- Bryant, C. E., Farnfield, B. A., & Janicke, H. J. (2003). Evaluation of the ability of carprofen and flunixin meglumine to inhibit activation of nuclear factor kappa B. *Am J Vet Res*, *64*(2), 211-215. doi:10.2460/ajvr.2003.64.211
- Brynskov, J., Foegh, P., Pedersen, G., Ellervik, C., Kirkegaard, T., Bingham, A., & Saermark, T. (2002). Tumour necrosis factor alpha converting enzyme (TACE) activity in the colonic mucosa of patients with inflammatory bowel disease. *Gut*, *51*(1), 37-43. doi:10.1136/gut.51.1.37
- Buckley, A., & Turner, J. R. (2018). Cell Biology of Tight Junction Barrier Regulation and Mucosal Disease. *Cold Spring Harb Perspect Biol*, *10*(1). doi:10.1101/cshperspect.a029314
- Bullen, T. F., Forrest, S., Campbell, F., Dodson, A. R., Hershman, M. J., Pritchard, D. M., . . . Watson, A. J. (2006). Characterization of epithelial cell shedding from human small intestine. *Lab Invest*, *86*(10), 1052-1063. doi:10.1038/labinvest.3700464
- Bunte, K., Smith, D. J., Chappell, M. J., Hassan-Smith, Z. K., Tomlinson, J. W., Arlt, W., & Tino, P. (2018). Learning pharmacokinetic models for in vivo glucocorticoid activation. *J Theor Biol*, *455*, 222-231. doi:10.1016/j.jtbi.2018.07.025
- Burge, K., Gunasekaran, A., Eckert, J., & Chaaban, H. (2019). Curcumin and Intestinal Inflammatory Diseases: Molecular Mechanisms of Protection. *Int J Mol Sci*, *20*(8). doi:10.3390/ijms20081912
- Burkitt, M. D., Hanedi, A. F., Duckworth, C. A., Williams, J. M., Tang, J. M., O'Reilly, L. A., . . . Pritchard, D. M. (2015). NF-kappaB1, NF-kappaB2 and c-Rel differentially regulate susceptibility to colitis-associated adenoma development in C57BL/6 mice. *J Pathol*, *236*(3), 326-336. doi:10.1002/path.4527

- Burkitt, M. D., Williams, J. M., Duckworth, C. A., O'Hara, A., Hanedi, A., Varro, A., . . . Pritchard, D. M. (2013). Signaling mediated by the NF-kappaB sub-units NF-kappaB1, NF-kappaB2 and c-Rel differentially regulate *Helicobacter felis*-induced gastric carcinogenesis in C57BL/6 mice. *Oncogene*, *32*(50), 5563-5573. doi:10.1038/onc.2013.334
- Burkitt, M. D., Williams, J. M., Townsend, T., Hough, R., Duckworth, C. A., & Pritchard, D. M. (2017). Mice lacking NF-kappaB1 exhibit marked DNA damage responses and more severe gastric pathology in response to intraperitoneal tamoxifen administration. *Cell Death Dis*, *8*(7), e2939. doi:10.1038/cddis.2017.332
- Burkly, L., Hession, C., Ogata, L., Reilly, C., Marconi, L. A., Olson, D., . . . Lo, D. (1995). Expression of relB is required for the development of thymic medulla and dendritic cells. *Nature*, *373*(6514), 531-536. doi:10.1038/373531a0
- Burkly, L. C., Michaelson, J. S., & Zheng, T. S. (2011). TWEAK/Fn14 pathway: an immunological switch for shaping tissue responses. *Immunol Rev*, *244*(1), 99-114. doi:10.1111/j.1600-065X.2011.01054.x
- Burns, A. J., Roberts, R. R., Bornstein, J. C., & Young, H. M. (2009). Development of the enteric nervous system and its role in intestinal motility during fetal and early postnatal stages. *Semin Pediatr Surg*, *18*(4), 196-205. doi:10.1053/j.sempedsurg.2009.07.001
- Buttke, T. M., & Sandstrom, P. A. (1994). Oxidative stress as a mediator of apoptosis. *Immunol Today*, *15*(1), 7-10. doi:10.1016/0167-5699(94)90018-3
- Butto, L. F., Pelletier, A., More, S. K., Zhao, N., Osme, A., Hager, C. L., . . . Dave, M. (2020). Intestinal Stem Cell Niche Defects Result in Impaired 3D Organoid Formation in Mouse Models of Crohn's Disease-like Ileitis. *Stem Cell Reports*, *15*(2), 389-407. doi:10.1016/j.stemcr.2020.06.017
- Butty, V. L., Roux-Lombard, P., Garbino, J., Dayer, J. M., Ricou, B., & Geneva Sepsis, N. (2003). Anti-inflammatory response after infusion of p55 soluble tumor necrosis factor receptor fusion protein for severe sepsis. *Eur Cytokine Netw*, *14*(1), 15-19.
- Caamano, J. H., Rizzo, C. A., Durham, S. K., Barton, D. S., Raventos-Suarez, C., Snapper, C. M., & Bravo, R. (1998). Nuclear factor (NF)-kappa B2 (p100/p52) is required for normal splenic microarchitecture and B cell-mediated immune responses. *J Exp Med*, *187*(2), 185-196. doi:10.1084/jem.187.2.185
- Cadigan, K. M., & Nusse, R. (1997). Wnt signaling: a common theme in animal development. *Genes Dev*, *11*(24), 3286-3305. doi:10.1101/gad.11.24.3286
- Cadwell, K., Patel, K. K., Komatsu, M., Virgin, H. W. t., & Stappenbeck, T. S. (2009). A common role for Atg16L1, Atg5 and Atg7 in small intestinal Paneth cells and Crohn disease. *Autophagy*, *5*(2), 250-252. doi:10.4161/auto.5.2.7560
- Calabresi, P. (1996). Results of the National Cancer Advisory Board evaluation of the National Cancer Program. *Cancer*, *78*(12), 2607-2608. doi:10.1002/(sici)1097-0142(19961215)78:12<2607::aid-cncr30>3.0.co;2-y
- Campbell, S., Burkly, L. C., Gao, H. X., Berman, J. W., Su, L., Browning, B., . . . Putterman, C. (2006). Proinflammatory effects of TWEAK/Fn14 interactions in glomerular mesangial cells. *J Immunol*, *176*(3), 1889-1898. doi:10.4049/jimmunol.176.3.1889
- Cande, C., Vahsen, N., Kouranti, I., Schmitt, E., Daugas, E., Spahr, C., . . . Kroemer, G. (2004). AIF and cyclophilin A cooperate in apoptosis-associated chromatinolysis. *Oncogene*, *23*(8), 1514-1521. doi:10.1038/sj.onc.1207279
- Cani, P. D., Bibiloni, R., Knauf, C., Waget, A., Neyrinck, A. M., Delzenne, N. M., & Burcelin, R. (2008). Changes in gut microbiota control metabolic

- endotoxemia-induced inflammation in high-fat diet-induced obesity and diabetes in mice. *Diabetes*, 57(6), 1470-1481. doi:10.2337/db07-1403
- Cao, Z., & Robinson, R. A. (2014). The role of proteomics in understanding biological mechanisms of sepsis. *Proteomics Clin Appl*, 8(1-2), 35-52. doi:10.1002/prca.201300101
- Capaldo, C. T., Farkas, A. E., Hilgarth, R. S., Krug, S. M., Wolf, M. F., Benedik, J. K., . . . Nusrat, A. (2014). Proinflammatory cytokine-induced tight junction remodeling through dynamic self-assembly of claudins. *Mol Biol Cell*, 25(18), 2710-2719. doi:10.1091/mbc.E14-02-0773
- Carmona-Gutierrez, D., Eisenberg, T., Buttner, S., Meisinger, C., Kroemer, G., & Madeo, F. (2010). Apoptosis in yeast: triggers, pathways, subroutines. *Cell Death Differ*, 17(5), 763-773. doi:10.1038/cdd.2009.219
- Cerovic, V., Bain, C. C., Mowat, A. M., & Milling, S. W. (2014). Intestinal macrophages and dendritic cells: what's the difference? *Trends Immunol*, 35(6), 270-277. doi:10.1016/j.it.2014.04.003
- Chan, E. Y. (2012). Regulation and function of uncoordinated-51 like kinase proteins. *Antioxid Redox Signal*, 17(5), 775-785. doi:10.1089/ars.2011.4396
- Chandel, N. S., Trzyna, W. C., McClintock, D. S., & Schumacker, P. T. (2000). Role of oxidants in NF-kappa B activation and TNF-alpha gene transcription induced by hypoxia and endotoxin. *J Immunol*, 165(2), 1013-1021. doi:10.4049/jimmunol.165.2.1013
- Chandramouli, K., & Qian, P. Y. (2009). Proteomics: challenges, techniques and possibilities to overcome biological sample complexity. *Hum Genomics Proteomics*, 2009. doi:10.4061/2009/239204
- Chavarria-Velazquez, C. O., Torres-Martinez, A. C., Montano, L. F., & Rendon-Huerta, E. P. (2018). TLR2 activation induced by *H. pylori* LPS promotes the differential expression of claudin-4, -6, -7 and -9 via either STAT3 and ERK1/2 in AGS cells. *Immunobiology*, 223(1), 38-48. doi:10.1016/j.imbio.2017.10.016
- Chen, L., Deng, H., Cui, H., Fang, J., Zuo, Z., Deng, J., . . . Zhao, L. (2018). Inflammatory responses and inflammation-associated diseases in organs. *Oncotarget*, 9(6), 7204-7218. doi:10.18632/oncotarget.23208
- Chen, S., Xia, Y., Zhu, G., Yan, J., Tan, C., Deng, B., . . . Ren, W. (2018). Glutamine supplementation improves intestinal cell proliferation and stem cell differentiation in weanling mice. *Food Nutr Res*, 62. doi:10.29219/fnr.v62.1439
- Chen, Y., Merzdorf, C., Paul, D. L., & Goodenough, D. A. (1997). COOH terminus of occludin is required for tight junction barrier function in early *Xenopus* embryos. *J Cell Biol*, 138(4), 891-899. doi:10.1083/jcb.138.4.891
- Cheng, E. H., Wei, M. C., Weiler, S., Flavell, R. A., Mak, T. W., Lindsten, T., & Korsmeyer, S. J. (2001). BCL-2, BCL-X(L) sequester BH3 domain-only molecules preventing BAX- and BAK-mediated mitochondrial apoptosis. *Mol Cell*, 8(3), 705-711. doi:10.1016/s1097-2765(01)00320-3
- Cheng, H. (1974). Origin, differentiation and renewal of the four main epithelial cell types in the mouse small intestine. IV. Paneth cells. *Am J Anat*, 141(4), 521-535. doi:10.1002/aja.1001410406
- Chicheportiche, Y., Bourdon, P. R., Xu, H., Hsu, Y. M., Scott, H., Hession, C., . . . Browning, J. L. (1997). TWEAK, a new secreted ligand in the tumor necrosis factor family that weakly induces apoptosis. *J Biol Chem*, 272(51), 32401-32410. doi:10.1074/jbc.272.51.32401
- Chieppa, M., Rescigno, M., Huang, A. Y., & Germain, R. N. (2006). Dynamic imaging of dendritic cell extension into the small bowel lumen in response to epithelial cell TLR engagement. *J Exp Med*, 203(13), 2841-2852. doi:10.1084/jem.20061884

- Cho, J. H., & Brant, S. R. (2011). Recent insights into the genetics of inflammatory bowel disease. *Gastroenterology*, *140*(6), 1704-1712. doi:10.1053/j.gastro.2011.02.046
- Chopra, M., Brandl, A., Siegmund, D., Mottok, A., Schafer, V., Biehl, M., . . . Wajant, H. (2015). Blocking TWEAK-Fn14 interaction inhibits hematopoietic stem cell transplantation-induced intestinal cell death and reduces GVHD. *Blood*, *126*(4), 437-444. doi:10.1182/blood-2015-01-620583
- Cildir, G., Low, K. C., & Tergaonkar, V. (2016). Noncanonical NF-kappaB Signaling in Health and Disease. *Trends Mol Med*, *22*(5), 414-429. doi:10.1016/j.molmed.2016.03.002
- Cipollone, F., Mezzetti, A., Porreca, E., Di Febbo, C., Nutini, M., Fazia, M., . . . Davi, G. (2002). Association between enhanced soluble CD40L and prothrombotic state in hypercholesterolemia: effects of statin therapy. *Circulation*, *106*(4), 399-402. doi:10.1161/01.cir.0000025419.95769.f0
- Clark, J. A., Clark, A. T., Hotchkiss, R. S., Buchman, T. G., & Coopersmith, C. M. (2008). Epidermal growth factor treatment decreases mortality and is associated with improved gut integrity in sepsis. *Shock*, *30*(1), 36-42. doi:10.1097/shk.0b013e31815D0820
- Clark, M. A., Plank, L. D., Connolly, A. B., Streat, S. J., Hill, A. A., Gupta, R., . . . Hill, G. L. (1998). Effect of a chimeric antibody to tumor necrosis factor-alpha on cytokine and physiologic responses in patients with severe sepsis--a randomized, clinical trial. *Crit Care Med*, *26*(10), 1650-1659. doi:10.1097/00003246-199810000-00016
- Clarke, K., & Chintanaboina, J. (2019). Allergic and Immunologic Perspectives of Inflammatory Bowel Disease. *Clin Rev Allergy Immunol*, *57*(2), 179-193. doi:10.1007/s12016-018-8690-3
- Clayburgh, D. R., Musch, M. W., Leitges, M., Fu, Y. X., & Turner, J. R. (2006). Coordinated epithelial NHE3 inhibition and barrier dysfunction are required for TNF-mediated diarrhea in vivo. *J Clin Invest*, *116*(10), 2682-2694. doi:10.1172/JCI29218
- Clayburgh, D. R., Musch, M. W., Leitges, M., Fu, Y. X., & Turner, J. R. (2006). Coordinated epithelial NHE3 inhibition and barrier dysfunction are required for TNF-mediated diarrhea in vivo. *J Clin Invest*, *116*(10), 2682-2694. doi:10.1172/JCI29218
- Cleary, R. A., Wang, R., Waqar, O., Singer, H. A., & Tang, D. D. (2014). Role of c-Abl tyrosine kinase in smooth muscle cell migration. *Am J Physiol Cell Physiol*, *306*(8), C753-761. doi:10.1152/ajpcell.00327.2013
- Clevers, H. C., & Bevins, C. L. (2013). Paneth cells: maestros of the small intestinal crypts. *Annu Rev Physiol*, *75*, 289-311. doi:10.1146/annurev-physiol-030212-183744
- Cohen, J. (2002). The immunopathogenesis of sepsis. *Nature*, *420*(6917), 885-891. doi:10.1038/nature01326
- Colbert, J. F., Schmidt, E. P., Faubel, S., & Ginde, A. A. (2017). Severe Sepsis Outcomes Among Hospitalizations With Inflammatory Bowel Disease. *Shock*, *47*(2), 128-131. doi:10.1097/SHK.0000000000000742
- Cole, L. A., & Kramer, P. R. (2016). *Human physiology, biochemistry, and basic medicine*. Amsterdam ; Boston: Elsevier/AP, Academic Press is an imprint of Elsevier.
- Collins, J. F., Honda, T., Knobel, S., Bulus, N. M., Conary, J., DuBois, R., & Ghishan, F. K. (1993). Molecular cloning, sequencing, tissue distribution, and functional expression of a Na⁺/H⁺ exchanger (NHE-2). *Proc Natl Acad Sci U S A*, *90*(9), 3938-3942. doi:10.1073/pnas.90.9.3938
- Conrad, U., Plagmann, I., Malchow, S., Sack, M., Floss, D. M., Kruglov, A. A., . . . Scheller, J. (2011). ELPylated anti-human TNF therapeutic single-domain

- antibodies for prevention of lethal septic shock. *Plant Biotechnol J*, 9(1), 22-31. doi:10.1111/j.1467-7652.2010.00523.x
- Conte, D., Holcik, M., Lefebvre, C. A., Lacasse, E., Picketts, D. J., Wright, K. E., & Korneluk, R. G. (2006). Inhibitor of apoptosis protein cIAP2 is essential for lipopolysaccharide-induced macrophage survival. *Mol Cell Biol*, 26(2), 699-708. doi:10.1128/MCB.26.2.699-708.2006
- Cook, M. J. (1965). *The anatomy of the laboratory mouse*. London, New York,: Academic Press.
- Corredor, J., Yan, F., Shen, C. C., Tong, W., John, S. K., Wilson, G., . . . Polk, D. B. (2003). Tumor necrosis factor regulates intestinal epithelial cell migration by receptor-dependent mechanisms. *Am J Physiol Cell Physiol*, 284(4), C953-961. doi:10.1152/ajpcell.00309.2002
- Coultas, L., Pellegrini, M., Visvader, J. E., Lindeman, G. J., Chen, L., Adams, J. M., . . . Strasser, A. (2003). Bfk: a novel weakly proapoptotic member of the Bcl-2 protein family with a BH3 and a BH2 region. *Cell Death Differ*, 10(2), 185-192. doi:10.1038/sj.cdd.4401204
- Crawley, S. W., Mooseker, M. S., & Tyska, M. J. (2014). Shaping the intestinal brush border. *J Cell Biol*, 207(4), 441-451. doi:10.1083/jcb.201407015
- Crawley, S. W., Shifrin, D. A., Jr., Grega-Larson, N. E., McConnell, R. E., Benesh, A. E., Mao, S., . . . Tyska, M. J. (2014). Intestinal brush border assembly driven by protocadherin-based intermicrovillar adhesion. *Cell*, 157(2), 433-446. doi:10.1016/j.cell.2014.01.067
- Croft, M. (2009). The role of TNF superfamily members in T-cell function and diseases. *Nat Rev Immunol*, 9(4), 271-285. doi:10.1038/nri2526
- Cronin, J., Kennedy, U., McCoy, S., An Fhaili, S. N., Crispino-O'Connell, G., Hayden, J., . . . O'Sullivan, R. (2012). Single dose oral dexamethasone versus multi-dose prednisolone in the treatment of acute exacerbations of asthma in children who attend the emergency department: study protocol for a randomized controlled trial. *Trials*, 13, 141. doi:10.1186/1745-6215-13-141
- Crowe, P. D., VanArsdale, T. L., Walter, B. N., Ware, C. F., Hession, C., Ehrenfels, B., . . . Smith, C. A. (1994). A lymphotoxin-beta-specific receptor. *Science*, 264(5159), 707-710. doi:10.1126/science.8171323
- Cuervo, A. M. (2004). Autophagy: in sickness and in health. *Trends Cell Biol*, 14(2), 70-77. doi:10.1016/j.tcb.2003.12.002
- Cutuli, S. L., Artigas, A., Fumagalli, R., Monti, G., Ranieri, V. M., Ronco, C., . . . Group, E. C. (2016). Polymyxin-B hemoperfusion in septic patients: analysis of a multicenter registry. *Ann Intensive Care*, 6(1), 77. doi:10.1186/s13613-016-0178-9
- Damas, P., Ledoux, D., Nys, M., Vrindts, Y., De Groote, D., Franchimont, P., & Lamy, M. (1992). Cytokine serum level during severe sepsis in human IL-6 as a marker of severity. *Ann Surg*, 215(4), 356-362. doi:10.1097/0000658-199204000-00009
- Damas, P., Reuter, A., Gysen, P., Demonty, J., Lamy, M., & Franchimont, P. (1989). Tumor necrosis factor and interleukin-1 serum levels during severe sepsis in humans. *Crit Care Med*, 17(10), 975-978. doi:10.1097/00003246-198910000-00001
- Danese, S., Sans, M., & Fiocchi, C. (2004). The CD40/CD40L costimulatory pathway in inflammatory bowel disease. *Gut*, 53(7), 1035-1043. doi:10.1136/gut.2003.026278
- Danese, S., Sans, M., & Fiocchi, C. (2004). The CD40/CD40L costimulatory pathway in inflammatory bowel disease. *Gut*, 53(7), 1035-1043. doi:10.1136/gut.2003.026278
- D'Arcy, M. S. (2019). Cell death: a review of the major forms of apoptosis, necrosis and autophagy. *Cell Biol Int*, 43(6), 582-592. doi:10.1002/cbin.11137

- Davis, R. J. (2000). Signal transduction by the JNK group of MAP kinases. *Cell*, 103(2), 239-252. doi:10.1016/s0092-8674(00)00116-1
- De Backer, D., Creteur, J., Preiser, J. C., Dubois, M. J., & Vincent, J. L. (2002). Microvascular blood flow is altered in patients with sepsis. *Am J Respir Crit Care Med*, 166(1), 98-104. doi:10.1164/rccm.200109-016oc
- de la Pompa, J. L., & Epstein, J. A. (2012). Coordinating tissue interactions: Notch signaling in cardiac development and disease. *Dev Cell*, 22(2), 244-254. doi:10.1016/j.devcel.2012.01.014
- De Togni, P., Goellner, J., Ruddle, N. H., Streeter, P. R., Fick, A., Mariathasan, S., . . . et al. (1994). Abnormal development of peripheral lymphoid organs in mice deficient in lymphotoxin. *Science*, 264(5159), 703-707. doi:10.1126/science.8171322
- De Wolf, I., Van Driessche, W., & Nagel, W. (1989). Forskolin activates gated Cl⁻ channels in frog skin. *Am J Physiol*, 256(6 Pt 1), C1239-1249. doi:10.1152/ajpcell.1989.256.6.C1239
- Debets, J. M., Kampmeijer, R., van der Linden, M. P., Buurman, W. A., & van der Linden, C. J. (1989). Plasma tumor necrosis factor and mortality in critically ill septic patients. *Crit Care Med*, 17(6), 489-494. doi:10.1097/00003246-198906000-00001
- Degenhardt, K., Mathew, R., Beaudoin, B., Bray, K., Anderson, D., Chen, G., . . . White, E. (2006). Autophagy promotes tumor cell survival and restricts necrosis, inflammation, and tumorigenesis. *Cancer Cell*, 10(1), 51-64. doi:10.1016/j.ccr.2006.06.001
- Degterev, A., Boyce, M., & Yuan, J. (2003). A decade of caspases. *Oncogene*, 22(53), 8543-8567. doi:10.1038/sj.onc.1207107
- Dejardin, E. (2006). The alternative NF-kappaB pathway from biochemistry to biology: pitfalls and promises for future drug development. *Biochem Pharmacol*, 72(9), 1161-1179. doi:10.1016/j.bcp.2006.08.007
- Dejardin, E., Droin, N. M., Delhase, M., Haas, E., Cao, Y., Makris, C., . . . Green, D. R. (2002). The lymphotoxin-beta receptor induces different patterns of gene expression via two NF-kappaB pathways. *Immunity*, 17(4), 525-535. doi:10.1016/s1074-7613(02)00423-5
- Dekkers, J. F., Wiegerinck, C. L., de Jonge, H. R., Bronsveld, I., Janssens, H. M., de Winter-de Groot, K. M., . . . Beekman, J. M. (2013). A functional CFTR assay using primary cystic fibrosis intestinal organoids. *Nat Med*, 19(7), 939-945. doi:10.1038/nm.3201
- Dellinger, R. P., Carlet, J. M., Masur, H., Gerlach, H., Calandra, T., Cohen, J., . . . Levy, M. M. (2004). Surviving Sepsis Campaign guidelines for management of severe sepsis and septic shock. *Intensive Care Med*, 30(4), 536-555. doi:10.1007/s00134-004-2210-z
- Dempsey, C. E., Dive, C., Fletcher, D. J., Barnes, F. A., Lobo, A., Bingle, C. D., . . . Renshaw, S. A. (2005). Expression of pro-apoptotic Bfk isoforms reduces during malignant transformation in the human gastrointestinal tract. *FEBS Lett*, 579(17), 3646-3650. doi:10.1016/j.febslet.2005.05.050
- Dessein, R., Gironella, M., Vignal, C., Peyrin-Biroulet, L., Sokol, H., Secher, T., . . . Chamailard, M. (2009). Toll-like receptor 2 is critical for induction of Reg3 beta expression and intestinal clearance of *Yersinia pseudotuberculosis*. *Gut*, 58(6), 771-776. doi:10.1136/gut.2008.168443
- Di Martino, L., Osme, A., Kossak-Gupta, S., Pizarro, T. T., & Cominelli, F. (2019). TWEAK/Fn14 Is Overexpressed in Crohn's Disease and Mediates Experimental Ileitis by Regulating Critical Innate and Adaptive Immune Pathways. *Cell Mol Gastroenterol Hepatol*, 8(3), 427-446. doi:10.1016/j.jcmgh.2019.05.009

- Diaz de Barboza, G., Guizzardi, S., & Tolosa de Talamoni, N. (2015). Molecular aspects of intestinal calcium absorption. *World J Gastroenterol*, *21*(23), 7142-7154. doi:10.3748/wjg.v21.i23.7142
- Dinarello, C. A. (2000). Proinflammatory cytokines. *Chest*, *118*(2), 503-508. doi:10.1378/chest.118.2.503
- Ding, L., Lu, Z., Foreman, O., Tatum, R., Lu, Q., Renegar, R., . . . Chen, Y. H. (2012). Inflammation and disruption of the mucosal architecture in claudin-7-deficient mice. *Gastroenterology*, *142*(2), 305-315. doi:10.1053/j.gastro.2011.10.025
- Dohi, T., Borodovsky, A., Wu, P., Shearstone, J. R., Kawashima, R., Runkel, L., . . . Burkly, L. C. (2009). TWEAK/Fn14 pathway: a nonredundant role in intestinal damage in mice through a TWEAK/intestinal epithelial cell axis. *Gastroenterology*, *136*(3), 912-923. doi:10.1053/j.gastro.2008.11.017
- Dohi, T., & Burkly, L. C. (2012). The TWEAK/Fn14 pathway as an aggravating and perpetuating factor in inflammatory diseases: focus on inflammatory bowel diseases. *J Leukoc Biol*, *92*(2), 265-279. doi:10.1189/jlb.0112042
- Doig, C. J., Sutherland, L. R., Sandham, J. D., Fick, G. H., Verhoef, M., & Meddings, J. B. (1998). Increased intestinal permeability is associated with the development of multiple organ dysfunction syndrome in critically ill ICU patients. *Am J Respir Crit Care Med*, *158*(2), 444-451. doi:10.1164/ajrccm.158.2.9710092
- Dominguez, J. A., Samocha, A. J., Liang, Z., Burd, E. M., Farris, A. B., & Coopersmith, C. M. (2013). Inhibition of IKKbeta in enterocytes exacerbates sepsis-induced intestinal injury and worsens mortality. *Crit Care Med*, *41*(10), e275-285. doi:10.1097/CCM.0b013e31828a44ed
- Donato, R., Cannon, B. R., Sorci, G., Riuzzi, F., Hsu, K., Weber, D. J., & Geczy, C. L. (2013). Functions of S100 proteins. *Curr Mol Med*, *13*(1), 24-57.
- Dorrington, M. G., & Fraser, I. D. C. (2019). NF-kappaB Signaling in Macrophages: Dynamics, Crosstalk, and Signal Integration. *Front Immunol*, *10*, 705. doi:10.3389/fimmu.2019.00705
- Dotti, I., Mora-Buch, R., Ferrer-Picon, E., Planell, N., Jung, P., Masamunt, M. C., . . . Salas, A. (2017). Alterations in the epithelial stem cell compartment could contribute to permanent changes in the mucosa of patients with ulcerative colitis. *Gut*, *66*(12), 2069-2079. doi:10.1136/gutjnl-2016-312609
- Dowlati, Y., Herrmann, N., Swardfager, W., Liu, H., Sham, L., Reim, E. K., & Lanctot, K. L. (2010). A meta-analysis of cytokines in major depression. *Biol Psychiatry*, *67*(5), 446-457. doi:10.1016/j.biopsych.2009.09.033
- Drake, R. L. (2019). *Gray's anatomy for students* (4th edition. ed.). Philadelphia, MO: Elsevier.
- D'Souza, B., Meloty-Kapella, L., & Weinmaster, G. (2010). Canonical and non-canonical Notch ligands. *Curr Top Dev Biol*, *92*, 73-129. doi:10.1016/S0070-2153(10)92003-6
- Du, C., Fang, M., Li, Y., Li, L., & Wang, X. (2000). Smac, a mitochondrial protein that promotes cytochrome c-dependent caspase activation by eliminating IAP inhibition. *Cell*, *102*(1), 33-42. doi:10.1016/s0092-8674(00)00008-8
- Duckworth, C. A., & Watson, A. J. (2011). Analysis of epithelial cell shedding and gaps in the intestinal epithelium. *Methods Mol Biol*, *763*, 105-114. doi:10.1007/978-1-61779-191-8_7
- Durand, A., Donahue, B., Peignon, G., Letourneur, F., Cagnard, N., Slomianny, C., . . . Romagnolo, B. (2012). Functional intestinal stem cells after Paneth cell ablation induced by the loss of transcription factor Math1 (Atoh1). *Proc Natl Acad Sci U S A*, *109*(23), 8965-8970. doi:10.1073/pnas.1201652109
- Ebnet, K., Suzuki, A., Ohno, S., & Vestweber, D. (2004). Junctional adhesion molecules (JAMs): more molecules with dual functions? *J Cell Sci*, *117*(Pt 1), 19-29. doi:10.1242/jcs.00930

- Eckmann, L., Nebelsiek, T., Fingerle, A. A., Dann, S. M., Mages, J., Lang, R., . . . Greten, F. R. (2008). Opposing functions of IKKbeta during acute and chronic intestinal inflammation. *Proc Natl Acad Sci U S A*, *105*(39), 15058-15063. doi:10.1073/pnas.0808216105
- Edwards, R. L., Luis, P. B., Varuzza, P. V., Joseph, A. I., Presley, S. H., Chaturvedi, R., & Schneider, C. (2017). The anti-inflammatory activity of curcumin is mediated by its oxidative metabolites. *J Biol Chem*, *292*(52), 21243-21252. doi:10.1074/jbc.RA117.000123
- Efrat, S., Leiser, M., Wu, Y. J., Fusco-DeMane, D., Emran, O. A., Surana, M., . . . Fleischer, N. (1994). Ribozyme-mediated attenuation of pancreatic beta-cell glucokinase expression in transgenic mice results in impaired glucose-induced insulin secretion. *Proc Natl Acad Sci U S A*, *91*(6), 2051-2055. doi:10.1073/pnas.91.6.2051
- Elmore, S. (2007). Apoptosis: a review of programmed cell death. *Toxicol Pathol*, *35*(4), 495-516. doi:10.1080/01926230701320337
- Elphick, D. A., & Mahida, Y. R. (2005). Paneth cells: their role in innate immunity and inflammatory disease. *Gut*, *54*(12), 1802-1809. doi:10.1136/gut.2005.068601
- Erlandsen, S. L., Parsons, J. A., & Taylor, T. D. (1974). Ultrastructural immunocytochemical localization of lysozyme in the Paneth cells of man. *J Histochem Cytochem*, *22*(6), 401-413. doi:10.1177/22.6.401
- Fabris, M., Visentini, D., De Re, V., Picierno, A., Maieron, R., Cannizzaro, R., . . . Tonutti, E. (2007). Elevated B cell-activating factor of the tumour necrosis factor family in coeliac disease. *Scand J Gastroenterol*, *42*(12), 1434-1439. doi:10.1080/00365520701452225
- Fan, Y., Zhang, G., Vong, C. T., & Ye, R. D. (2020). Serum amyloid A3 confers protection against acute lung injury in *Pseudomonas aeruginosa*-infected mice. *Am J Physiol Lung Cell Mol Physiol*, *318*(2), L314-L322. doi:10.1152/ajplung.00309.2019
- Fatehullah, A., Tan, S. H., & Barker, N. (2016). Organoids as an in vitro model of human development and disease. *Nat Cell Biol*, *18*(3), 246-254. doi:10.1038/ncb3312
- Fatehullah, A., Tan, S. H., & Barker, N. (2016). Organoids as an in vitro model of human development and disease. *Nat Cell Biol*, *18*(3), 246-254. doi:10.1038/ncb3312
- Faure, E., Equils, O., Sieling, P. A., Thomas, L., Zhang, F. X., Kirschning, C. J., . . . Arditi, M. (2000). Bacterial lipopolysaccharide activates NF-kappaB through toll-like receptor 4 (TLR-4) in cultured human dermal endothelial cells. Differential expression of TLR-4 and TLR-2 in endothelial cells. *J Biol Chem*, *275*(15), 11058-11063. doi:10.1074/jbc.275.15.11058
- Faustman, D., & Davis, M. (2010). TNF receptor 2 pathway: drug target for autoimmune diseases. *Nat Rev Drug Discov*, *9*(6), 482-493. doi:10.1038/nrd3030
- Feldman, G. J., Mullin, J. M., & Ryan, M. P. (2005). Occludin: structure, function and regulation. *Adv Drug Deliv Rev*, *57*(6), 883-917. doi:10.1016/j.addr.2005.01.009
- Ferrajoli, A., Keating, M. J., Manshour, T., Giles, F. J., Dey, A., Estrov, Z., . . . Albitar, M. (2002). The clinical significance of tumor necrosis factor-alpha plasma level in patients having chronic lymphocytic leukemia. *Blood*, *100*(4), 1215-1219.
- Ferraris, R. P., & Diamond, J. (1997). Regulation of intestinal sugar transport. *Physiol Rev*, *77*(1), 257-302. doi:10.1152/physrev.1997.77.1.257
- Fink, M. P., & Heard, S. O. (1990). Laboratory models of sepsis and septic shock. *J Surg Res*, *49*(2), 186-196. doi:10.1016/0022-4804(90)90260-9

- Flanagan, D. J., Austin, C. R., Vincan, E., & Phesse, T. J. (2018). Wnt Signalling in Gastrointestinal Epithelial Stem Cells. *Genes (Basel)*, *9*(4). doi:10.3390/genes9040178
- Fleischmann-Struzek, C., Goldfarb, D. M., Schlattmann, P., Schlapbach, L. J., Reinhart, K., & Kisson, N. (2018). The global burden of paediatric and neonatal sepsis: a systematic review. *Lancet Respir Med*, *6*(3), 223-230. doi:10.1016/S2213-2600(18)30063-8
- Flynn, D. C. (2001). Adaptor proteins. *Oncogene*, *20*(44), 6270-6272. doi:10.1038/sj.onc.1204769
- Fong, Y., Tracey, K. J., Moldawer, L. L., Hesse, D. G., Manogue, K. B., Kenney, J. S., . . . et al. (1989). Antibodies to cachectin/tumor necrosis factor reduce interleukin 1 beta and interleukin 6 appearance during lethal bacteremia. *J Exp Med*, *170*(5), 1627-1633. doi:10.1084/jem.170.5.1627
- Force, W. R., Glass, A. A., Benedict, C. A., Cheung, T. C., Lama, J., & Ware, C. F. (2000). Discrete signaling regions in the lymphotoxin-beta receptor for tumor necrosis factor receptor-associated factor binding, subcellular localization, and activation of cell death and NF-kappaB pathways. *J Biol Chem*, *275*(15), 11121-11129. doi:10.1074/jbc.275.15.11121
- Formigli, L., Papucci, L., Tani, A., Schiavone, N., Tempestini, A., Orlandini, G. E., . . . Orlandini, S. Z. (2000). Aponecrosis: morphological and biochemical exploration of a syncretic process of cell death sharing apoptosis and necrosis. *J Cell Physiol*, *182*(1), 41-49. doi:10.1002/(SICI)1097-4652(200001)182:1<41::AID-JCP5>3.0.CO;2-7
- Frey, M. R., Edelblum, K. L., Mullane, M. T., Liang, D., & Polk, D. B. (2009). The ErbB4 growth factor receptor is required for colon epithelial cell survival in the presence of TNF. *Gastroenterology*, *136*(1), 217-226. doi:10.1053/j.gastro.2008.09.023
- Frisch, S. M., & Francis, H. (1994). Disruption of epithelial cell-matrix interactions induces apoptosis. *J Cell Biol*, *124*(4), 619-626. doi:10.1083/jcb.124.4.619
- Fukuyama, S., Hiroi, T., Yokota, Y., Rennert, P. D., Yanagita, M., Kinoshita, N., . . . Kiyono, H. (2002). Initiation of NALT organogenesis is independent of the IL-7R, LTbetaR, and NIK signaling pathways but requires the Id2 gene and CD3(-)CD4(+)CD45(+) cells. *Immunity*, *17*(1), 31-40. doi:10.1016/s1074-7613(02)00339-4
- Fulda, S., & Debatin, K. M. (2006). Extrinsic versus intrinsic apoptosis pathways in anticancer chemotherapy. *Oncogene*, *25*(34), 4798-4811. doi:10.1038/sj.onc.1209608
- Furness, J. B., Kunze, W. A., & Clerc, N. (1999). Nutrient tasting and signaling mechanisms in the gut. II. The intestine as a sensory organ: neural, endocrine, and immune responses. *Am J Physiol*, *277*(5), G922-928. doi:10.1152/ajpgi.1999.277.5.G922
- Furriols, M., & Bray, S. (2001). A model Notch response element detects Suppressor of Hairless-dependent molecular switch. *Curr Biol*, *11*(1), 60-64. doi:10.1016/s0960-9822(00)00044-0
- Furuse, M., Fujita, K., Hiiragi, T., Fujimoto, K., & Tsukita, S. (1998). Claudin-1 and -2: novel integral membrane proteins localizing at tight junctions with no sequence similarity to occludin. *J Cell Biol*, *141*(7), 1539-1550. doi:10.1083/jcb.141.7.1539
- Furuse, M., Hirase, T., Itoh, M., Nagafuchi, A., Yonemura, S., Tsukita, S., & Tsukita, S. (1993). Occludin: a novel integral membrane protein localizing at tight junctions. *J Cell Biol*, *123*(6 Pt 2), 1777-1788. doi:10.1083/jcb.123.6.1777
- Furuta, K., Ikeda, M., Nakayama, Y., Nakamura, K., Tanaka, M., Hamasaki, N., . . . August, J. T. (2001). Expression of lysosome-associated membrane proteins in human colorectal neoplasms and inflammatory diseases. *Am J Pathol*, *159*(2), 449-455. doi:10.1016/S0002-9440(10)61716-6

- Gallagher, J., Fisher, C., Sherman, B., Munger, M., Meyers, B., Ellison, T., . . . Velagapudi, R. (2001). A multicenter, open-label, prospective, randomized, dose-ranging pharmacokinetic study of the anti-TNF-alpha antibody afelimomab in patients with sepsis syndrome. *Intensive Care Med*, 27(7), 1169-1178. doi:10.1007/s001340100973
- Ganeff, C., Remouchamps, C., Boutaffala, L., Benezech, C., Galopin, G., Vandepaer, S., . . . Dejardin, E. (2011). Induction of the alternative NF-kappaB pathway by lymphotoxin alphabeta (LTalphabeta) relies on internalization of LTbeta receptor. *Mol Cell Biol*, 31(21), 4319-4334. doi:10.1128/MCB.05033-11
- Gasbarrini, G., & Montalto, M. (1999). Structure and function of tight junctions. Role in intestinal barrier. *Ital J Gastroenterol Hepatol*, 31(6), 481-488.
- Gatto, M., Iaccarino, L., Ghirardello, A., Bassi, N., Pontisso, P., Punzi, L., . . . Doria, A. (2013). Serpins, immunity and autoimmunity: old molecules, new functions. *Clin Rev Allergy Immunol*, 45(2), 267-280. doi:10.1007/s12016-013-8353-3
- Gauvin, R., Chen, Y. C., Lee, J. W., Soman, P., Zorlutuna, P., Nichol, J. W., . . . Khademhosseini, A. (2012). Microfabrication of complex porous tissue engineering scaffolds using 3D projection stereolithography. *Biomaterials*, 33(15), 3824-3834. doi:10.1016/j.biomaterials.2012.01.048
- Gebert, N., Cheng, C. W., Kirkpatrick, J. M., Di Fraia, D., Yun, J., Schadel, P., . . . Ori, A. (2020). Region-Specific Proteome Changes of the Intestinal Epithelium during Aging and Dietary Restriction. *Cell Rep*, 31(4), 107565. doi:10.1016/j.celrep.2020.107565
- Gelbmann, C. M., Leeb, S. N., Vogl, D., Maendel, M., Herfarth, H., Scholmerich, J., . . . Rogler, G. (2003). Inducible CD40 expression mediates NFkappaB activation and cytokine secretion in human colonic fibroblasts. *Gut*, 52(10), 1448-1456. doi:10.1136/gut.52.10.1448
- Gerbe, F., Brulin, B., Makrini, L., Legraverend, C., & Jay, P. (2009). DCAMKL-1 expression identifies Tuft cells rather than stem cells in the adult mouse intestinal epithelium. *Gastroenterology*, 137(6), 2179-2180; author reply 2180-2171. doi:10.1053/j.gastro.2009.06.072
- Gerbe, F., Legraverend, C., & Jay, P. (2012). The intestinal epithelium tuft cells: specification and function. *Cell Mol Life Sci*, 69(17), 2907-2917. doi:10.1007/s00018-012-0984-7
- Gerbe, F., van Es, J. H., Makrini, L., Brulin, B., Mellitzer, G., Robine, S., . . . Jay, P. (2011). Distinct ATOH1 and Neurog3 requirements define tuft cells as a new secretory cell type in the intestinal epithelium. *J Cell Biol*, 192(5), 767-780. doi:10.1083/jcb.201010127
- Gerthoffer, W. T. (2008). Migration of airway smooth muscle cells. *Proc Am Thorac Soc*, 5(1), 97-105. doi:10.1513/pats.200704-051VS
- Ghosh, S., Gifford, A. M., Riviere, L. R., Tempst, P., Nolan, G. P., & Baltimore, D. (1990). Cloning of the p50 DNA binding subunit of NF-kappa B: homology to rel and dorsal. *Cell*, 62(5), 1019-1029. doi:10.1016/0092-8674(90)90276-k
- Ghosh, S., May, M. J., & Kopp, E. B. (1998). NF-kappa B and Rel proteins: evolutionarily conserved mediators of immune responses. *Annu Rev Immunol*, 16, 225-260. doi:10.1146/annurev.immunol.16.1.225
- Giammanco, A., Cefalu, A. B., Noto, D., & Aversa, M. R. (2015). The pathophysiology of intestinal lipoprotein production. *Front Physiol*, 6, 61. doi:10.3389/fphys.2015.00061
- Gibbison, B., Lopez-Lopez, J. A., Higgins, J. P., Miller, T., Angelini, G. D., Lightman, S. L., & Annane, D. (2017). Corticosteroids in septic shock: a systematic review and network meta-analysis. *Crit Care*, 21(1), 78. doi:10.1186/s13054-017-1659-4

- Giles, D. A., Zahner, S., Krause, P., Van Der Gracht, E., Riffelmacher, T., Morris, V., . . . Kronenberg, M. (2018). The Tumor Necrosis Factor Superfamily Members TNFSF14 (LIGHT), Lymphotoxin beta and Lymphotoxin beta Receptor Interact to Regulate Intestinal Inflammation. *Front Immunol*, *9*, 2585. doi:10.3389/fimmu.2018.02585
- Gilmore, T. D. (2006). Introduction to NF-kappaB: players, pathways, perspectives. *Oncogene*, *25*(51), 6680-6684. doi:10.1038/sj.onc.1209954
- Gindzienska-Sieskiewicz, E., Distler, O., Reszec, J., Jordan, S., Bielecki, P., Sieskiewicz, A., . . . Kowal-Bielecka, O. (2019). Increased expression of the TNF superfamily member LIGHT/TNFSF14 and its receptors (HVEM and LTssR) in patients with systemic sclerosis. *Rheumatology (Oxford)*, *58*(3), 502-510. doi:10.1093/rheumatology/key348
- Girardin, E., Grau, G. E., Dayer, J. M., Roux-Lombard, P., & Lambert, P. H. (1988). Tumor necrosis factor and interleukin-1 in the serum of children with severe infectious purpura. *N Engl J Med*, *319*(7), 397-400. doi:10.1056/NEJM198808183190703
- Gold, J. A., Parsey, M., Hoshino, Y., Hoshino, S., Nolan, A., Yee, H., . . . Weiden, M. D. (2003). CD40 contributes to lethality in acute sepsis: in vivo role for CD40 in innate immunity. *Infect Immun*, *71*(6), 3521-3528. doi:10.1128/iai.71.6.3521-3528.2003
- Goldstein, J. C., Waterhouse, N. J., Juin, P., Evan, G. I., & Green, D. R. (2000). The coordinate release of cytochrome c during apoptosis is rapid, complete and kinetically invariant. *Nat Cell Biol*, *2*(3), 156-162. doi:10.1038/35004029
- Gordon, A. C., Waheed, U., Hansen, T. K., Hitman, G. A., Garrard, C. S., Turner, M. W., . . . Hinds, C. J. (2006). Mannose-binding lectin polymorphisms in severe sepsis: relationship to levels, incidence, and outcome. *Shock*, *25*(1), 88-93. doi:10.1097/01.shk.0000186928.57109.8d
- Gordon, M. D., & Nusse, R. (2006). Wnt signaling: multiple pathways, multiple receptors, and multiple transcription factors. *J Biol Chem*, *281*(32), 22429-22433. doi:10.1074/jbc.R600015200
- Goren, I., Brom, A., Yanai, H., Dagan, A., Segal, G., & Israel, A. (2020). Risk of bacteremia in hospitalised patients with inflammatory bowel disease: a 9-year cohort study. *United European Gastroenterol J*, *8*(2), 195-203. doi:10.1177/2050640619874524
- Grammer, A. C., & Lipsky, P. E. (2000). CD40-mediated regulation of immune responses by TRAF-dependent and TRAF-independent signaling mechanisms. *Adv Immunol*, *76*, 61-178. doi:10.1016/s0065-2776(01)76019-1
- Granger, S. W., & Rickert, S. (2003). LIGHT-HVEM signaling and the regulation of T cell-mediated immunity. *Cytokine Growth Factor Rev*, *14*(3-4), 289-296. doi:10.1016/s1359-6101(03)00031-5
- Graves, P. R., & Haystead, T. A. (2002). Molecular biologist's guide to proteomics. *Microbiol Mol Biol Rev*, *66*(1), 39-63; table of contents. doi:10.1128/mmbr.66.1.39-63.2002
- Gremel, G., Wanders, A., Cedernaes, J., Fagerberg, L., Hallstrom, B., Edlund, K., . . . Ponten, F. (2015). The human gastrointestinal tract-specific transcriptome and proteome as defined by RNA sequencing and antibody-based profiling. *J Gastroenterol*, *50*(1), 46-57. doi:10.1007/s00535-014-0958-7
- Greten, F. R., Eckmann, L., Greten, T. F., Park, J. M., Li, Z. W., Egan, L. J., . . . Karin, M. (2004). IKKbeta links inflammation and tumorigenesis in a mouse model of colitis-associated cancer. *Cell*, *118*(3), 285-296. doi:10.1016/j.cell.2004.07.013
- Grimstad, T., Skoie, I. M., Doerner, J., Isaksen, K., Karlsen, L., Aabakken, L., . . . Putterman, C. (2017). TWEAK is not elevated in patients with newly

- diagnosed inflammatory bowel disease. *Scand J Gastroenterol*, 52(4), 420-424. doi:10.1080/00365521.2016.1273382
- Groppe, J., Greenwald, J., Wiater, E., Rodriguez-Leon, J., Economides, A. N., Kwiatkowski, W., . . . Choe, S. (2002). Structural basis of BMP signalling inhibition by the cystine knot protein Noggin. *Nature*, 420(6916), 636-642. doi:10.1038/nature01245
- Guan, Y., Watson, A. J., Marchiando, A. M., Bradford, E., Shen, L., Turner, J. R., & Montrose, M. H. (2011). Redistribution of the tight junction protein ZO-1 during physiological shedding of mouse intestinal epithelial cells. *Am J Physiol Cell Physiol*, 300(6), C1404-1414. doi:10.1152/ajpcell.00270.2010
- Gubernatorova, E. O., & Tumanov, A. V. (2016). Tumor Necrosis Factor and Lymphotoxin in Regulation of Intestinal Inflammation. *Biochemistry (Mosc)*, 81(11), 1309-1325. doi:10.1134/S0006297916110092
- Guma, M., Stepniak, D., Shaked, H., Spehlmann, M. E., Shenouda, S., Cheroutre, H., . . . Karin, M. (2011). Constitutive intestinal NF-kappaB does not trigger destructive inflammation unless accompanied by MAPK activation. *J Exp Med*, 208(9), 1889-1900. doi:10.1084/jem.20110242
- Gunawardene, A. R., Corfe, B. M., & Staton, C. A. (2011). Classification and functions of enteroendocrine cells of the lower gastrointestinal tract. *Int J Exp Pathol*, 92(4), 219-231. doi:10.1111/j.1365-2613.2011.00767.x
- Gunther, C., Buchen, B., He, G. W., Hornef, M., Torow, N., Neumann, H., . . . Becker, C. (2015). Caspase-8 controls the gut response to microbial challenges by Tnf-alpha-dependent and independent pathways. *Gut*, 64(4), 601-610. doi:10.1136/gutjnl-2014-307226
- Gunzel, D., & Yu, A. S. (2013). Claudins and the modulation of tight junction permeability. *Physiol Rev*, 93(2), 525-569. doi:10.1152/physrev.00019.2012
- Gutierrez, M. G., Mishra, B. B., Jordao, L., Elliott, E., Anes, E., & Griffiths, G. (2008). NF-kappa B activation controls phagolysosome fusion-mediated killing of mycobacteria by macrophages. *J Immunol*, 181(4), 2651-2663. doi:10.4049/jimmunol.181.4.2651
- Hall, P. A., Coates, P. J., Ansari, B., & Hopwood, D. (1994). Regulation of cell number in the mammalian gastrointestinal tract: the importance of apoptosis. *J Cell Sci*, 107 (Pt 12), 3569-3577.
- Hamada, M., Abe, M., Miyake, T., Kawasaki, K., Tada, F., Furukawa, S., . . . Onji, M. (2011). B cell-activating factor controls the production of adipokines and induces insulin resistance. *Obesity (Silver Spring)*, 19(10), 1915-1922. doi:10.1038/oby.2011.165
- Han, M. K., Baker, M., Zhang, Y., Yang, C., Zhang, M., Garg, P., . . . Merlin, D. (2018). Overexpression of CD98 in intestinal epithelium dysregulates miRNAs and their targeted proteins along the ileal villus-crypt axis. *Sci Rep*, 8(1), 16220. doi:10.1038/s41598-018-34474-9
- Han, N. Y., Choi, W., Park, J. M., Kim, E. H., Lee, H., & Hahm, K. B. (2013). Label-free quantification for discovering novel biomarkers in the diagnosis and assessment of disease activity in inflammatory bowel disease. *J Dig Dis*, 14(4), 166-174. doi:10.1111/1751-2980.12035
- Han, Y. P., Nien, Y. D., & Garner, W. L. (2002). Tumor necrosis factor-alpha-induced proteolytic activation of pro-matrix metalloproteinase-9 by human skin is controlled by down-regulating tissue inhibitor of metalloproteinase-1 and mediated by tissue-associated chymotrypsin-like proteinase. *J Biol Chem*, 277(30), 27319-27327. doi:10.1074/jbc.M202842200
- Han, Y. P., Tuan, T. L., Wu, H., Hughes, M., & Garner, W. L. (2001). TNF-alpha stimulates activation of pro-MMP2 in human skin through NF-(kappa)B mediated induction of MT1-MMP. *J Cell Sci*, 114(Pt 1), 131-139.
- Hannoush, R. N. (2015). Synthetic protein lipidation. *Curr Opin Chem Biol*, 28, 39-46. doi:10.1016/j.cbpa.2015.05.025

- Hardie, E. M., Kolata, R. J., & Rawlings, C. A. (1983). Canine septic peritonitis: treatment with flunixin meglumine. *Circ Shock*, *11*(2), 159-173.
- Harrop, J. A., Reddy, M., Dede, K., Brigham-Burke, M., Lyn, S., Tan, K. B., . . . Truneh, A. (1998). Antibodies to TR2 (herpesvirus entry mediator), a new member of the TNF receptor superfamily, block T cell proliferation, expression of activation markers, and production of cytokines. *J Immunol*, *161*(4), 1786-1794.
- Haskill, S., Beg, A. A., Tompkins, S. M., Morris, J. S., Yurochko, A. D., Sampson-Johannes, A., . . . Baldwin, A. S., Jr. (1991). Characterization of an immediate-early gene induced in adherent monocytes that encodes I kappa B-like activity. *Cell*, *65*(7), 1281-1289. doi:10.1016/0092-8674(91)90022-q
- Hausser, F., Chakraborty, S., Halbgebauer, R., & Huber-Lang, M. (2019). Challenge to the Intestinal Mucosa During Sepsis. *Front Immunol*, *10*, 891. doi:10.3389/fimmu.2019.00891
- Haybaeck, J., Zeller, N., Wolf, M. J., Weber, A., Wagner, U., Kurrer, M. O., . . . Heikenwalder, M. (2009). A lymphotoxin-driven pathway to hepatocellular carcinoma. *Cancer Cell*, *16*(4), 295-308. doi:10.1016/j.ccr.2009.08.021
- Hayden, M. S., & Ghosh, S. (2004). Signaling to NF-kappaB. *Genes Dev*, *18*(18), 2195-2224. doi:10.1101/gad.1228704
- Hayden, M. S., & Ghosh, S. (2008). Shared principles in NF-kappaB signaling. *Cell*, *132*(3), 344-362. doi:10.1016/j.cell.2008.01.020
- Hayden, M. S., West, A. P., & Ghosh, S. (2006). NF-kappaB and the immune response. *Oncogene*, *25*(51), 6758-6780. doi:10.1038/sj.onc.1209943
- He, X., Semenov, M., Tamai, K., & Zeng, X. (2004). LDL receptor-related proteins 5 and 6 in Wnt/beta-catenin signaling: arrows point the way. *Development*, *131*(8), 1663-1677. doi:10.1242/dev.01117
- Heeschen, C., Dimmeler, S., Hamm, C. W., van den Brand, M. J., Boersma, E., Zeiher, A. M., . . . Investigators, C. S. (2003). Soluble CD40 ligand in acute coronary syndromes. *N Engl J Med*, *348*(12), 1104-1111. doi:10.1056/NEJMoa022600
- Hehner, S. P., Hofmann, T. G., Droge, W., & Schmitz, M. L. (1999). The antiinflammatory sesquiterpene lactone parthenolide inhibits NF-kappa B by targeting the I kappa B kinase complex. *J Immunol*, *163*(10), 5617-5623.
- Heinrich, P. C., Behrmann, I., Muller-Newen, G., Schaper, F., & Graeve, L. (1998). Interleukin-6-type cytokine signalling through the gp130/Jak/STAT pathway. *Biochem J*, *334* (Pt 2), 297-314. doi:10.1042/bj3340297
- Heming, N., Sivanandamoorthy, S., Meng, P., Bounab, R., & Annane, D. (2018). Immune Effects of Corticosteroids in Sepsis. *Front Immunol*, *9*, 1736. doi:10.3389/fimmu.2018.01736
- Herfarth, H. H., Bocker, U., Janardhanam, R., & Sartor, R. B. (1998). Subtherapeutic corticosteroids potentiate the ability of interleukin 10 to prevent chronic inflammation in rats. *Gastroenterology*, *115*(4), 856-865. doi:10.1016/s0016-5085(98)70257-4
- Hesse, D. G., Tracey, K. J., Fong, Y., Manogue, K. R., Palladino, M. A., Jr., Cerami, A., . . . Lowry, S. F. (1988). Cytokine appearance in human endotoxemia and primate bacteremia. *Surg Gynecol Obstet*, *166*(2), 147-153.
- Hilliard, V. C., Frey, M. R., Dempsey, P. J., Peek, R. M., Jr., & Polk, D. B. (2011). TNF-alpha converting enzyme-mediated ErbB4 transactivation by TNF promotes colonic epithelial cell survival. *Am J Physiol Gastrointest Liver Physiol*, *301*(2), G338-346. doi:10.1152/ajpgi.00057.2011
- Hinkelbein, J., Feldmann, R. E., Jr., Schubert, C., Peterka, A., Schelshorn, D., Maurer, M. H., & Kalenka, A. (2009). Alterations in rat serum proteome and metabolome as putative disease markers in sepsis. *J Trauma*, *66*(4), 1065-1075. doi:10.1097/TA.0b013e3181958ad7

- Hollander, D. (1999). Intestinal permeability, leaky gut, and intestinal disorders. *Curr Gastroenterol Rep*, 1(5), 410-416. doi:10.1007/s11894-999-0023-5
- Holler, N., Zaru, R., Micheau, O., Thome, M., Attinger, A., Valitutti, S., . . . Tschopp, J. (2000). Fas triggers an alternative, caspase-8-independent cell death pathway using the kinase RIP as effector molecule. *Nat Immunol*, 1(6), 489-495. doi:10.1038/82732
- Holmes, J. L., Van Itallie, C. M., Rasmussen, J. E., & Anderson, J. M. (2006). Claudin profiling in the mouse during postnatal intestinal development and along the gastrointestinal tract reveals complex expression patterns. *Gene Expr Patterns*, 6(6), 581-588. doi:10.1016/j.modgep.2005.12.001
- Holst, J. J., Skak-Nielsen, T., Orskov, C., & Seier-Poulsen, S. (1992). Vagal control of the release of somatostatin, vasoactive intestinal polypeptide, gastrin-releasing peptide, and HCl from porcine non-antral stomach. *Scand J Gastroenterol*, 27(8), 677-685. doi:10.3109/00365529209000139
- Hotchkiss, R. S., & Karl, I. E. (2003). The pathophysiology and treatment of sepsis. *N Engl J Med*, 348(2), 138-150. doi:10.1056/NEJMra021333
- Huang, M., Cai, S., & Su, J. (2019). The Pathogenesis of Sepsis and Potential Therapeutic Targets. *Int J Mol Sci*, 20(21). doi:10.3390/ijms20215376
- Huch, M., Knoblich, J. A., Lutolf, M. P., & Martinez-Arias, A. (2017). The hope and the hype of organoid research. *Development*, 144(6), 938-941. doi:10.1242/dev.150201
- Hynds, R. E., & Giangreco, A. (2013). Concise review: the relevance of human stem cell-derived organoid models for epithelial translational medicine. *Stem Cells*, 31(3), 417-422. doi:10.1002/stem.1290
- Ijiri, K., & Potten, C. S. (1983). Response of intestinal cells of differing topographical and hierarchical status to ten cytotoxic drugs and five sources of radiation. *Br J Cancer*, 47(2), 175-185. doi:10.1038/bjc.1983.25
- Ijiri, K., & Potten, C. S. (1987). Further studies on the response of intestinal crypt cells of different hierarchical status to eighteen different cytotoxic agents. *Br J Cancer*, 55(2), 113-123. doi:10.1038/bjc.1987.25
- Inoue, J., Kerr, L. D., Kakizuka, A., & Verma, I. M. (1992). I kappa B gamma, a 70 kd protein identical to the C-terminal half of p110 NF-kappa B: a new member of the I kappa B family. *Cell*, 68(6), 1109-1120. doi:10.1016/0092-8674(92)90082-n
- Inoue, J., Kerr, L. D., Kakizuka, A., & Verma, I. M. (1992). I kappa B gamma, a 70 kd protein identical to the C-terminal half of p110 NF-kappa B: a new member of the I kappa B family. *Cell*, 68(6), 1109-1120. doi:10.1016/0092-8674(92)90082-n
- Irmeler, M., Thome, M., Hahne, M., Schneider, P., Hofmann, K., Steiner, V., . . . Tschopp, J. (1997). Inhibition of death receptor signals by cellular FLIP. *Nature*, 388(6638), 190-195. doi:10.1038/40657
- Isaacs, K. L., Sartor, R. B., & Haskill, S. (1992). Cytokine messenger RNA profiles in inflammatory bowel disease mucosa detected by polymerase chain reaction amplification. *Gastroenterology*, 103(5), 1587-1595. doi:10.1016/0016-5085(92)91182-4
- Ito, K., Barnes, P. J., & Adcock, I. M. (2000). Glucocorticoid receptor recruitment of histone deacetylase 2 inhibits interleukin-1beta-induced histone H4 acetylation on lysines 8 and 12. *Mol Cell Biol*, 20(18), 6891-6903. doi:10.1128/mcb.20.18.6891-6903.2000
- Itoh, M., Sasaki, H., Furuse, M., Ozaki, H., Kita, T., & Tsukita, S. (2001). Junctional adhesion molecule (JAM) binds to PAR-3: a possible mechanism for the recruitment of PAR-3 to tight junctions. *J Cell Biol*, 154(3), 491-497. doi:10.1083/jcb.200103047
- Iwagami, M., Yasunaga, H., Doi, K., Horiguchi, H., Fushimi, K., Matsubara, T., . . . Noiri, E. (2014). Postoperative polymyxin B hemoperfusion and mortality in

- patients with abdominal septic shock: a propensity-matched analysis. *Crit Care Med*, 42(5), 1187-1193. doi:10.1097/CCM.0000000000000150
- Izumi, Y., Hirose, T., Tamai, Y., Hirai, S., Nagashima, Y., Fujimoto, T., . . . Ohno, S. (1998). An atypical PKC directly associates and colocalizes at the epithelial tight junction with ASIP, a mammalian homologue of *Caenorhabditis elegans* polarity protein PAR-3. *J Cell Biol*, 143(1), 95-106. doi:10.1083/jcb.143.1.95
- Jabati, S., Fareed, J., Liles, J., Otto, A., Hoppensteadt, D., Bontekoe, J., . . . Syed, M. (2018). Biomarkers of Inflammation, Thrombogenesis, and Collagen Turnover in Patients With Atrial Fibrillation. *Clin Appl Thromb Hemost*, 24(5), 718-723. doi:10.1177/1076029618761006
- Jacob, A., Wu, R., Zhou, M., & Wang, P. (2007). Mechanism of the Anti-inflammatory Effect of Curcumin: PPAR-gamma Activation. *PPAR Res*, 2007, 89369. doi:10.1155/2007/89369
- Jacobs, M. D., & Harrison, S. C. (1998). Structure of an I kappa B alpha/NF-kappa B complex. *Cell*, 95(6), 749-758. doi:10.1016/s0092-8674(00)81698-0
- Jager, R., Lowery, R. P., Calvanese, A. V., Joy, J. M., Purpura, M., & Wilson, J. M. (2014). Comparative absorption of curcumin formulations. *Nutr J*, 13, 11. doi:10.1186/1475-2891-13-11
- Jakubowski, A., Ambrose, C., Parr, M., Lincecum, J. M., Wang, M. Z., Zheng, T. S., . . . Burkly, L. C. (2005). TWEAK induces liver progenitor cell proliferation. *J Clin Invest*, 115(9), 2330-2340. doi:10.1172/JCI23486
- Janda, C. Y., Waghray, D., Levin, A. M., Thomas, C., & Garcia, K. C. (2012). Structural basis of Wnt recognition by Frizzled. *Science*, 337(6090), 59-64. doi:10.1126/science.1222879
- Jang, S. W., Lim, S. G., Suk, K., & Lee, W. H. (2015). Activation of lymphotoxin-beta receptor enhances the LPS-induced expression of IL-8 through NF-kappa B and IRF-1. *Immunol Lett*, 165(2), 63-69. doi:10.1016/j.imlet.2015.04.001
- Jensen, S. R., Schoof, E. M., Wheeler, S. E., Hvid, H., Ahnfelt-Ronne, J., Hansen, B. F., . . . Brubaker, P. L. (2017). Quantitative Proteomics of Intestinal Mucosa From Male Mice Lacking Intestinal Epithelial Insulin Receptors. *Endocrinology*, 158(8), 2470-2485. doi:10.1210/en.2017-00194
- Jeon, M. K., Klaus, C., Kaemmerer, E., & Gassler, N. (2013). Intestinal barrier: Molecular pathways and modifiers. *World J Gastrointest Pathophysiol*, 4(4), 94-99. doi:10.4291/wjgp.v4.i4.94
- Jin, S., Hansson, E. M., Tikka, S., Lanner, F., Sahlgren, C., Farnebo, F., . . . Lendahl, U. (2008). Notch signaling regulates platelet-derived growth factor receptor-beta expression in vascular smooth muscle cells. *Circ Res*, 102(12), 1483-1491. doi:10.1161/CIRCRESAHA.107.167965
- Jin, Y. R., & Yoon, J. K. (2012). The R-spondin family of proteins: emerging regulators of WNT signaling. *Int J Biochem Cell Biol*, 44(12), 2278-2287. doi:10.1016/j.biocel.2012.09.006
- Johansson, M. E., Phillipson, M., Petersson, J., Velcich, A., Holm, L., & Hansson, G. C. (2008). The inner of the two Muc2 mucin-dependent mucus layers in colon is devoid of bacteria. *Proc Natl Acad Sci U S A*, 105(39), 15064-15069. doi:10.1073/pnas.0803124105
- Jones, L. G., Vaida, A., Thompson, L. M., Ikuomola, F. I., Caamano, J. H., Burkitt, M. D., . . . Duckworth, C. A. (2019). NF-kappa B2 signalling in enteroids modulates enterocyte responses to secreted factors from bone marrow-derived dendritic cells. *Cell Death Dis*, 10(12), 896. doi:10.1038/s41419-019-2129-5
- Julian, M. W., Bao, S., Knoell, D. L., Fahy, R. J., Shao, G., & Crouser, E. D. (2011). Intestinal epithelium is more susceptible to cytopathic injury and altered

- permeability than the lung epithelium in the context of acute sepsis. *Int J Exp Pathol*, 92(5), 366-376. doi:10.1111/j.1365-2613.2011.00783.x
- Jung, H., Leal-Ekman, J. S., Lu, Q., & Stappenbeck, T. S. (2019). Atg14 protects the intestinal epithelium from TNF-triggered villus atrophy. *Autophagy*, 15(11), 1990-2001. doi:10.1080/15548627.2019.1596495
- Jungbeck, M., Stopfer, P., Bataille, F., Nedospasov, S. A., Mannel, D. N., & Hehlhans, T. (2008). Blocking lymphotoxin beta receptor signalling exacerbates acute DSS-induced intestinal inflammation--opposite functions for surface lymphotoxin expressed by T and B lymphocytes. *Mol Immunol*, 45(1), 34-41. doi:10.1016/j.molimm.2007.05.007
- Junqueira, L. C. U. a., Carneiro, J., & Contopoulos, A. N. Basic histology. In *A Concise medical library for practitioner and student* (pp. 11 volumes). Los Altos, Calif. Norwalk, Conn. New York: Lange Medical Publications Appleton & Lange Lange Medical Books/McGraw Hill McGraw Hill.
- Jurgensmeier, J. M., Krajewski, S., Armstrong, R. C., Wilson, G. M., Oltersdorf, T., Fritz, L. C., . . . Otilie, S. (1997). Bax- and Bak-induced cell death in the fission yeast *Schizosaccharomyces pombe*. *Mol Biol Cell*, 8(2), 325-339. doi:10.1091/mbc.8.2.325
- Kallen, K. J., zum Buschenfelde, K. H., & Rose-John, S. (1997). The therapeutic potential of interleukin-6 hyperagonists and antagonists. *Expert Opin Investig Drugs*, 6(3), 237-266. doi:10.1517/13543784.6.3.237
- Kang, S. J., Wang, S., Hara, H., Peterson, E. P., Namura, S., Amin-Hanjani, S., . . . Yuan, J. (2000). Dual role of caspase-11 in mediating activation of caspase-1 and caspase-3 under pathological conditions. *J Cell Biol*, 149(3), 613-622. doi:10.1083/jcb.149.3.613
- Karin, M. (1998). New twists in gene regulation by glucocorticoid receptor: is DNA binding dispensable? *Cell*, 93(4), 487-490. doi:10.1016/s0092-8674(00)81177-0
- Karin, M., Cao, Y., Greten, F. R., & Li, Z. W. (2002). NF-kappaB in cancer: from innocent bystander to major culprit. *Nat Rev Cancer*, 2(4), 301-310. doi:10.1038/nrc780
- Kato, A., Truong-Tran, A. Q., Scott, A. L., Matsumoto, K., & Schleimer, R. P. (2006). Airway epithelial cells produce B cell-activating factor of TNF family by an IFN-beta-dependent mechanism. *J Immunol*, 177(10), 7164-7172. doi:10.4049/jimmunol.177.10.7164
- Kattah, M. G., Shao, L., Rosli, Y. Y., Shimizu, H., Whang, M. I., Advincula, R., . . . Ma, A. (2018). A20 and ABIN-1 synergistically preserve intestinal epithelial cell survival. *J Exp Med*, 215(7), 1839-1852. doi:10.1084/jem.20180198
- Kaufmann, I., Briegel, J., Schliephake, F., Hoelzl, A., Chouker, A., Hummel, T., . . . Thiel, M. (2008). Stress doses of hydrocortisone in septic shock: beneficial effects on opsonization-dependent neutrophil functions. *Intensive Care Med*, 34(2), 344-349. doi:10.1007/s00134-007-0868-8
- Kawai, T., & Akira, S. (2010). The role of pattern-recognition receptors in innate immunity: update on Toll-like receptors. *Nat Immunol*, 11(5), 373-384. doi:10.1038/ni.1863
- Kawashima, R., Kawamura, Y. I., Oshio, T., Son, A., Yamazaki, M., Hagiwara, T., . . . Dohi, T. (2011). Interleukin-13 damages intestinal mucosa via TWEAK and Fn14 in mice—a pathway associated with ulcerative colitis. *Gastroenterology*, 141(6), 2119-2129 e2118. doi:10.1053/j.gastro.2011.08.040
- Keh, D., Boehnke, T., Weber-Cartens, S., Schulz, C., Ahlers, O., Bercker, S., . . . Gerlach, H. (2003). Immunologic and hemodynamic effects of "low-dose"

- hydrocortisone in septic shock: a double-blind, randomized, placebo-controlled, crossover study. *Am J Respir Crit Care Med*, 167(4), 512-520. doi:10.1164/rccm.200205-446OC
- Keh, D., Boehnke, T., Weber-Cartens, S., Schulz, C., Ahlers, O., Bercker, S., . . . Gerlach, H. (2003). Immunologic and hemodynamic effects of "low-dose" hydrocortisone in septic shock: a double-blind, randomized, placebo-controlled, crossover study. *Am J Respir Crit Care Med*, 167(4), 512-520. doi:10.1164/rccm.200205-446OC
- Kelliher, M. A., Grimm, S., Ishida, Y., Kuo, F., Stanger, B. Z., & Leder, P. (1998). The death domain kinase RIP mediates the TNF-induced NF-kappaB signal. *Immunity*, 8(3), 297-303. doi:10.1016/s1074-7613(00)80535-x
- Kelsen, J. R., Dawany, N., Conrad, M. A., Karakasheva, T. A., Maurer, K., Wei, J. M., . . . Hamilton, K. E. (2020). Colonoids From Patients With Pediatric Inflammatory Bowel Disease Exhibit Decreased Growth Associated With Inflammation Severity and Durable Upregulation of Antigen Presentation Genes. *Inflamm Bowel Dis*. doi:10.1093/ibd/izaa145
- Kelstrup, C. D., Bekker-Jensen, D. B., Arrey, T. N., Hogrebe, A., Harder, A., & Olsen, J. V. (2018). Performance Evaluation of the Q Exactive HF-X for Shotgun Proteomics. *J Proteome Res*, 17(1), 727-738. doi:10.1021/acs.jproteome.7b00602
- Kiesslich, R., Duckworth, C. A., Moussata, D., Gloeckner, A., Lim, L. G., Goetz, M., . . . Watson, A. J. (2012). Local barrier dysfunction identified by confocal laser endomicroscopy predicts relapse in inflammatory bowel disease. *Gut*, 61(8), 1146-1153. doi:10.1136/gutjnl-2011-300695
- Kiesslich, R., Goetz, M., Angus, E. M., Hu, Q., Guan, Y., Potten, C., . . . Watson, A. J. (2007). Identification of epithelial gaps in human small and large intestine by confocal endomicroscopy. *Gastroenterology*, 133(6), 1769-1778. doi:10.1053/j.gastro.2007.09.011
- Kim, K. A., Wagle, M., Tran, K., Zhan, X., Dixon, M. A., Liu, S., . . . Abo, A. (2008). R-Spondin family members regulate the Wnt pathway by a common mechanism. *Mol Biol Cell*, 19(6), 2588-2596. doi:10.1091/mbc.E08-02-0187
- Knoop, K. A., & Newberry, R. D. (2018). Goblet cells: multifaceted players in immunity at mucosal surfaces. *Mucosal Immunol*, 11(6), 1551-1557. doi:10.1038/s41385-018-0039-y
- Knutson, M. D. (2017). Iron transport proteins: Gateways of cellular and systemic iron homeostasis. *J Biol Chem*, 292(31), 12735-12743. doi:10.1074/jbc.R117.786632
- Kohn, A. D., & Moon, R. T. (2005). Wnt and calcium signaling: beta-catenin-independent pathways. *Cell Calcium*, 38(3-4), 439-446. doi:10.1016/j.ceca.2005.06.022
- Komatsu, M., Kobayashi, D., Saito, K., Furuya, D., Yagihashi, A., Araake, H., . . . Watanabe, N. (2001). Tumor necrosis factor-alpha in serum of patients with inflammatory bowel disease as measured by a highly sensitive immuno-PCR. *Clin Chem*, 47(7), 1297-1301.
- Komatsu, M., Kobayashi, D., Saito, K., Furuya, D., Yagihashi, A., Araake, H., . . . Watanabe, N. (2001). Tumor necrosis factor-alpha in serum of patients with inflammatory bowel disease as measured by a highly sensitive immuno-PCR. *Clin Chem*, 47(7), 1297-1301.
- Komiya, Y., & Habas, R. (2008). Wnt signal transduction pathways. *Organogenesis*, 4(2), 68-75. doi:10.4161/org.4.2.5851
- Konigsson, K., Torneke, K., Engeland, I. V., Odensvik, K., & Kindahl, H. (2003). Pharmacokinetics and pharmacodynamic effects of flunixin after intravenous, intramuscular and oral administration to dairy goats. *Acta Vet Scand*, 44(3-4), 153-159. doi:10.1186/1751-0147-44-153

- Kontgen, F., Grumont, R. J., Strasser, A., Metcalf, D., Li, R., Tarlinton, D., & Gerondakis, S. (1995). Mice lacking the c-rel proto-oncogene exhibit defects in lymphocyte proliferation, humoral immunity, and interleukin-2 expression. *Genes Dev*, *9*(16), 1965-1977. doi:10.1101/gad.9.16.1965
- Kopan, R. (2012). Notch signaling. *Cold Spring Harb Perspect Biol*, *4*(10). doi:10.1101/cshperspect.a011213
- Koss, K., Satsangi, J., Welsh, K. I., & Jewell, D. P. (2000). Is interleukin-6 important in inflammatory bowel disease? *Genes Immun*, *1*(3), 207-212. doi:10.1038/sj.gene.6363658
- Kovalenko, A., Chable-Bessia, C., Cantarella, G., Israel, A., Wallach, D., & Courtois, G. (2003). The tumour suppressor CYLD negatively regulates NF-kappaB signalling by deubiquitination. *Nature*, *424*(6950), 801-805. doi:10.1038/nature01802
- Krasnodembskaya, A., Samarani, G., Song, Y., Zhuo, H., Su, X., Lee, J. W., . . . Matthay, M. A. (2012). Human mesenchymal stem cells reduce mortality and bacteremia in gram-negative sepsis in mice in part by enhancing the phagocytic activity of blood monocytes. *Am J Physiol Lung Cell Mol Physiol*, *302*(10), L1003-1013. doi:10.1152/ajplung.00180.2011
- Krause, P., Zahner, S. P., Kim, G., Shaikh, R. B., Steinberg, M. W., & Kronenberg, M. (2014). The tumor necrosis factor family member TNFSF14 (LIGHT) is required for resolution of intestinal inflammation in mice. *Gastroenterology*, *146*(7), 1752-1762 e1754. doi:10.1053/j.gastro.2014.02.010
- Kroemer, G., Galluzzi, L., Vandenabeele, P., Abrams, J., Alnemri, E. S., Baehrecke, E. H., . . . Nomenclature Committee on Cell, D. (2009). Classification of cell death: recommendations of the Nomenclature Committee on Cell Death 2009. *Cell Death Differ*, *16*(1), 3-11. doi:10.1038/cdd.2008.150
- Kucuk, C., Sozuer, E., Gursoy, S., Canoz, O., Artis, T., Akcan, A., . . . Muhtaroglu, S. (2006). Treatment with Met-RANTES decreases bacterial translocation in experimental colitis. *Am J Surg*, *191*(1), 77-83. doi:10.1016/j.amjsurg.2005.10.005
- Kumar, A., Roberts, D., Wood, K. E., Light, B., Parrillo, J. E., Sharma, S., . . . Cheang, M. (2006). Duration of hypotension before initiation of effective antimicrobial therapy is the critical determinant of survival in human septic shock. *Crit Care Med*, *34*(6), 1589-1596. doi:10.1097/01.CCM.0000217961.75225.E9
- Kuppen, P. J., Jonges, L. E., van de Velde, C. J., Vahrmeijer, A. L., Tollenaar, R. A., Borel Rinkes, I. H., & Eggermont, A. M. (1997). Liver and tumour tissue concentrations of TNF-alpha in cancer patients treated with TNF-alpha and melphalan by isolated liver perfusion. *Br J Cancer*, *75*(10), 1497-1500. doi:10.1038/bjc.1997.255
- Lai, N., Min, Q., Xiong, E., Liu, J., Zhang, L., Yasuda, S., & Wang, J. Y. (2019). A tetrameric form of CD40 ligand with potent biological activities in both mouse and human primary B cells. *Mol Immunol*, *105*, 173-180. doi:10.1016/j.molimm.2018.11.018
- Lal-Nag, M., & Morin, P. J. (2009). The claudins. *Genome Biol*, *10*(8), 235. doi:10.1186/gb-2009-10-8-235
- Lamkanfi, M. (2011). Emerging inflammasome effector mechanisms. *Nat Rev Immunol*, *11*(3), 213-220. doi:10.1038/nri2936
- Lancaster, M. A., & Knoblich, J. A. (2014). Organogenesis in a dish: modeling development and disease using organoid technologies. *Science*, *345*(6194), 1247125. doi:10.1126/science.1247125
- Lane, K., Van Valen, D., DeFelice, M. M., Macklin, D. N., Kudo, T., Jaimovich, A., . . . Covert, M. W. (2017). Measuring Signaling and RNA-Seq in the Same Cell Links Gene Expression to Dynamic Patterns of NF-kappaB Activation. *Cell Syst*, *4*(4), 458-469 e455. doi:10.1016/j.cels.2017.03.010

- Lang, I., Fullsack, S., Wyzgol, A., Fick, A., Trebing, J., Arana, J. A., . . . Wajant, H. (2016). Binding Studies of TNF Receptor Superfamily (TNFRSF) Receptors on Intact Cells. *J Biol Chem*, *291*(10), 5022-5037. doi:10.1074/jbc.M115.683946
- Lapchak, P. H., Ioannou, A., Kannan, L., Rani, P., Dalle Lucca, J. J., & Tsokos, G. C. (2012). Platelet-associated CD40/CD154 mediates remote tissue damage after mesenteric ischemia/reperfusion injury. *PLoS One*, *7*(2), e32260. doi:10.1371/journal.pone.0032260
- Larmonier, C. B., Laubitz, D., Thurston, R. D., Bucknam, A. L., Hill, F. M., Midura-Kiela, M., . . . Ghishan, F. K. (2011). NHE3 modulates the severity of colitis in IL-10-deficient mice. *Am J Physiol Gastrointest Liver Physiol*, *300*(6), G998-G1009. doi:10.1152/ajpgi.00073.2011
- Lassus, P., Opitz-Araya, X., & Lazebnik, Y. (2002). Requirement for caspase-2 in stress-induced apoptosis before mitochondrial permeabilization. *Science*, *297*(5585), 1352-1354. doi:10.1126/science.1074721
- Last, R. J., & McMinn, R. M. H. (1994). *Last's anatomy, regional and applied* (9th ed.). Edinburgh ; New York: Churchill Livingstone.
- Laubitz, D., Harrison, C. A., Midura-Kiela, M. T., Ramalingam, R., Larmonier, C. B., Chase, J. H., . . . Kiela, P. R. (2016). Reduced Epithelial Na⁺/H⁺ Exchange Drives Gut Microbial Dysbiosis and Promotes Inflammatory Response in T Cell-Mediated Murine Colitis. *PLoS One*, *11*(4), e0152044. doi:10.1371/journal.pone.0152044
- Lee, H. J., & Zheng, J. J. (2010). PDZ domains and their binding partners: structure, specificity, and modification. *Cell Commun Signal*, *8*, 8. doi:10.1186/1478-811X-8-8
- Lee, J. W., & Juliano, R. L. (2000). alpha5beta1 integrin protects intestinal epithelial cells from apoptosis through a phosphatidylinositol 3-kinase and protein kinase B-dependent pathway. *Mol Biol Cell*, *11*(6), 1973-1987. doi:10.1091/mbc.11.6.1973
- Lee, J. W., Wang, P., Kattah, M. G., Youssef, S., Steinman, L., DeFea, K., & Straus, D. S. (2008). Differential regulation of chemokines by IL-17 in colonic epithelial cells. *J Immunol*, *181*(9), 6536-6545. doi:10.4049/jimmunol.181.9.6536
- Lee, W. H., Seo, D., Lim, S. G., & Suk, K. (2019). Reverse Signaling of Tumor Necrosis Factor Superfamily Proteins in Macrophages and Microglia: Superfamily Portrait in the Neuroimmune Interface. *Front Immunol*, *10*, 262. doi:10.3389/fimmu.2019.00262
- Legras, A., Giraudeau, B., Jonville-Bera, A. P., Camus, C., Francois, B., Runge, I., . . . Autret-Leca, E. (2009). A multicentre case-control study of nonsteroidal anti-inflammatory drugs as a risk factor for severe sepsis and septic shock. *Crit Care*, *13*(2), R43. doi:10.1186/cc7766
- Lennernas, H., Skrtic, S., & Johannsson, G. (2008). Replacement therapy of oral hydrocortisone in adrenal insufficiency: the influence of gastrointestinal factors. *Expert Opin Drug Metab Toxicol*, *4*(6), 749-758. doi:10.1517/17425255.4.6.749
- Leppkes, M., Roulis, M., Neurath, M. F., Kollias, G., & Becker, C. (2014). Pleiotropic functions of TNF-alpha in the regulation of the intestinal epithelial response to inflammation. *Int Immunol*, *26*(9), 509-515. doi:10.1093/intimm/dxu051
- Lerebours, F., Vacher, S., Andrieu, C., Espie, M., Marty, M., Lidereau, R., & Bieche, I. (2008). NF-kappa B genes have a major role in inflammatory breast cancer. *BMC Cancer*, *8*, 41. doi:10.1186/1471-2407-8-41
- Lesley, R., Kelly, L. M., Xu, Y., & Cyster, J. G. (2006). Naive CD4 T cells constitutively express CD40L and augment autoreactive B cell survival. *Proc Natl Acad Sci U S A*, *103*(28), 10717-10722. doi:10.1073/pnas.0601539103

- Ley, R. E., Peterson, D. A., & Gordon, J. I. (2006). Ecological and evolutionary forces shaping microbial diversity in the human intestine. *Cell*, *124*(4), 837-848. doi:10.1016/j.cell.2006.02.017
- Li, L. Y., Luo, X., & Wang, X. (2001). Endonuclease G is an apoptotic DNase when released from mitochondria. *Nature*, *412*(6842), 95-99. doi:10.1038/35083620
- Li, P., Nijhawan, D., Budihardjo, I., Srinivasula, S. M., Ahmad, M., Alnemri, E. S., & Wang, X. (1997). Cytochrome c and dATP-dependent formation of Apaf-1/caspase-9 complex initiates an apoptotic protease cascade. *Cell*, *91*(4), 479-489. doi:10.1016/s0092-8674(00)80434-1
- Li, Q., Zhang, Q., Wang, C., Liu, X., Li, N., & Li, J. (2009). Disruption of tight junctions during polymicrobial sepsis in vivo. *J Pathol*, *218*(2), 210-221. doi:10.1002/path.2525
- Li, X., Su, J., Cui, X., Li, Y., Barochia, A., & Eichacker, P. Q. (2009). Can we predict the effects of NF-kappaB inhibition in sepsis? Studies with parthenolide and ethyl pyruvate. *Expert Opin Investig Drugs*, *18*(8), 1047-1060. doi:10.1517/13543780903018880
- Liang, S. C., Tan, X. Y., Luxenberg, D. P., Karim, R., Dunussi-Joannopoulos, K., Collins, M., & Fouser, L. A. (2006). Interleukin (IL)-22 and IL-17 are coexpressed by Th17 cells and cooperatively enhance expression of antimicrobial peptides. *J Exp Med*, *203*(10), 2271-2279. doi:10.1084/jem.20061308
- Lim, S. G., Suk, K., & Lee, W. H. (2013). Reverse signaling from LIGHT promotes pro-inflammatory responses in the human monocytic leukemia cell line, THP-1. *Cell Immunol*, *285*(1-2), 10-17. doi:10.1016/j.cellimm.2013.08.002
- Lindon, J. C., Tranter, G. E., & Koppenaal, D. W. (2017). *Encyclopedia of spectroscopy and spectrometry* (Third edition. ed.). Amsterdam ; Boston: Elsevier/AP, Academic Press is an imprint of Elsevier.
- Liu, F., Bardhan, K., Yang, D., Thangaraju, M., Ganapathy, V., Waller, J. L., . . . Liu, K. (2012). NF-kappaB directly regulates Fas transcription to modulate Fas-mediated apoptosis and tumor suppression. *J Biol Chem*, *287*(30), 25530-25540. doi:10.1074/jbc.M112.356279
- Liu, J. Z., van Sommeren, S., Huang, H., Ng, S. C., Alberts, R., Takahashi, A., . . . Weersma, R. K. (2015). Association analyses identify 38 susceptibility loci for inflammatory bowel disease and highlight shared genetic risk across populations. *Nat Genet*, *47*(9), 979-986. doi:10.1038/ng.3359
- Liu, X., Zheng, X., Wang, N., Cao, H., Lu, Y., Long, Y., . . . Zheng, J. (2011). Kukoamine B, a novel dual inhibitor of LPS and CpG DNA, is a potential candidate for sepsis treatment. *Br J Pharmacol*, *162*(6), 1274-1290. doi:10.1111/j.1476-5381.2010.01114.x
- Liu, Y. F., Yang, C. W., Liu, H., Sui, S. G., & Li, X. D. (2017). Efficacy and Therapeutic Potential of Curcumin Against Sepsis-Induced Chronic Lung Injury in Male Albino Rats. *J Nutr Health Aging*, *21*(3), 307-313. doi:10.1007/s12603-016-0722-1
- Locksley, R. M., Killeen, N., & Lenardo, M. J. (2001). The TNF and TNF receptor superfamilies: integrating mammalian biology. *Cell*, *104*(4), 487-501. doi:10.1016/s0092-8674(01)00237-9
- Loddo, I., & Romano, C. (2015). Inflammatory Bowel Disease: Genetics, Epigenetics, and Pathogenesis. *Front Immunol*, *6*, 551. doi:10.3389/fimmu.2015.00551
- Lodish, H. F. (2008). *Molecular cell biology* (6th ed.). New York: W.H. Freeman.
- Logan, C. Y., & Nusse, R. (2004). The Wnt signaling pathway in development and disease. *Annu Rev Cell Dev Biol*, *20*, 781-810. doi:10.1146/annurev.cellbio.20.010403.113126

- Loh, K., Chia, J. A., Greco, S., Cozzi, S. J., Buttenshaw, R. L., Bond, C. E., . . . Whitehall, V. L. (2008). Bone morphogenetic protein 3 inactivation is an early and frequent event in colorectal cancer development. *Genes Chromosomes Cancer*, *47*(6), 449-460. doi:10.1002/gcc.20552
- Lorenz, J. N., Nieman, M., Sabo, J., Sanford, L. P., Hawkins, J. A., Elitsur, N., . . . Cohen, M. B. (2003). Uroguanylin knockout mice have increased blood pressure and impaired natriuretic response to enteral NaCl load. *J Clin Invest*, *112*(8), 1244-1254. doi:10.1172/JCI18743
- Lu, J., Yang, Y., Guo, G., Liu, Y., Zhang, Z., Dong, S., . . . Huang, Q. (2017). IKBKE regulates cell proliferation and epithelial-mesenchymal transition of human malignant glioma via the Hippo pathway. *Oncotarget*, *8*(30), 49502-49514. doi:10.18632/oncotarget.17738
- Ludwiczek, O., Kaser, A., & Tilg, H. (2003). Plasma levels of soluble CD40 ligand are elevated in inflammatory bowel diseases. *Int J Colorectal Dis*, *18*(2), 142-147. doi:10.1007/s00384-002-0425-4
- Luftig, M., Yasui, T., Soni, V., Kang, M. S., Jacobson, N., Cahir-McFarland, E., . . . Kieff, E. (2004). Epstein-Barr virus latent infection membrane protein 1 TRAF-binding site induces NIK/IKK alpha-dependent noncanonical NF-kappaB activation. *Proc Natl Acad Sci U S A*, *101*(1), 141-146. doi:10.1073/pnas.2237183100
- Lundell, A. C., Nordstrom, I., Andersson, K., Lundqvist, C., Telemo, E., Nava, S., . . . Rudin, A. (2017). IFN type I and II induce BAFF secretion from human decidual stromal cells. *Sci Rep*, *7*, 39904. doi:10.1038/srep39904
- Luu, L., Matthews, Z. J., Armstrong, S. D., Powell, P. P., Wileman, T., Wastling, J. M., & Coombes, J. L. (2018). Proteomic Profiling of Enteroid Cultures Skewed toward Development of Specific Epithelial Lineages. *Proteomics*, *18*(16), e1800132. doi:10.1002/pmic.201800132
- Lv, S., Han, M., Yi, R., Kwon, S., Dai, C., & Wang, R. (2014). Anti-TNF-alpha therapy for patients with sepsis: a systematic meta-analysis. *Int J Clin Pract*, *68*(4), 520-528. doi:10.1111/ijcp.12382
- Lyss, G., Knorre, A., Schmidt, T. J., Pahl, H. L., & Merfort, I. (1998). The anti-inflammatory sesquiterpene lactone helenalin inhibits the transcription factor NF-kappaB by directly targeting p65. *J Biol Chem*, *273*(50), 33508-33516. doi:10.1074/jbc.273.50.33508
- Ma, T. Y., Boivin, M. A., Ye, D., Pedram, A., & Said, H. M. (2005). Mechanism of TNF- α modulation of Caco-2 intestinal epithelial tight junction barrier: role of myosin light-chain kinase protein expression. *Am J Physiol Gastrointest Liver Physiol*, *288*(3), G422-430. doi:10.1152/ajpgi.00412.2004
- MacEwan, D. J. (2015). TWEAKing for a fight with GVHD. *Blood*, *126*(4), 429-430. doi:10.1182/blood-2015-06-649517
- Mach, F., Schonbeck, U., Sukhova, G. K., Bourcier, T., Bonnefoy, J. Y., Pober, J. S., & Libby, P. (1997). Functional CD40 ligand is expressed on human vascular endothelial cells, smooth muscle cells, and macrophages: implications for CD40-CD40 ligand signaling in atherosclerosis. *Proc Natl Acad Sci U S A*, *94*(5), 1931-1936. doi:10.1073/pnas.94.5.1931
- Mackay, F., Browning, J. L., Lawton, P., Shah, S. A., Comiskey, M., Bhan, A. K., . . . Simpson, S. J. (1998). Both the lymphotoxin and tumor necrosis factor pathways are involved in experimental murine models of colitis. *Gastroenterology*, *115*(6), 1464-1475. doi:10.1016/s0016-5085(98)70025-3
- Mackay, F., & Leung, H. (2006). The role of the BAFF/APRIL system on T cell function. *Semin Immunol*, *18*(5), 284-289. doi:10.1016/j.smim.2006.04.005
- Macpherson, A. J., & McCoy, K. (2007). APRIL in the intestine: a good destination for immunoglobulin A(2). *Immunity*, *26*(6), 755-757. doi:10.1016/j.immuni.2007.06.003

- Madara, J. L. (1990). Maintenance of the macromolecular barrier at cell extrusion sites in intestinal epithelium: physiological rearrangement of tight junctions. *J Membr Biol*, 116(2), 177-184. doi:10.1007/BF01868675
- Madison, B. B., Braunstein, K., Kuizon, E., Portman, K., Qiao, X. T., & Gumucio, D. L. (2005). Epithelial hedgehog signals pattern the intestinal crypt-villus axis. *Development*, 132(2), 279-289. doi:10.1242/dev.01576
- Malmstrom, E., Kilsgard, O., Hauri, S., Smeds, E., Herwald, H., Malmstrom, L., & Malmstrom, J. (2016). Large-scale inference of protein tissue origin in gram-positive sepsis plasma using quantitative targeted proteomics. *Nat Commun*, 7, 10261. doi:10.1038/ncomms10261
- Mana, P., Linares, D., Silva, D. G., Fordham, S., Scheu, S., Pfeffer, K., . . . Bertram, E. M. (2013). LIGHT (TNFSF14/CD258) is a decisive factor for recovery from experimental autoimmune encephalomyelitis. *J Immunol*, 191(1), 154-163. doi:10.4049/jimmunol.1203016
- Mankertz, J., & Schulzke, J. D. (2007). Altered permeability in inflammatory bowel disease: pathophysiology and clinical implications. *Curr Opin Gastroenterol*, 23(4), 379-383. doi:10.1097/MOG.0b013e32816aa392
- Marcelino, J., Sciortino, C. M., Romero, M. F., Ulatowski, L. M., Ballock, R. T., Economides, A. N., . . . Warman, M. L. (2001). Human disease-causing NOG missense mutations: effects on noggin secretion, dimer formation, and bone morphogenetic protein binding. *Proc Natl Acad Sci U S A*, 98(20), 11353-11358. doi:10.1073/pnas.201367598
- Marchiando, A. M., Shen, L., Graham, W. V., Edelblum, K. L., Duckworth, C. A., Guan, Y., . . . Watson, A. J. (2011). The epithelial barrier is maintained by in vivo tight junction expansion during pathologic intestinal epithelial shedding. *Gastroenterology*, 140(4), 1208-1218 e1201-1202. doi:10.1053/j.gastro.2011.01.004
- Marik, P. E., Khangoora, V., Rivera, R., Hooper, M. H., & Catravas, J. (2017). Hydrocortisone, Vitamin C, and Thiamine for the Treatment of Severe Sepsis and Septic Shock: A Retrospective Before-After Study. *Chest*, 151(6), 1229-1238. doi:10.1016/j.chest.2016.11.036
- Marik, P. E., & Taeb, A. M. (2017). SIRS, qSOFA and new sepsis definition. *J Thorac Dis*, 9(4), 943-945. doi:10.21037/jtd.2017.03.125
- Martin, L., Koczera, P., Simons, N., Zechendorf, E., Hoeger, J., Marx, G., & Schuerholz, T. (2016). The Human Host Defense Ribonucleases 1, 3 and 7 Are Elevated in Patients with Sepsis after Major Surgery--A Pilot Study. *Int J Mol Sci*, 17(3), 294. doi:10.3390/ijms17030294
- Martins, T. B., Rose, J. W., Jaskowski, T. D., Wilson, A. R., Husebye, D., Seraj, H. S., & Hill, H. R. (2011). Analysis of proinflammatory and anti-inflammatory cytokine serum concentrations in patients with multiple sclerosis by using a multiplexed immunoassay. *Am J Clin Pathol*, 136(5), 696-704. doi:10.1309/AJCP7UBK8IBVMVNR
- Matsuda, M., Kubo, A., Furuse, M., & Tsukita, S. (2004). A peculiar internalization of claudins, tight junction-specific adhesion molecules, during the intercellular movement of epithelial cells. *J Cell Sci*, 117(Pt 7), 1247-1257. doi:10.1242/jcs.00972
- Matsumoto, H., Ogura, H., Shimizu, K., Ikeda, M., Hirose, T., Matsuura, H., . . . Shimazu, T. (2018). The clinical importance of a cytokine network in the acute phase of sepsis. *Sci Rep*, 8(1), 13995. doi:10.1038/s41598-018-32275-8
- Mauri, D. N., Ebner, R., Montgomery, R. I., Kochel, K. D., Cheung, T. C., Yu, G. L., . . . Ware, C. F. (1998). LIGHT, a new member of the TNF superfamily, and lymphotoxin alpha are ligands for herpesvirus entry mediator. *Immunity*, 8(1), 21-30. doi:10.1016/s1074-7613(00)80455-0

- Mauro, C., Pacifico, F., Lavorgna, A., Mellone, S., Iannetti, A., Acquaviva, R., . . . Leonardi, A. (2006). ABIN-1 binds to NEMO/IKKgamma and co-operates with A20 in inhibiting NF-kappaB. *J Biol Chem*, *281*(27), 18482-18488. doi:10.1074/jbc.M601502200
- Mayhew, T. M., Myklebust, R., Whybrow, A., & Jenkins, R. (1999). Epithelial integrity, cell death and cell loss in mammalian small intestine. *Histol Histopathol*, *14*(1), 257-267. doi:10.14670/HH-14.257
- Mayr, F. B., Yende, S., & Angus, D. C. (2014). Epidemiology of severe sepsis. *Virulence*, *5*(1), 4-11. doi:10.4161/viru.27372
- Mazor, R. L., Menendez, I. Y., Ryan, M. A., Fiedler, M. A., & Wong, H. R. (2000). Sesquiterpene lactones are potent inhibitors of interleukin 8 gene expression in cultured human respiratory epithelium. *Cytokine*, *12*(3), 239-245. doi:10.1006/cyto.1999.0526
- McGovern, D. P., Kugathasan, S., & Cho, J. H. (2015). Genetics of Inflammatory Bowel Diseases. *Gastroenterology*, *149*(5), 1163-1176 e1162. doi:10.1053/j.gastro.2015.08.001
- McIlwraith, C. W., Frisbie, D. D., Kawcak, C. E., & Weeren, R. v. (2016). *Joint disease in the horse* (Second edition. ed.). St. Louis, Missouri: Elsevier.
- McKinley, E. T., Sui, Y., Al-Kofahi, Y., Millis, B. A., Tyska, M. J., Roland, J. T., . . . Coffey, R. J. (2017). Optimized multiplex immunofluorescence single-cell analysis reveals tuft cell heterogeneity. *JCI Insight*, *2*(11). doi:10.1172/jci.insight.93487
- McKinley, M. P., & O'Loughlin, V. D. (2008). *Human anatomy* (2nd ed.). Boston: McGraw-Hill Higher Education.
- Medvedev, A. E., Espevik, T., Ranges, G., & Sundan, A. (1996). Distinct roles of the two tumor necrosis factor (TNF) receptors in modulating TNF and lymphotoxin alpha effects. *J Biol Chem*, *271*(16), 9778-9784. doi:10.1074/jbc.271.16.9778
- Meighan-Mantha, R. L., Hsu, D. K., Guo, Y., Brown, S. A., Feng, S. L., Peifley, K. A., . . . Winkles, J. A. (1999). The mitogen-inducible Fn14 gene encodes a type I transmembrane protein that modulates fibroblast adhesion and migration. *J Biol Chem*, *274*(46), 33166-33176. doi:10.1074/jbc.274.46.33166
- Merga, Y. J., O'Hara, A., Burkitt, M. D., Duckworth, C. A., Probert, C. S., Campbell, B. J., & Pritchard, D. M. (2016). Importance of the alternative NF-kappaB activation pathway in inflammation-associated gastrointestinal carcinogenesis. *Am J Physiol Gastrointest Liver Physiol*, *310*(11), G1081-1090. doi:10.1152/ajpgi.00026.2016
- Michel, N. A., Zirlik, A., & Wolf, D. (2017). CD40L and Its Receptors in Atherothrombosis-An Update. *Front Cardiovasc Med*, *4*, 40. doi:10.3389/fcvm.2017.00040
- Michie, H. R., Manogue, K. R., Spriggs, D. R., Revhaug, A., O'Dwyer, S., Dinarello, C. A., . . . Wilmore, D. W. (1988). Detection of circulating tumor necrosis factor after endotoxin administration. *N Engl J Med*, *318*(23), 1481-1486. doi:10.1056/NEJM198806093182301
- Michielan, A., & D'Inca, R. (2015). Intestinal Permeability in Inflammatory Bowel Disease: Pathogenesis, Clinical Evaluation, and Therapy of Leaky Gut. *Mediators Inflamm*, *2015*, 628157. doi:10.1155/2015/628157
- Middendorp, S., Schneeberger, K., Wiegerinck, C. L., Mokry, M., Akkerman, R. D., van Wijngaarden, S., . . . Nieuwenhuis, E. E. (2014). Adult stem cells in the small intestine are intrinsically programmed with their location-specific function. *Stem Cells*, *32*(5), 1083-1091. doi:10.1002/stem.1655
- Mikuda, N., Schmidt-Ullrich, R., Kargel, E., Golusda, L., Wolf, J., Hopken, U. E., . . . Kolesnichenko, M. (2020). Deficiency in IkappaBalpha in the intestinal

- epithelium leads to spontaneous inflammation and mediates apoptosis in the gut. *J Pathol*, 251(2), 160-174. doi:10.1002/path.5437
- Miller, H., Zhang, J., Kuolee, R., Patel, G. B., & Chen, W. (2007). Intestinal M cells: the fallible sentinels? *World J Gastroenterol*, 13(10), 1477-1486. doi:10.3748/wjg.v13.i10.1477
- Miller, S. C., Huang, R., Sakamuru, S., Shukla, S. J., Attene-Ramos, M. S., Shinn, P., . . . Xia, M. (2010). Identification of known drugs that act as inhibitors of NF-kappaB signaling and their mechanism of action. *Biochem Pharmacol*, 79(9), 1272-1280. doi:10.1016/j.bcp.2009.12.021
- Mineta, K., Yamamoto, Y., Yamazaki, Y., Tanaka, H., Tada, Y., Saito, K., . . . Tsukita, S. (2011). Predicted expansion of the claudin multigene family. *FEBS Lett*, 585(4), 606-612. doi:10.1016/j.febslet.2011.01.028
- Mizoguchi, E., Mizoguchi, A., Takedatsu, H., Cario, E., de Jong, Y. P., Ooi, C. J., . . . Bhan, A. K. (2002). Role of tumor necrosis factor receptor 2 (TNFR2) in colonic epithelial hyperplasia and chronic intestinal inflammation in mice. *Gastroenterology*, 122(1), 134-144. doi:10.1053/gast.2002.30347
- Mizushima, N. (2007). Autophagy: process and function. *Genes Dev*, 21(22), 2861-2873. doi:10.1101/gad.1599207
- M'Koma, A. E., Seeley, E. H., Washington, M. K., Schwartz, D. A., Muldoon, R. L., Herline, A. J., . . . Caprioli, R. M. (2011). Proteomic profiling of mucosal and submucosal colonic tissues yields protein signatures that differentiate the inflammatory colitides. *Inflamm Bowel Dis*, 17(4), 875-883. doi:10.1002/ibd.21442
- Moore, F., Buonocore, S., Aksoy, E., Ouled-Haddou, N., Goriely, S., Lazarova, E., . . . Flamand, V. (2007). An alternative pathway of NF-kappaB activation results in maturation and T cell priming activity of dendritic cells overexpressing a mutated IkappaBalpha. *J Immunol*, 178(3), 1301-1311. doi:10.4049/jimmunol.178.3.1301
- Moss, M. L., Jin, S. L., Milla, M. E., Bickett, D. M., Burkhart, W., Carter, H. L., . . . et al. (1997). Cloning of a disintegrin metalloproteinase that processes precursor tumour-necrosis factor-alpha. *Nature*, 385(6618), 733-736. doi:10.1038/385733a0
- Moulton, D. E., Crandall, W., Lakhani, R., & Lowe, M. E. (2004). Expression of a novel cadherin in the mouse and human intestine. *Pediatr Res*, 55(6), 927-934. doi:10.1203/01.PDR.0000125260.46861.32
- Mowat, A. M., & Agace, W. W. (2014). Regional specialization within the intestinal immune system. *Nat Rev Immunol*, 14(10), 667-685. doi:10.1038/nri3738
- Mudter, J., & Neurath, M. F. (2007). Il-6 signaling in inflammatory bowel disease: pathophysiological role and clinical relevance. *Inflamm Bowel Dis*, 13(8), 1016-1023. doi:10.1002/ibd.20148
- Murch, S. H., Braegger, C. P., Walker-Smith, J. A., & MacDonald, T. T. (1993). Location of tumour necrosis factor alpha by immunohistochemistry in chronic inflammatory bowel disease. *Gut*, 34(12), 1705-1709. doi:10.1136/gut.34.12.1705
- Muzio, M., Chinnaiyan, A. M., Kischkel, F. C., O'Rourke, K., Shevchenko, A., Ni, J., . . . Dixit, V. M. (1996). FLICE, a novel FADD-homologous ICE/CED-3-like protease, is recruited to the CD95 (Fas/APO-1) death-inducing signaling complex. *Cell*, 85(6), 817-827. doi:10.1016/s0092-8674(00)81266-0
- Nagata, S. (2000). Apoptotic DNA fragmentation. *Exp Cell Res*, 256(1), 12-18. doi:10.1006/excr.2000.4834
- Nakagawa, T., Zhu, H., Morishima, N., Li, E., Xu, J., Yankner, B. A., & Yuan, J. (2000). Caspase-12 mediates endoplasmic-reticulum-specific apoptosis and cytotoxicity by amyloid-beta. *Nature*, 403(6765), 98-103. doi:10.1038/47513
- Nasdala, I., Wolburg-Buchholz, K., Wolburg, H., Kuhn, A., Ebnet, K., Brachtendorf, G., . . . Butz, S. (2002). A transmembrane tight junction protein selectively

- expressed on endothelial cells and platelets. *J Biol Chem*, 277(18), 16294-16303. doi:10.1074/jbc.M111999200
- Navale, A. M., & Paranjape, A. N. (2016). Glucose transporters: physiological and pathological roles. *Biophys Rev*, 8(1), 5-9. doi:10.1007/s12551-015-0186-2
- Nedwin, G. E., Naylor, S. L., Sakaguchi, A. Y., Smith, D., Jarrett-Nedwin, J., Pennica, D., . . . Gray, P. W. (1985). Human lymphotoxin and tumor necrosis factor genes: structure, homology and chromosomal localization. *Nucleic Acids Res*, 13(17), 6361-6373. doi:10.1093/nar/13.17.6361
- Nelson, K. M., Dahlin, J. L., Bisson, J., Graham, J., Pauli, G. F., & Walters, M. A. (2017). The Essential Medicinal Chemistry of Curcumin. *J Med Chem*, 60(5), 1620-1637. doi:10.1021/acs.jmedchem.6b00975
- Nenci, A., Becker, C., Wullaert, A., Gareus, R., van Loo, G., Danese, S., . . . Pasparakis, M. (2007). Epithelial NEMO links innate immunity to chronic intestinal inflammation. *Nature*, 446(7135), 557-561. doi:10.1038/nature05698
- Neufert, C., Becker, C., Tureci, O., Waldner, M. J., Backert, I., Floh, K., . . . Neurath, M. F. (2013). Tumor fibroblast-derived epiregulin promotes growth of colitis-associated neoplasms through ERK. *J Clin Invest*, 123(4), 1428-1443. doi:10.1172/JCI63748
- Neugut, A. I., Jacobson, J. S., Suh, S., Mukherjee, R., & Arber, N. (1998). The epidemiology of cancer of the small bowel. *Cancer Epidemiol Biomarkers Prev*, 7(3), 243-251.
- Neurath, M. F., Pettersson, S., Meyer zum Buschenfelde, K. H., & Strober, W. (1996). Local administration of antisense phosphorothioate oligonucleotides to the p65 subunit of NF-kappa B abrogates established experimental colitis in mice. *Nat Med*, 2(9), 998-1004. doi:10.1038/nm0996-998
- Neutra, M. R., Mantis, N. J., & Kraehenbuhl, J. P. (2001). Collaboration of epithelial cells with organized mucosal lymphoid tissues. *Nat Immunol*, 2(11), 1004-1009. doi:10.1038/ni1101-1004
- Newton, K., & Dixit, V. M. (2012). Signaling in innate immunity and inflammation. *Cold Spring Harb Perspect Biol*, 4(3). doi:10.1101/cshperspect.a006049
- Ng, L. G., Mackay, C. R., & Mackay, F. (2005). The BAFF/APRIL system: life beyond B lymphocytes. *Mol Immunol*, 42(7), 763-772. doi:10.1016/j.molimm.2004.06.041
- Ngo, V. N., Korner, H., Gunn, M. D., Schmidt, K. N., Riminton, D. S., Cooper, M. D., . . . Cyster, J. G. (1999). Lymphotoxin alpha/beta and tumor necrosis factor are required for stromal cell expression of homing chemokines in B and T cell areas of the spleen. *J Exp Med*, 189(2), 403-412. doi:10.1084/jem.189.2.403
- Nicholls, S., Stephens, S., Braegger, C. P., Walker-Smith, J. A., & MacDonald, T. T. (1993). Cytokines in stools of children with inflammatory bowel disease or infective diarrhoea. *J Clin Pathol*, 46(8), 757-760. doi:10.1136/jcp.46.8.757
- Nicholls, S., Stephens, S., Braegger, C. P., Walker-Smith, J. A., & MacDonald, T. T. (1993). Cytokines in stools of children with inflammatory bowel disease or infective diarrhoea. *J Clin Pathol*, 46(8), 757-760. doi:10.1136/jcp.46.8.757
- Niisato, N., & Marunaka, Y. (2001). Forskolin activation of apical Cl⁻ channel and Na⁺/K⁺/2Cl⁻ cotransporter via a PTK-dependent pathway in renal epithelium. *Biochem Biophys Res Commun*, 285(4), 880-884. doi:10.1006/bbrc.2001.5251
- Nijman, S. M., Luna-Vargas, M. P., Velds, A., Brummelkamp, T. R., Dirac, A. M., Sixma, T. K., & Bernards, R. (2005). A genomic and functional inventory of deubiquitinating enzymes. *Cell*, 123(5), 773-786. doi:10.1016/j.cell.2005.11.007
- Nomme, J., Fanning, A. S., Caffrey, M., Lye, M. F., Anderson, J. M., & Lavie, A. (2011). The Src homology 3 domain is required for junctional adhesion

- molecule binding to the third PDZ domain of the scaffolding protein ZO-1. *J Biol Chem*, 286(50), 43352-43360. doi:10.1074/jbc.M111.304089
- Notarangelo, L. D., Duse, M., & Ugazio, A. G. (1992). Immunodeficiency with hyper-IgM (HIM). *Immunodeficiency Rev*, 3(2), 101-121.
- Ogata, A., & Tanaka, T. (2012). Tocilizumab for the treatment of rheumatoid arthritis and other systemic autoimmune diseases: current perspectives and future directions. *Int J Rheumatol*, 2012, 946048. doi:10.1155/2012/946048
- Ogura, Y., Bonen, D. K., Inohara, N., Nicolae, D. L., Chen, F. F., Ramos, R., . . . Cho, J. H. (2001). A frameshift mutation in NOD2 associated with susceptibility to Crohn's disease. *Nature*, 411(6837), 603-606. doi:10.1038/35079114
- O'Hara, A. M., & Shanahan, F. (2006). The gut flora as a forgotten organ. *EMBO Rep*, 7(7), 688-693. doi:10.1038/sj.embor.7400731
- Okumura, R., & Takeda, K. (2017). Roles of intestinal epithelial cells in the maintenance of gut homeostasis. *Exp Mol Med*, 49(5), e338. doi:10.1038/emm.2017.20
- Opal, S. M., Laterre, P. F., Francois, B., LaRosa, S. P., Angus, D. C., Mira, J. P., . . . Group, A. S. (2013). Effect of eritoran, an antagonist of MD2-TLR4, on mortality in patients with severe sepsis: the ACCESS randomized trial. *JAMA*, 309(11), 1154-1162. doi:10.1001/jama.2013.2194
- Ostermann, G., Weber, K. S., Zerneck, A., Schroder, A., & Weber, C. (2002). JAM-1 is a ligand of the beta(2) integrin LFA-1 involved in transendothelial migration of leukocytes. *Nat Immunol*, 3(2), 151-158. doi:10.1038/ni755
- Otterdal, K., Haukeland, J. W., Yndestad, A., Dahl, T. B., Holm, S., Segers, F. M., . . . Aukrust, P. (2015). Increased Serum Levels of LIGHT/TNFSF14 in Nonalcoholic Fatty Liver Disease: Possible Role in Hepatic Inflammation. *Clin Transl Gastroenterol*, 6, e95. doi:10.1038/ctg.2015.23
- Owen, R. L., & Jones, A. L. (1974). Epithelial cell specialization within human Peyer's patches: an ultrastructural study of intestinal lymphoid follicles. *Gastroenterology*, 66(2), 189-203.
- Ozoren, N., Inohara, N., & Nunez, G. (2009). A putative role for human BFK in DNA damage-induced apoptosis. *Biotechnol J*, 4(7), 1046-1054. doi:10.1002/biot.200900091
- Pahl, H. L. (1999). Activators and target genes of Rel/NF-kappaB transcription factors. *Oncogene*, 18(49), 6853-6866. doi:10.1038/sj.onc.1203239
- Palomero, T., Lim, W. K., Odom, D. T., Sulis, M. L., Real, P. J., Margolin, A., . . . Ferrando, A. A. (2006). NOTCH1 directly regulates c-MYC and activates a feed-forward-loop transcriptional network promoting leukemic cell growth. *Proc Natl Acad Sci U S A*, 103(48), 18261-18266. doi:10.1073/pnas.0606108103
- Papich, M. G. (2016). *Saunders handbook of veterinary drugs : small and large animal* (Fourth edition. ed.). St. Louis, Missouri: Elsevier.
- Park, E., Kim, G. H., Choi, S. C., & Han, J. K. (2006). Role of PKA as a negative regulator of PCP signaling pathway during *Xenopus* gastrulation movements. *Dev Biol*, 292(2), 344-357. doi:10.1016/j.ydbio.2006.01.011
- Park, J. S., Kwok, S. K., Lim, M. A., Oh, H. J., Kim, E. K., Jhun, J. Y., . . . Cho, M. L. (2013). TWEAK promotes osteoclastogenesis in rheumatoid arthritis. *Am J Pathol*, 183(3), 857-867. doi:10.1016/j.ajpath.2013.05.027
- Parween, S., DiNardo, G., Baj, F., Zhang, C., Gilardi, G., & Pandey, A. V. (2020). Differential effects of variations in human P450 oxidoreductase on the aromatase activity of CYP19A1 polymorphisms R264C and R264H. *J Steroid Biochem Mol Biol*, 196, 105507. doi:10.1016/j.jsbmb.2019.105507
- Pattison, A. M., Barton, J. R., Entezari, A. A., Zalewski, A., Rappaport, J. A., Snook, A. E., & Waldman, S. A. (2020). Silencing the intestinal GUCY2C tumor

- suppressor axis requires APC loss of heterozygosity. *Cancer Biol Ther*, 21(9), 799-805. doi:10.1080/15384047.2020.1779005
- Pearce, S. C., Al-Jawadi, A., Kishida, K., Yu, S., Hu, M., Fritzky, L. F., . . . Ferraris, R. P. (2018). Marked differences in tight junction composition and macromolecular permeability among different intestinal cell types. *BMC Biol*, 16(1), 19. doi:10.1186/s12915-018-0481-z
- Pekalski, J., Zuk, P. J., Kochanczyk, M., Junkin, M., Kellogg, R., Tay, S., & Lipniacki, T. (2013). Spontaneous NF-kappaB activation by autocrine TNFalpha signaling: a computational analysis. *PLoS One*, 8(11), e78887. doi:10.1371/journal.pone.0078887
- Pelekanou, V., Kampa, M., Kafousi, M., Darivianaki, K., Sanidas, E., Tsiftsis, D. D., . . . Castanas, E. (2008). Expression of TNF-superfamily members BAFF and APRIL in breast cancer: immunohistochemical study in 52 invasive ductal breast carcinomas. *BMC Cancer*, 8, 76. doi:10.1186/1471-2407-8-76
- Pennica, D., Nedwin, G. E., Hayflick, J. S., Seeburg, P. H., Derynck, R., Palladino, M. A., . . . Goeddel, D. V. (1984). Human tumour necrosis factor: precursor structure, expression and homology to lymphotoxin. *Nature*, 312(5996), 724-729. doi:10.1038/312724a0
- Perkins, N. D. (2007). Integrating cell-signalling pathways with NF-kappaB and IKK function. *Nat Rev Mol Cell Biol*, 8(1), 49-62. doi:10.1038/nrm2083
- Perrot-Applanat, M., Vacher, S., Toullec, A., Pelaez, I., Velasco, G., Cormier, F., . . . Bieche, I. (2011). Similar NF-kappaB gene signatures in TNF-alpha treated human endothelial cells and breast tumor biopsies. *PLoS One*, 6(7), e21589. doi:10.1371/journal.pone.0021589
- Peterson, E. J., Clements, J. L., Fang, N., & Koretzky, G. A. (1998). Adaptor proteins in lymphocyte antigen-receptor signaling. *Curr Opin Immunol*, 10(3), 337-344. doi:10.1016/s0952-7915(98)80173-8
- Pickert, G., Neufert, C., Leppkes, M., Zheng, Y., Wittkopf, N., Warntjen, M., . . . Becker, C. (2009). STAT3 links IL-22 signaling in intestinal epithelial cells to mucosal wound healing. *J Exp Med*, 206(7), 1465-1472. doi:10.1084/jem.20082683
- Piguet, P. F., Vesin, C., Guo, J., Donati, Y., & Barazzone, C. (1998). TNF-induced enterocyte apoptosis in mice is mediated by the TNF receptor 1 and does not require p53. *Eur J Immunol*, 28(11), 3499-3505. doi:10.1002/(SICI)1521-4141(199811)28:11<3499::AID-IMMU3499>3.0.CO;2-Q
- Pinto, D., Gregorieff, A., Begthel, H., & Clevers, H. (2003). Canonical Wnt signals are essential for homeostasis of the intestinal epithelium. *Genes Dev*, 17(14), 1709-1713. doi:10.1101/gad.267103
- Piton, G., Manzon, C., Cypriani, B., Carbonnel, F., & Capellier, G. (2011). Acute intestinal failure in critically ill patients: is plasma citrulline the right marker? *Intensive Care Med*, 37(6), 911-917. doi:10.1007/s00134-011-2172-x
- Plevy, S. E., Landers, C. J., Prehn, J., Carramanzana, N. M., Deem, R. L., Shealy, D., & Targan, S. R. (1997). A role for TNF-alpha and mucosal T helper-1 cytokines in the pathogenesis of Crohn's disease. *J Immunol*, 159(12), 6276-6282.
- Plubell, D. L., Wilmarth, P. A., Zhao, Y., Fenton, A. M., Minnier, J., Reddy, A. P., . . . Pamir, N. (2017). Extended Multiplexing of Tandem Mass Tags (TMT) Labeling Reveals Age and High Fat Diet Specific Proteome Changes in Mouse Epididymal Adipose Tissue. *Mol Cell Proteomics*, 16(5), 873-890. doi:10.1074/mcp.M116.065524
- Portillo, J. A., Feliciano, L. M., Okenka, G., Heinzl, F., Subauste, M. C., & Subauste, C. S. (2012). CD40 and tumour necrosis factor-alpha co-operate to up-regulate inducible nitric oxide synthase expression in macrophages. *Immunology*, 135(2), 140-150. doi:10.1111/j.1365-2567.2011.03519.x

- Potten, C. S. (1977). Extreme sensitivity of some intestinal crypt cells to X and gamma irradiation. *Nature*, 269(5628), 518-521. doi:10.1038/269518a0
- Potten, C. S. (1990). A comprehensive study of the radiobiological response of the murine (BDF1) small intestine. *Int J Radiat Biol*, 58(6), 925-973. doi:10.1080/09553009014552281
- Potten, C. S., Gandara, R., Mahida, Y. R., Loeffler, M., & Wright, N. A. (2009). The stem cells of small intestinal crypts: where are they? *Cell Prolif*, 42(6), 731-750. doi:10.1111/j.1365-2184.2009.00642.x
- Potten, C. S., & Grant, H. K. (1998). The relationship between ionizing radiation-induced apoptosis and stem cells in the small and large intestine. *Br J Cancer*, 78(8), 993-1003. doi:10.1038/bjc.1998.618
- Potten, C. S., & Loeffler, M. (1990). Stem cells: attributes, cycles, spirals, pitfalls and uncertainties. Lessons for and from the crypt. *Development*, 110(4), 1001-1020.
- Potten, C. S., Wilson, J. W., & Booth, C. (1997). Regulation and significance of apoptosis in the stem cells of the gastrointestinal epithelium. *Stem Cells*, 15(2), 82-93. doi:10.1002/stem.150082
- Pourdast, A., Sanaei, M., Jafari, S., Mohammadi, M., Khalili, H., Shafiee, G., . . . Mohraz, M. (2017). Effect of Septimeb(TM) as a new natural extract on severe sepsis: A randomized clinical trial. *Caspian J Intern Med*, 8(1), 35-43.
- Pritchard, D. M., Watson, A. J., Potten, C. S., Jackman, A. L., & Hickman, J. A. (1997). Inhibition by uridine but not thymidine of p53-dependent intestinal apoptosis initiated by 5-fluorouracil: evidence for the involvement of RNA perturbation. *Proc Natl Acad Sci U S A*, 94(5), 1795-1799. doi:10.1073/pnas.94.5.1795
- Punchard, N. A., Greenfield, S. M., & Thompson, R. P. (1992). Mechanism of action of 5-aminosalicylic acid. *Mediators Inflamm*, 1(3), 151-165. doi:10.1155/S0962935192000243
- Qi, Z., & Chen, Y. G. (2015). Regulation of intestinal stem cell fate specification. *Sci China Life Sci*, 58(6), 570-578. doi:10.1007/s11427-015-4859-7
- Qin, C., Qiu, K., Sun, W., Jiao, N., Zhang, X., Che, L., . . . Yin, J. (2016). A proteomic adaptation of small intestinal mucosa in response to dietary protein limitation. *Sci Rep*, 6, 36888. doi:10.1038/srep36888
- Qiu, Z., He, Y., Ming, H., Lei, S., Leng, Y., & Xia, Z. Y. (2019). Lipopolysaccharide (LPS) Aggravates High Glucose- and Hypoxia/Reoxygenation-Induced Injury through Activating ROS-Dependent NLRP3 Inflammasome-Mediated Pyroptosis in H9C2 Cardiomyocytes. *J Diabetes Res*, 2019, 8151836. doi:10.1155/2019/8151836
- Qu, Y., Zhao, G., & Li, H. (2017). Forward and Reverse Signaling Mediated by Transmembrane Tumor Necrosis Factor-Alpha and TNF Receptor 2: Potential Roles in an Immunosuppressive Tumor Microenvironment. *Front Immunol*, 8, 1675. doi:10.3389/fimmu.2017.01675
- Quaglio, A. E., Castilho, A. C., & Di Stasi, L. C. (2015). Experimental evidence of heparanase, Hsp70 and NF-kappaB gene expression on the response of anti-inflammatory drugs in TNBS-induced colonic inflammation. *Life Sci*, 141, 179-187. doi:10.1016/j.lfs.2015.09.023
- Raffray, M., & Cohen, G. M. (1997). Apoptosis and necrosis in toxicology: a continuum or distinct modes of cell death? *Pharmacol Ther*, 75(3), 153-177. doi:10.1016/s0163-7258(97)00037-5
- Rakoff-Nahoum, S., Hao, L., & Medzhitov, R. (2006). Role of toll-like receptors in spontaneous commensal-dependent colitis. *Immunity*, 25(2), 319-329. doi:10.1016/j.immuni.2006.06.010
- Ranganathan, P., Weaver, K. L., & Capobianco, A. J. (2011). Notch signalling in solid tumours: a little bit of everything but not all the time. *Nat Rev Cancer*, 11(5), 338-351. doi:10.1038/nrc3035

- Rao, P., & Kadesch, T. (2003). The intracellular form of notch blocks transforming growth factor beta-mediated growth arrest in Mv1Lu epithelial cells. *Mol Cell Biol*, 23(18), 6694-6701. doi:10.1128/mcb.23.18.6694-6701.2003
- Raymond, S. L., Holden, D. C., Mira, J. C., Stortz, J. A., Loftus, T. J., Mohr, A. M., . . . Efron, P. A. (2017). Microbial recognition and danger signals in sepsis and trauma. *Biochim Biophys Acta Mol Basis Dis*, 1863(10 Pt B), 2564-2573. doi:10.1016/j.bbadis.2017.01.013
- Reed, J. C. (1999). Dysregulation of apoptosis in cancer. *J Clin Oncol*, 17(9), 2941-2953. doi:10.1200/JCO.1999.17.9.2941
- Rees, W. D., Stahl, M., Jacobson, K., Bressler, B., Sly, L. M., Vallance, B. A., & Steiner, T. S. (2020). Enteroids Derived From Inflammatory Bowel Disease Patients Display Dysregulated Endoplasmic Reticulum Stress Pathways, Leading to Differential Inflammatory Responses and Dendritic Cell Maturation. *J Crohns Colitis*, 14(7), 948-961. doi:10.1093/ecco-jcc/jjz194
- Reinecker, H. C., Steffen, M., Witthoef, T., Pflueger, I., Schreiber, S., MacDermott, R. P., & Raedler, A. (1993). Enhanced secretion of tumour necrosis factor-alpha, IL-6, and IL-1 beta by isolated lamina propria mononuclear cells from patients with ulcerative colitis and Crohn's disease. *Clin Exp Immunol*, 94(1), 174-181. doi:10.1111/j.1365-2249.1993.tb05997.x
- Reinhart, K., Daniels, R., Kisson, N., Machado, F. R., Schachter, R. D., & Finfer, S. (2017). Recognizing Sepsis as a Global Health Priority - A WHO Resolution. *N Engl J Med*, 377(5), 414-417. doi:10.1056/NEJMp1707170
- Reinisch, W., Gasche, C., Tillinger, W., Wyatt, J., Lichtenberger, C., Willheim, M., . . . Lochs, H. (1999). Clinical relevance of serum interleukin-6 in Crohn's disease: single point measurements, therapy monitoring, and prediction of clinical relapse. *Am J Gastroenterol*, 94(8), 2156-2164. doi:10.1111/j.1572-0241.1999.01288.x
- Rescigno, M., Urbano, M., Valzasina, B., Francolini, M., Rotta, G., Bonasio, R., . . . Ricciardi-Castagnoli, P. (2001). Dendritic cells express tight junction proteins and penetrate gut epithelial monolayers to sample bacteria. *Nat Immunol*, 2(4), 361-367. doi:10.1038/86373
- Ritsma, L., Ellenbroek, S. I. J., Zomer, A., Snippert, H. J., de Sauvage, F. J., Simons, B. D., . . . van Rheenen, J. (2014). Intestinal crypt homeostasis revealed at single-stem-cell level by in vivo live imaging. *Nature*, 507(7492), 362-365. doi:10.1038/nature12972
- Rizvi, M., Pathak, D., Freedman, J. E., & Chakrabarti, S. (2008). CD40-CD40 ligand interactions in oxidative stress, inflammation and vascular disease. *Trends Mol Med*, 14(12), 530-538. doi:10.1016/j.molmed.2008.09.006
- Roach, D. R., Briscoe, H., Saunders, B., France, M. P., Riminton, S., & Britton, W. J. (2001). Secreted lymphotoxin-alpha is essential for the control of an intracellular bacterial infection. *J Exp Med*, 193(2), 239-246. doi:10.1084/jem.193.2.239
- Rock, K. L., & Kono, H. (2008). The inflammatory response to cell death. *Annu Rev Pathol*, 3, 99-126. doi:10.1146/annurev.pathmechdis.3.121806.151456
- Russell, R. C., Tian, Y., Yuan, H., Park, H. W., Chang, Y. Y., Kim, J., . . . Guan, K. L. (2013). ULK1 induces autophagy by phosphorylating Beclin-1 and activating VPS34 lipid kinase. *Nat Cell Biol*, 15(7), 741-750. doi:10.1038/ncb2757
- Saelens, X., Festjens, N., Vande Walle, L., van Gurp, M., van Loo, G., & Vandenabeele, P. (2004). Toxic proteins released from mitochondria in cell death. *Oncogene*, 23(16), 2861-2874. doi:10.1038/sj.onc.1207523
- Saha, S., Jing, X., Park, S. Y., Wang, S., Li, X., Gupta, D., & Dziarski, R. (2010). Peptidoglycan recognition proteins protect mice from experimental colitis by promoting normal gut flora and preventing induction of interferon-gamma. *Cell Host Microbe*, 8(2), 147-162. doi:10.1016/j.chom.2010.07.005

- Saito, A., Suzuki, H. I., Horie, M., Ohshima, M., Morishita, Y., Abiko, Y., & Nagase, T. (2013). An integrated expression profiling reveals target genes of TGF-beta and TNF-alpha possibly mediated by microRNAs in lung cancer cells. *PLoS One*, *8*(2), e56587. doi:10.1371/journal.pone.0056587
- Sakai, J., & Akkoyunlu, M. (2017). The Role of BAFF System Molecules in Host Response to Pathogens. *Clin Microbiol Rev*, *30*(4), 991-1014. doi:10.1128/CMR.00046-17
- Salim, S. Y., & Soderholm, J. D. (2011). Importance of disrupted intestinal barrier in inflammatory bowel diseases. *Inflamm Bowel Dis*, *17*(1), 362-381. doi:10.1002/ibd.21403
- Sanz, A. B., Sanchez-Nino, M. D., Ramos, A. M., Moreno, J. A., Santamaria, B., Ruiz-Ortega, M., . . . Ortiz, A. (2010). NF-kappaB in renal inflammation. *J Am Soc Nephrol*, *21*(8), 1254-1262. doi:10.1681/ASN.2010020218
- Sartor, R. B. (2004). Therapeutic manipulation of the enteric microflora in inflammatory bowel diseases: antibiotics, probiotics, and prebiotics. *Gastroenterology*, *126*(6), 1620-1633. doi:10.1053/j.gastro.2004.03.024
- Sasaki, N., Sachs, N., Wiebrands, K., Ellenbroek, S. I., Fumagalli, A., Lyubimova, A., . . . Clevers, H. (2016). Reg4+ deep crypt secretory cells function as epithelial niche for Lgr5+ stem cells in colon. *Proc Natl Acad Sci U S A*, *113*(37), E5399-5407. doi:10.1073/pnas.1607327113
- Sathawane, D., Kharat, R. S., Halder, S., Roy, S., Swami, R., Patel, R., & Saha, B. (2013). Monocyte CD40 expression in head and neck squamous cell carcinoma (HNSCC). *Hum Immunol*, *74*(1), 1-5. doi:10.1016/j.humimm.2012.09.004
- Sato, T., & Clevers, H. (2013). Growing self-organizing mini-guts from a single intestinal stem cell: mechanism and applications. *Science*, *340*(6137), 1190-1194. doi:10.1126/science.1234852
- Sato, T., Stange, D. E., Ferrante, M., Vries, R. G., Van Es, J. H., Van den Brink, S., . . . Clevers, H. (2011). Long-term expansion of epithelial organoids from human colon, adenoma, adenocarcinoma, and Barrett's epithelium. *Gastroenterology*, *141*(5), 1762-1772. doi:10.1053/j.gastro.2011.07.050
- Sato, T., Vries, R. G., Snippert, H. J., van de Wetering, M., Barker, N., Stange, D. E., . . . Clevers, H. (2009). Single Lgr5 stem cells build crypt-villus structures in vitro without a mesenchymal niche. *Nature*, *459*(7244), 262-265. doi:10.1038/nature07935
- Say, L., Chou, D., Gemmill, A., Tuncalp, O., Moller, A. B., Daniels, J., . . . Alkema, L. (2014). Global causes of maternal death: a WHO systematic analysis. *Lancet Glob Health*, *2*(6), e323-333. doi:10.1016/S2214-109X(14)70227-X
- Schaumann, R., Schlick, T., Schaper, M., & Shah, P. M. (1997). Is TNF-alpha a prognostic factor in patients with sepsis? *Clin Microbiol Infect*, *3*(1), 24-31. doi:10.1111/j.1469-0691.1997.tb00247.x
- Schepers, A. G., Vries, R., van den Born, M., van de Wetering, M., & Clevers, H. (2011). Lgr5 intestinal stem cells have high telomerase activity and randomly segregate their chromosomes. *EMBO J*, *30*(6), 1104-1109. doi:10.1038/emboj.2011.26
- Schijvens, A. M., Ter Heine, R., de Wildt, S. N., & Schreuder, M. F. (2019). Pharmacology and pharmacogenetics of prednisone and prednisolone in patients with nephrotic syndrome. *Pediatr Nephrol*, *34*(3), 389-403. doi:10.1007/s00467-018-3929-z
- Schmid-Schonbein, G. W., Penn, A., & Kistler, E. (2011). The Autodigestion Hypothesis in Shock and Multi-Organ Failure: Degrading Protease Activity. *Bol Soc Port Hemorreol Microcirc*, *26*(3), 6-15.
- Schmitz, H., Fromm, M., Bode, H., Scholz, P., Riecken, E. O., & Schulzke, J. D. (1996). Tumor necrosis factor-alpha induces Cl- and K+ secretion in human

- distal colon driven by prostaglandin E2. *Am J Physiol*, 271(4 Pt 1), G669-674. doi:10.1152/ajpgi.1996.271.4.G669
- Schneeberger, E. E., & Lynch, R. D. (2004). The tight junction: a multifunctional complex. *Am J Physiol Cell Physiol*, 286(6), C1213-1228. doi:10.1152/ajpcell.00558.2003
- Schneider, P., MacKay, F., Steiner, V., Hofmann, K., Bodmer, J. L., Holler, N., . . . Tschopp, J. (1999). BAFF, a novel ligand of the tumor necrosis factor family, stimulates B cell growth. *J Exp Med*, 189(11), 1747-1756. doi:10.1084/jem.189.11.1747
- Schonbeck, U., & Libby, P. (2001). The CD40/CD154 receptor/ligand dyad. *Cell Mol Life Sci*, 58(1), 4-43. doi:10.1007/pl00000776
- Schonbeck, U., & Libby, P. (2001). The CD40/CD154 receptor/ligand dyad. *Cell Mol Life Sci*, 58(1), 4-43. doi:10.1007/pl00000776
- Schreiber, S., Nikolaus, S., & Hampe, J. (1998). Activation of nuclear factor kappa B inflammatory bowel disease. *Gut*, 42(4), 477-484. doi:10.1136/gut.42.4.477
- Schulte, G., & Bryja, V. (2007). The Frizzled family of unconventional G-protein-coupled receptors. *Trends Pharmacol Sci*, 28(10), 518-525. doi:10.1016/j.tips.2007.09.001
- Schulzke, J. D., Ploeger, S., Amasheh, M., Fromm, A., Zeissig, S., Troeger, H., . . . Fromm, M. (2009). Epithelial tight junctions in intestinal inflammation. *Ann N Y Acad Sci*, 1165, 294-300. doi:10.1111/j.1749-6632.2009.04062.x
- Schwartz, N., Rubinstein, T., Burkly, L. C., Collins, C. E., Blanco, I., Su, L., . . . Putterman, C. (2009). Urinary TWEAK as a biomarker of lupus nephritis: a multicenter cohort study. *Arthritis Res Ther*, 11(5), R143. doi:10.1186/ar2816
- Schwarz, B. T., Wang, F., Shen, L., Clayburgh, D. R., Su, L., Wang, Y., . . . Turner, J. R. (2007). LIGHT signals directly to intestinal epithelia to cause barrier dysfunction via cytoskeletal and endocytic mechanisms. *Gastroenterology*, 132(7), 2383-2394. doi:10.1053/j.gastro.2007.02.052
- Sellon, R. K., Tonkonogy, S., Schultz, M., Dieleman, L. A., Grenther, W., Balish, E., . . . Sartor, R. B. (1998). Resident enteric bacteria are necessary for development of spontaneous colitis and immune system activation in interleukin-10-deficient mice. *Infect Immun*, 66(11), 5224-5231. doi:10.1128/IAI.66.11.5224-5231.1998
- Sen, R., & Baltimore, D. (1986). Multiple nuclear factors interact with the immunoglobulin enhancer sequences. *Cell*, 46(5), 705-716. doi:10.1016/0092-8674(86)90346-6
- Serramito-Gomez, I., Boada-Romero, E., Slowicka, K., Vereecke, L., Van Loo, G., & Pimentel-Muinos, F. X. (2019). The anti-inflammatory protein TNFAIP3/A20 binds the WD40 domain of ATG16L1 to control the autophagic response, NFkB/NF-kappaB activation and intestinal homeostasis. *Autophagy*, 15(9), 1657-1659. doi:10.1080/15548627.2019.1628549
- Sha, T., Iizawa, Y., & Li, M. (2011). Combination of imipenem and TAK-242, a Toll-like receptor 4 signal transduction inhibitor, improves survival in a murine model of polymicrobial sepsis. *Shock*, 35(2), 205-209. doi:10.1097/SHK.0b013e3181f48942
- Sha, W. C., Liou, H. C., Tuomanen, E. I., & Baltimore, D. (1995). Targeted disruption of the p50 subunit of NF-kappa B leads to multifocal defects in immune responses. *Cell*, 80(2), 321-330. doi:10.1016/0092-8674(95)90415-8
- Shao, L., Oshima, S., Duong, B., Advincula, R., Barrera, J., Malynn, B. A., & Ma, A. (2013). A20 restricts wnt signaling in intestinal epithelial cells and

- suppresses colon carcinogenesis. *PLoS One*, 8(5), e62223. doi:10.1371/journal.pone.0062223
- Shao, Y., Chen, F., Chen, Y., Zhang, W., Lin, Y., Cai, Y., . . . Cui, L. (2017). Association between genetic polymorphisms in the autophagy-related 5 gene promoter and the risk of sepsis. *Sci Rep*, 7(1), 9399. doi:10.1038/s41598-017-09978-5
- Sharma, N. K., & Salomao, R. (2017). Sepsis Through the Eyes of Proteomics: The Progress in the Last Decade. *Shock*, 47(1S Suppl 1), 17-25. doi:10.1097/SHK.0000000000000698
- Sharma, V. M., Draheim, K. M., & Kelliher, M. A. (2007). The Notch1/c-Myc pathway in T cell leukemia. *Cell Cycle*, 6(8), 927-930. doi:10.4161/cc.6.8.4134
- Sheehan, M., Wong, H. R., Hake, P. W., & Zingarelli, B. (2003). Parthenolide improves systemic hemodynamics and decreases tissue leukosequestration in rats with polymicrobial sepsis. *Crit Care Med*, 31(9), 2263-2270. doi:10.1097/01.CCM.0000085186.14867.F7
- Shen, L., Weber, C. R., & Turner, J. R. (2008). The tight junction protein complex undergoes rapid and continuous molecular remodeling at steady state. *J Cell Biol*, 181(4), 683-695. doi:10.1083/jcb.200711165
- Shen, M., Zhou, L., Zhou, P., Zhou, W., & Lin, X. (2017). Lymphotoxin beta receptor activation promotes mRNA expression of RelA and pro-inflammatory cytokines TNFalpha and IL-1beta in bladder cancer cells. *Mol Med Rep*, 16(1), 937-942. doi:10.3892/mmr.2017.6676
- Shen, X. F., Cao, K., Jiang, J. P., Guan, W. X., & Du, J. F. (2017). Neutrophil dysregulation during sepsis: an overview and update. *J Cell Mol Med*, 21(9), 1687-1697. doi:10.1111/jcmm.13112
- Shiels, H., Li, X., Schumacker, P. T., Maltepe, E., Padrid, P. A., Sperling, A., . . . Lindsten, T. (2000). TRAF4 deficiency leads to tracheal malformation with resulting alterations in air flow to the lungs. *Am J Pathol*, 157(2), 679-688. doi:10.1016/S0002-9440(10)64578-6
- Shifrin, D. A., Jr., McConnell, R. E., Nambiar, R., Higginbotham, J. N., Coffey, R. J., & Tyska, M. J. (2012). Enterocyte microvillus-derived vesicles detoxify bacterial products and regulate epithelial-microbial interactions. *Curr Biol*, 22(7), 627-631. doi:10.1016/j.cub.2012.02.022
- Shin, J. H., & Seeley, R. J. (2019). Reg3 Proteins as Gut Hormones? *Endocrinology*, 160(6), 1506-1514. doi:10.1210/en.2019-00073
- Shinoda, T., Shinya, N., Ito, K., Ohsawa, N., Terada, T., Hirata, K., . . . Shirouzu, M. (2016). Structural basis for disruption of claudin assembly in tight junctions by an enterotoxin. *Sci Rep*, 6, 33632. doi:10.1038/srep33632
- Shirey, K. A., Lai, W., Scott, A. J., Lipsky, M., Mistry, P., Pletneva, L. M., . . . Vogel, S. N. (2013). The TLR4 antagonist Eritoran protects mice from lethal influenza infection. *Nature*, 497(7450), 498-502. doi:10.1038/nature12118
- Shukla, P., Rao, G. M., Pandey, G., Sharma, S., Mittapelly, N., Shegokar, R., & Mishra, P. R. (2014). Therapeutic interventions in sepsis: current and anticipated pharmacological agents. *Br J Pharmacol*, 171(22), 5011-5031. doi:10.1111/bph.12829
- Siddiqui, A. M., Cui, X., Wu, R., Dong, W., Zhou, M., Hu, M., . . . Wang, P. (2006). The anti-inflammatory effect of curcumin in an experimental model of sepsis is mediated by up-regulation of peroxisome proliferator-activated receptor-gamma. *Crit Care Med*, 34(7), 1874-1882. doi:10.1097/01.CCM.0000221921.71300.BF
- Siegel, R. M., Chan, F. K., Chun, H. J., & Lenardo, M. J. (2000). The multifaceted role of Fas signaling in immune cell homeostasis and autoimmunity. *Nat Immunol*, 1(6), 469-474. doi:10.1038/82712

- Silva, A. T., Bayston, K. F., & Cohen, J. (1990). Prophylactic and therapeutic effects of a monoclonal antibody to tumor necrosis factor-alpha in experimental gram-negative shock. *J Infect Dis*, *162*(2), 421-427. doi:10.1093/infdis/162.2.421
- Silva, L. S., Catalao, C. H., Felippotti, T. T., Oliveira-Pelegrin, G. R., Petenusci, S., de Freitas, L. A., & Rocha, M. J. (2017). Curcumin suppresses inflammatory cytokines and heat shock protein 70 release and improves metabolic parameters during experimental sepsis. *Pharm Biol*, *55*(1), 269-276. doi:10.1080/13880209.2016.1260598
- Singer, M., Deutschman, C. S., Seymour, C. W., Shankar-Hari, M., Annane, D., Bauer, M., . . . Angus, D. C. (2016). The Third International Consensus Definitions for Sepsis and Septic Shock (Sepsis-3). *JAMA*, *315*(8), 801-810. doi:10.1001/jama.2016.0287
- Sinnatamby, C. S., & Last, R. J. (2011). *Last's anatomy : regional and applied* (12th ed.). Edinburgh ; New York: Churchill Livingstone/Elsevier.
- Slee, E. A., Adrain, C., & Martin, S. J. (2001). Executioner caspase-3, -6, and -7 perform distinct, non-redundant roles during the demolition phase of apoptosis. *J Biol Chem*, *276*(10), 7320-7326. doi:10.1074/jbc.M008363200
- Slusarski, D. C., Yang-Snyder, J., Busa, W. B., & Moon, R. T. (1997). Modulation of embryonic intracellular Ca²⁺ signaling by Wnt-5A. *Dev Biol*, *182*(1), 114-120. doi:10.1006/dbio.1996.8463
- Smulski, C. R., Decossas, M., Chekkat, N., Beyrath, J., Willen, L., Guichard, G., . . . Fournel, S. (2017). Hetero-oligomerization between the TNF receptor superfamily members CD40, Fas and TRAILR2 modulate CD40 signalling. *Cell Death Dis*, *8*(2), e2601. doi:10.1038/cddis.2017.22
- Snoeck, V., Goddeeris, B., & Cox, E. (2005). The role of enterocytes in the intestinal barrier function and antigen uptake. *Microbes Infect*, *7*(7-8), 997-1004. doi:10.1016/j.micinf.2005.04.003
- Sohma, M. (1983). Ultrastructure of the absorptive cells in the small intestine of the rat during starvation. *Anat Embryol (Berl)*, *168*(3), 331-339. doi:10.1007/BF00304271
- Son, A., Oshio, T., Kawamura, Y. I., Hagiwara, T., Yamazaki, M., Inagaki-Ohara, K., . . . Dohi, T. (2013). TWEAK/Fn14 pathway promotes a T helper 2-type chronic colitis with fibrosis in mice. *Mucosal Immunol*, *6*(6), 1131-1142. doi:10.1038/mi.2013.10
- Song, D., Zong, X., Zhang, H., Wang, T., Yi, H., Luan, C., & Wang, Y. (2015). Antimicrobial peptide Cathelicidin-BF prevents intestinal barrier dysfunction in a mouse model of endotoxemia. *Int Immunopharmacol*, *25*(1), 141-147. doi:10.1016/j.intimp.2015.01.017
- Song, W. B., Wang, Y. Y., Meng, F. S., Zhang, Q. H., Zeng, J. Y., Xiao, L. P., . . . Zhang, Z. S. (2010). Curcumin protects intestinal mucosal barrier function of rat enteritis via activation of MKP-1 and attenuation of p38 and NF-kappaB activation. *PLoS One*, *5*(9), e12969. doi:10.1371/journal.pone.0012969
- Sotillo, J., Ferreira, I., Potriquet, J., Laha, T., Navarro, S., Loukas, A., & Mulvenna, J. (2017). Changes in protein expression after treatment with *Ancylostoma caninum* excretory/secretory products in a mouse model of colitis. *Sci Rep*, *7*, 41883. doi:10.1038/srep41883
- Specian, R. D., & Neutra, M. R. (1980). Mechanism of rapid mucus secretion in goblet cells stimulated by acetylcholine. *J Cell Biol*, *85*(3), 626-640. doi:10.1083/jcb.85.3.626
- Spit, M., Koo, B. K., & Maurice, M. M. (2018). Tales from the crypt: intestinal niche signals in tissue renewal, plasticity and cancer. *Open Biol*, *8*(9). doi:10.1098/rsob.180120

- Spooner, C. E., Markowitz, N. P., & Saravolatz, L. D. (1992). The role of tumor necrosis factor in sepsis. *Clin Immunol Immunopathol*, 62(1 Pt 2), S11-17. doi:10.1016/0090-1229(92)90036-n
- Srinivasula, S. M., Ahmad, M., Fernandes-Alnemri, T., Litwack, G., & Alnemri, E. S. (1996). Molecular ordering of the Fas-apoptotic pathway: the Fas/APO-1 protease Mch5 is a CrmA-inhibitable protease that activates multiple Ced-3/ICE-like cysteine proteases. *Proc Natl Acad Sci U S A*, 93(25), 14486-14491. doi:10.1073/pnas.93.25.14486
- Stadnyk, A. W. (2002). Intestinal epithelial cells as a source of inflammatory cytokines and chemokines. *Can J Gastroenterol*, 16(4), 241-246. doi:10.1155/2002/941087
- Starr, A. E., Deeke, S. A., Ning, Z., Chiang, C. K., Zhang, X., Mottawea, W., . . . Figeys, D. (2017). Proteomic analysis of ascending colon biopsies from a paediatric inflammatory bowel disease inception cohort identifies protein biomarkers that differentiate Crohn's disease from UC. *Gut*, 66(9), 1573-1583. doi:10.1136/gutjnl-2015-310705
- Stelzner, M., Helmrich, M., Dunn, J. C., Henning, S. J., Houchen, C. W., Kuo, C., . . . Consortium, N. I. H. I. S. C. (2012). A nomenclature for intestinal in vitro cultures. *Am J Physiol Gastrointest Liver Physiol*, 302(12), G1359-1363. doi:10.1152/ajpgi.00493.2011
- Steri, M., Orru, V., Idda, M. L., Pitzalis, M., Pala, M., Zara, I., . . . Cucca, F. (2017). Overexpression of the Cytokine BAFF and Autoimmunity Risk. *N Engl J Med*, 376(17), 1615-1626. doi:10.1056/NEJMoa1610528
- Stuber, E., Strober, W., & Neurath, M. (1996). Blocking the CD40L-CD40 interaction in vivo specifically prevents the priming of T helper 1 cells through the inhibition of interleukin 12 secretion. *J Exp Med*, 183(2), 693-698. doi:10.1084/jem.183.2.693
- Sun, S. C. (2011). Non-canonical NF-kappaB signaling pathway. *Cell Res*, 21(1), 71-85. doi:10.1038/cr.2010.177
- Susin, S. A., Daugas, E., Ravagnan, L., Samejima, K., Zamzami, N., Loeffler, M., . . . Kroemer, G. (2000). Two distinct pathways leading to nuclear apoptosis. *J Exp Med*, 192(4), 571-580. doi:10.1084/jem.192.4.571
- Suzuki, Y., Imai, Y., Nakayama, H., Takahashi, K., Takio, K., & Takahashi, R. (2001). A serine protease, HtrA2, is released from the mitochondria and interacts with XIAP, inducing cell death. *Mol Cell*, 8(3), 613-621. doi:10.1016/s1097-2765(01)00341-0
- Swardfager, W., Lanctot, K., Rothenburg, L., Wong, A., Cappell, J., & Herrmann, N. (2010). A meta-analysis of cytokines in Alzheimer's disease. *Biol Psychiatry*, 68(10), 930-941. doi:10.1016/j.biopsych.2010.06.012
- Tait, S. W., & Green, D. R. (2008). Caspase-independent cell death: leaving the set without the final cut. *Oncogene*, 27(50), 6452-6461. doi:10.1038/onc.2008.311
- Tak, P. P., & Firestein, G. S. (2001). NF-kappaB: a key role in inflammatory diseases. *J Clin Invest*, 107(1), 7-11. doi:10.1172/JCI11830
- Takeuchi, O., & Akira, S. (2010). Pattern recognition receptors and inflammation. *Cell*, 140(6), 805-820. doi:10.1016/j.cell.2010.01.022
- Tamada, K., Shimozaki, K., Chapoval, A. I., Zhu, G., Sica, G., Flies, D., . . . Chen, L. (2000). Modulation of T-cell-mediated immunity in tumor and graft-versus-host disease models through the LIGHT co-stimulatory pathway. *Nat Med*, 6(3), 283-289. doi:10.1038/73136
- Tamura, A., Kitano, Y., Hata, M., Katsuno, T., Moriwaki, K., Sasaki, H., . . . Tsukita, S. (2008). Megaintestine in claudin-15-deficient mice. *Gastroenterology*, 134(2), 523-534. doi:10.1053/j.gastro.2007.11.040
- Tanaka, H., Takechi, M., Kiyonari, H., Shioi, G., Tamura, A., & Tsukita, S. (2015). Intestinal deletion of Claudin-7 enhances paracellular organic solute flux and

- initiates colonic inflammation in mice. *Gut*, *64*(10), 1529-1538. doi:10.1136/gutjnl-2014-308419
- Tanaka, T., Narazaki, M., & Kishimoto, T. (2014). IL-6 in inflammation, immunity, and disease. *Cold Spring Harb Perspect Biol*, *6*(10), a016295. doi:10.1101/cshperspect.a016295
- Tang, B., Zhong, Z., Qiu, Z., Wu, H. P., Hu, J. Y., Ma, J. P., & Wu, J. P. (2019). Serum soluble TWEAK levels in severe traumatic brain injury and its prognostic significance. *Clin Chim Acta*, *495*, 227-232. doi:10.1016/j.cca.2019.04.070
- Tang, J., Chen, X., Tu, W., Guo, Y., Zhao, Z., Xue, Q., . . . Liu, Y. (2011). Propofol inhibits the activation of p38 through up-regulating the expression of annexin A1 to exert its anti-inflammation effect. *PLoS One*, *6*(12), e27890. doi:10.1371/journal.pone.0027890
- Targan, S. R., Hanauer, S. B., van Deventer, S. J., Mayer, L., Present, D. H., Braakman, T., . . . Rutgeerts, P. J. (1997). A short-term study of chimeric monoclonal antibody cA2 to tumor necrosis factor alpha for Crohn's disease. Crohn's Disease cA2 Study Group. *N Engl J Med*, *337*(15), 1029-1035. doi:10.1056/NEJM199710093371502
- Taupin, D., & Podolsky, D. K. (2003). Trefoil factors: initiators of mucosal healing. *Nat Rev Mol Cell Biol*, *4*(9), 721-732. doi:10.1038/nrm1203
- Tetikcok, R., Kayaoglu, H. A., Ozsoy, Z., Yenidogan, E., Ozkan, N., Celik, A., . . . Ersoy, O. F. (2016). The Effect of Peritoneal Prednisolone Lavage in Bacterial Peritonitis: An Experimental Study. *Wounds*, *28*(10), 354-359.
- Theiss, A. L., Simmons, J. G., Jobin, C., & Lund, P. K. (2005). Tumor necrosis factor (TNF) alpha increases collagen accumulation and proliferation in intestinal myofibroblasts via TNF receptor 2. *J Biol Chem*, *280*(43), 36099-36109. doi:10.1074/jbc.M505291200
- Thuny, F., Textoris, J., Amara, A. B., Filali, A. E., Capo, C., Habib, G., . . . Mege, J. L. (2012). The gene expression analysis of blood reveals S100A11 and AQP9 as potential biomarkers of infective endocarditis. *PLoS One*, *7*(2), e31490. doi:10.1371/journal.pone.0031490
- Tickenbrock, L., Muller-Tidow, C., Berdel, W. E., & Serve, H. (2006). Emerging Flt3 kinase inhibitors in the treatment of leukaemia. *Expert Opin Emerg Drugs*, *11*(1), 153-165. doi:10.1517/14728214.11.1.153
- Tipsmark, C. K., Kiilerich, P., Nilsen, T. O., Ebbesson, L. O., Stefansson, S. O., & Madsen, S. S. (2008). Branchial expression patterns of claudin isoforms in Atlantic salmon during seawater acclimation and smoltification. *Am J Physiol Regul Integr Comp Physiol*, *294*(5), R1563-1574. doi:10.1152/ajpregu.00915.2007
- Toden, S., Theiss, A. L., Wang, X., & Goel, A. (2017). Essential turmeric oils enhance anti-inflammatory efficacy of curcumin in dextran sulfate sodium-induced colitis. *Sci Rep*, *7*(1), 814. doi:10.1038/s41598-017-00812-6
- Tracey, K. J., Fong, Y., Hesse, D. G., Manogue, K. R., Lee, A. T., Kuo, G. C., . . . Cerami, A. (1987). Anti-cachectin/TNF monoclonal antibodies prevent septic shock during lethal bacteraemia. *Nature*, *330*(6149), 662-664. doi:10.1038/330662a0
- Tran, N. L., McDonough, W. S., Donohue, P. J., Winkles, J. A., Berens, T. J., Ross, K. R., . . . Berens, M. E. (2003). The human Fn14 receptor gene is up-regulated in migrating glioma cells in vitro and overexpressed in advanced glial tumors. *Am J Pathol*, *162*(4), 1313-1321. doi:10.1016/S0002-9440(10)63927-2
- Trevaskis, N. L., Kaminskis, L. M., & Porter, C. J. (2015). From sewer to saviour - targeting the lymphatic system to promote drug exposure and activity. *Nat Rev Drug Discov*, *14*(11), 781-803. doi:10.1038/nrd4608

- Tsertsvadze, A., Royle, P., & McCarthy, N. (2015). Community-onset sepsis and its public health burden: protocol of a systematic review. *Syst Rev*, 4, 119. doi:10.1186/s13643-015-0103-6
- Tsukita, S., Yamazaki, Y., Katsuno, T., Tamura, A., & Tsukita, S. (2008). Tight junction-based epithelial microenvironment and cell proliferation. *Oncogene*, 27(55), 6930-6938. doi:10.1038/onc.2008.344
- Tumanov, A. V., Koroleva, E. P., Guo, X., Wang, Y., Kruglov, A., Nedospasov, S., & Fu, Y. X. (2011). Lymphotoxin controls the IL-22 protection pathway in gut innate lymphoid cells during mucosal pathogen challenge. *Cell Host Microbe*, 10(1), 44-53. doi:10.1016/j.chom.2011.06.002
- Turnbaugh, P. J., Ley, R. E., Hamady, M., Fraser-Liggett, C. M., Knight, R., & Gordon, J. I. (2007). The human microbiome project. *Nature*, 449(7164), 804-810. doi:10.1038/nature06244
- Turner, J. R. (2009). Intestinal mucosal barrier function in health and disease. *Nat Rev Immunol*, 9(11), 799-809. doi:10.1038/nri2653
- Uchiyama, K., Naito, Y., Takagi, T., Mizushima, K., Hirai, Y., Hayashi, N., . . . Yoshikawa, T. (2012). Serpin B1 protects colonic epithelial cell via blockage of neutrophil elastase activity and its expression is enhanced in patients with ulcerative colitis. *Am J Physiol Gastrointest Liver Physiol*, 302(10), G1163-1170. doi:10.1152/ajpgi.00292.2011
- Uhlig, H. H. (2013). Monogenic diseases associated with intestinal inflammation: implications for the understanding of inflammatory bowel disease. *Gut*, 62(12), 1795-1805. doi:10.1136/gutjnl-2012-303956
- Ulluwishewa, D., Anderson, R. C., McNabb, W. C., Moughan, P. J., Wells, J. M., & Roy, N. C. (2011). Regulation of tight junction permeability by intestinal bacteria and dietary components. *J Nutr*, 141(5), 769-776. doi:10.3945/jn.110.135657
- Upadhyay, V., & Fu, Y. X. (2013). Lymphotoxin signalling in immune homeostasis and the control of microorganisms. *Nat Rev Immunol*, 13(4), 270-279. doi:10.1038/nri3406
- van Amerongen, R., Fuerer, C., Mizutani, M., & Nusse, R. (2012). Wnt5a can both activate and repress Wnt/beta-catenin signaling during mouse embryonic development. *Dev Biol*, 369(1), 101-114. doi:10.1016/j.ydbio.2012.06.020
- van der Bruggen, T., Nijenhuis, S., van Raaij, E., Verhoef, J., & van Asbeck, B. S. (1999). Lipopolysaccharide-induced tumor necrosis factor alpha production by human monocytes involves the raf-1/MEK1-MEK2/ERK1-ERK2 pathway. *Infect Immun*, 67(8), 3824-3829. doi:10.1128/IAI.67.8.3824-3829.1999
- van der Meulen, T., Donaldson, C. J., Caceres, E., Hunter, A. E., Cowing-Zitron, C., Pound, L. D., . . . Huising, M. O. (2015). Urocortin3 mediates somatostatin-dependent negative feedback control of insulin secretion. *Nat Med*, 21(7), 769-776. doi:10.1038/nm.3872
- van Es, J. H., & Clevers, H. (2005). Notch and Wnt inhibitors as potential new drugs for intestinal neoplastic disease. *Trends Mol Med*, 11(11), 496-502. doi:10.1016/j.molmed.2005.09.008
- van Gent, D., Sharp, P., Morgan, K., & Kalsheker, N. (2003). Serpins: structure, function and molecular evolution. *Int J Biochem Cell Biol*, 35(11), 1536-1547. doi:10.1016/s1357-2725(03)00134-1
- van Kooten, C., & Banchereau, J. (2000). CD40-CD40 ligand. *J Leukoc Biol*, 67(1), 2-17. doi:10.1002/jlb.67.1.2
- van Kuijk, A. W., Wijbrandts, C. A., Vinkenoog, M., Zheng, T. S., Reedquist, K. A., & Tak, P. P. (2010). TWEAK and its receptor Fn14 in the synovium of patients with rheumatoid arthritis compared to psoriatic arthritis and its response to tumour necrosis factor blockade. *Ann Rheum Dis*, 69(1), 301-304. doi:10.1136/ard.2008.090548

- Vanden Berghe, T., Linkermann, A., Jouan-Lanhouet, S., Walczak, H., & Vandenabeele, P. (2014). Regulated necrosis: the expanding network of non-apoptotic cell death pathways. *Nat Rev Mol Cell Biol*, *15*(2), 135-147. doi:10.1038/nrm3737
- Vane, J. R., Botting, J. H., & Botting, R. M. (1996). *Improved non-steroid anti-inflammatory drugs COX-2 enzyme inhibitors : proceedings of a conference held on October 10-11, 1995, at Regent's College, London*. Dordrecht ; Boston: Kluwer Academic Publishers.
- Vazquez-Frias, R., Gutierrez-Reyes, G., Urban-Reyes, M., Velazquez-Guadarrama, N., Fortoul-van der Goes, T. I., Reyes-Lopez, A., & Consuelo-Sanchez, A. (2015). Proinflammatory and anti-inflammatory cytokine profile in pediatric patients with irritable bowel syndrome. *Rev Gastroenterol Mex*, *80*(1), 6-12. doi:10.1016/j.rgmx.2014.11.001
- Venet, F., & Monneret, G. (2018). Advances in the understanding and treatment of sepsis-induced immunosuppression. *Nat Rev Nephrol*, *14*(2), 121-137. doi:10.1038/nrneph.2017.165
- Ventham, N. T., Kennedy, N. A., Nimmo, E. R., & Satsangi, J. (2013). Beyond gene discovery in inflammatory bowel disease: the emerging role of epigenetics. *Gastroenterology*, *145*(2), 293-308. doi:10.1053/j.gastro.2013.05.050
- Verhagen, A. M., Ekert, P. G., Pakusch, M., Silke, J., Connolly, L. M., Reid, G. E., . . . Vaux, D. L. (2000). Identification of DIABLO, a mammalian protein that promotes apoptosis by binding to and antagonizing IAP proteins. *Cell*, *102*(1), 43-53. doi:10.1016/s0092-8674(00)00009-x
- Verhelst, K., Gardam, S., Borghi, A., Kreike, M., Carpentier, I., & Beyaert, R. (2015). XEDAR activates the non-canonical NF-kappaB pathway. *Biochem Biophys Res Commun*, *465*(2), 275-280. doi:10.1016/j.bbrc.2015.08.019
- Verma, I. M. (2004). Nuclear factor (NF)-kappaB proteins: therapeutic targets. *Ann Rheum Dis*, *63 Suppl 2*, ii57-ii61. doi:10.1136/ard.2004.028266
- Victor, F. C., & Gottlieb, A. B. (2002). TNF-alpha and apoptosis: implications for the pathogenesis and treatment of psoriasis. *J Drugs Dermatol*, *1*(3), 264-275.
- Vincent, F. B., Saulep-Easton, D., Figgett, W. A., Fairfax, K. A., & Mackay, F. (2013). The BAFF/APRIL system: emerging functions beyond B cell biology and autoimmunity. *Cytokine Growth Factor Rev*, *24*(3), 203-215. doi:10.1016/j.cytogfr.2013.04.003
- Vit, O., & Petrak, J. (2017). Integral membrane proteins in proteomics. How to break open the black box? *J Proteomics*, *153*, 8-20. doi:10.1016/j.jprot.2016.08.006
- Vlantis, K., Wullaert, A., Polykratis, A., Kondylis, V., Dannappel, M., Schwarzer, R., . . . Pasparakis, M. (2016). NEMO Prevents RIP Kinase 1-Mediated Epithelial Cell Death and Chronic Intestinal Inflammation by NF-kappaB-Dependent and -Independent Functions. *Immunity*, *44*(3), 553-567. doi:10.1016/j.immuni.2016.02.020
- Waage, A., Halstensen, A., & Espevik, T. (1987). Association between tumour necrosis factor in serum and fatal outcome in patients with meningococcal disease. *Lancet*, *1*(8529), 355-357. doi:10.1016/s0140-6736(87)91728-4
- Wallach, T. E., & Bayrer, J. R. (2017). Intestinal Organoids: New Frontiers in the Study of Intestinal Disease and Physiology. *J Pediatr Gastroenterol Nutr*, *64*(2), 180-185. doi:10.1097/MPG.0000000000001411
- Wallin, E., & von Heijne, G. (1998). Genome-wide analysis of integral membrane proteins from eubacterial, archaean, and eukaryotic organisms. *Protein Sci*, *7*(4), 1029-1038. doi:10.1002/pro.5560070420
- Wan, F., & Lenardo, M. J. (2009). Specification of DNA binding activity of NF-kappaB proteins. *Cold Spring Harb Perspect Biol*, *1*(4), a000067. doi:10.1101/cshperspect.a000067

- Wang, F., Graham, W. V., Wang, Y., Witkowski, E. D., Schwarz, B. T., & Turner, J. R. (2005). Interferon-gamma and tumor necrosis factor-alpha synergize to induce intestinal epithelial barrier dysfunction by up-regulating myosin light chain kinase expression. *Am J Pathol*, *166*(2), 409-419. doi:10.1016/s0002-9440(10)62264-x
- Wang, L., Bastarache, J. A., & Ware, L. B. (2008). The coagulation cascade in sepsis. *Curr Pharm Des*, *14*(19), 1860-1869. doi:10.2174/138161208784980581
- Wang, M. J., Yang, H. Y., Zhang, H., Zhou, X., Liu, R. P., & Mi, Y. Y. (2016). TNFAIP3 gene rs10499194, rs13207033 polymorphisms decrease the risk of rheumatoid arthritis. *Oncotarget*, *7*(50), 82933-82942. doi:10.18632/oncotarget.12638
- Wang, X., & Lin, Y. (2008). Tumor necrosis factor and cancer, buddies or foes? *Acta Pharmacol Sin*, *29*(11), 1275-1288. doi:10.1111/j.1745-7254.2008.00889.x
- Wang, Y., Koroleva, E. P., Kruglov, A. A., Kuprash, D. V., Nedospasov, S. A., Fu, Y. X., & Tumanov, A. V. (2010). Lymphotoxin beta receptor signaling in intestinal epithelial cells orchestrates innate immune responses against mucosal bacterial infection. *Immunity*, *32*(3), 403-413. doi:10.1016/j.immuni.2010.02.011
- Wang, Y., Meng, A., Lang, H., Brown, S. A., Konopa, J. L., Kindy, M. S., . . . Zhou, D. (2004). Activation of nuclear factor kappaB In vivo selectively protects the murine small intestine against ionizing radiation-induced damage. *Cancer Res*, *64*(17), 6240-6246. doi:10.1158/0008-5472.CAN-04-0591
- Wannemuehler, T. J., Manukyan, M. C., Brewster, B. D., Rouch, J., Poynter, J. A., Wang, Y., & Meldrum, D. R. (2012). Advances in mesenchymal stem cell research in sepsis. *J Surg Res*, *173*(1), 113-126. doi:10.1016/j.jss.2011.09.053
- Ward-Kavanagh, L. K., Lin, W. W., Sedy, J. R., & Ware, C. F. (2016). The TNF Receptor Superfamily in Co-stimulating and Co-inhibitory Responses. *Immunity*, *44*(5), 1005-1019. doi:10.1016/j.immuni.2016.04.019
- Waters, J. P., Pober, J. S., & Bradley, J. R. (2013). Tumour necrosis factor and cancer. *J Pathol*, *230*(3), 241-248. doi:10.1002/path.4188
- Watson, A. J., Duckworth, C. A., Guan, Y., & Montrose, M. H. (2009). Mechanisms of epithelial cell shedding in the Mammalian intestine and maintenance of barrier function. *Ann N Y Acad Sci*, *1165*, 135-142. doi:10.1111/j.1749-6632.2009.04027.x
- Watson, A. J., & Hughes, K. R. (2012). TNF-alpha-induced intestinal epithelial cell shedding: implications for intestinal barrier function. *Ann N Y Acad Sci*, *1258*, 1-8. doi:10.1111/j.1749-6632.2012.06523.x
- Wei, J., & Feng, J. (2010). Signaling pathways associated with inflammatory bowel disease. *Recent Pat Inflamm Allergy Drug Discov*, *4*(2), 105-117. doi:10.2174/187221310791163071
- Werner, S. L., Barken, D., & Hoffmann, A. (2005). Stimulus specificity of gene expression programs determined by temporal control of IKK activity. *Science*, *309*(5742), 1857-1861. doi:10.1126/science.1113319
- Werner, T., Sweetman, G., Savitski, M. F., Mathieson, T., Bantscheff, M., & Savitski, M. M. (2014). Ion coalescence of neutron encoded TMT 10-plex reporter ions. *Anal Chem*, *86*(7), 3594-3601. doi:10.1021/ac500140s
- White, G. L., Archer, L. T., Beller, B. K., & Hinshaw, L. B. (1978). Increased survival with methylprednisolone treatment in canine endotoxin shock. *J Surg Res*, *25*(4), 357-364. doi:10.1016/0022-4804(78)90131-2
- Wiley, S. R., Cassiano, L., Lofton, T., Davis-Smith, T., Winkles, J. A., Lindner, V., . . . Fanslow, W. C. (2001). A novel TNF receptor family member binds

- TWEAK and is implicated in angiogenesis. *Immunity*, 15(5), 837-846. doi:10.1016/s1074-7613(01)00232-1
- Wilkins, M. R., Sanchez, J. C., Gooley, A. A., Appel, R. D., Humphery-Smith, I., Hochstrasser, D. F., & Williams, K. L. (1996). Progress with proteome projects: why all proteins expressed by a genome should be identified and how to do it. *Biotechnol Genet Eng Rev*, 13, 19-50. doi:10.1080/02648725.1996.10647923
- Williams, J. M., Duckworth, C. A., Burkitt, M. D., Watson, A. J., Campbell, B. J., & Pritchard, D. M. (2015). Epithelial cell shedding and barrier function: a matter of life and death at the small intestinal villus tip. *Vet Pathol*, 52(3), 445-455. doi:10.1177/0300985814559404
- Williams, J. M., Duckworth, C. A., Watson, A. J., Frey, M. R., Miguel, J. C., Burkitt, M. D., . . . Pritchard, D. M. (2013). A mouse model of pathological small intestinal epithelial cell apoptosis and shedding induced by systemic administration of lipopolysaccharide. *Dis Model Mech*, 6(6), 1388-1399. doi:10.1242/dmm.013284
- Willott, E., Balda, M. S., Fanning, A. S., Jameson, B., Van Itallie, C., & Anderson, J. M. (1993). The tight junction protein ZO-1 is homologous to the Drosophila discs-large tumor suppressor protein of septate junctions. *Proc Natl Acad Sci U S A*, 90(16), 7834-7838. doi:10.1073/pnas.90.16.7834
- Winkles, J. A. (2008). The TWEAK-Fn14 cytokine-receptor axis: discovery, biology and therapeutic targeting. *Nat Rev Drug Discov*, 7(5), 411-425. doi:10.1038/nrd2488
- Wodarz, A., & Nusse, R. (1998). Mechanisms of Wnt signaling in development. *Annu Rev Cell Dev Biol*, 14, 59-88. doi:10.1146/annurev.cellbio.14.1.59
- Wolczyk, D., Zaremba-Czogalla, M., Hryniewicz-Jankowska, A., Tabola, R., Grabowski, K., Sikorski, A. F., & Augoff, K. (2016). TNF-alpha promotes breast cancer cell migration and enhances the concentration of membrane-associated proteases in lipid rafts. *Cell Oncol (Dordr)*, 39(4), 353-363. doi:10.1007/s13402-016-0280-x
- Wong, V. W., Stange, D. E., Page, M. E., Buczacki, S., Wabik, A., Itami, S., . . . Jensen, K. B. (2012). Lrig1 controls intestinal stem-cell homeostasis by negative regulation of ErbB signalling. *Nat Cell Biol*, 14(4), 401-408. doi:10.1038/ncb2464
- Wullaert, A., Bonnet, M. C., & Pasparakis, M. (2011). NF-kappaB in the regulation of epithelial homeostasis and inflammation. *Cell Res*, 21(1), 146-158. doi:10.1038/cr.2010.175
- Xavier, R. J., & Podolsky, D. K. (2007). Unravelling the pathogenesis of inflammatory bowel disease. *Nature*, 448(7152), 427-434. doi:10.1038/nature06005
- Xiao, Y., Lu, Y., Wang, Y., Yan, W., & Cai, W. (2019). Deficiency in intestinal epithelial Reg4 ameliorates intestinal inflammation and alters the colonic bacterial composition. *Mucosal Immunol*, 12(4), 919-929. doi:10.1038/s41385-019-0161-5
- Xu, C., Wang, K., Ding, Y. H., Li, W. J., & Ding, L. (2019). Claudin-7 gene knockout causes destruction of intestinal structure and animal death in mice. *World J Gastroenterol*, 25(5), 584-599. doi:10.3748/wjg.v25.i5.584
- Xu, G., & Shi, Y. (2007). Apoptosis signaling pathways and lymphocyte homeostasis. *Cell Res*, 17(9), 759-771. doi:10.1038/cr.2007.52
- Yagami, T., Yamamoto, Y., & Koma, H. (2019). Pathophysiological Roles of Intracellular Proteases in Neuronal Development and Neurological Diseases. *Mol Neurobiol*, 56(5), 3090-3112. doi:10.1007/s12035-018-1277-4

- Yamazaki, Y., Okawa, K., Yano, T., Tsukita, S., & Tsukita, S. (2008). Optimized proteomic analysis on gels of cell-cell adhering junctional membrane proteins. *Biochemistry*, *47*(19), 5378-5386. doi:10.1021/bi8002567
- Yang, J., Andre, P., Ye, L., & Yang, Y. Z. (2015). The Hedgehog signalling pathway in bone formation. *Int J Oral Sci*, *7*(2), 73-79. doi:10.1038/ijos.2015.14
- Yang, L., Liu, C., Zhao, W., He, C., Ding, J., Dai, R., . . . Meng, H. (2018). Impaired Autophagy in Intestinal Epithelial Cells Alters Gut Microbiota and Host Immune Responses. *Appl Environ Microbiol*, *84*(18). doi:10.1128/AEM.00880-18
- Yang, R., Miki, K., Oksala, N., Nakao, A., Lindgren, L., Killeen, M. E., . . . Tenhunen, J. (2009). Bile high-mobility group box 1 contributes to gut barrier dysfunction in experimental endotoxemia. *Am J Physiol Regul Integr Comp Physiol*, *297*(2), R362-369. doi:10.1152/ajpregu.00184.2009
- Yao, J., Mackman, N., Edgington, T. S., & Fan, S. T. (1997). Lipopolysaccharide induction of the tumor necrosis factor-alpha promoter in human monocytic cells. Regulation by Egr-1, c-Jun, and NF-kappaB transcription factors. *J Biol Chem*, *272*(28), 17795-17801. doi:10.1074/jbc.272.28.17795
- Yarmolinsky, M. B. (1995). Programmed cell death in bacterial populations. *Science*, *267*(5199), 836-837. doi:10.1126/science.7846528
- Ye, D., Ma, I., & Ma, T. Y. (2006). Molecular mechanism of tumor necrosis factor-alpha modulation of intestinal epithelial tight junction barrier. *Am J Physiol Gastrointest Liver Physiol*, *290*(3), G496-504. doi:10.1152/ajpgi.00318.2005
- Yoo, J. H., & Donowitz, M. (2019). Intestinal enteroids/organoids: A novel platform for drug discovery in inflammatory bowel diseases. *World J Gastroenterol*, *25*(30), 4125-4147. doi:10.3748/wjg.v25.i30.4125
- Yoseph, B. P., Klingensmith, N. J., Liang, Z., Breed, E. R., Burd, E. M., Mittal, R., . . . Coopersmith, C. M. (2016). Mechanisms of Intestinal Barrier Dysfunction in Sepsis. *Shock*, *46*(1), 52-59. doi:10.1097/SHK.0000000000000565
- Yoshikawa, Y., Nakayama, T., Saito, K., Hui, P., Morita, A., Sato, N., . . . Usami, R. (2007). Haplotype-based case-control study of the association between the guanylate cyclase activator 2B (GUCA2B, Uroguanylin) gene and essential hypertension. *Hypertens Res*, *30*(9), 789-796. doi:10.1291/hypres.30.789
- Young, J., Yu, X., Wolslegel, K., Nguyen, A., Kung, C., Chiang, E., . . . Grogan, J. L. (2010). Lymphotoxin-alpha-beta heterotrimers are cleaved by metalloproteinases and contribute to synovitis in rheumatoid arthritis. *Cytokine*, *51*(1), 78-86. doi:10.1016/j.cyto.2010.03.003
- Yu, F. S., Yin, J., Xu, K., & Huang, J. (2010). Growth factors and corneal epithelial wound healing. *Brain Res Bull*, *81*(2-3), 229-235. doi:10.1016/j.brainresbull.2009.08.024
- Yu, K. Y., Kwon, B., Ni, J., Zhai, Y., Ebner, R., & Kwon, B. S. (1999). A newly identified member of tumor necrosis factor receptor superfamily (TR6) suppresses LIGHT-mediated apoptosis. *J Biol Chem*, *274*(20), 13733-13736. doi:10.1074/jbc.274.20.13733
- Yuan, J., & Horvitz, H. R. (2004). A first insight into the molecular mechanisms of apoptosis. *Cell*, *116*(2 Suppl), S53-56, 51 p following S59. doi:10.1016/s0092-8674(04)00028-5
- Zachary, J. F., & McGavin, M. D. (2012). *Pathologic basis of veterinary disease* (5th ed.). St.Louis, Mo.: Elsevier.
- Zambrano, S., De Toma, I., Piffer, A., Bianchi, M. E., & Agresti, A. (2016). NF-kappaB oscillations translate into functionally related patterns of gene expression. *Elife*, *5*, e09100. doi:10.7554/eLife.09100
- Zhang, C., Yan, J., Xiao, Y., Shen, Y., Wang, J., Ge, W., & Chen, Y. (2017). Inhibition of Autophagic Degradation Process Contributes to Claudin-2 Expression Increase and Epithelial Tight Junction Dysfunction in TNF-alpha Treated Cell Monolayers. *Int J Mol Sci*, *18*(1). doi:10.3390/ijms18010157

- Zhang, H., Nan, W., Wang, S., Zhang, T., Si, H., Wang, D., . . . Li, G. (2016). Epidermal growth factor promotes proliferation of dermal papilla cells via Notch signaling pathway. *Biochimie*, *127*, 10-18. doi:10.1016/j.biochi.2016.04.015
- Zhang, J. M., & An, J. (2007). Cytokines, inflammation, and pain. *Int Anesthesiol Clin*, *45*(2), 27-37. doi:10.1097/AIA.0b013e318034194e
- Zhang, L., Sun, J., Wang, B., Ren, J. C., Su, W., & Zhang, T. (2015). MicroRNA-10b Triggers the Epithelial-Mesenchymal Transition (EMT) of Laryngeal Carcinoma Hep-2 Cells by Directly Targeting the E-cadherin. *Appl Biochem Biotechnol*, *176*(1), 33-44. doi:10.1007/s12010-015-1505-6
- Zhang, P., Liu, X., Guo, A., Xiong, J., Fu, Y., & Zou, K. (2016). B Cell-Activating Factor as a New Potential Marker in Inflammatory Bowel Disease. *Dig Dis Sci*, *61*(9), 2608-2618. doi:10.1007/s10620-016-4136-z
- Zhang, Q., Raouf, M., Chen, Y., Sumi, Y., Sursal, T., Junger, W., . . . Hauser, C. J. (2010). Circulating mitochondrial DAMPs cause inflammatory responses to injury. *Nature*, *464*(7285), 104-107. doi:10.1038/nature08780
- Zhang, X., Wu, J., Ye, B., Wang, Q., Xie, X., & Shen, H. (2016). Protective effect of curcumin on TNBS-induced intestinal inflammation is mediated through the JAK/STAT pathway. *BMC Complement Altern Med*, *16*(1), 299. doi:10.1186/s12906-016-1273-z
- Zhang, Y., Chen, D., Wang, F., Li, X., Xue, X., Jiang, M., . . . Liang, J. (2019). Comparison of the efficiency of different enemas on patients with distal ulcerative colitis. *Cell Prolif*, *52*(2), e12559. doi:10.1111/cpr.12559
- Zhao, G. J., Li, D., Zhao, Q., Lian, J., Hu, T. T., Hong, G. L., . . . Lu, Z. Q. (2016). Prognostic Value of Plasma Tight-Junction Proteins for Sepsis in Emergency Department: An Observational Study. *Shock*, *45*(3), 326-332. doi:10.1097/SHK.0000000000000524
- Zhou, Z., Ren, J., Liu, H., Gu, G., & Li, J. (2011). Serum proteomic analysis from bacteremic and leucopenic rabbits. *J Surg Res*, *171*(2), 749-754. doi:10.1016/j.jss.2010.04.056
- Zhu, Y., Brannstrom, M., Janson, P. O., & Sundfeldt, K. (2006). Differences in expression patterns of the tight junction proteins, claudin 1, 3, 4 and 5, in human ovarian surface epithelium as compared to epithelia in inclusion cysts and epithelial ovarian tumours. *Int J Cancer*, *118*(8), 1884-1891. doi:10.1002/ijc.21506
- Zihni, C., Mills, C., Matter, K., & Balda, M. S. (2016). Tight junctions: from simple barriers to multifunctional molecular gates. *Nat Rev Mol Cell Biol*, *17*(9), 564-580. doi:10.1038/nrm.2016.80
- Zou, G. M., & Hu, W. Y. (2005). LIGHT regulates CD86 expression on dendritic cells through NF-kappaB, but not JNK/AP-1 signal transduction pathway. *J Cell Physiol*, *205*(3), 437-443. doi:10.1002/jcp.20420
- Zou, H., Li, Y., Liu, X., & Wang, X. (1999). An APAF-1-cytochrome c multimeric complex is a functional apoptosome that activates procaspase-9. *J Biol Chem*, *274*(17), 11549-11556. doi:10.1074/jbc.274.17.11549
- Zuo, C., Sheng, X., Ma, M., Xia, M., & Ouyang, L. (2016). ISG15 in the tumorigenesis and treatment of cancer: An emerging role in malignancies of the digestive system. *Oncotarget*, *7*(45), 74393-74409. doi:10.18632/oncotarget.11911
- Zwanzger, P., Domschke, K., & Bradwejn, J. (2012). Neuronal network of panic disorder: the role of the neuropeptide cholecystokinin. *Depress Anxiety*, *29*(9), 762-774. doi:10.1002/da.21919

9 Outputs



[Cell Death Dis.](#) 2019 Dec; 10(12): 896.

Published online 2019 Nov 26. doi: [10.1038/s41419-019-2129-5](https://doi.org/10.1038/s41419-019-2129-5)

PMCID: PMC6879761

PMID: [31772152](https://pubmed.ncbi.nlm.nih.gov/31772152/)

NF- κ B2 signalling in enteroids modulates enterocyte responses to secreted factors from bone marrow-derived dendritic cells

[Lauren G. Jones](#),¹ [Andra Vaida](#),¹ [Louise M. Thompson](#),¹ [Felix I. Ikuomola](#),¹ [Jorge H. Caamaño](#),² [Michael D. Burkitt](#),¹ [Fabio Miyajima](#),^{3,4} [Jonathan M. Williams](#),⁵ [Barry J. Campbell](#),¹ [D. Mark Pritchard](#),¹ and [Carrie A. Duckworth](#)¹✉

Abstract

Alternative pathway NF- κ B signalling regulates susceptibility towards developing inflammatory bowel disease (IBD), colitis-associated cancer and sepsis-associated intestinal epithelial cell apoptosis and shedding. However, the cell populations responsible for the perturbed alternative pathway NF- κ B signalling in intestinal mucosal pathology remain unclear. In order to investigate the contribution of the epithelial compartment, we have tested whether NF- κ B2 regulated transcription in intestinal epithelial cells controls the intestinal epithelial response to cytokines that are known to disrupt intestinal barrier permeability. Enteroids were generated from the proximal, middle and distal regions of small intestine (SI) from C57BL/6J wild-type mice and displayed region-specific morphology that was maintained during sub-culture. Enteroids treated with 100 ng/mL TNF were compared with corresponding regions of SI from C57BL/6J mice treated systemically with 0.33 mg/kg TNF for 1.5 h. TNF-induced apoptosis in all regions of the intestine in vitro and in vivo but resulted in Paneth cell degranulation only in proximal tissue-derived SI and enteroids. TNF also resulted in increased enteroid sphericity (quantified as circularity from two-dimensional bright field images). This response was dose and time-dependent and correlated with active caspase-3 immunopositivity. Proximal tissue-derived enteroids generated from *Nfkb2*^{-/-} mice showed a significantly blunted circularity response following the addition of TNF, IFN γ , lipopolysaccharide (LPS) activated C57BL/6J-derived bone marrow-derived dendritic cells (BMDC) and secreted factors from LPS-activated BMDCs. However, *Nfkb1*^{-/-} mouse-derived enteroids showed no significant changes in response to these stimuli. In conclusion, the selection of SI region is important when designing enteroid studies as region-specific identity and response to stimuli such as TNF are maintained in culture. Intestinal epithelial cells are at least partially responsible for regulating their own fate by modulating NF- κ B2 signalling in response to stimuli known to be involved in multiple intestinal and systemic diseases. Future studies are warranted to investigate the therapeutic potential of intestinal epithelial NF- κ B2 inhibition.

Subject terms: Intestinal stem cells, Inflammatory bowel disease, Experimental models of disease, Immunopathogenesis, Sepsis

Introduction

The intestine is lined by a single layer of columnar epithelial cells that function to maintain a barrier between luminal contents and the body^{1,2}. Barrier function is maintained by the tight regulation of intestinal epithelial cell proliferation, apoptosis and cell shedding rates which are themselves modulated by several factors, including age, genetic background, dietary components, intestinal microbiota, enterally and parenterally administered drugs and other environmental factors³. Dysregulation of these cellular processes results in the break-down of the intestinal barrier and this is thought to be a contributing factor to the development of multiple diseases. We have recently shown that defective intestinal barrier function caused by cell shedding in the terminal ileum predicts relapse of inflammatory bowel disease (IBD) in humans⁴. Defects in intestinal barrier function may also be involved in the pathogenesis of systemic conditions, such as metabolic endotoxaemia and sepsis^{5,6}.

Several pro-inflammatory cytokines are present at increased concentrations in the circulation, intestinal lumen and lamina propria of the intestine during active IBD, infectious diarrhoea, coeliac disease and sepsis⁷⁻¹². Tumour necrosis factor (TNF) is a well characterised cytokine that is produced in these conditions and is a key mediator of mucosal pathology^{3,13}. Elevated TNF concentrations in excess of 63 ng/g stool have been documented in humans in response to *Shigella flexneri* infection¹¹. Anti-TNF therapies are also widely used clinically to ameliorate active Crohn's disease¹⁴.

We have recently shown that the administration of lipopolysaccharide (LPS) or its downstream effector, TNF, by intraperitoneal injection to mice results in a massive induction of epithelial apoptosis and cell shedding from the SI villus tip within 1.5 h^{4,15-17}. This rapid onset of active caspase-3 positively stained shedding cells subsequently resulted in villus atrophy and was accompanied by fluid effusion into the SI lumen and diarrhoea, but was largely diminished at 3 h post LPS injection¹⁷. However, increased efflux of FITC-dextran (FD4) from the intestinal lumen into the circulation following LPS treatment was observed at later time-points¹⁷, suggesting that defects in intestinal barrier function persist once cell shedding and apoptosis have subsided, until complete restitution of the epithelium has been achieved. The regenerative capacity of the intestinal epithelium is remarkable. Cell turnover in the epithelium is normally around 5 days with around 1400 cells shed from a single mouse villus tip per day¹⁸. We would therefore anticipate that barrier function could take up to 5 days to be restored following extensive epithelial cell loss by apoptosis and cell shedding once inflammatory stimuli such as TNF and interferon γ (IFN γ) have been removed. Understanding the mechanisms underpinning intestinal epithelial cell protection from cytokine-mediated injury will enable the future development of therapeutics for several intestinal and systemic diseases.

The NF- κ B family of transcription factors consists of 5 members (NF- κ B2 (p52), RelB, NF- κ B1 (p50), c-Rel, and RelA (p65)) and regulate multiple cellular processes¹⁹. We have recently identified components of the alternative NF- κ B signalling pathway that are important in modulating the susceptibility to IBD, colitis-associated cancer and intestinal epithelial apoptosis and cell shedding in mice. *Nfkb2*^{-/-} mice were resistant to dextran sulphate sodium (DSS)-induced colitis and azoxymethane/DSS-induced colonic adenoma formation²⁰ and were also resistant

to the induction of LPS and TNF-induced SI apoptosis and cell shedding in vivo^{16,17}. Infection studies have also shown that *Nfkb2*^{-/-} mice have a reduced ability to clear the gut helminth *Trichuris muris*²¹ and the gastric pathogen *Helicobacter felis*, the latter observation being associated with reduced gastric preneoplastic pathology owing to a defective immune response²². The complex in vivo nature of these studies to date, has made it impossible to determine the importance of each cellular compartment (e.g., immune or epithelial) in regulating the intestinal response to damage-inducing stimuli. The majority of studies characterising alternative pathway NF-κB signalling are also focused on immune cell mechanisms which may be differentially regulated in other cellular compartments. Therefore, we have now generated a SI enteroid model to assess the interactions between the intestinal epithelium and specific immune cell derived cytokines that are known to be elevated in intestinal and systemic disease, and to determine the importance of epithelial cell-specific alternative pathway NF-κB signalling in regulating the epithelial cell response to cytokine-induced pathology.

Dendritic cells are present throughout the lamina propria of the gut and contribute to innate and adaptive immunity thus regulating gut homeostasis. Direct bidirectional interaction of dendritic cells with the epithelium is believed to maintain the dendritic cell population in a tolerogenic state and this protects the intestinal epithelium from inappropriate immune cell-derived attack²³. Whilst dendritic cells are the most potent antigen presenting cell population, they are also activated by pro-inflammatory cytokines or oxidative stress and are conditioned by their surrounding microenvironment²⁴. Cytokines and chemokines released by dendritic cells along with other lamina propria immune cell populations can modulate intestinal barrier integrity, intestinal cell proliferation and cell death²⁵. Our previous whole mouse global *Nfkb2* knockout studies^{17,20,22} have limited our ability to dissect the importance of alternative pathway NF-κB signalling within epithelial and immune compartments in regulating the susceptibility of the intestinal epithelium to cytokine-induced injury. We therefore generated a bone marrow-derived dendritic cell (BMDC) reconstituted intestinal organoid model to assess the role of NF-κB2 in regulating intestinal epithelial cell-specific responses to secreted factors from BMDCs.

We hypothesise that *Nfkb2* activation within intestinal epithelial cells sensitises them to the induction of apoptosis by pro-inflammatory cytokines that are upregulated in intestinal tissues and systemically during active intestinal disease and bacteraemia. We have therefore explored whether *Nfkb2* inhibition within intestinal epithelia could be a potential therapeutic approach to ameliorating inflammation-associated intestinal disease using a novel reconstituted intestinal organoid co-culture model.

Results

Regional differences are observed in enteroid morphology

The small intestine (SI) displays regional differences in structure and function. The expression of several genes is altered along the cephalocaudal axis in vivo and this region-specific identity has previously been shown to be maintained in enteroid culture^{26,27}. We therefore generated organoids from proximal, middle and distal 2 cm segments of murine SI from female C57BL/6J mice and assessed their morphological changes over 10 consecutive passages. Enteroids derived from the three distinct areas displayed morphological differences between regions and these did not alter following repeated passage. At days 3–5 post passage, proximal SI

derived enteroids had the longest ($116 \pm 3 \mu\text{m}$) and most abundant crypt domains ($7.22 \pm 0.26/\text{enteroid}$) with smooth surfaces and a polarised Paneth cell distribution at the base of crypts, whilst the distal SI derived enteroids had a smaller number of crypt domains ($4.04 \pm 1.02/\text{enteroid}$) which were shorter ($89 \pm 4 \mu\text{m}$) and displayed a more rounded and rugged appearance with a less polarised Paneth cell distribution with these differentiated cells also being found further along the crypt axes (Fig. (Fig.1a).1a). Middle SI derived enteroids had 5.22 ± 1.90 crypts per enteroid that were $91 \pm 11 \mu\text{m}$ in length and showed the greatest degree of variation in crypt length and number and Paneth cell distribution, suggestive of an intermediate phenotype.

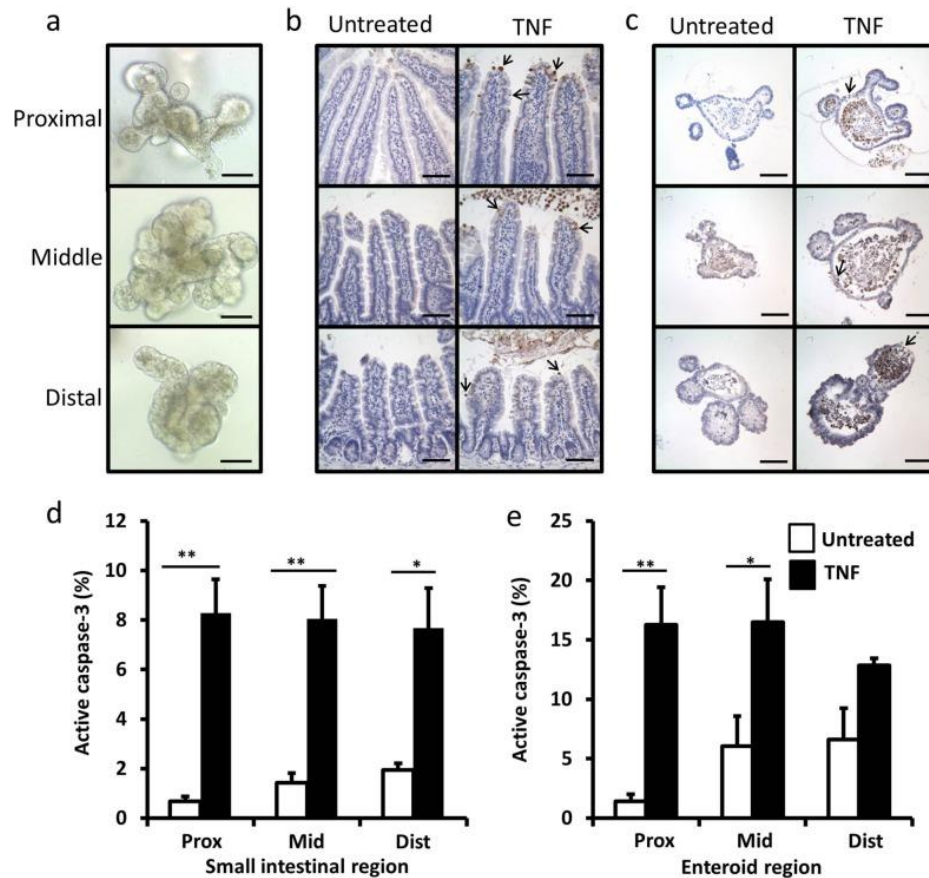


Fig. 1

Enteroids show regional differences in morphology and respond to TNF similarly to native SI tissue.

Bright field micrographs of enteroids derived from proximal, middle and distal sections of C57BL/6J SI (a). Proximal, middle and distal sections of SI tissue taken from untreated and TNF (0.33 mg/kg, 1.5 h) treated C57BL/6J mice (b) and enteroids generated from proximal, middle and distal regions of SI untreated or treated with TNF (100 ng/mL 24 h) (c) immunohistochemically stained for active caspase-3. Quantification of active caspase-3 positive epithelial cells from untreated (white) and TNF treated (black) SI epithelia (d) and enteroid culture (e). For animal study, quantified from $n = 6$ mice per group; for enteroid study $n = 6$, $N = 3$, $*p < 0.05$, $**p < 0.01$. Scale bars = $100 \mu\text{m}$.

TNF induces enteroid apoptosis and Paneth cell depletion, but does not modulate enteroid proliferation

We previously identified subtle regional differences in the murine SI in vivo in response to intraperitoneally administered LPS. A greater extent of villus blunting was observed in the proximal SI compared with other SI regions¹⁷. We therefore investigated the apoptotic and proliferative responses to a downstream effector of LPS, TNF, in region-specific enteroid cultures compared to histological sections taken from the same regions of the intestine in vivo. Baseline amounts of apoptosis in both untreated SI and in enteroid culture regardless of region were low, however, a small increase in the percentage of active caspase-3 positive cells was observed along the cephalocaudal axis in both systems (Fig. [1b–e](#)). As expected, intraperitoneal injection of 0.33 mg/kg TNF-induced a significant increase in apoptotic cells at the villus tip after 1.5 h (Fig. [1b, d](#)), whilst 100 ng/ml TNF-induced apoptosis to a similar extent in enteroids after 24 h (Fig. [1c, e](#)).

Paneth cells are important for maintaining the intestinal stem cell niche, although the exact mechanisms by which this cell population supports the proliferative capacity and number of neighbouring crypt base columnar cells remain unknown. However, TNF has previously been shown to induce Paneth cell dysfunction in vivo²⁸, and this could potentially impact on the regenerative capacity of the intestinal epithelium. We therefore investigated whether TNF modulated Paneth cell number in SI tissue and in enteroids as this could impact on crypt-villus growth dynamics. TNF administration caused a more marked and significant reduction in Paneth cell number in the proximal SI and proximal tissue-derived enteroids compared with other SI regions (Fig. [2a, b](#)) suggesting that TNF may modulate the intestinal stem cell niche in different ways within the proximal SI compared with other intestinal regions. Olfactomedin-4 (Olfm4) is a putative active stem cell marker that also labels early transit-amplifying cells. Olfm4 expression was not altered in SI tissues treated with TNF but due to the distribution differences in cellular location of Olfm4 observed in enteroids, Olfm4 expressing cells were not possible to quantify reliably (Supplementary Fig. [1](#)). We also wanted to test whether another abundant secretory cell type was affected by the addition of TNF and found that the goblet cell population in different regions of SI and in enteroids was not modulated by the addition of TNF (Supplementary Fig. [2](#)).

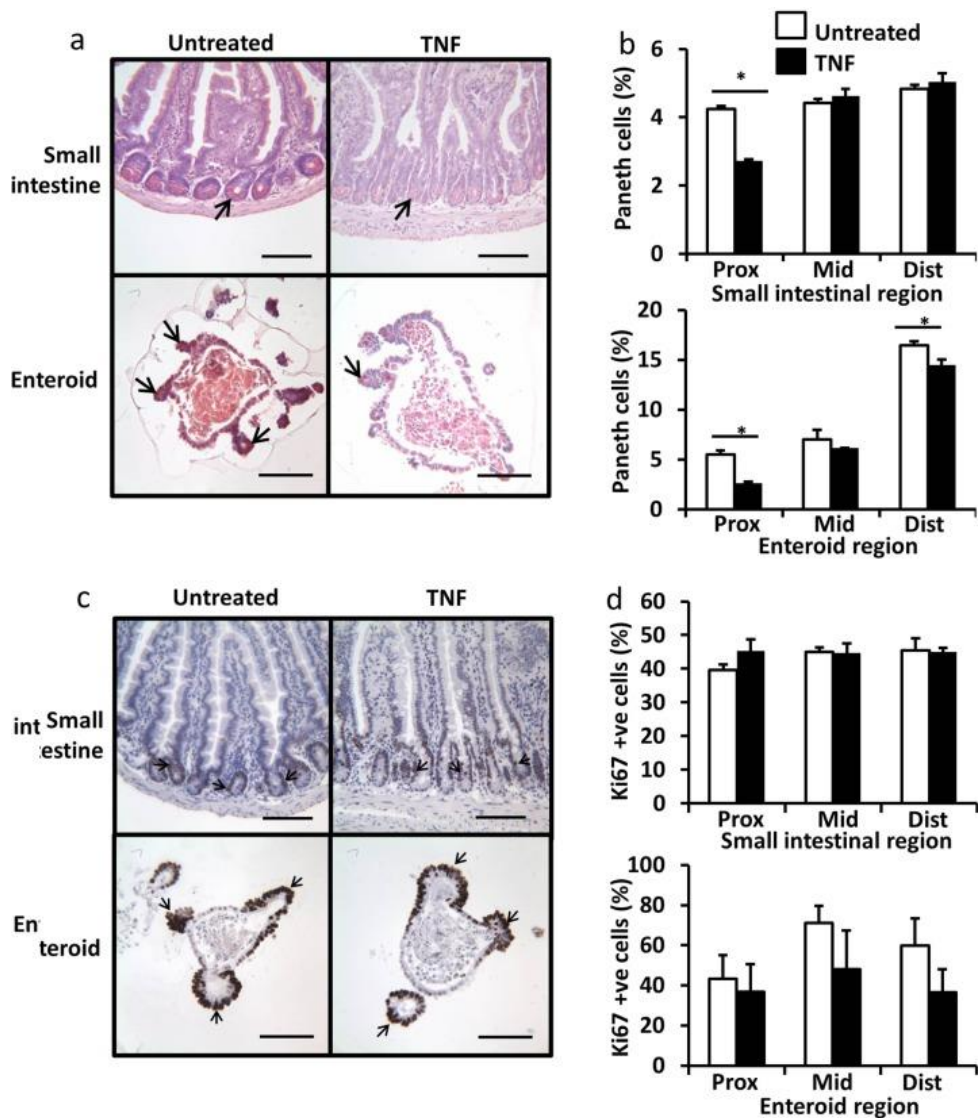


Fig. 2

TNF causes Paneth cell degranulation in proximal SI but does not change the rate of cell proliferation.

Proximal SI and enteroids stained with Sirius red (a). Percentage of Sirius red stained Paneth cells in untreated (white) and TNF treated (black) proximal, middle and distal derived SI (top) and enteroids (bottom) (b). Proximal SI and enteroids stained with Ki67 (c). Percentage of Ki67 stained epithelial cells in untreated (white) and TNF treated (black) proximal, middle and distal derived SI (top) and enteroids (bottom) (d). For animal study quantified from $n = 6$ mice per group, for enteroid study $n = 6$, $N = 3$, $*p < 0.05$. Scale bars = 100 μm .

Proliferation in the SI in vivo occurs within the transit-amplifying region of the crypt; a distinctly different part of the crypt-villus axis to the villus tip, which is the region most susceptible to apoptosis in response to systemically administered TNF. As we have shown that TNF causes apoptosis and Paneth cell depletion at the dose and time-points tested in mice in vivo and in enteroids, we wanted to determine whether this treatment had any impact on intestinal proliferation. Proliferation indicated by Ki67 positively stained nuclei was identified in the crypt domains of whole SI tissue and enteroids. TNF treatment had no significant effect on cellular proliferation either in vivo or in enteroid culture, in any of the three SI regions at the doses and time

points that showed an increased apoptotic response and Paneth cell depletion (Fig. [2c, d](#)).

Apoptosis and resultant cell shedding into the lumen correlate positively with enteroid circularity

Villus shortening occurs *in vivo* as a result of an increased rate of apoptosis and cell shedding from the villus tip with no compensatory increase in cellular proliferation (Figs. ([Figs.11](#) and [and22](#))¹⁷). Similar atrophy also occurs in enteroid cultures. As a result of cell loss by apoptosis with no accompanying change in cellular proliferation (Figs. ([Figs.11](#) and [and2](#)),²), cells are shed into the enteroid lumen and these are not immediately replaced. Junctional complexes hold remaining epithelial cells together whilst there is likely pressure from the build-up of apoptotic bodies within enteroid lumens. This results in the enteroids gaining a more spherical morphology. We have quantified this enteroid ‘rounding’ in terms of circularity from 2-dimensional images and have validated this as a reproducible and robust method of cell death analysis in enteroids following cytokine treatment (materials and methods). Three days post passage, untreated enteroids had circularity values of ~0.35, however, circularity increased to ~0.65 48 h following 100 ng/mL TNF and ~0.9 with conditioned media from LPS-activated BMDCs in C57BL/6J proximal tissue-derived enteroids (Fig. ([Fig.3a](#)),[3a](#)). We validated the reproducibility of the scoring method by assessment of intra-scorer variability where the same person (L.J.) scored images from the same 12 enteroids with a range of different circularities 1 week apart (Fig. ([Fig.3b](#)),[3b](#)), and inter-scorer variability where two different blinded scorers (L.J. and C.D.) assessed enteroid circularity from the same 12 enteroid images (Fig. ([Fig.3c](#)),[3c](#)). We also determined that there was no correlation between enteroid area and circularity as long as organoids were above a critical size at the start of each experiment, which equated to 3 days post passage or an initial baseline circularity value <0.4 (Fig. ([Fig.3d](#)),[3d](#)).

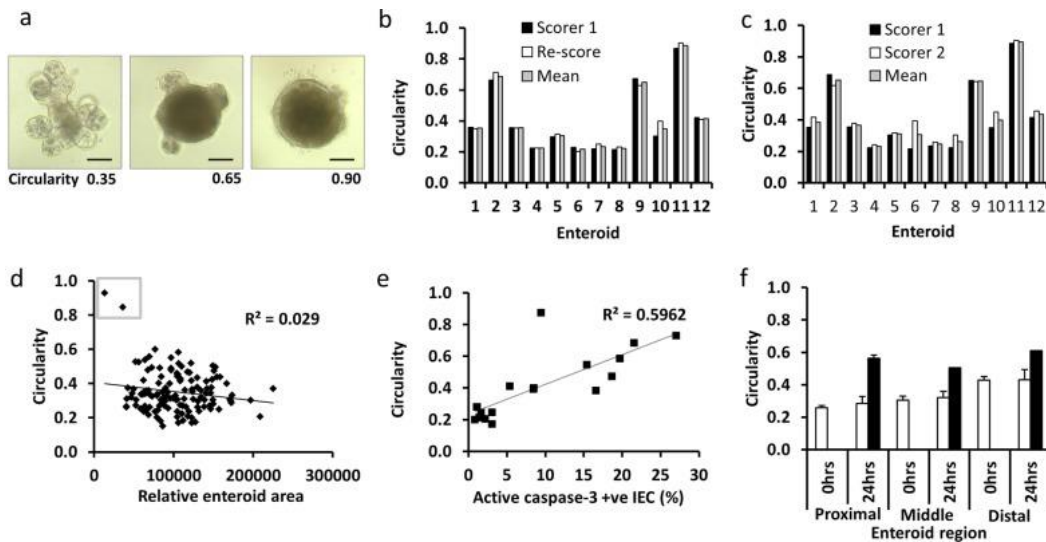


Fig. 3

Validation of circularity assessment as a marker of TNF-induced apoptosis in enteroid culture.

Light micrograph examples of proximal tissue-derived enteroids either untreated 3 days post passage (left), 48 h following 100 ng/ml TNF (middle) and 48 h following treatment with CM from LPS-activated BMDCs (right) traced in yellow using Image

J (a). Quantification of circularity from 12 different enteroids administered with a range of treatments over different experiments and re-scored by the same observer (b) and by an independent second observer (c). Correlation between relative enteroid area and circularity for 130 individual enteroids at baseline (d), small organoids at baseline have high circularity values and need to be excluded from further analysis (grey box). Percentage active-caspase 3 positive cells were correlated with enteroid circularity from organoids selected at 0, 24 and 48 h post treatment with 100 ng/ml TNF (e). Change in circularity between three enteroid regions at baseline (white bars) and 24 h after 100 ng/ml TNF (black bars). Scale bars = 100 μ m.

To further validate the assessment of circularity as a reliable indicator of cytokine-induced cell death in proximal tissue-derived enteroids, we observed a good positive correlation ($R^2 = 0.6$) between enteroid circularity and active caspase-3 immunohistochemical staining (Fig. (Fig.3e).3e). TNF activates apoptosis via caspase-8 and active caspase-8 is observed at the villus tip during intestinal cell shedding²⁹. Active caspase-8 was not detected at later time-points during enteroid studies (Supplementary Fig. 3). As enteroids derived from the middle or distal segments of the SI displayed a more rounded appearance in culture at baseline (Fig. (Fig.1a),1a), they also showed a blunted response to TNF in terms of increased circularity compared with proximal tissue-derived enteroids (Fig. (Fig.3f).3f). Future studies should therefore consider the use of the circularity method for determining enteroid response to injury, however this method is not suitable for comparing responses between enteroid regions. We therefore used proximal tissue-derived enteroids for the remainder of this study.

Alternative NF- κ B pathway signalling in small intestinal epithelial cells regulates the response to cytokine-induced injury

We have previously shown that *Nfkb2*^{-/-} mice are resistant to TNF-induced villus tip apoptosis and cell shedding compared with their wild-type C57BL/6J counterparts¹⁷. However, the mechanism responsible for this resistance could not be determined during these in vivo studies as it was impossible to quantify the contribution of specific cellular compartments such as epithelial cells or immune cells. Using proximal tissue-derived enteroids, we have now assessed the importance of NF- κ B2 signalling specifically in the epithelial cell compartment in response to TNF and IFN γ stimulation. Both TNF and IFN γ caused C57BL/6J and *Nfkb1*^{-/-} mouse-derived enteroids to undergo morphological changes and round up over a 24-h period, with further noticeable rounding after 48 h (Fig. 4a, b). This response was however blunted in *Nfkb2*^{-/-} enteroids (Fig. (Fig.4c).4c). A dose-dependent increase in circularity was observed in C57BL/6J and *Nfkb1*^{-/-} enteroids from 1 to 1000 ng/mL TNF and from 0.1 to 100 ng/mL IFN γ at both 24- and 48-h post treatment, however, no such increase was observed in *Nfkb2*^{-/-} enteroids (Fig. 5a–f) suggesting that alternative pathway NF- κ B activation is an important modulator of the intestinal epithelial cell response to injury.

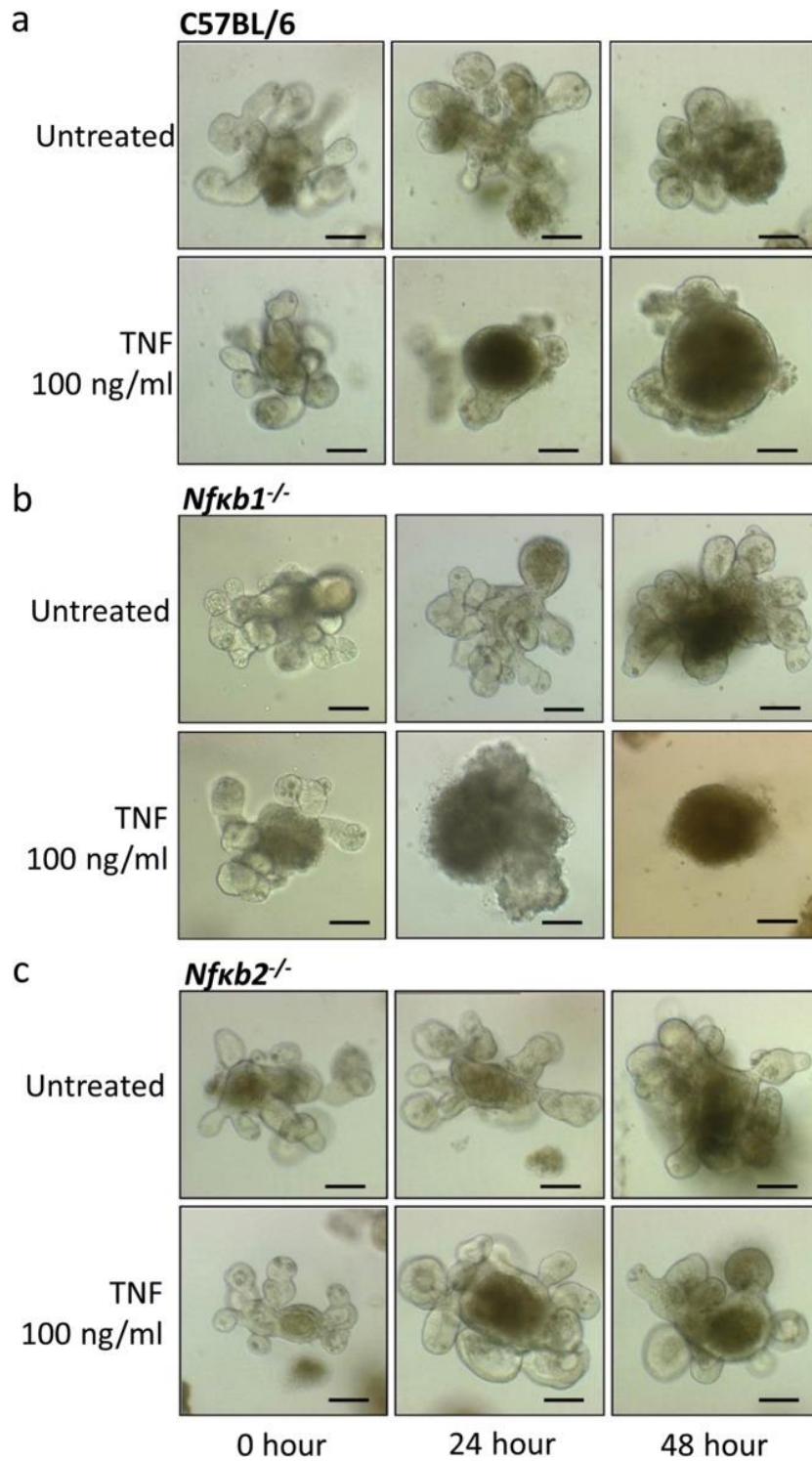


Fig. 4
TNF induces circularity of C57BL/6 but not *Nfkb2*^{-/-} enteroids.

TNF (100 ng/mL) induces enteroid rounding of C57BL/6J (a) and *Nfkb1*^{-/-} (b) proximal tissue-derived enteroids but not *Nfkb2*^{-/-} proximal tissue-derived enteroids (c) at 24 and 48 h time points following treatment. Scale bars = 100 μm.

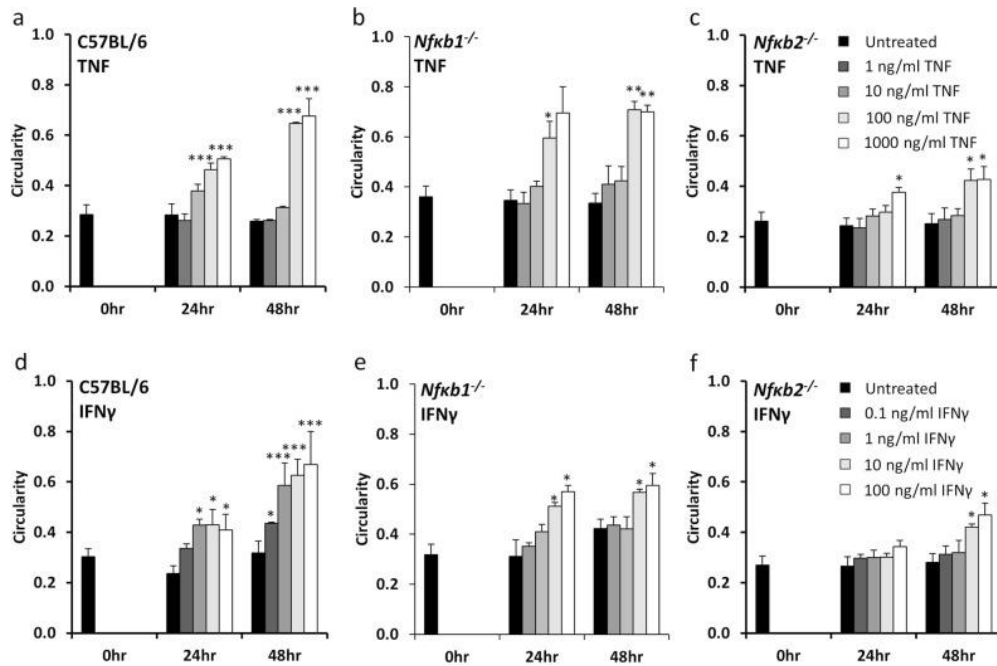


Fig. 5
TNF and IFN γ -induced circularity is blunted in *Nfkb2*^{-/-} enteroids.

Enteroid circularity is dose-dependently increased at 24 and 48 h time-points by treatment with TNF (a–c) and IFN γ (d–f) in C57BL/6J-derived enteroids (a, d) and *Nfkb1*^{-/-} enteroids (b, e), but is blunted in *Nfkb2*^{-/-} enteroids (c, f). *N* = 4, *n* = 6, **p* < 0.05, ***p* < 0.01, ****p* < 0.001 compared with untreated of the same genotype at the same time point.

LPS-activated bone marrow-derived dendritic cells induce enteroid rounding in a co-culture model and this is inhibited by epithelial NF- κ B2 deletion

LPS administration to mice in vivo resulted in abundant villus tip apoptosis and cell shedding 1.5 h following intraperitoneal injection. We have previously shown *Tnfr1*^{-/-} and *Tlr4*^{-/-} mice to be resistant to LPS-induced cell shedding, suggesting that LPS acts via TLR4 on immune cells to induce ligands that bind the TNFR1 on epithelial cells to initiate the shedding process¹⁷. Dendritic cells have important functions in the innate and adaptive immune systems and are activated by LPS. We therefore co-cultured C57BL/6J-derived BMDCs with C57BL/6J, *Nfkb1*^{-/-} or *Nfkb2*^{-/-} enteroids and tested BMDCs that had or had not been activated by LPS. The direct application of 1 μ g/mL LPS or unstimulated BMDCs had no morphological effect on any enteroid genotype (Fig. (Fig.6a)6a) and we did not observe any significant differences in enteroid circularity following treatment (Fig. 6b–d). Interestingly, co-culture of C57BL/6J and *Nfkb1*^{-/-} enteroids with LPS-activated BMDCs resulted in enteroid rounding (Fig. (Fig.6a)6a) and a significant increase in enteroid circularity at both 24- and 48-h post treatment (Fig. 6b, c). However, *Nfkb2*^{-/-} enteroids were resistant to rounding and showed no significant increase in circularity in co-culture with LPS-activated BMDCs at 24 or 48 h (Fig. 6a, d). This suggests that NF- κ B2 signalling specifically in intestinal epithelial cells is modulated by the interaction with dendritic cells.

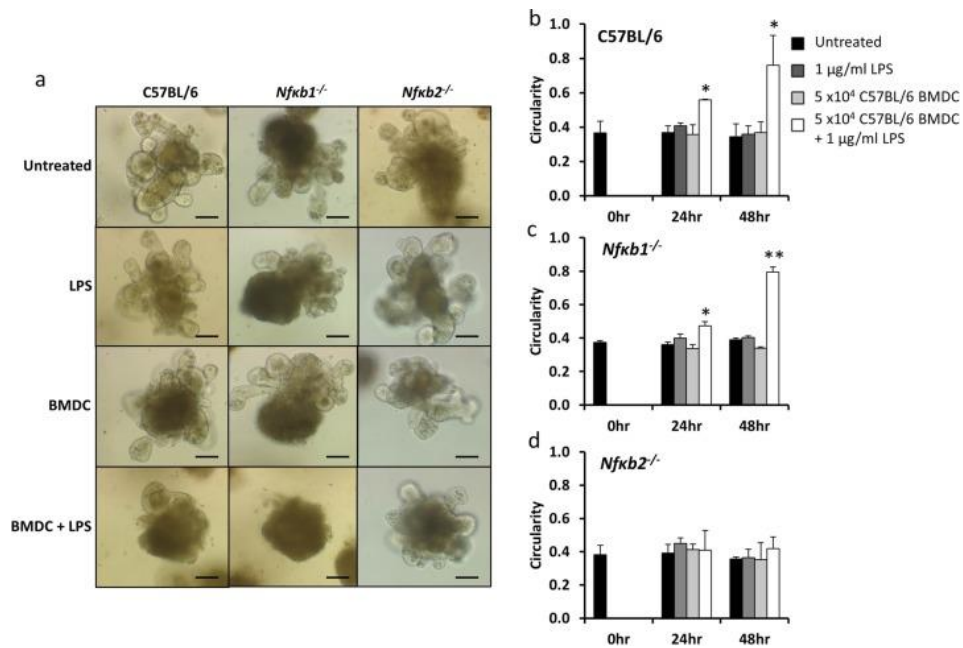


Fig. 6

***Nfkb2*^{-/-} enteroids showed a blunted response to co-culture with LPS activated BMDCs.**

Enteroids were generated from the proximal SI of C57BL/6J, *Nfkb1*^{-/-} and *Nfkb2*^{-/-} mice and were either left untreated, treated with 1 µg/ml LPS, 5 × 10⁴ C57BL/6J-derived BMDC or 5 × 10⁴ C57BL/6J-derived BMDC plus 1 µg/ml LPS and subjected to light microscopy at 48 h (a). Circularity assessment was conducted at 0, 24 and 48 h time points for each stimulus in C57BL/6J (b), *Nfkb1*^{-/-} (c) and *Nfkb2*^{-/-} (d) enteroids. *N* = 3, *n* = 6, **p* < 0.05, ***p* < 0.01 compared with untreated of the same enteroid genotype at the same time point. Scale bars = 100 µm.

Secreted factors from LPS-activated bone marrow-derived dendritic cells are responsible for organoid injury

We sought to determine whether the direct action of BMDC secreted factors on epithelial cells were responsible for the observed increase in C57BL/6J-derived enteroid circularity following stimulation with LPS. Conditioned media from unstimulated and LPS-stimulated BMDCs was placed onto C57BL/6J enteroids. Conditioned media from BMDCs did not induce an increase in enteroid circularity, however, conditioned media from LPS-activated BMDCs induced a significant increase in enteroid circularity at both 24- and 48-h post treatment (Fig. 7a, b). We assessed the cytokines that had been secreted by BMDCs into this conditioned media following stimulation with LPS and determined that several pro-inflammatory cytokines were upregulated. Initial analysis suggested that the amounts of IL-2, IL-4, IL-5 and IL-23 produced were minimal or below the lower limit of detection, hence these cytokines were not considered in subsequent experiments. TNF was upregulated in response to LPS and reached maximal concentrations of around 1 ng/mL (Table (Table1).1). However, this concentration was not high enough to stimulate an increase in enteroid circularity alone (Figs. (Figs.44 and and5).5). Significant increases in IL-6, IL-1β, IL-17A and IL-15 were also detected in the media of LPS-activated BMDCs in co-culture with enteroids and these cytokines may therefore have contributed to the observed increase in enteroid circularity. Secreted factors from dendritic cells are therefore able to modulate intestinal epithelial cell response to injury, which can be modelled in an enteroid system.

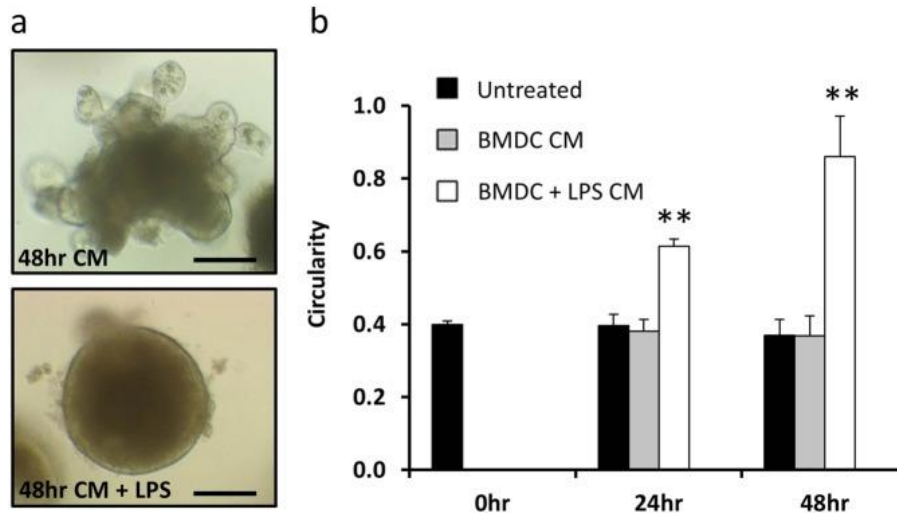


Fig. 7

Conditioned media from LPS-activated BMDCs induced enteroid rounding.

Enteroids derived from the proximal SI of C57BL/6J mice were untreated or treated with 50% conditioned media (CM) generated from 1×10^5 BMDC/ml that were previously either untreated or treated with 1 μ g/ml LPS for 48 h (a). Circularity assessment of enteroids was conducted at 0, 24 and 48 h time points for each stimulus (b). $N = 3$, $n = 6$, $**p < 0.01$ compared with untreated at the same time point. Scale bars = 100 μ m.

Table 1

Cytokines produced by C57BL/6J proximal tissue-derived enteroids, enteroids in co-culture with unstimulated BMDCs and enteroids in co-culture with LPS (1 μ g/ml) activated BMDCs.

Cytokine	Enteroid (pg/ml)	Enteroid + BMDC (pg/ml)	Enteroid + BMDC + LPS (pg/ml)
IFN- γ	0.09 \pm 0.02	0.05 \pm 0.02	ND
IL-10	ND	98.42 \pm 43.94	51.18 \pm 30.89
IL-12 p70	ND	2.35 \pm 2.03	320.85 \pm 94.57
IL-15	0.40 \pm 0.40	10.81 \pm 6.37	186.74 \pm 42.01*
IL-17A	0.01 \pm 0.01	0.01 \pm 0.01	1.51 \pm 0.28*
IL-1 β	ND	0.61 \pm 0.28	42.90 \pm 5.36*
IL-33	0.60 \pm 0.15	0.30 \pm 0.19	4.97 \pm 2.92
IL-6	2.14 \pm 0.82	31.61 \pm 14.81	43967.35 \pm 4220.72*
KC/GRO	4.16 \pm 0.55	5.52 \pm 1.96	103.43 \pm 30.89
TNF	2.29 \pm 0.51	180.37 \pm 78.95	806.86 \pm 335.23

Analysis from three independent experiments in duplicate, data presented \pm SEM. ND = not detected. * $p < 0.05$ between enteroid + BMDC + LPS and enteroid + BMDC groups

Discussion

Recent advances have enabled long-term three-dimensional culture of the mammalian SI epithelium³⁰⁻³². However, many published studies have not considered the differences that exist in structure and function between different anatomical regions of the SI in vivo. The duodenum, jejunum and ileum are each specialised compartments which have distinct absorptive and secretory functions^{26,33-36}. Previous studies in human and mouse enteroids have indicated that cultures retain their region-specific identities following multiple passage, in the absence of mesenchymal cell signalling or other niche factors²⁷. For instance, the Gata 4 transcription factor is highly expressed in all epithelial cells of the duodenum, but shows greatly reduced expression further down the cephalocaudal axis, with no expression being detected in the terminal ileum^{26,27}. Gata 4 has been shown to activate jejunal-specific genes such as *Clnd2* (encoding Claudin-2 protein) but represses ileal-specific genes such as *Slc10a2* (solute carrier family 10, member 2) and *Fabp6* (encoding fatty acid binding protein 6)^{26,37}. Overexpression of Claudin-2 has been associated with inflammatory bowel disease and coeliac disease³⁸ and is also upregulated in the intestine within 1 h of experimentally induced sepsis³⁹. Regional differences in susceptibility occur for each of these pathologies and this is likely to result from differences in gene expression and environmental cues.

We therefore considered SI location when establishing enteroids and have identified variations in growth dynamics between three different regions of the intestine at baseline and following TNF treatment. These differences were also observed in parallel in vivo studies. In particular, Paneth cell numbers were increased from proximal to distal SI in vivo and in enteroid culture and we noted a greater amount of Paneth cell degranulation in the proximal SI both in vitro and in vivo in response to TNF. Previous studies have indicated that there is a greater degree of LPS-induced SI shedding and villus atrophy in the proximal SI compared with other regions¹⁷, however, loss of Paneth cell function within the crypt domains may also contribute to an alteration in the SI stem cell niche, thus perturbing cell production and dynamics further along the crypt-villus axis. We did not observe differences in the proliferative compartment along the length of the intestine by Ki67 immunohistochemistry (IHC), however, a large population of cells are labelled by Ki67 in both systems and more subtle differences in the proliferative compartment may be apparent by using more sensitive detection methods. It was difficult to compare the overall growth rate of organoids between the three regions, however, distal tissue-derived enteroids were more difficult to establish than those from other regions of the SI and displayed morphological differences that were maintained for greater than ten passages. Therefore, future studies should consider that following successive culture, proximal tissue-derived enteroids may outcompete distal tissue-derived derived enteroids in a mixed population.

One of the major cytokines that is responsible for the development of IBD and which is a major contributor to the cytokine storm and multiple organ dysfunction (including the gut epithelium) that occurs in sepsis is TNF^{4,7,17}. The direct impact of TNF on enteroid morphology was striking. Over a period of 48 h, enteroids adopted a rounded appearance and many became almost spherical. This altered morphology was a likely result of increased apoptosis and cell shedding into the enteroid lumen. Analogous to bubble formation, a spherical appearance may result from the line of least tension across tight and adherens junctions with pressure build up from shed cellular debris and secretions within the enteroid lumen. The observed change in enteroid morphology was assessed by measuring circularity and this correlated linearly with active caspase-3 expression, thus validating the technique as a method for analysing cell death in this setting. This technique is

much quicker than other similarly reported methods such as the assessment of branching morphogenesis by assessing the number and length of crypt buds⁴⁰. The circularity assessment method is therefore useful for determining dose and time points for further investigations of a mechanistic nature, but requires optimisation and validation for each culture media formulation and damaging stimulus. The mechanisms of rounding are unlikely to be the same for all stimuli, however, this assay is particularly useful to determining the morphological impact on intestinal epithelia. Active caspase-3 is relatively stable compared with other caspases and has a half-life of 8–11 h⁴¹ and was detectable following TNF treatment for the entire time-course of our experiments. We also assessed the expression of active caspase-8 and whilst this was observed at the villus tip at early time-points as in previous studies²⁹, this caspase is much less stable, cleaved components p43 having a half-life of 63 ± 5 min and p18 having a much shorter half-life of 7 ± 1 min⁴² and was not detected over the whole time-course of our experiments in enteroids, thus active caspase-8 activity did not positively correlate with enteroid circularity.

Upregulation of *NF- κ B* mRNA has been observed in colitis-associated dysplasia and carcinoma⁴³. Our previous in vivo studies have also demonstrated that *Nfkb2*^{-/-} mice are less susceptible to the induction of experimental colitis, colitis-associated cancer and LPS-induced SI cell shedding^{17,20}. However, the role of the intestinal epithelium in contributing to this protection was previously unclear as *Nfkb2*^{-/-} mice have a perturbed immune system that could have also contributed to the altered phenotype⁴⁴. We have now demonstrated that *Nfkb2*^{-/-} proximal SI epithelium is resistant to TNF and IFN γ induced pathology in enteroids in the absence of contributions from the other cellular compartments that are present in vivo. This suggests that NF- κ B signalling is an important determinant of intestinal epithelial cell homeostasis. A range of concentrations of cytokines was tested in our experiments and alterations in circularity were noted at concentrations greater than 10 ng/ml TNF and 0.1 ng/ml IFN γ . These concentrations are higher than those detected in the circulation and tissues of human patients, however, faecal concentrations have been noted between 1 and 100 ng/g and are in line with the concentrations used in this study¹¹. Murine TNF is a known regulator of both classical and alternative pathway NF- κ B signalling and is likely to mediate its effects via TNFR1 and 2 ligation. However, it was surprising to also observe a decreased sensitivity to IFN γ in *Nfkb2*^{-/-} enteroids, though this is likely to be via an indirect mechanism resulting in the production of an NF- κ B activator such as BAFF⁴⁵. In addition to TNF and IFN γ , many cytokines contribute to the development of intestinal pathologies. We generated a co-culture model incorporating enteroids and BMDCs and showed that these cell populations could co-exist without any change to enteroid morphology. However, upon activation by LPS, BMDCs induced significant morphological changes in wild-type enteroids, whereas *Nfkb2*^{-/-} enteroids were seemingly protected. Cytokines generated in the model included TNF and IFN γ but both were produced at much lower concentrations than were required alone to induce circularity changes in enteroids and were similar to those observed in patients with pathology. This suggests that other secreted factors may also act synergistically with TNF and IFN γ to induce enteroid rounding in this setting. IL-6 was produced in abundance and could therefore contribute to modulating epithelial cell dynamics. An in-depth investigation of the BMDC secretome and assessment of cytokine combinations is now warranted to determine how the intestinal mucosal microenvironment regulates epithelial cell dynamics in combination with genetic susceptibility that may modulate the threshold for cytokines to induce a pathological response.

These data suggest that the NF- κ B2 signalling pathway, specifically in intestinal epithelial cells, may be targetable to ameliorate intestinal and systemic inflammation.

Materials and methods

Animals

Ten- to 12-week old wild-type C57BL/6J (Charles River, Margate, UK) and *Nfkb1*^{-/-} and *Nfkb2*^{-/-} mice^{44,46}, bred on the C57BL/6J genetic background were maintained at the University of Liverpool under a 12:12 h light dark cycle and fed a standard pelleted diet. All mice were euthanized by cervical dislocation with ethical approval under UK Home Office legislation (Animals Scientific Procedures Act 1986) and local ethical approval.

TNF treatment

Six female C57BL/6J mice were administered 0.33 mg/kg murine recombinant TNF (Peprotech Ltd., London, UK) by intraperitoneal injection and euthanized 1.5 h later. Six untreated female C57BL/6J were used as controls, mice were randomly allocated to two groups prior to treatment. SIs were excised, flushed with phosphate-buffered saline (PBS) pH 7.4 and fixed in 10% v/v neutral buffered formalin maintaining orientation using previously described methods⁴⁷.

Tissue preparation and scoring

Formalin-fixed SI was divided up into proximal, middle and distal thirds and bundled using methods previously described⁴⁷⁻⁴⁹. Bundles were routinely processed, embedded in paraffin wax in the transverse orientation and 4 μ m thick tissue sections were stained with haematoxylin and eosin (H&E), direct red 80 (both from Sigma, Dorset, UK) or prepared for IHC.

For the quantification of apoptotic and proliferative intestinal epithelial cells in immunostained tissue sections, individual epithelial cells were counted from the base of the crypt to the mid-point of the villus tip in 20 well-orientated hemi crypt-hemi villi at 400x magnification from 6 mice per group (group sizes of 6 were estimated to be needed from previous studies to provide appropriate statistical power and the scorer was blinded to animal identifier at the time of analysis)¹⁷. For the quantification of apoptotic and proliferative intestinal epithelial cells in immunostained enteroid sections, individual cells were counted in the total circumference of 6 whole enteroids from at least 3 independent replicate studies at 400x magnification. Labelled cells were counted if in continuation with the epithelial monolayer. Intestinal epithelial cells were categorised according to the following criteria:

1. Normal if there was no or weak non-specific brown staining.
2. Apoptotic/mitotic if there was defined positive staining confined to cytoplasmic or nuclear borders.

IHC and histochemical staining

Tissue and enteroid sections were deparaffinised and rehydrated. Standard histochemical techniques were used for H&E, direct red 80 (Sirius red) and alcian

blue staining, the latter two being counterstained with haematoxylin to identify nuclei for quantification. Immunohistochemically stained slides were subjected to 1% v/v hydrogen peroxide in methanol to block endogenous peroxidases, followed by heat-mediated antigen retrieval in 0.01 M citrate acid buffer (pH 6) and then blocked with 1% w/v bovine serum albumin (Sigma, Dorset, UK). Rabbit polyclonal primary antibodies against active caspase-3 (AF835; R&D Systems, Abingdon, UK), Ki67 (AB15580; Abcam, Cambridge, UK) and olfactomedin-4 (#39141; Cell Signalling Technology, UK) were applied at 2.5, 2 and 0.25 µg/mL, respectively to sections for 2 h and visualisation was completed using an anti-rabbit Envision kit (Dako, Cambridge, UK) polymer followed by peroxidase substrate 3,3'-diaminobenzidine (DAB) (Sigma, Dorset, UK) using the manufacturer's instructions. Sections were counterstained with haematoxylin.

Bone marrow-derived dendritic cell extraction and culture

Femurs and tibias were harvested from male C57BL/6J wild-type mice and were mechanically cleaned to remove any surrounding tissues. Bones were transferred into 70% v/v ethanol for 2 min to sterilise their outsides. Bones were clipped at the top and bottom and a 24 G needle was used to flush out the bone marrow through a 40 µm cell sieve. Red blood cells were lysed, cells were quantified and resuspended in dendritic cell differentiation solution (RPMI containing GM-CSF (20 ng/ml), β-mercaptoethanol (50 µM), 10% w/v FCS, 1% w/v glutamine, 1% w/v penicillin/streptomycin; all from Sigma, Dorset, UK) in 10 cm petri dishes at a concentration of 2.5×10^5 /mL and plated at 20 mL/plate. Fresh media was added to dishes 4 days following and non-adherent BMDCs were used in experiments 7 days following isolation and differentiation.

BMDC conditioned media was generated by plating BMDCs in complete RPMI media as described above at concentrations of 1×10^3 , 1×10^4 , 1×10^5 BMDC/mL. BMDCs were removed from culture media by centrifugation after 48 h and supernatants were immediately used in enteroid assays.

Enteroid culture

Extraction and culture of SI crypts was carried out as previously described³² with modifications as indicated below. Male 10-week-old C57BL/6J mice were killed and the SI was rapidly removed and flushed with ice-cold PBS. The most proximal, middle and most distal 2 cm segments were isolated separately, opened out longitudinally, cut into 1 cm lengths and placed into PBS. Intestinal segments were washed 10 times in ice-cold PBS and incubated with ice-cold chelation buffer (20 mL of 2 mM EDTA in PBS) at 4 °C with constant gentle agitation for 30 min. Chelation buffer was then replaced with 20 mL shaking buffer (43.3 mM sucrose, 59.4 mM sorbitol; Sigma, Dorset, UK) and shaken gently for 30 s to remove the majority of villi. Shaking buffer was replaced with fresh shaking buffer (20 mL) and crypts were then detached from the basal membrane by vigorous shaking by hand for 2 min. The crypt-enriched supernatant was filtered through a 70 µm cell strainer (BD Biosciences Heidelberg, Germany) and quantified using microscopy. The filtered crypts were centrifuged at $200 \times g$ (4 °C, 10 min) and resuspended at 10,000 crypts/mL in Matrigel (BD Biosciences) containing growth factors; epidermal growth factor (50 ng/mL), R-spondin-1 (500 ng/mL) and Noggin (100 ng/mL) (R&D Systems). Approximately, 500 crypts in 50 µL Matrigel were seeded per well of a pre-warmed 24-well flat-bottomed plate and incubated at 37 °C for 10 min to polymerise the Matrigel. Finally, 500 µL of minigut culture medium was added to each well (advanced DMEM/F12, 1% l-glutamine, 1% Pen/Strep, 10 mM HEPES,

10 mM N2 supplement, 50 mM B27 supplement (Invitrogen)) and crypts were cultured at 37 °C in a 95% air, 5% CO₂ atmosphere.

All enteroids were passaged at least once prior to use in an experiment. Passage was carried out weekly at a 1:4 split ratio. Media was removed and enteroids in Matrigel were resuspended in PBS and mechanically dissociated into crypts by passing through a 27 G needle. Dissociated enteroids were then centrifuged at 200 × *g* (4 °C, 10 min), resuspended in fresh Matrigel containing growth factors and plated as above. Culture medium was changed and replaced with new media containing growth factors every 4 days.

Enteroid treatments

C57BL/6J, *Nfkb1*^{-/-} and *NFkb2*^{-/-} enteroids (passage 2–12) were treated 3 days following passage by adding murine recombinant TNF (1–1000 ng/mL; PeproTech Ltd., London, UK), IFN γ (01–100 ng/mL; Peprotech Ltd.), C57BL/6J BMDCs (5 × 10⁴/well) with or without 1 μ g/mL LPS diluted in 50% minigut media (containing 2× growth factors) and 50% complete BMDC media or conditioned media from BMDCs. High power images of 3 enteroids/well, conducted in duplicate were taken at 0, 24 and 48 h for circularity measurements and enteroids were harvested for histological analysis as described below.

Enteroid histology

Following treatment with TNF, media was removed and replaced with 500 μ L cell recovery solution (Corning, New York, USA) and agitated at 4 °C until the Matrigel was dispersed. Enteroids were then fixed in 2% v/v neutral buffered formalin. After 1-h fixation enteroids were centrifuged at 100×*g* for 1 min. The supernatant was discarded and 80–120 μ L of pre-warmed Histogel™ (Thermo Scientific, Massachusetts, USA) was mixed carefully with enteroids and transferred directly onto a section of Micropore™ surgical tape forming a button when set. Sections of tape with Histogel were transferred into embedding cassettes and routinely processed and embedded in paraffin wax. Sections of Histogel containing enteroids (4 μ m thick) were stained with H&E, direct red 80, or prepared for IHC as described above.

Enteroid circularity assessment

Bright field microscopy was used to monitor enteroid development from crypt isolation and throughout subsequent passages and treatments. Images were taken using an Axiovert 25 microscope (Zeiss) and a 20× objective lens with a Hitachi HV-C20A camera. Enteroid morphology was assessed throughout experiments using 2D bright field images and a software-based formula for calculating circularity: 4π (area)/perimeter². Two-dimensional images of enteroids were traced (three representative images per well conducted in duplicate) and analysis was conducted by recording enteroid area, perimeter and circularity using the analyse and measure function in ImageJ software⁵⁰. Circularity values are possible between 0 and 1, with a score of 1 indicating a perfect circle. The circularity scoring method was adapted for enteroids from a previously reported system in mammary epithelial cultures⁵¹.

Cytokine analysis

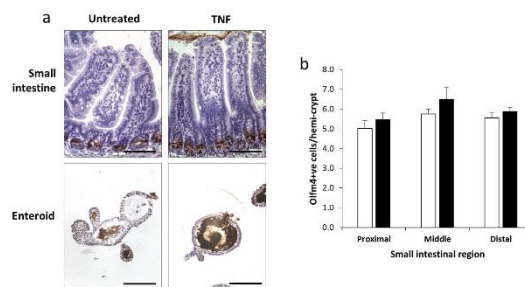
Media was removed from enteroids and enteroids in co-culture with BMDCs with and without LPS treatment 48 h post culture and centrifuged to remove debris. Samples were immediately frozen at -80°C until further analysis and defrosted only once for further usage. Samples were run in duplicate and a multiplexing capable analysis platform selected for simultaneous cytokine profiling (QuickPlex SQ 120, Meso Scale Discovery, USA). The U-plex mouse cytokine assay system was employed for the analysis of a panel of markers as per manufacturer's instructions. Cytokines analysed were: IFN γ , TNF, KC/GRO, IL-1 β , IL-2, IL-4, IL-5, IL-6, IL-10, IL-12 p70, IL-15, IL-17, IL-23 and IL-33. Quantitative measurement of each marker was achieved using a four-parameter logistic regression method.

Statistical analysis

Student's *t* tests were carried out on normally distributed data within proximal, middle and distal regions of the SI and for cytokine production between LPS-treated BMDCs and untreated BMDCs. All additional normally distributed data were analysed by one-way ANOVA versus control group followed by Holm–Sidak post hoc analysis. Statistical tests that achieved $p < 0.05$ were considered significant.

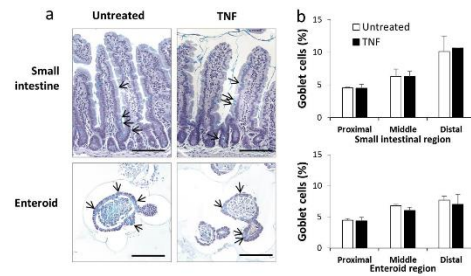
Supplemental Figure legends

Supplemental figure 1: TNF does not modulate Olfm4 expression in small intestine at the time-points tested. Untreated and TNF treated proximal SI and enteroids stained for Olfm4 (a). Percentage of Olfm4 stained cells in untreated (white) and TNF treated (black) proximal, middle and distal small intestine (b). For animal study quantified from $n=3$ mice per group.



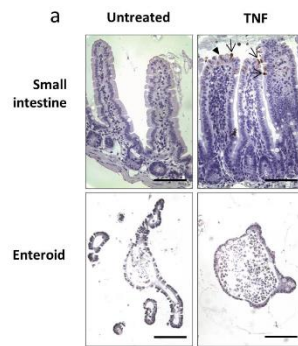
Supplemental figure 1

Supplemental figure 2: TNF does not reduce goblet cell number at the time-points tested. Proximal SI and enteroids stained with alcian blue (a). Percentage of alcian blue stained goblet cells in untreated (white) and TNF treated (black) proximal, middle and distal derived small intestine (top) and enteroids (bottom)(b). For animal study quantified from $n=3$ mice per group, for enteroid study $n=6$, $N=3$.



Supplemental figure 2

Supplemental figure 3: TNF activates caspase-8 in the small intestinal epithelium but is short lived. Proximal SI and enteroids stained for active caspase-8. Arrows indicate active caspase-8 positive cells with shedding morphology, and arrow heads indicate active caspase-8 positive cells without shedding morphology (a).



Supplemental figure 3